UNIVERSIDADE DE LISBOA
Faculdade de Medicina

The Role of Post-Translational Modifications on the Oligomerization, Aggregation and Toxicity of Mutant Huntingtin

Joana Margarida Marques Branco dos Santos

Orientadores: Doutor Federico Herrera Garcia
Prof. Doutor Tiago Fleming de Oliveira Outeiro
Prof. Doutor Flaviano Giorgini

Tese especialmente elaborada para obtenção do grau de Doutor em Ciências Biomédicas, na especialidade de Neurociências

2018

UNIVERSIDADE DE LISBOA
Faculdade de Medicina

The Role of Post-Translational Modifications on the Oligomerization, Aggregation and Toxicity of Mutant Huntingtin

Joana Margarida Marques Branco dos Santos

Orientadores: Doutor Federico Herrera Garcia
Prof. Doutor Tiago Fleming de Oliveira Outeiro
Prof. Doutor Flaviano Giorgini

Tese especialmente elaborada para obtenção do grau de Doutor em Ciências Biomédicas, na especialidade de Neurociências

Júri

Presidente: Professor Doutor José Luís Bliebernicht Ducla Soares, Professor Catedrático em regime de tenure e Vice-Presidente do Conselho Científico da Faculdade de Mecinina da Universidade de Lisboa.

Vogais:

- Prof. Dr. Ir. *Nollen*, *Ellen Alexandra Adriënne*, Professor of Faculty of Medical Sciences Aging Biology, University of Groningen (Holanda),
- Doutora Ana Cristina Carvalho Rego, Professora Auxiliar com Agregação da Faculdade de Medicina da Universidade de Coimbra,
- Doutora Cecília Maria Pereira Rodrigues, Professora Catedrática da Faculdade de Farmácia da Universidade de Lisboa,
- Doutor Cláudio Emanuel Moneira Gomes, Professor Associado com Agregação da Faculdade de Ciências da Universidade de Lisboa,
- Doutor Federico Herrera Garcia, Professor Auxiliar da Faculdade de Ciências da Universidade de Lisboa (orientador),
- Doutora Luísa Maria Vaqueiro Lopes, Professora Associada Convidada da Faculdade de Medicina da Universidade de Lisboa.

Instituição Financiadora: Fundação para a Ciência e Tecnologia (SFRH/BD/85275/2012)

2018

Todas as informações efectuadas no presente documento são da exclusiva responsabilidade da sua autora, não cabendo qualquer responsabilidade à Faculdade de Medicina da Universidade de Lisboa pelos conteúdos nele apresentados.

A impressão desta tese foi aprovada pelo Conselho Científico da Faculdade de Medicina de Lisboa em reunião de 12 de Outubro de 2018.

I declare that this dissertation is based on work developed during my PhD research project, except where otherwise stated. Experimental work was performed mainly at Instituto de Tecnologia Química e Biológica António Xavier, Universidade Nova de Lisboa, in Oeiras, Portugal and the Department of Genetics and Genome Biology, University of Leicester, in Leicester, United Kingdom. The initial part of the work involving mammalian cell models (described in Chapter III, 3.1 and 3.3) was developed at Instituto de Medicina Molecular – Faculdade de Medicina, Universidade de Lisboa, in Lisbon, Portugal. Doctor Federico Herrera, Prof. Doctor Tiago Fleming Outeiro and Prof. Doctor Flaviano Giorgini supervised all work.

Financial support was provided by Fundação para a Ciência e a Tecnologia (FCT), Portugal, through the PhD fellowship SFRH/BD/85275/2012 and FCT/MCTES (Ref. CBQ/04612/ICL3535, to Doctor Federico Herrera and Doctor Pedro Domingos). Doctor Federico Herrera and Prof. Doctor Tiago Outeiro were supported by a seed grant from the European Huntington Disease Network (EHDN). Doctor Federico Herrera is currently supported by Project LISBOA-01-0145-FEDER-007660 (Cellular Structural and Molecular Microbiology) funded by FEDER funds through COMPETE2020 - Programa Operacional Competitividade e Internacionalização (POCI) and by national funds through FCT (Ref. IF/00094/2013). Prof. Doctor Tiago Outeiro is supported by the DFG Center for Nanoscale Microscopy and Molecular Physiology of the Brain. Prof. Doctor Flaviano Giorgini thanks the Medical Research Council (MRC) for infrastructure supporting this work.

Aos meus pais.

Ao meu irmão.

"*For pure joy, I look at a small painting by Arbit Blatas. An ocean liner is at the center of the composition, perhaps ready to depart. It holds the promise of discovery.*"

António Damásio, *in* "Self comes to mind".

Table of contents

Acknowledgements/Agradecimentos

A PhD is a long journey of self discovery, yet a challenge that is hardly exceeded by oneself. This thesis represents not only my work, it was a group effort in which extraordinary researchers have participated and contributed, in one way or another, to the person I am today, both at scientific and personal levels.

My deepest gratitude goes to my supervisor Dr. Federico Herrera, who made this thesis a reality in every way possible. Our journey together started in 2011, when I joined Professor Tiago Outeiro lab (UNCM). Fede was determinant for my growth as a master student and now, as a PhD. I thank Fede for guiding me throughout my PhD, and for sharing with me his valuable scientific and technical knowledge. Fede taught me everything I know about scientific writing, being always very careful and going deeply through all details of the present thesis and other scientific publications. I am sincerely grateful to Fede for his patience and for giving me the time and space I needed to independently grow and develop my own scientific ideas/opinions. Mostly, I thank Fede for the constructive and fair criticism, which was sometimes hard to hear, but essential to get to the final stage of my PhD. Thank you for motivating me to finish this thesis, for all the support and advice in the critical and hard times of my PhD, and especially for all the precious time you have dedicated to discuss and supervise my work.

O meu profundo agradecimento ao Professor Dr. Tiago Outeiro, a quem devo o início da minha jornada neste maravilhoso mundo da ciência e, como tal, parte do meu percurso científico. O Tiago abriu-me as portas do seu laboratório oferecendo-me a possibilidade de trabalhar com investigadores excepcionais, num ambiente de sólida construção de conhecimento científico. Muito obrigado por toda a ajuda, disponibilidade e sábias diretrizes que em muito contribuíram para a minha investigação e para a consolidação deste trabalho.

I owe my sincere gratitude to Professor Dr. Flaviano Giorgini, who gave me the opportunity to work in his lab for two wonderful years (Leicester, UK), and probably the most productive times of my PhD. Flav is one of the rare supervisors who always have wise words to share and to guide his students in such a stressful and demanding period of ours science careers. I found in Flav an inspiring and rigorous scientist, who helped me to see the bright side of my work, even when I thought I had no results or new developments to discuss with him and my colleagues in Leicester. He helped to organize and develop my scientific thinking, to make rational sense of my results, and to reach quality in the

production of scientific data. I am deeply thankful to Flav for the meaningful scientific discussions, for trusting in my work, and for motivating me to never give up on accomplishing my goals.

Devo também um especial agradecimento ao Dr. Pedro Domingos pela preciosa colaboração e por proporcionar todo o apoio técnico e intelectual necessários ao meu trabalho com *Drosophila*. Obrigado por fazer parte do meu comité de tese e por me receber no seu laboratório ao longo destes dois últimos anos de PhD. Agradeço a disponibilidade em me ajudar e receber sempre que tive dúvidas.

Um sincero agradecimento à Dra Luísa Lopes e ao meu querido colega Dr. Hugo Vicente Miranda pelo tempo dispensado como membros do meu comité de tese. O excepcional input científico que me facultaram foi fundamental para o foco e desenrolar da minha investigação. Ao Hugo, muito obrigado por todo o apoio tanto a nível profissional como pessoal, é com muito carinho que guardo todos os conselhos que certamente me guiarão no futuro.

Aos colegas do grupo UNCM, a todos sem exceção, com quem tive a honra de trabalhar e que me proporcionaram momentos de constante inspiração e espírito de entreajuda. Devo também um agradecimento aos colegas do laboratório "Cell Structure and Dynamics", no ITQB, dos quais teria que destacar o Ricardo Vilela e a Joana Ferreira pelo companheirismo, apoio e confidências. Ainda do ITQB, à Yolanda Pires, que contribuiu e ajudou em algumas das últimas experiências do meu PhD. Obrigado pela amizade e companhia nas longas horas de microscopia. Um obrigado também à Cristiana Santos.

To my colleagues and friends in Leicester, who supported me in all possible ways. Special thanks to Carlo Breda, who introduced me to *Drosophila* and helped me to think and design experiments. To Ane, Usha, Marcela and Daniel for always making me feel at home.

I am grateful to all collaborators, whose names are mentioned in the results chapter of the present thesis. I would also like to thank the people from IMM and IGC facilities for the technical support with some of the experiments.

A toda a minha família, pela preocupação e interesse no meu trabalho. Por acreditarem nos meus sonhos e confiarem nas minhas escolhas. Ao meu irmão, por todo o seu entusiasmo por ciência. À Inês e à Filipa, amigas e confidentes desde os tempos de mestrado. À Maria, por estar sempre presente e por vibrar com todos os meus sucessos.

Summary

Neurodegenerative diseases (NDs) present major health and economic challenges to modern societies. No treatments can currently stop, delay or reverse the progression of such devastating disorders. The development of effective therapeutics is particularly complicated because the molecular underpinnings of NDs are still far from being understood. A possible clue could come from the fact that a large number of NDs display protein misfolding and aggregation as pathophysiological hallmarks. Understanding factors which modulate the aggregate formation process and the mechanisms by which protein intermediates exert cellular toxicity could advance our knowledge of disease pathogenesis and represents a possible intervention point in our search for effective therapies. Recent years have seen several rational targets for therapeutic development being generated from a combination of cell culture studies and analysis of genetically tractable animals. Here we used a cell model exploiting bimolecular fluorescence complementation (BiFC) and *Drosophila* models to study the molecular basis of Huntington's disease (HD).

HD is a hereditary neurodegenerative disorder generally affecting individuals of 40-50 years of age, although the most severe forms of the disease can appear in children and adolescents. HD causes death invariably 15-20 years after the first symptoms, with patients and their families experiencing incalculable pain and suffering throughout the course of the disease. The causative mutation encodes a polyglutamine expansion in the huntingtin (HTT) protein, which modulates its aggregation and cytotoxicity by still unclear mechanisms. Although HD is genetically well defined, unidentified genetic and/or environmental factors may also play a role in disease development and progression.

The present thesis aimed to (i) characterize the effect of specific post-translational modifications (PTMs) upon mutant HTT aggregation dynamics and toxicity, as well as (ii) investigate the putative regulatory role of protein phosphatases in these processes, and (iii) understand how interactions between mutant HTT and other aggregation-prone proteins may modulate disease pathogenesis.

We started by determining the relative contribution of each of the three phosphorylatable residues (T3, S13 and S16) in the N-terminal region of HTT towards its aggregation and toxicity. By using single phosphomimic (D) and phosphoresistant (A) BiFC mutants, we found that all of the D mutants completely abolished the formation of large insoluble species, while having little effect on oligomerization and toxicity. When combined with non-phosphorylated forms of mutant HTT, D mutants differentially

affected HTT aggregation dynamics in living cells, with T3 phosphorylation having the most dominant effect. Analyses of transgenic *Drosophila* mutants further supported T3 as a critical modulator of mutant HTT aggregation, with both larvae and adult fly tissues from T3D mutants exhibiting lower number of aggregates compared to non-mutated counterpart.

Since N-terminal phosphorylation strikingly prevented HTT aggregation, we investigated specific protein phosphatases as potential modulators of HTT aggregation and toxicity in both mammalian cells and *Drosophila*. An initial pharmacological screen in our BiFC cell model identified three phosphatase inhibitors (PP1, PP2A and Cdc25) as potential suppressors of HTT aggregation. Subsequent RNAi experiments *in vivo* showed that PP1 downregulation prevented the deposition of HTT inclusions in adult fly dopaminergic neurons, whereas both PP2 and Cdc25 knockdown did not produce overt phenotypes. Interestingly, downregulation of PP1 in flies caused severe age-dependent neurodegeneration. Together, these findings indicate that PP1 modulates HTT aggregation and toxicity in opposite ways, which further support the current notion that large inclusions are not the toxic factors in HD and other NDs.

The formation of advanced glycation-end products (AGEs) as result of the interaction between proteins and reducing sugars is referred to as protein glycation. Such irreversible PTM is found in various disease-associated proteins, and is thought to contribute to the pathogenesis of NDs. Here, we provide the first *in vivo* evidence on the deleterious impact of glycation on HTT biology and HD. Pharmacological or genetic modulation of protein glycation led to increased accumulation of AGEs in mutant HTT-expressing flies and exacerbated phenotypes related to both early and late stages of HD. In particular, we showed that treatment with increasing doses of a potent glycation agent - methylglyoxal (MGO) - accelerated neuronal loss in adult animals and negatively affected the development of photoreceptor neurons. Genetic suppression of the MGO pathway resulted in impaired development, reduced lifespan and increased neurodegeneration of HD flies. In humans, increased blood glucose levels activate the MGO pathway, which would implicate altered glucose metabolism (e.g. diabetes) as an environment risk factor for HD development.

Aberrant protein-protein interactions can compromise normal cell function and contribute to cytotoxicity in NDs. Here, we explored the effects of mutant HTT interactions with other aggregation-prone proteins on each other's behavior. We showed that mutant HTT interacts and co-aggregates with alpha-synuclein (α-syn), Tau and the Rnq1 prion protein in living human cells, altering their subcellular localization and

aggregation patterns. While *in vivo* α-syn and Tau studies were carried out by various collaborators, we set out to elucidate the interplay between the Rnq1 prion protein and mutant HTT. In yeast, the Q/N-rich Rnq1 prion protein is required for mutant HTT aggregation and toxicity. Because the human genome encodes multiple proteins enriched in Q/N domains, we hypothesized that they may function as modifiers of disease pathogenesis. *Drosophila* expressing Rnq1 showed a significant increase in age-dependent neuronal loss and motor dysfunction. Furthermore, as occurs in yeast, we found that Rnq1 potentiates mutant HTT toxicity in *Drosophila*. Together, our results are consistent with the existence of two mechanisms for HTT toxicity, one related to toxicity of the aggregation process itself, and the other related to the sequestration of molecules required for normal cell function.

Overall, our findings provide new insights into HD pathology by uncovering novel aspects of mutant HTT aggregation and toxicity. We expect these studies to contribute to a better understanding of the mechanisms underlying the pathogenesis of HD and other human protein misfolding disorders, and thus lay the groundwork for effective therapeutic strategies for these devastating disorders.

Keywords: Huntington's disease, huntingtin, phosphorylation, glycation, prion proteins.

Resumo

As doenças neurodegenerativas (DNs) apresentam grandes desafios económicos e para a saúde nas sociedades modernas. Atualmente, não existem tratamentos capazes de parar, atrasar ou reverter a progressão destas doenças devastadoras. Os fundamentos moleculares de DNs ainda estão longe de serem compreendidos, o que complica o desenvolvimento de terapias eficazes. Um grande número de DNs é caracterizada pela alteração da conformação normal de proteínas (*misfolding)* e sua acumulação em agregados proteicos (agregação). Assim, compreender quais os intervenientes no processo de formação de agregados, e os mecanismos pelos quais as espécies intermédias, resultantes do processo, exercem toxicidade celular, pode facultar avanços no nosso conhecimento sobre a patogénese de NDs e, representa um ponto de inflexão na nossa busca por terapias eficientes. Nos últimos anos têm surgido vários potenciais alvos terapêuticos através de estudos em culturas celulares e da análise de modelos animais de fácil manipulação genética. Neste trabalho, utilizámos modelos celulares, baseados no método de complementação biomolecular por fluorescência (BiFC), e modelos de *Drosophila* para estudar os mecanismos associados à doença de Huntington (DH).

A DH é uma doença neurodegenerativa hereditária que afeta geralmente indivíduos entre os 40-50 anos de idade, embora formas mais graves da doença possam surgir em crianças e adolescentes. Esta doença leva à morte 15-20 anos após o aparecimento dos primeiros sintomas, causando dor e sofrimento incalculáveis a pacientes e famílias ao longo de todo esse período. A mutação genética responsável pela DH resulta na expansão anormal de uma região rica em glutaminas na proteína huntingtina (HTT). Essa região modula a agregação e a toxicidade celular da proteína por mecanismos ainda não totalmente conhecidos. Apesar da DH ser uma doença de causa genética definida, outros factores genéticos e/ou ambientais podem afectar o seu desenvolvimento e progressão.

Esta tese teve como principais objectivos (i) caracterizar o efeito de modificações pós-traducionais específicas na dinâmica de agregação da HTT bem como na sua toxicidade, (ii) investigar o potencial papel regulador de fosfatases nesses processos, e (iii) compreender como interações entre a HTT e outras proteínas com propensão para agregar podem contribuir para a patogénese da doença.

Começámos por determinar o papel de cada um dos três resíduos fosforiláveis (T3, S13 e S16) da região N-terminal da HTT na agregação e toxicidade da proteína. Através da utilização de mutantes BiFC que imitam o estado de fosforilação (D) ou não-fosforilação

(A) nos respectivos resíduos, verificou-se que a fosforilação constitutiva de qualquer um dos resíduos resultou na ausência total de grandes espécies insolúveis nas células. No entanto, estes mutantes produziram pouco efeito sobre a oligomerização e toxicidade da HTT. Estes resultados indicam que a fosforilação da região N-terminal da HTT desempenha um papel-chave na agregação da proteína. Combinações de mutantes fosforilados com mutantes resistentes à fosforilação levaram a alterações na dinâmica de agregação da HTT em células vivas, onde T3D exerceu um efeito dominante sobre todos os mutantes resistentes à fosforilação, impedindo assim a formação de agregados. Em *Drosophila,* mutantes T3D exibiram um menor número de agregados em relação ao controlo, evidenciando assim o resíduo T3 como um modulator crítico da agregação da HTT.

Uma vez que a fosforilação da região N-terminal da HTT produziu um efeito supressor notável sobre a agregação da proteína, procurámos de seguida identificar fosfatases específicas como potenciais reguladores da agregação e toxicidade da HTT em células de mamífero e *Drosophila*. Um *screening* farmacológico inicial permitiu-nos identificar três inibidores de fosfatases (PP1, PP2A e Cdc25) como possíveis supressores da agregação da HTT. Experiências subsequentes de interferência de RNA contra PP1 em *Drosophila* resultaram na diminuição de agregados em neurónios dopaminérgicos da mosca adulta, enquanto que, tanto a inibição de PP2 como Cdc25 não produziu qualquer alteração no fenótipo de agregação esperado da HTT. Curiosamente, a inibição de PP1 em *Drosophila* agravou severamente a perda neuronal dependente da idade. Estas novas descobertas indicam que PP1 modula de forma oposta a agregação e toxicidade da HTT, o que vai de encontro à hipótese atual de que grandes agregados proteicos não constituem os factores tóxicos na DH e noutras DNs.

A formação de produtos finais da glicação avançada (AGEs) como resultado da interação entre proteínas e açúcares redutores é conhecida como "glicação proteica". Esta modificação pós-traducional irreversível ocorre em várias proteínas associadas a doenças, e pensa-se estar envolvida na patogénese de DNs. Nesta tese, oferecemos a primeira evidência *in vivo* sobre o impacto negativo da glicação na biologia da HTT e na DH. Ao manipular farmacologicamente ou geneticamente a glicação proteica observámos a acumulação de AGEs num modelo de *Drosophila* da DH, sendo que tanto fenótipos relacionados com estágios precoces e tardios da DH tiveram uma manifestação exacerbada nestes animais. Em particular, demonstrámos que o tratamento com doses crescentes de um potente agente de glicação, o metilglioxal (MGO), resultou na perda neuronal

prematura em animais adultos e afetou negativamente o desenvolvimento dos neurónios fotorreceptores. A estimulação genética da via do MGO prejudicou o desenvolvimento, a sobrevida e a integridade neuronal destes animais modelo da DH. Nos seres humanos, níveis aumentados de glicose no sangue levam à ativação da via do MGO, sugerindo que alterações no metabolismo da glicose (por exemplo, diabetes) podem constituir um factor de risco ambiental para o desenvolvimento da doença.

Interações proteicas aberrantes podem comprometer a função celular normal e contribuir para a toxicidade celular em DNs. Neste trabalho, explorámos os efeitos de interações entre a HTT e outras proteínas propensas à agregação no contexto celular e em modelos animais. Foi demonstrado que a HTT é capaz de interagir e co-agregar com as proteínas alfa-sinucleína (α-syn), Tau e a proteína prião Rnq1, alterando a sua localização e padrão de agregação em células vivas. Estudos *in vivo* da interação com α-syn ou Tau foram realizados por vários colaboradores, enquanto que o nosso trabalho focou-se na interação entre a HTT e a proteína prião Rnq1. Em levedura, este proteína rica em regiões Q/N é necessária para a agregação e toxicidade da HTT. Uma vez que, o nosso genoma codifica múltiplas proteínas enriquecidas em domínios Q/N, colocámos a hipótese de que estas proteínas poderiam eventualmente desempenhar um papel na patogénese da DH. Quando expressa em *Drosophila*, Rnq1 provocou um aumento significativo da perda neuronal associada à idade, e disfunção motora. Além disso, como ocorre em levedura, também a expressão de Rnq1 em *Drosophila* resultou no aumento da toxicidade da HTT. Na sua totalidade, os nossos resultados são consistentes com a existência de dois mecanismos de toxicidade da HTT, um relacionado com a toxicidade do próprio processo de formação de agregados e, outro relacionado com o "sequestro" de moléculas essenciais à normal função celular.

O presente estudo põe a descoberto novos aspectos sobre a agregação e toxicidade da HTT, possibilitando deste modo um melhor conhecimento da patologia da DH. Esperamos que este trabalho possa contribuir para desvendar os mecanismos moleculares responsáveis pela patogénese da DH e de outras doenças humanas associadas ao *misfolding* de proteínas, e assim, estabelecer as bases para o desenvolvimento de estratégias terapêuticas eficientes contra estas doenças devastadoras.

Palavras-chave: Doença de Huntington, huntingtina, fosforilação, glicação, proteínas prião.

List of thesis publications

The work present in this thesis was reported in the following journals, book and scientific meetings:

Publications

Peer-reviewed articles

Branco-Santos J, Staniforth GL, Maddison DC, Breda C, Domingos PM, Steinert JR, Kyriacou CP, Outeiro TF, Herrera F, Tuite MF, Giorgini F. Prion proteins modulate mutant huntingtin mediated neurotoxicity. (*under review)*

Branco-Santos J, Herrera F, Poças GM, Pires-Afonso Y, Giorgini F, Domingos PM, Outeiro TF (2017). Protein phosphatase 1 regulates hungtingtin exon 1 aggregation and toxicity. *Human Molecular Genetics*, 26: 3763-3775.

Vicente Miranda H, Gomes MA, Branco-Santos J, Breda C, Lázaro DF, Lopes LV, Herrera F, Giorgini F, Outeiro TF (2016). Glycation potentiates neurodegeneration in models of Huntington's disease. *Scientific Reports*, 18 (6): 36798.

Poças GM, Branco-Santos J, Herrera F, Outeiro TF, Domingos PM (2014). α-Synuclein modifies mutant huntingtin aggregation and neurotoxicity in Drosophila. *Human Molecular Genetics*, 24: 1898-1907.

Book chapter

Herrera F, Gonçalves S, Branco-Santos J, Outeiro TF (2014). Studying the molecular determinants of protein oligomerization in neurodegenerative disorders by bimolecular fluorescence complementation. In: *Bio-nanoimaging in protein misfolding and aggregation* (pp. 133-145, Part II, Chapter 12), Vladimir N Uversky and Yuri L Lyubchenko. Elsevier Inc. doi: 10.1016/B978-0-12-394431-3.00012-2.

Communications in scientific meetings

Oral communications

Branco-Santos J, Poças GM, Pires-Afonso Y, Giorgini F, Domingos PM, Herrera F, Outeiro TF (2016). Single N-terminal phosphorylation modulates mutant huntingtin aggregation and toxicity. 7th ITQB NOVA PhD Students' Meeting. November 23-25. ITQB. Oeiras, Portugal. Oral presentation.

Branco-Santos J, Poças GM, Pires-Afonso Y, Giorgini F, Domingos PM, Herrera F, Outeiro TF (2016). Single N-terminal phosphorylation modulates mutant huntingtin aggregation and toxicity. 1st Cedoc Symposium on Chronic Diseases. June 30 - July 1. NOVA Medical School, Faculty of Medical Sciences. Lisbon, Portugal. Selected short talk.

Branco-Santos J, Poças GM, Pires-Afonso Y, Giorgini F, Domingos PM, Herrera F, Outeiro TF (2016). The Role of protein phosphatases in mutant huntingtin aggregation and toxicity. Understanding the molecular brain in health and disease symposium. June 29. Faculty of Sciences, University of Lisbon. Lisbon, Portugal. Selected short talk.

Branco-Santos J, Staniforth GL, Maddison DC, Breda C, Herrera F, Outeiro TF, Tuite MF, Giorgini F (2014). The Role of Post-Translational Modifications in Huntington's Disease Pathogenesis. Post-Graduate Research Students Seminar, Department of Genetics, University of Leicester. Leicester, U.K. Oral presentation.

Branco-Santos J, Staniforth GL, Maddison DC, Breda C, Herrera F, Outeiro TF, Tuite MF, Giorgini F (2014). The Role of Aggregation-Prone Proteins in Huntington's Disease Pathogenesis. University of Kent. Kent, U.K. Oral presentation.

Poster communications

Branco-Santos J, Staniforth GL, Maddison DC, Breda C, Herrera F, Outeiro TF, Tuite MF, Giorgini F (2017). Prion-like proteins alter mutant huntingtin aggregation and neurotoxicity in models of Huntington's disease. Proteostasis EMBO Workshop. November 17-21. Ericeira, Portugal.

Branco-Santos J, Poças GM, Pires-Afonso Y, Giorgini F, Domingos PM, Herrera F, Outeiro TF (2017). Protein phosphatase 1 modulates mutant huntingtin aggregation and toxicity. Portuguese Drosophila Meeting 2017. September 8-9. Tomar, Portugal.

Branco-Santos J, Poças GM, Pires-Afonso Y, Giorgini F, Domingos PM, Herrera F, Outeiro TF (2017). Protein phosphatase 1 modulates mutant huntingtin aggregation and toxicity. Ciência 2017. July 3-5. Lisbon Congress Center, Lisbon, Portugal

Branco-Santos J, Poças GM, Pires-Afonso Y, Giorgini F, Domingos PM, Herrera F, Outeiro TF (2017). Protein phosphatase 1 modulates mutant huntingtin aggregation and toxicity. XV Meeting of the Portuguese Society for Neuroscience 2017. May 25-26. Braga, Portugal.

Branco-Santos J, Poças GM, Pires-Afonso Y, Giorgini F, Domingos PM, Herrera F, Outeiro TF (2016). Single N-terminal phosphorylation modulates mutant huntingtin aggregation and toxicity. Ciência 2016. July 4-6. Lisbon Congress Center, Lisbon, Portugal.

Branco-Santos J, Poças G, Letra-Vilela R, Silva-Almeida C, Outeiro T, Silvestre-Ferreira J, Pires-Afonso Y, Domingos P, Herrera F (2016). Co-aggregation of huntingtin with other neurodegeneration-related proteins: effect on aggregation patterns and toxiciy. 1st Cedoc Symposium on Chronic Diseases. June 30- July 1. NOVA Medical School, Faculty of Medical Sciences. Lisbon, Portugal.

Branco-Santos J, Poças GM, Pires-Afonso Y, Giorgini F, Domingos PM, Herrera F, Outeiro TF (2016). Single N-terminal phosphorylation modulates mutant huntingtin aggregation and toxicity. X PhD CAML Meeting. March 30 – April 1. Lisboa, Portugal.

Branco-Santos J, Giorgini F, Outeiro TF, Herrera F (2015). Exploring the role of phosphorylation in huntingtin aggregation dynamics. XIV Meeting of the Portuguese Society for Neuroscience. June 4-5, July 1. Póvoa de Varzim, Portugal.

Branco-Santos J, Herrera F, Outeiro TF, Giorgini F (2014). The Role of Huntingtin Post-translational Modifications in Huntington's Disease Pathogenesis. Neuroscience & Behaviour Symposium. December 3. Leicester, United Kingdom.

Vicente Miranda H, Gomes M, Branco-Santos J, Giorgini F, Outeiro TF (2014). Glycation modulates huntingtin aggregation and toxicity. European Huntington's Disease Network Plenary Meeting. September 19-21. Barcelona, Spain.

Branco-Santos J, Herrera F, Outeiro TF, Giorgini F (2014). Exploring the Role of Phosphorylation in Huntingtin Aggregation Dynamics. European Huntington's Disease Network Plenary Meeting. September 19-21. Barcelona, Spain.

Branco-Santos J, Staniforth G, Breda C, Herrera F, Outeiro TF, Tuite M, Giorgini F (2014). Aggregation-prone Proteins Exacerbate Huntingtin Toxicity in Yeast and Drosophila. European Huntington's Disease Network Plenary Meeting. September 19-21. Barcelona, Spain.

Branco-Santos J, Herrera F, Outeiro TF (2013). The Role of N-terminal Phosphorylation on Mutant Huntingtin Oligomerization, Aggregation and Toxicity. EMBO Young Scientists Forum. July 15-16. Lisbon, Portugal.

Branco-Santos J, Herrera F, Outeiro TF (2013). The Role of N-terminal Phosphorylation on Mutant Huntingtin Oligomerization, Aggregation and Toxicity. XIII Meeting of the Portuguese Society for Neuroscience. May 30-31, July 1. Luso, Portugal.

Herrera F, Branco-Santos J, Outeiro TF (2012). N-terminal phosphorylation of mutant huntingtin prevents the formation of large aggregates and toxicity but not oligomerization. European Huntington´s Disease Network Meeting. September 14-16. Stockholm, Sweden.

List of abbreviations

3-HK 3-hydroxykynurenine
α-syn Alpha-synuclein
Aβ Beta amyloid peptide
AD Alzheimer's disease
AGE Advanced glycation-end product
ALP Autophagy lysosome pathway
ALS Amyotrophic lateral sclerosis
AMP Adenosine monophosphate
APP Amyloid precursor protein
AU Arbitrary units
BAC Bacterial artificial chromosome
BDNF Brain-derived neurotrophic factor
bFGF Basic fibroblast growth factor
BiFC Bimolecular complementation assay
CAG Cytosine-adenine-guanine triplet
cAMP Cyclic adenosine monophosphate
CBP CREB-binding protein
Cdc25 Cell division cycle 25 phosphatase
Cdk5 Cyclin-dependent kinase 5
cDNA Complementary DNA
CHIP C terminus of HSC70-interacting protein
CK2 Casein kinase 2
CNS Central nervous system
Cp Crossing point-PCR-cycle
CREB cAMP response element binding
DAM *Drosophila* Activity Monitoring
DARPP-32 Dopamine- and cAMP-regulated phosphoprotein, 32 kDa
DLB Dementia with Lewy bodies
DN Down's syndrome
DPP Deep pseudopupil
DRPLA Dentatorubral pallidoluysian atrophy
EDTA Ethylenediaminetetraacetic acid
eGFP Enhanced green fluorescent protein
Elav Embryonic lethal, abnormal visual
ER Endoplasmic reticulum
ERK Extracellular signal-regulated kinase
FBS Fetal bovine serum
FRAP Fluorescence recovery after photobleaching
FRET/FLIM Fluorescence resonance energy transfer/Fluorescence lifetime imaging
FT Filter trap
GABA Gamma aminobutyric acid
GAL Galactose
GAPDH Glyceraldehyde 3-phosphate dehydrogenase
GdnHCL Guanidine hydrochloride
GFP Green fluorescent protein
Glo Glyoxalase
GLT1 Glutamate transporter 1
GM1 Monosialotetrahexosylganglioside
GMR Glass multiple reporter
GSK3 Glycogen synthase kinase 3
GTP Guanosine 5'-triphosphate
HAP1 Huntingtin-associated protein 1
HD Huntington's disease
HEAT Huntingtin, elongation factor 3, protein phosphatase 2A, TOR1
Hip1 Huntingtin interacting protein 1
Hippi Hip-1 protein interactor
HSC Heat-shock cognate
HSP Heat-shock protein
HTT Huntingtin
HTTex1 Huntingtin exon 1
ICC Immunocytochemistry
IKK IκB kinase
IP Immunoprecipitation
IPOD Insoluble protein deposit
IT15 Interesting transcript 15 gene
KMO Kynurenine 3-monooxygenase
KP Kynurenine pathway
KYNA Kynurenic acid
LDH Lactate dehydrogenase

LRRK2 Leucine-rich repeat kinase 2

MAPK Mitogen-activated protein kinase

MGO Methylglyoxal

MoPrP Murine prion protein

mRNA Messenger ribonucleic acid

MSK1 Mitogen- and stress-activated protein kinase 1

MSN Medium spiny neuron

N17 N-terminal sequence of 17 amino acids

NAD Nicotinamide adenine dinucleotide

ND Neurodegenerative disease

NFT Neurofibrillary tangles

NF-Y Nuclear factor Y

NGF Nerve growth factor

NMDA N-methyl-D-aspartic acid

PACSIN1 Protein kinase C and casein kinase 2 substrate in neurons

PAGE Polyacrylamide gel electrophoresis

Pak2 p21-activated kinase 2

PBS Phosphate buffer saline

PCR Polymerase chain reaction

PD Parkinson's disease

PMD Protein misfolding disorder

polyQ Polyglutamine

PP1/PP2 Protein phosphatase 1/Protein phosphatase 2

PRD Proline-rich domain

PRL-3 Phosphatase of regenerating liver 3

PrP Prion protein

PRNP Prion protein gene

PTM Post-translational modification

QPCR Quantitative polymerase chain reaction

QUIN Quinolinic acid

RAGE Receptor for advanced glycation-end product

Rh Rhodopsin

Rhes Ras homologue enriched in the *Striatum*

RNA Ribonucleic acid

RNAi Ribonucleic acid interference

ROI Region of interest

ROS Reactive oxygen species

Rpm Revolutions per minute

RT Room temperature

S13 Serine-13

S16 Serine-16

SBMA Spinal and bulbar muscular atrophy

SCA Spinocerebellar ataxia

SD Standard deviation

SDS Sodium dodecyl sulfate

SEM Standard error

SGK Serum and glucocorticoid-induced kinase

SNCA Synuclein alpha gene

SOD1 Superoxide dismutase 1

SUMO Small Ubiquitin-like Modifier

T3 Threonine-3

TARGET Temporal and regional gene expression targeting

TDP-43 Trans-activator regulatory DNA-binding protein 43

TH Tyrosine hydroxylase

TNT Tunneling nanotube

Tpi Triose phosphate isomerase

TRP Tryptophan

TSE Transmissible spongiform encephalopathy

UAS Upstream activating sequence

UPS Ubiquitin-proteasome system

WT Wild-type

YEPD Yeast extract peptone dextrose

YNB Yeast nitrogen base

I.

Introduction

This chapter contains parts of the following publication:
Herrera F, Gonçalves S, Branco-Santos J, Outeiro TF (2014). Studying the molecular determinants of protein oligomerization in neurodegenerative disorders by bimolecular fluorescence complementation. In: *Bio-nanoimaging in protein misfolding and aggregation* (pp. 133-145, Part II, Chapter 12), Vladimir N Uversky and Yuri L Lyubchenko. Elsevier Inc. doi: 10.1016/B978-0-12-394431-3.00012-2.

1.1. Protein Misfolding and Neurodegeneration

The correct folding of proteins into a unique three-dimensional structure is essential for normal function and stability. Protein folding starts at ribosomes, where proteins are synthesized as linear chains of amino acids that subsequently undergo various conformational changes to achieve native and functional state. Intermediate conformers are thermodynamically unstable due to the exposure of hydrophobic residues that are normally buried in the native structure. Such hydrophobic surfaces become the object of several off-pathway interactions favoring protein aggregation, a highly dynamic process that starts with the association of two misfolded monomers (dimerization) and can progress towards the formation of a wide range of structures with variable size, stability and solubility (Balchin *et al*., 2016) (Figure 1). Under normal conditions, cells are capable of maintaining proteome homeostasis, i.e. proteostasis, via a complex quality-control system that acts either by refolding or degrading misfolded proteins (Figure 1). This system involves a tight cooperation between molecular chaperones, which mediate protein folding and conformational repair, and proteolytic pathways, which get rid of misfolded proteins when repair fails. However, once formed, higher ordered aggregate structures are extremely stable and highly resistant to degradation, while recruiting other proteins into the aggregation process. Although folding intermediates often aggregate in normal conditions, protein misfolding can increase in the presence of particular cellular stress conditions, leading to the exhaustion of the protein-quality control system. Accumulation of misfolded proteins and aggregates can have deleterious effects on cells (Sweeney *et al*., 2017, Tyedmers *et al*., 2010a). The maintenance of protein integrity is crucial for normal cell function and viability, and imbalance of the proteostasis network underlies many fatal diseases, including cancer, diabetes and neurodegenerative disorders. Proteome integrity declines with aging, which is also a major risk factor for a significant number of human diseases associated with protein misfolding and aggregation, commonly termed protein misfolding disorders (PMDs) (Balchin *et al*., 2016) (Table I).

Many neurodegenerative disorders are PMDs, including Alzheimer's (AD), Parkinson's (PD) or Huntington's (HD) diseases. In these disorders, relatively specific proteins abnormally aggregate into β-sheet fibrils (amyloid) and deposit in particular regions of the brain. However, amyloid deposits are not exclusive to the central nervous system (CNS) and can also appear in peripheral tissues (Table I). The composition and

location of protein aggregates, as well as the neurons that are selectively killed and the clinical symptoms are characteristic of each disorder (Table I). For example, beta amyloid peptide (Aβ) plaques and Tau intracellular tangles in AD are found in the hippocampus, amygdala and cortex regions that regulate memory, emotions and thinking. Alpha-synuclein (α-syn) is the primary component of Lewy bodies in PD, which is characterized by the loss of dopaminergic neurons in the *Substantia nigra*. Polyglutamine diseases such as HD and some spinocerebellar ataxias develop due to an abnormal expansion of polyglutamine amino acid sequences (polyQ) in the huntingtin (HTT) and ataxin proteins, respectively. Huntingtin aggregates are initially found in the striatum, while ataxin aggregates are found in the cerebellum, and degeneration of these regions is responsible for the motor symptoms that characterize these disorders. Rapid spongiform degeneration of brain tissue in prion disorders is thought to occur via the intracellular propagation of pathogenic conformers of the prion protein (PrP^{Sc}) (Kumar *et al.*, 2016, Ross and Poirier, 2004).

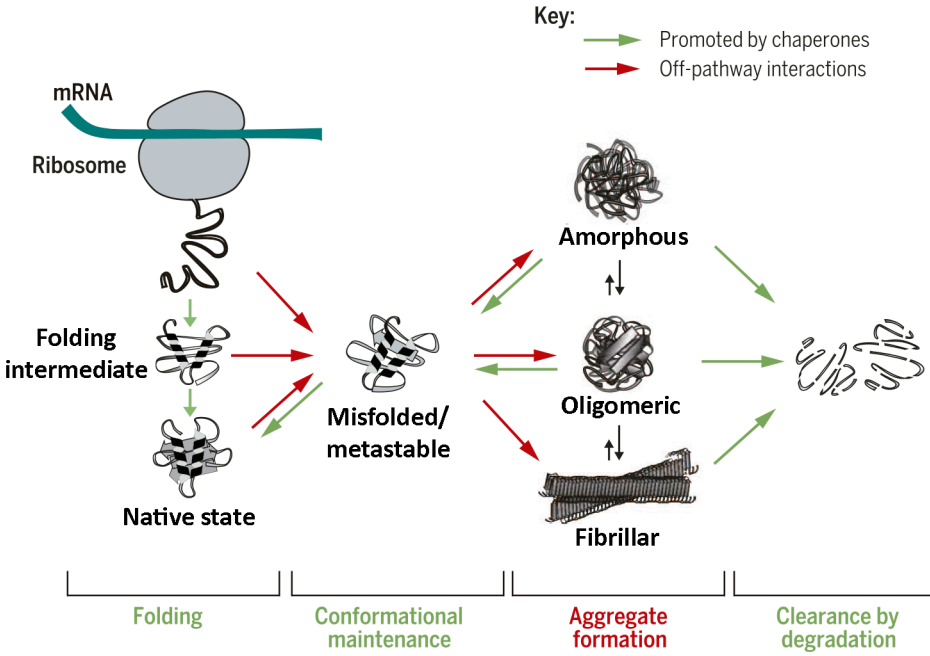

Figure 1. Protein folding, misfolding and aggregation. Molecular chaperones promote *de novo* folding, assist the refolding and proteolytic degradation of misfolded proteins, and prevent harmful interactions with other cellular and molecular factors. Genetic and environmental stressors may accelerate protein misfolding and aggregation, resulting in the accumulation of potentially toxic species that can have a wide range of morphologies and physical-chemical features. In normal conditions, intermediate aggregate species are targeted for degradation via the ubiquitin-proteasome or the autophagic-lysosomal systems. However, when the concentration of misfolded and/or aggregated proteins exceeds the capacity of the

proteome quality-control system, proper functioning of multiple cellular processes become affected, which may ultimately result in premature cell death. Adapted from (Balchin *et al*., 2016).

Table I. Protein misfolding diseases: histopathological features

Neurodegenerative diseases				
Disease	**Location**	**Aggregate types**	**Major protein components**	**References**
Parkinson's Disease	Substantia nigra, Cerebral cortex	Cytoplasmic Lewy Bodies	α-synuclein Ubiquitin LRRK2	(Conway *et al.*, 1998, Forloni *et al.*, 2002, Nussbaum and Polymeropoulos, 1997, Tan *et al.*, 2009, Zhu *et al.*, 2006)
Alzheimer's Disease	Neocortex, Limbic region	Extracellular amyloid plaques and intracellular Tau tangles	β-amyloid HSP90 Tau protein Ubiquitin	(Agorogiannis *et al.*, 2004, Cataldo *et al.*, 2003, Forloni *et al.*, 2002, Liao *et al.*, 2004)
Huntington's Disease	Striatal and cortical areas	Nuclear and cytoplasmic aggregates	Huntingtin Ubiquitin	(Agorogiannis *et al.*, 2004, Arrasate *et al.*, 2004, The Huntington's Disease Collaborative Research Group, 1993)
Spinocerebellar Ataxias	Cerebellum, Spinal Cord and Brainstem	Cytoplasmic or intranuclear inclusions	Ataxins CACNA1A Tau protein TBP ATN1	(Hayashi *et al.*, 2003, Houlden *et al.*, 2007, Huynh *et al.*, 1999, Zhuchenko *et al.*, 1997)
Friedrich Ataxia	Dentate nucleus, Dorsal root ganglia	Cytoplasmatic inclusions in neurons	Frataxin	(Koeppen, 2011)
Amyotrophic lateral sclerosis	Motor neurons	Cytoplasmatic aggregates in neurons and astrocytes	SOD I TDP-43 FUS/TLS Ubiquitin	(Arai *et al.*, 2006, Kwiatkowski *et al.*, 2009, Niwa *et al.*, 2002)
Alexander's Disease	Astrocytes	Rosenthal fibers	GFAP CRYAB HSP27 Plectin	(Brenner *et al.*, 2001, Iwaki *et al.*, 1993, Tian *et al.*, 2006)
Fragile X Syndrome	Neocortex, Hippocampus	Intranuclear inclusions	FMRP Ubiquitin	(Koukoui and Chaudhuri, 2007)
Transmissible spongiform encephalopathies (TSEs) or prion diseases	Cerebral cortex	Fibrillar amyloid deposits	Prion protein (PrP) MAP2 α-synuclein β-amyloid Tau protein	(Ben-Gedalya *et al.*, 2011, Haik *et al.*, 2002, Kovacs *et al.*, 2017, Miyazono *et al.*, 1992, Zhang and Dong, 2012)
Familial amyloid polyneuropathy	Sensory and motor nerve fibers, Autonomic ganglions	Amyloid deposits	Transthyretin	(Fong and Vieira, 2013)
Prolactinomas	Pituitary gland	Amyloid deposits	Prolactin	(Hinton *et al.*, 1997)

(Continued)

Table I. Protein misfolding diseases: histopathological features (cont.)

Peripheral diseases				
Disease	**Location**	**Aggregate types**	**Composition**	**References**
Aortic medial amyloid	Circulatory System	Amyloid deposits	Medin	(Madine and Middleton, 2010)
Atherosclerosis	Circulatory System	Amyloid deposits	Apolipoprotein A1	(Teoh *et al.*, 2011)
Cardiac arrhythmias, Isolated atrial amyloidosis	Circulatory System	Atrial amyloid deposits	Atrial natriuretic factor	(Steiner and Hajkova, 2006)
Cerebral amyloid angiopathy	Circulatory System	Amyloid deposits	β-amyloid, Cystatin	(Revesz *et al.*, 2009)
Diabetes mellitus type 2	Pancreas	Amyloid deposits	Amylin	(Tomita, 2012)
Dialysis related amyloidosis	Systemic	Amyloid deposits in osteoarticular structures	β2-microglobulin	(Heegaard, 2009)
Finnish amyloidosis	Systemic	Amyloid deposits	Gelsolin	(Solomon *et al.*, 2012)
Hereditary non-neuropathic systemic amyloidosis	Systemic	Amyloid deposits	Lysozyme	(Pepys *et al.*, 1993)
Lattice corneal dystrophy	Eye	Amyloid deposits	Keratoepithelin	(Ozawa *et al.*, 2011)
Medullary carcinoma of the thyroid	Thyroid gland	Nuclear, cytoplasmic and extracellular amyloid deposits	Calcitonin	(Stamatakos *et al.*, 2011)
Rheumatoid arthritis	Bones and joints	B and T cell aggregates	Serum amyloid A	(Weyand, 2007)
Sporadic Inclusion Body Myositis	Muscle	Multiprotein aggregates: Aβ42, Tau, α-synuclein	S-IBM	(Askanas *et al.*, 2012)
Systemic AL amyloidosis	Systemic	Amyloid deposits	Immunoglobulin light chain AL	(Merlini *et al.*, 2011)

Mechanisms of protein aggregation

Amyloid fibril formation

Protein aggregation occurs via a complex seeding-nucleation mechanism involving the formation of small oligomers, amorphous aggregates of various sizes, protofibrils and mature fibrils organized as cross-β-sheet amyloid structures. The initial step of aggregation involves the formation of a nucleus typically consisting in misfolded monomers that self-associate to form soluble oligomeric species of different sizes and structures. The process evolves through the addition of intermediate species that further accumulate as a globular oligomeric structure or protofibril. The formation of such structures increases thermodynamic stability and marks the rate-limiting step of the aggregation process. Once a nucleus is formed, fibrils grow exponentially by elongation reactions ultimately resulting

in higher-order aggregates, including amyloid fibrils, in which β-sheets run perpendicular to the long fibril axis. These cross-β-sheet aggregates can then seed polymerization by inducing conformational conversion of proximal monomers into amyloid structures in a process similar to that occurring during prion propagation. Fibril fragmentation results in the release of fibril ends which enables the formation of secondary nucleation sites, and can therefore accelerate aggregation (Eisele *et al*., 2015, Knowles *et al*., 2014) (Figure 2). Thus, the conversion of a soluble molecule into an amyloid conformation can be triggered by two mechanisms that can act independently and complement each other – nucleation or seeding from preformed aggregates. The latter might constitute an important step for spreading of amyloid species within and between cells and is currently thought to contribute to the progression of pathology in neurodegenerative diseases. Indeed, such a prion-like phenomenon was first observed with the PrP^{Sc} conformer in transmissible spongiform encephalopathies (TSEs), but it has recently been extended to non-infectious disease-associated proteins, including Aβ, Tau, α-syn, SOD1, TDP-43 and mutant HTT (Costanzo and Zurzolo, 2013, Brundin *et al*., 2010, Stopschinski and Diamond, 2017).

Causes of protein misfolding and aggregation

Despite the fact that the cross-β-sheet is a common structure of aggregates formed by several disease-associated proteins (Table I), the initial trigger of protein misfolding remains unclear in most cases. Internal conditions that have been identified to drive protein misfolding include mutations, translational errors and covalent modifications of proteins due to proteolytic cleavage, posttranslational modifications (PTMs) and oxidative stress.

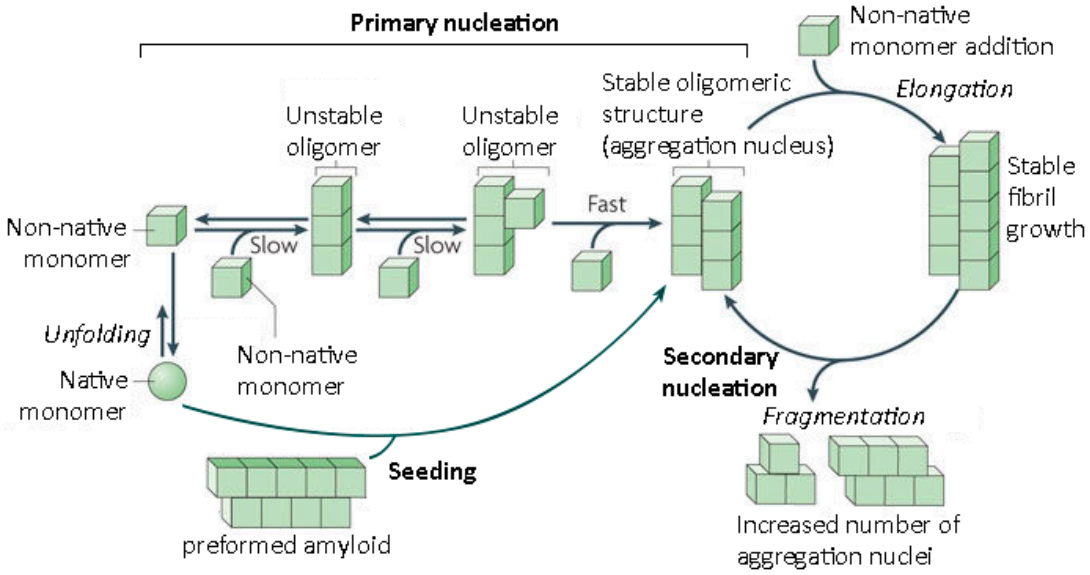

Figure 2. Aggregate formation process. Amyloid formation may occur via nucleated and/or seeded polymerization. Nucleated polymerization involves the formation of an aggregation nucleus consisting in β-sheet rich intermediates, typically soluble oligomers or protofibrils. This primary nucleation event is characterized by slow assembly kinetics, being highly dependent on protein concentration. However, once misfolded species are converted into more stable intermediates, rapid fibril growth can take place through the recruitment of soluble monomers. The growing fibril has an intrinsic tendency to further assemble into an amyloid-like structure, in which β-strands are rearranged in a perpendicular orientation to the axis of the fiber, giving rise to larger insoluble species (cross-β aggregates). Protein aggregation may imply secondary processes that greatly increase the size and number of aggregates. Such processes are primarily catalyzed by proteolytic reactions involving the formation of new aggregation nuclei (secondary nucleation), and the generation of seeds that induce the misfolding and incorporation of native molecules into β-sheet conformations (seeding). Adapted from (Brundin *et al*., 2010).

The probability of protein aggregation increases with increasing protein concentration, whether it is caused by increased gene expression or by decreased protein degradation and recycling. For example, duplications and triplications of the genes encoding α-syn or amyloid precursor protein (APP) cause early deposition of Aβ plaques and α-syn intracellular inclusions, respectively (Cataldo *et al*., 2003, Chartier-Harlin *et al*., 2004, Lemere *et al*., 1996). In Down's syndrome (DS), the triplication of APP on chromosome 21 is widely accepted as the underlying mechanism through which DS individuals progressively develop Aβ deposits and other features of AD (Wiseman *et al*., 2015). The abnormal expansion of a triplet cytosine-adenine-guanine (CAG) repeat in the coding regions of at least 9 unrelated genes leads to the production of polyQ-expanded proteins with high aggregation propensities. Such mutated proteins are the causative agents of a group of neurodegenerative disorders termed as polyglutaminopathies. To date, this family of diseases include one recessive inherited disorder, the X-linked spinal and bulbar muscular atrophy (SBMA), and eight dominantly inherited disorders: six spinocerebellar ataxias (SCA) types 1, 2, 3 (also known as Machado-Joseph disease) 6, 7 and 17; dentatorubral pallidoluysian atrophy (DRPLA); and HD (Fan *et al*., 2014). HD is caused by the expansion of a CAG repeat in the first exon of the *HTT* gene, also known as *IT15* (The Huntington's Disease Collaborative Research Group, 1993). The CAG expansion size in all diseases correlates with the age of onset, extent of protein aggregation and disease severity (Fan *et al*., 2014). Moreover, single-point mutations in SNCA, Parkin, and LRRK2, among a few other genes, lead invariably to protein misfolding and aggregation in cell and animal models of PD (Conway *et al*., 1998, Forloni *et al*., 2002, Hattori and

Mizuno, 2004, Nussbaum and Polymeropoulos, 1997). Presenilin mutations are associated with extracellular amyloid deposits in familial AD (De Strooper, 2007). Mutations in superoxide dismutase, TDP-43 or FUS induce the aggregation and toxicity of these proteins in familial amyotrophic lateral sclerosis (ALS) (Durham *et al.*, 1997, Kwiatkowski *et al.*, 2009, Liscic *et al.*, 2008). Although prion diseases are typically sporadic or acquired by infection, over 60 mutations in the *PRNP* gene are now recognized to cause premature PrP truncation and accumulation of the pathogenic conformer (PrP^{Sc}) (Mead and Reilly, 2015). The generation of aggregation-prone peptides can also result from proteolytic degradation of larger precursor proteins. Amyloid fibrils are known to be composed of relatively short peptides or proteolytic fragments. The role of proteolysis is well established in AD pathogenesis, being the toxic Aβ peptide generated from APP via successive aspartyl protease-mediated cleavage (Esler and Wolfe, 2001). Proteolytic cleavage promotes the aggregation of other disease-related proteins, such as α-syn, Tau and HTT, by liberating fragments that are more prone to misfold and can then seed aggregation of the full-length protein (Graham *et al.*, 2006, Li *et al.*, 2005, Wellington *et al.*, 2002, Yin and Kuret, 2006).

Protein aggregation is also influenced by phosphorylation and other PTMs. While neurofibrillary tangles and Lewy bodies are mostly composed of hyperphosphorylated Tau and serine-129-phosphorylated α-syn, respectively (Tenreiro *et al.*, 2014), phosphorylation of mutant HTT on its N-terminal region prevents the formation of large inclusions in different cell and animal models (Branco-Santos *et al.*, 2017, Gu *et al.*, 2009). Phosphorylation may also serve as a recognition signal for further modifications, such as catalytic cleavage and ubiquitination (Thompson *et al.*, 2009). Likewise, oxidation leads to irreversible modifications of protein residues, being also implicated in modulating aggregation of disease-associated proteins (Rochet, 2007, Tyedmers *et al.*, 2010a).

Environmental factors such as aging and diet may also potentiate aberrant protein covalent modifications, and decrease the ability of the cell to clear misfolded proteins (Balchin *et al.*, 2016). Cellular defense mechanisms against protein accumulation primarily involve the ubiquitin-proteasome system (UPS), whereby abnormal proteins are ubiquitinated and transported to the proteasome for their degradation (Figure 3). Alternatively, misfolded proteins are processed by chaperone-mediated autophagy, a clearance mechanism in which targeted proteins are translocated into the lysosome with the assistance of molecular chaperones, such as the heat shock cognate protein (Hsc70) (Kuiper *et al.*, 2017, Rochet, 2007, Taylor *et al.*, 2002) (Figure 3). The autophagy-

lysosome system comprises another two mechanisms capable of removing cytosolic components: micro- and macroautophagy. In microautophagy, non-degraded proteins are directly sequestered by engulfment of the lysosomal membrane. When degradation and primary clearance mechanisms fail, protein aggregates are deposited in a specific cellular compartment located near the nucleus, known as aggresome in mammalian cells or IPOD in yeast cells (Tyedmers *et al*., 2010a) (Figure 3). The formation of such transient deposits or inclusion bodies is thought to constitute an attempt of the cell to avoid potential toxic interactions between protein aggregates and other cytosolic proteins or organelles until they can be cleared (Balchin *et al*., 2016, Tyedmers *et al*., 2010a). Although proteasomes can be stimulated to degrade large inclusions (Myeku *et al*., 2016), they are normally cleared by macroautophagy in a process involving the formation of double-membrane vesicular bodies termed autophagosomes that scavenge protein aggregates along with damaged organelles and other cellular debris (Rochet, 2007). Examples of aggregated proteins that may be processed via aggresome formation and macroautophagy are α-syn and polyQ-containing proteins (Tanaka *et al*., 2004b, Taylor *et al*., 2003). It has been hypothesized that the impairment of cellular proteostasis pathways is both a cause and a consequence of protein aggregation, thereby creating a vicious cycle that ultimately leads to cell death. Support for this idea comes from the observation that cytosolic aggregates compromise protein folding and degradation by sequestering components of the chaperone network and proteasome subunits (Hipp *et al*., 2014, Park *et al*., 2013). On the other hand, the presence of ubiquitinated aggregates in PMDs suggests that they are targeted for degradation but the UPS is unable to function, resulting in their accumulation (Hipp *et al*., 2012).

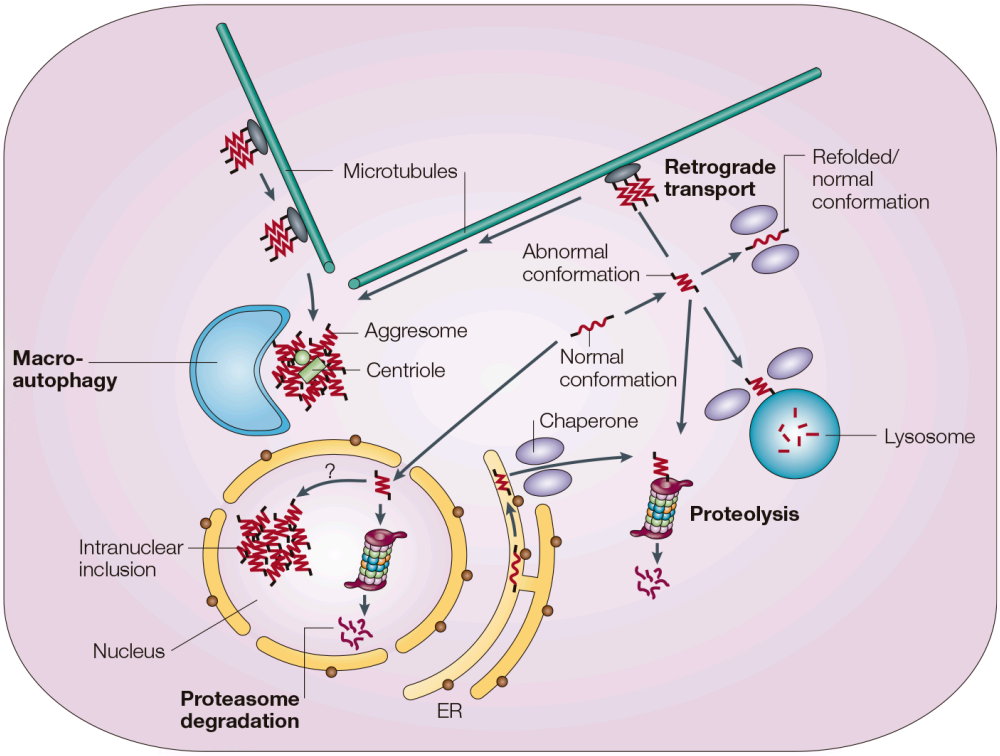

Figure 3. Cellular defense mechanisms against protein accumulation. Molecular chaperones and the ubiquitin-proteasome system are the primary routes of protein turnover, being responsible for refolding processes and degradation of unfolded proteins, respectively. Proteasome degradation can occur in the cytoplasm or in the nucleus. Misfolded proteins retained in the ER and/or other organelles can be stabilized by chaperones (e.g., CHIP) and transported to the cytoplasm for proteasome degradation. When a protein does not turnover rapidly, molecular chaperones are called into action to assist in its delivering to the lysosome, a clearance mechanism known as chaperone-mediated autophagy. If all this fails and misfolded proteins start to accumulate in the cytoplasm, they can be sequestered by microtubule-mediated transport and deposited near the centriole forming an aggresome, where they remain until the cell can discard them through macroautophagy. Obtained from (Ross and Poirier, 2005).

Molecular basis of neurodegeneration

The fact that large proteinaceous deposits can be easily observed in affected patient tissues led to the initial assumption that these species are the causative agents of neurodegeneration. However, neuronal death does not always correlate with the presence of amyloid fibrils (Saudou *et al.*, 1998, Slow *et al.*, 2005, Tsvetkov *et al.*, 2013). There is now increasing evidence suggesting that some intracellular inclusions are formed as a part of a physiological response to excess misfolded protein, being neuroprotective rather than neurotoxic (Arrasate *et al.*, 2004, Bodner *et al.*, 2006, Winner *et al.*, 2011). While large aggregates occupy specific cellular sites and do not move substantially, oligomeric species

are able to move more freely within cells and across membranes. Their solubility and dynamic properties should, in theory, allow them to interfere with biological processes more effectively than larger, more static protein inclusions. In fact, intermediate species expose sticky hydrophobic surfaces and form intermolecular hydrogen bonds, which increase their propensity to engage in aberrant interactions with proteins, lipids, nucleic acids and carbohydrates (Eisele *et al*., 2015). Protein misfolding and aggregation compromise important cellular processes for normal brain function and neuronal survival, including transcription, synaptic signaling, vesicular trafficking and mitochondrial function (Chiti and Dobson, 2006, Sweeney *et al*., 2017, Taylor *et al*., 2002). In addition, accumulation of misfolded proteins can lead to the extracellular release of reactive oxygen species (ROS) and induce stress response pathways. Chronic microglia and astrocyte activation promotes the production of chemokines and pro-inflammatory cytokines that generally lead to death of nearby neurons (Ben Haim *et al*., 2015, Gentleman, 2013), hence contributing to spreading neurodegeneration and disease progression. On the other hand, extracellular aggregates have been shown to directly bind glial cells and impair the microglial M2 phenotype, considered to be neuroprotective owing to release of neurotrophic and growth factors (Heppner *et al*., 2015).

Although aggregation-prone proteins appear to act primarily by toxic gain-of-function, in some cases, loss-of-function events may also contribute to disease pathogenesis. According to this hypothesis, neuronal dysfunction can be caused by the loss of normal activity of aggregation-prone proteins upon self-assembly and/or depletion of vital regulatory and signaling proteins that get sequestered into the inclusions. Experimental support in this regard is provided by knockout studies, in which deletion of genes encoding disease-related proteins results in premature death or accelerates neurodegenerative phenotypes of disease-model organisms. Knockout of endogenous HTT leads to early embryonic lethality in mice (Duyao *et al*., 1995, Nasir *et al*., 1995, Zeitlin *et al*., 1995), and exacerbates brain degeneration and motor deficits in adult HD flies (Zhang *et al*., 2009). Loss-of-function effects are also observed for the cellular prion protein (PrP^{C}) (Sakudo and Onodera, 2014), APP (Senechal *et al*., 2008), SOD1 (Reaume *et al*., 1996) and three syn isoforms (Greten-Harrison *et al*., 2010). Interestingly, diffusion of human α-syn fibrils to different brain regions occurs more readily in α-syn null mice, suggesting that loss of the endogenous protein influences interneuronal transfer of oligomeric α-syn and leads to advanced brain pathology (Helwig *et al*., 2016). Altogether, these observations raise the possibility that loss of normal protein function may be involved not only in

disease development but also in its progression.

Spreading of protein aggregation in neurodegeneration

As mentioned above, transneuronal propagation of toxicity may occur through a seeding mechanism in which soluble oligomeric species are capable of crossing cellular membranes and act as seeds for the generation of amyloid-like aggregates in different areas of the brain. This concept of prion-like aggregation has been hypothesized to have an important role in driving pathogenesis of many PMDs (Brundin *et al*., 2010), but remains a matter of intense debate. On one hand, there is currently no evidence that more common neurodegenerative disorders are transmissible between individuals (Irwin *et al*., 2013, Stopschinski and Diamond, 2017). On the other hand, pathophysiological studies of AD, PD, ALS and HD patient brains reveal unique but stereotypical patterns of pathology spread between interconnected brain regions, suggesting a similar mechanism of disease progression based on non-cell autonomous dissemination of protein aggregates (Brettschneider *et al*., 2015, Pecho-Vrieseling *et al*., 2014). Experimental evidence for prion-like seeding and spreading of toxic aggregates comes mainly from animal models. In AD transgenic mice, intracerebral injection of either *in vitro* purified fibrils or disease-affected brain homogenates can induce progressive spread of Aβ or Tau aggregation (Clavaguera *et al*., 2009, Clavaguera *et al*., 2013, Kane *et al*., 2000). Similarly, α-syn was shown to propagate from neurons to other neurons (Desplats *et al*., 2009) and glial cells (Lee *et al*., 2010), following a PD-like cascade of neuropathology that evolves along specific neuronal networks to neighboring anatomical structures (Luk *et al*., 2012, Rey *et al*., 2016). While pathological protein propagation in AD and PD is relatively well documented, evidence for prion-like spreading of mutant HTT (Babcock and Ganetzky, 2015, Herrera *et al*., 2011, Pearce *et al*., 2015), SOD1 (Ayers *et al*., 2016) and other disease-causing proteins has only recently begun to emerge. The intercellular processes underlying spreading of protein aggregates are still under investigation, although common mechanisms of release and uptake of biomolecules, such as endocytosis, exocytosis and receptor-mediated phagocytosis, are likely to be involved (Pearce, 2017). In addition, misfolded proteins can be transferred directly by cell-to-cell contact via tunneling nanotubes (TNTs) (Gousset *et al*., 2009, Wang *et al*., 2011) or be internalized by passive diffusion across lipid membranes (Cecchi and Stefani, 2013, Ren *et al*., 2009, van Rooijen *et al*., 2009). Extracellular aggregates of Aβ (Resenberger *et al*., 2011) and α-syn (Ferreira *et al*., 2017) were recently found to physically interact with PrP^c at the cell membrane,

initiating a cascade of toxic events that leads to synaptic dysfunction and subsequent neuronal death. These exciting findings may suggest the existence of a cell receptor-mediated mechanism for neurotoxicity spread that could explain, at least in part, why some neurons are more vulnerable to toxic extracellular species.

Seeding and aggregation typically occurs for the same type of aggregation-prone protein (Rajan *et al*., 2001). However, several studies have shown that misfolding of one disease-causing protein can induce misfolding an aggregation of other aggregation-prone proteins (Guo *et al*., 2013, Katorcha *et al*., 2017, Vasconcelos *et al*., 2016). Such cross-seeding properties can contribute to neuropathology and are implicated as one possible reason for the heterogeneity of neurodegenerative diseases. Indeed, aggregates of different proteins can be observed in patients with overlapped symptoms (Galpern and Lang, 2006, Miyazono *et al*., 1992, Vital *et al*., 2007). Furthermore, we and others have found that co-aggregation of otherwise unrelated proteins alters protein subcellular localization and aggregation patterns (Blum *et al*., 2015, Herrera and Outeiro, 2012), and potentiates cytotoxicity and neurodegeneration (Pocas *et al*., 2015, Sajjad *et al*., 2014).

Over the last decade, researchers have focused on developing therapeutic strategies targeting protein aggregation, but very few have shown significant benefits in clinical trials (Eisele *et al*., 2015, Sweeney *et al*., 2017). This is in part because we still lack deep understanding of the processes underlying disease pathogenesis. A major challenge would be to determine which species are toxic to which cells and under which conditions. Protein aggregates exist in a wide variety of structures that show different levels of neurotoxicity and afflict different neuronal populations. Despite the fact that oligomeric species are currently considered to be at the core of proteotoxic interactions and seeding mechanisms, amyloid-β structures represent a more readily accessible target for novel therapeutic intervention due partly to the absence, until recently, of suitable experimental models for the study and detection of soluble intermediate species in living cells (Goncalves *et al*., 2010, Herrera *et al*., 2014). The availability of such models should contribute to a better understanding of the initial events triggering aggregation of aberrant proteins, and is expected to prove useful in our search for promising disease-modifying candidates that could be modulated before irreversible spreading of protein pathology and neuronal loss. Furthermore, although neurodegenerative disorders share common histopathological features, the cellular pathways and molecular mechanisms involved in neurotoxicity may differ. Thus, because selective neuronal vulnerability is likely dependent on specific

protein-protein interactions (Yang and Hu, 2016), identifying molecular partners of disease-causing proteins and understanding how such interactions are modulated by environmental changes could provide new insights into the pathogenesis of neurodegenerative disorders. In the scope of the present thesis, current understanding of HD pathogenesis is detailed bellow, with particular emphasis on post-translational modifications and aberrant protein-protein interactions underlying mutant HTT aggregation and toxicity.

1.2. Huntington's Disease

Etiology and clinical symptoms

HD was first described in 1872 by George Huntington as a choreiform movement disorder (Huntington, 1872). Although rare, HD is the most common inherited neurodegenerative disorder affecting 5 to 10 individuals per 100,000 in western populations, with many more people at risk of developing symptoms (Bates *et al*., 2015, Labbadia and Morimoto, 2013). HD has an autosomal dominant pattern of inheritance, and men and women have the same probability of developing the disease. The most prominent clinical feature is the inability to control muscles, which manifests early in the course of the disease as involuntary movements, giving the patient characteristic irregular "dance-like movements" known as chorea. As HD progresses, chorea stabilizes and fine motor impairment (dystonia, bradykinesia and rigidity) starts to appear. Such motor symptoms are correlated with progressive neuronal loss in the striatum and related basal ganglia structures, although other regions of the brain are also affected (Bates *et al*., 2015, Ross *et al*., 2014) (Figure 4A). Imaging studies suggest that neurodegeneration initiates in the cerebral cortex and extends to subcortical regions involved in sensory signals and regulatory functions (Brundin *et al*., 2010), which could explain the appearance of cognitive and neuropsychiatric disturbances years before the motor symptoms (Stout *et al*., 2011). Changes in cognition and behavior generally include personality changes often accompanied by social disengagement and disinhibition, irritability, apathy, sleep problems and depression. Learning can also be impaired but language and episodic memory are not affected, in contrast to AD. Most HD patients also experience peripheral symptoms such as extreme fatigue and weight loss (Carroll *et al*., 2015, van der Burg *et al*., 2009). These symptoms are generally associated with changes in muscular, circulatory and digestive systems that affect quality of life and, in some cases, constitute the primary cause of death. Indeed, more than half of the HD population dies from aspiration pneumonia followed by cardiovascular disease (Heemskerk and Roos, 2012, Sorensen and Fenger, 1992). Non-neurological complications of HD may also include gastrointestinal dysfunction (van der Burg *et al*., 2011), skeletal-muscle atrophy (Lodi *et al*., 2000, Ribchester *et al*., 2004) and osteoporosis (Goodman and Barker, 2011). Moreover, HD patients are at higher risk of developing diabetes *mellitus* and hyperglycemia (Farrer, 1985). These peripheral

abnormalities are presumably caused by HTT-induced defects as intranuclear inclusions alongside with a decline in glucose tolerance and decreased insulin production are seen in pancreatic islet cells of HD mice (Andreassen *et al*., 2002, Hurlbert *et al*., 1999). Due to the nonspecific nature of these early-stage features, HD can be initially confounded with other CNS disorders. Patients and their families are frequently left without proper medical follow-up and counseling until the time of diagnosis, that typically occurs when motor difficulties begin. In the future, studies on peripheral pathology might pave the way for early diagnosis in HD and new markers to monitor disease progression.

HD is caused by abnormal expansion of a CAG repeat located in the beginning of the *HTT* gene, located on the short arm of chromosome 4 (4p16.3). The size of expanded CAG has a strong inverse correlation with the age of disease onset (Figure 4B), and can also influence disease progression and severity (Rosenblatt *et al*., 2012). Healthy individuals carry between 16 and 27 CAG repeats, while 36 repeats or more are associated with manifested HD. However, repeats of 36-40 CAG are incompletely penantrant which often leads to uncertainty in clinical diagnosis. Full penetrance is observed when CAG length is expanded over 40 repeats with mutation carriers invariably developing motor signs of HD. Disease onset occurs most frequently in midlife, approximately at 40 years of age, while juvenile cases have been reported with CAG lengths over 55 repeats (Bates *et al*., 2015, Rubinsztein, 2002). Individuals with 27 to 35 CAG repeats are essentially asymptomatic, although the disease can appear in future generations owing to meiotic instability of such intermediate alleles. However, there is a large part of the interindividual variability that is not explained by differences in CAG repeat extension between patients, and that may be due to genetic, epigenetic or environmental factors, such as sport or nutrition (Gusella and MacDonald, 2009).

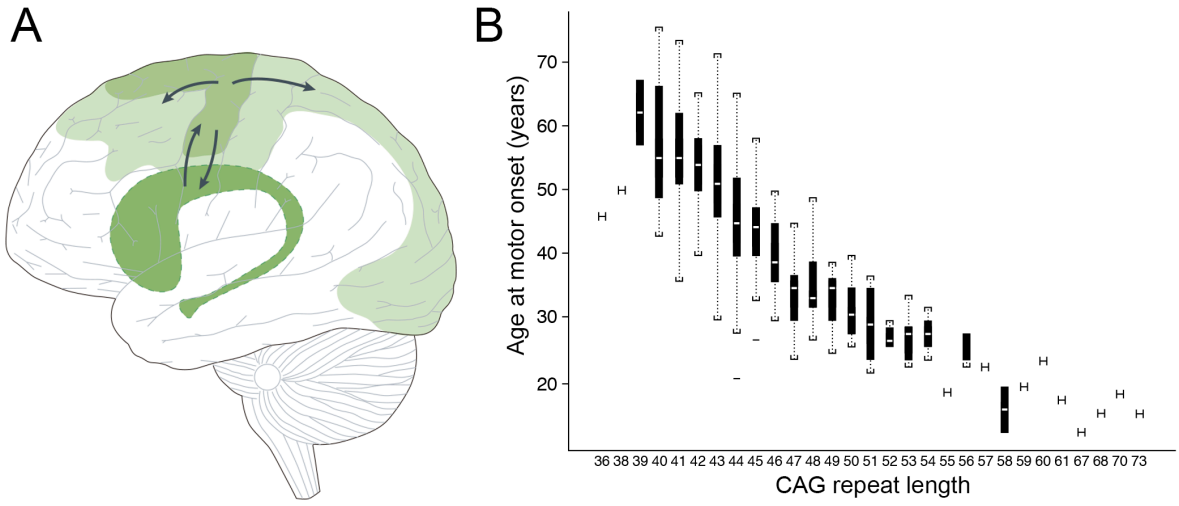

Figure 4. Clinical and histopathological hallmarks of HD. (A) HD is characterized by the accumulation of mutant HTT associated with neurotoxicity in specific brain regions. The medium spiny neurons of the basal ganglia are particularly vulnerable to mutant HTT toxicity (darkest green). However, cortical degeneration appears to precede neuronal loss in the striatum and might be observed 15 years before first symptoms emerge. Neurodegeneration progresses gradually throughout the brain affecting subcortical regions, although to a lesser extent (lighter green). The specific pattern of spreading of neurodegeneration gives HD a combination of motor, cognitive and behavioral features that have some similarity with other disorders involving corticostriatal atrophy, such as dementia and PD. Extracted from (Brundin *et al*., 2010). (B) HD is caused by an abnormal expansion of a CAG repeat in an autosomal dominant gene, with longer expansions causing greater HTT aggregation and earlier onset of pathology. Despite the strong correlation between CAG repeat number and disease onset, wide variation in age of onset can be observed for the same CAG repeat length. Such differences have been attributed to genetic and/or environmental factors that may modulate disease pathogenesis. Median value for each repeat size is indicated as a white line; Interval of 95% confidence is indicated as the black box; Range is indicated by brackets; Outliers are indicated by black lines. Extracted from (Rubinsztein, 2002).

HD is a fatal disorder, with patients having 15 to 20 years of life expectancy after the first signs of motor dysfunction (Foroud *et al*., 1999). Currently, there is no effective treatment for this devastating disease, and existing drugs only alleviate symptoms (Kim and Kim, 2014, Ross *et al*., 2014). Drugs aiming at modifying disease pathogenesis should be considered for therapeutic strategies against HD. Thus, research on the mechanisms underlying HD may lay the groundwork for the development of novel therapies that can alter the course of HD.

Huntingtin protein and molecular pathogenesis of HD

Huntingtin structure, function and pathobiology

The *HTT* gene is extremely large and consists of 67 exons and 180 kb, encoding for a large protein of 3144 amino acids (~350 kDa). The pathogenic CAG expansion, located in the first exon of the gene, is translated as an abnormally elongated polyglutamine (polyQ) tract in the HTT protein. HTT is widely expressed throughout all body tissues, although its expression is particularly high in the brain. At the cellular level, normal HTT is mostly found in the cytoplasm as a soluble unfolded monomer (Bates *et al*., 2015, The Huntington's Disease Collaborative Research Group, 1993). However, the existence of a nuclear export signal in its C-terminal indicates that HTT can shuttle between the nucleus and cytoplasm under certain conditions (Xia *et al*., 2003). While some biochemical and

mechanistic roles of wild-type HTT have been uncovered, its specific cellular function remains elusive. This is mainly due to the large size of the protein, that makes isolation and analysis very difficult, and to the large number of HTT interacting partners (Table II).

Table II. Selected HTT interactors and modifiers of HTT aggregation and toxicity

Interactor/ modifier	Function	Secondary partners	PolyQ length dependence	HTT aggregation	HTT toxicity	References
α-Adaptin C/HYP-J	Endocytosis		Yes	n.d.	n.d.	(Faber *et al.*, 1998)
α-syn	Unknown		n.d.	enhancer	enhancer	(Charles *et al.*, 2000, Herrera and Outeiro, 2012, Pocas *et al.*, 2015, Tomas-Zapico *et al.*, 2012)
ADMR1	Ubiquitin receptor, proteasome activity		Yes	suppressor	suppressor	(Huang and Her, 2016)
AIFM1	Mitochondrial apoptosis-inducing factor		No	n.d.	enhancer	(Ratovitski *et al.*, 2012)
Arfaptin 2	Cytoskeletal remodeling	Ras-related GTPases	n.d.	enhancer	enhancer	(Peters *et al.*, 2002, Rangone *et al.*, 2005)
CA150	Transcription co-activator		No	suppressor	suppressor	(Arango *et al.*, 2006, Holbert *et al.*, 2001)
Calmodulin	Calcium-binding protein	TG2	Yes	enhancer	enhancer	(Bao *et al.*, 1996, Dudek *et al.*, 2008, Zainelli *et al.*, 2004)
Caprin-1	RNA-binding translational repressor, stress granule-associated protein	G3BP	No	n.d.	n.d.	(Ratovitski *et al.*, 2012)
Caspase-3	Pro-apoptotic		Yes	n.d.	enhancer	(Zhang *et al.*, 2006)
CBP	Transcription co-activator		Yes	n.d.	n.d.	(Cong *et al.*, 2005, Steffan *et al.*, 2000)
CBS	Generation of cystein		No	n.d.	n.d.	(Boutell *et al.*, 1998)
CIP4	Signal transduction		Yes	n.d.	(-)	(Holbert *et al.*, 2003)
CtBP	Transcription co-repressor		Yes	n.d.	n.d.	(Kegel *et al.*, 2002)
DNAJB1	HSP40 molecular chaperone	HSP70	n.d.	n.d.	suppressor	(Kuo *et al.*, 2013, Park *et al.*, 2013)
DNAJB6, DNAJB8	HSP40 molecular chaperones	HDAC4	n.d.	suppressor	suppressor	(Gillis *et al.*, 2013, Hageman *et al.*, 2010, Mansson *et al.*, 2014)
E2-25K/HIP2	Ubiquitin-conjugating enzyme		No	enhancer	enhancer	(de Pril *et al.*, 2007, Kalchman *et al.*, 1996)
FIP2	Cell morphogenesis	Rab8	n.d.	n.d.	n.d.	(Hattula and Peranen, 2000, Qin *et al.*, 2004)
FUS/TLS	RNA/DNA-binding protein		No	(-)	suppressor	(Doi *et al.*, 2010, Kino *et al.*, 2016)
GIT1	G protein-coupled receptor kinase		n.d.	enhancer	n.d.	(Goehler *et al.*, 2004)
GRB2	Epidermal growth factor receptor-binding protein	Foxd3	Yes	suppressor	n.d.	(Baksi *et al.*, 2013, Liu *et al.*, 1997)

(Continued)

Table II. Selected HTT interactors and modifiers of HTT aggregation and toxicity (cont.)

Interactor/ modifier	Function	Secondary partners	PolyQ length dependence	HTT aggregation	HTT toxicity	References
HAP1	Membrane trafficking, autophagy	dynactin	Yes	n.d.	n.d.	(Li *et al.*, 1995, Wong and Holzbaur, 2014)
HAP40	Endosome motility	Rab5	n.d.	enhancer	enhancer	(Guo *et al.*, 2018, Huang and Her, 2016, Pal *et al.*, 2006)
HIP1	Endocytosis, pro-apoptotic		Yes	(-)	enhancer	(Gervais *et al.*, 2002, Kalchman *et al.*, 1997, Qin *et al.*, 2004, Wanker *et al.*, 1997)
HIP14/HYP-H	palmitoyl transferase, traffic, endocytosis		Yes	suppressor	suppressor	(Faber *et al.*, 1998, Singaraja *et al.*, 2002, Yanai *et al.*, 2006)
HYPA/FBP11	RNA splicing	MeCP2	Yes	n.d.	n.d.	(Faber *et al.*, 1998)
HYPB/SETD 2	Lysine methyltransferase, RNA splicing		n.d.	n.d.	n.d.	(Gao *et al.*, 2014)
HYPK	Chaperone-like activity		No	suppressor	suppressor	(Raychaudhuri *et al.*, 2008)
HSP70	Molecular chaperone involved in endocytosis and apoptosis	Clathrin	No	suppressor	suppressor	(Monsellier *et al.*, 2015, Yu *et al.*, 2014)
$InsP_3R1$	Calcium release channel	HAP1A	Yes	n.d.	n.d.	(Tang *et al.*, 2003)
ITSN	Endocytosis, signal transduction	JNK	No	enhancer	enhancer	(Scappini *et al.*, 2007)
MLF1, MLF2	Myeloid leukemia factors		Yes	suppressor	suppressor	(Banerjee *et al.*, 2017)
mSin3a	Transcription co-repressor		Yes	n.d.	n.d.	(Boutell *et al.*, 1999, Steffan *et al.*, 2000)
N-CoR	Nuclear receptor co-repressor		Yes	n.d.	n.d.	(Boutell *et al.*, 1999)
NF-Y	Transcription factor		Yes	n.d.	n.d.	(Yamanaka *et al.*, 2008)
NFκ B	Transcription factor		n.d.	n.d.	n.d.	(Takano and Gusella, 2002)
p53	Transcription factor, pro-apoptotic (tumor suppressor)		No	(-)	enhancer	(Bae *et al.*, 2005, Steffan *et al.*, 2000)
PAK1, PAK2	Cytoskeleton dynamics, anti-apoptotic		Yes	enhancer	enhancer	(Luo *et al.*, 2008, Luo and Rubinsztein, 2009)
PACSIN1	Endocytosis, cell morphogenesis		Yes	n.d.	n.d.	(Modregger *et al.*, 2002)
PFN2	Actin-binding protein, endocytosis	Dynamin 1, Clathrin, Synapsin, Rock2 NAP1 NSF/Sec18	Yes	suppressor	suppressor	(Burnett *et al.*, 2008, Goehler *et al.*, 2004, Posey *et al.*, 2018)
PrP^C	Unknown		n.d.	suppressor	suppressor	(Lee *et al.*, 2007)
PSD-95	Synaptic scaffolding protein		Yes	n.d.	suppressor	(Sun *et al.*, 2001)
Rab5	Autophagosome formation		n.d.	suppressor	suppressor	(Ravikumar *et al.*, 2008)
RasGAP	Ras GTPase activating protein		n.d.	n.d.	n.d.	(Liu *et al.*, 1997)
REST/NRSF	Transcription repressor	NRSE	Yes	n.d.	n.d.	(Zuccato *et al.*, 2003)
SH3GL3/endophilin-A3	Vesicle trafficking, endocytosis		Yes	enhancer	n.d.	(Qin *et al.*, 2004, Sittler *et al.*, 1998)

(Continued)

Table II. Selected HTT interactors and modifiers of HTT aggregation and toxicity (cont.)

Interactor/ modifier	Function	Secondary partners	PolyQ length dependence	HTT aggregation	HTT toxicity	References
SP1	Transcription activator	NGFR	Yes	suppressor	suppressor	(Dunah *et al.*, 2002, Li *et al.*, 2002b)
TAFII-130	Transcription co-activator		No	n.d.	suppressor	(Dunah *et al.*, 2002)
TATA-binding protein	Transcription factor		Yes	n.d.	n.d.	(Huang *et al.*, 1998, van Roon-Mom *et al.*, 2002)
Tau	Microtubule-associated protein		Yes	suppressor	enhancer	(Blum *et al.*, 2015, Fernandez-Nogales *et al.*, 2014, Vuono *et al.*, 2015)
TDP-43	RNA/DNA-binding protein	PGNR	n.d.	n.d.	enhancer	(Fuentealba *et al.*, 2010, Schwab *et al.*, 2008, Tauffenberger *et al.*, 2013)
Tpr	Nuclear export protein		Yes	n.d.	n.d.	(Cornett *et al.*, 2005)
TRiC	Chaperonin, *de novo* folding,		No	suppressor	suppressor	(Darrow *et al.*, 2015, Shahmoradian *et al.*, 2013, Tam *et al.*, 2006, Tam *et al.*, 2009)
tTG	Tissue transglutaminase		Yes	(-)	enhancer	(Bailey and Johnson, 2005, Chun *et al.*, 2001a, Chun *et al.*, 2001b)
USP19	Deubiquitinating enzyme	HSP90	No	enhancer	n.d.	(He *et al.*, 2017)

Adapted and completed from (Borrell-Pages *et al.*, 2006, Giorgini and Muchowski, 2005, Harjes and Wanker, 2003, Yang and Hu, 2016, Zuchner and Brundin, 2008). n.d., not determined; (-), no effect.

Normal HTT protein is implicated as a scaffold in various cellular processes, including vesicular trafficking (Li *et al.*, 1995, Strehlow *et al.*, 2007) and gene transcription (Zuccato *et al.*, 2003). Furthermore, the critical role of HTT in CNS development (Duyao *et al.*, 1995, Henshall *et al.*, 2009, Nasir *et al.*, 1995, Zeitlin *et al.*, 1995) is likely to be associated to its ability in inhibiting apoptosis, acting as a neuroprotective agent (Gervais *et al.*, 2002, Leavitt *et al.*, 2006, Luo and Rubinsztein, 2009, Zhang *et al.*, 2006). Depletion of wild-type HTT in mice leads to embryonic lethality (Duyao *et al.*, 1995, Nasir *et al.*, 1995, Zeitlin *et al.*, 1995), while a reduction of 50% in its levels of expression results in abnormal brain development (Auerbach *et al.*, 2001, White *et al.*, 1997). A subsequent study using zebrafish further suggests a role for HTT in the formation of the CNS, with morphological defects being evident in specific nerve cells (Henshall *et al.*, 2009). Further investigation on the underlying mechanisms responsible for such deleterious phenotypes point at an anti-apoptotic function of HTT (Zeitlin *et al.*, 1995). This anti-apoptotic function is independent of the polyQ length (Ho *et al.*, 2001,

Leavitt *et al*., 2001) and possibly related to HTT´s ability to sequester pro-apoptotic proteins (Gervais *et al*., 2002) and/or inhibit specific caspases (Zhang *et al*., 2006). The huntingtin interacting protein 1 (Hip1) is a pro-apoptotic protein capable of inducing caspase-3-mediated cell death and activating the pro-caspase 8 apoptotic pathway (Gervais *et al*., 2002, Hackam *et al*., 2000). Hip-1 activity is dependent on its interaction with Hippi (Hip-1 protein interactor). However, wild-type HTT sequesters Hip-1, reducing its availability to form pro-apoptotic complexes (Gervais *et al*., 2002). Furthermore, wild-type HTT physically interacts with caspase-3 *in vitro*, while its overexpression *in vivo* is concomitant with a decrease in caspase-3 activity and ameliorated neurodegenerative phenotypes (Zhang *et al*., 2006). Wild-type HTT could also prevent neuronal death by promoting specific pro-survival pathways. HTT protects against stress damage by preventing caspase-mediated cleavage of p21-activated kinase 2 (Pak2). Full-length Pak2 stimulates cell survival and growth, but it can be converted into a pro-apoptotic factor under particular stress conditions, via activation by caspase-3 and -8. Wilt-type HTT specifically binds to Pak2, interfering with its cleavage (Luo and Rubinsztein, 2009).

Structurally, HTT is composed of multiple regions of HEAT repeats that consist of 40 or more amino acids assembling into a hydrophobic α-helical conformation (Figure 5). The role of these domains in HTT biology is not clear, although they have been suggested as binding motifs for protein-protein interactions. Intrinsically disordered regions found to have a large number of PTM sites intercalate with the clusters of HEAT repeats. Of particular interest is the N-terminus segment encoded by exon 1 (HTTex1). This region contains a sequence of 17 amino acids (N17) preceding the polyQ tract and a proline-rich domain (PRD) of 51 amino acids after the polyQ tract (Figure 5). The importance of HTTex1 lies on the observation that expression of expanded polyQ-containing HTTex1 is sufficient to cause HD-like phenotypes in animal models (Bates *et al*., 1998, Mangiarini *et al*., 1996). Moreover, small N-terminal fragments of mutant HTT have been found in human post-mortem brains (Kim *et al*., 2001, Lunkes *et al*., 2002), suggesting that the generation of N-terminal fragments containing HTTex1 is a key step in HD pathogenesis. Although aberrant RNA splicing of mutant HTT can give rise to a truncated form of about 100 amino acids (Sathasivam *et al*., 2013), the generation of toxic fragments containing HTTex1 generally occurs through protease-mediated cleavage. HTT can be cleaved at arginine-167 and aspartate-586 by caspase-6 and at aspartates 513 and 552 by caspase-3. Caspase-2 and -8 were also found to target aspartates 552 or 586, respectively. In addition, three calpain cleavage sites are predicted at leucine-437, threonine-469 and serine-536.

Both wild-type and mutant HTT can undergo proteolytic cleavage (Goffredo *et al*., 2002, Kim *et al*., 2001). However, such modification appears to be more relevant in a disease context since mutant HTT aggregation is facilitated by its cleavage. In a mouse model of HD, proteolysis of full-length mutant HTT into HTTex1-containing fragments promotes protein aggregation and occurs prior to detection of behavioral deficits (Landles *et al*., 2010). Furthermore, such cleavage events may also promote toxic effects since N-terminal fragments are likely more toxic than full-length mutant HTT (Graham *et al*., 2006). Pharmacological inhibition of caspase-6 decreases intracellular levels of HTT proteolytic fragments and prevents mutant HTT-induced toxicity in both cells and animals (Aharony *et al*., 2015). However, such approach is unlikely to prove effective in HD treatment as other caspases may function as alternate enzymes and liberate similar toxic fragments, in the absence of caspase-6 (Wong *et al*., 2015a).

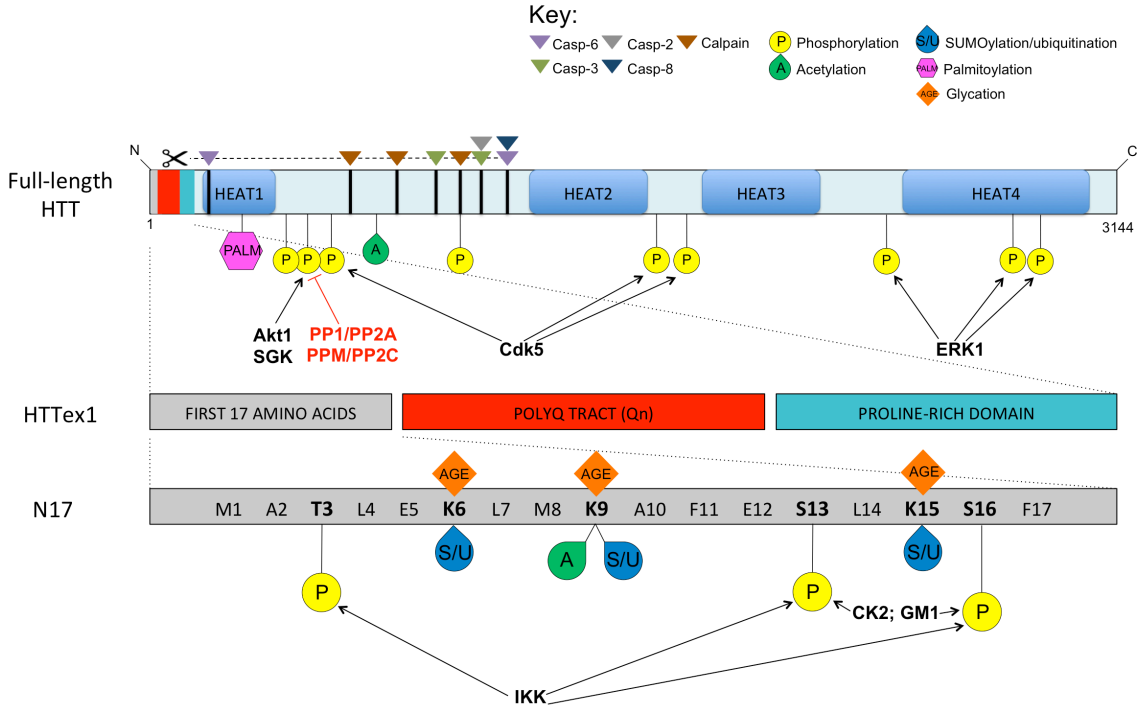

Figure 5. Schematic representation of HTT and its post-translational modification sites. HTT has a polyQ stretch at the N-terminus that is flanked by its first 17 amino acids (N17) and by a proline-rich domain (PRD). This region (HTTex1) corresponds to exon 1 and is followed by a series of clusters of highly repeated sequences, known as HEAT domains, which confer an intrinsic disorderly nature to the protein. Between these HEAT repeats are a number of cleavage sites and several other PTMs. Predicted cleavage sites are marked by inverted triangles. Caspase-2, -3, -6 and -8 sites are indicated in grey, green, purple and dark blue, respectively. Calpain cleavage sites are shown in brown. SUMO-1 and ubiquitin enzymes compete for the same lysine (K) sites, indicated in blue oval. Lysine residues are also putative targets for protein glycation (orange diamond). Additional PTMs include phosphorylation (yellow circles), acetylation (green oval) and palmitoylation (purple hexagon). To date, seven specific kinases responsible for HTT

phosphorylation have been identified (in black), while only two families of phosphatases are demonstrated to target HTT at serine (S)-421 (in red).

Although abnormally expanded polyQ is pointed as the major responsible for HTT aggregation (DiFiglia *et al*., 1997, Li and Li, 1998, Scherzinger *et al*., 1999), several lines of evidence indicate that the amino acid sequences flanking the polyQ tract (N17 and PRD) may also play a role in this process. N17 and PRD seem to affect HTT aggregation in opposite ways (Chen and Wolynes, 2017, Crick *et al*., 2013). Synthetic polyQ peptides lacking the N17 domain show slower aggregation kinetics, whereas PRD deletion results in increased aggregation propensity (Tam *et al*., 2009, Thakur *et al*., 2009). It has been hypothesized that the N17 domain triggers the initial steps of polyQ aggregation by facilitating primary nucleation events. The N17 domain features an amphipathic α-helix with a characteristic coiled-coil structure (Rossetti *et al*., 2011). However, when the polyQ tract is expanded, N17 can undergo conformational changes and self-associate into α-helix-rich tetramers that may act as a nucleus for fibril formation (Fiumara *et al*., 2010, Jayaraman *et al*., 2012). Such self-association process would expose the hydrophobic face of N17 and shorten the distance between the adjacent polyQ tract thus favoring inter-domain interactions and accelerating polyQ aggregation (Kelley *et al*., 2009, Liebman and Meredith, 2010, Williamson *et al*., 2010). N17 generally stands at the edge of the amyloid structure (Hoop *et al*., 2014, Sivanandam *et al*., 2011), which in theory could allow it to sequester truncated monomers for fibril elongation and/or to participate in secondary nucleation events (Jayaraman *et al*., 2012). Initial steps of HTT aggregation can be suppressed by several chaperones found to directly bind the N17 domain, further supporting a role for N17 in HTT aggregate formation (Monsellier *et al*., 2015, Tam *et al*., 2009). In contrast, PRD stabilizes aggregation-prone conformations adopted by the polyQ stretch (Bhattacharyya *et al*., 2006, Darnell *et al*., 2007). Although the PRD is thought to inhibit N17 nucleation when at a proximal position (Caron *et al*., 2013), this positive effect is minimized by the loss of flexibility of expanded polyQ repeats, which prevents possible interactions between the PRD and N17.

Compelling evidence suggest that regions flanking the polyQ stretch may also modulate HTT toxicity (Dehay and Bertolotti, 2006, Duennwald *et al*., 2006b, Lin *et al*., 2017). Deletion of PRD leads to the conversion of benign large aggregates into smaller toxic species (Dehay and Bertolotti, 2006). Those smaller aggregates often display undefined boundaries, which would favor polyQ interactions with other proteins in the

cellular environment (Duennwald *et al*., 2006b). In agreement with the idea that PRD may function to attenuate HTT toxicity is the fact that this sequence recruits protein interactors that are associated with increased proteasomal degradation of mutant HTT and reduced neuronal loss (Southwell *et al*., 2008). Conversely, N17 has been shown to target HTT aggregates to lipid membranes, setting the basis for potential toxic interactions between cellular compartments (Burke *et al*., 2013a, Kegel *et al*., 2005, Rockabrand *et al*., 2007). Such a role for N17 is attributed to its amphipathic α-helix, which confers lipid-binding properties to the protein (Kegel *et al*., 2005). N17 also contains a functionally active nuclear export signal (NES) being suggested to modulate HTT cellular localization and trafficking (Cornett *et al*., 2005, Zheng *et al*., 2013). Abnormal expansion of the polyQ or specific mutations within the N17 domain lead to HTT nuclear accumulation and cytotoxicity (Atwal *et al*., 2007, Cornett *et al*., 2005, Zheng *et al*., 2013). Despite the high degree of sequence conservation throughout mammalian evolution, polyQ-flanking regions do not seem to be required for normal HTT function (Andre *et al*., 2017, Gu *et al*., 2015, Neveklovska *et al*., 2012). They might have rather evolved along with polyQ stretches to modulate their pathogenicity as suggested by their significant role in mutant HTT aggregation and toxicity.

Huntingtin post-translational modifications

In addition to proteolytic cleavage (mention above), HTT can be modified by several other PTMs, including phosphorylation, acetylation, ubiquitination, SUMOylation, palmitoylation, glycosylation, transglutamination and protein glycation (Figure 5). Known phosphorylation sites at HTTex1 include one threonine and two serine residues (threonine-3, serine-13 and -16), but several other phopho-serine sites are found beyond HTTex1, including serine-419, -421, -434, -536, -1181, -1201, -2076, -2653 and -2657. The IκB kinase (IKK) phosphorylates the three phospho-residues contained in HTTex1 (Bustamante *et al*., 2015, Thompson *et al*., 2009). Casein kinase 2 (CK2) (Atwal *et al*., 2011) and GM1 ganglioside (Di Pardo *et al*., 2012) are also suggested as HTTex1 serine-specific kinases. Downstream of HTTex1, both Akt1 (Humbert *et al*., 2002) and the serum and glucocorticoid-induced kinase (SGK) (Rangone *et al*., 2004) target phosphorylation of serine-421, whereas its dephosphorylation is catalyzed by phosphatases of the PPP family (PP1 and PP2A) (Metzler *et al*., 2010) or by metal-dependent phosphatases of the PPM family (PP2C) (Marion *et al*., 2014). Other kinases such as the cyclin-dependent kinase 5 (Cdk5) (Anne *et al*., 2007, Luo *et al*., 2005) and a kinase of the mitogen-activated protein

kinase (MAPK) family, the ERK1 (Schilling *et al*., 2006), have also been implicated in HTT phosphorylation. Most HTT phosphorylation events are thought to have a neuroprotective effect, although this assumption is still controversial (Ehrnhoefer *et al*., 2011). Lysine-444 is the best characterized site for acetylation that, similar to phosphorylation, is suggested to confer neuroprotection against mutant HTT toxicity (Cong *et al*., 2011, Jeong *et al*., 2009). In addition, HTTex1 contains other potential acetylation sites that are also targeted by SUMO or ubiquitin E3 ligases (Kalchman *et al*., 1996, Subramaniam *et al*., 2009). The covalent attachment of fatty acids is catalyzed by palmitoyl transferases at cysteine-214. While diminished palmitoylation is associated with increased mutant HTT aggregation and toxicity (Yanai *et al*., 2006), suppression of HTT glycosylation results in decreased neuronal loss and enhanced clearance of protein aggregates via autophagy (Kumar *et al*., 2014). Likewise, increased levels of transglutaminases are found in particular HD brain regions, suggesting a potential enzymatic imbalance accounting for selective neuronal vulnerability to mutant HTT (Kahlem *et al*., 1998).

N17 PTMs as key modulators of HD pathogenesis

The reversible covalent addition of a functional group to a protein can modulate its biological function and its interaction with other molecules. Therefore, PTMs play a critical role in maintaining normal cell biology, but also influence pathological processes in many neurodegenerative diseases.

The N17 domain provides multiple sites of regulatory PTMs (Figure 5) that can modify HTT conformation and affect protein stability, modulating the propensity of misfolded HTT to form aggregates as well as its subcellular localization, clearance and toxicity. Phosphorylation is a major PTM occurring on N17, where threonine-3 (T3), serine-13 (S13) and serine-16 (S16) were found to be phosphorylated *in vivo* (Aiken *et al*., 2009, Di Pardo *et al*., 2012, Thompson *et al*., 2009). These events seem to be less predominant in a disease context, as expanded HTTex1 shows lower levels of N17 phosphorylation than normal HTTex1 (Aiken *et al*., 2009, Atwal *et al*., 2011, Cariulo *et al*., 2017a). Mounting evidence suggests that N17 phosphorylation is associated with reduced HTT accumulation and neurotoxicity (Atwal *et al*., 2011, Cariulo *et al*., 2017a, Chiki *et al*., 2017, Di Pardo *et al*., 2012, Mishra *et al*., 2012, Thompson *et al*., 2009). Phosphorylation of N17 serine residues by IKK promotes proteasome- and lysosome-mediated turnover of wild-type HTT fragments. However, mutant HTT molecules are

inefficiently targeted for degradation, a process that was related with lower IKK activity (Thompson *et al*., 2009). Impairment of such IKK-dependent cleavage mechanisms would result in increased accumulation of mutant HTT and ultimately lead to the loss of striatal neurons observed in mutant HTTex1 transfected mice (Thompson *et al*., 2009). Experimental support for this hypothesis comes from a later study showing that IKK inhibition increases the accumulation of amyloid fibrils in striatal neurons expressing expanded HTTex1 (Caron *et al*., 2014). A very recent report indicates that T3 can also be targeted by IKK (Bustamante *et al*., 2015), although this finding has not been confirmed *in vivo*. Other kinases have been suggested to regulate N17 phosphorylation at S13 and S16 (Atwal *et al*., 2011, Di Pardo *et al*., 2012). Pharmacological inhibition of CK2 leads to diminished N17 phosphorylation and greater mutant HTT toxicity, suggesting a protective role of S13/S16 phosphorylation (Atwal *et al*., 2011). GM1 ganglioside induces phosphorylation of both S13 and S16 while normalizing levels of a neurotransmission-associated factor and restoring motor function in a mouse HD model (Di Pardo *et al*., 2012).

Additional evidence for the neuroprotective function of N17 phosphorylation is provided by experiments using animal models carrying phosphomimetic (E/D) or phosphoresistant (A) mutations in either full-length HTT (Gu *et al*., 2009) or HTTex1 (Aiken *et al*., 2009, Gu *et al*., 2009, Thompson *et al*., 2009). Serine to aspartate (S→D) substitutions in a mouse HD model based on bacterial artificial chromosome (BAC) expression reverted motor and psychiatric disease-related phenotypes to that of healthy controls (Gu *et al*., 2009). Constitutive double S13/S16 phosphorylation also prevented the accumulation of mutant HTT aggregates and associated neuropathology in striatum and cortical layers of the brain (Gu *et al*., 2009). Marsh and colleagues showed that mimicking T3 phosphorylation ameliorates polyQ-mediated toxicity in a *Drosophila* HD model, but increases the amount of insoluble HTTex1 species (Aiken *et al*., 2009). This is consistent with the emerging view that not all aggregates are toxic, and differential effects of distinct aggregates may depend on the molecular context, including factors that are either intrinsic or extrinsic to the HTT protein. Recent studies on HTTex1 peptides demonstrated that inducing phosphorylation (Arndt *et al*., 2015, Bustamante *et al*., 2015, Cariulo *et al*., 2017a), or adding a negative charge (D) (Chiki *et al*., 2017) to the T3 residue disrupts the N17 amphipathic α-helical structure leading to a decreased ability to form α-helix-rich tetramers that are required for amyloid nucleation and fibril elongation. However, the

inhibitory effect of T3D on mutant HTT aggregation propensity can be reversed by modifications in adjacent N17 residues (Chiki *et al*., 2017). Similarly, phosphomimetic mutations at S13 and S16 diminish the α-helical content of mutant HTTex1 (Atwal *et al*., 2011, Mishra *et al*., 2012) and stabilize inter-domain interactions between N17 and PRD (Caron *et al*., 2013). The slower aggregation kinetics observed for phospho-serine HTT peptides (Caron *et al*., 2013, Gu *et al*., 2009, Mishra *et al*., 2012) seem to be due to reduced stability of transient oligomers rather than changes in monomer conformations, indicating that N17 phosphorylation may inflict a kinetic and/or thermodynamic barrier to the initial phases of oligomerization (Mishra *et al*., 2012).

Phosphorylation can regulate secondary modifications such as acetylation, ubiquitination and SUMOylation. For example, IKK-mediated phosphorylation of N17 serine residues reduces HTTex1 poly-ubiquitination while promoting its poly-SUMOylation and acetylation (Thompson *et al*., 2009). SUMO-1 (small ubiquitin-like modifier) or ubiquitin can modify HTT at identical lysine residues (K6, K9 and K15). SUMOylation stabilizes HTTex1, reduces its aggregation and increases its toxicity (Steffan *et al*., 2004), whereas ubiquitination enhances aggregation and reduces toxicity by targeting soluble HTT molecules for proteasomal degradation (Jana *et al*., 2005, Zucchelli *et al*., 2011). Analysis of wild-type HTT purified peptides by mass spectrometry showed that acetylation of K9 can occur concomitantly with Ser13 phosphorylation (Thompson *et al*., 2009). Acetylation of K9 does not seem to directly affect HTT aggregation (Chiki *et al*., 2017), and its role on HD pathogenesis remains poorly understood. Acetylation can also occur beyond HTTex1 as the acetyltransferase CREB-binding protein (CBP) was found to target K444, promoting the autophagic clearance of mutant HTT and preventing its toxicity *in vivo* (Jeong et al., 2009). Because acetylation is emerging as an important regulatory cellular mechanism for protein stability and turnover in health and disease (Glozak *et al*., 2005, Ravikumar *et al*., 2004, Yamamoto *et al*., 2006), one may speculate a similar role for N17 acetylation. In agreement with this idea, IKK is found to directly interact with CBP in the nucleus suggesting a possible link between IKK-mediated phosphorylation of N17 and CBP activity (Verma *et al*., 2004). N17 serine phosphorylation is indeed associated with increased HTTex1 nuclear accumulation (Atwal *et al*., 2011, Havel *et al*., 2011), which would in turn allow CBP-mediated acetylation, facilitating HTT traffic into autophagosomes (Jeong *et al*., 2009).

In summary, current evidence indicates that PTMs occurring within the N17 region are critical players in HD pathogenesis. Because PTMs are catalyzed by enzymes, they

may hold great potential as druggable targets for therapeutic interventions. However, many questions remain to be answered. For example, it is not yet clear whether altered pathway-modifying PTMs are a cause or a consequence of mutant HTT misfolding and subsequent toxicity. We also still lack evidence about what protein phosphatases, if any, may modulate N17 phosphorylation and whether they would affect its aggregation and toxicity. Understanding how N17 PTMs impact on HTT behavior and modulate each other, as well as identifying molecular pathways involved in these processes, will provide deeper insight into HD pathogenesis and may therefore open novel avenues for treatment of this devastating disorder.

Cell and non-cell autonomous mechanisms of striatal degeneration in HD

Despite the ubiquitous expression of HTT, selective striatal degeneration accounts for up to 95% of the cell loss observed within the brain of patients and animal models of HD. Such striatal vulnerability to mutant HTT-induced toxicity is attributed to particular biochemical and structural characteristics of the medium spiny neurons (MSNs) and/or to their functional connectivity within the complex neuronal networks of the striatum. These neurons are GABAergic cells that project to the *Globus pallidus* and S*ubstantia nigra*, and receive glutamatergic and dopaminergic input from the cortex and *Substantia nigra*, respectively (Ehrlich, 2012, Ross and Tabrizi, 2011). Various cell autonomous and non-cell-autonomous mechanisms for MSN-preferential degeneration have been suggested, including reduced availability of neuronal survival factors such as neurotrophins and heat-shock proteins, glutamatergic excitotoxicity, and MSN-specific SUMOylation of HTT mediated by a Ras homologue enriched in the *Striatum* (Rhes) (Figure 6).

Loss of neuronal survival factors

In HD, loss of the brain-derived neurotrophic factor (BDNF) underlies synaptic dysfunction and impaired survival of MSNs. BDNF is produced in the cortex and anterogradely transported along the cortico-striatal tract to the MSNs, with the wild-type HTT playing an important role in mRNA synthesis and vesicular transport of BDNF (Gauthier *et al*., 2004, Zuccato *et al*., 2003). However, when the polyQ tract is abnormally expanded, HTT loses the ability to sequester the repressor element-1 silencing transcription factor/neuron-restrictive silencer factor (REST/NRSF) complex in the

cytoplasm, which is then translocated into the nucleus thereby leading to transcriptional repression of *BDNF* and other neuronal genes (Zuccato *et al*., 2001). Furthermore, axonal transport and release of BDNF from cortical neurons to their terminals within the striatum is also impaired in HD due to aberrant mutant HTT interactions with the huntingtin-associated protein 1 (HAP1). HAP1 and dynactin are part of an important motor protein complex for intracellular trafficking in neuronal cells. Sequestration of HAP1 into mutant HTT inclusions leads to disruption of the HAP1/dynactin complex, disturbing the transport of BDNF vesicles along microtubules (Gauthier *et al*., 2004). Notably, BDNF vesicle traffic deficits appear to be a specific pathogenic mechanism of HD, since proteins involved in other neurodegenerative disorders do not affect BDNF transport (Gauthier *et al*., 2004). In support of this, mimicking phosphorylation of mutant HTT on S421 restores the binding of molecular motors to microtubules, which may indicate the existence of an upstream HTT-related signaling pathway for controlling BDNF transport (Colin *et al*., 2008). Conversely, lower levels of BDNF in the synaptic cleft may induce the expression of particular caspases in striatal neurons, thereby contributing to the generation of cytotoxic HTT fragments, and ultimately, cell death (Hermel *et al*., 2004). Ellerby et al. showed that removal of BDNF from the extracellular medium of primary striatal cultures leads to enhanced caspase-2 gene transcription by a still unknown mechanism. Caspase-2 expression is indeed increased in striatal and cortical post-mortem HD tissues from both patients and transgenic mice (Hermel *et al*., 2004). Furthermore, caspase-2 associates with full-length mutant HTT promoting its cleavage and hence modulating HTT cytotoxicity (Hermel *et al*., 2004). This study also suggests a mutual relation between mutant HTT and BDNF loss, and implicates caspase-2 in HD-mediated striatal cell death. This is consistent with the preferential accumulation of mutant HTT cytotoxic fragments in striatal neurons (Li *et al*., 2000).

Additional neurotrophic agents may also play significant roles for MSN survival by conferring neuroprotection against oxidative stress (Maksimovic *et al*., 2001, Maksimovic *et al*., 2002) and glutamate-induced excitotoxicity (Freese *et al*., 1992, Frim *et al*., 1993, Nakao *et al*., 1996, Schumacher *et al*., 1991). Neural implants of either nerve growth factor (NGF)- or basic fibroblast growth factor (bFGF)-producing cells prevented striatal loss in adult rats subjected to excitotoxic insults, whereas grafting of BDNF-secreting cells showed no protection in this model (Frim *et al*., 1993). Furthermore, treatment of striatal cultures with NGF and bFGF can regulate the levels of wild-type HTT in a dose-dependent manner, suggesting a gain-of-function mechanism of neuroprotection (Haque and Isacson,

2000).

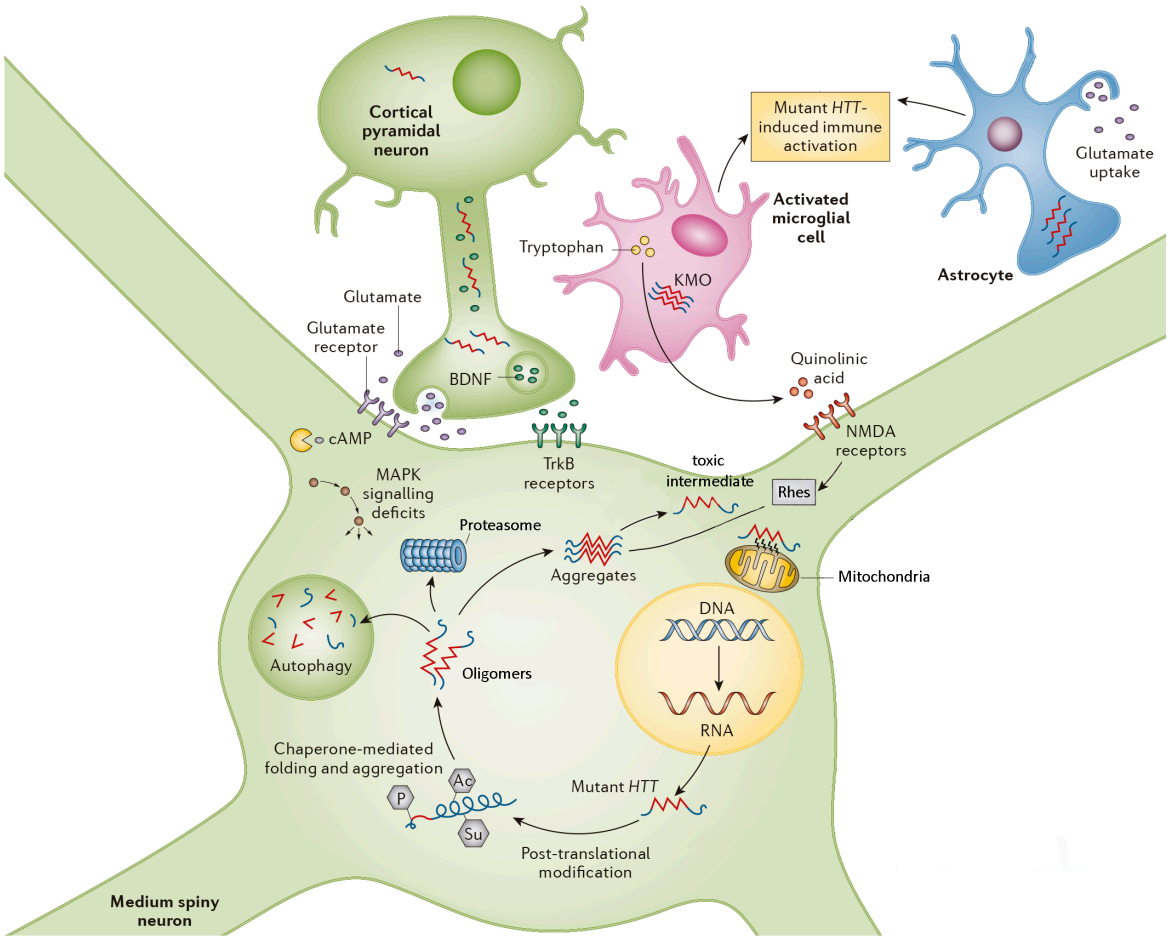

Figure 6. Mechanisms underlying striatal vulnerability in HD. Given the diversity of HTT molecular interactions, its misfolding and aggregation can culminate with the disruption of essential cellular processes, such as transcription, intracellular signaling, mitochondrial activity, autophagy and proteasomal function. Although mutant HTT is likely to contribute predominantly to neuronal pathology, other cells might also become affected thereby triggering a cascade of pathological events that lead to dysfunctional cell-to-cell interaction mechanisms and ultimately neuronal death. These non-cell autonomous pathogenic mechanisms include excitotoxicity, dysregulation of the kynurenine pathway, neuroinflammation and spread of mutant HTT toxic species in a prion-like fashion. Adapted from (Bates *et al.*, 2015).

Heat-shock proteins in HD

Heat-shock proteins (HSPs) play important roles in the maintenance of protein homeostasis essential for cell survival in both health and disease (Hartl *et al.*, 2011, Sakahira *et al.*, 2002). In the HD context, heat-shock proteins HSP70 and HSP40 prevent the formation of HTT aggregates (Muchowski *et al.*, 2000, Wacker *et al.*, 2004) via direct interaction with the N17 domain (Monsellier *et al.*, 2015). HSP70/40 specifically binds to

N17 acting as a shield in pro-aggregation interactions between N17 and flanking regions (Monsellier *et al*., 2015). In addition, it alters structural conformations of pre-formed HTT fibrils, rendering them less toxic (Monsellier *et al*., 2015). Reduced levels of HSP70 and co-chaperones of the DNAJ/HSP40 family are associated with increased HTT aggregation and toxicity (Hageman *et al*., 2010, Tagawa *et al*., 2007), while their overexpression prevents toxicity (Jana *et al*., 2000) and neurodegenerative phenotypes in *Drosophila* models of HD (Chan *et al*., 2000, Kazemi-Esfarjani and Benzer, 2000). Interestingly, HSP70 is upregulated in rat brain-derived cells found to be particularly resistant to HD pathology, but not in cortical and striatal neurons (Tagawa *et al*., 2007). The underlying mechanism seems to involve a positive feedback loop between mutant HTT and p53 gene expression (Bae *et al*., 2005, Feng *et al*., 2006, Tagawa *et al*., 2007) which in turn inhibits the transcriptional regulation of HSP70 in vulnerable neurons (Tagawa *et al*., 2007). However, this might not be exclusive since mutant HTT may also interfere with HSP70 expression via sequestration of the NF-Y transcriptional factor (Yamanaka *et al*., 2008). The consequences of HSP70 loss in striatal neurons may also involve impaired endocytosis (Yu *et al*., 2014) and increased caspase-3-mediated cell death (Zhou *et al*., 2001). It is important to note that downregulation of striatal HSP70 levels and its co-chaperones may also occur during normal aging (Gleixner *et al*., 2014). This could explain, in part, the age-dependent enhanced sensitivity of striatal neurons to mutant HTT.

Glutamatergic excitotoxicity

Impairment of cortico-striatal synapses has also been linked to excitotoxicity. Glutamate is a major component of the CNS, serving as the primary excitatory neurotransmitter for synaptic plasticity stimulation and thereby being associated with learning and memory functions. Such biological processes depend on glutamate binding and activation of NMDA receptors (NMDAR). NMDARs mediate calcium influx to the cell, triggering a cascade of downstream regulatory events involved in mitochondrial activity, transcription, cellular responses to oxidative stress and programmed cell death pathways. Overstimulation of NMDAR or stimulation of extrasynaptic NMDAR due to excessive glutamate levels can lead to excitotoxic cell death, in a mechanism thought to be central to many neurodegenerative disorders (Labbadia and Morimoto, 2013, Roze *et al*., 2011, Zuccato *et al*., 2010). There are increased levels of glutamate in the HD striatum due to reduced glial glutamate uptake (Behrens *et al*., 2002, Hassel *et al*., 2008, Lievens *et al*., 2001, Miller *et al*., 2008). Mutant HTT accumulates in the nucleus of astrocytes and

downregulates the glutamate transporter GLT1 from their surface (Shin *et al*., 2005) by blocking the association of its promoter with the Sp1 transcription factor (Bradford *et al*., 2009). This culminates with a deficient glutamate uptake and increased excitotoxicity in cell and animal models of HD (Shin *et al*., 2005). Altered levels of *GLT1* mRNA in mice occur after the appearance of HTT aggregates in astrocytes (Lievens *et al*., 2001), suggesting that excitotoxicity might not be a cause but a consequence of HD pathology. Notably, mRNA levels of *GLT1* are also found to be decreased in the striatum from HD patients (Arzberger *et al*., 1997).

The quinolinic acid hypothesis

MSNs express higher levels of NMDAR relative to spared interneurons, which could also contribute to excitotoxicity and may account for the preferential loss of MSNs in HD (Raymond *et al*., 2011). NMDAR trafficking is increased in HD-striatal neurons as a consequence of aberrant interaction between mutant HTT and post-synaptic proteins required for NMDAR stability (Fan *et al*., 2009). Secondary metabolites derived from the kynurenine pathway (KP) of tryptophan degradation can also affect NMDAR activity (Figure 7). Altered tryptophan metabolism has been implicated in HD and other neurodegenerative disorders, with elevated levels of neurotoxic KP metabolites being correlated with increased oxidative stress and excitotoxicity (Maddison and Giorgini, 2015). The mechanisms underlying KP activation in HD are not completely understood. However, it was recently demonstrated that expression of mutant HTT stimulates the transcription and release of proinflammatory cytokines in microglial cells (Crotti *et al*., 2014, Kierdorf *et al*., 2013). Therefore, microglial activation could lead to increased levels of downstream KP metabolites, in particular quinolinic acid (QUIN), a strong agonist of NMDAR. Furthermore, induction of proinflammatory cell response can influence the enzymatic activity of kynurenine 3-monooxygenase (KMO) (Giorgini *et al*., 2008), which determines the balance between neurotoxic and neuroprotective KP metabolites (Giorgini et al., 2005). Strikingly, treatment with KMO inhibitors can prevent the toxic effects of mutant HTT *in vivo*, revealing KMO as a promising potential target for HD therapy (Campesan *et al*., 2011, Giorgini *et al*., 2005, Zwilling *et al*., 2011).

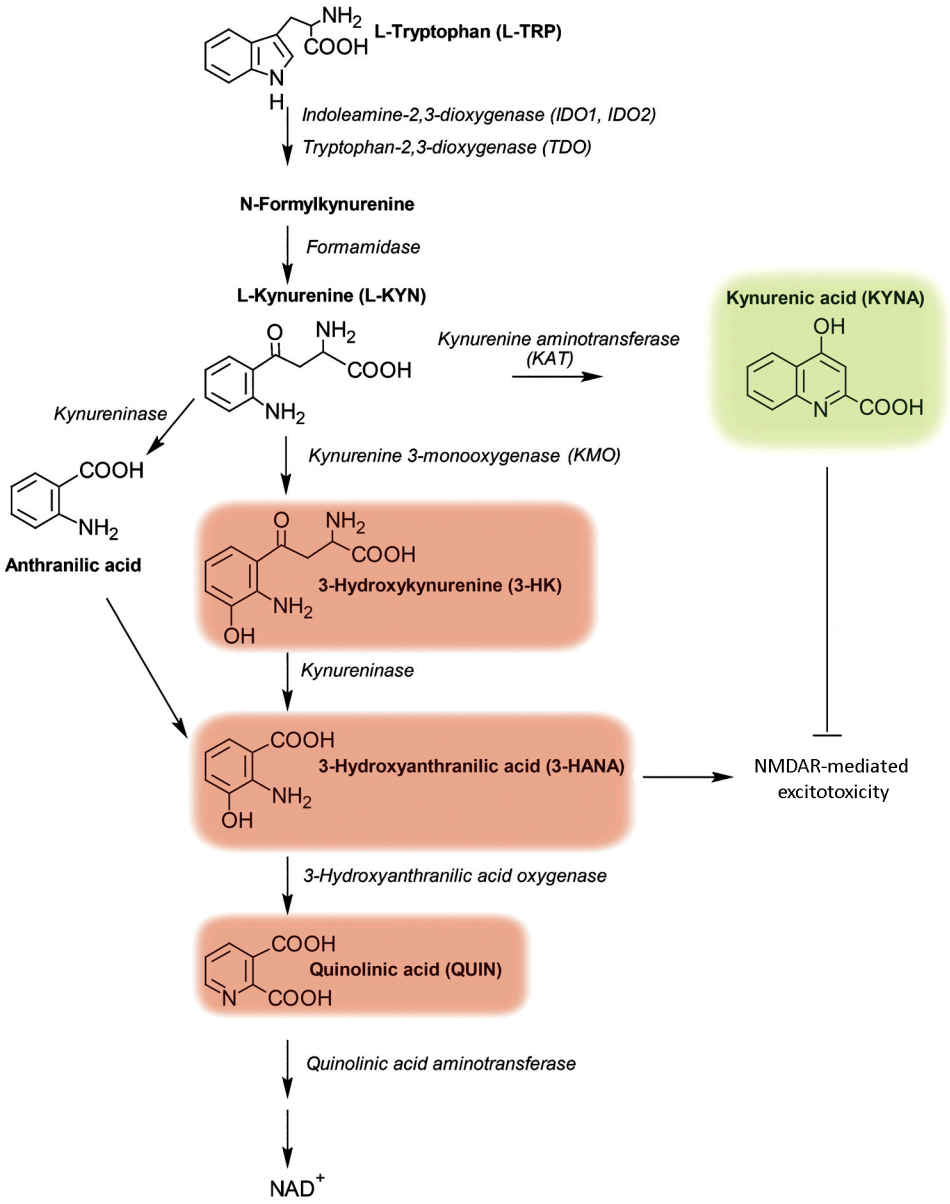

Figure 7. Schematic representation of the kynurenine pathway in mammals. The KP serves as the primary route of L-TRP degradation in mammals. This route ultimately leads to the synthesis of NAD^+, a vital coenzyme for the maintenance of cellular energy homeostasis. The KP contains four neuroactive compounds derived from L-KYN. Both KAT and KMO enzymes can metabolize L-KYN, resulting in the production of neuroprotective (KYNA, highlighted in green) or neurotoxic (3-HK, 3-HANA and QUIN, highlighted in red) metabolites, respectively. While the mechanistic chemistry behind 3-HK and 3-HANA neurotoxicity is still poorly understood, QUIN and KYNA metabolites have been hypothesized to play a role in excitotoxicity via regulation of NMDAR activity. QUIN selectively activates NMDARs whereas KYNA acts as an antagonist of the receptor by blocking its glycine co-agonist site. Image from (Maddison and Giorgini, 2015).

Altered striatal signaling pathways in HD

The small GTP binding protein Rhes is highly expressed in the striatum, where it

preferentially binds to mutant HTT acting as a SUMO E3 ligase, thereby inducing HTT SUMOylation while reducing its ubiquitination. Ultimately, Rhes leads to disaggregation of non-toxic aggregates of mutant HTT and reduces proteasomal degradation of soluble neurotoxic species (Subramaniam *et al*., 2009). Experimental evidence suggests that Rhes activity is controlled by extrasynaptic NMDARs, which once blocked cause downregulation of Rhes and decrease the levels of non-toxic HTT inclusions in cultured striatal cells (Okamoto *et al*., 2009). The same study further proposes a possible link between extrasynaptic NMDARs, mutant HTT and mitochondria-mediated cell death. In physiological conditions, NMDAR-mediated calcium influx activates MAPK signaling along with the protein phosphatase MSK1, which targets cyclic AMP (cAMP)-response element binding protein (CREB). CREB is a critical factor for mitochondrial gene transcription, thus playing an essential role in mitochondrial biogenesis and function (Roze *et al*., 2011). Excessive extrasynaptic NMDAR activity in mutant HTT-expressing neurons leads to inhibition of MAPK signaling, CREB phosphorylation and increased cell death (Okamoto *et al*., 2009).

Remarkably, interrelated signaling pathways resulting in HTTex1 phosphorylation are specifically altered in the striatum, which may also contribute to the spatial distribution of toxicity observed in HD. Compelling evidence indicates that regulation of dopaminergic and cAMP-regulated phosphoprotein (DARPP-32) activity in the striatum provides an indirect modulatory mechanism of HTTex1 phosphorylation (Di Pardo *et al*., 2012, Metzler *et al*., 2010). DARPP-32 has been identified as a key integrator of glutamate and dopamine signaling in MSNs, serving as a neuroprotective agent against NMDA-induced excitotoxicity by acting as a potent inhibitor of PP1 (Svenningsson *et al*., 2004). The loss of DARPP-32 expression in a mouse HD model correlates with increased PP1 activity and decreased S421 HTT phosphorylation, which in turn confers enhanced striatal vulnerability to excitotoxicity (Metzler *et al*., 2010). Interestingly, normal levels of DARPP-32 striatal expression can be restored by GM1-mediated phosphorylation of N17 (Di Pardo *et al*., 2012), suggesting a bidirectional relation between DARPP-32 and HTT. Finally, the protein kinase C and casein kinase 2 substrate in neurons (PACSIN1), also known as syndapin 1, has been shown to overlap with molecular mechanisms of synaptic transmission known to be affected in HD, such as NMDAR recycling, neuronal spine formation and microtubule organization (Zuccato *et al*., 2010). Moreover, PACSIN1 is required for HTT structural stability via direct interactions with the N17 and PRD domains (Caron *et al*., 2013). However, such interactions are affected by increased length of the

polyQ stretch and/or by decreased overall phosphorylation levels via treatment with CK2 inhibitors. Given that both N17 and PACSIN1 are substrates for CK2 (Plomann *et al*., 1998), it has been hypothesized that PACSIN1 may affect HTT conformation and stability, and potentially its aggregation and toxicity, in conjugation with striatal-specific signaling events (Atwal *et al*., 2011, Caron *et al*., 2013).

Intercellular transmission of mutant huntingtin

Current studies indicate that spatiotemporal patterns of neurodegenerative disease progression are highly selective, which may imply a role for neuronal connection-mediated propagation of protein misfolding in pathology. In the particular case of HD, there is increasing consensus that mutant HTT is able to spread between cells in several different ways, which may underlie non-cell autonomous mechanisms of striatal vulnerability. First evidence came from post-mortem human studies. Neuronal grafts of striatal tissue transplanted intracerebrally into HD patients about a decade before death exhibited markers of inflammation and excitotoxicity, as well as disease-like degeneration with preferential loss of projection neurons in comparison to interneurons (Cicchetti *et al*., 2009). Later work from the same authors confirmed the presence of mutant HTT aggregates within the transplanted tissue, suggesting a potential mechanism of intercellular transfer between host cells and grafted neurons (Cicchetti *et al*., 2014). Studies in cell and animal models further indicate that the spread of mutant HTT from one cell to another might take place in HD (Babcock and Ganetzky, 2015, Pearce *et al*., 2015, Pecho-Vrieseling *et al*., 2014). Although synaptic transfer and lysosomal exocytosis have been implicated in transmission of Aβ, Tau and α-syn aggregates, this seems not to be the case of HTT in HD (Costanzo and Zurzolo, 2013, Victoria and Zurzolo, 2017). Unlike other aggregation-prone proteins, mutant HTT does not appear to associate with membrane vesicles upon cellular internalization, which precludes potential exo- and endocytic mechanisms of transfer (Ren *et al*., 2009). Instead, extracellular mutant HTT aggregates can directly bind to the cell surface, being readily taken up into the cytosol and subsequently gaining access to the nucleus and other cellular compartments. Internalized aggregates can be transmitted across dividing cells and persist in culture for over 80 generations, although the fraction of cells exhibiting this phenotype remained low (Ren *et al*., 2009). Similarly, experiments in living cells showed low rate movement of mutant HTT between cells (Herrera *et al*., 2011). Nonetheless, this phenomenon can be further accelerated upon selective lysis of the donor cells (Ren *et al*., 2009), which could suggest a

possible link between cell death and widespread HTT aggregation in the brain. Another proposed mechanism for interneuronal transmission of mutant HTT aggregates is the formation of TNTs (Costanzo *et al*., 2013). These structures are long thin actin-containing bridges that allow cell-to-cell contacts for the exchange of molecules and organelles under both physiological and pathological conditions (Victoria and Zurzolo, 2017). An increase in TNT formation can occur as a result of oxidative stress (Wang *et al*., 2011) and accumulation of HTT aggregates (Costanzo *et al*., 2013). TNT formation might be induced as a cell attempt to get rid of aggregated toxic species, presumably via activation of ROS-induced stress pathways (Victoria and Zurzolo, 2017). In *Drosophila*, phagocytic uptake of neuronal HTT is followed by its accumulation and aggregation in the glial cytoplasm (Pearce *et al*., 2015). This process is hypothesized as a neuroprotective clearance mechanism against the spread of mutant HTT toxicity (Pearce *et al*., 2015, Pearce, 2017). However, another hypothesis would be that phagocytic glia might serve as an alternative route for spreading of HTT aggregates hence accounting for non-cell autonomous-associated toxicity (Victoria and Zurzolo, 2017). This is supported by the observation that selective expression of mutant HTT in astrocytes induces early neuronal dysfunction (Meunier *et al*., 2016) and increased gliosis (Bradford *et al*., 2009), being sufficient for causing HD-related phenotypes in mice (Bradford *et al*., 2009). Moreover, mice with both neuronal and glial expression of mutant HTT develop HTT aggregates in their astroglial brain cells (Bradford *et al*., 2010, Lievens *et al*., 2001) prior to astrocyte dysfunction and excitotoxicity (Lievens *et al*., 2001). Thus, suggesting a positive feed-forward loop between HTT aggregation and glia-related neurotoxicity that may accelerate disease progression (Bradford *et al*., 2010).

1.3. Model Systems of Neurodegenerative Diseases

Neurodegeneration can result from a variety of environmental and genetic factors. Although common neurodegenerative disorders appear to occur mostly sporadically, the identification of causative gene mutations through human genome-wide association studies has facilitated a better understanding of molecular mechanisms underlying these disorders. Indeed, the discovery of APP, SNCA, HTT and TDP-43 gene mutations has been instrumental in developing experimental models of AD, PD, HD and ALS, respectively. These disease models range from yeast and *C. elegans* (nematode) to mammals and human cell culture systems, typically exhibiting many features of familial forms of the human disease, clinically very similar to sporadic cases. However, none of the existing models fully recapitulates the human disease and the choice of a particular model may depend on the question under investigation. As such, the use of different models as complementary tools for dissecting the pathogenesis of disease should be considered if results are to be extrapolated or generalized to humans (Narayan *et al.*, 2014). In this section, the bimolecular fluorescence complementation assay and its application to the study of aberrant protein oligomerization in neurodegenerative disorders is discussed, as well as the use of *Drosophila melanogaster* as a model organism to study neurodegenerative and motor disorders such as HD.

Bimolecular fluorescence complementation: a cell-based assay for studying protein oligomerization

Since its discovery in 1958 by Frederic M Richards (Richards, 1958), protein complementation has been widely used for the development of biological assays (Shekhawat and Ghosh, 2011). Such assays rely on the principle that most proteins can be digested into two or more fragments without activity once isolated, but that recover activity when they are mixed together in certain conditions (Kerppola, 2008). Complementation properties of fluorescent proteins were first described in the beginning of this century. The green fluorescent protein (GFP) was used to develop a protein reassembly system based on antiparallel leucine zipper heterodimer formation for the detection of artificial protein-protein interactions in bacteria (Ghosh *et al.*, 2000). Kerppola and colleagues then used fluorescence complementation for the analysis of protein-protein

interactions in mammalian cells and named the method bimolecular fluorescence complementation (BiFC) assay (Hu *et al*., 2002). This assay involves the fusion of two non-fluorescent fragments of a reporter protein to the proteins of interest which, when interacting, form a fluorescence complex by bringing the reporter fragments back together and reconstituting the activity of the reporter protein (Figure 8A). In the following decade, BiFC systems evolved considerably. There are currently BiFC systems with virtually every fluorescent protein in the spectrum, and their advantages and disadvantages have been extensively analyzed. Probably the greatest advantage of BiFC assays over other complementation assays is the fact that they enable the direct visualization of protein interactions in living cells, without the need for staining with exogenous molecules (Chen *et al*., 2006a, Kerppola, 2008). However, the formation of fluorescent protein complexes is fundamentally irreversible and does not occur instantly, requiring a maturation period in the range of minutes. Such features complicate the visualization of dynamic reversible interactions, but they can be useful for trapping and visualization of rare complexes. For example, in the context of neurodegenerative diseases, the stabilization of certain protein-protein interactions facilitates the study of transient species forming during the aggregation process, such as dimers and/or small oligomers (Herrera *et al*., 2011, Outeiro *et al*., 2008). Another potential limitation of some fluorescent proteins is that their activity is restored more efficiently at temperatures below 30ºC, which is not ideal for mammalian cell studies. This disadvantage is now overcome with the availability of third generation-fluorescent proteins, such as Venus or Cerulean (Nagai *et al*., 2002). These variants are brighter and able to efficiently reconstitute the fluorophore at 37ºC. Finally, original BiFC systems were limited to the study of the interaction between two proteins, but current multicolor BiFC systems allow the analysis of multiple protein-protein interactions simultaneously (Hu and Kerppola, 2003). Multicolor BiFC is based on the fact that N-terminal fragments from different GFP-derived proteins have different excitation/emission spectra when combined with the same C-terminal fragment. As such, each protein interaction produces a different type of fluorescence that can be measured simultaneously in the same cell. Alternatively, BiFC systems can be combined with other methods, in particular FRET/FLIM, to analyze the interaction between more than two proteins simultaneously (Shyu *et al*., 2008).

As mentioned above, the BiFC system has also proven useful as a cellular model of neurodegenerative disorders. We and others have developed BiFC models for the visualization of toxic aggregation-prone proteins in living cells, including α-syn (Outeiro

et al., 2008), HTT (Herrera *et al*., 2011, Lajoie and Snapp, 2010), APP (Chen *et al*., 2006a) and Tau (Blum *et al*., 2015, Chun *et al*., 2011). Besides their feasibility, and in contrast with other techniques, these systems make it possible to monitor closely the first steps of aggregation, i.e. oligomerization, owing to the fact that monomers, soluble oligomeric species and large inclusion bodies are visually distinguishable (Figure 8B). Monomers are not fluorescent and only dimers, oligomers and larger inclusions produce fluorescence. Fluorescence from dimers and oligomers is homogeneously distributed, while large inclusions are foci of concentrated, intense fluorescence. This allows the determination of the number, size and subcellular location of large inclusions and the assessment of the dynamics of oligomeric species and inclusions of different sizes over time, for example. Because dimers and oligomers cannot be distinguished by this method, further toxicity and biochemical assays should complement the initial BiFC results, in order to characterize both the nature and toxicity of oligomeric species and the levels of expression of the constructs. If insoluble aggregates are formed, Triton-X-soluble and -insoluble fractions, sucrose gradients or filter trap assays can be used to more accurately characterize larger inclusions (Goncalves *et al*., 2010, Herrera *et al*., 2011).

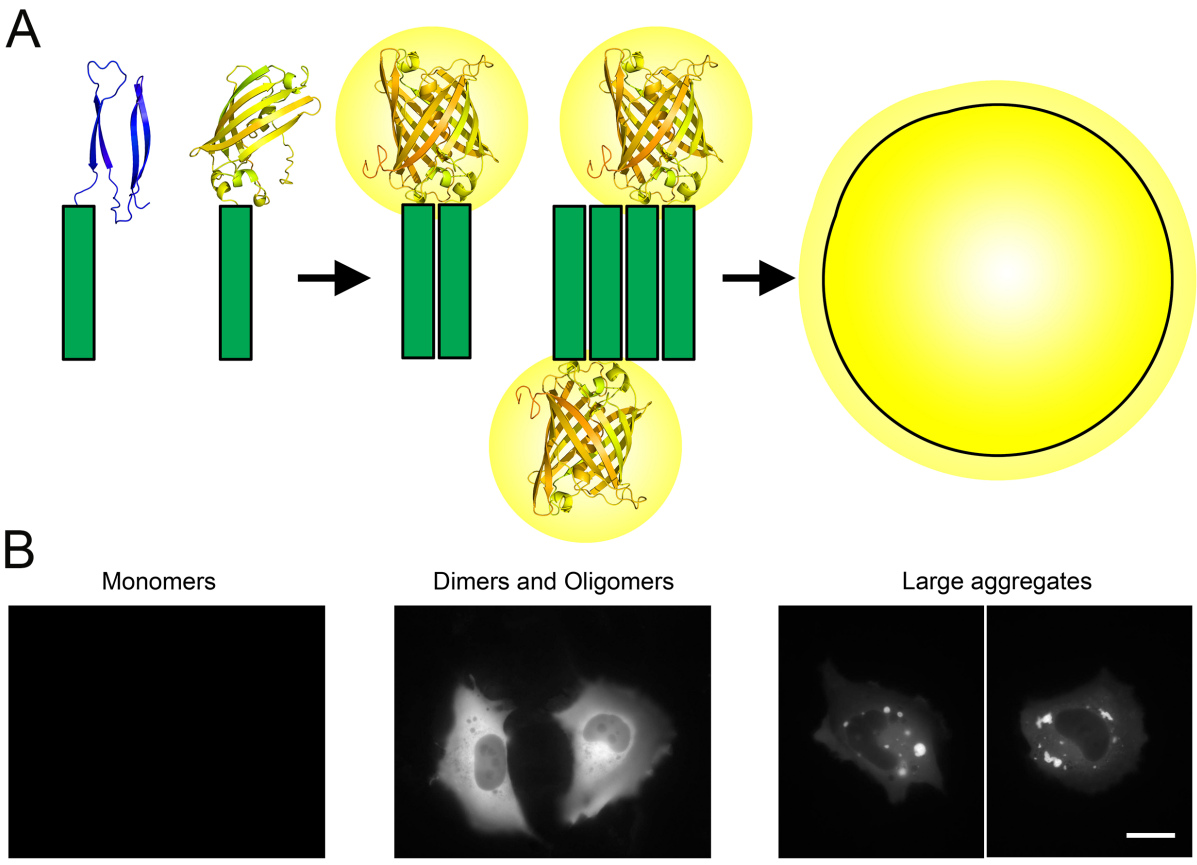

Figure 8. BiFC models of neurodegenerative disorders. (A) The non-fluorescent halves of a reporter

protein are fused to two proteins of interest (green bars). If the proteins dimerize, the non-fluorescent fragments are close enough to each other to reconstitute the fluorophore. The resulted fluorescence is then directly proportional to the amount of dimers/oligomers within cells and can be easily measured by conventional methods such as flow cytometry, western blotting and fluorescence microscopy. (B) While monomers do not show fluorescence, dimers and oligomers show a homogeneously distributed fluorescence in the subcellular compartment where they are formed; larger inclusions are observed as brighter regions with different morphologies that 'scavenge' fluorescence from the rest of the cell. The localization of oligomers and aggregates depends on the protein of interest and the particular experimental conditions. In the HTT-Venus BiFC model, fluorescence is mostly restricted to the cytoplasm and aggregates are very frequent. Scale bar: 20 μm. Obtained from (Herrera *et al*., 2014).

Another possible use for the BiFC system in the study of neurodegenerative disorders is the characterization of aberrant interactions between different disease-related proteins. Using this method, we found that both α-syn (Herrera and Outeiro, 2012, Pocas *et al*., 2015), Tau (Blum *et al*., 2015) and DJ-1 (Sajjad *et al*., 2014) co-aggregate with mutant HTT and alter its aggregation pattern in living cells, suggesting that alterations of these proteins may also contribute to HD pathogenesis. We have also used successfully our HTT-Venus BiFC system to show cell-to-cell transmission of mutant HTT in living cells by flow cytometry (Herrera *et al*., 2011). In that study, two independent populations of cells were transfected with each of the BiFC constructs. When these cell populations were isolated, they did not display fluorescence, as determined by flow cytometry. However, when cell populations were mixed, some fluorescent cells appeared, demonstrating the traffic of mutant HTT between cells.

In summary, the use of BiFC along with other complementary methodologies provides a promising approach for the search of novel molecular targets involved protein misfolding and aggregation. Moreover, the BiFC assay constitutes a simple and easy tool for performing high-throughput genetic and pharmacological screens in a predictable, timely and cost-effective manner (Amaral *et al*., 2013).

Modeling HD in *Drosophila melanogaster*

The fact that HD has a monogenic origin has enabled the development of reliable models for exploring different aspects of HTT aggregation and toxicity. Bioinformatic analyses and the cloning of the HD gene from ancient organisms have revealed a strong homology of the *HTT* sequence across evolution. Similarities can be found among

mammals, but also in more distant relatives such as *Drosophila melanogaster*. In contrast to mammals, the fruit fly offers great advantages in terms of rapid generation and low cost maintenance, and it is therefore being extensively used to model HD and other human neurodegenerative disorders. Remarkably, more than 75% of genes identified in human diseases have counterparts in *Drosophila* (Chien et al., 2002), and fundamental cellular processes related to neurobiology are similar between *Drosophila* and humans, including synaptic transmission, synaptogenesis, subcellular trafficking and age-related cell death. Moreover, critical signalling pathways involved in brain development are also conserved due to a common evolutionary origin for the CNS of invertebrates and vertebrates (Hirth and Reichert, 1999). Despite its simpler nervous system as compared to humans, the fruit fly is capable of performing multiple tasks involving learning and memory functions, and show complex sleep and motor behaviours (Ambegaokar *et al*., 2010, Lessing and Bonini, 2009). Additional features of *Drosophila* make it an attractive organism for use in genetic and pharmacological screenings of potential modifiers of neurodegeneration. First, it has a life cycle of only 2-weeks and relatively short lifespan, although one single cross may give rise to a large number of genetically identical individuals (Hirth, 2010). This allows the study of disease development and progression within the same population, in a statistically significant manner. Second, its well-known anatomy displays unique features such as compound eyes that enable rapid and detailed experimentation in the search of phenotypic suppressors or enhancers (Hirth, 2010). Flies also feature both blood-brain and blood-retinal barriers established by septate junctions formed between glial cells or between cone and pigment cells, respectively, which prevent passive entrance of small molecules to their CNS, including endogenous factors, environmental toxins and drugs (Pinsonneault *et al*., 2011). This characteristic offers the possibility of accurately assessing efficacy of candidate drugs for brain pathologies. Finally, the simplicity and manipulability of the fly genome - comprised in only four pairs of chromosomes - have allowed the development of powerful genetic tools for dissecting disease mechanisms. Indeed, the ease of creating gene deletions, insertions, knock-downs or transgenics, in comparison to mammals, is probably the most important reason for the successful use of *Drosophila* to model and study human neurodegenerative diseases (Venken *et al*., 2011).

The GAL4/UAS (upstream activating sequence) system provides an efficient way to spatially and temporally control the expression of transgenes in *Drosophila* (Figure 9). This binary approach requires two transgenic lines: the driver line that expresses GAL4, a transcriptional activator protein from yeast, in a specific tissue (i.e. under the control of a

tissue- or cell-specific promoter), and a second line containing a UAS-dependent transgene. The generation of UAS lines has been achieved by taking advantage of the naturally found transposable element in *Drosophila*, the P-element. P-elements can be engineered to carry foreign sequences thus allowing for integration of a single UAS-dependent transgene at random locations in the fly genome. Although this system favours the creation of several independent transgenic lines harbouring the same UAS construct, one should be aware that expression levels of the transgene and consequent severity of a degenerative phenotype might vary between lines due to chromatin position effects. The development of a new high-efficient genomic integration system based on phiC31 integrase-mediated DNA recombination has made it possible to overcome disadvantages of the former system by allowing site-specific insertions in the genome, and thereby providing a particular expression profile of the transgene. Once the UAS line carrying the transgene of interest is established, it can then be crossed together with a driver GAL4 line to induce transgene expression. GAL4 specifically bind to UAS activating the transcription of the reporter gene, which is expressed in the progeny, in a tissue-specific manner. Ubiquitous expression of polyQ-expanded HTTex1 by *actinGAL4* or *tubulinGAL4* drivers is extremely toxic causing almost complete pre-adult fly lethality (Green and Giorgini, 2012). To overcome potential deleterious effects of the transgenes, tissue-specific drivers can be employed. This also confers a particular advantage in the study of neurodegenerative disease owing to the possibility of addressing cell-type specific toxicity of disease-associated proteins. In addition, the temperature-sensitivity of the GAL4/UAS system provided by the TARGET (temporal and regional gene expression targeting) method allows the temporal control of transgene expression. This method relies on the antagonistic action of a yeast temperature-sensitive protein, the GAL80, over GAL4 expression. When combined with GAL4/UAS constructs at temperatures above 29ºC, GAL80 is inactivated resulting in derepression of GAL4 activity and consequent onset of the UAS-dependent transgene expression (Elliott and Brand, 2008). The strength of this technique is illustrated in a study showing that polyQ-containing proteins being expressed in old flies are more prone to form toxic amyloids than those from younger individuals, suggesting that different protein aggregation patterns may be related to age. These observations have led to the conclusion that age-related changes in aggregate characteristics may help to explain the late-onset nature of HD and other polyglutamine diseases (Tonoki *et al*., 2011).

Besides its utility in mis-expression studies, the GAL4/UAS system also applies to RNA interference (RNAi) knockdown studies, in which expression of the *Drosophila* homologue of a certain human gene is reduced allowing loss-of-function analyses (Duffy, 2002). Indeed, the use of similar approaches in *Drosophila* has provided hints to the physiological role of the HTT protein. For example, it has been shown that null mutants for the *Drosophila* HD gene (dhtt) display no obvious developmental defects, but their mobility is strongly compromised later in life and they have significantly lower longevity (Zhang *et al*., 2009). Dhtt knockout phenotypes may result from disruption of normal synaptic function and axonal trafficking in the absence of HTT (Zhang *et al*., 2009). Following the same approach, recent studies have also implied HTT as a scaffold for selective autophagy (Rui *et al*., 2015) and as an epigenetic modulator for chromatin organization during development (Dietz *et al*., 2015).

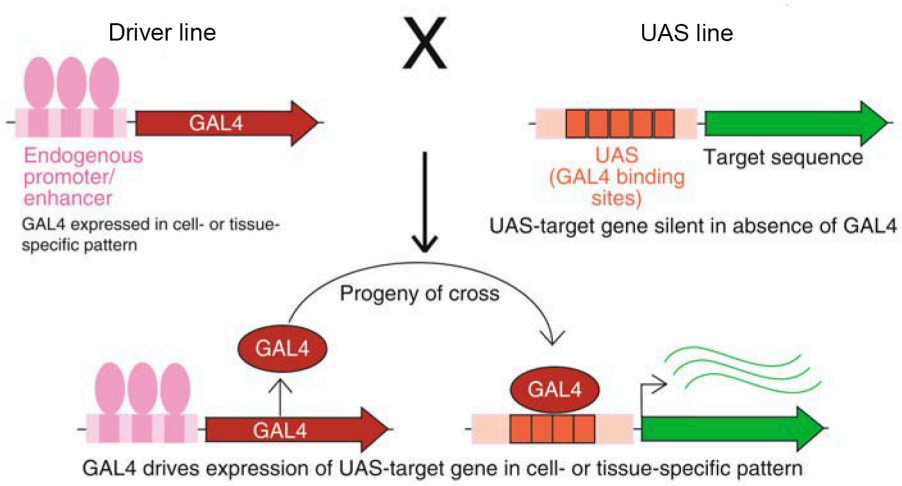

Figure 9. Modeling human neurodegenerative disease in *Drosophila*. The GAL4/UAS binary system allows the ectopic expression of any given sequence, including a protein coding sequence from a human disease-associated gene or a noncoding RNA. This system is based upon crossing two independent transgenic lines, one line expressing a tissue-specific GAL4 promoter [e.g., *elav* (embryonic lethal, abnormal visual), *GMR* (glass multiple reporter) and *Rh* (rhodopsin)], and another line carrying a transgene of interest under the control of several copies of the UAS sequence. In the latter, the transgene of interest is inserted in a pUAST vector downstream of the UAS, and then injected into *Drosophila* embryos by well-established techniques. Because transcription of the transgene requires the presence of GAL4, the two components are brought together in the progeny of a simple genetic cross, whereby triggering the expression of the transgene in a tissue-specific manner. Obtained from (Elliott and Brand, 2008).

Although the *HTT* gene is well conserved throughout evolution, the *Drosophila* homolog does not contain a sequence of CAG repeats (Li *et al*., 1999). As such, and

because HD is thought to be caused primarily by toxic dominant gain-of-function mechanisms, the simple expression of the human polyQ-expanded HTT protein has been used as a strategy to accurately model the disease in this organism (Green and Giorgini, 2012, Krench and Littleton, 2013). Most common drivers used to model HD in *Drosophila* include *elavGAL4*, *GMRGAL4* and the rhabdomere-specific driver Rhodopsin (*RhGAL4*). The *elavGAL4* driver is broadly expressed throughout the nervous system in both neurons and glial cells from embryogenesis onward (Berger *et al*., 2007). Pan-neuronal expression of mutant HTT by the *elavGAL4* driver causes pronounced neurodegenerative phenotypes in the eye or CNS, including degeneration of photoreceptor neurons often accompanied by developmental defects and reduced lifespan. The *Drosophila* eye is a compound structure in which about 750 units, called ommatidia, are arranged in a highly regular pattern. Each ommatidium contains eight light-sensitive neurons (rhabdomeres) composed of rhodopsin molecules, seven of which are visible under the light microscope (Green and Giorgini, 2012). Flies expressing HTTex1 containing 93Q under the control of the *elavGAL4* driver exhibit progressive rhabdomere loss that can be easily quantified using the well-established pseudopupil assay (Figure 10). The *GMRGAL4* and *RhGAL4* drivers can also be employed to assess neurodegeneration in the *Drosophila* compound eye. Given their eye-specific expression, these drivers allow the study of highly toxic constructs that would be lethal if they were more broadly expressed. Furthermore, *GMRGAL4*-driven mutant HTT flies yield a typically "rough" eye phenotype that can be readily observed without the need for quantitative measurements, thereby providing an appropriate model for genetic enhancer/suppressor screens (Marsh *et al*., 2003, Pocas *et al*., 2015).

Larva eye imaginal discs preparations are another advantage of the model, allowing imaging of fluorescent-tagged proteins *in vivo* (Branco-Santos *et al*., 2017, Pocas *et al*., 2015). Development of photoreceptor cells begins in the third larva stage, where the eye imaginal discs complete their growth (Marsh *et al*., 2003). By using transgenic *Drosophila* lines encoding mCherry-tagged wild-type or mutant versions of HTTex1, we recently showed that GMR-driven expression of polyQ-expanded HTTex1 produced a large number of aggregates within larval eye imaginal discs. On the contrary, no inclusion bodies were observed in wild-type HTT expressing larvae, although its diffused pattern of expression was suggestive of the presence of soluble oligomeric species. Such phenotypes are similar to those seen in human cells (Branco-Santos *et al*., 2017, Herrera *et al*., 2011), which further indicate that *Drosophila* may share common mechanisms of polyQ pathogenesis. Other tissue-specific drivers may prove useful in mimicking behavioral

aspects of HD in *Drosophila*. This is the case of the *c164GAL4,* a motor neuron-specific driver widely used to study motor dysfunction in *Drosophila* models of HD and other diseases affecting fine control of movements. Motor performance in *Drosophila* can be assayed by standardized behavioral testing of adult negative geotactic responses or larval crawling activity. While adult HD flies exhibit progressive loss of normal motor function as evidenced by their inefficient ability to climb or fly to the top a tube in a specified amount of time (Branco-Santos *et al*., unpublished work), HD larvae perform greater crawling activity but weaker exploratory behavior of the surrounding environment relative to controls (Steinert *et al*., 2012) (Figure 11). Although apparently contradictory, both phenotypes denote altered innate behaviors indicative of extensive cellular toxicity and/or changes in metabolism. Larval crawling assays are particularly useful when expression or deletion of a gene causes lethality in pupal or adult stages and they allow to screen directly for chemical compounds that may act on early stages of the disease.

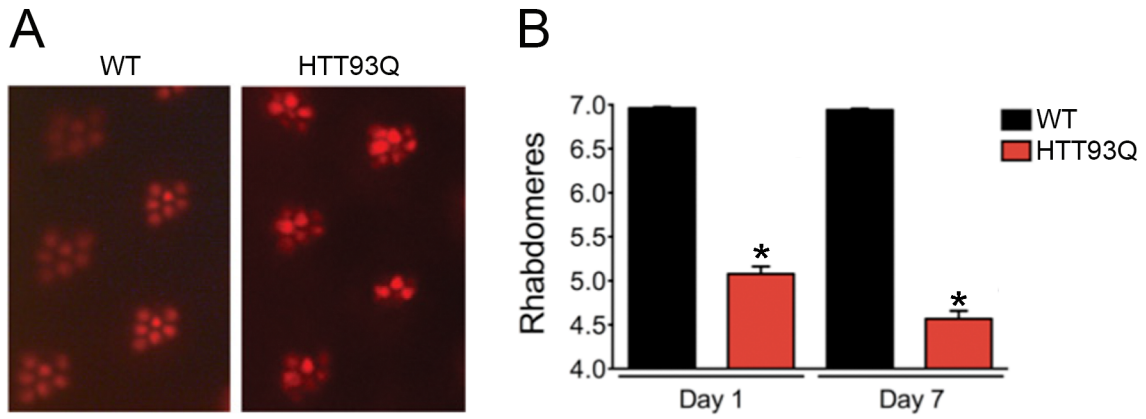

Figure 10. Assaying neurodegeneration in *Drosophila* HD models. The light microscopy-based pseudopupil assay enables the quantification of photoreceptor neurons in the adult fly eye, being frequently used to assess polyQ-mediated neurotoxicity in *Drosophila*. (A) Representative images from wild-type (WT) and *elav*-driven HTTex1 flies carrying 93Q (HTT93Q). Images obtained from (Green and Giorgini, 2012). (B) Quantification of mean rhabdomeres (± SEM) per ommatidium. A normal fly (WT) typically has 7 visible photoreceptors in each ommatidia, whereas HD flies exhibit an average of 5 rhabdomeres at one day of age, with that number being significantly reduced over time, in an age-dependent manner. Statistical analysis by two-way ANOVA, n=30 flies per genotype, *p<0.0001.

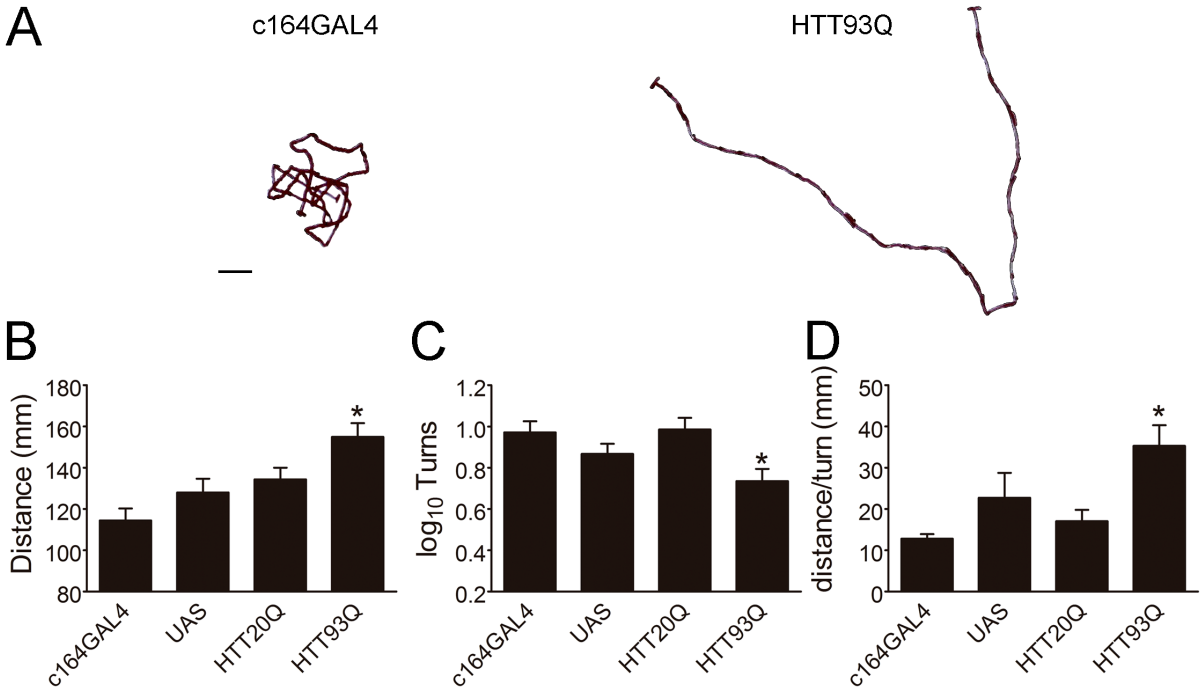

Figure 11. Larval crawling behavior defects in a *Drosophila* model of HD. (A) Representative pattern of crawling behavior in control (c164GAL4) and larvae overexpressing HTT93Q in motor neurons, via the c164 promoter. HTT93Q larvae typically exhibit a weaker exploratory behavior when compared to HTT20Q as observed by a significant decrease in number of turns (C) and a correlated significant increase in distance travelled (B). Greater crawling activity of HD larvae is demonstrated by a significant increase in distance/turn in comparison to control larvae (D). Data are mean ± SEM. *significant versus HTT20Q, $p<0.05$. Scale bar, 10 mm. (Branco-Santos *et al*., unpublished work).

II.

Aims

The most common histopathological hallmark of HD is the presence of intracellular HTT aggregates associated with neuronal loss in the striatum and deep layers of the cortex. These inclusions are generated by the misfolding and subsequent aggregation and intracellular accumulation of mutant HTT. Although the precise molecular mechanisms underlying HD pathogenesis are still not clear, a suite of intramolecular and intermolecular factors have been identified and associated with HTT aggregation and toxicity. Current evidence indicates that PTMs and specific protein-protein interactions play a key role in HD pathogenesis. Identifying the intracellular pathways involved in HTT PTMs and understanding how these modifications and/or other proteins modulate HTT aggregation and toxicity may provide further insight into the molecular basis of this devastating disorder. Thus, by taking advantage of a series of BiFC systems and *Drosophila* models of HD, the aims of the present PhD work were to:

1) Explore the role of specific PTMs on mutant HTT oligomerization, aggregation and toxicity (Chapter III, section A)

- Characterize single HTT N-terminal phosphomutants *in vitro* and *in vivo;*
- Identify specific protein phosphatases involved in mutant HTT N-terminal phosphorylation, aggregation and toxicity *in vitro* and *in vivo*;
- Determine the effect of protein glycation on mutant HTT toxicity in vivo.

2) Understand how aberrant protein-protein interactions may modulate HD pathogenesis (Chapter III, section B)

- Study the effect of aggregation-prone proteins upon mutant HTT aggregation and toxicity;
- Unravel molecular pathways involved in mutant HTT toxicity mediated by prion-like proteins.

III.

Results

This chapter contains parts of the following publications:
Branco-Santos J[§], Herrera F[§]*, Poças GM, Pires-Afonso Y, Giorgini F, Domingos PM*, Outeiro TF* (2017) Protein phosphatase 1 regulates huntingtin exon 1 aggregation and toxicity. *Human Molecular Genetics*, 26**,** 3763-3775

Vicente Miranda H, Gomes MA, Branco-Santos J, Breda C, Lázaro DF, Lopes LV, Herrera F, Giorgini F, Outeiro TF (2016) Glycation potentiates neurodegeneration in models of Huntington's disease. *Scientific Reports*, 18 (6): 36798.

Poças GM, Branco-Santos J, Herrera F, Outeiro TF, Domingos PM (2014) α-Synuclein modifies mutant huntingtin aggregation and neurotoxicity in Drosophila. *Human Molecular Genetics*, 24 (7): 1898-907

This chapter also includes results of the following manuscript (*under review*):
Prion proteins modulate mutant huntingtin mediated neurotoxicity
Branco-Santos J, Staniforth GL, Maddison DC, Breda C, Domingos PM, Steinert JR, Kyriacou CP, Outeiro TF, Herrera F, Tuite MF, Giorgini F

[§]Contributed equally to this work
*Co-corresponding authors

A.

Post-translational modifications in Huntington's disease: new insights into the mechanisms of mutant huntingtin aggregation and toxicity

3.1. The role of N-terminal phosphorylation and protein phosphatases on huntingtin oligomerization, aggregation and toxicity

Abstract

Huntington's disease (HD) is an incurable and fatal neurodegenerative disorder characterized by the accumulation of mutant huntingtin protein (HTT) into intracellular proteinaceous inclusions in specific brain tissues. The first 17 amino acids of the huntingtin protein (N17) undergo several post-translational modifications that modulate the propensity of huntingtin to form aggregates, and alter its subcellular localization, clearance and toxicity. In this study, our aim was to understand how single phosphorylation events in N17 regulate huntingtin oligomerization, aggregation and toxicity, and to identify protein phosphatases that could be involved in these processes. Using a bimolecular fluorescence complementation (BiFC) assay, we showed that expression of single phosphomimic mutations within N17 phosphorylatable residues (T3, S13 or S16) completely abolished HTT aggregation in human cells. In *Drosophila,* mimicking phosphorylation at T3 decreased HTT aggregation in larvae and adult dopaminergic neurons. Interestingly, pharmacological or genetic inhibition of protein phosphatase 1 (PP1) prevented HTT aggregation in both human cells and *Drosophila* while increasing neurotoxicity in flies. In summary, our findings provide novel insights into the role of N17 phosphorylation in HD pathogenesis.

Introduction

Huntington's disease (HD) is characterized by the loss of medium spiny neurons in the striatum. The main histopathological hallmark of HD is the misfolding and subsequent intracellular aggregation of a mutant form of huntingtin (HTT) (Rochet, 2007). HTT is a very large protein (~350 kDa), but expression of exon 1 is sufficient to produce HD-like features in various cellular and animal models (Bates *et al*., 1998, Bates *et al*., 2015, Mangiarini *et al*., 1996). HTT exon 1 (HTTex1) contains a polyglutamine (polyQ) tract that, in normal conditions, is constituted by 6 to 35 glutamine residues. An expansion of

the polyQ tract beyond 35 glutamines induces the misfolding and aggregation of mutant HTT and causes HD (Ambrose CM and Hummerich H, 1994, The Huntington's Disease Collaborative Research Group, 1993). Mutant HTT with longer polyQ expansions is more prone to aggregate, and leads to earlier onset of the disease (Bates *et al*., 2015, DiFiglia *et al*., 1997, Krobitsch and Lindquist, 2000).

The polyQ tract is preceded by an N-terminal sequence of 17 amino acids (N17 domain) that is highly conserved, suggesting that this domain plays an important role in the function of HTT (Atwal *et al*., 2007, Burke *et al*., 2013b, Cornett *et al*., 2005, Kuiper *et al*., 2017, Michalek *et al*., 2013, Rockabrand *et al*., 2007, Xia *et al*., 2003). The N17 domain plays a key role in the aggregation pathway of HTT, where the protein associates first into alpha-helical oligomers and acts as a seed to concentrate and facilitate the formation of larger aggregates and fibrils (Crick *et al*., 2013, Jayaraman *et al*., 2012, Thakur *et al*., 2009, Wetzel, 2006, Williamson *et al*., 2010). Deletion or posttranslational modifications, such as phosphorylation, ubiquitination and SUMOylation, in the N17 produce striking effects in the stability and aggregation of HTT, as well as in cell viability (Aiken *et al*., 2009, Choudhury and Bhattacharyya, 2015, Gu *et al*., 2009, Gu *et al*., 2015, Havel *et al*., 2011, Jana *et al*., 2005, Maiuri *et al*., 2013, Mishra *et al*., 2012, Steffan *et al*., 2001, Steffan *et al*., 2004, Thompson *et al*., 2009, Veldman *et al*., 2015, Zheng *et al*., 2013, Zucchelli *et al*., 2011). The N17 domain has 3 phosphorylatable amino acid residues – threonine at position 3 (T3), and serine residues at positions 13 and 16 (S13 and S16). Constitutive phosphorylation of T3 enhances mutant HTT aggregation, but its role in HTT toxicity remains unclear (Aiken *et al*., 2009). Previous studies have focused on double S13/S16 phosphorylation (Atwal *et al*., 2011, Caron *et al*., 2014, Di Pardo *et al*., 2012, Gu *et al*., 2009, Khoshnan *et al*., 2004, Thompson *et al*., 2009), despite the fact that double S13/S16 phosphorylation is less frequent than single T3 or S13 phosphorylation (Bustamante *et al*., 2015, Huang *et al*., 2015), and that overexpression of particular kinases is required in order to achieve double S13/S16 phosphorylation (Thompson *et al*., 2009).

Single phosphorylation and phosphomimetic modifications in S13 or S16 modulates the formation of HTT fibrils and reduces the oligomerization rate in cell-free systems, just as the double S13/S16 phosphorylation does *in vitro* and *in vivo* (Gu *et al*., 2009, Havel *et al*., 2011, Mishra *et al*., 2012, Thompson *et al*., 2009). Casein Kinase 2 (CK2) inhibitors reduce S13/S16 phosphorylation and enhance toxicity (Atwal *et al*., 2011), while GM1 ganglioside induces S13/S16 phosphorylation and restores motor and molecular deficits in HD mice (Di Pardo *et al*., 2012). IKK, a kinase involved in inflammatory responses, also

regulates T3 and S13/S16 phosphorylation and modulates HTT aggregation (Atwal *et al*., 2011, Bustamante *et al*., 2015, Caron *et al*., 2013, Thompson *et al*., 2009). While several protein phosphatases control HTT dephosphorylation beyond exon 1 and modulate its toxicity (Ermak *et al*., 2009, Marion *et al*., 2014, Pardo *et al*., 2006, Pineda *et al*., 2009, Rosenstock *et al*., 2011), it is not known which protein phosphatases, if any, regulate phosphorylation of the N17 domain.

Here, we elucidate the contribution of single N17 phosphorylation events towards HTTex1 oligomerization, aggregation and toxicity in cell cultures and a *Drosophila* HS model. We screened a collection of protein phosphatase chemical inhibitors to identify modulators of HTTex1 oligomerization, aggregation and toxicity. Inhibition of PP1 prevents HTTex1 aggregation but not oligomerization in human cells. In addition, downregulation of PP1 in *Drosophila* neurons reduces HTTex1 aggregation and increases its toxicity. In total, our findings point to a critical role of T3 phosphorylation in HTTex1 aggregation and support the targeting of PP1 for therapeutic interventions in HD.

Results

Single N-terminal phosphomutants modulate mutant huntingtin aggregation in human cells

In order to investigate the contribution of each phosphorylatable residue (T3, S13 and S16) within the N17 towards HTTex1 aggregation, we first interrogated whether single N17 phosphorylation events modulate aggregate formation. We employed our HTTex1-Venus BiFC system for the visualization of both oligomeric species and inclusion bodies of HTTex1 in living cells, which we have previously described (Herrera *et al*., 2011). Using the 97QHTTex1-Venus constructs as templates, we introduced point mutations in each of the phosphorylatable residues within the N17, changing these amino acids to either alanine or aspartic acid (Figure 12A). Mutations to alanine (A, phosphoresistant) resemble biophysical properties of a constitutive unphosphorylated state, and mutations to aspartate (D, phosphomimic) confer a negative charge to the residue, mimicking phosphorylation. Importantly, these phosphomutants behave like phosphorylated peptides in terms of their intramolecular conformation and aggregation in cell-free systems and primary neuronal cultures (Caron *et al*., 2013, Chiki *et al*., 2017, Havel *et al*., 2011, Mishra *et al*., 2012).

As described in Chapter I, expanded (97Q) HTTex1 BiFC pairs produce more oligomers and inclusion bodies than wild-type (19Q) HTTex1 BiFC pairs (Figure 12B). In accordance, HTTex1 is known to exist as tetramers but not monomers (Sahoo *et al*., 2016). These phenotypes were further confirmed by protein immunoblot and dot blot analysis (Figure 12D), where 97QHTTex1 appears as large SDS-insoluble aggregates (filter trap, FT) and oligomeric species of variable sizes (Native-PAGE), and 19QHTTex1 accumulates essentially as single-size oligomers. The aggregation pattern of non-mutated 97QHTTex1 was compared with that of phosphoresistant (T3A, S13A, S16A) or phosphomimic (T3D, S13D, S16D) mutant forms of 97QHTTex1 (Figure 12B-D and Figure S1, Supplemental information I). While phosphoresistant mutants (T3A, S13A and S16A) showed essentially the same aggregation pattern as non-mutated 97QHTTex1, phosphomimic mutants (T3D, S13D and S16D) completely abolished the formation of 97QHTTex1 aggregates. However, the absence of aggregates was accompanied by the formation of intermediate species in similar levels to the non-mutated 97QHTTex1 BiFC pair as determined by flow cytometry analysis (Figure S2, Supplemental information I), suggesting that N17 phosphorylation redirects aggregation down to a different assembly pathway. Consistent with this, previous reports show that N17 phosphorylation alters aggregate morphologies, resulting in both reduced aggregation kinetics and increased susceptibility for degradation (Arndt *et al*., 2015, Chiki *et al*., 2017, Mishra *et al*., 2012, Thompson *et al*., 2009).

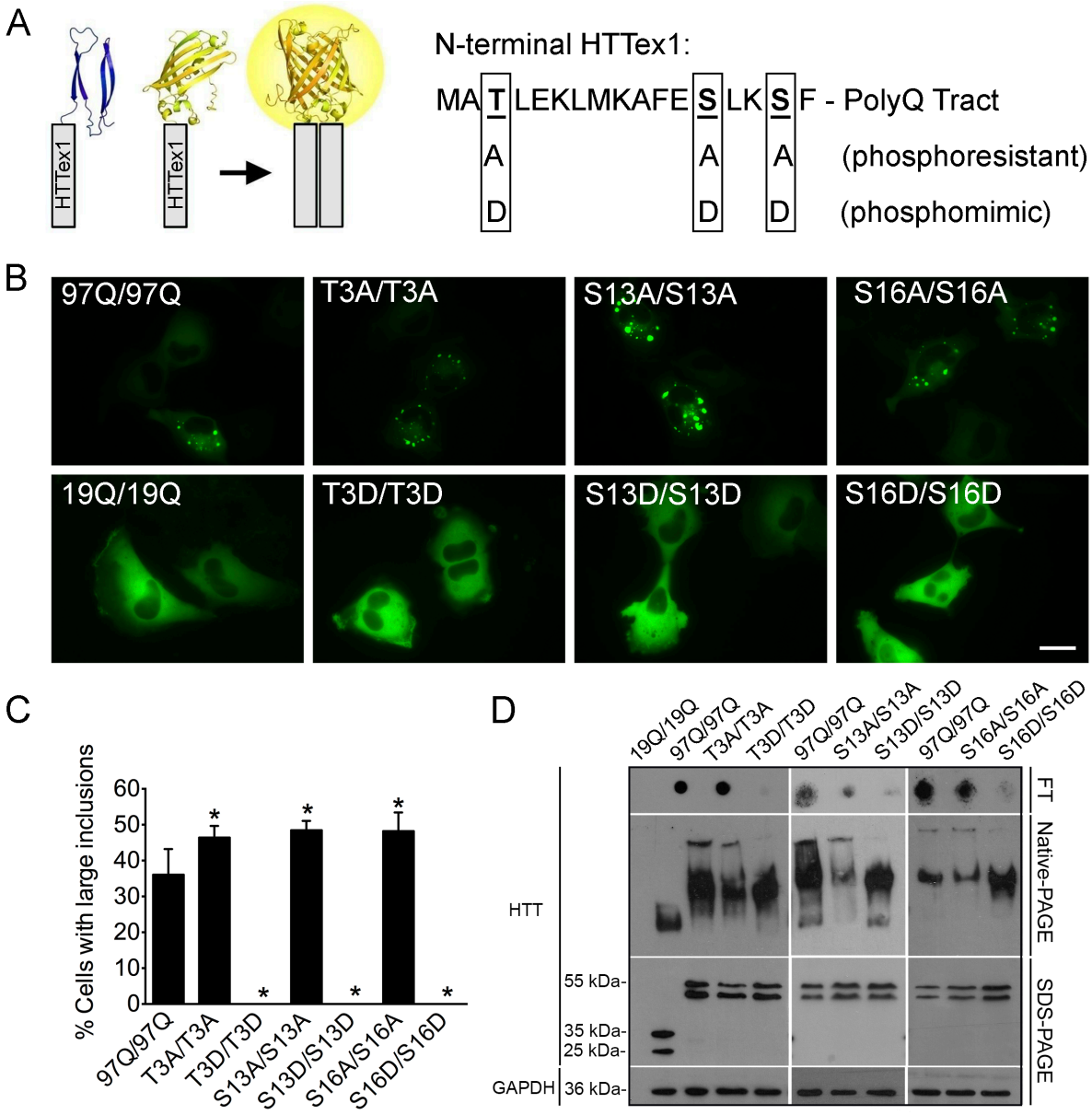

Figure 12. Single N17 phosphomimic mutations modulate 97QHTTex1 aggregation but not oligomerization in human H4 glioma cells. (A) HTTex1 (gray bars) was fused to two non-fluorescent halves of the Venus protein. When HTTex1 dimerizes, Venus recovers fluorescence. The three N17 phosphorylatable residues were mutated to mimic phosphorylation or dephosphorylation. (B) Cells transfected with phosphoresistant BiFC pairs resemble the non-mutated 97QHTTex1 phenotype in terms of aggregation, while phosphomimic pairs showed a total absence of aggregates. (C) Quantitative analyses of microscopy pictures. *significant versus 97Q/97Q, $p<0.05$. (D) Filter trap assays (FT) were consistent with microscopy results. Phosphomimic pairs did not produce insoluble aggregates (FT), but showed similar levels of oligomeric species (Native-PAGE) comparing to non-mutated 97QHTTex1. Expression levels of each pair were evaluated by SDS-PAGE. Scale bar, 20 μm.

Threonine-3 is a critical modulator of mutant huntingtin aggregation

Phosphorylation is a dynamic process that could differently affect various subpopulations of any given protein within a cell. Thus, we predicted that, in normal conditions, mixed pools of phosphorylated and unphosphorylated HTT may co-exist in cells. Taking advantage of the unique features of our BiFC system, we asked whether different combinations of phosphomimic and phosphoresistant mutants could interact and affect 97QHTTex1 aggregation. We transfected H4 cells with all possible pairwise combinations of phosphomutants and non-mutated counterparts (Table III).

Strikingly, combinations of different phosphomimic pairs did not produce any inclusions, independently of the mutated residues (Table III). On the other hand, combinations of phosphomimics with phosphoresistant (Table III) or non-mutated versions (Table III and Figure S3, Supplemental information I) resulted in intermediate patterns of aggregation that were dependent on the residue mutated. Importantly, combinations containing T3D resulted in total absence (0%) of cells with inclusions, whereas combinations with S13D or S16D resulted in 14.1-17.1% or 19.8-29.1% of cells with inclusions, respectively, which was significantly less than that of the non-mutated 97QHTTex1 pair (36.1%). Further analysis of cells expressing these combinations showed that the S13D/97Q combination decreased the number of inclusions per cell (Figure S3C and D, Supplemental information I) but had no effect on inclusion diameter (Figure S3E, Supplemental information I). No differences were observed in the number or size of S16D/97Q inclusions (Figure S3C-E, Supplemental information I). In addition, analysis of total cell fluorescence showed that all combinations of phosphomimic with non-mutated 97QHTTex1 oligomerized and produced similar levels of oligomeric species as those formed solely by non-mutated 97QHTTex1 (Figure S4, Supplemental information I). These results strongly suggest that mixed phospho-HTTex1 molecules interact and co-aggregate in living cells at different extents, depending on the phosphorylated residue, being T3D the most restrictive modification for preventing HTTex1 aggregation.

Table III. Percentage of cells containing HTTex1 inclusions (average±SEM) when transfected with different combinations of HTTex1-Venus BiFC constructs.

		Venus 2						
		T3D	S13D	S16D	T3A	S13A	S16A	97Q
Venus 1	T3D	0	0	0	0	0	0	0
	S13D		0	0	22.0±3.4	17.1±2.3	14.5±1.2	14.1±1.3
	S16D			0	27.5±1.5	29.1±3.6	19.8±3.0	22.9±1.0
	T3A				46.4±1.3	43.5±3.6	45.9±2.5	34.5±2.2
	S13A					48.5±1.3	35.3±2.4	37.8±1.9
	S16A						48.2±2.6	36.6±6.1
	97Q							36.1±2.2

While combinations of phosphoresistant mutants with non-mutated 97QHTTex1 did not modify inclusion body formation, combinations of different phosphoresistant pairs generally resulted in increased percentage of cells displaying inclusions (43.5-48.5%) versus the non-mutated 97QHTTex1 pair, with the exception of the S13A/S16A combination (35.3%) (Table III). Interestingly, pairs of BiFC plasmids containing T3A and S13A mutations (double mutant) resulted in 49% of cells with inclusions (data not shown), similar to T3A (46.4%) or S13A (48.5%) pairs, indicating that additional dephosphorylation events on these residues do not enhance aggregation.

N17 phosphorylation has been shown to modulate neurotoxicity in several HD models by preventing HTT aggregation (Gu *et al*., 2009, Khoshnan *et al*., 2004), although this finding remains controversial (Aiken *et al*., 2009, Atwal *et al*., 2011, Thompson *et al*., 2009). Given that we demonstrated that N17 phosphomutants modulate HTTex1 aggregation in our cell model, we next evaluated whether N17 phosphomutants affected HTTex1 cytotoxicity. We assessed cytotoxicity by measuring the levels of lactate dehydrogenase (LDH) release from cells as an indicator of cell membrane integrity (Figure 13 and Figure S5, Supplemental information I). Only T3D pairs decreased significantly 97QHTTex1 cytotoxicity at 24 h post-transfection (Figure 13A). The levels of LDH activity produced by T3D pairs were further measured at 48 h and 72 h after transfection, which revealed a trend towards a decrease in 97QHTTex1 cytotoxicity, although no significant differences were detected (Figure S5, Supplemental information I). S13 and S16 phosphomutants had no effect on HTTex1 cytotoxicity at 24 h (Figure 13A), 48 h or 72 h post-transfection (data not shown). Interestingly, T3D was no longer able to prevent HTTex1 cytotoxicity when combined with unphosphorylated molecules of 97QHTTex1

(Figure 13B). No differences were observed when S13D or S16D was co-expressed with non-mutated 97QHTTex1 (Figure 13B).

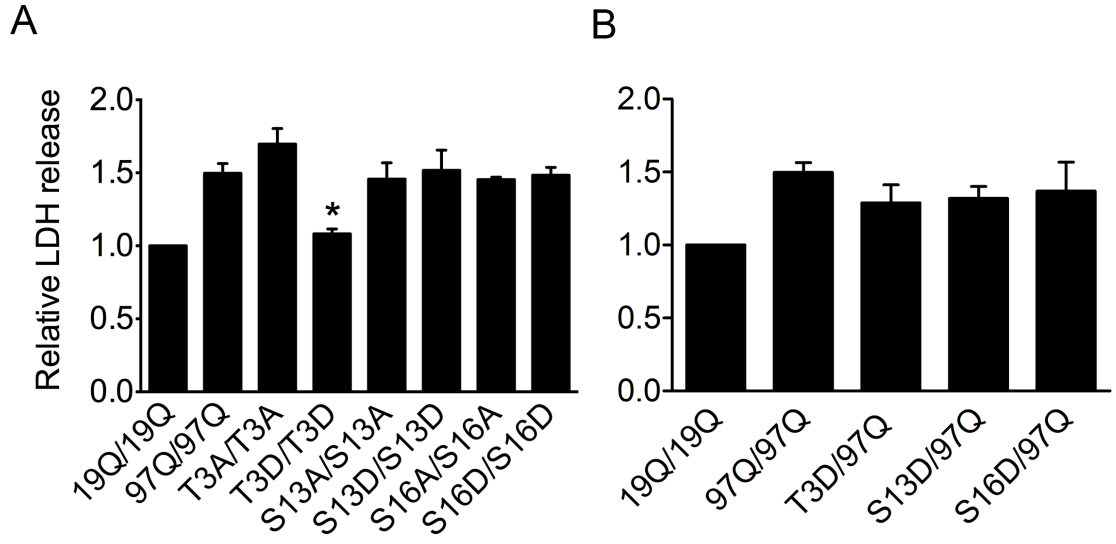

Figure 13. T3 phosphomimic prevents 97QHTTex1 cytotoxicity. Cytotoxicity produced by phosphomutants BiFC pairs (A) or combinations of phosphomimic mutants with non-mutated 97QHTTex1 (B), measured at 24 h post-transfection. Levels of released LDH activity were normalized versus the 19Q/19Q control. *significant versus 97Q/97Q, $p<0.05$.

These observations reinforce the significance of T3 residue for HD pathogenesis and indicate that, in our cell model, HTTex1 cytotoxicity is not directly associated with its oligomerization or aggregation, since changes in N17's phosphorylation state had striking effects on aggregation but very limited or no effects on cytotoxicity.

Serine-13 or -16 phosphorylation modifies the dynamics of mutant huntingtin aggregates

As mentioned above, N17 phosphorylation can influence the morphology of HTT aggregates (Gu *et al*., 2009, Mishra *et al*., 2012) as well as the rate of inclusion body formation (Caron *et al*., 2014). To further investigate the properties of the different 97QHTTex1 inclusions in our cell model, we used fluorescence recovery after photobleaching (FRAP) analysis. This microscopy-based approach assesses protein kinetics properties in living cells by measuring the movement of unbleached fluorescent proteins into a small region of interest (ROI) that was irreversibly photobleached with high-intensity light (Lippincott-Schwartz *et al*., 2001). Thus, fluorescence intensity after photobleaching is directly proportional to dynamics of protein assemblies and/or exchange of proteins between ROI and its surrounding area. Using this technique, we compared the

dynamics of inclusions formed exclusively by non-mutated 97QHTTex1 and phosphomimic- or phosphoresistant-containing inclusions (Figure 14). Fluorescence recovery of 97QHTTex1 inclusions containing S13D or S16D mutants occurred rapidly relative to inclusions formed solely by non-mutated 97QHTTex1 (Figure 14A and B), indicating a higher exchange of HTTex1 molecules. In contrast, inclusions formed by non-mutated 97QHTTex1 and phosphoresistant mutants showed significantly slower fluorescence recovery, with the exception of the S16A/97Q combination (Figure 14C). Interestingly, phosphomimic-containing inclusions mostly displayed a fluid-like behavior, appearing rather continuous with the cytosolic fluorescence (Figure 14D), as opposed to the more rigid behavior of the inclusions formed by combinations containing phosphoresistant mutants or non-mutated 97QHTTex1 BiFC pairs (data not shown).

Expanded HTTex1 enters a multistep aggregation pathway where globular intermediates self-associate to form more tightly packed inclusions (Duim *et al*., 2014). These two types of inclusions differ in their dynamic properties, being globular intermediates highly mobile and constantly exchanged between soluble phases (Caron *et al*., 2014, Thakur *et al*., 2009). Our results suggest that phosphomimic-containing inclusions are more similar to large dynamic oligomers than to mature aggregates, and support the idea that aggregates may be mainly composed of unphosphorylated HTT molecules, consistent with data indicating that disease-causing HTT is hypophosphorylated in the N17 region (Aiken *et al*., 2009, Atwal *et al*., 2011).

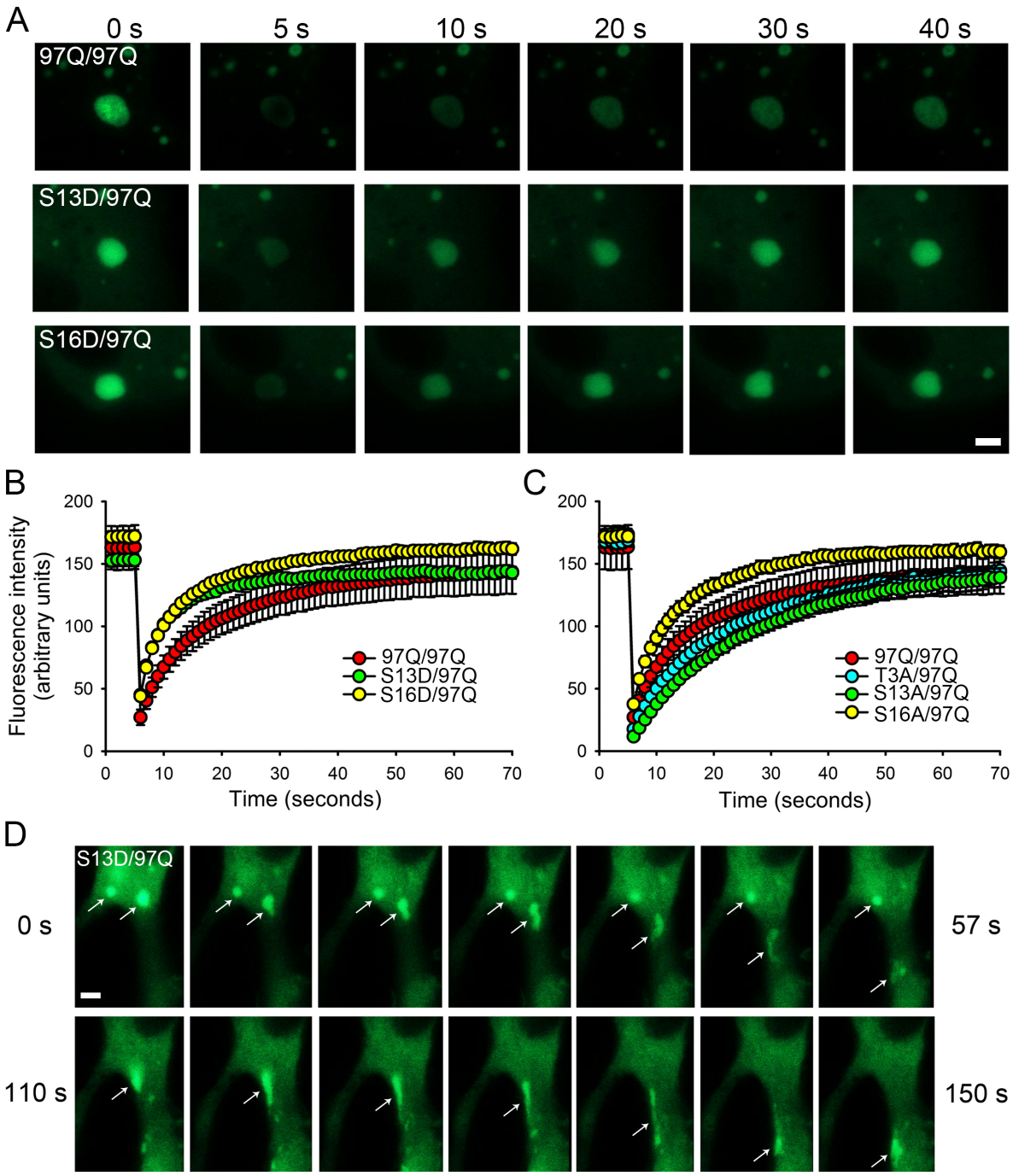

Figure 14. Phosphomimic-containing inclusions of 97QHTTex1 are more dynamic. (A) Time lapse of FRAP experiments on aggregates containing non-mutated 97QHTTex1 alone or in combination with phosphomimic mutant in H4 glioma cells. T3D mutants produced no aggregates under any circumstance. (B) Aggregates containing S13D or S16D mutants recovered significantly faster than the non-mutated 97QHTTex1 pair. (C) Aggregates combining non-mutated 97QHTTex1 with T3A or S13A recovered more slowly than aggregates made only of non-mutated 97QHTTex1, with the exception of the S16A/97Q combination. (D) Time lapse of aggregates formed by non-mutated 97QHTTex1 and S13D. Aggregates containing phosphomimic versions are highly dynamic and flexible, and move (arrow indicates moving aggregate in each frame) through the cell with more freedom than aggregates formed by non-mutated 97QHTTex1 pair (data not shown). Scale bars, 20 μm.

N-terminal phosphorylation modulates mutant huntingtin aggregation in Drosophila

To further explore the role of N17 phosphorylation on HTTex1 aggregation, we tested how single phosphoresistant or phosphomimic mutants modulate the formation of inclusion bodies in *Drosophila*. We generated flies expressing either wild-type (19Q), non-mutated (97Q) control or different phosphomutant versions of 97QHTTex1 fused to mCherry in adult dopaminergic neurons, under the control of *THGAL4* (Figure 15A-G), or in larval imaginal discs using the eye-specific *GMRGAL4* driver (Figure S6, Supplemental information). Wild-type 19QHTTex1-mCherry produced a diffuse pattern of distribution in both larval eye imaginal discs (Figure S6A, Supplemental information) and adult dopaminergic neurons (data not shown), indicating the presence of soluble oligomeric species. On the other hand, Non-mutated 97QHTTex1-mCherry accumulated mostly as large inclusion bodies, showing a high number of inclusions in both larval and fly tissues (Figure 15A and Figure S6B, Supplemental information I). This is consistent with our results in human cell lines. Surprisingly, all phosphomutants produced inclusion bodies that varied substantially in their number, morphology and localization, depending on tissue specificity. In the larval eye imaginal discs, all phosphomutants showed fewer inclusion bodies than non-mutated 97QHTTex1 (Figure S6, Supplemental information I), with the exception of S13D mutant that increased aggregation (Figure S6F and I, Supplemental information I). In adult dopaminergic neurons, both T3A (Figure 15B) and T3D (Figure 15E) mutants generated lower number of inclusions versus non-mutated 97QHTTex1 (Figure 15O), which was also accompanied by wider expression of intermediate species. In contrast, S13D (Figure 15F) and S16D (Figure 15G) showed a significantly higher number of aggregates (Figure 15O), with S13D also displaying larger inclusions in comparison to those formed by the non-mutated counterpart. Inclusions formed by S16D mutant were also localized in cell nuclei, in agreement with previous studies suggesting that S16 phosphorylation promotes nuclear translocation of HTTex1 (Atwal *et al*., 2011, Havel *et al*., 2011). S13A (Figure 15C) and S16A (Figure 15D) mutants produced as many inclusions as non-mutated 97QHTTex1 (Figure 15O).

Together with our results in cells, these findings further indicate that single N17 phosphorylation modulates 97QHTTex1 aggregation, although the final outcome can depend on the biological context.

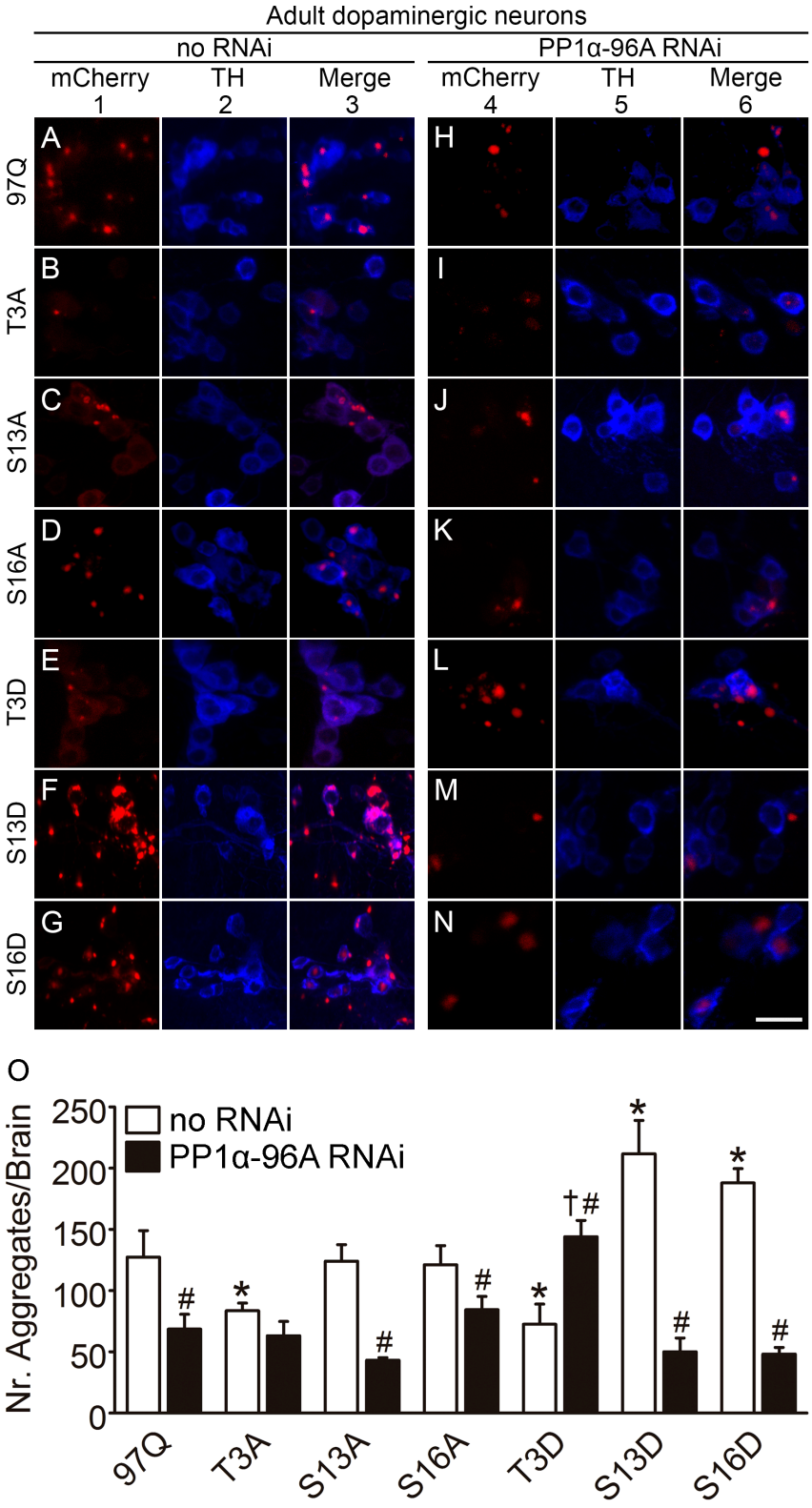

Figure 15. PP1 knockdown prevents 97QHTTex1 aggregation in *Drosophila*. Confocal microscopy images of dopaminergic neurons in adult *Drosophila* brains expressing non-mutated 97QHTTex1-mCherry or the different phosphomutants (A-G) under the control of *THGAL4*. (H-N) Co-expression of *PP1α-96A* RNAi with non-mutated 97QHTTex1-mCherry or phosphomutants. 97HTTex1-mCherry is shown in red (column 1 and 4), and dopaminergic cells (column 2 and 5, anti-TH) are shown in

blue. Any mutation at T3 residue prevented 97HTTex1 aggregation (B and E), while phosphomimic mutations at S13 or S16 produced a significant increase of 97HTTex1 inclusion bodies (F and G). *PP1α-96A* RNAi decreased the number of 97HTTex1 inclusions, with the exception of T3A (I), where no change was observed, and T3D (L) expressing flies that showed a significant increase in 97HTTex1 aggregation, all in comparison to the respective no RNAi expressing genotype. (O) Quantification of average number of aggregates (±SEM) in each brain. *significant versus THGAL4>UAS-97QHTTex1-mCherry, #significant versus the correspondent "no RNAi" transgenic control (white bars), †significant versus THGAL4>UAS-97QHTTex1-mCherry/UAS-*PP1α-96A* RNAi, $p<0.05$. Scale bar, 10 μm.

Protein phosphatase inhibitors regulate mutant huntingtin aggregation and toxicity

We next aimed at characterizing the molecular pathways involved in HTTex1 oligomerization, aggregation and toxicity. Others have identified several kinases that modulate N17 phosphorylation and hence HTTex1 aggregation and toxicity (Atwal *et al*., 2011, Bustamante *et al*., 2015, Thompson *et al*., 2009). However, the protein phosphatases that could be involved in these processes remain unknown. To address this question, we screened a library of 33 phosphatase chemical inhibitors in our BiFC cellular model for their effect on 97QHTTex1 aggregation and oligomerization, by means of filter trap assays and flow cytometry, respectively (Figure 16 and Table S1, Supplemental information I). We identified three groups of phosphatases (PP1/PP2A, CD45 and Cdc25) which inhibition decreased 97QHTTex1 aggregation in human cells when compared to controls treated with DMSO (Figure 16A, B01, B02, B07, B08, C04 and C05). Furthermore, these compounds were validated by fluorescence microscopy analyses, where a consistent decrease in the number of cells forming inclusions was observed (Figure 16B). Interestingly, cells treated with the three selected inhibitors also showed a slight reduction in average fluorescence, indicating a decrease towards the production of oligomeric species, although the formation of large aggregates was affected to a greater degree (Figure 16A, B01, B02, B07, B08 and C04). We also observed an overall reduction in fluorescence levels for 28 out of the 33 inhibitors assayed. However, the few exceptions where a striking decrease was observed (C06, D01 and D03) were due to a reduction in HTTex1 expression or toxicity of the compound (Table S1 and Figure S7, Supplemental information I). CD45 inhibitors resulted in decreased levels of HTTex1 expression and were lately excluded from our study. PP1/PP2A and Cdc25 inhibitors did not decrease cell viability or HTTex1 protein levels (Table S1 and Figure S7, Supplemental information I).

To further characterize PP1/PP2A and Cdc25 inhibitors, we tested the effect of those compounds in adult compound eye of *Drosophila* expressing pan-neuronally

93QHTTex1 under the control of elavGAL4. The *Drosophila* eye is composed by photoreceptor neurons, known as rhabdomeres, which are regularly arranged in clusters of eight to form highly organized individual structures called ommatidia. Seven rhabdomeres per ommatidia are visible in cross-section, and can then be scored using the light microscopy-based pseudopupil assay (Green and Giorgini, 2012). We assessed neurodegeneration of treated or non-treated HD flies, by scoring degeneration of rhabdomeres (Figure 16C). When expressed in the fly nervous system, 93QHTTex1 causes progressive photoreceptor loss. Interestingly, while Cdc25 inhibition enhanced neurodegeneration in our *Drosophila* HD model, PP1/PP2A inhibitor treatment ameliorated 93QHTTex1 neurotoxicity in a dose-dependent manner, being able to completely reversed this phenotype (Figure 16C, 93QHTTex1 Day 7 treated with 100 μM of B02 compound versus 93QHTTex1 Day 0 non-treated). However, we also observed that treatment with PP1/PP2A inhibitors strongly compromised the survival of our HD flies (data not shown), so we cannot exclude the possibility of an artifact or compensatory mechanism responses.

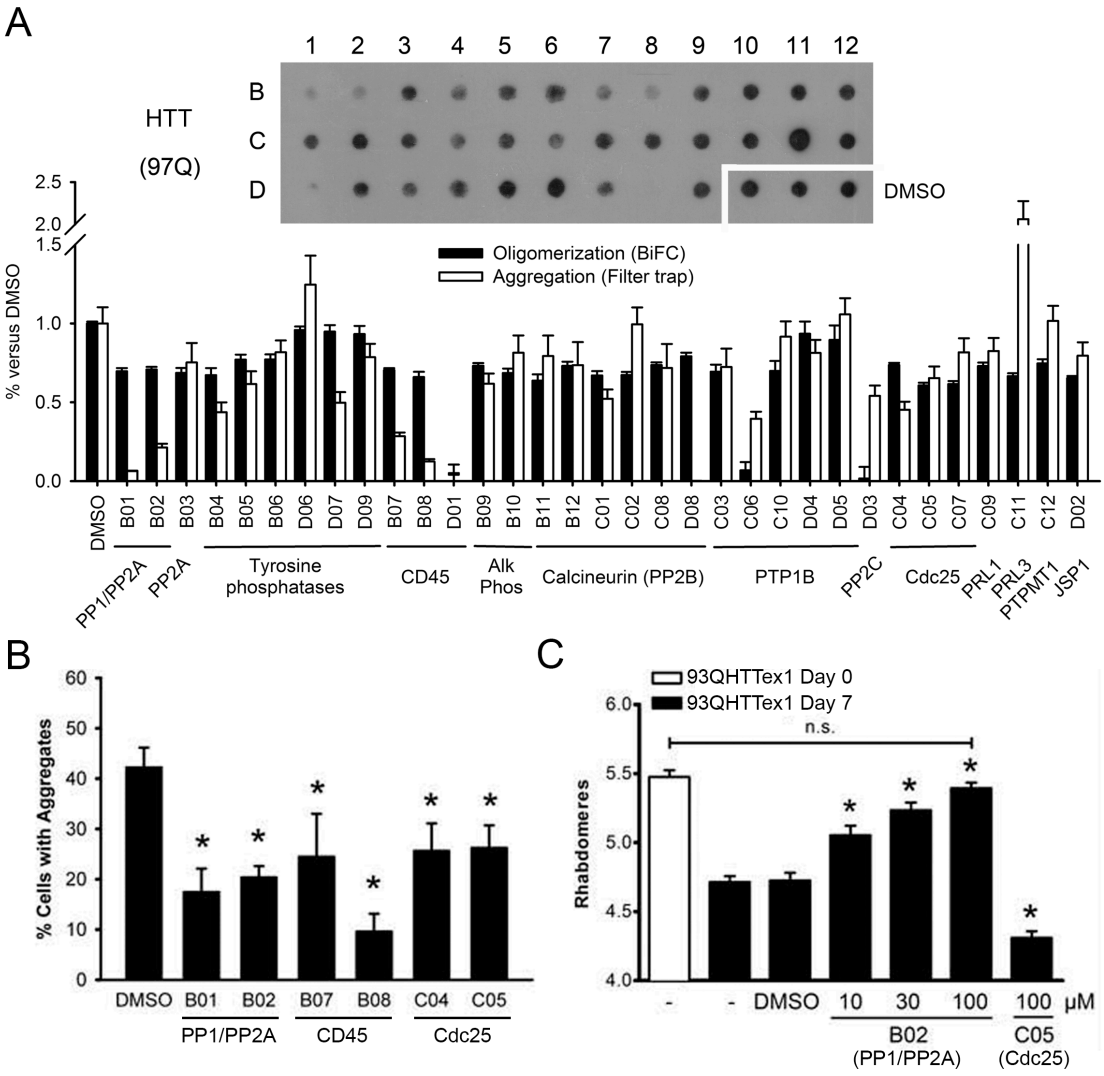

Figure 16. Protein phosphatase inhibitors regulate HTTex1 aggregation in human cells and neurotoxicity in *Drosophila*. (A) Representative filter trap of protein extracts from H4 cells transfected with non-mutated 97QHTTex1 BiFC constructs and treated with chemical inhibitors of protein phosphatases. The graph shows oligomerization levels as determined by flow cytometry (black bars) and aggregation levels as determined by optic density of filter trap dots (white bars). The names of phosphatase inhibitors (Enzo Life Sciences) and the concentrations used are described in Table S1. (B) Selected inhibitors PP1/PP2A (B01 and B02) and Cdc25 (C04 and C05) also reduced the percentage of H4 cells with large 97QHTTex1 inclusions as determined by quantitative analyses of microscopy pictures. (C) Quantification of mean rhabdomeres (±SEM) in adult flies expressing 93QHTTex1 pan-neuronally after 7 days of treatment with increasing concentrations of a PP1/PP2A inhibitor (B02) or with a single-dose of 100 µM of a Cdc25 inhibitor (C05). PP1/PP2A inhibition prevented HTTex1 neurotoxicity in a dose-response manner, while Cdc25 inhibition potentiated neuronal loss as it decreased the number of rhabdomeres comparing to 93QHTTex1 flies treated with DMSO. *significant versus DMSO treated flies, $p<0.05$; n.s., not significant.

Protein phosphatase 1 modulates mutant huntingtin aggregation and neurotoxicity in Drosophila

Next, we assessed whether genetic inhibition of the selected protein phosphatases regulate HTTex1 aggregation in *Drosophila*. We used an RNAi knockdown approach to downregulate homologues of PP1, PP2A or Cdc25 in flies expressing 97QHTTex1-mCherry in dopaminergic neurons (Figure 15, columns 4-6, and Figure S8, Supplemental information I). Downregulation of *string,* the fly homologue for Cdc25, or PP2A had no effect on 97QHTTex1 aggregation (Figure S8, Supplemental information I), while PP1 knockdown flies (Figure 15H and O) showed significantly fewer aggregates per brain when compared to 97QHTTex1 no RNAi control (Figure 15A and O). In order to exclude the possibility that suppression of aggregation upon PP1 silencing was due to titration of GAL4/UAS activity, we compared single UAS-97QHTTex1-mCherry expressing flies versus flies carrying double UAS constructs. As expected, the titration control expressing both UAS-97QHTTex1-mCherry and UAS-*lacZ* constructs displayed similar aggregation phenotype to single UAS-97QHTTex1-mCherry expressing flies (Figure S9, Supplemental information I). Strikingly, PP1 downregulation in phosphomutant backgrounds (Figure 15J, K, M and N) also resulted in decreased 97QHTTex1 aggregation, with the exception of T3A (Figure 15I) and T3D (Figure 15L). When co-expressed with T3A, PP1 RNAi did not cause significant changes in the number of aggregates (Figure 15O), which could indicate that PP1 modulates HTTex1 aggregation by targeting T3 dephosphorylation. On the other hand, PP1 knockdown increased aggregation in T3D mutants relative to its no RNAi counterpart. Interestingly, the aggregation levels observed in T3D background upon PP1 inhibition were also significantly higher than those seen in PP1 knockdown brains expressing non-mutated 97QHTTex1. Since HTTex1 does not contain any phosphorylatable residue beyond N17 domain, these results denote a potential cumulative effect of PP1 RNAi on 97QHTTex1 aggregation concomitant with S13 and/or S16 phosphorylation.

We further explored the effects of PP1 silencing in our *Drosophila* model by assaying neurodegeneration of photoreceptor neurons in living animals (Figure 17). Importantly, genetic inhibition of PP1 did not compromise rhabdomere viability in flies expressing wild-type (19Q) HTTex1 under the control of Rh1GAL4 (Figure 17A, column 4 and D), but significantly enhanced 97QHTTex1 neurotoxicity, further reducing the number of rhabdomeres in an age-dependent manner (Figure 17A-C, column 5 and D). This is consistent with the toxicity of PP1 pharmacological inhibitors that we observed in

flies. PP2A or *string* RNAi had no effect in the number of rhabdomeres upon co-expression with either 19QHTTex1 or 97QHTTex1 (Figure S8, Supplemental information I).

In total, our data suggest that PP1 has a role in modulating the formation of HTTex1 aggregates in both cell and *Drosophila* models of HD, which may be mostly mediated by T3 phosphorylation state. Furthermore, PP1 seems to regulate *Drosophila* neuronal loss but only in a disease context, suggesting that 97QHTTex1 aggregation and neurotoxicity may be related in our HD fly model.

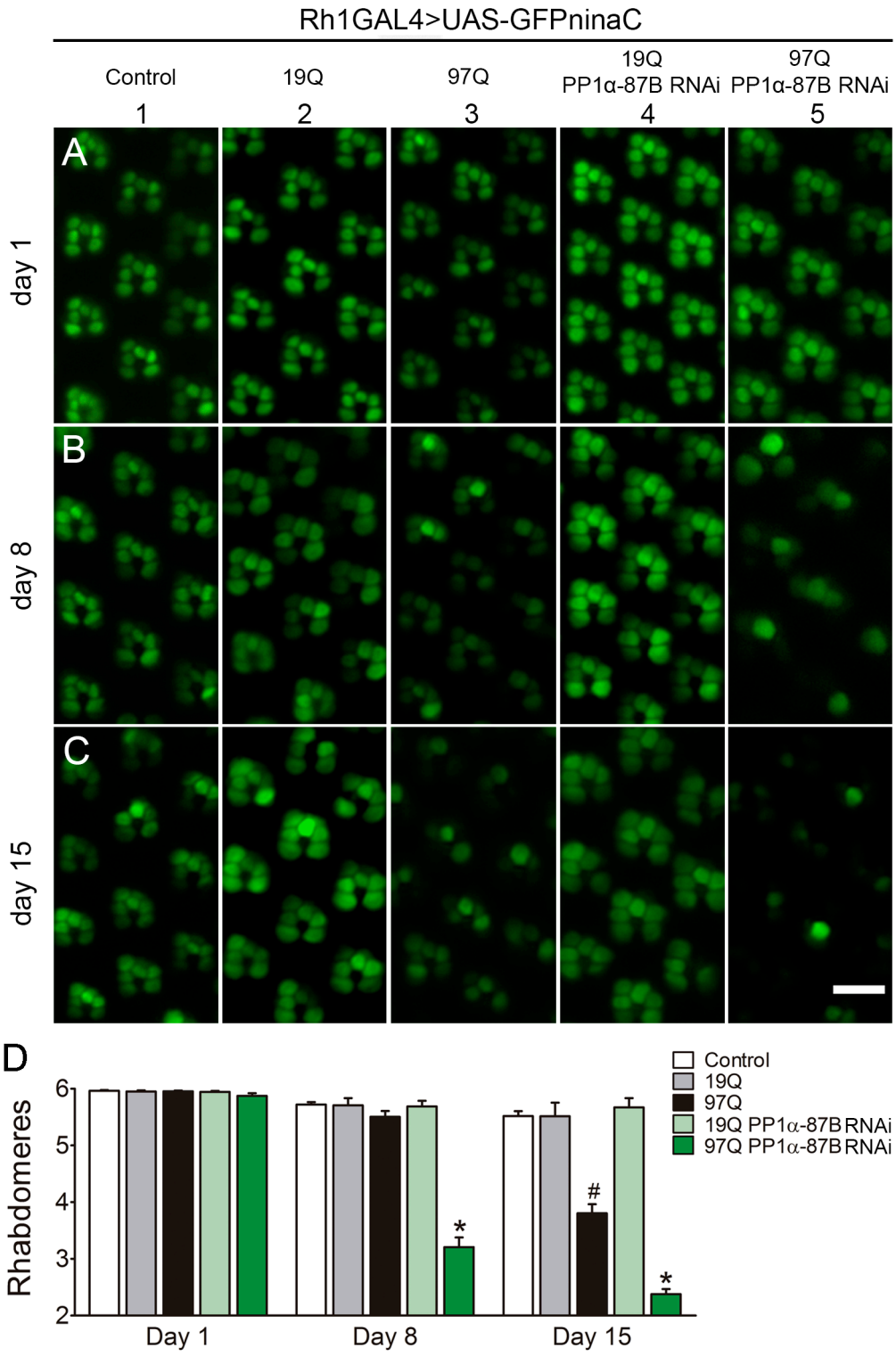

Figure 17. Downregulation of PP1 potentiates 97QHTTex1 neurotoxicity in adult photoreceptor neurons. (A-C) Representative pictures of photoreceptors observed by water immersion live imaging of the retinas. Wild-type flies, HD flies and flies expressing *PP1α-87B* RNAi together with 19QHTTex1 or 97QHTTex1 were analyzed at day 1, 8 and 15 post-eclosion. Wild-type and 19QHTTex1 expressing flies showed normal retinal morphology as the 6 outer photoreceptors were visible per ommatidium (columns 1 and 2). Flies expressing 97QHTTex1 exhibited age-dependent neurodegeneration

with progressive loss of rhabdomeres from 8 to 15 days after eclosion (B and C, column 3). *PP1α-87B* downregulation caused increased neurotoxicity in flies expressing 97QHTTex1 (B and C, column 5) and did not affect photoreceptor integrity of 19QHTTex1 flies (column 4). Visualization of the rhabdomeres was performed using Rh1Gal4>UAS-GFP^{ninaC}, as described in methods section. (D) Quantification of mean rhabdomeres (±SEM) per ommatidium. *significant versus Rh1GAL4>UAS-GFP^{ninaC}/UAS-97QHTTex1-mCherry, #significant versus Rh1GAL4>UAS-GFP^{ninaC}/UAS-97QHTTex1-mCherry at day 1 and day 8, $p<0.05$. Scale bar, 10 μm.

Discussion

Protein misfolding and aggregation are intimately involved in the pathogenesis of HD and other neurodegenerative disorders. Despite extensive research in the field, the precise molecular mechanisms by which misfolded proteins aggregate and form toxic species remain elusive. Increasing evidence suggests that targeting phosphorylation events in the N17 domain of mutant HTT can influence the pathological behavior of the protein (Atwal *et al*., 2011, Di Pardo *et al*., 2012, Havel *et al*., 2011, Khoshnan *et al*., 2004, Thompson *et al*., 2009). However, the significance of single N17 phosphorylation events in HTT oligomerization, aggregation and toxicity is still poorly understood.

Here, we report that single N17 phosphorylation can prevent HTTex1 aggregation, but not oligomerization. We propose that each residue has a different "strength" in modulating HTTex1 aggregation. Importantly, we found that PP1 can control HTTex1 aggregation and toxicity, suggesting that N17 phosphorylation might be regulated by this protein phosphatase. The fact that single N17 phosphorylation events are sufficient to abolish HTTex1 aggregation could be very important from an HD therapeutic perspective, since a single N17 phosphorylation could provide a simpler molecular target than double phosphorylation.

We showed that single phosphomimic mutations at T3, S13 or S16 allow 97QHTTex1 to oligomerize but not to form large inclusions in human cells (Figure 12 and Figure S2, Supplemental information I). Double S13/S16 phosphorylation prevents aggregation both *in vitro* and *in vivo*, and toxicity *in vivo* (Gu *et al*., 2015, Mishra *et al*., 2012). However, double S13/S16 phosphorylation is less abundant than single phosphorylation events (Bustamante *et al*., 2015), and may require the overexpression of specific kinases (Thompson *et al*., 2009), which may confound therapeutic efforts based on this approach. Although some studies reported on the effect of single S13 or S16

phosphorylation events on HTTex1 intracellular localization, they did not focus on HTTex1 oligomerization, aggregation or toxicity (Atwal *et al*., 2011, Havel *et al*., 2011). Results from cell-free systems indicate that single S13- or S16-phosphorylated HTTex1 behave similarly to double S13/S16-phosphorylated HTTex1 in terms of aggregation, being unable to form mature fibrils (Mishra *et al*., 2012). Our findings in living human cells provide additional biological support for those *in vitro* studies.

The unique properties of our BiFC cellular model allowed us to analyze the relative contribution of each phosphorylatable residue towards HTTex1 oligomerization and aggregation. We found that T3D completely abolished 97QHTTex1 aggregation in the presence of any other phosphomutant or non-mutated 97QHTTex1 molecules, while S13D or S16D only had a partial reduction effect (Table III and Figure S3, Supplemental information I). Our results are consistent with a recent report showing that bona-fide T3 phosphorylation decreases the aggregation propensity of mutant HTT (Cariulo *et al*., 2017a). Interestingly, HD samples display low levels of T3 phosphorylation (Cariulo *et al*., 2017a), while higher abundance of T3-phosphorylated pools is detected in normal contexts (Bustamante *et al*., 2015, Huang *et al*., 2015). Altogether, these findings highlight the relevance of this residue in modulating the aggregation of HTTex1, and strongly support T3 as a promising target for HD intervention (Aiken *et al*., 2009). Our results also suggest that HTTex1 might be predominantly unphosphorylated under pathological conditions (Aiken *et al*., 2009, Atwal *et al*., 2011), as phosphoresistant combinations behave more similarly to the non-mutated 97QHTTex1 pair than to the phosphomimics in terms of aggregation (Figure 12 and Table III).

Previous *in vitro* studies demonstrate that N17 phosphorylation inhibits β-sheet conformation of mutant HTTex1 and suppresses its fibrillization, stabilizing the α-helical structure of the N17 domain which could lead to altered aggregation dynamics (Caron *et al*., 2013, Chiki *et al*., 2017). In FRAP experiments, we show that combinations of phosphomimic and non-mutated 97QHTTex1 induced the formation of inclusions that were more dynamic, diffuse and fluid than regular 97QHTTex1 aggregates, resembling an intermediate stage between oligomers and mature inclusions (Figure 14). Additionally, non-mutated 97QHTTex1 pairs did not aggregate to the same extent as the phosphoresistant combinations (Figure 12C and Table III). Thus, we propose a model where unphosphorylated HTTex1 fragments oligomerize and form inclusions that grow into mature fibrils until enough phosphorylated HTTex1 molecules are intercalated in the

structure to interfere with the process, acting as a 'brake'. This could explain the existence of aggregates of various sizes and morphologies.

Genetic and pharmacological inhibition of PP1 resulted in lower 97QHTTex1 aggregation and increased toxicity (Figure 15-17). Protein phosphatases PP2B/3 (Calcineurin), PP2C and PP1/PP2A have been also shown to regulate HTT phosphorylation at several residues beyond exon 1, as well as HTT toxicity (Ermak *et al*., 2009, Marion *et al*., 2014, Pardo *et al*., 2006, Pineda *et al*., 2009, Rosenstock *et al*., 2011). It is important to note that HTTex1 does not contain any phosphorylatable residue beyond the N17 domain and, therefore, any direct effect of protein phosphatases should happen on T3, S13 or S16. Our results indicate that PP1 affects 97QHTTex1 aggregation by regulating T3 phosphorylation. In *Drosophila* dopaminergic neurons, PP1 knockdown in serine-phosphomutant backgrounds leads to a decrease in 97QHTTex1 aggregation, regardless the type of mutation – phosphomimic or phosphoresistant - on these residues (Figure 15O). Moreover, PP1 RNAi does not cause any further reduction of 97QHTTex1 aggregation when co-expressed with T3A mutant. Together, these data suggest that the effect of PP1 inhibition on HTTex1 aggregation is primarily mediated by T3 phosphorylation. However, an increase in 97QHTTex1 aggregation is observed when PP1 RNAi is co-expressed with T3D mutant (Figure 15L and O), indicating that S13 and S16 might also be target for PP1 regulation. Since S13D or S16D increase 97QHTTex1 aggregation (Figure 15F, G and O), we hypothesize that PP1 modulates S13 or S16 phosphorylation upon T3 phosphorylation. In fact, it is likely that different N17 mutations may contribute to subsequent phosphorylation events in other residues. For example, IKK-mediated S16 phosphorylation is facilitated by previous phosphorylation of S13 (Thompson *et al*., 2009), and we have observed that phosphomimic T3D mutation completely blocks S13/S16 phosphoryation.

Interestingly, the striking decrease in 97QHTTex1 aggregation observed when PP1 RNAi was co-expressed with S13D or S16D mutants versus S13D or S16D alone (no RNAi) (Figure 15O) suggests that T3 phosphorylation is dominant over S13 or S16 phosphorylation. Our human cell data also supports this hypothesis, since S13D or S16D BiFC combinations with non-mutated 97QHTTex1 still shows aggregates, while T3D BiFC combinations with any other mutant completely abolishes aggregation (Table III and Figure S3, Supplemental information I).

Huntingtin N17 phosphorylation modulates neurotoxicity in several HD models by preventing HTT aggregation (Gu *et al*., 2009). However, this finding is still under intense

debate (Aiken *et al*., 2009, Atwal *et al*., 2011, Thompson *et al*., 2009). Currently, there is still debate on whether large, insoluble aggregates are the cause of neuropathology or a by-product of accumulated misfolded HTT. Though these aggregates were originally thought to be neurotoxic, accumulating evidence suggests that the formation of large aggregates might be part of a protective cellular mechanism to sequester soluble toxic species (Arrasate *et al*., 2004, Bodner *et al*., 2006, Kuemmerle *et al*., 1999, Slow *et al*., 2005). Our data here suggest that modulation of HTTex1 neurotoxicity by N17 phosphorylation and the appearance of large aggregates are not necessarily related. Interestingly, polyQ-dependent toxicity varies widely depending on the cellular environment and cell-type specificity, indicating that additional factors may contribute to HTTex1 toxicity (Tsvetkov *et al*., 2013). Moreover, studies on other post-translational modifications in the N17 region reveal a complex cross-talk among them in modulating aggregation, and suggest that neurotoxicity may be due to different mechanisms dependent upon the modifier site (Steffan *et al*., 2004, Thompson *et al*., 2009).

Altered PP1 activity has been linked to a variety of diseases, including several neurodegenerative disorders, such as AD and PD (Braithwaite *et al*., 2012, Gong *et al*., 1995, Lobbestael *et al*., 2013). In fact, PP1 is normally highly expressed in the brain, and is particularly abundant in medium spiny neurons, known to be significantly affected in HD (da Cruz e Silva *et al*., 1995b). Based on these findings, it is possible that PP1 malfunction increases the susceptibility of certain types of neurons to mutant HTTex1-induced degeneration. Not surprisingly, inhibition of PP1 resulted in increased age-dependent neuronal loss in our *Drosophila* HD model, suggesting that PP1 activity imbalance might precede HTTex1 neurotoxicity. Despite considerable efforts to develop specific chemical activators of PP1 (Chatterjee *et al*., 2012, Tappan and Chamberlin, 2008), further investigations will be necessary to clarify the relationship between PP1 activity impairment, aggregation and neurotoxicity in the context of HD and other polyQ misfolding disorders.

In summary, our results support a strong role for single N17 phosphorylation events on HTTex1 aggregation, dynamics and toxicity, and uncover the regulatory role of PP1 in these events. Ultimately, our study opens novel avenues for the therapeutic targeting of PP1 and N17 phosphorylation in HD.

Materials and methods I

In vitro experiments

Cell cultures, plasmids and treatments

Human H4 glioma cells (ATCC HTB-148, LGC Standards, Barcelona, Spain) were maintained in OPTI-MEM I culture medium (Gibco, TermoFisher Scientific, Carlsbad, CA, USA) supplemented with 10% (v/v) Fetal Bovine Serum (FBS) and 1% (w/v) of a penicillin/streptomycin commercial antibiotic mixture (Gibco, TermoFisher Scientific, Carlsbad, CA, USA), under controlled conditions of temperature and humidity (37ºC, 5% CO_2). Different types of cell culture dishes were used for cell seeding depending on the application. For flow cytometry and toxicity assays, cells were grown on 6-well plates (35 mm diameter, Techno Plastic Cultures AG, Switzerland). For microscopy, cells were seeded on glass-bottom 35 mm dishes (10 mm glass surface diameter, MatTek Corporation, Ashland, MA, USA). And for protein extraction (PAGE and filter trap assays) cells were seeded on 100 mm dishes (Techno Plastic Cultures AG, Switzerland). For all experiments, cells were counted and seeded at a density of 10,000 cells/cm^2 regardless dish size. Generation of 19QHTTex1- and 97QHTTex1-Venus BiFC constructs was described elsewhere (Herrera *et al*., 2011). Phosphomimic (T3, S13 or S16 mutated to Aspartic acid) and phosphoresistant (T3, S13 or S16 mutated to Alanine) constructs were produced by PCR-based site-directed mutagenesis using 97QHTTex1-Venus plasmids as templates. Plasmid transfection was performed by means of the X-tremeGene 9 reagent (Roche diagnostics, Mannheim, Germany), following manufacturer's instructions. Twenty-four hours after transfection, cells were collected and analyzed for oligomerization, aggregation and toxicity as described below. Pharmacological inhibition of protein phosphatases was performed using a phosphatase inhibitor library (Enzo Life Sciences, Lausen, Switzerland). Briefly, cells were treated with 33 different phosphatase inhibitors upon transfection of 97QHTTex1 BiFC constructs. Phosphatase inhibitors were dissolved in DMSO and added to culture medium at variable concentrations, according to the IC50s described in manufacturer's instructions (Table S1, Supplemental information I).

Flow cytometry

Transfection efficiency and fluorescence levels were determined by flow cytometry analyses. Cells were washed with Ca^{2+} and Mg^{2+} free phosphate buffer saline (PBS)

(Gibco, TermoFisher Scientific, Carlsbad, CA, USA) and collected by trypsinization (0.05% w/v trypsin, 5 min, 37ºC) into BD Falcon Round-Bottom tubes (BD Biosciences, San Jose, CA, USA). Cell pellets were resuspended in PBS and analyzed by means of a LSR Fortessa flow cytometer (Beckton Dickinson, Franklin Lakes, NJ, USA). Ten thousand cells were examined per experimental group. The FlowJo software (Tree Star Inc., Ashland, OR, USA) was used for data analysis and representation.

Fluorescence microscopy and FRAP experiments

The visualization of intracellular BiFC fluorescent aggregates was accessed in living cell cultures using an Axiovert 200M widefield fluorescence microscope equipped with a CCD camera (Carl Zeiss MicroImaging GmbH, Germany). Pictures of a total of 100-150 cells per sample were scored for aggregate quantification. FRAP experiments were performed using a META LSM 510 confocal microscope. Briefly, protein aggregates were focused at the central focal plane and adjusted to avoid pixel saturation. Experiments lasted for 70-150 s, taking one picture every second. After establishing the basal signal, aggregates were bleached using the 488 nm laser line at 100% laser transmission on a circular region of interest (ROI) with a diameter of 30 pixels (1.31 μm radius) for 5 s (10 iterations). Fluorescence recovery was then monitored for 60-140 s with LSM software. Data analyses were carried out using the ImageJ free software (http://rsbweb.nih.gov/ij/).

Protein extraction and Immunoblotting

Total protein levels and formation of oligomeric species were measured by means of SDS- or Native-PAGE immunoblotting, respectively. Proteins were extracted in native or denaturing conditions according to the requirements of each technique. Briefly, cells were washed with PBS 1X and collected by scraping. Cells were incubated with lysis buffer and sonicated for 10 sec at 5 mA using a Soniprep 150 sonicator (Albra, Milano, Italy). For denaturalizing conditions, the lysis buffer was 1% Triton X-100, 150 mM NaCl, 50 mM Tris pH 7.4, supplemented with a protease inhibitor cocktail (Roche diagnostics, Mannheim, Germany). For native conditions, the lysis buffer was 173 mM NaCl, 50 mM Tris pH 7.4, 5 mM EDTA, also supplemented with protease inhibitor cocktail. Proteins were collected after cell lysate centrifugation at 10,000xg for 10 min at 4ºC and quantified by means of the BCA Protein Assay Kit (ThermoFisher Scientific, Waltham, MA, USA), following manufacturer's instructions. For SDS- or Native-PAGE immunoblotting, 15 µg of total protein extracts were prepared and separated by electrophoresis using a 12% SDS-

polyacrylamide gel or a 5% SDS-free-polyacrylamide gel, respectively. For denaturing conditions, samples were boiled in standard loading buffer (200 mM Tris-HCl pH 6.8, 8% SDS, 40% glycerol, 6.3% β-mercaptoethanol, 0.4% bromophenol blue) for 5 min at 95ºC. For native conditions, extracts were mixed with SDS- and mercaptoethanol free loading buffer (200 mM Tris-HCl pH 6.8; 40% glycerol; 0.4% bromophenol blue) and the boiling step was omitted. Proteins were transferred onto PVDF membranes and blocked with 5% (w/v) non-fat dry milk in Tris-HCl buffer saline-Tween solution (TBS-T) (150 mM NaCl, 50 mM Tris pH 7.4, 0.5% Tween-20) for 1 h at room temperature. Membranes were incubated with primary antibodies against HTT (1:500, Millipore, Billerica, MA, USA) and GAPDH (1:30000, Ambion, Austin, TX, USA) as specified. A secondary mouse IgG Horseradish Peroxidase-linked antibody (1:10000, GE Healthcare Life Sciences, Uppsala, Sweden) was used for 1 h incubation at room temperature. Immunoblots were developed with enhanced chemiluminescence reagents (Millipore, Billerica, MA, USA) and exposed to X-ray films. The relative intensities of protein bands were measured using the Image J software. Protein expression levels were calculated by densitometry analyses and normalized to the GAPDH loading control.

Filter trap assays

Cells were pelleted by centrifugation at 700xg for 10 min and cell lysates collected in native conditions as described above. One hundred μg of native protein extracts were mixed with SDS to a final concentration of 0.4% (w/v). Samples were loaded on a dot-blotting device and filtered by vacuum through cellulose acetate membranes (0.22 μm pore; GE Water & Process Technologies, Fairfield, CT, USA), previously incubated with 1% (w/v) SDS solution in PBS. After filtration, membranes were washed twice and processed for immublotting detection of HTT, as described above. In these conditions, only large SDS-insoluble aggregates are retained in the filter and therefore HTT signal is proportional to the presence of large insoluble species. Analyses and quantification of blots signal were performed using ImageJ software.

Toxicity assays

Cell toxicity was assayed by measuring the release of lactate dehydrogenase (LDH) from damaged cells into extracellular medium using the LDH Cytotoxicity Detection Kit (Clontech Laboratories Inc., Mountain View, CA, USA), following manufacturer's instructions. Briefly, 5 μl of cell culture medium was collected and extracellular levels of

LDH measured at 492 nm using an Infinite M200 plate reader (Tecan, Männedorf, Switzerland). For statistical analysis, absorbance values were obtained in triplicate for all the different experimental groups and normalized versus the 19Q/19Q control.

Drosophila **experiments**

Drosophila stocks, genetics and crosses

Flies were maintained at 25ºC and raised on standard cornmeal medium in a light/dark cycle of 12 hours. We generated eight constructs encoding for different versions of HTTex1 fused to mCherry: a wild-type version with a polyQ tail containing 19 glutamines, a mutant version with 97 glutamines, and six constructs encoding phosphomutant versions (T3A/D, S13A/D and S16A/D) with 97 glutamines. To establish transgenic UAS-HTTex1-mCherry lines, our constructs were cloned into pWalium10-roe by the Gateway cloning technology (ThermoFisher Scientific, Waltham, MA, USA), and then injected into y^1w^{1118} embryos using phiC31 integrase-mediated DNA recombination (BestGene strain #9723, attP landing site located at the 2L-28E7 genomic region). The UAS-93QHTTex1 line (P463) was a gift from J. Lawrence Marsh and Leslie Thompson (University of California, Irvine) (Steffan *et al*., 2001). For genetic knockdown experiments in *Drosophila,* we employed UAS-RNAi-targeted lines of four different fly genes encoding specific phosphatases: *string* (homolog of cdc25 phosphatase, BL34831, HMS00146), *PP1α -87B* (alpha-2 isoform of PP1 catalytic subunit, BL32414, HMS00409), *PP1α-96A* (alpha-1 isoform of PP1 catalytic subunit, BL42641, HMS02477) and *PP2A-29B* (different isoforms of PP2A regulatory subunit, BL43283, HMS01921). RNAi stocks were obtained from the TRiP (Transgenic RNAi Project) library (Ni *et al*., 2011, Perkins *et al*., 2015), courtesy of the Bloomington *Drosophila* Stock Center (Indiana University, Bloomington, IN, USA). TRiP transgenic fly strains were generated by phiC31-targeted site-specific integration of shRNA Valium20 vectors at genomic attP40 or attP2 landing sites on the second and third chromosomes, respectively (strain BL42641, attp40 (2L-25C6); strains BL34831, BL32414 and BL43283, attP2 (3L-68A4)). Four different driver lines were used: *THGAL4* (active in DA neurons, under the control of the tyrosine hydroxylase promoter), elavGAL4 (c155) (transiently active in the nervous system), *GMRGAL4* (active in the eye) and *Rh1GAL4* (active in the photoreceptors R1-R6, under the control of rhodopsin1 promoter). To analyze the effect RNAi downregulation of specific phosphatases upon HTTex1 aggregation in adult brains, UAS-97QHTTex1-mCherry/CyO;Sb/TM6B and Sco/CyO;THGAL4/TM6B were established and crossed

together to generate UAS-97QHTTex1-mCherry/CyO;THGAL4/TM6B progeny, then crossed with UAS-RNAi-targeted lines. Adult flies carrying UAS-97QHTTex1-mCherry/+;THGAL4/UAS-*string*RNAi, UAS-97QHTTex1-mCherry/+;THGAL4/UAS-*PP1-87B*RNAi, UAS-97QHTTex1-mCherry/UAS-*PP1α-96A*;THGAL4/+ and UAS-97QHTTex1-mCherry/+;THGAL4/UAS-*PP2A-29B*RNAi were selected and analyzed (Figure 18A). Unless specified otherwise, flies carrying UAS-*lacZ* targeted to the same location were used as controls. For deep pseudopupil (DPP) analysis, Rh1GAL4;UAS-GFP^{ninaC}/UAS-19QHTTex1-mCherry;UAS-*PP1-87B*RNAi/+ and Rh1GAL4;UAS-GFP^{ninaC}/UAS-97QHTTex1-mCherry;UAS-*PP1-87B*RNAi/+ adult flies were obtained by crossing the Rh1GAL4;UAS-GFP^{ninaC} with UAS-19QHTTex1-mCherry/CyO;UAS-*PP1-87B*RNAi or UAS-97QHTTex1-mCherry/CyO;UAS-*PP1-87B*RNAi established stocks, respectively (Figure 18B). Rh1GAL4;UAS-GFP^{ninaC}, Rh1GAL4;UAS-GFP^{ninaC}/UAS-19QHTTex1-mCherry;UAS-GFP and Rh1GAL4;UAS-GFP^{ninaC}/UAS-97QHTTex1-mCherry;UAS-GFP were used as controls.

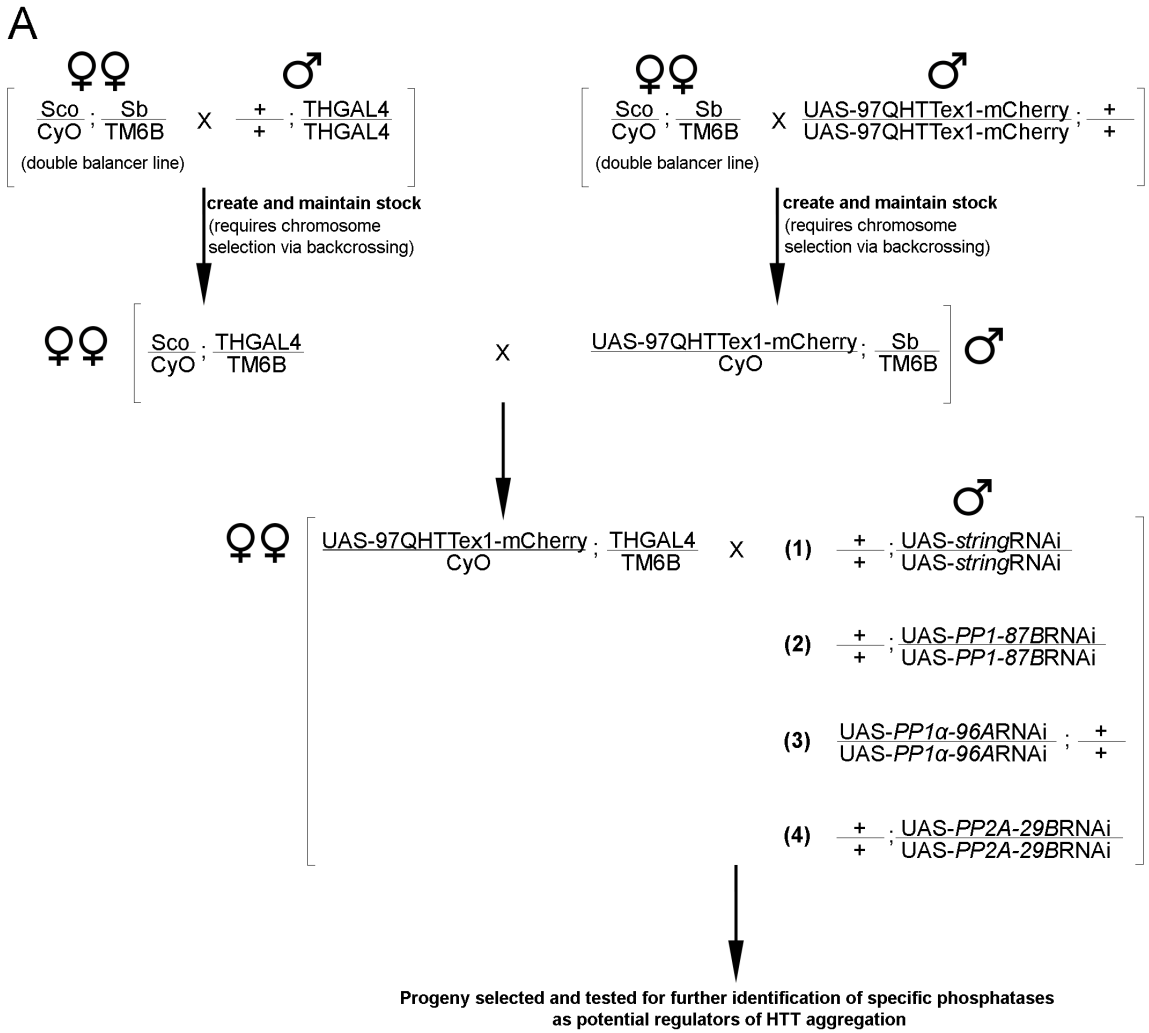

(Continue in the next page)

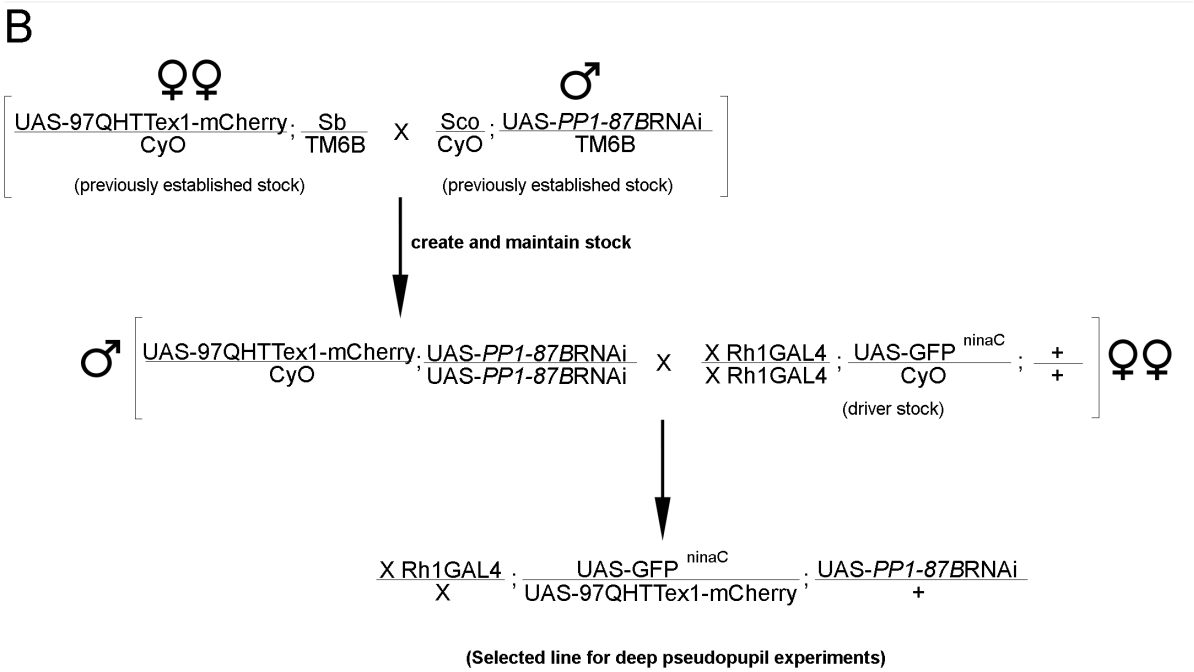

Figure 18. *Drosophila* crossing schemes for screen for phosphatases as regulators of mutant HTT aggregation and toxicity. (A) Female virgins from a double balancer stock are crossed to original TH driver and UAS-97QHTTex1-mCherry lines in order to establish balanced stocks of those lines. Balancing original lines is a common practice in *Drosophila* laboratories. The use of balancer chromosomes prevents crossing-over events during meiosis thereby allowing for the maintenance of mutant fly stocks without the risk of losing the transgene over time, through successive generations. Once established, flies from the two different stocks are crossed together to generate a final stock-expressing mutant HTT via the GAL4/UAS system. Virgins are then collected and used in a series of 4 independent crosses with UAS-RNAi targeted lines, ensuring the knockdown of a specific phosphatase in fly dopaminergic neurons where mutant HTT is being expressed. The effect of phosphatase knockdown on mutant HTT aggregation was evaluated by means of immunohistochemistry. (B) In this scheme, a stock carrying both mutant HTT and an RNAi-targeted phosphatase construct is established. Expression of both UAS-dependent transgenes is induced upon crossing with an *Rh1GAL4* driver carrying also a GFP^{ninaC} construct, which allows fluorescence visualization of rhabdomeres. Flies from the resulting F1 progeny expressing the three UAS-dependent transgenes are selected and subsequently used for deep pseudopupil analyses of rhabdomere loss. Sco (Scutoid), dominant marker manifested in a specific pattern of loss of bristles from the head and thorax of the adult fly. CyO (Curly "O", Oster 1956), second balancer chromosome carrying a dominant mutation, which causes curly wings. Sb (Stubble), dominant marker for shorter bristles. TM6B (Third multiply-inverted 6B), third balancer chromosome carrying the dominant mutation Tubby (Tb), which is manifested as physically shortened pupae and 3rd instar larvae phenotypes. X, chromosome X.

Immunohistochemistry and Confocal microscopy

For confocal imaging of adult brains, 10-days-old flies were dissected and brains prepared as previously described (Wu and Luo, 2006). Briefly, adult flies were

anesthetized with CO_2 and brains isolated in PBS 1X from the head cuticles before being fixed in 4% paraformaldehyde-containing PBS. Dopaminergic neurons were stained by incubation for 48 h at 4°C with mouse anti-TH antibody (1:100, Immunostar, Hudson, WI, USA) in PBST (1X PBS, 0.3% Triton X-100) containing 5% (v/v) normal goat serum. Samples were washed three times for 15 min in PBST. Mouse anti-Cy5 (1:200, Jackson ImmunoResearch, West Grove, PA, USA) was diluted in PBST with 5% (v/v) normal goat serum and used as secondary antibody by incubation for 24 h at 4ºC. For immunohistochemistry in larvae, eye imaginal discs of 3rd instar larvae were dissected in PBS 1X and fixed for 1 h in 4% paraformaldehyde as described elsewhere (Purves and Brachmann, 2007). Samples were then washed three times for 15 min in PBST and incubated overnight at 4ºC with rat anti-Elav antibody (1:100, Developmental Studies Hybridoma Bank, University of Iowa, USA). Imaginal discs were washed three times for 15 min in PBST and incubated for 2 h with rat anti-Cy5 secondary antibody (1:200, Jackson ImmunoResearch, West Grove, PA, USA). Finally, all samples were subjected to a last step of washing and mounted in 80% glycerol PBS solution, followed by confocal microscopy analysis. Z-stack images were acquired using a LSM 710 Meta Zeiss confocal microscope (resolution of 1024 × 1024, slice thickness of 1 μm, frame average of 2). Z-projections were generated and merged using ImageJ free software and images were prepared for publication on Adobe Photoshop CS6 (Adobe Systems Incorporated, San Jose, CA, USA). For quantification of aggregates, mCherry Z-stack images were analyzed by means of the Fiji software (Schindelin *et al*., 2012) and aggregation was measured using the 3D Objects Counter plugin (Bolte and Cordelieres, 2006). Briefly, the minimum threshold value was defined as 0.144 μm^3 to exclude signal from soluble HTT in the count. The volume (μm^3) occupied per each aggregate, the average number of aggregates and the corresponding standard deviations were calculated for at least 5 imaginal discs or adult brains per genotype.

Live Imaging of adult Drosophila eye

DPP analysis was performed in living animals as previously described (Pichaud and Desplan, 2001, Pocas *et al*., 2015). Briefly, flies at age of 1, 8 or 15 days were anaesthetized with CO_2 and then placed on a 50 mm petri dish, previously poured with 2% agarose at 40ºC. Once the agarose was solidified, the anesthetized flies were covered with cool water to keep anaesthetic conditions. Adult compound eye integrity of at least 5 flies per genotype was examined by fluorescence microscopy with a water immersion objective

(HC APO L40X/0.80W U-V-I, Leica Microsystems, Wetzlar, Germany). Images were obtained using a Leica DM5500 B microscope (Leica Microsystems, Wetzlar, Germany) and an Andor Luca R DL-604M camera (Andor Technology Ltd., Belfast, UK). For quantitative analysis, images were analyzed using Image J free software and number of fluorescing rhabdomeres was scored for >15 ommatidia per fly.

Phosphatase Inhibitors Treatment and Pseudopupil analysis

Adult flies expressing 93QHTTex1 in the nervous system were collected upon eclosion and transferred to fresh vials of food previously supplemented with different concentrations of a PP2A inhibitor (compound B2, Table S1, Supplemental information I) (10, 30 or 100 μM) or a Cdc25 inhibitor (compound C5, Table S1, Supplemental information I) (100 μM). Briefly, compounds were dissolved in DMSO (0.1% final) and added to standard maize media at required doses. Flies were introduced to the media after eclosion and moved daily onto new vials containing freshly made food with appropriate concentrations of the compound. Pseudopupil analysis was performed after 7 days of treatment with PP2A or Cdc25 inhibitors as previously described (Campesan *et al*., 2011). Newly emerged untreated flies (0 day-old) and 7 day-old untreated or 0.1% DMSO treated flies were also analyzed for changes in rhabdomere number. Briefly, fly heads were carefully removed and fixed to glass slides using fingernail polish and rhabdomeres were analyzed at 500x magnification using an Olympus BH2 microscope. The number of visible rhabdomeres was scored for >50 ommatidia per fly, and at least 15 flies were examined per condition.

Statistics

GraphPad Prism 5 (GraphPad Software Inc., La Jolla, CA, USA) or Sigmaplot software (Systat Software, Inc., San Jose, CA, USA) were used to perform the statistical analysis and graphical representation of data. *In vitro* results are shown as the average ± standard deviation (SD) of at least 3 independent experiments and *Drosophila* results as the average ± standard error (SEM), unless specified otherwise. Cell culture data was analyzed by means of a one-way ANOVA followed by a post-hoc Tukey test for average comparison. Aggregate quantification and pseudopupil assays in *Drosophila* were analyzed by means of a one-way ANOVA followed by a Student-Newman-Keuls post-hoc test. DPP assays were analyzed by means of a two-way ANOVA followed by a Bonferroni post-hoc test. Results were in all cases considered significant only when $p<0.05$.

Acknowledgements

We thank J. Lawrence Marsh and Leslie Thompson for the UAS-93QHTTex1 line. We are also grateful to the Bioimaging Unit from Instituto de Medicina Molecular and the Advance Imaging Unit from Gulbenkian Science Institute for support with imaging.

Contribution

JBS carried out the mutagenesis experiments and phosphomutant aggregation and toxicity studies in BiFC cellular model, the feeding experiments with phosphatase inhibitors in flies, the knockdown experiments in *Drosophila,* and all data analysis. FH performed the FRAP experiments and the screening with protein phosphatase inhibitors in mammalian cells. GMP, YPA and JBS generated and established the phosphomutant fly lines. JBS and YPA carried out the dissections, immunohistochemistry and confocal microscopy of larvae and adult phosphomutant samples. JBS and FH wrote the manuscript.

3.2. Glycation modulates mutant huntingtin toxicity in *Drosophila*

Abstract

Protein glycation is an age-dependent post-translational modification associated with several neurodegenerative disorders, including Alzheimer's and Parkinson's diseases. This non-enzymatic reaction occurring between reducing sugars and free amino-groups from proteins interferes with the folding and the aggregation process of proteins such as amyloid-beta and alpha-synuclein. As methylglyoxal (MGO) is the most important glycation agent, being present in all cell types, we asked whether MGO-mediated glycation might also play a role in huntingtin (HTT) biology, the causative protein in Huntington's disease (HD). We have previously observed that glycation increased the aggregation of mutant HTT exon 1 (HTTex1) fragments associated with HD, in yeast and mammalian cell models. Here, we studied the effect of glycation on mutant HTT neurotoxicity in fruit flies. Notably, treatment of flies expressing a mutant version of HTTex1 (93QHTTex1) with MGO enhanced neuronal loss in a dose-dependent manner. Furthermore, increased glycation levels resulted in compromised viability during both developmental and adult stages of the fruit fly, impairing eclosion and decreasing lifespan. Overall, our study provides evidence that glycation modulates mutant HTTex1-related toxicity, and suggests it may constitute a novel target for therapeutic intervention in HD.

Introduction

The formation of advanced glycation-end products (AGEs) has been implicated in several pathological conditions as well as in physiological aging. AGEs result from a non-enzymatic reaction between reducing sugars and proteins, named Maillard's reaction also known as glycation. This process is reported to have deleterious effects on proteins, being associated with loss of protein activity and aggregation (Kulkarni *et al*., 2013). Indeed, various proteins and enzymes of clinical significance are found to be glycated in patients, including those linked to neurodegenerative diseases such as Aβ, α-syn, Tau and prions (Vicente Miranda and Outeiro, 2010, Vicente Miranda *et al*., 2016a). In AD and PD, glycation interferes with normal biology of Aβ (Chen *et al*., 2006b, Li *et al*., 2013) and α-

syn (Vicente Miranda *et al*., 2017), respectively, leading to increased protein accumulation and concomitant cytotoxicity. Moreover, glycation could induce aberrant signaling via a specific membrane receptor for AGEs (RAGE), resulting in increased oxidative stress and inflammation through the formation of ROS. Aβ itself is a ligand of RAGE, forming a positive feedback loop to augment oxidative damage in the brain (Chen *et al*., 2007). Importantly, RAGE-specific inhibitors have been shown to reduce Aβ-mediated toxicity in models of AD (Crunkhorn, 2012). Therefore, pharmacological interventions targeting glycation may emerge as valuable approaches for the treatment of AD and potentially, other neurodegenerative conditions.

Methylglyoxal (MGO) is an unavoidable by-product of glycolysis and the most reactive glycation agent. It is mainly produced by the non-enzymatic decomposition of the phosphate group of the triose phosphates (glyceraldeyde 3-phosphate and dihydroxyacetone phosphate) (Figure 19) (Vicente Miranda *et al*., 2016a). MGO can also arise from the interconversion between glyceraldeyde 3-phosphate and dihydroxyacetone phosphate by the triose phosphate isomerase (Tpi), where the enediolate intermediate may leak from the active site of Tpi in a paracatalytical reaction (Richard, 1991). Moreover, decreased Tpi activity results in an accumulation of dihydroxyacetone phosphate and MGO (Guix *et al*., 2009, Orosz *et al*., 2009). MGO is detoxified by the glyoxalase system, involving the enzymes glyoxalases I (Glo1) and II (Glo2), and by aldose reductases (Vicente Miranda *et al*., 2013). Previous reports showed that Glo1 inactivation induces a strong increase in MGO levels in yeast (Gomes *et al*., 2005). TPI deficiency increases the levels of dihydroxyacetone phosphate (Ciriacy and Breitenbach, 1979) and, consequently, increases the levels of MGO (Hollan *et al*., 1993, Phillips and Thornalley, 1993). TPI deficiency in humans results in increased levels of MGO (Ahmed *et al*., 2003).

Although no direct correlation between glycation and the pathogenesis of HD has been established thus far, levels of RAGE are increased in HD brains (Ma and Nicholson, 2004) and in mouse models (Anzilotti *et al*., 2012). In addition, we found that glycation promotes aggregation and cytotoxicity in yeast and mammalian cell models expressing mutant HTT exon 1 fragments (HTTex1) (Vicente Miranda *et al*., 2016b). Here, we further investigate the role of protein glycation on mutant HTT toxicity *in vivo*, using a *Drosophila* HD model.

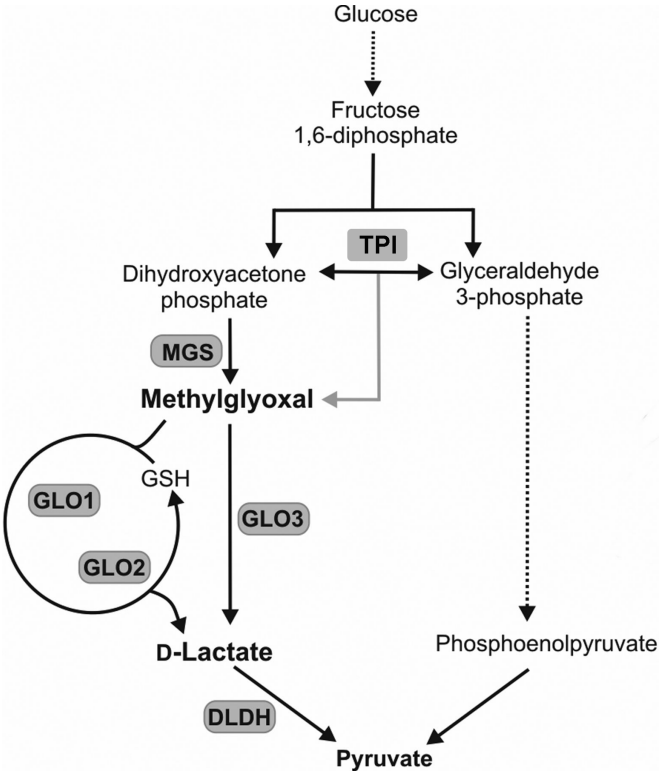

Figure 19. Methylglyoxal pathway. The methylglyoxal (MGO) pathway is an alternative metabolic route of glycolysis, where pyruvate is formed and subsequently catalyzed in mitochondria via the Krebs cycle for energy production. The excessive intake of glucose by a cell is the most important process for activation of the MGO pathway, although MGO can also be generated by lipid peroxidation and amino acid catabolism. MGO is a highly reactive dycarbonyl compound that binds to free amino-groups of proteins such as lysine, arginine and cysteine, thereby inducing the formation of an unstable Schiff's base. This modification is reversible, although the Schiff's base undergoes further intramolecular rearrangements and reactions, giving rise to irreversibly bounded compounds, the so-called AGEs. Notably, MGO is one of the substrates of the glyoxalase system that functions to protect cells from dicarbonyl-mediated AGE formation. TPI, triose phosphate isomerase. MGS, methylglyoxal synthase. GLO, glyoxalase enzymes. GSH, glutathione. DLDH, D-lactate dehydrogenase. Extracted from (Sousa Silva *et al*., 2013).

Results

MGO treatment exarcerbates neurodegeneration in a Drosophila model of HD

Using a versatile yeast model of HD and a human neuroglioma cell line (H4 cells), we recently observed that pharmacological or genetic modulation of the MGO pathway affects mutant HTT aggregation and toxicity (Vicente Miranda *et al*., 2016b). Deletion of genes encoding for enzymes involved in MGO metabolism, Glo1 or Tpi, induced HTT intracellular accumulation and formation of inclusion bodies in yeast cells (Vicente Miranda *et al*., 2016b). Importantly, Glo1 and Tpi knockout yeast strains are known to produce higher amounts of MGO and to accumulate AGEs (Gomes *et al*., 2005, Hollan *et al*., 1993, Phillips and Thornalley, 1993). These findings were further validated in human H4 cells, in which MGO treatment potentiated mutant HTT aggregation, an effect that was accompanied by defective autophagic clearance of HTT and enhanced cytotoxicity (Vicente Miranda *et al*., 2016b). To determine the effects of MGO-mediated glycation *in vivo,* we employed a *Drosophila* model of HD, described above (see Chapter I and Chapter

III, 3.1). This model is based upon the pan-neuronal expression of HTTex1 containing either normal (20QHTTex1) or expanded (93QHTTex1) polyQ stretches via the GAL4/UAS system (Steffan *et al*., 2001). Flies expressing 93QHTTex1 under the control of *elavGAL4* exhibit a variety of HD-relevant phenotypes, including degeneration of the photoreceptor neurons (rhabdomeres), locomotor defects, decreased lifespan, and impaired emergence of the adult fly from the pupal case (eclosion) (Breda *et al*., 2016, Campesan *et al*., 2011, Green and Giorgini, 2012, Mason *et al*., 2013). Moreover, *elavGAL4* drives expression of HTT at all developmental and adult fly stages (Berger *et al*., 2007), allowing for the assessment of MGO effects on early and late disease-like changes. Thus, we interrogated whether MGO-mediated glycation could contribute to mutant HTT-related neurotoxicity in different stages of the fly life cycle. For that purpose, both larvae and adult HD flies were treated with increasing concentrations of MGO. Flies expressing 93QHTTex1 pan-neuronally display severe age-dependent neurodegeneration, with some neuronal loss being evident already upon eclosion (day 0) (Figure 20). After treatment with increasing concentrations of MGO during 7 days post-eclosion, HD adult flies showed greater reduction in the number of rhabdomeres per ommatidium in comparison to their untreated counterparts (Figure 20A). Notably, this effect was dependent on the dose of MGO added to the fly food (see Material and methods II for details), which indicates a successful administration of MGO through feeding. In addition, treatment of 93QHTTex1 larvae also resulted in a dose-dependent reduction in the number of rhabdomeres upon eclosion (Figure 20B). Notably, MGO was toxic only in disease context, as treatment of control fly lines did not produce any effect (Figure S10, Supplemental information II).

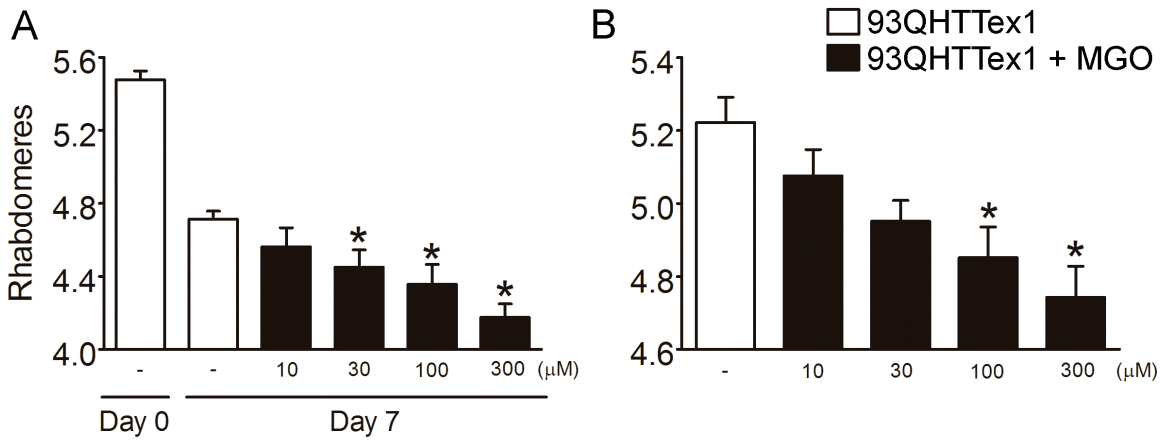

Figure 20. MGO treatment exacerbates neurodegeneration in HD transgenic flies. MGO significantly increases neuronal loss in adult (A) and developing flies (B) with pan-neuronal expression of

93QHTTex1, in a dose-response manner. Quantification of mean rhabdomeres (±SEM) per ommatidium. *Significance of differences versus untreated 7 day-old flies (A) or newly emerged flies (B), $p<0.05$.

Genetic modulation of the MGO pathway alters mutant huntingtin-induced defects in vivo

Next, we asked whether genetic modulation of glycation via knockdown of Glo1 or Tpi altered 93QHTTex1-induced defects *in vivo*. We employed an RNAi approach to downregulate Glo1 or Tpi in *Drosophila*. The Glo1 knockdown line was generated using the phiC31 integrase system to insert an RNAi sequence into specific attP target sites in the genome (Groth *et al*., 2004), whereas Tpi knockdown was engineered via traditional P-element-mediated mutagenesis, where the RNAi construct is inserted randomly into the genome. As such, two independent Tpi knowdown lines (Tpia and Tpib) were used in order to discard off-target effects or other artifacts. We first confirmed that silencing of Tpi or Glo1 increased overall glycation levels in 93QHTTex1-expressing flies (Figure S11, Supplemental information II). Moreover, a consistent increase in the levels of AGEs was detected in HTT protein by immunoprecipitation (Figure S11, Supplemental information II). Downregulation of either Glo1 or Tpi in WT background flies did not cause neurotoxicity as measured by the pseudopupil assay (Figure S12, Supplemental information II). However, when Glo1 or Tpi was knocked down in flies expressing 93QHTTex1, a significant increase in neuronal loss was observed at both 0 and 7 days post-eclosion, in comparison to their relative titration controls (Figure 21A and B). Downregulation of Glo1 or Tpi also affects development and survival of HD flies (Figure 21C-F). In this *Drosophila* HD model, pan-neuronal expression of normal polyQ stretches (20QHTTex1) causes a fly to live for up to 80 days, while 93QHTTex1 flies suffer a striking reduction of ~60 days in their lifespan (Figure S13, Supplemental information II). Downregulation of Glo1, but not Tpi, caused a further reduction in the lifespan of flies expressing 93QHTTex1 (Figure 21C and D). To assess viability in 93QHTTex1 developing flies under glycation conditions, we measured the eclosion ratio between pupa-emerging flies expressing both 93QHTTex and Glo1 or Tpi RNAi and their non-expressing siblings (see Materials and methods II for details). Pre-eclosion lethality of 93QHTTex1 flies was significantly increased when either Glo1 (Figure 21E) or Tpi (Figure 21F) was knocked down.

Overall, the results strongly suggest that glycation can act as an important environmental modifier of HTT toxicity, and thus influence HD onset and/or progression.

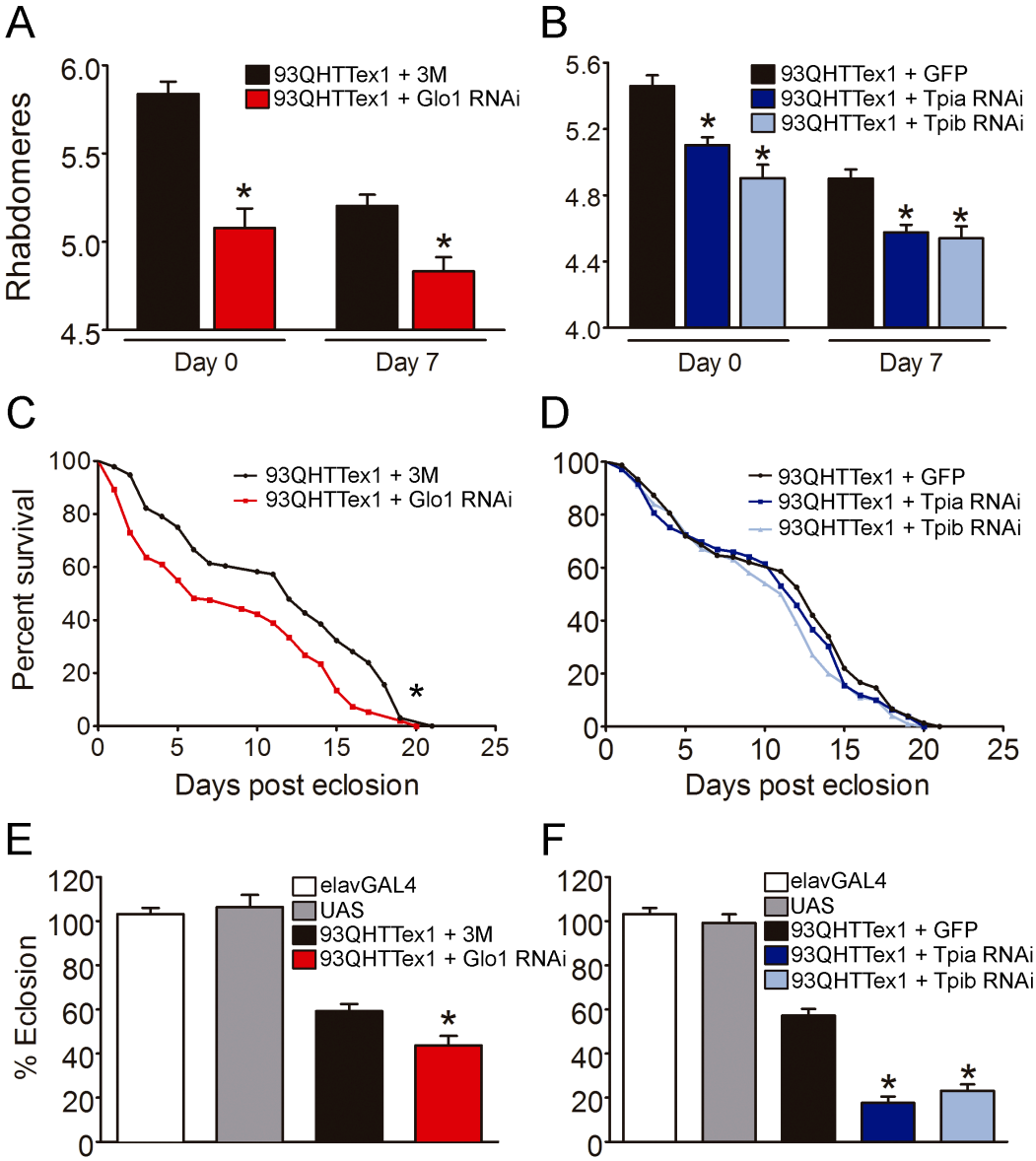

Figure 21. Downregulation of Glo1 or Tpi potentiates mutant HTT toxicity in *Drosophila*. Flies expressing 93QHTTex1 pan-neuronally and knocked down for Glo1 or Tpi were assayed for neurodegeneration (A, B), longevity (C, D) and eclosion rates (E, F). HD flies carrying either Glo1 RNAi (A) or Tpi RNAi (B) showed increased neuronal loss in comparison to respective controls. Number of rhabdomeres per ommatidium was evaluated at day 0 and day 7 post-eclosion. Survival rate was evaluated in flies with pan-neuronal knockdown of Glo1 (C) or Tpi (D) in mutant HTT backgrounds. Mean survival in days: 93QHTTex1 + 3M = 12; 93QHTTex1 + Glo1 RNAi = 6; 93QHTTex1 + GFP = 13; 93QHTTex1 + Tpia RNAi = 12; 93QHTTex1 + Tpib RNAi = 11.5. RNAi silencing of Glo1 (E) or Tpi (F) caused a reduction in the percentage of flies emerging from the pupal case. Flies carrying a single copy of the driver (elavGAL4) or, two copies of UAS constructs (UAS) in the absence of GAL4, are shown as controls. For all experiments, 93QHTTex1 + 3M or 93QHTTex1 + GFP flies were used as titration controls for Glo1 and Tpi silencing lines, respectively. Data in all panels are mean ± SEM. *Significant versus the respective titration control, $p<0.05$.

Discussion

The precise mechanisms through which HTT mutations cause HD are still unknown. However, accumulation of HTT plays an important role in the disease and strategies aimed at reducing its levels constitute attractive strategies for therapeutic intervention and are currently being explored in ongoing clinical trials (Wild and Tabrizi, 2014). Different post-translational modifications (PTMs) are known to modulate the levels, aggregation propensity and clearance of HTT, and could thereby play a role in HD pathogenesis (Ehrnhoefer *et al*., 2011, Krainc, 2010, Saudou and Humbert, 2016). For example, phosphorylation of HTT on Ser13 and Ser16 is protective in mouse models of HD (Gu *et al*., 2009), enhancing the clearance of HTT via the proteasome and chaperone-mediated autophagy (Thompson *et al*., 2009). Acetylation of Lys9 and Lys444 promotes HTT clearance via the autophagy lysosome pathway (ALP) (Jeong *et al*., 2009). On the other hand, SUMOylation leads to HTT accumulation and translocation into the nucleus (Steffan *et al*., 2004).

We have previously found that both pharmacological and genetic induction of glycation plays a deleterious role in yeast and mammalian cell models of HD by decreasing HTT clearance, increasing the intracellular levels of HTT and enhancing its aggregation and toxicity, either directly or indirectly (through the increase in the levels of HTT) (Vicente Miranda *et al*., 2016b). Impaired clearance of HTT via the proteasome was previously associated with HD (Labbadia and Morimoto, 2013). Interestingly, our previous results in mammalian cells point for opposite effects of glycation on normal (25Q) versus mutant (104Q) HTTex1 variants. While glycation impairs the activation of the ALP system in cells expressing 25Q HTTex1, the ALP system is highly induced in the presence of glycated mutant HTTex1 (Vicente Miranda *et al*., 2016b). This increased ALP activation suggests a compensatory mechanism for the cell to cope with aggregated HTT that is normally cleared via the ALP system (Nixon, 2013, Yamamoto *et al*., 2006).

Although activation of autophagy could clear aggregated proteins and is considered an important therapeutic approach for several neurodegenerative disorders (Rubinsztein *et al*., 2012), it could also lead to neuronal death in certain conditions (Puyal *et al*., 2012). It is therefore possible that increasing levels of glycation could contribute to mutant HTT cytotoxicity via overactivation of the ALP (Vicente Miranda *et al*., 2016b). Interestingly, in this previous study we also observed that glycation reduces the extracellular release of

mutant HTT, which may account for its intracellular accumulation, increased aggregation and toxicity.

Diabetes is a risk factor for neurodegenerative diseases such as AD and PD (Vicente Miranda and Outeiro, 2010, Vicente Miranda *et al*., 2016a). A major consequence of diabetes is glucose metabolism imbalance and consequent hyperglycemia. Glucose and its byproducts have the ability to react with amino groups, forming AGEs that can impact the function of target proteins. Glycation exacerbates the accumulation, aggregation and toxicity of Aβ and α-syn (Li *et al*., 2013, Vicente Miranda *et al*., 2017). Glycation could therefore constitute a common mechanism contributing to the development of neurodegenerative diseases by acting as a "second hit" that tips the proteostasis balance of cells, causing dysfunction of multiple essential cellular pathways, and leading to premature death. Consistently with this hypothesis, antidiabetic drugs have been shown to be protective in HD pre-clinical trials. For example, metformin was shown to prolong the survival of HD male mice (Ma *et al*., 2007); and exendin-4 decreased HTT aggregation, suppressed cellular pathology in both brain and pancreas, improved motor function, and extended survival in a mouse model of HD (Martin *et al*., 2009). The prevalence of diabetes is higher in HD patients (Farrer, 1985, Podolsky *et al*., 1972), HD brains differentially express several proteins linked to type-2 diabetes (Schonberger *et al*., 2013), and mouse models of HD develop hyperglycemia (Hurlbert *et al*., 1999, Jenkins *et al*., 2000), possibly due to the accumulation of intranuclear HTT inclusions in pancreatic β cells that produce insulin (Andreassen *et al*., 2002, Bjorkqvist *et al*., 2005). However, whether diabetes is a contributing factor or a consequence of HD is still unclear, as is the role of HTT glycation.

In this study, we demonstrate for the first time that glycation potentiates mutant HTT toxicity *in vivo,* as shown by the worsening of several disease-relevant phenotypes in a *Drosophila* model of HD (Figure 20 and 21). Feeding of mutant HTTex1-expressing flies with MGO reduced the number of rhabdomeres per omatidium, demonstrating a dose-dependent and selective effect. Such deleterious effect was also observed upon eclosion, suggesting that glycation exacerbates HTT toxicity during development. Importantly, genetic manipulation of pathways controlling MGO levels, through Glo1 or Tpi1 knockdown, also resulted in increased neurotoxicity and reduced survival. In Tpi RNAi flies, we observed a significant reduction in eclosion, and in Glo1 RNAi flies we observed a significant reduction in both eclosion and survival rate. Altogether, our results suggest that hyperglycemia, and the subsequent glycation of proteins including HTT, could not

only be a consequence but also a contributing factor in HD pathogenesis.

Interestingly, we recently showed that DJ-1 overexpression protects against HTT toxicity in yeast and fruit flies (Sajjad *et al*., 2014). Although mutations in the DJ-1 gene are associated with recessive forms of PD, DJ-1 was also described as an anti-MGO enzyme with glyoxalase activity (Lee *et al*., 2012). Moreover, DJ-1 is suggested to act as a protein deglycase that repairs MGO-glycated proteins (Richarme *et al*., 2015), although this finding remains controversial, as loss of *Drosophila* DJ-1 does not further contribute to MGO-induced AGE accumulation (Pfaff *et al*., 2017). Our studies are consistent with a potential protective role of human DJ-1, further supporting a connection between protein glycation and HD.

In summary, the present data obtained in flies serve as a strong complement to our previous findings in yeast and mammalian cell models of HD, further suggesting that protein glycation could contribute to HTT dysfunction and that its modulation may constitute a novel target for therapeutic intervention in HD.

Materials and methods II

Drosophila lines

Flies were raised on standard maize media at 25ºC in l2 h light/dark cycle. The UAS-20QHTT and UAS-93QHTT exon 1 flies were kindly provided by J. Lawrence Marsh and Leslie Thompson (University of California, Irvine) (Steffan *et al*., 2001). RNAi transgenic lines were obtained from the Vienna *Drosophila* Resource Center (VDRC, Vienna, Austria) for genetic silencing of glyoxalase I (*Glo1*) or triose phosphatase isomerase (*Tpi*). The *Glo1* knockdown line (v101560, KK109109) was generated using the phiC31-integrase system, which target the RNAi transgene to a specific landing site on the second chromosome (P{attP,y^+,$w^{3'}$}VIE-260B (2L:22019296)) (Dietzl *et al*., 2007). For *Tpi* silencing, we employed two lines from the GD library, *Tpia* (v25643, GD10138) and *Tpib* (v25644, GD10138) (Mummery-Widmer *et al*., 2009), where the RNAi construct is inserted randomly into the genome via traditional P-element-mediated mutagenesis. The *elavGAL4* driver (c155) and the UAS-eGFP (BL5431) stocks were obtained from the Bloomington *Drosophila* Stock Center (Indiana University, Bloomington, IN, USA). Flies carrying UAS-3M (empty vector located in the KK site) and UAS-eGFP were used as titration controls for the RNAi knockdown experiments.

Immunoprecipitation and immunoblot analysis

Total glycation levels and formation of AGEs in *Glo1* or *Tpi* knockdown HD flies were measured by standard western blotting or immunoprecipitation (IP), respectively. One hundred heads of 7 days-old flies were isolated as described in (Campesan *et al*., 2011), with minor modifications. Flies were frozen in liquid nitrogen and heads separated by vigorous vortexing. Heads were collected into new eppendorfs and homogenized using a sterile plastic pestle (Sigma-Aldrich, St. Louis, MO, USA) in NP40 buffer (0.5% NP40, 10 mM Tris-HCl pH 7.5, 150 mM NaCl, 5 mM EDTA) containing protease inhibitors (Complete Mini, Roche diagnostics, Mannheim, Germany). Total protein lysates were obtained by centrifugation at 2000 rpm, for 1 min at 4ºC and quantified by means of the BCA Protein Assay Kit (ThermoFisher Scientific, Waltham, MA, USA), following manufacturer's instructions. For IP experiments, 93QHTTex1 was pulled down from 750 μg of total protein extracts as we previously described (Guerreiro *et al*., 2013), and immunoprecipitated with 10 μl of anti-HTT antibody (Millipore, Billerica, MA, USA). Total protein lysates and IP samples were analyzed by immunoblotting using the following antibodies: anti-AGEs (1:500, Cosmo Bio, Tokyo, Japan), anti-HTT (1:1000, Millipore, Billerica, MA, USA) and anti-α-tubulin (1:15000, Sigma-Aldrich, St. Louis, MO, USA).

MGO treatment

To access glycation-mediated effects in different stages of *Drosophila* HD development, both larva and adult flies were treated with increasing concentrations of MGO. MGO was purified as previously described (Gomes *et al*., 2005), dissolved in H_2O and added to maize media at the required doses (10, 30, 100 or 300 μM). For treatment during development, parental lines were crossed and flies were grown on maize media previously supplemented with different concentrations of MGO. F1 progeny was collected upon eclosion and analyzed for eclosion ratio and photoreceptor loss as described above. Adult feeding experiments were performed as described in Materials and methods I. Briefly, newly emerged flies were transferred to MGO-supplemented food and moved daily to new vials with appropriate MGO concentration. Rhabdomere number was scored after 7 days of treatment.

Pseudopupil analysis

Neurodegeneration was assayed by measuring the number of visible rabdomeres per ommatidium as described above (see Materials and methods I), and at least twelve flies were examined per condition at day 0 or 7 post-eclosion.

Eclosion and longevity assays

Fruit fly viability was determined by measuring the percentage of eclosion, as previously described (Breda *et al*., 2016). For RNAi knockdown experiments, males carrying the sex-linked *elavGAL4* driver were crossed to virgin females carrying UAS-*Glo1*RNAi; UAS-93QHTTex1 or UAS-*Tpi*RNAi; UAS-93QHTTex1 in order to generate female expressing the desired genotype and wild-type control males in the progeny. For MGO feeding experiments, the *elavGAL4* males were crossed to virgin females homozygous for the UAS-20QHTTex1 or the UAS-93QHTTex1 transgene, and flies were allowed to lay eggs on vials with or without treatment. At least ten independent crosses were set up per condition and parental flies were removed 5 days after mating. The number of female or male flies emerging in the F1 generation was scored over 10 days post-eclosion and eclosion percent per vial was calculated using the following ratio: (number of female/number of male flies)*100. For longevity analysis, one hundred newly emerged female flies were collected per genotype and kept in groups of 10 in separate vials. Flies were moved to fresh food every 2-3 days and the number of living flies was scored daily.

Statistics

Statistical analysis was performed using Prism 6 (GraphPad Software Inc., La Jolla, CA, USA). For eclosion and rhabdomere quantification, analyses were carried out using ANOVA with the Newman-Keuls post-hoc test. For longevity, survival curves were generated and analyzed using the Kaplan-Meier method and log-rank statistics. All data is represented as the average ± standard error (SEM), and results were considered significant only when $p<0.05$.

Acknowledgements

We thank Professor Rui Moreira and Dr. Susana Lucas for MGO purification. Authors were supported by: HVM (Fundação para a Ciência e Tecnologia (FCT), Portugal

SFRH/BPD/64702/2009 and SFRH/BPD/109347/2015); JBS (SFRH/BD/85275/2012); FH (SFRH/BPD/63530/2009 and IF/00094/2013); TFO (EMBO Installation Grant; Marie Curie IRG, Neurofold). TFO is supported by the DFG Center for Nanoscale Microscopy and Molecular Physiology of the Brain (CNMPB). FG is supported by grants from the Medical Research Council (MRC) and the CHDI Foundation, Inc.

Contribution

Experiments in *Drosophila* were performed by JBS and analyzed by JBS and CB under the supervision of FG. HVM carried out protein extraction from fly heads and immunoprecipitation assays. HVM and TFO wrote the manuscript. JBS and CB reviewed the manuscript.

B.

Interplay between mutant huntingtin and other aggregation-prone proteins for Huntington's disease pathogenesis

3.3. Co-aggregation between huntingtin and alpha-synuclein in living cells

Abstract

Protein misfolding and aggregation underlies the pathogenesis of several neurodegenerative disorders. Although the proteins causing these diseases are unique, growing evidence indicates that they can co-aggregate and modify one another's behavior, suggesting this process may contribute to the overlap in clinical symptoms across different neurodegenerative disorders. Unraveling how such interactions occur and interfere with protein aggregate properties may provide opportunities for developing therapies. Here, we used a bimolecular fluorescence complementation (BiFC) assay to study interactions between a toxic huntingtin fragment (97QHTTex1), which causes Huntington's disease, and other aggregation-prone proteins, in living human cells. We showed that 97QHTTex1 interacts and co-aggregates with both alpha-synuclein (α-syn) and Tau, whose abnormalities were originally thought to be exclusively related with Parkinson's and Alzheimer's disease, respectively. Interactions of either α-syn or Tau with 97QHTTex1 altered its pattern of aggregation and cellular distribution, although toxicity of the resulting aggregates was not further increased. Strikingly, we found that N-terminal phosphorylation of HTTex1 can prevent co-aggregation between 97QHTTex1 and α-syn, but not their ability to form hetero-dimers or higher oligomeric species. Altogether, our results further support that co-aggregation of otherwise unrelated disease-causing proteins might contribute to the development of mixed neuropathologies, pointing for a critical role of post-translational modifications in modulating these processes.

Introduction

Neurodegenerative disorders such AD, PD or HD are generally characterized by the gradual loss of motor and/or cognitive functions, attributed to the death of specific neurons in the central nervous system. While an AD patient typically exhibits severe hippocampal degeneration accompanied by cognitive impairment and dementia, PD and HD are disorders of the basal ganglia characterized by behavior and motor defects.

Interestingly, clinical observations have reported a substantial overlap among neurodegenerative disorders, with some patients showing co-occurrence of symptoms characteristic of more than one disease (Rahimi and Kovacs, 2014). Additionally, there seems to be a cross-talk between different diseases. For example, PD and HD patients are at increased risk of developing dementia (Leverenz *et al*., 2009, Tyebji and Hannan, 2017), and individuals primarily diagnosed with dementia may also develop parkinsonism (Horvath *et al*., 2014). Despite intensive research in the field, the complexity and heterogeneity of neurodegenerative disorders are still poorly understood.

The presence of amyloid-like proteinaceous inclusions is a common feature among several neurodegenerative diseases, which have been histopatologically classified according to the nature and localization of these inclusions in the brain. In HD, cytoplasmic and intranuclear aggregates containing an abnormal expanded polyQ protein (HTT) are typically found in medium spiny neurons of the striatum. AD can be classified as an amyloidopathy as well as a tauopathy, being characterized by the formation of both Aβ extracellular plaques and intracellular inclusions composed of hyperphosphorylated Tau in the form of neurofibrillary tangles (NFTs). The accumulation of α-syn into Lewy bodies is one of the hallmarks of PD hence belonging to a group of neuropathologies termed as synucleinopathies. Nevertheless, Tau positive inclusions are also described in synucleinopathies and vice-versa, suggesting that the presence of mixed proteinaceous inclusions may contribute to clinical heterogeneity, and perhaps, disease development and progression (Kotzbauer *et al*., 2004). In particular, the co-occurrence of Tau and α-syn deposits has been found in patients with Dementia with Lewy bodies (DLB) (Colom-Cadena *et al*., 2013, Ishizawa *et al*., 2003), whereas α-syn localizes to NFTs of AD (Marui *et al*., 2000, Takeda *et al*., 2000).

Relevant findings have also emerged from *in vitro* and *in vivo* studies. The direct interaction between α-syn and Tau is first described in a report from 1999, where the researchers show that α-syn co-localizes with Tau in axons promoting its phosphorylation via activation of the protein kinase A (Jensen *et al*., 1999). Moreover, α-syn is shown to contain a specific binding site for Tau at its C-terminus, further suggesting that these proteins may work together on mechanisms of neurodegeneration (Jensen *et al*., 1999). Consistently, co-aggregation of α-syn and Tau is associated with increased toxicity in cellular and *Drosophila* models of disease (Badiola *et al*., 2011, Roy and Jackson, 2014).

Importantly, α-syn interactions are not restricted to Tau, and may also occur between other aggregation-prone proteins, including HTT (Charles *et al*., 2000, Furlong *et al*., 2000, Herrera and Outeiro, 2012, Masliah *et al*., 2001, Zondler *et al*., 2014). Immunohistochemical analysis of tissues from both cortex and striatum of patients and mouse models of HD revealed α-syn as a component of polyglutamine aggregates (Charles *et al*., 2000). Intriguingly, overexpression of α-syn potentiates the formation of mutant HTT aggregates in cultured human cells, even when co-aggregation does not occur (Furlong *et al*., 2000). Notably, we showed that α-syn interacts and co-aggregates with HTT in living human cells, resulting in an altered HTT aggregation pattern (Herrera and Outeiro, 2012).

In the last decade, evidence linking Tau aggregation and HD neuropathology has also begun to emerge (Gratuze *et al*., 2016). A post-mortem study has reported co-localization of Tau and HTT aggregates in the striatum of an HD patient (Caparros-Lefebvre *et al*., 2009). At the cellular level, we recently showed that HTT directly interacts with Tau enhancing its phosphorylation, and that these interactions change the aggregation profile of HTT (Blum *et al*., 2015). Likewise, we found that Tau is hyperphosphorylated in a mouse model of HD (Blum *et al*., 2015), what is also observed by a similar study from other laboratory (Gratuze *et al*., 2015).

Altogether, these observations indicate that neurodegenerative diseases involve co-aggregation of different protein species, which may also include post-translational modified species. PTMs can alter protein structure and could, in theory, play a role in co-aggregation processes. Given that we found that PTMs modulate HTT aggregation (Chapter III, section A), we postulated that it might also interfere in HTT ability to interact and co-aggregate with other aggregation-prone proteins. Here, we investigated the effects of single phosphorylation events in the N-terminal region of HTTex1 upon mutant HTT interactions with both α-syn and Tau.

Results

Alpha-synuclein modifies mutant huntingtin aggregation pattern

We started by characterizing the effect of α-syn upon mutant HTT oligomerization, aggregation and toxicity in mammalian cells. By employing a Venus-based BiFC approach, a pair of constructs encoding either a wild-type (19Q) or a mutant (97Q)

HTTex1 fragment, or α-syn fused to non-fluorescence halves of the Venus protein was transfected into H4 human glioma cells (Figure S14A, Supplemental information III). In this system, HTTex1 is located at the N-terminus of both Venus halves (V1 and V2), whereas α-syn is located at the C-terminus of V1 or at the N-terminus of V2. The Syn-V1 construct also contains a serine/glycine linker between V1 and α-syn in order to improve the flexibility of the fusion protein. As described in Chapter I, interaction between proteins of interest would bring the two Venus halves together, reconstituting the functional fluorophore and thereby emitting fluorescence. Importantly, these combinations of plasmids were previously generated and tested in our laboratory for production of fluorescence and dimerization efficiency (Herrera *et al*., 2011, Herrera and Outeiro, 2012). Flow cytometry analyses showed that transfection of all Venus BiFC pairs produced fluorescence (Figure S14B and C, Supplemental information III), indicating the formation of dimers/oligomers. This was further confirmed by microscopy, whereby HTTex1 BiFC pairs are visualized mostly in the cytoplasm (Figure 22A, 19Q/19Q and 97Q/97Q) and α-syn spreading both through nucleus and cytosol (Figure 22A, Syn/Syn). While mutant HTT forms oligomeric species and large inclusions (Figure 22A, 97Q/97Q), α-syn accumulates as dimers and/or oligomers, with no aggregates being formed (Figure 22A, Syn/Syn). Consistently, filter trap assays indicated the presence of SDS-insoluble aggregates in 97Q/97Q cells, but not in cells transfected with the α-syn BiFC pair (Figure 22F, FT). In addition, oligomeric species of variable size were detected in both mutant HTT and α-syn expressing cells (Figure 22F, Native-PAGE).

Co-transfection of α-syn-V2 with either 19QHTTex1-V1 or 97QHTTex1-V1 plasmid produced fluorescence as determined by flow cytometry (Figure S14B and C, Supplemental information III). This suggests that α-syn can interact directly with both wild-type and mutant HTTex1, although it appears more prone to form dimers/oligomers with the mutant version (Figure S14B and C, Supplemental information III). Interestingly, when combined with mutant HTT, α-syn loses its nuclear location (Figure 22A, 97Q/Syn). This could be explained by the existence of a cytoplasmatic location-related domain in HTTex1 (Yan *et al*., 2011), which once interacting with α-syn would sequester it in the cytosol. Notably, combination of mutant HTT and α-syn BiFC constructs also resulted in the occurrence of large inclusions (Figure 22A, 97Q/Syn). However, further analysis of microscopy pictures revealed a change in the pattern of mutant HTT aggregation (Figure 22B-D), with significantly fewer but larger aggregates being generated in the presence of α-syn. Filter trap assays showed a reduction in the formation of large aggregates

containing HTTex1 in 97Q/Syn cells versus 97Q/97Q cells (Figure 22F, FT), which was accompanied by a slight increase in the amount of HTTex1 oligomers (Figure 22F, Native-PAGE). Moreover, α-syn co-expression with mutant HTT led to decreased levels of α-syn oligomeric species in comparison to the α-syn BiFC pair (Figure 22F, Native-PAGE).

Since, in our cellular model, α-syn and HTT interact modifying each other's patterns of oligomerization and aggregation, we next asked whether such cellular phenotypic changes would correlate with altered cytotoxicity levels. We used the LDH assay (described in Chapter III, 3.1) to measure the cytotoxicity levels produced by H4 cells after 24h of being transfected with different combinations of BiFC constructs (Figure 22E). As previously reported, transfection of the 97QHTTex1 BiFC pair significantly increase cytotoxicity versus the wild-type counterpart (Herrera *et al*., 2011). A significant increase in cytotoxicity was also observed in cells transfected with the α-syn BiFC pair (Figure 22E). However, and in spite of the clear changes induced by α-syn on mutant HTT aggregation pattern and vice-versa, no changes were observed on cell viability when these two proteins were expressed together, even at 72 after transfection (data not shown).

Overall, the results are consistent with a previous report from our laboratory (Herrera and Outeiro, 2012), further suggesting HTT and α-syn as interplayers in mechanisms of neurodegenerative disease.

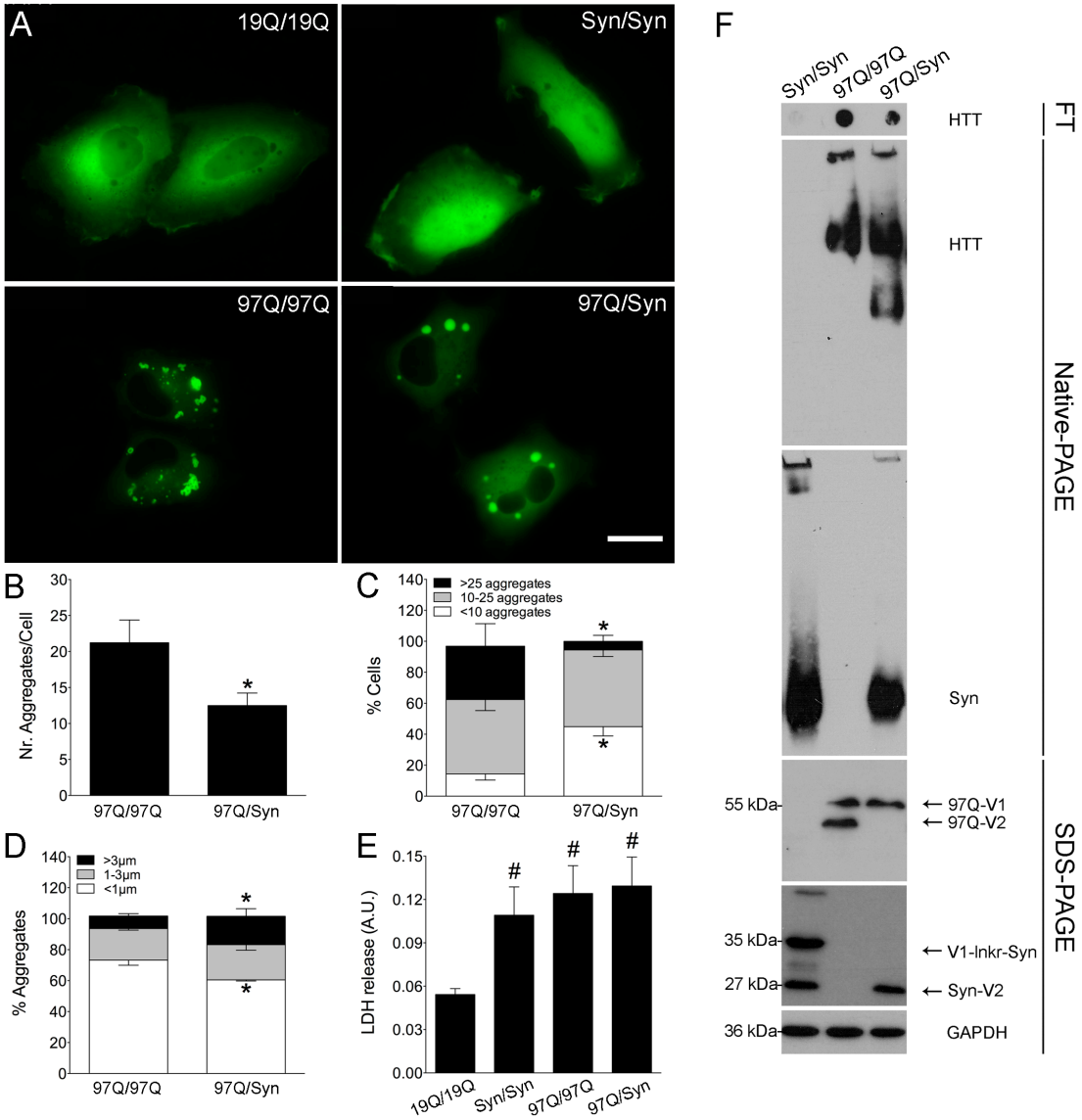

Figure 22. α-syn co-aggregates with mutant HTT and alters its aggregation pattern. (A) Cells transfected with 19QHTTex1-Venus BiFC pair of plasmids (19Q/19Q) show homogeneous fluorescence indicative of oligomeric species, while 97QHTTex1-Venus BiFC pair (97Q/97Q) produces both oligomeric species and large intracellular fluorescent aggregates with variable size and morphology. HTT location is primarily cytosolic. α-syn-Venus BiFC pair (Syn/Syn) produces homogeneous fluorescence distributed throughout all cellular compartments, including the nucleus. When α-syn and 97QHTTex1 BiFC constructs were combined, there is a change in the aggregation pattern of both proteins, quantified in B-D. Co-transfection of 97QHTTex1 with α-syn BiFC constructs decreases the average number of aggregates per cell (B, C), and increases the average size of aggregates (D). (E) The α-syn pair or the 97QHTTex1 pair are more toxic than the wild-type HTTex1 pair (19Q/19Q) and combining α-syn with 97QHTTex1 does not enhance toxicity in this model. *significant versus 97Q/97Q, #significant versus 19Q/19Q, $p<0.05$. Scale bar, 20 µm. AU, arbitrary units. (F) Filter trap (FT) assays showed that both 97Q/97Q and 97Q/Syn produced SDS-insoluble aggregates. Immunoblotting of total protein extracts under native conditions (Native-PAGE) indicated the generation of oligomeric species of variable size. Expression levels of each construct were evaluated by SDS-PAGE and GAPDH used as loading control.

Co-aggregation between huntingtin and alpha-synuclein is dependent on N-terminal phosphorylation state

In Chapter III, section A we demonstrated that single phosphorylation events in N-terminal region comprising the first 17 amino acids of HTTex1 (N17) modulate protein aggregation. In particular, by employing HTTex1-Venus BiFC plasmids carrying single phosphomimic mutations within the 3 phosphorylatable residues of N17 (T3, S13, S16), we showed that phospho-HTTex1 molecules interact and co-aggregate with unphosphorylated HTTex1, depending on the residue mutated (Figure S3, Supplemental information I). To investigate the influence of HTTex1 phosphorylation on its interactions with α-syn, we transfected H4 cells with different combinations of phosphomimic mutants and α-syn (Figure 23). We observed that phosphorylated HTTex1 interacted with α-syn to the same extent as non-phosphorylated HTTex1 molecules (97Q/Syn combination), producing similar levels of fluorescence (flow cytometry assays, data not shown). However, co-expression of different phosphomimic mutants with α-syn resulted in mixed patterns of aggregation (Figure 23A), with a residue-dependent reduction in the percentage of cells with inclusions being shown (Figure 23B). Notably, such aggregation profiles resembled that of cells co-transfected with the correspondent phosphomimic mutant and non-mutated 97QHTTex1 BiFC constructs (Figure S3, Supplemental information I). This suggests that, in addition to regulating the formation of pure HTTex1 aggregates, N17 phosphorylation may also play a role in co-aggregation processes occurring between HTT and other aggregation-prone proteins.

To further test the above hypothesis, we asked whether the modulatory effect of HTTex1 phosphomutants on aggregate formation could be extended to the Tau protein. Tau is an abundant neuronal protein, known to function as a microtubule stabilizer, thus being frequently found to localize to microtubule and actin networks (Elie *et al*., 2015). We have previously shown that mutant HTT interacts with Tau affecting its normal cellular distribution (Blum *et al*., 2015). In particular, using BiFC-based cellular models, we observed that, when co-expressed with Tau, mutant HTTex1 is recruited to the microtubules inducing Tau aggregation (Blum *et al*., 2015) (Figure 23A, 97Q/Tau). Concomitantly, mutant HTTex1 aggregation pattern was also altered, often leading to the formation of one single inclusion per cell (Blum *et al*., 2015) (Figure 23A, 97Q/Tau). Interestingly, most HTT/Tau inclusions were morphologically distinct from pure HTTex1 aggregates, assembling into a ring-like structure (Blum *et al*., 2015) (Figure 23A, T3D/Tau). While the 97QHTTex1 BiFC pair induces the formation of inclusions in 30-

40% of transfected cells (Herrera *et al*., 2011) (Figure 23B), 97Q/Tau inclusions are found in 15-17% of co-transfected cells (Blum *et al*., 2015) (Figure 23C). Strikingly, no changes in the percentage of cells showing large inclusions were observed when Tau was combined with the different phosphomimic mutants of HTTex1 (Figure 23C).

In summary, these observations further support a role for N17 phosphorylation in modulating HTTex1 aggregation, and suggest that it might also modulate HTTex1 protein-protein interactions. Furthermore, our results strongly indicate that T3 phosphorylation is particularly important in preventing the formation, not only of pure HTTex1 aggregates, but also mixed aggregates containing HTTex1 and α-syn. Nevertheless, this effect appears to be protein-specific, as N17 phosphorylation did not affect interactions between Tau and HTTex1.

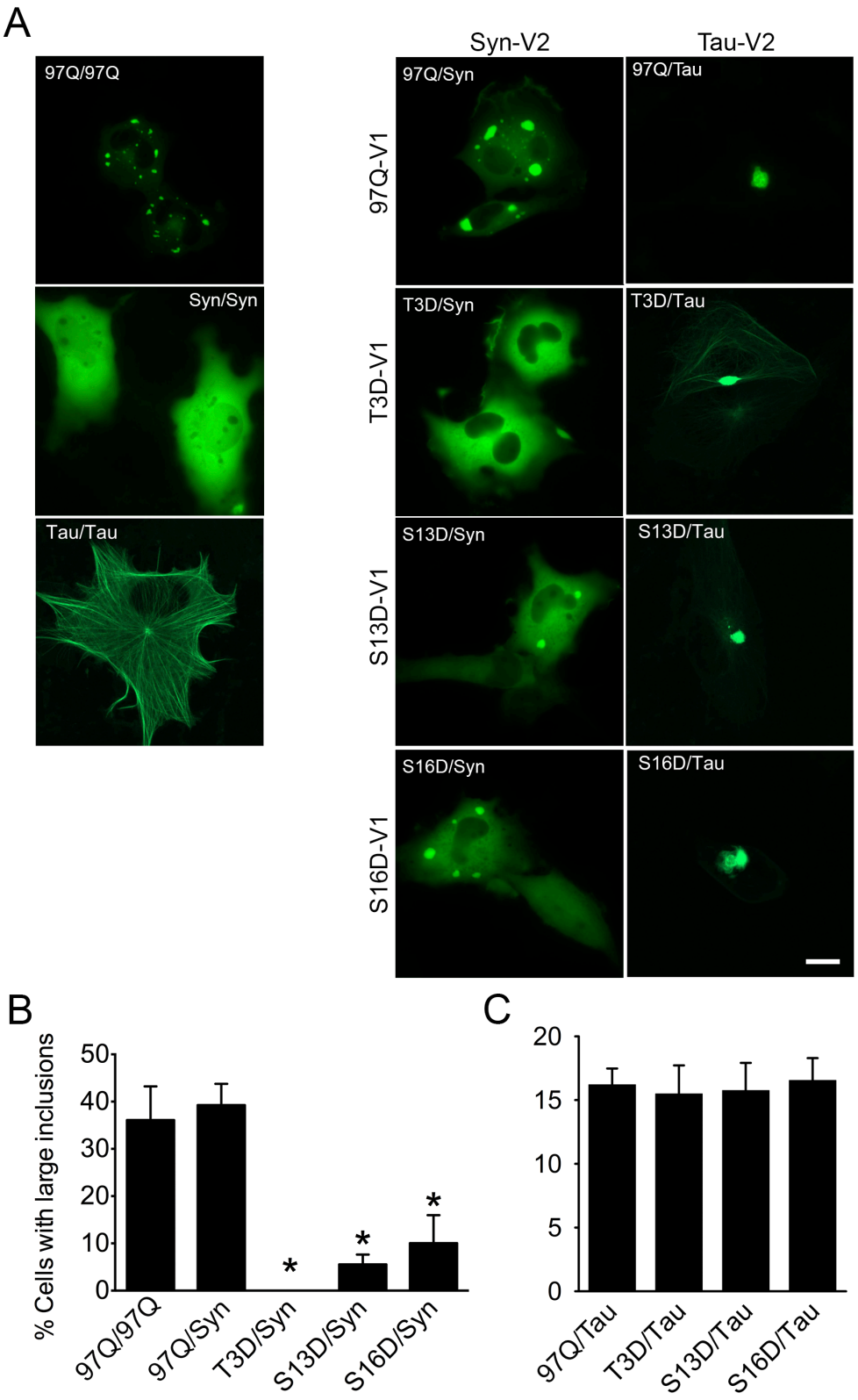

Figure 23. N17 phosphorylation interferes with mutant HTT and α-syn co-aggregation. (A) Combinations of 97QHTTex1-Venus BiFC contructs with α-syn revealed different co-aggregation responses to phosphomimic constructs, with T3D being the most restrictive in reducing aggregation. On the other hand, Tau co-aggregated with 97QHTTex1 regardless of the N17 mutation. B and C, Percentage of cells containing large inclusions as determined by quantitative analysis of microscopy pictures. *significant versus 97Q/Syn, $p<0.05$. Scale bar, 20 μm.

Discussion

Most neurodegenerative disorders are typically characterized by the aggregation of one or two specific proteins in the brain. In AD, PD and HD, much of the aggregated protein consist of Aβ, α-syn or HTT, respectively. However, accumulating evidence indicates that aggregation-prone proteins can co-aggregate increasing the possibility for neurotoxicity and disease (Badiola *et al*., 2011, Clinton *et al*., 2010, Corrochano *et al*., 2012a, Pocas *et al*., 2015, Roy and Jackson, 2014, Tomas-Zapico *et al*., 2012). Indeed, since no protein acts in isolation, the interplay of diverse aggregation-prone proteins may influence disease onset, progression and severity, and is implicated as one possible reason for the heterogeneity of neurodegenerative diseases.

Interactions between particular aggregation-prone proteins can influence aggregation propensity and its outcomes, resulting in the formation of morphologically distinct intermediates that may differ in their ability to cause cell dysfunction and thus affect neurodegenerative processes (Morales *et al*., 2013, Sarell *et al*., 2013). In the present study, we further discuss the consequences of HTT interactions with either α-syn or Tau upon the properties of the resulting aggregates, including their morphology and solubility, subcellular localization, and toxicity. In addition, we provide evidence for a modulatory role of N17 phosphorylation on mutant HTT co-aggregation propensity.

Both α-syn and Tau are expressed predominantly in the brain, more abundantly within nerve terminals, being involved in similar neuronal processes such as synaptic transmission and plasticity (Guo *et al*., 2017, Si *et al*., 2017). At a cellular and molecular level, endogenous α-syn is mostly present in the cytoplasm as an unfolded monomer, but it can also exist as a tetramer (Bartels *et al*., 2011, Dettmer *et al*., 2013). Tau is a microtubule-associated protein that promptly forms intracellular fibril structures when hyperphosphorylated (Guo *et al*., 2017). The fact that these two proteins share similar locations and functions suggests that interactions between them may be relevant for neuropathology. Moreover, the presence of aggregation-prone proteins within the same cellular compartments or in functionally connected brain areas may facilitate the occurrence of cross-seeding events (Morales *et al*., 2013, Sarell *et al*., 2013). Indeed, the aggregation potential of Tau is greatly enhanced in the presence of α-syn oligomers (Giasson *et al*., 2003, Kotzbauer *et al*., 2004, Waxman and Giasson, 2011). Similarly, when at low concentrations, α-syn requires Tau to initiate fibril formation (Giasson *et al*.,

2003). Additional evidence for a significant role of α-syn/Tau interactions in neurodegeneration comes from experiments in different animal models (Emmer *et al*., 2011, Roy and Jackson, 2014). Following the same line of thought, and considering that HTT is also a cytoplasmic protein, it is possible that HTT directly interacts with α-syn and/or Tau, and interferes with their normal cellular functions by cross-seeding their aggregation and/or recruiting them into HTT inclusions. Our study supports this idea by showing that co-expression of mutant HTT with either α-syn or Tau in human living cells leads to the formation of mixed cytosolic inclusions and altered patterns of protein subcellular distribution. In contrast with a report showing that mutant HTT aggregation is accelerated in the presence of overexpressed α-syn (Furlong *et al*., 2000), our results indicate that although α-syn can alter the aggregation profile of mutant HTT, no further HTT aggregation is observed when the two proteins are co-expressed at similar levels (Figure 22). However, while more HTT oligomeric species were formed, α-syn oligomerization was diminished, suggesting a dynamic system, where mutant HTT readily aggregates with α-syn becoming less available to form pure HTT aggregates. Indeed, cells expressing only mutant HTT produced similar levels of oligomerization versus cells expressing both mutant HTT and α-syn (Figure S14, Supplemental information III), indicating that mutant HTT molecules are as likely to interact with α-syn as with each other. These results might have clinical relevance as it suggest that a HD patient with no mutations in the SNCA gene affecting α-syn expression could also be at risk of developing α-syn pathology.

In mammalian neurons, endogenous α-syn is primarily located in the cytoplasm (Huang *et al*., 2011). However, its existence has also been reported in the nucleus (Li *et al*., 2002a, Zhong *et al*., 2010), where α-syn is thought to promote toxicity independent of its aggregation (Goers *et al*., 2003, Kontopoulos *et al*., 2006). In our BiFC-based cell model, α-syn oligomerizes in the nucleus and produces cytotoxicity, while no inclusion bodies are formed (Figure 22). When co-expressed with mutant HTT, α-syn changed its subcellular distribution being sequestered in the cytosol. This could suggest that cross-seeding events between these two proteins preferentially occur in the cytoplasm. Consistent with this idea, the formation of HTT aggregates is greatly dependent on its cytosolic localization, with less aggregates being formed when HTT is localized to other cellular compartments (Yan *et al*., 2011).

Strikingly, no changes in cytotoxicity were observed when mutant HTT was combined with α-syn (Figure 22E). Given that oligomeric species are likely more toxic

than large insoluble species (Arrasate *et al*., 2004, Bodner *et al*., 2006, Eisele *et al*., 2015, Winner *et al*., 2011), it would be expected that higher levels of HTT oligomerization, observed in the presence of α-syn (Figure 22F), would lead to increased cytotoxicity. However, there are other cellular events occurring simultaneously that may be acting against such an expected outcome. In particular, the presence of α-syn oligomers in the nucleus was abolished as well as their overall levels decreased (Figure 22A and F). Other possible explanations may include the idea that, in our BiFC-based cell model, HTT oligomerization and cytotoxicity may not be necessary related (Chapter III, 3.1), and not least, because co-aggregation of HTT and α-syn may affect the stability of forming intermediates, resulting in a prolonged lifetime of potential toxic species, that would be difficult to catch in such early assays. Interestingly, *in vitro* studies show that mixed oligomeric species are more stable than homo-oligomers being incapable of further assembly, hence accumulating in a time-dependent manner (Fung *et al*., 2004, Lashuel *et al*., 2003). This enrichment of potential toxic species over time may be responsible for accelerating disease progression in patients with mixed neuropathologies (Tsigelny *et al*., 2008). Subsequent experiments in *Drosophila* revealed a synergistic worsening of HD- and PD-related phenotypes in flies co-expressing α-syn and mutant HTT (Pocas *et al*., 2015). In this study, we established new *Drosophila* lines carrying UAS transgenes encoding either α-syn-EGFP or a mCherry-tagged mutant HTTex1 fragment. Immunohistochemistry analyses of different *Drosophila* tissues demonstrated that mutant HTT co-localizes with α-syn in adult fly dopaminergic neurons, and axonal projections of photoreceptor neurons in larval brains. Such physical interactions between these two proteins resulted in the generation of both soluble and insoluble species. Moreover, flies with neuronal expression of both mutant HTT and α-syn exhibited early motor impairment, decreased lifespan and premature neuronal loss (Pocas *et al*., 2015). Whether such deleterious phenotypes are a direct consequence of cross-seeding events resulting in a gradual accumulation of intermediate toxic species, or the result of a loss of normal α-syn function that becomes sequestered within HTT aggregates, remains to be clarified. Previous studies using mouse models of HD show that α-syn depletion ameliorates disease-relevant phenotypes while decreasing the number of inclusions in the brain (Corrochano *et al*., 2012a, Tomas-Zapico *et al*., 2012). At a cellular level, these animals display increased number of autophagosomes in comparison to HD animals expressing normal levels of endogenous α-syn (Corrochano *et al*., 2012a, Corrochano *et al*., 2012b). These observations could suggest that the presence of both α-syn and mutant HTT triggers the occurrence of cross-

seeding events thereby accelerating protein misfolding and aggregation, which would ultimately result in saturation of the autophagy-lysosome system with a consequent increase in cellular stress and toxicity.

Notably, a previous study from our laboratory provides the first evidence for a direct interaction between HTT and Tau in living cells (Blum *et al*., 2015). Co-expression of mutant HTT and Tau leads to slower aggregation rate, with less cells showing inclusions as well as less aggregates being formed per cell (Blum *et al*., 2015) (Figure 23). These inclusions are dynamically and morphologically distinct from pure HTT aggregates, appearing as static ring-like structures (Blum *et al*., 2015). Although the biological significance of such structural changes remains unclear, it has been hypothesized that increased cytotoxicity may arise when the rearrangement of globular species into ring-like structures exceed a certain threshold (Pires *et al*., 2012). Importantly, in the presence of mutant HTT, Tau displays increased levels of phosphorylation, which is probably related to a deregulation of protein phosphatase/kinase activity (Blum *et al*., 2015, Gratuze *et al*., 2015). These observations indicate that both direct and indirect mechanisms of protein aggregation might be involved in the formation of Tau inclusions observed in HD.

Further support for the existence of indirect processes in the cross-talk between aggregation-prone proteins comes from studies on Aβ interactions with Tau. Although the ability of Aβ to induce Tau neuropathology is clearly demonstrated *in vivo* (Clinton *et al*., 2010, Gotz *et al*., 2001, Vasconcelos *et al*., 2016), it seems that Tau aggregates do not have the same effect over Aβ (Gotz *et al*., 2001, Lewis *et al*., 2001). It has been hypothesized that Aβ deposition occurring prior to Tau pathology can trigger the activation of certain kinases responsible for Tau phosphorylation, which in turn, induces misfolding and aggregation of this protein (Ferrer, 2004, Guo *et al*., 2006, Oddo *et al*., 2004). Together with the existence of a spatial dissociation between Aβ and Tau inclusions in AD, these findings suggest that, in some cases, the formation of different proteinaceous inclusions in the brain may be mediated by altered signaling pathways rather than cross-seeding events.

On the other hand, Tau phosphorylation may also affect its ability to co-aggregate (Guo *et al*., 2006, Nubling *et al*., 2012). McGeer and colleagues show that Aβ binds to non-phosphorylated Tau forming soluble oligomers *in vitro* (Guo et al., 2006). Such Aβ/Tau interactions induce GSK3β-mediated Tau phosphorylation, that then decreases Aβ binding affinity, and prevents further assembly of Aβ/Tau oligomers into larger species (Guo *et al*., 2006). Remarkably, prior phosphorylation of Tau in specific threonine and

serine residues inhibits Aβ/Tau interactions, suggesting that initial steps of co-aggregation may be mediated by particular Tau phosphorylation events (Guo *et al*., 2006). On the contrary, Tau phosphorylation enhances co-aggregation of Tau and α-syn (Nubling *et al*., 2012). Thus, it seems that PTMs can be crucial in determining the propensity of a protein to cross-seed and form mixed aggregates. Another striking example is the existence of prion (PrP^{c}) strains with different glycosylation patterns that differ in their ability to initiate its own conformation conversion to infectious prion (PrP^{Sc}) (Collinge, 2001). The present study provides further evidence for an important role of specific PTMs in modulating co-aggregation processes, although the outcome may vary depending on the interacting proteins. In particular, we propose that single N-terminal phosphorylation of HTT modulates its co-aggregation with α-syn but not Tau (Figure 23). Moreover, our results indicate common mechanisms of both HTT aggregation and HTT cross-seeding interactions with α-syn, whereby T3 phosphorylation plays an inhibitory role. Since a significant amount of HTT molecules are found in an unphosphorylated state in HD (Aiken *et al*., 2009, Atwal *et al*., 2011), this might help to explain the high propensity of mutant HTT to interact with α-syn (Figure S14, Supplemental information III), and the coincidence of HTT and α-syn in HD brain deposits (Charles *et al*., 2000). Such a mechanism would not exclude a direct association between increased levels of a certain aggregation-prone protein, in the cellular environment, and the likelihood of co-aggregation occurring (Sarell *et al*., 2013).

In summary, our results support that HTT interactions with α-syn (and Tau) might contribute to the development and spreading of neurodegeneration in HD, and that HTT phosphorylation state might determine the efficiency of such cross-seeding events.

Materials and methods III

Cell culture and plasmids

Human H4 glioma cells (ATCC HTB-148, LGC Standards, Barcelona, Spain) were maintained and seeded as described in Materials and methods I. Generation of HTTex1- and Tau-Venus BiFC constructs was described in detail elsewhere (Blum *et al*., 2015, Herrera *et al*., 2011). α-syn-Venus BiFC plasmids were a kind gift from Pamela J. McLean (Department of Neurology, Alzheimer's Disease Research Unit, Massachusetts General Hospital, MA, USA). Mutagenesis experiments for creating phosphomimic point

mutations within HTTex1-Venus plasmids are detailed in Materials and methods I. Cells were co-transfected with the different combinations of plasmids using X-tremeGene 9 reagent (Roche diagnostics, Mannheim, Germany), and 24 h later, prepared for flow cytometry, miscroscopy, toxicity or immunoblotting.

Protein interaction, oligomerization and aggregation were determined by flow cytometry, fluorescence microscopy, immunoblotting and filter trap assays as described in Materials and methods I. Toxicity assays were carried out also as described above (see Materials and methods I).

Statistics

Statistical analyses were performed using the GraphPad Prism 5 software (GraphPad Software Inc., La Jolla, CA, USA). All graphs show the average ± standard deviation (SD) of at least 3 independent experiments. Differences between mean values were determined by one-way ANOVA followed by a Tukey post-hoc test. Statistical significance was accepted when $p<0.05$.

Acknowledgements

We thank Pamela J. McLean for the α-syn-Venus BiFC plasmids.

Contribution

JBS carried out mutagenesis for obtaining phosphomimic HTTex1 BiFC constructs, and performed the experiments and data analysis presented on Figure 22 and Figure 23A, left panel. FH cloned HTTex1- and Tau-Venus BiFC plasmids and carried out co-expression experiments with phosphomimic HTT- and Tau BiFC constructs (Figure 23A, right panel, and C).

3.4. Prion proteins modulate mutant huntingtin mediated neurotoxicity

Abstract

Several studies have shown that misfolding of one disease-causing protein can induce misfolding an aggregation of other aggregation-prone proteins. Such cross-seeding properties can contribute to neuropathology and disease progression. Therefore, understanding how interactions between different types of aggregation-prone proteins may influence toxicity will be crucial for a deeper understanding of the molecular mechanisms underlying the pathogenesis of neurodegenerative disorders. In yeast, a suite of aggregation-prone proteins modulates the toxicity of mutant huntingtin (HTT). In particular, the Rnq1 protein (which forms the [*PIN*$^+$] prion) is required for maximal mutant HTT toxicity and aggregation. Here, we investigated the effects of Rnq1 on mutant HTT-dependent phenotypes using *Drosophila* and mammalian cell models of Huntington's disease (HD). We found that Rnq1 exacerbates several disease-relevant phenotypes in a *Drosophila* HD model. Similar results were observed with co-expression of mutant HTT and either wild-type or disease-associated P101L mouse prion protein (MoPrP). Furthermore, we found that Rnq1 physically interacts with mutant HTT in mammalian cells, dramatically increasing its aggregation. As humans express many proteins with prion-like domains, these data suggest that prion-like proteins may play a critical role in HD pathogenesis and that of other neurodegenerative disorders.

Our past work has found that modulating levels of neuroactive kynurenine pathway metabolites via inhibition of kynurenine 3-monooxygenase (KMO) ameliorates disease-relevant phenotypes in flies expressing HTT, alpha-synuclein, and amyloid-beta. We find here that KMO inhibition is also protective against Rnq1-mediated toxicity in flies, suggesting convergent mechanisms contributing to cellular toxicity in these models of protein misfolding. Altogether, our findings provide new insights into HD pathology and further support KMO as a promising therapeutic target for human protein misfolding disorders.

Introduction

The progressive accumulation of protein aggregates in the brain is a common hallmark of fatal neurodegenerative disorders including AD, PD and HD. Growing evidence suggest that these aggregates are able to seed protein misfolding in a process similar to the spreading of prion proteins in transmissible prion disorders (Stopschinski and Diamond, 2017). However, the events leading to the formation of toxic species and their propagation in brain cells remain elusive. Intriguingly, the co-existence of aggregated forms of distinct disease-associated proteins in patient brains have been observed (Rahimi and Kovacs, 2014), suggesting that cross-seeding interactions among various aggregation-prone proteins might contribute to the pathogenesis and progression of different neurodegenerative disorders. In fact, prion-like proteins have been reported to mediate toxicity and propagation of Aβ aggregates (Kostylev *et al*., 2015, Salazar and Strittmatter, 2017), and to interact with α-syn, thereby inducing synaptic dysfunction in transgenic PD mice (Ferreira *et al*., 2017). Conversely, α-syn is capable of cross-seeding prion protein aggregation and pathology (Katorcha *et al*., 2017). Identifying molecular factors involved in these cross-seeding processes is essential to better understanding the pathogenesis of these devastating disorders.

Prion proteins are infectious amyloids, capable of converting natively folded proteins into prion-like conformers that can self-propagate between cells and among individuals of the same or different species (Colby and Prusiner, 2011, Aguzzi and Rajendran, 2009). Recent studies have found a suite of aggregation-prone proteins containing yeast prion-like domains that can modulate polyQ toxicity (Duennwald *et al*., 2006a, Duennwald *et al*., 2006b, Kantcheva *et al*., 2014, Kayatekin *et al*., 2014, Mason *et al*., 2013, Ripaud *et al*., 2014). Prion-like domains are typically enriched for glutamine (Q) and asparagine (N) residues (King *et al*., 2012) that are essential for prion-like propagation and amyloid formation (Bruce and Chernoff, 2011, Wickner *et al*., 2008). However, different combinations of Q/N-rich proteins may determine different polyQ pathobiology (Sabate *et al*., 2015, Toombs *et al*., 2010). Deletion of genes encoding Q-rich proteins abolishes polyQ toxicity and their overexpression can convert nontoxic HTT species into toxic species (Duennwald *et al*., 2006a). Intriguingly, overexpression of other Q-rich peptides can also suppress polyQ toxicity (Ripaud *et al*., 2014). Furthermore, N-rich domains enhance polyQ aggregation and toxicity whereas the association of Q-rich

proteins with mutant HTT alters physical properties of HTT aggregates (Kayatekin *et al*., 2014), which may reduce their ability to sequester nuclear proteins and other aggregation-prone factors (Ripaud *et al*., 2014).

The Rnq1 protein is a transferable epigenetic modifier of protein function in yeast, which contains a Q/N-rich region in its C-terminal region (residues 153-405) (Bruce and Chernoff, 2011, Perrett and Jones, 2008, Sondheimer and Lindquist, 2000). Despite the fact that the physiological function of the soluble protein is not known, the prion state of Rnq1 ([*PIN*$^+$]) is required for *de novo* formation and propagation of other yeast prion proteins (Derkatch *et al*., 1997, Derkatch *et al*., 2000, Derkatch *et al*., 2001, Derkatch *et al*., 2004, Osherovich and Weissman, 2001, Resende *et al*., 2003). Strikingly, mounting evidence suggests a role for Rnq1 in yeast cell toxicity mediated by misfolded proteins (Duennwald *et al*., 2006a, Meriin *et al*., 2002). For example, in the yeast model of HD, downregulation of the *RNQ1* gene suppresses HTT aggregation and toxicity (Meriin *et al*., 2002), and the effect of other Q-rich proteins upon polyQ aggregation and toxicity require Rnq1 in its [*PIN*$^+$] prion conformation (Duennwald *et al*., 2006a). Although no orthologue of Rnq1 is present in higher eukaryotes, hundreds of genes containing yeast prion-like regions have been identified in the human genome (Alberti *et al*., 2009, King *et al*., 2012), and therefore may serve as a simple model for understanding how prion-like proteins may modulate mutant HTT aggregation and toxicity.

The fruit fly has been widely exploited for the study of many protein-misfolding disorders, including polyQ-related disorders such as HD (Campesan *et al*., 2011, Green *et al*., 2012, Gunawardena *et al*., 2003, Jackson *et al*., 1998, Lee *et al*., 2004, Steffan *et al*., 2001, Steinert *et al*., 2012) and prion disorders (Choi *et al*., 2010, Deleault *et al*., 2003, Fernandez-Funez *et al*., 2010, Gavin *et al*., 2006, Murali *et al*., 2014, Robinson *et al*., 2014, Steinert *et al*., 2012). These *Drosophila* models resemble aspects of the corresponding human diseases and provide multiple experimental advantages that have allowed the identification of new molecular pathways underling disease pathogenesis. Unlike yeast models, fruit flies yield the multifactorial and age-dependent components thus serving as a better model to investigate the role of prion-like proteins on HD and other human protein misfolding disorders. In the present study, we generated a transgenic *Drosophila* model expressing Rnq1 to determine the effects of prion-like proteins during normal aging, and to elucidate further its contribution towards expanded polyQ-related toxicity. In addition, we employed the bimolecular fluorescence complementation (BiFC) assay (Herrera *et al*., 2011) to study the interaction between Rnq1 and mutant HTT in

living cells. Our results highlight prion-like proteins as probable players in the complex and dynamic network of protein-protein interactions that regulate mutant HTT misfolding, and thereby HD pathogenesis, and further support the potential therapeutic value of kynurenine 3-monooxygenase (KMO) inhibition in HD and other human pathologies involving protein misfolding and aggregation.

Results

Rnq1 exhibits prion-like properties in transgenic flies

In order to investigate whether previous observations in yeast involving Rnq1 (Bruce and Chernoff, 2011, Duennwald *et al*., 2006a, Kantcheva *et al*., 2014, Meriin *et al*., 2002, Ripaud *et al*., 2014, Wickner *et al*., 2008) are relevant in animal models, we generated transgenic flies carrying UAS-*RNQ1* and initially placed it under the control of the ubiquitously expressed *daGal4* driver using the GAL4/UAS system (see Materials and methods IV) (Brand and Perrimon, 1993). We confirmed Rnq1 expression in the 1M and 6M lines via QPCR (Figure S15, Supplemental information IV). To test whether the *RNQ1* transgenic flies produce Rnq1 with prion-inducing properties, we employed an adaptation of a prion-based *in vivo* transformation assay in yeast (Tanaka *et al*., 2004a). This assay exploits the [*PIN*$^+$] prion requirement for the *de novo* formation of the Sup35-based [*PSI*$^+$] prion that can in turn be induced by overexpression of Sup35 or its prion-forming region NM (Derkatch *et al*., 1997). The presence of the [*PSI*$^+$] prion can be detected by suppression of a nonsense mutation (*ade1-14*) in the *ADE1* gene that promotes phenotypic change in color (red to white; Ade$^-$ to Ade$^+$) in prion-containing [*PSI*$^+$] cells. Cells lacking the [*PSI*$^+$] prion are therefore unable to grow on a medium lacking adenine and appear red due to efficient translation termination at the premature UGA stop codon in the *ade1-14* allele. In contrast, aggregation of Sup35 into its [*PSI*$^+$]-aggregated form often leads to read-through of the *ade1-14* mutation detectable as growth of white/pink colonies on defined medium lacking adenine.

Brain homogenates were prepared from 56 day-old Rnq1-expressing and control *elavGAL4* flies and added to prion-free [*pin*$^-$][*psi*$^-$] cells along with the *URA3*-based plasmid p6442 that allows for overexpression of the Sup35NM domain. After selecting p6442 Ura$^+$ transformed cells, those that concomitantly acquire the [*PIN*$^+$] prion from the

protein extract show induction of the [*PSI*$^+$] prion when the Sup35 prion-forming domain (Sup35NM) is overexpressed (Sideri *et al*., 2011).

Forty-eight independent Ura$^+$ transformed colonies were isolated in each experiment and the *de novo* prion formation was scored as the number of Ura$^+$ colonies able to give rise to guanidine hydrochloride (GdnHCl)-curable [*PSI*$^+$] colonies (Figure 24A). GdnHCl is a reversible inhibitor of the Hsp104 chaperone that prevents continued [*PSI*$^+$] propagation leading to the generation of red [*psi*$^-$] colonies (Derkatch *et al*., 2000, Tuite *et al*., 1981). p6442-induced formation [*PSI*$^+$] was detected in less than 10% of control [*pin*$^-$] [*psi*$^-$] cells, a figure comparable to previous reported frequencies (Sideri *et al*., 2011). Co-transformation with protein lysates prepared from a [*PIN*$^+$] yeast strain increased the frequency of [*PSI*$^+$] colonies up to 20.1% confirming that the *de novo* formation of [*PSI*$^+$] is induced by [*PIN*$^+$] infection (Patel and Liebman, 2007). A high molecular weight pellet fraction prepared from Rnq1-expressing fly extracts, yielded the highest frequency of [*PSI*$^+$]-generating cells (34.4%), with similar infectivity observed for the crude fraction of the same fly lysate (31.9%). Notably, extracts prepared from flies not expressing Rnq1 (i.e. *elavGAL4*) gave a lower number of [*PSI*$^+$]-forming cells than those expressing Rnq1 (18.2% vs 33.2%). It is interesting to note, however, that transformation with crude and pellet extracts from *elavGAL4* driver control flies resulted in modest prion induction independent of Rnq1 expression (19.4% and 17%, respectively) (Figure 24A), suggesting the existence of an intrinsic activity in the fly that can drive the formation of the [*PSI*$^+$] prion.

To further explore the infectivity of fly produced Rnq1 molecules, Rnq1-induced [*PSI*$^+$] events were normalized to the *elavGAL4* background (Figure 24B). We observed a trend ($p=0.0624$) towards increased [*PSI*$^+$] conversion upon transformation using high molecular weight Rnq1 pellet over background. Notably, [*PSI*$^+$] formation was significantly elevated ~2-fold when total Rnq1-dependent (crude plus pellet) [*PSI*$^+$] events were considered (Rnq1 total). These data suggest that Rnq1 molecules synthesized in flies can seed the formation of the [*PSI*$^+$] prion, possibly by contributing to [*PSI*$^+$] propagation to the same extent as higher-order Rnq1 assemblies. This further supports the role of Rnq1 as an infectious agent with the ability to self-propagate between different species, acting as a seed for the *de novo* formation of misfolded prion-like proteins.

A **Frequency of [*PSI*$^+$] formation**

Seed	No. [*PSI*$^+$] colonies			Average % Infectivity
	Assay 1	Assay 2	Assay 3	
None	5	1	8	9.7
[*PIN*$^+$] yeast	11	8	10	20.1
elavGAL4 crude	7	7	14	19.4
elavGAL4 pellet	3	10	12	17
elavGAL4 total	*10*	*17*	*26*	*18.2*
Rnq1Dm crude	9	18	19	31.9
Rnq1Dm pellet	13	14	23	34.4
Rnq1Dm total	*22*	*32*	*42*	*33.2*

No., number of; Dm, *Drosophila melanogaster*

B

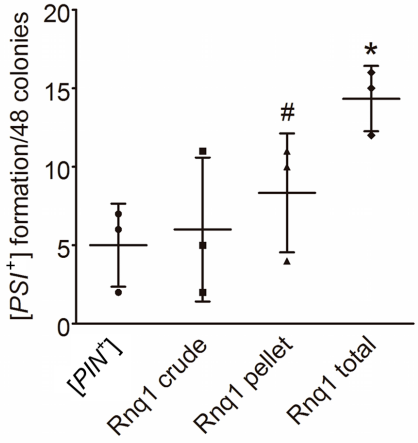

Figure 24. Brain extracts from Rnq1 expressing flies increase *de novo* formation of the [*PSI*$^+$] prion in yeast. (A) The infection potential of the fly-expressed Rnq1 was assayed in yeast cells by means of yeast prion transformation (95). Protein extracts from aged Rnq1 expressing flies were introduced into sphaeroplasts prepared from an *ura3* [*pin*$^-$][*psi*$^-$] yeast strain by co-transformation with the plasmid p6442 (*pCUP1-SUP35NM-URA3*). Following a period of overexpression of Sup35NM to induce the formation of the [*PSI*$^+$] prion, colonies formed from [*PSI*$^+$] cells were scored using a nonsense suppressible *ade1-14* allele by growth on medium lacking adenine and confirmed by loss of the white [*PSI*$^+$] phenotype following growth in the presence of 4 mM GdnHCl. "Total" represents grouped measurements of pellet and crude samples from the same fly brain lysates. Average % infectivity refers to the frequency (%) of [*PSI*$^+$] cells formed per 48 Ura+ transformants analyzed. (B) Total Rnq1 was significantly more infectious in comparison to protein Total *elavGAL4* flies not expressing Rnq1. For each condition, the number of [*PSI*$^+$] colonies arising in controls (e.g. None, *elavGAL4*) was subtracted from the experimental colonies (e.g. [*PIN*$^+$], Rnq1) in order to eliminate background effects, and a one sample t test was employed for analyses (see Materials and methods IV). The data illustrate the three independent assay values upon normalization and their mean ± SD. *p<0.05; $^{\#}$p=0.0624.

Rnq1 expression induces age-dependent neurodegeneration and causes motor dysfunction in Drosophila

The presence of misfolded prion proteins in humans is associated with a range of brain pathologies (Mead and Reilly, 2015, Rahimi and Kovacs, 2014), although the importance of the physiological role of the prion protein has not yet been fully established. In yeast, prions can confer phenotypic benefits to the host, and are thought to play a role as functional amyloidogenic proteins in certain conditions (Eaglestone *et al*., 1999, Stein and True, 2011, True and Lindquist, 2000, True *et al*., 2004), while in other paradigms overexpression can lead to severe toxicity (Douglas *et al*., 2008). To investigate the effect of Rnq1 expression in *Drosophila*, we drove expression of Rnq1 pan-neuronally with the *elavGAL4* driver or in motor neurons using the *c164GAL4* driver, and assayed for

neurodegenerative phenotypes and behavior impairments in adult flies and larvae (Figure 25 and 26). We assessed neurodegeneration of Rnq1-expressing flies by scoring degeneration of adult rhabdomeres at different time-points, from day 1 to day 56. When expressed under the control of *elavGAL4*, Rnq1 caused photoreceptor loss in an age-dependent manner (Figure 25A). A significant decrease in rhabdomere number was observed in RNQ1-1M flies at 21 days, and neuronal loss progressively increased in older flies (genotype x age interaction, $p<0.05$, Figure 25A). We found a similar trend in RNQ1-6M flies, although these decreases were only significant at 56 days of age (Figure 25A). This is consistent with *Drosophila* models of PD (Feany and Bender, 2000) and prion diseases (Fernandez-Funez *et al*., 2010), where neurodegeneration is observed only in aging animals.

While young control flies exhibit strong negative geotactic responses manifested by their ability to rapidly climb to the top of a vial, a decline in motor performance is observed as they age (Figure 25B) (Breda *et al*., 2015, Breda *et al*., 2016). We found that both RNQ1-1M and RNQ1-6M transgenic flies developed premature motor dysfunction, showing a decline in climbing ability relative to controls at every time point tested (Figure 25B). Furthermore, Rnq1-related degenerative changes were not restricted to the brain, as analysis of total motor activity in *c164GAL4*-driven Rnq1 flies revealed a reduction of ~21-36% in movement compared to driver and *UAS* controls (Figure 25C). Interestingly, a significant decrease in activity in the dark was observed for the Rnq1 flies versus controls (Figure 25D), which was accompanied by greater sleep-like behavior (Figure S16, Supplemental information IV).

Next, we asked whether Rnq1 expression could compromise behavior during early developmental stages. Third instar larvae display innate crawling behavior characterized by periods of movements in a specific direction followed by pauses during which the surrounding area is explored and direction may be altered (turns) (Wang *et al*., 1997). Expression of Rnq1 either in the nervous system (Figure 26A-D) or specifically in motor neurons (Figure 26E-G) resulted in abnormal larval crawling behavior. Interestingly, our Rnq1 expressing larvae displayed nearly identical crawling phenotypes to those previously observed in HD larvae (Steinert *et al*., 2012) (Figure 26B, C, E and F), which resulted in fewer turns and greater crawling activity relative to controls (Figure 26D and G).

Together with our prion infectivity observations, these results suggest that although Rnq1 has no detrimental effects on fruit fly viability and survival (Figure S17, Supplemental information IV), it promotes neuronal dysfunction during development,

suggesting the occurrence of early prion-like protein misfolding events that precede neuronal loss in older individuals.

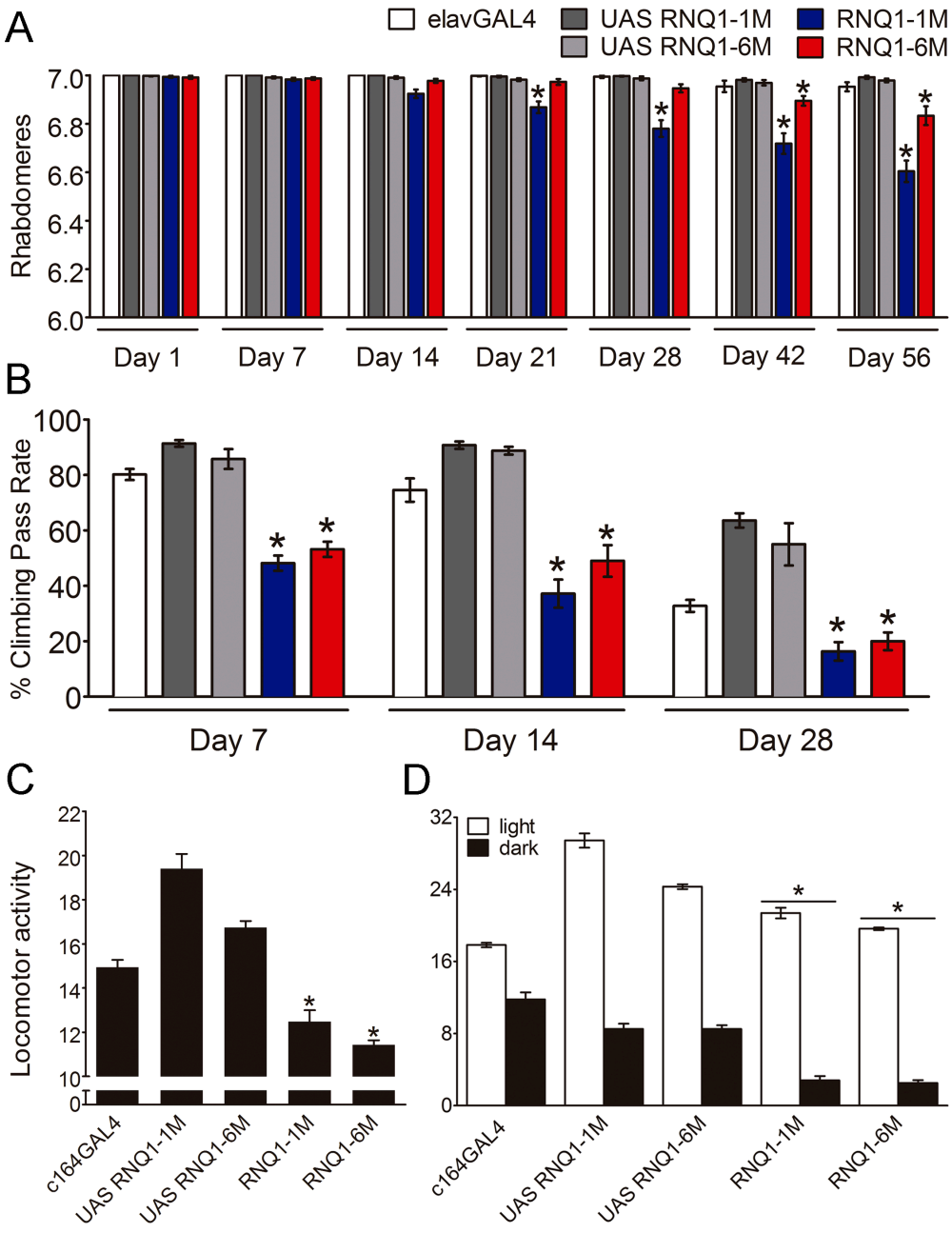

Figure 25. *RNQ1* transgenic flies exhibit age-dependent neurodegeneration and early motor dysfunction. (A) Neuronal loss caused by Rnq1 pan-neuronal expression was assessed in aged RNQ1-1M or RNQ1-6M *Drosophila* lines at different time-points (1, 7, 14, 21, 28, 42 or 56 days post-eclosion). (B) Climbing activity of Rnq1 expressing flies under the control of *elavGAL4*. Fifty flies from each group were examined in 10 consecutive climbing assay tests at day 7, 14 or 28 post-eclosion. Values on the Y-axis represent the percentage of flies that successfully climbed above the threshold line of 8 cm within 10 s. (C, D) Total locomotor activity was assayed in new-emerged flies, using Trikinetics *Drosophila* monitors. Flies expressing Rnq1 in the motor neurons showed reduced overall activity in comparison to controls (C).

Analysis of mean activity levels during 12 h light/dark cycles reveals that decreased activity levels occur during the dark phase (D). Locomotor activity is represented as the average number of infrared beam crossings per 30 min of recording interval over 7 days in 12 h light/dark cycles. Comparisons are versus *elavGAL4* or *c164GAL4* and respective UAS controls, *p<0.05. All data are shown as the mean ± SEM.

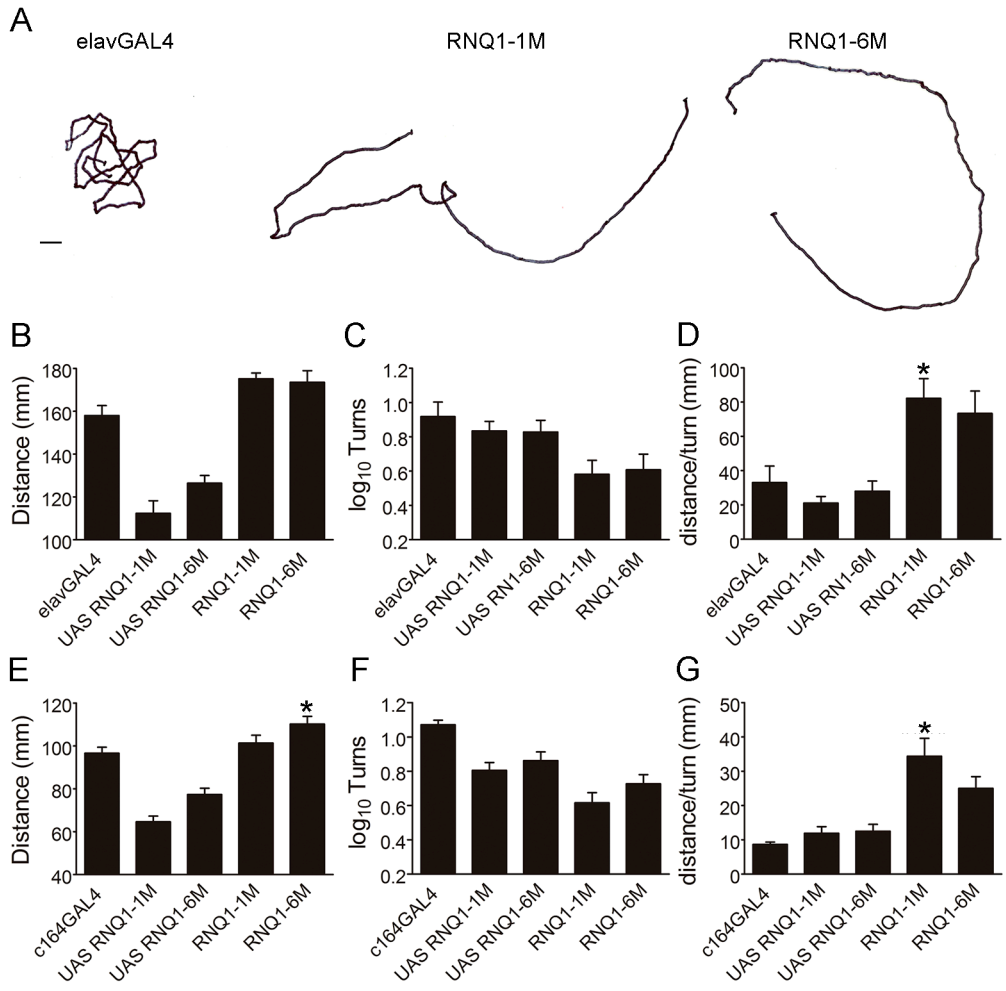

Figure 26. Rnq1 expression induces abnormal larval crawling. (A) Representative crawling behavior produced by *elavGAL4* control and pan-neuronal RNQ1-1M or RNQ1-6M expression in third instar larvae. Larva crawling activity was manually monitored for 2 min in a temperature controlled room and expressed as crawling distance travelled (mm) (B, E), number of turns (C, F) and distance/turns (D, G) in larvae expressing Rnq1 driven to all nervous system (B-D) or specifically to motor neurons (E-G) by the *elav* or the *c164* promoter, respectively. Comparisons are versus *elavGAL4* or *c164GAL4* and respective UAS controls, *p<0.05. Data are mean ± SEM.

Prion-like proteins exacerbate disease-relevant phenotypes in a Drosophila model of HD

Since Rnq1 increases mutant HTT toxicity in yeast (Meriin *et al*., 2002), we sought to extend these findings by using a well-characterized *Drosophila* model of HD, in which the expression of a mutant HTT exon 1 encoding fragment (93QHTTex1) is directed to the

nervous system of the fruit fly using *elavGAL4* (Steffan *et al*., 2001) (also described in Chapter I and III, section A). We found that Rnq1 expression potentiated 93QHTTex1 phenotypes in *Drosophila* (Figure 27). Co-expression of Rnq1 with 93QHTTex1 resulted in a significant increase in neuronal loss at day 1 (Figure 27A) and day 7 post-eclosion (Figure 27A and B). We also observed a 3-day reduction in the lifespan of flies expressing both 93QHTTex1 and RNQ1-1M transgenes versus the UAS titration control (GFP + HTT) (Figure 27C), while RNQ1-6M + HTT co-expressing flies exhibited a modest reduction in lifespan relative to control flies (Figure 27D). Moreover, the eclosion of 93QHTTex1 expressing flies was significantly decreased in the presence of Rnq1 (Figure 27E and F), indicating that Rnq1 promotes developmental defects during late metamorphosis that further compromise the emergence of adult HD flies. Rnq1-induced toxic effects on viability of HD flies appear to reflect potentiation of mutant HTT toxicity and not solely additive effects, as Rnq1 expression did not affect eclosion or survival in wild-type backgrounds (Figure S17, Supplemental information IV). In order to investigate Rnq1 effects upon 93QHTTex1 toxicity during early developmental stages, we assessed the motor behavior of third instar larvae. Specific expression of Rnq1 in motor neurons using the *c164GAL4* driver led to significant defects in locomotion in comparison to controls, and a modest enhancement of motor impairments in HD larvae (Figure 28). These data provide additional evidence supporting Rnq1 as a modulator of mutant HTT toxicity, and suggest a potential role for prion-like proteins in HD pathology.

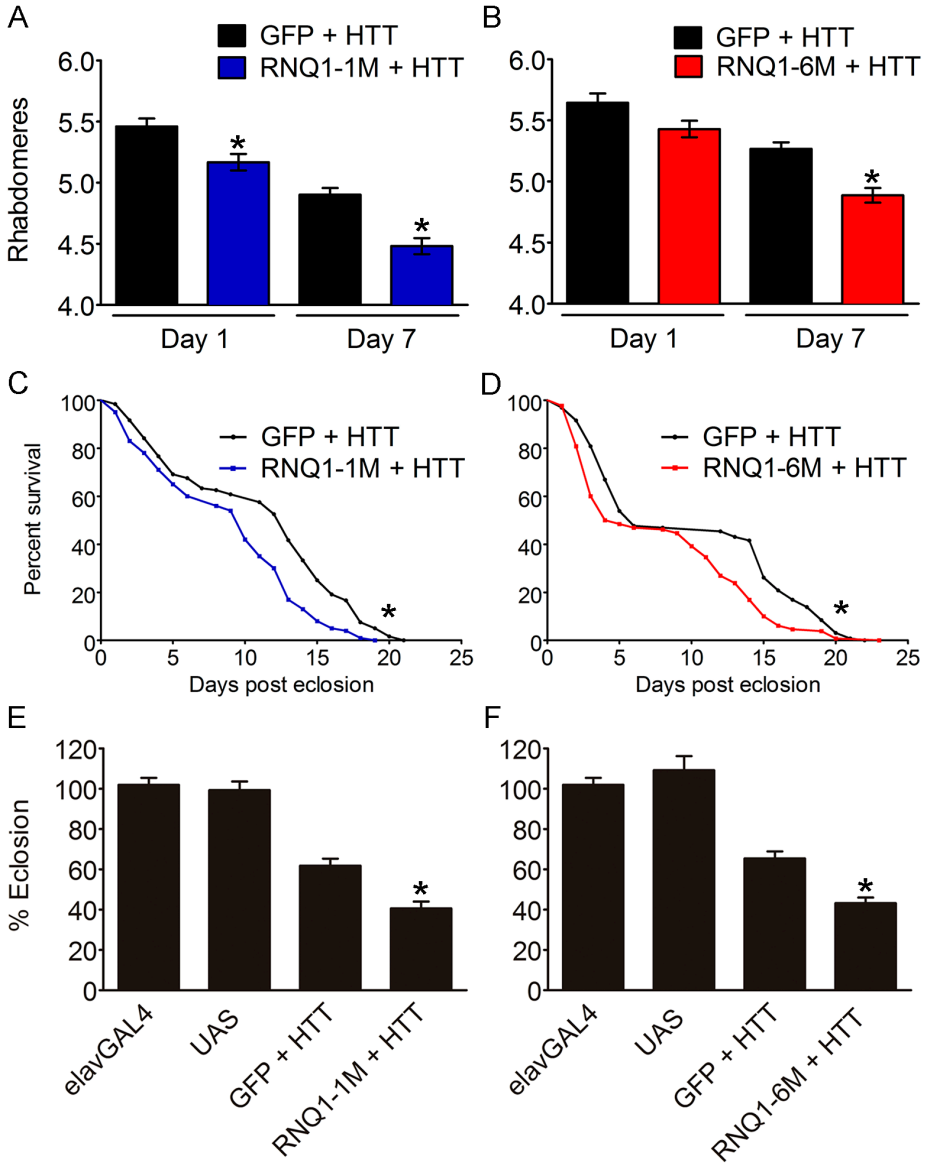

Figure 27. Rnq1 expression potentiates mutant HTT toxicity in *Drosophila*. Transgenic fly lines exhibiting pan-neuronal expression of 93QHTTex1 and RNQ1 (RNQ1-1M + HTT, left panels; RNQ1-6M + HTT, right panels) were analyzed for photoreceptor number (A, B), survival (C, D) and viability (E, F). (A, B) Quantification of mean rhabdomeres (±SEM) per ommatidium at day 1 or day 7 after eclosion. Rnq1 and 93QHTTex1 co-expressing flies showed significantly increased neurotoxicity when compared to GFP + HTT flies. (C, D) Rnq1 expression reduces lifespan of HD transgenic flies. Values on the Y-axis represent the percentage of flies alive at each time point analyzed. The mean values indicate the number of days it took for half of the flies to die (50% survival): GFP + HTT (mean = 13 days, left panel, C; mean = 6 days, right panel, D), RNQ1-1M + HTT (mean = 10 days), RNQ1-6M + HTT (mean = 4.5 days). (E, F) Percentage of eclosion (mean ratio of female/male flies ± SEM per vial). Female progeny express 93QHTTex1 pan-neuronally, whereas male progeny are wild-type. The ratio of female/male flies per vial (expected ratio 1:1) emerging over a 10 day period reveals a substantial deficit of 93QHTTex1 expressing females relative to male controls. The eclosion deficit caused by 93QHTTex1 expression is significantly enhanced by the presence of Rnq1. Comparisons are versus GFP + HTT, *$p<0.05$.

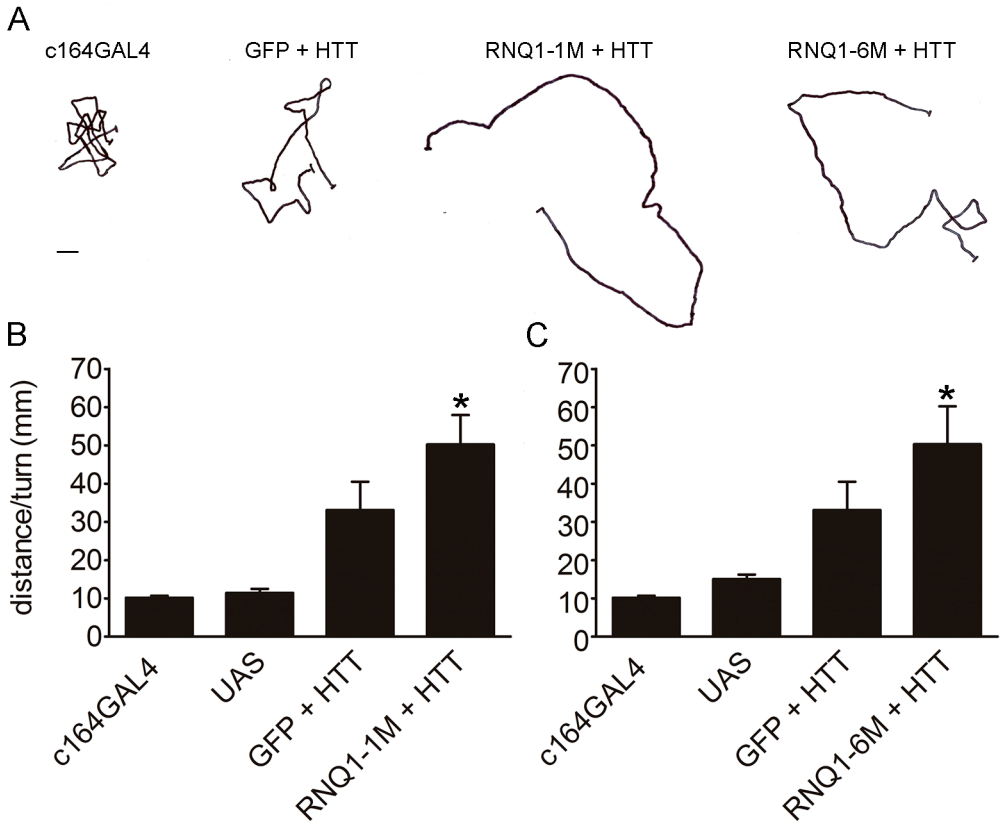

Figure 28. Rnq1 expression enhances defective locomotor behavior of HD third instar larvae. (A) Representative crawling traces of control (*c164GAL4*) and larvae expressing GFP + HTT, RNQ1-1M + HTT or RNQ1-6M + HTT in motor neurons via the *c164GAL4* driver. (B, C) Co-expression of Rnq1 and 93QHTTex1 induce greater larval crawling activity as observed by a significant increase in distance travelled (mm) in comparison to GFP + HTT (left panel). Data are mean distance/turn (mm) ± SEM. Comparisons are versus both *c164GAL4* and respective UAS-*RNQ1* control, *p<0.05. Scale bar, 10 mm.

To further support these findings, we interrogated whether the murine prion protein (MoPrP) could induce similar neuropathology in our *Drosophila* HD model. Mammalian prions are associated with transmissible spongiform encephalopathies (Colby and Prusiner, 2011) and are found to co-exist with other aggregation-prone proteins in neurodegenerative disease-affected brains (Adjou *et al*., 2007, Haik *et al*., 2002, Miyazono *et al*., 1992, Rahimi and Kovacs, 2014). Consistent with a previous study showing that MoPrP exacerbates expanded polyQ-dependent morphological defects in *Drosophila* eyes (Park *et al*., 2011), we found that both the wild-type version of MoPrP (WT PrP), as well as MoPrP containing a human prion disease-associated mutation (P101L PrP), enhanced rhabdomere degeneration in 93QHTTex1 flies (Figure 29A). However, WT PrP had no effect on survival (Figure 29B) or eclosion (Figure 29C), while P101L PrP expression significantly impaired lifespan (Figure 29B) and development (Figure 29D) of HD flies. The differences

in viability outcome measures could be explained by the low propensity of WT PrP to accumulate in *Drosophila* brain neurons (Deleault *et al*., 2003). In contrast, P101L PrP rapidly accumulates as misfolded prion-like conformers (Gavin *et al*., 2006), which may increase the rate of protein misfolding and sequestration into toxic aggregates, thus resulting in accelerated neuropathology and premature death in larval and adult stages. Interestingly, MoPrP expression had no toxic effects on normal aging (Figure S18A, Supplemental information IV) and development (Figure S18C and D, Supplemental information IV) of wild-type background flies, while affecting their long-term survival (Figure S18B, Supplemental information IV).

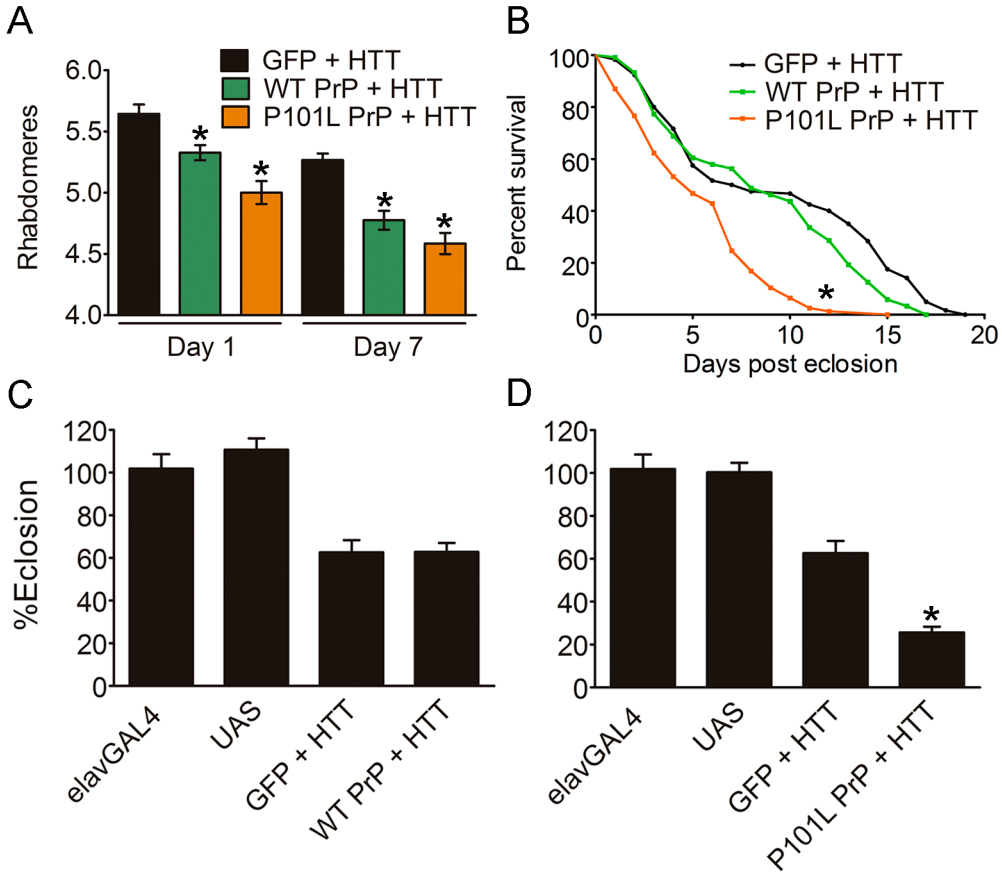

Figure 29. Expression of murine prion protein exacerbates disease-relevant phenotypes in HD transgenic flies. (A) Expression of either wild-type (WT) or mutated (P101L) PrP caused an increased in neuronal loss of 93QHTTex1 transgenic flies. Data are represented as the number of rhabdomeres per ommatidium (mean ± SEM). (B) Expression of P101L PrP decreased lifespan of HD flies by ~2.5 days and WT PrP did not alter survival rate. GFP + HTT (mean = 7.5 days), WT PrP + HTT (mean = 8 days), P101L PrP + HTT (mean = 5 days). Murine P101L PrP (D) impairs fly viability during development as observed by the increased eclosion deficit of pan-neuronal 93QHTTex1 expressing flies. Comparisons are versus GFP + HTT, *p<0.05.

Rnq1 interacts and forms inclusions with mutant huntingtin in living mammalian cells

It is widely accepted that Rnq1 modulates polyQ aggregation in yeast cells (Kantcheva *et al*., 2014, Meriin *et al*., 2002), but the molecular mechanisms underlying this effect are unclear. Whether Rnq1 prion formation precedes polyQ aggregation serving as a nucleation-promoting factor for amyloid replication, or indirectly acts on polyQ aggregation after it has already been established needs to be clarified. The BiFC assay is commonly used for studying protein-protein interactions in living cells and serves as a robust tool to visualize the initial steps of aggregate formation, including the dimerization or oligomerization of misfolding-prone proteins (Goncalves *et al*., 2010). To further explore the role of Rnq1 on mutant HTT aggregation, we employed our recently developed HTTex1 BiFC cellular model, based on the fusion of two non-fluorescent halves of the Venus fluorescent reporter to HTTex1 constructs (Herrera *et al*., 2011, Herrera and Outeiro, 2012). Different combinations of wild-type (19Q) or mutant (97Q) HTTex1, as well as RNQ1-Venus BiFC plasmids (Figure 30A) were transfected into mammalian cells and the recovered emitting fluorescence was assessed by flow cytometry as an indication of direct protein interactions. Similar to our previous reports (Herrera *et al*., 2011), 97QHTTex1-Venus BiFC pairs caused increased levels of fluorescence in comparison to 19QHTTex1-Venus BiFC pairs (Figure 30B and C), suggestive of higher rates of dimerization/oligomerization. Co-transfection of RNQ1- and 97QHTTex1-Venus plasmids produced fluorescence as measured by the number of fluorescent cells (Figure 30B) and average fluorescence intensity (Figure 30C), suggesting a direct physical interaction between the two proteins, though much reduced in comparison to 97QHTTex1-Venus BiFC pairs. Analysis of 97QHTTex1-transfected cells by fluorescence microscopy confirmed the presence of both cytosolic oligomeric species and large aggregates, visualized as homogenously distributed fluorescence and very bright foci, respectively (Figure 30D) (Herrera *et al*., 2011). When co-transfected with RNQ1, 97QHTTex1 changed its subcellular localization, accumulating as oligomeric species in all cell compartments, including the nucleus (Figure S19, Supplemental information IV). Moreover, Rnq1 co-aggregated with 97QHTTex1 generally altering its aggregation pattern towards the formation of fewer but larger aggregates in the cytosol (Figure 30E). These aggregates were often visualized as amorphous intracellular inclusions with no defined boundaries, suggesting that Rnq1 might alter aggregate morphology to facilitate toxic interactions (Duennwald *et al*., 2006a, Giorgini *et al*., 2005).

In spite of the increased propensity of heterogeneous polyQ aggregates formed by unrelated Q-rich proteins to translocate to the nucleus in mammalian cells (Preisinger *et al*., 1999), no RNQ1/97Q aggregates were observed within the nucleus (Figure 30E and Figure S19, Supplemental information IV). The biophysical properties of forming aggregates were then analyzed by means of filter trap assays. We found that the amount of large SDS-insoluble aggregates composed of mutant HTT was significantly enhanced in cells transfected with both RNQ1 and 97QHTTex1 BiFC constructs (Figure 30F and H). This effect is even more notable if we consider that only one copy of 97QHTTex1 was being expressed in the RNQ1/97Q group (Figure 30G and I). Unexpectedly, we were unable to detect Rnq1 protein levels by standard immunoblot procedures using an anti-Rnq1 antibody (Santa Cruz Biotechnology Inc., Dallas, Texas, USA) (data not shown), suggesting that Rnq1 might adopt a different conformation once expressed in mammalian cells, masking the epitopes recognized by the antibodies. To overcome this, we carried out immunocytochemistry (ICC) in RNQ1 and 97QHTTex1 co-transfected cells, which was more sensitive, allowing the detection of Rnq1 throughout the cell and within BiFC aggregates (Figure 30J). In total, these results suggest that Rnq1 likely associates with HTT and accelerates polyQ aggregation. However, mutant HTT appears to be more prone to dimerize/oligomerize than to interact with Rnq1, indicating that this interaction is likely rather transient - consistent with the occurrence of highly stable Rnq1 prion conformations (Patel and Liebman, 2007).

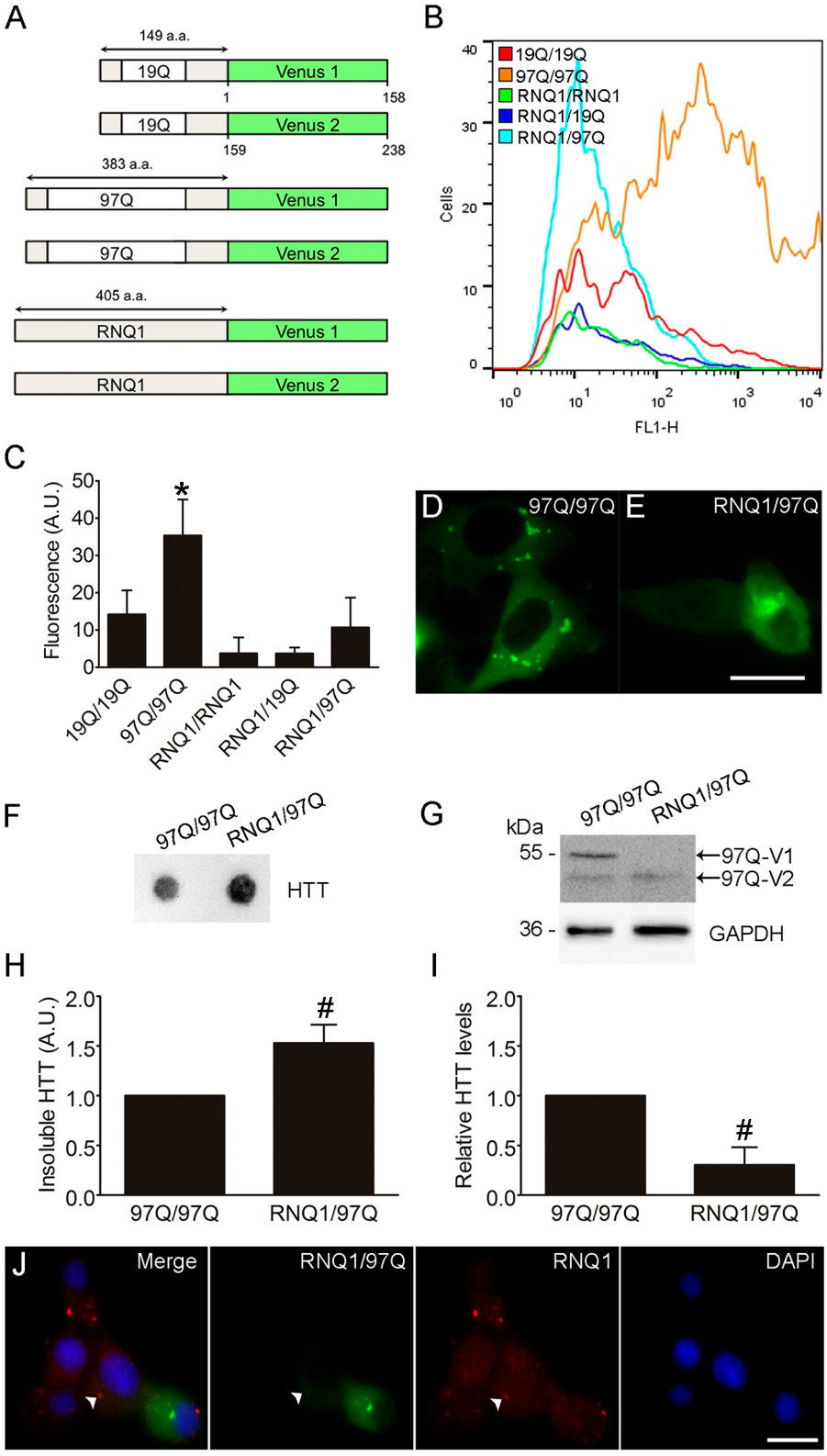

Figure 30. Rnq1 interacts with mutant HTT and alters its aggregation in living cells. (A) Schematic representation of HTTex1 and RNQ1 BiFC constructs. (B-E) Cells were transfected with the indicated pairs of BiFC constructs, and analyzed for fluorescence levels (B, C) and formation of large inclusions (D-J) by flow cytometry or widefield fluorescence microscopy, respectively. Co-transfection of RNQ1-Venus and 97QHTTex1-Venus plasmids causes an increased number of fluorescent cells (B) and

similar average fluorescence to the 19Q/19Q control, indicating the generation of RNQ1/97Q dimers (C). The 97QHTTex1 BiFC pair is mostly localized in the cytosol as both diffuse fluorescence and large inclusions (D). Co-transfection of RNQ1-Venus and 97QHTTex1-Venus plasmids results in the cytosolic accumulation of larger insoluble species (E). (F) Representative filter trap assay and (G) immunoblotting (SDS-PAGE) of total protein extracts under native conditions. (H) Quantification of HTT SDS-insoluble species and (I) corresponding HTT protein expression levels. (J) Rnq1 antibody (1:500, Santa Cruz Biotechnology Inc., Dallas, Texas, USA) (in red) localizes to RNQ1/97Q BiFC inclusions (in green) (white arrows). Data is mean ± SD. *significant versus 19Q/19Q, #significant versus 97Q/97Q, $p < 0.05$. Scale bars, 20 μm. AU, arbitrary units.

Kynurenine pathway metabolism contributes to Rnq1 neurotoxicity in Drosophila

We were next interested in exploring the mechanisms downstream of Rnq1 expression that contribute to the neurotoxicity observed. We have previously shown that dysregulation of kynurenine pathway (KP) metabolism contributes to neurodegeneration in flies expressing mutant HTT, α-syn, and Aβ (Breda *et al*., 2016, Campesan *et al*., 2011). The KP is the primary route of tryptophan degradation in mammals, and contains several potent neuroactive and immunomodulatory intermediates – e.g. kynurenic acid (KYNA), 3-hydroxykynurenine (3-HK), and quinolinic acid (QUIN) - which have been implicated in numerous neurodegenerative disorders, including HD. Genetic or pharmacological inhibition of kynurenine 3-monooxygenase (KMO) modulates the levels of these neuroactive metabolites, thereby ameliorating disease-relevant phenotypes in models of HD, PD and AD (Breda *et al*., 2016, Campesan *et al*., 2011, Giorgini *et al*., 2005, Giorgini *et al*., 2008, Maddison and Giorgini, 2015, Zwilling *et al*., 2011). Since Rnq1 expression enhanced HD-relevant phenotypes in *Drosophila*, we hypothesized that KP dysfunction may also be involved in prion-like-mediated toxicity.

In order to address this question, we used RNAi to silence *cinnabar* (*cn*), the fly homolog for the KMO gene, in Rnq1-expressing flies. Since *cn* is located on the 2nd chromosome, we first characterized two transgenic lines encoding *RNQ1* on the 3rd chromosome (RNQ1-2M and RNQ1-3M) in order to simplify the genetic crosses. In agreement with the experiments described above (Figure 25 and 26), pan-neuronal Rnq1 expression caused neurodegeneration (Figure S20A, Supplemental information IV) and climbing impairments (Figure S20B, Supplemental information IV) in both RNQ1-2M and RNQ1-3M transgenic flies. Additionally, expression of Rnq1 in motor neurons using the *c164* driver resulted in abnormal larvae crawling behavior (Figure S20C and D, Supplemental information IV). Although rhabdomere degeneration in these transgenic

lines is more modest (Figure 31A and Figure S21A, Supplemental information IV), we found that *cn* downregulation was able to rescue the observed neuronal loss in aged RNQ1-2M (Figure 31A) and RNQ1-3M flies (Figure S21A, Supplemental information IV). KMO inhibition also significantly ameliorated climbing performance of Rnq1 expressing flies compared with the corresponding controls (Figure 31B and Figure S21B, Supplemental information IV). These observations suggest the KP plays a role in Rnq1 toxicity, indicating a possible overlap between the mechanisms of mutant HTT and Rnq1 toxicity.

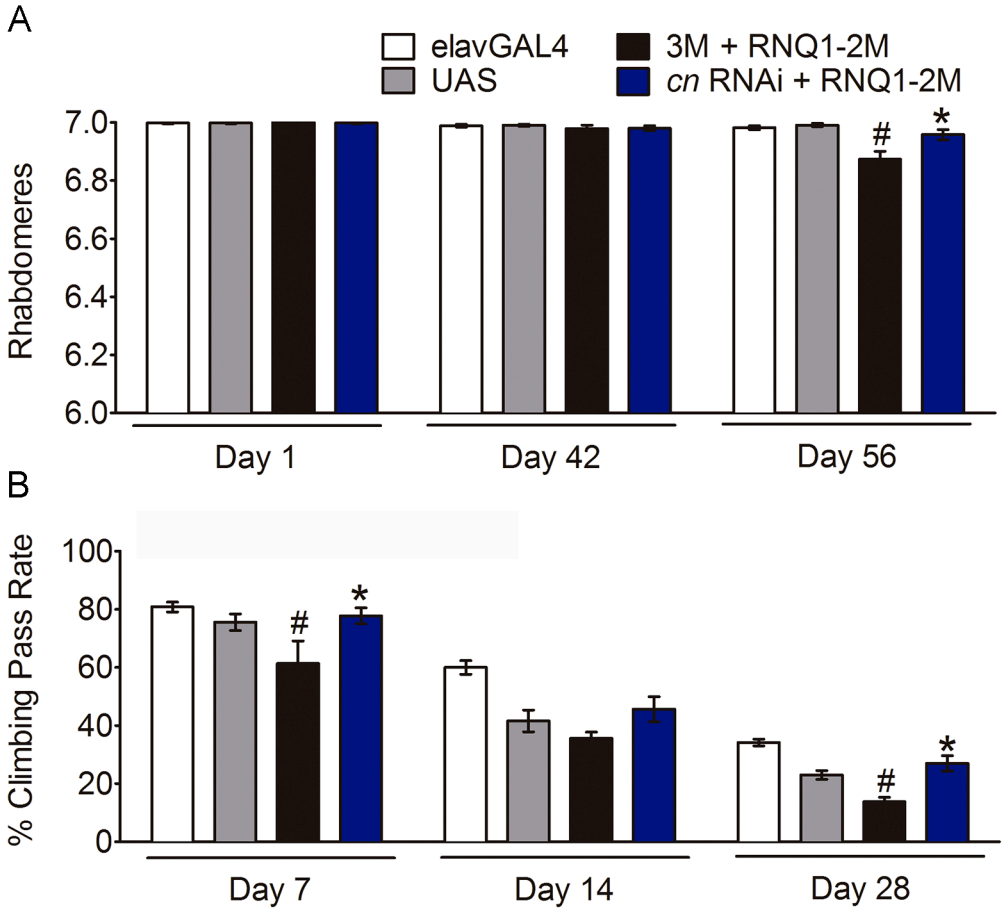

Figure 31. KMO genetic inhibition ameliorates neurodegeneration and locomotor impairments of *RNQ1* transgenic flies. (A) Average number of rhabdomeres per ommatidium. Downregulation of the *Drosophila* KMO gene *cinnabar* (*cn*) rescues neuronal loss exhibited by aged *elav*-driven Rnq1 expressing flies. (B) Climbing deficits are significantly rescued when *cn* is knocked down in pan-neuronal Rnq1 expressing flies. All data are mean ± SEM. *significant versus 3M + RNQ1-2M, #significant versus *elavGAL4* and UAS 3M + RNQ1-2M controls, $p<0.05$.

Discussion

Misfolding of specific proteins into pathological conformations and their accumulation in the brain is a common feature of nearly all neurodegenerative disorders. As such, developing therapeutic approaches have focused on treating these disorders by preventing the formation and deposition of amyloid peptides. However, neuronal toxicity is not always associated with protein aggregation and may depend on the proteome composition and particular cellular environments. Recent studies have suggested prion-like proteins as co-factors in the misfolding of other aggregation-prone proteins and subsequent extracellular spreading of toxic aggregates (Salazar and Strittmatter, 2017, Urrea *et al*., 2017), which is thought to precede neurodegeneration and the appearance of clinical symptoms (Brundin *et al*., 2010). Thus, in addition to directly blocking amyloid formation, a better understanding on how these molecular species contribute to neurotoxicity may aid in the development of more effective therapies.

The Rnq1 prion is central to mutant HTT-mediated toxicity in yeast (Mason and Giorgini, 2011) and the yeast Sup35 prion domain has been found to modulate polyQ toxicity in flies (Li *et al*., 2007), suggesting that abnormal expression of proteins containing Q/N-rich regions could be involved in HD pathogenesis. Here, we have extended these findings by generating transgenic *Drosophila* lines that express Rnq1 which may induce the formation of molecules with prion-like properties. We show that Rnq1 elicits several disease-relevant phenotypes throughout the *Drosophila* lifecycle, ultimately leading to premature neuronal loss in aging flies. We propose that Rnq1 enhances mutant HTT-induced toxicity by altering the morphology of polyQ-containing aggregates, making them more accessible to toxic interactions.

Behavioral assessments showed that Rnq1 expression caused an early and rapid decline in adult motor function and enhanced sleep, which did not parallel the degeneration of fly photoreceptors (Figure 25 and Figure S16, Supplemental information IV). Indeed, significant neuronal loss was only detected in advanced stages of aging, indicating that Rnq1 may induce functional defects that occur prior to neuronal death. As mitochondrial function is found to be impaired in models of prion disease (Sikora *et al*., 2009, Siskova *et al*., 2010), it is possible that the low locomotor performance of Rnq1 expressing flies is due to early neuronal dysfunction involving altered mitochondrial metabolism that ultimately leads to neurodegeneration. In addition, as the flies age, Rnq1 molecules could

undergo prion-like conformational changes accumulating as pathogenic amyloids and/or amplifying misfolded forms of other molecules, thereby increasing neuronal vulnerability. This is supported by the high infectious potential of brain homogenates from aged Rnq1 expressing flies (Figure 24). Our interpretation is in accordance with reports from other *Drosophila* models of protein misfolding-related disorders showing that pre-fibrillar protein conformations cause altered locomotor activity and sleep disturbances in young flies prior to neuronal degeneration (Gajula Balija *et al*., 2011, Karpinar *et al*., 2009), suggesting that these phenotypes may be caused by early impairment of neuronal function rather than neuronal death.

Although Rnq1 expression did not compromise viability of wild-type flies (Figure S17, Supplemental information IV), their normal development was affected as indicated by abnormal larval crawling phenotypes (Figure 26). In the context of protein misfolding disorders, differences in crawling phenotypes have been associated with protein-specific patterns of aggregation and distribution throughout neurons (Jakubowski *et al*., 2012). For example, expression of α-syn causes larvae to crawl shorter distances (Breda *et al*., 2015), whereas mutant HTT expressing larvae typically exhibit weaker exploratory crawling behavior, but greater crawling distances when compared to wild-type larvae (Steinert *et al*., 2012). Rnq1 expression resulted in greater larval crawling activity, which is in accordance with a previous report on the murine prion-expressing larvae (Robinson *et al*., 2014), and may indicate a possible similarity between prion- and polyQ-like patterns of aggregation, and downstream consequences of these events.

The presence of Rnq1 prion conformers has been linked to cytotoxicity of polyQ aggregates (Duennwald *et al*., 2006a, Meriin *et al*., 2002). This toxicity may arise from the recruitment of essential proteins during prion amyloidogenesis or alternatively, through direct interaction between prion-like proteins and polyQ aggregates which could convert each to novel toxic conformations. Our experiments in *Drosophila* indicate that Rnq1 enhances mutant HTT toxicity (Figure 27 and 28), perhaps via direct interactions between these proteins and consequent alteration in aggregation and cellular distribution (Figure 30). Similarly, previous studies in yeast demonstrate that Rnq1 co-localizes with mutant HTT, facilitating the translocation of soluble HTT into the nucleus (Douglas *et al*., 2009), and leading to the formation of distinct types of polyQ aggregates in the cytoplasm (Duennwald *et al*., 2006a). While the accumulation of HTT in the nucleus is directly related with cytotoxicity (Douglas *et al*., 2009), the combination of mutant HTT with other Q-rich proteins can lead to toxic and non-toxic outcomes, depending on the interacting

protein and on the nature of this interaction (Duennwald *et al*., 2006b, Duennwald *et al*., 2006a, Kayatekin *et al*., 2014, Ripaud *et al*., 2014). Nevertheless, there are likely common features of misfolding and aggregation that would determine the toxicity of polyQ aggregates.

Interactions between Rnq1 and mutant HTT resulted in the formation of large aggregates, whose appearance was different from the aggregates formed exclusively by mutant HTT. In addition, cells expressing both Rnq1 and mutant HTT often exhibited an amorphous structure forming at a single location in the cytoplasm. Interestingly, we noted that some of these large heterogeneous structures were visualized as a condensed collection of many small aggregates (Figure S19, Supplemental information IV), which could explain the increased amount of SDS-insoluble species seen in filter traps. Thus, one may speculate that prion-like proteins might contribute to the formation of toxic polyQ aggregates through two complementary mechanisms of action. First, they could increase the rate of polyQ aggregation by acting as mediators for highly efficient conversion of mutant HTT misfolding. Therefore, the rapid production of aggregation-prone misfolded molecules may exceed the capacity of cellular defense mechanisms (Johnston *et al*., 1998), resulting in accumulation into amorphous aggregates with larger surface areas, hence potentially becoming more susceptible to toxic interactions with other cellular factors or organelles (Duennwald *et al*., 2006a, Giorgini *et al*., 2005). In addition, prion-like proteins impair autophagy in the context of HD (Park *et al*., 2011), which could account for enhanced polyQ aggregation and toxicity. Second, it is possible that the unique properties of Rnq1 would allow the fragmentation of co-aggregates promoting their assembly into small aggregates organized in highly compacted structures.

The *de novo* prion formation in yeast underlies aggregate fragmentation mediated by molecular chaperones. In particular, Hsp104 is required for prion maintenance and seeding of polyQ aggregates (Meriin *et al*., 2002), suggesting that molecular chaperones may intercalate into co-aggregated structures via Rnq1 to control the release of "seeds" that would trigger prion-like spreading of toxic misfolded forms to neighboring cells. Evidence suggesting that Rnq1 contains a site for Sis1 binding, and that the Hsp40-Sis1 complex is essential for prion propagation (Douglas *et al*., 2008), supports such a role for Rnq1 in polyQ aggregate propagation. Notably, *Drosophila* has a homolog for Sis1 (*DROJ1*) (Lopez *et al*., 2003), suggesting that a similar mechanism might occur in our *Drosophila* HD model upon expression of Rnq1 to facilitate prion-like transmission of HTT aggregates in the fly brain (Babcock and Ganetzky, 2015, Pearce *et al*., 2015), and

would at least partially account for the enhanced neurotoxicity observed. Although small polyQ aggregates consisting of β-sheet structures are more likely to bind to cell surfaces, and therefore to be transferred between cells (Trevino *et al*., 2012), we cannot exclude the possibility that toxicity may also derive from the difficulty to eliminate such stable aggregates (Douglas *et al*., 2009) via the ubiquitin-proteasome system (Collinge and Clarke, 2007).

We observed that both types of aggregates formed in our mammalian cell system were usually localized adjacent to the nucleus. Prion-like proteins are found to co-aggregate with mutant HTT in specific yeast subcellular locations (Kayatekin *et al*., 2014), known as quality control compartments for the deposition of misfolded proteins (Kaganovich *et al*., 2008), and more recently, suggested as potential maturation sites for the *de novo* prion induction (Tyedmers *et al*., 2010b). This latter study proposed a model in which aggregated proteins are concentrated and converted to highly fragmented prions at the perivacuolar insoluble protein deposit (IPOD) – a yeast cellular compartment for sequestration of protein aggregates - therefore suggesting a novel site for cross-seeding activity. Because these compartments are conserved from yeast to mammals (Kaganovich *et al*., 2008), it is likely that similar processes involving prion-like misfolding events may also occur in mammalian cells and higher eukaryotes.

Importantly, we found that KMO inhibition by RNAi completely reversed behavioral defects of Rnq1 expressing flies (Figure 31 and Figure S21, Supplemental information IV). Altered levels of KP metabolites have been implicated in the pathogenesis of several neurodegenerative disorders, including HD (Maddison and Giorgini, 2015). Since the identification of the yeast gene encoding KMO as a potent loss of function suppressor of mutant HTT toxicity (Giorgini *et al*., 2005), many studies have shown the efficacy of KMO inhibition in other protein misfolding neurodegeneration models (e.g. α-syn, Aβ) (Breda *et al*., 2016, Campesan *et al*., 2011, Zwilling *et al*., 2011). Here we observed that knocking down *cn* ameliorated climbing impairments and age-dependent neurodegeneration of Rnq1 expressing flies, suggesting that alterations in KP metabolism may contribute to prion-mediated toxicity in manner similar to other misfolded proteins, suggesting convergent downstream pathways contributing to disease phenotypes.

Compelling evidence for a relevant role of prion-like proteins in the pathogenesis of neurodegenerative disorders has come from recent studies linking progressive misfolding and neurotoxicity with cross-seeding activity of otherwise unrelated proteins

(Ferreira *et al*., 2017, Katorcha *et al*., 2017, Salazar and Strittmatter, 2017). The current study strongly supports a *trans* effect of prion-like proteins on mutant HTT toxicity (Duennwald *et al*., 2006a), and opens novel avenues for understanding the underlying mechanisms of neurodegeneration.

Materials and methods IV

Yeast experiments

Yeast strains and growth conditions

The [*PIN*$^+$][*psi*$^-$] and [*pin*$^-$][*psi*$^-$] variants carrying a premature nonsense mutation (*ade1-14*) in the *ADE1* gene were derivatives of the wild-type yeast strain 74D-694 (*MATa ade1-14 trp1-289 his3*-200 *ura3-52 leu2-3,112*). The plasmid p6442 (*CUP1*, *SUP35*NM-GFP, *URA3* selectable marker) was used in prion co-transformation experiments for the *de novo* induction of [*PSI*$^+$]. Stains were grown overnight at 30°C with constant shaking at 200 rpm in yeast extract peptone dextrose (YEPD) complete medium (2% w/v glucose, 2% w/v bactopeptone, 1% w/v yeast extract) or minimal yeast nitrogen base (YNB) medium (0.67% w/v YNB without amino acids, 2% w/v glucose) supplemented with appropriate amino acids and bases, but lacking one or more defined components. For prion elimination, guanidine hydrochloride (Sigma-Aldrich, St. Louis, MO, USA) was added to a final concentration of 5 mM.

Preparation of yeast and Drosophila protein extracts

Total yeast cell extracts were obtained from a [*PIN*$^+$][*psi*$^-$] variant strain. Briefly, cells were harvested by centrifugation at 2500 rpm for 10 min at RT. The resulting cell pellet was resuspended in 50 µl yeast buffer (1X PBS, 100 mM NaCl, 2 mM PMSF, 0.1 mM pepstatin A) supplemented with EDTA-free protease inhibitor cocktail (Roche diagnostics, Mannheim, Germany), and cell extracts were collected using glass bead lysis and stored at -80ºC. *Drosophila* protein extracts were obtained as described in Material and methods II. Briefly, heads of 56-day-old flies were isolated and homogenized using standard procedures (Campesan *et al*., 2011). The homogenate was centrifuged at maximum speed for 10 min at 4ºC, and total protein lysate transferred into a new tube. Crude and pellet fly extracts were separated by centrifugation at 80,000 rpm for 60 min at 4ºC. The resulting supernatant was taken as the crude fraction and the remaining pellet

(pellet fraction) was resuspended in 10 µl yeast buffer containing protease inhibitors. Protein concentration was measured using Bradford's Reagent (Sigma-Aldrich, St. Louis, MO, USA) and 300 µg of each sample was used for co-transformation experiments in yeast spheroplasts.

Yeast transformation and analysis of prion formation

Spheroplasts of [*pin*-][*psi*-] cells were used as hosts for measuring the infectivity protein extracts prepared from the [PIN^+][psi^-] yeast strain and either *elavGAL4* or RNQ1 transgenic flies. Briefly, spheroplasts of the [*pin*-][*psi*-] yeast were generated using lyticase as described previously (Tanaka *et al*., 2004a) and maintained at 4 ºC in STC buffer (1.2 M sorbitol, 10 mM $CaCl_2$, 10 mM Tris-HCl pH 7.5). Protein extracts and p6442 plasmid were co-transfected into yeast sphaeroplasts using a transformation mix containing 40% PEG-(4000) and 100 µg salmon sperm DNA. Plasmid uptake was selected by incubation for 3 days at 30 ºC on a uracil (Ura)-lacking sorbitol medium. Subsequently, one hundred Ura^+ colonies were induced for *SUP35* overexpression by overnight growth in -Ura selective YNB medium supplemented with 50 µM copper sulphate. The *de novo* formation of [PSI^+] was scored following incubation for 3 weeks at room temperature on adenine (Ade)-lacking YNB medium. Forty-eight Ade^+ white transformants were further tested for [PSI^+] conversion by guanidine curability (Tuite *et al*., 1981). [PSI^+] formation was calculated based on the mean of three independent experiments. Thirty fly heads per genotype were used for each experiment, in a total of 90 fly heads per genotype.

Drosophila experiments

Fly stocks and genetics

Fruit flies were maintained on standard maize food at 25ºC in a light/dark cycle of 12:12 h. The *elavGAL4* (c155), *daGAL4* (55849) and UAS-eGFP (5431) stocks were obtained from the Bloomington *Drosophila* Stock Center (Indiana University, Bloomington, IN, USA). The *c164GAL4* driver was a gift from Juan Botas (Baylor College of Medicine, Houston, TX, USA) (Torroja *et al*., 1999). The UAS-93QHTT exon 1 flies were a gift from J. Lawrence Marsh and Leslie Thompson (University of California, Irvine) (Steffan *et al*., 2001). For the generation of UAS-*RNQ1* lines, the full-length gene encoding *RNQ1* was amplified and cloned into the pTW vector using Gateway Cloning Technology (Invitrogen, ThermoFisher Scientific, Carlsbad, CA, USA). The resulting pTW-*UASRNQ1* construct was confirmed by DNA sequencing, and then injected into w^{1118}

embryos by means of P-element transformation (BestGene Inc, Chino Hills, CA, USA). Two UAS transgenic lines carrying *RNQ1* targeted randomly in the 2nd chromosome (RNQ1-1M and -6M lines) were generated and further confirmed for the presence of *RNQ1* transgene by PCR-based genotyping using the following primers: 5'CCACAGTGATGACACACTC3' and 5'CTGACCCTGTTGTTGATG3' (Sigma-Aldrich, St. Louis, MO, USA). Expression of *RNQ1* was confirmed for both RNQ1-1M and RNQ1-6M lines by QPCR. The UAS-MoPrP^{WT} and UAS-MoPrP^{P101L} lines, referred to in Figure 29 as WT PrP or P101L PrP, respectively, were kindly provided by Prof. Patrick J. Dolph (Dartmouth College Hanover, USA) (Gavin *et al*., 2006). For analysis of MoPrP-mediated toxicity in HD flies, a recombined line carrying both P101L PrP and 93QHTTex1 transgenes in the 3rd chromosome was generated by meiotic recombination (Sherizen *et al*., 2005) upon crossing of UAS-MoPrP^{P101L} males with UAS-93QHTTex1 female virgins. The UAS-MoPrP^{P101L} UAS-93QHTTex1 homozygous line was validated by PCR-based genotyping for the presence of both transgenes. For all experiments, the UAS-eGFP and UAS-3M flies were used as titration controls, unless otherwise stated.

Quantitative reverse transcription PCR

The RNQ1-1M and RNQ1-6M lines were crossed to the *daGAL4* driver line for ubiquitous expression of the *RNQ1* transgene in the F1 progeny. Samples of 30 flies per genotype were then collected and processed for RNA extraction by means of the TRIzol reagent (Invitrogen, ThermoFisher Scientific, Carlsbad, CA USA), following manufacturer's instructions. RNA samples were purified by genomic DNA removal using Turbo DNAse (Ambion, ThermoFisher Scientific, Waltham, MA, USA) according to the manufacturer's protocol. cDNA was synthesized by reverse transcription reaction using the QuantiTect Reverve Transcription kit (Qiagen, Hilden, Germany). Samples were then prepared for quantitative PCR reactions using Maxima SYBR Green Master Mix (ThermoFisher Scientific, Waltham, MA, USA). Two pairs of primers were used for cDNA quantification of either *RNQ1* or the fly *rpl32* housekeeping gene: 5'TTCCATGGCAAGTTCCTACC3' and 5'CATTCTGTTGCGGTCTACCA3' for RNQ1; 5'AGCATACAGGCCCAAGATCG3' and 5'TGTTGTCGATACCCTTGGGC3' for *rpl32*. Primers were analyzed for efficiency and specificity by melting curve analysis using several dilutions of genomic DNA in triplicate. Total reaction volume was 20 µl, including 12.5 µl SYBR Green, 13.5 ng cDNA and 0.3 µM of each primer. Control reactions without reverse transcriptase were included to ensure that genomic DNA was efficiently removed

from RNA. Reactions were run in 96-well plates using a LightCycler 480 Real-Time PCR System (Roche diagnostics, Mannheim, Germany). Four biological replicates were used for each genotype and qPCR reactions were performed in quadruplicate. The amplification efficiency of each reaction was calculated using the qpcR package in R Studio (Ritz and Spiess, 2008) by fitting sigmoidal curves to the raw fluorescence data, using the *pcrbatch* function. Rnq1 expression lines were normalized to each corresponding UAS control, calculated using the *ratiobatch* function with the Cp value of rp49 used as an internal control for each sample. Statistical significance of relative expression levels was tested using a pairwise-reallocation test based upon that used by REST software (Pfaffl *et al*., 2002), where Cp and efficiency values were permutated within control and treatment groups.

Quantification of photoreceptor neurons

Neuronal loss was determined using the pseudopupil assay as described in Materials and methods I. For analysis of prion-mediated toxicity in wild-type background, *elavGAL4*>UAS-*RNQ1* was examined over 8 weeks, being handled for pseudopupil analysis once per week. To assess the effects of prion protein expression upon HTT toxicity, flies expressing either *RNQ1* or MoPrP and 93QHTTex1 in the nervous system were scored for rhabdomere number at day 1 and day 7 post-eclosion. Pan-neuronal RNQ1 expressing flies carring *cn* RNAi were examined at 1 day-, 42 days- and 56 days-old. A minimum number of 12 flies were examined per condition.

Larval crawling and climbing assays

Motor behavior of 3rd instar larvae was assayed by means of larval crawling assays as previously described (Steinert *et al*., 2012). Briefly, crosses were set up on standard maize food mixed with 0.05% bromophenol blue (FisherBiotech, Loughborough, UK). 3rd instar larvae stage were distinguished by the deep blue color of their intestines (Maroni and Laurie-Ahlberg, 1983). Young, deep blue-colored wandering larvae were selected, washed in distilled water and placed on a 145 mm petri dish containing solidified 0.8% agarose. Larvae were allowed to crawl for 2 min at 25ºC. Larval tracks and number of turns were manually monitored, and the distance crawled by each larva was calculated by measuring track length using Image J software (http://rsbweb.nih.gov/ij/). The log number of turns [$\log_{10}(n + 1)$], where "n" represents the actual number of turns performed by the larva, was calculated to ensure a normalized distribution of the data. At least 30 larvae were analyzed

for each genotype. Motor function of adult flies was analyzed via negative geotaxis response assays as previously described (Breda *et al*., 2015). Briefly, 50-60 female flies carrying the desired genotypes were placed in groups of 10 into 18.4 cm length-empty tubes, and left to acclimatize for 10 min at 25ºC. Flies were then gently tapped to the bottom of the tube and allowed to fly or climb the sides of the tube for 10 sec. The climbing pass rate was measured as the number of flies that passed an 8 cm height threshold line. Climbing tests were repeated 10 times for each tube, with 5-6 tubes containing 10 flies each analyzed per genotype. The same groups of flies were scored for climbing activity at days 7, 14 and 28 post-eclosion.

Eclosion and longevity assays

Eclosion and longevity assays were performed as detailed in Materials and methods II.

Motor and sleep activity

Motor activity was monitored using the *Drosophila* Activity Monitoring (DAM) system (Trikinetics, Waltham, MA, USA), as described (Mason *et al*., 2013). Briefly, male flies expressing *RNQ1* in the motor neurons were collected upon eclosion and placed individually into the DAM activity tubes. The DAM system contains 32 channels, with each connected to a single tube, in which the activity of individual flies is measured when movement breaks an infrared beam that bisects the tube. The activity of thirty-two flies per genotype was individually recorded over 7 days in 12 h light/dark cycles. Only flies surviving for at least 5 days in the activity tubes were analyzed. Total motor activity was assayed as the average number of infrared beam crossings per 30 min of recording interval (bin) over the 7 days. Sleep activity was measured in parallel with locomotor activity for the same groups of flies, as described in (Joiner *et al*., 2006). For sleep analysis, movements were recorded in 5 min bin length and rest was defined as a bout of 5 or more minutes of complete inactivity.

In vitro experiments

BiFC constructs and cell cultures

The generation of HTTex1-Venus BiFC constructs have been described in detail elsewhere (Herrera *et al*., 2011). RNQ1-Venus BiFC constructs were produced by PCR-based subcloning of *RNQ1* full-length gene into the Venus BiFC vectors. Briefly, an

expression plasmid for untagged *RNQ1* was used as template to extract the *RNQ1* open reading frame. The resulting PCR-amplified *RNQ1* was integrated into AflII and XhoI sites of pCS2 plasmids containing the Venus N-terminal (Venus 1, amino acids 1-158) or C-terminal (Venus 2, amino acids 159-238) sequences. RNQ1-Venus 1 and RNQ1-Venus 2 plasmid sequences were confirmed by DNA sequencing (LIGHTrun sequencing, GATC Biotech, Constance, Germany). The mouse CAD neuronal cell line was purchased from Sigma-Aldrich (St. Louis, MO, USA) and HT22 mouse hippocampal cells were kindly provided by David Schubert (The Salk Institute for Biological Studies, CA, USA). Cells were maintained in Dulbecco's minimum essential medium (DMEM) (Lonza, Basel, Switzerland) supplemented with 10% (v/v) Fetal Bovine Serum (FBS) (Gibco, TermoFisher Scientific, Carlsbad, CA, USA), 2 mM glutamine and 1X commercial penicillin/streptomycin solution (Sigma-Aldrich, St. Louis, MO, USA) and grown under undifferentiated conditions in an incubator with controlled atmosphere at 37ºC and 5% CO_2. For flow cytometry, protein extraction or microscopy analyses, cells were seeded at a constant density of 7500 cells/cm^2 in 6-well plates, 100 mm dishes (Corning-Costar, Tewksbury, MA, USA) or 35 mm glass bottom dishes (ibidi, Munich, Germany) respectively. Twenty-four hours after seeding, cells were co-transfected with different combinations of Venus BiFC plasmids using the Lipofectamine 2000 transfection reagent (Invitrogen, ThermoFisher Scientific, Carlsbad, CA, USA), following manufacturer's instructions. Twenty-four hours after transfection, cells were collected and processed according to the requirements of each analytical method.

Flow cytometry

The BiFC interaction analysis, i.e. dimerization/oligomerization, was performed by means of flow cytometry as described in Materials and methods I with minor modifications. Samples were analyzed using a BD FACSCalibur flow cytometer (Beckton Dickinson, Franklin Lakes, NJ, USA), and graphs prepared in FlowJo software (Tree Star Inc., Ashland, OR, USA).

Cell imaging and immunocytochemistry

For co-aggregation and co-localization studies, living cell cultures were imaged using a Nikon Eclipse TE2000-S high throughput microscope equipped with a Hamamatsu Flash 2.8 sCMOS camera (Bridgewater, NJ, USA) and pictures analyzed by means of the Image J free software (http://rsbweb.nih.gov/ij/). For immunocytochemistry, cells were

prepared as described in (Steffan *et al*., 2001). Briefly, cells were washed and fixed for 10 min with 4% (w/v) paraformaldehyde PBS solution. Samples were then washed three times and incubated for 5 min in PBST (0.1% Triton X-100, PBS 1X) to allow permeabilization of cell membranes. After three wash steps, cells were incubated for 45 min in blocking buffer (1% BSA, PBST), and exposed overnight at 4ºC to anti-RNQ1 primary antibody (1:500, Santa Cruz Biotechnology Inc., Dallas, Texas, USA), previously diluted in blocking buffer. Subsequently, cells were washed three times, incubated for 1 h at RT with anti-goat TRITC-conjugated secondary antibody in blocking buffer, and washed again three times. Nuclei were stained by incubation for 5 min with 0.1% Hoesch in PBS solution and samples subjected to a final wash step before microscopy fluorescence analysis. All procedure was carried in the dark and all wash steps were performed in PBS 1X. The secondary antibody used was kindly provided by Florence Janody (Instituto Gulbenkian de Ciência, Oeiras, Portugal).

Immunoblotting and filter retardation assay

Total protein lysates were obtained in native conditions and processed for immunoblotting or filter retardation assay as described in Materials and methods I. Immunoblotting was performed according to standard methods and membranes were probed against HTT (1:500, Millipore, Billerica, MA, USA) and GAPDH (1:30000, Ambion, Austin, TX, USA). Insoluble HTT levels were determined by means of filter retardation assay as described in Materials and methods I. Briefly, aggregates that are insoluble in SDS and larger than 0.22 μm are retained in cellulose acetate membranes and can then be detected using standard immunoblotting procedures. HTT insoluble species were immunoblotted with anti-HTT antibody. Analyses and quantification of relative intensity signal of protein blots were performed by means of the Image J software.

Statistics

Graphs and statistical analyses were performed with Prism 6 Software (GraphPad Software Inc., La Jolla, CA, USA). Results from the yeast and mammalian experiments are shown as average ± standard deviation (SD) of at least three independent experiments, unless specified otherwise. For statistical analysis of the yeast data, background [PSI^+] events in respective controls were subtracted from the Rnq1-expressing flies or [PIN^+] yeast lysates and comparisons were made using single sample t-tests versus the predicted value of 0. Analyses of the mammalian results were performed using one-way ANOVA

followed by the Tukey test for comparison of mean values, aside from the filter blot/immunoblot experiments where a one-sample t-test was employed post-normalization. *Drosophila* data are represented as the average ± standard error (SEM), and analyses were carried out by ANOVA with the Tukey *post-hoc* test, with the exception of longevity experiments that were analyzed by means of a Log-rank test. Statistical significance was accepted when $p<0.05$.

Acknowledgements

We are grateful to David Schubert for HT22 cell line, Florence Janody for TRITC-conjugated antibody, and Lígia Teixeira for valuable equipment that allowed work with mammalian cells. We thank J. Lawrence Marsh, Leslie Thompson, Juan Botas and Patrick J. Dolph for transgenic lines. We also thank the Bloomington *Drosophila* Stock Center and Vienna *Drosophila* Resource Center for fly stocks, and BestGene for the generation of *RNQ1* transgenic lines. We acknowledge the Imaging and Cytometry Unit at Instituto Gulbenkian de Ciência for support with imaging and flow cytometry, respectively.

Contribution

JBS, DCM and CB performed the *Drosophila* experiments. Mammalian cell experiments were performed by JBS under the supervision of FH, who also cloned HTTex1 and RNQ1 BiFC constructs. GLS performed the experiments in yeast and cloned the pTW-UAS-*RNQ1* construct. JBS, FG, GLS and DCM analyzed the data. JBS wrote the manuscript.

IV.

Conclusions and Future perspectives

Neurodegenerative diseases (NDs) affect millions of people worldwide. The economic and social costs are extremely high, and are estimated to increase over time owing to the growing size of the elderly population. Although the vast majority of cases are observed in older people, these disorders can affect any age group, and they start likely years or decades before the first clear symptoms appear. Because of the long latency period and lack of early symptoms, NDs are generally diagnosed in very advanced phases of the pathology. This issue makes very difficult the search for treatments that modify the course of the disease, as any experimental therapy arrives when a majority of neurons is already death and the ageing brain has a very limited regenerative capacity. Thus, available treatments still act at a symptomatic level only. A common pathological hallmark among NDs is the formation of misfolded protein aggregates accompanied by neuronal dysfunction and death. Therapeutic options that target different steps of protein aggregation and degradation are currently being explored. However, the events leading to aberrant protein accumulation, and the particular cellular contexts influencing the formation of toxic aggregates remain unclear.

HD is relatively easy to model because, unlike most PD and AD cases, it has a monogenetic origin, and there is a direct association between the presence of mutant HTT and the development of the disease. HD is thus proving useful for the study of common molecular mechanisms underlying neurodegeneration, as well as for the identification of potential disease-modifying targets in NDs. Here, we used mammalian cell and *Drosophila* models of HD to study intra- and intermolecular factors involved in the oligomerization, aggregation and toxicity of mutant HTT. Although the expanded polyQ tract in HTT is the critical determinant of HD pathogenesis, the precise disease manifestations and their timing are clearly influenced by additional factors. We and others have found that the aggregation propensity of mutant HTT is indeed modulated by secondary events such as PTMs and/or aberrant interactions with a wide range of proteins and other cellular components, which may vary between neuronal populations and individuals. Advancing our understanding of these phenomena should precede any potential therapeutic approach for HD, and would provide relevant information about the normal function of HTT, a protein essential for normal development and cell survival.

Huntingtin phosphorylation is relevant to HD pathology

The lower levels of HTT phosphorylation in the cortex and striatum from HD mice compared to other regions of the brain (Warby *et al*., 2005) suggests a role for

phosphorylation/dephosphorylation events in disease pathogenesis, and may indicate the existence of altered phosphorylation-modifying pathways in HD-affected neurons that could be potentially targeted against neurotoxicity. A significant number of studies demonstrate the neuroprotective potential of constitutive serine phosphorylation of mutant HTT in several models of HD (Atwal *et al*., 2011, Di Pardo *et al*., 2012, Gu *et al*., 2009, Humbert *et al*., 2002, Thompson *et al*., 2009), and point at specific kinases (Atwal *et al*., 2011, Di Pardo *et al*., 2012, Thompson *et al*., 2009, Warby *et al*., 2005) and phosphatases (Ermak *et al*., 2009, Metzler *et al*., 2010, Pardo *et al*., 2006, Pineda *et al*., 2009, Rosenstock *et al*., 2011) as promising targets for drug development. We expanded this list by identifying PP1 as a modulator of HTTex1 aggregation and toxicity (Chapter III, 3.1). The fact that PP1 is the first protein phosphatase to be described in the literature (Branco-Santos *et al*., 2017) as being involved in mutant HTTex1 behavior is of potential therapeutic significance, since the amount of HTTex1-containing fragments is likely to be increased in HD-affected neurons (Li *et al*., 2000) as a result of increased caspase activity (Hermel *et al*., 2004).

PP1 in the context of HD and other neurodegenerative disorders

PP1 belongs to a family of threonine/serine specific protein phosphatases and is highly enriched in the brain, particularly in MSNs (da Cruz e Silva *et al*., 1995b). This phosphatase is composed of one catalytic subunit that exists in three distinct isoforms (PP1α, β and γ). The single PP1 catalytic subunit can form holoenzyme complexes with more than 200 regulatory partners, which target PP1 to specific subcellular locations whereby influencing its substrate specificity and function (Bollen *et al*., 2010, Chatterjee and Kohn, 2013). PP1 is thus involved in a multiplicity of cellular signaling events and, together with PP2A, it accounts for more than 90% of the protein phosphatase activity in eukaryotes (Virshup and Shenolikar, 2009). Its precise role in NDs is not well defined and varies between different experimental models and conditions. Selective inhibition of a PP1 regulatory subunit involved in ER stress protects cells from misfolded protein toxicity and prevents disease development in mouse models of amyotrophic lateral sclerosis (Das *et al*., 2015). In AD, PP1 inhibition leads to secretion of non-amyloidogenic APP fragments (da Cruz e Silva *et al*., 1995a). Exposure to Aβ toxic peptides affects PP1 expression differentially, depending on the cell type (Amador *et al*., 2004). Tau directly interacts with PP1 in normal conditions, targeting PP1 to the microtubules. In turn PP1 plays a role in maintaining microtubule stability by regulating Tau phosphorylation and possibly other

microtubule-associated proteins (Liao *et al*., 1998). A potent inhibitor of PP1 is found to be upregulated in patient and mouse AD brains, wherein specifically co-localizes with Tau neurofibrillary tangles (Raha-Chowdhury *et al*., 2005). PP1 inhibition correlates with Tau hyperphosphorylation and memory impairment in AD rats (Sun *et al*., 2003), while inefficient inhibition of PP1 by DARPP-32 is associated with reduced synaptic plasticity and memory loss (Cho *et al*., 2015). Tau hyperphosphorylation leads to PP1 overstimulation, which could represent an attempt of the cell to restore normal levels of Tau phosphorylation. Instead, increased PP1 activity leads to activation of GSK3, a kinase associated with fibrillar Tau pathology and axonal deficits (Braithwaite *et al*., 2012). These studies suggest that both inhibition and overstimulation of PP1 may account for neuronal dysfunction, while minimal repression seems to be necessary for normal cognition. Notably, PP1 exerts differential control of neuronal viability when activated in different brain regions. While PP1 potentiates synaptic activity and promotes cell survival in the hippocampus, it exacerbates NMDAR-induced pathways in response to excitotoxicity and other stress stimuli in cortico-striatal connections (Arias *et al*., 2002, Mansuy and Shenolikar, 2006). Loss of the PP1 inhibitor DARPP-32 in HD mice results in decreased serine-421 HTT phosphorylation and reduced neuroprotection against excitotoxicity (Metzler *et al*., 2010). Excitotoxicity involved a positive feedback loop mechanism, in which overstimulation of NMDAR triggered GSK3 activation via PP1, resulting in amplification of PP1-mediated signaling and subsequent inhibition of CREB transcription (Szatmari *et al*., 2005). However, in physiological conditions, loss of PP1 leads to CREB hyperphosphorylation, followed by proteosomal degradation (Taylor *et al*., 2000). These observations indicate that the precise role of PP1 depends on its interaction with particular regulatory subunits, which may vary between cell types and pathophysiological or experimental conditions. In fact, PP1 holoenzyme complexes are highly selective (Chatterjee and Kohn, 2013). Therefore, if PP1 is to be considered a therapeutic target in NDs, it is essential to identify specific regulatory partners that associate with the PP1 catalytic subunit in particular cellular environments and/or in response to specific insults.

The putative relationship between PP1 and N17 phosphorylation

We showed that single N17 phosphorylation of mutant HTTex1 reduces its aggregation, while having no effect on oligomerization (Chapter III, 3.1). Consistently, treatment of mammalian cells with PP1 inhibitors prevented the formation of large HTTex1 aggregates but did not alter the levels of oligomers. A similar effect was observed

in *Drosophila* dopaminergic neurons, with genetic downregulation of PP1 resulting in decreased number of HTTex1 large aggregates. However, specific downregulation of PP1 in photoreceptor neurons led to their premature death. Since each parameter was better studied in different cell populations, we cannot establish a direct connection between HTTex1 aggregation, toxicity and PP1 downregulation. Our interpretation is that decreased PP1 activity in HD cells might result in increased levels of HTTex1 phosphorylation, which induce conformational changes that interfere with the ability of HTTex1 oligomers to assembly into large insoluble species, thereby increasing their availability to engage in toxic interactions. Ultimately, this would lead to neuronal degeneration via direct or indirect activation of apoptotic signaling pathways (Saudou *et al*., 1998). This is in agreement with the "toxic oligomer hypothesis", which argues that neuronal protection might be conferred either by preventing the initial oligomer formation or accelerating their sequestration into forming neutral inclusion bodies (Arrasate *et al*., 2004, Bodner *et al*., 2006, Kuemmerle *et al*., 1999, Slow *et al*., 2005). In line with this hypothesis, T3D fly mutants displayed an impressive phenotype of motor dysfunction (data not shown) in spite of the low deposition of inclusion bodies in their brains. Together with the striatal-enrichment of PP1 in healthy brains (da Cruz e Silva *et al*., 1995b), the decreased levels of T3 phosphorylation in pre-manifested disease models of HD (Cariulo *et al*., 2017b) suggests that an imbalance of PP1 activity and T3 phosphorylation levels could trigger a series of pathological events and instigate the development of HD. The modulatory role of T3 phosphorylation on HTTex1 α-helicity (Ansaloni *et al*., 2014, Chiki *et al*., 2017) and the demonstrated impact of this modification on mutant HTT aggregation propensity (Chapter III, 3.1) (Cariulo *et al*., 2017b) lead us to speculate that phosphorylation of T3 might attenuate the effect of expanded polyQ on HTTex1 conformation. An increased content of HTTex1 phosphorylated fragments within forming oligomeric structures would affect their structural stability, thereby preventing further stages of the aggregation process. Indeed, T3 phosphorylation decreases conformational rigidity of mutant HTTex1, while having no effect on soluble wild-type HTT (Cariulo *et al*., 2017b).

However, it is important to note that our results may not imply a direct action of PP1 on N17 residues. It is also plausible that PP1 downregulation could have an indirect effect on mutant HTTex1 aggregation, while promoting downstream events of toxicity. For example, the deleterious effect of PP1 downregulation may be due to a potential role of the *Drosophila* PP1α-87B isoform in maintaining structural integrity of photoreceptor neurons (Bennett *et al*., 2006, Dombradi *et al*., 1990, Kirchner *et al*., 2007a, Kirchner *et al*.,

2007b). In this scenario, expression of mutant HTT would converge to determine cellular collapse thereby accelerating neurodegeneration. The two hypotheses are not mutually exclusive, and further studies will clarify whether PP1 directly regulates N17 phosphorylation and whether there are N17-specific PP1 regulatory subunits. Such findings could open new venues for the development of drugs with a high degree of specificity. We also proposed that T3 phosphorylation plays a dominant effect over S13 and S16 modifications on mutant HTTex1 aggregation (discussed on Chapter III, 3.1). Thus, future investigations should also focus on deciphering the molecular pathways that influence T3 phosphorylation in the context of polyQ expansion, as they could provide more effective therapeutic targets for promoting the formation of species with lower cytotoxicity. Finally, it could be interesting to further explore the role of PRL-3 on HD pathogenesis. In our cell BiFC-based phosphatase inhibitor screen, PRL-3 showed to be a strong modulator of mutant HTTex1 aggregation, with its inhibition leading to a dramatic increase of HTT insoluble species. PRL-3 is a tyrosine phosphatase, fact that allowed us to exclude any direct modulation of N17 phosphorylation by this phosphatase, but it would be interesting to understand the underpinnings of a pathway that seems to enhance HTT aggregation.

The role of AGEs in huntingtin aggregation and toxicity

PP1 activation has been repeatedly proposed as a potential approach to treat *Diabetes mellitus* type 2 (Kuehnen *et al*., 2011, Reither *et al*., 2013, Sato *et al*., 1998), one of the most debilitating peripheral complications of HD (Carroll *et al*., 2015, van der Burg *et al*., 2009). Downregulation of PP1 activity in human pancreatic β cells is associated with impairment of glucose-induced insulin secretion through a mechanism involving decreased calcium influx into cells (Kuehnen *et al*., 2011). In HD, the progressive accumulation of mutant HTT in pancreatic β cells results in age-dependent decrease of insulin production and disruption of glucose intake (Andreassen *et al*., 2002, Bjorkqvist *et al*., 2005, Hurlbert *et al*., 1999). Glucose is the major energy supply of neurons. However, imbalance of glucose metabolism drives the formation of glycation agents, which aberrantly interact with functional proteins inducing the formation of AGEs, and AGEs have deleterious effects on proteins associated with NDs (Chen *et al*., 2006b, Choi *et al*., 2004, Li *et al*., 2013, Vicente Miranda *et al*., 2017). In the current work, we established a relationship between mutant HTTex1 glycation and neurotoxicity *in vivo* (Chapter III, 3.2). Accumulation of AGEs can induce inflammatory responses and oxidative stress via RAGE

(Vicente Miranda and Outeiro, 2010). Upregulation of RAGE promotes Tau hyperphosphorylation and aggregation, and impairs synaptic transmission through activation of GSK3 and MAPKs. Conversely, glycated Tau induces RAGE-mediated ROS production and subsequent Aβ secretion in AD models (Kulkarni *et al*., 2013). Inhibiting or suppressing AGE-RAGE aberrant signaling is a promising therapeutic strategy against age-related diseases, but so far they have failed to demonstrate safety and efficacy in phase 1 clinical trials (Galasko *et al*., 2014). A threonine/serine kinase, the p58-regulated/activated protein kinase (PRAK), was recently identified as a novel binding partner of the RAGE cytoplasmic domain, regulating downstream autophagic signaling in response to Aβ-RAGE interaction (Kim *et al*., 2016). Since a complex kinase/phosphatase signaling is likely involved in RAGE mediated-processes, it would be interesting to investigate a possible link between PP1 malfunction and glycation-related toxicity in HD. We previously found that the autophagy lysosome pathway (APL) is activated in the presence of glycated mutant HTT (Vicente Miranda *et al*., 2016b). Phosphatase activity is required for APL induction in cell stress conditions (Wong *et al*., 2015b). We think it could be important to measure the activity levels of specific kinases and phosphatases involved in HTT aggregation and toxicity, as well as HTT phosphorylation levels, under glycation conditions. Would an increase in AGEs trigger PP1 activation as a first line of defense against the accumulation of toxic species? Could a continuous exposure to reducing sugars result in chronic reactions and overstimulation of PP1, ultimately leading to dephosphorylation of HTT species and their subsequent aggregation, to the point where cell loss is irreversible? Would such AGE-RAGE signaling transduction occur specifically in striatal neurons thus constituting a novel mechanism of striatal vulnerability in HD? Achieving a tight control of PP1 activity in glycation-affected CNS, in addition to peripheral tissues, could be of extreme clinical importance since it would mean the use of a single drug to treat multiple symptoms of HD.

Another potential approach to overcome glycation-induced stress and cytotoxicity is to reduce the accumulation of AGEs. Increased levels of glycation exacerbated mutant HTT-induced defects in young flies, suggesting that the deposition of glycated HTT species may occur in early stages of HD development (Chapter III, 3.2). However, several questions remain to be answered. For example, it is not yet clear whether the toxicity seen in HD models subjected to glycating conditions is a direct consequence of enhanced HTTex1 aggregation or just a result of the high reactivity of glycated species. Likewise, the specific HTTex1 residues where AGEs are formed remain to be identified, and

therefore we are still unable to know whether such modifications would be sufficient to initiate aggregate formation. Mounting evidence suggests that HTTex1 accumulation might occur as a secondary event promoted by disruption of the proteostasis network by age-associated glycation. Although glycation is reported to induce chaperone activity (Nagaraj *et al*., 2003, New *et al*., 1998, Oya-Ito *et al*., 2006) and to stimulate the APL system in a cell model of HD (Vicente Miranda *et al*., 2016b), glycated HTTex1 fragments could be more difficult to degrade thus leading to their accumulation in a time-dependent manner. This is demonstrated by a reduced capacity of the cells to clear mutant HTTex1 when treated with glycation agents (Vicente Miranda *et al*., 2016b). A recent study from our laboratory shows that glycation promotes α-syn oligomerization, while blocking ubiquitin-mediated proteasome degradation and autophagy (Vicente Miranda *et al*., 2017). Protein aggregation and decay of the protein quality control system could therefore constitute concomitant events in glycation-related toxicity. An important question arising from these observations is how interplay between glycation and other PTMs can influence HTT aggregation propensity and clearance. Since lysines are the preferential targets of glycation (Vicente Miranda and Outeiro, 2010), and because modifications in HTT lysine residues are known to regulate protein degradation and clearance (Jeong *et al*., 2009), glycation agents could compete with acetyltransferases, ubiquitin or SUMO for HTT lysine residues thus playing a role in modulating these processes. Notably, phosphorylation of S13 and S16 by IKK regulates modifications on adjacent lysine residues (Thompson *et al*., 2009). It would be interesting to investigate the influence of N17 phosphorylation/dephosphorylation events upon lysine-targeting glycation.

While a direct relationship between diabetes and NDs is yet to be clearly established, the studies discussed above indicate protein glycation as an environmental risk factor for disease development and progression. Anti-glycation agents may prove beneficial for HD patients, at least for those suffering from hyperglycemia and diabetic complications. In addition, preventive approaches based on dietary restriction may also delay the onset of disease, as well as improve the quality-of-life of symptomatic HD patients. Dietary energy restriction in a mouse HD model protects against mutant HTT-related neurodegeneration while preserving BDNF levels in cortico-striatal synapses. Importantly, glucose metabolism of these animals was improved, motor deficits were delayed, and their lifespan was increased (Duan *et al*., 2003). Aerobic exercise is also known to positively impact glucose levels and improve insulin sensitivity, and may therefore constitute a good complementary therapy. Wheel-running HD mice exhibited

delayed onset of motor and cognitive deficits (Pang *et al*., 2006). In the future, it will be important to understand the nature of the link between AGEs, peripheral pathology and neurodegeneration. Furthermore, since there is evidence for the presence of mutant HTT in cerebrospinal fluid (Wild *et al*., 2015), the detection of AGEs in circulating HTT could constitute a potential biomarker for premanifest and early progression of HD.

Protein-protein interactions as modifiers of huntingtin aggregation and toxicity

The observation of heterologous aggregates composed by apparently unrelated proteins in patient brains has opened up a new chapter of research regarding the mechanisms underlying differential progression of NDs. An age-dependent increase of protein misfolding as result of proteasome decay is a view widely acknowledged in the field, and is pointed as a possible explanation for the appearance of mixed aggregates. Such theory reasons that the accumulation of certain misfolded proteins, such polyQ-containing proteins, can compromise the entire proteostatic network, thereby triggering the misfolding of unrelated proteins that would otherwise fold normally. Increased levels of misfolded proteins in the cellular environment would facilitate the occurrence of co-aggregation processes and accelerate disease progression. However, in addition to increased protein concentrations, other factors may determine co-aggregation propensity and its outcomes (Kostylev *et al*., 2015, Sarell *et al*., 2013, Shattuck *et al*., 2017, Stewart and Radford, 2017). The presence of aggregation-prone proteins itself in a particular subcellular location can initiate co-aggregation events. Intrinsic properties of aggregation-prone proteins may dictate its fate in cross-seeding interactions. Further supporting this notion, we showed that HTTex1 co-aggregates with other disease-causing proteins, in some cases depending on its phosphorylation state (Chapter III, section B). The ability of phosphorylated HTTex1 molecules to co-assemble into large insoluble structures appears to be highly selective. In particular, N17 phosphorylation prevents further co-aggregation processes between mutant HTT and α-syn, while having no effect upon HTT-Tau interactions. As such, specific PTMs in HTT might constitute interesting targets for controlling efficiency of cross-seeding and should be object of further study. Since different cell types may comprise different pools of HTT molecules, this could explain why the spread of HD pathology is facilitated in certain types of neurons, and leads to the intriguing possibility that PTMs might affect the location and timescale of disease progression. It has also been postulated that sequence similarity between aggregation-prone proteins increases the chance for cross-seeding events. We showed that Rnq1, a

yeast prion that is highly enriched in Q/N domains, interacts with mutant HTT in human living cells (Chapter III, 3.4). Although not naturally present in mammalian systems, Rnq1 was able to promote dramatic changes in mutant HTT aggregation profile, raising the possibility that human proteins with similar properties could function as modifiers of HTT aggregation.

Once demonstrated that specific aggregation-prone proteins interact with mutant HTT and affect its aggregation properties, it is important to understand whether such aberrant interactions can impact on mutant HTT toxicity and thus influence disease development and/or progression. While our collaborators explored the downstream consequences of mutant HTT interactions with α-syn (Pocas *et al*., 2015) or Tau (Blum *et al*., 2015) in *Drosophila* and mouse models, respectively (discussed in Chapter III, 3.3), we sought to determine the effect of Rnq1 expression in *Drosophila*, during normal aging or in HD-like context (Chapter III, 3.4). We showed that expression of Rnq1 is sufficient to cause neuronal dysfunction and degeneration in aging flies. The relevance of this finding stems from the fact that human cells express many proteins enriched with Q/N domains (Alberti *et al*., 2009, King *et al*., 2012). Furthermore, such proteins with prion-like properties are abundant in nature and may serve as critical environmental risk factors in predisposed individuals with ND (Lundmark *et al*., 2005). Westermark and colleagues show that naturally occurring amyloid-like fibrils act as seeds to accelerate amyloidogenesis in mice (Lundmark *et al*., 2005). Our data here offer an important proof-of-concept demonstration of the role of Q/N-rich proteins as enhancers of mutant HTT aggregation and toxicity. We propose that these proteins may function as HTT amyloid precursors together with co-chaperones, although additional experiments are needed to prove the involvement of chaperones in such cross-seeding phenomena. Expression of polyQ peptides in *C. elegans* perturbs protein-folding homeostasis and causes co-aggregation with Q/N-rich proteins associated with developmental deficits (Satyal *et al*., 2000). A specific molecular chaperone that modulates seeding and formation of polyQ aggregates (Meriin *et al*., 2002) was able to reduce aggregation and improve development, while expression of other chaperones had no effect (Satyal *et al*., 2000). Indeed, subsequent studies have shown that specific chaperones can function in early stages of protein aggregation and alter the toxic properties of oligomers by promoting their assembly into fewer but larger insoluble species (Douglas *et al*., 2008, Mannini *et al*., 2012, Sajjad *et al*., 2014). However, such mechanisms of action of molecular chaperones remain unclear with the existence of conflicting data (Muchowski *et al*., 2000). The balance between

molecular chaperones and factors that enhance protein misfolding and aggregation may determine the final outcome. Chaperones associate with co-chaperones to mediate seeding and propagation of prion proteins (Arslan *et al*., 2015, Telling *et al*., 1995). Genetic manipulation of the *Drosophila* cellular co-factor DROJ1 with chaperone-like activity may help to establish such prion model of aggregation in HD (Davis and Sindi, 2016, Lopez *et al*., 2003). In addition to deregulation of the proteostasis network, it is important to investigate whether exposure to Q/N-rich proteins can trigger early mechanisms of cellular dysfunction thus contributing to enhanced cell vulnerability to mutant HTT. Downregulation of the *Drosophila* KMO gene in Rnq1 expressing flies ameliorated motor defects and neurodegeneration, suggesting that impaired KP metabolism may contribute to neuronal dysfunction and toxicity observed in these flies. We are currently performing measurements of overall mitochondrial metabolism and transcription in our Rnq1 flies, which will provide further insight into the underlying mechanisms of Rnq1-mediated toxicity.

Final remarks

Resolving the biochemical properties of different molecules in the total HTT population, in a particular set of neurons (e.g. MSNs in the striatum), could be crucial to understand their relative contribution to HD pathology. In the future, monitoring the amount of Q/N-rich and other aggregation-prone proteins in humans, in the context of both physiological aging and disease, may provide opportunities for the development of sensitive predictive tools of HD progression.

In summary, the results discussed here suggest that i) pathway-modifying PTMs in HTT (e.g. phosphorylation and glycation), ii) the presence of specific factors in the cell environment (e.g. PP1, Q/N-rich proteins), and iii) the recruitment of proteins essential for normal cell function (e.g. α-syn and Tau) may affect significantly disease development and progression, and constitute areas of research of particular interest for advancing our knowledge of HD pathogenesis. The next big challenge will be to integrate current findings into meaningful pathways. Only a comprehensive approach of the putative molecular targets could push forward the rational development of therapeutics against a monogenetic disorder with as much interindividual variability as HD.

V.

Appendix

This chapter contains additional results published in the following articles:
Branco-Santos J[§], Herrera F[§]*, Poças GM, Pires-Afonso Y, Giorgini F, Domingos PM*, Outeiro TF* (2017). Protein phosphatase 1 regulates huntingtin exon 1 aggregation and toxicity. *Human Molecular Genetics*, 26**,** 3763-3775.

Vicente Miranda H, Gomes MA, Branco-Santos J, Breda C, Lázaro DF, Lopes LV, Herrera F, Giorgini F, Outeiro TF (2016). Glycation potentiates neurodegeneration in models of Huntington's disease. *Scientific Reports*, 18 (6): 36798.

This chapter also includes supplemental information of the following manuscript (*under review):*
Prion proteins modulate mutant huntingtin mediated neurotoxicity
Branco-Santos J, Staniforth GL, Maddison DC, Breda C, Domingos PM, Steinert JR, Kyriacou CP, Outeiro TF, Herrera F, Tuite MF, Giorgini F

[§]Contributed equally to this work
*Co-corresponding authors

Supplemental information I

Inventory

Table S1. Name, concentration, description, toxicity and effect on HTTex1 expression of the phosphatase inhibitor library.

Code	Name	Concentration	Compound description	Toxic	Inhibits HTTex1 expression
B1	Cantharidic acid	1 μM	PP1 and PP2A	No	No
B2	Cantharidin	1 μM	PP1 and PP2A	No	No
B3	Endothall	5 μM	PP2A	No	No
B4	Benzylphosphonic acid	5 μM	Tyrosine phosphatases	No	No
B5	L-p-Bromotetramisole oxalate	10 μM	Tyrosine phosphatases	No	No
B6	RK-682	10 μM	Tyrosine phosphatases	Yes	Yes
B7	RWJ-60475	5 μM	CD45 tyrosine phosphatase	No	Yes
B8	RWJ-60475 (AM)3	5 μM	CD45 tyrosine phosphatase (cell permeable)	No	No
B9	Levamisole HCl	10 μM	Mammalian alkaline phosphatase	No	No
B10	Tetramisole HCl	10 μM	Mammalian alkaline phosphatase	No	No
B11	Cypermethrin	1 μM	Calcineurin (PP2B)	No	No
B12	Deltamethrin	1 μM	Calcineurin (PP2B)	No	No
C1	Fenvalerate	5 μM	Calcineurin (PP2B)	No	No
C2	Tyrphostin 8	10 μM	Calcineurin (PP2B)	No	No
C3	CinnGel	5 μM	PTP1B	No	No
C4	NSC-95397	5 μM	Cdc25	No	No
C5	BN-82002	5 μM	Cdc25	No	No
C6	Shikonin	10 μM	PTP1B	Yes	No
C7	NSC-663284	1 μM	CDC25	No	No
C8	Cyclosporin A	1 μM	Calcineurin (PP2B)	No	No
C9	Pentamidine	10 μM	PRL1	No	No
C10	BVT-948	5 μM	Tyrosine phosphatases	No	No
C11	B4-Rhodanine	1 μM	PRL3	No	No
C12	Alexidine·2HCl	1 μM	PTPMT1	No	No
D1	9,10-Phenanthrenequinone	10 μM	CD45 tyrosine phosphatase	Yes	No
D2	BML-260	10 μM	JSP-1	No	No
D3	Sanguinarine chloride	10 μM	PP2C	Yes	No
D4	BML-267	10 μM	PTP1B	No	No
D5	BML-267 Ester	10 μM	PTP1B (cell permeable)	No	No
D6	OBA	10 μM	Tyrosine phosphatases	No	No
D7	OBA Ester	10 μM	Tyrosine phosphatases (cell permeable)	No	No
D8	Gossypol	10 μM	Calcineurin (PP2B)	No	Yes
D9	Alendronate	10 μM	Tyrosine phosphatases	No	No

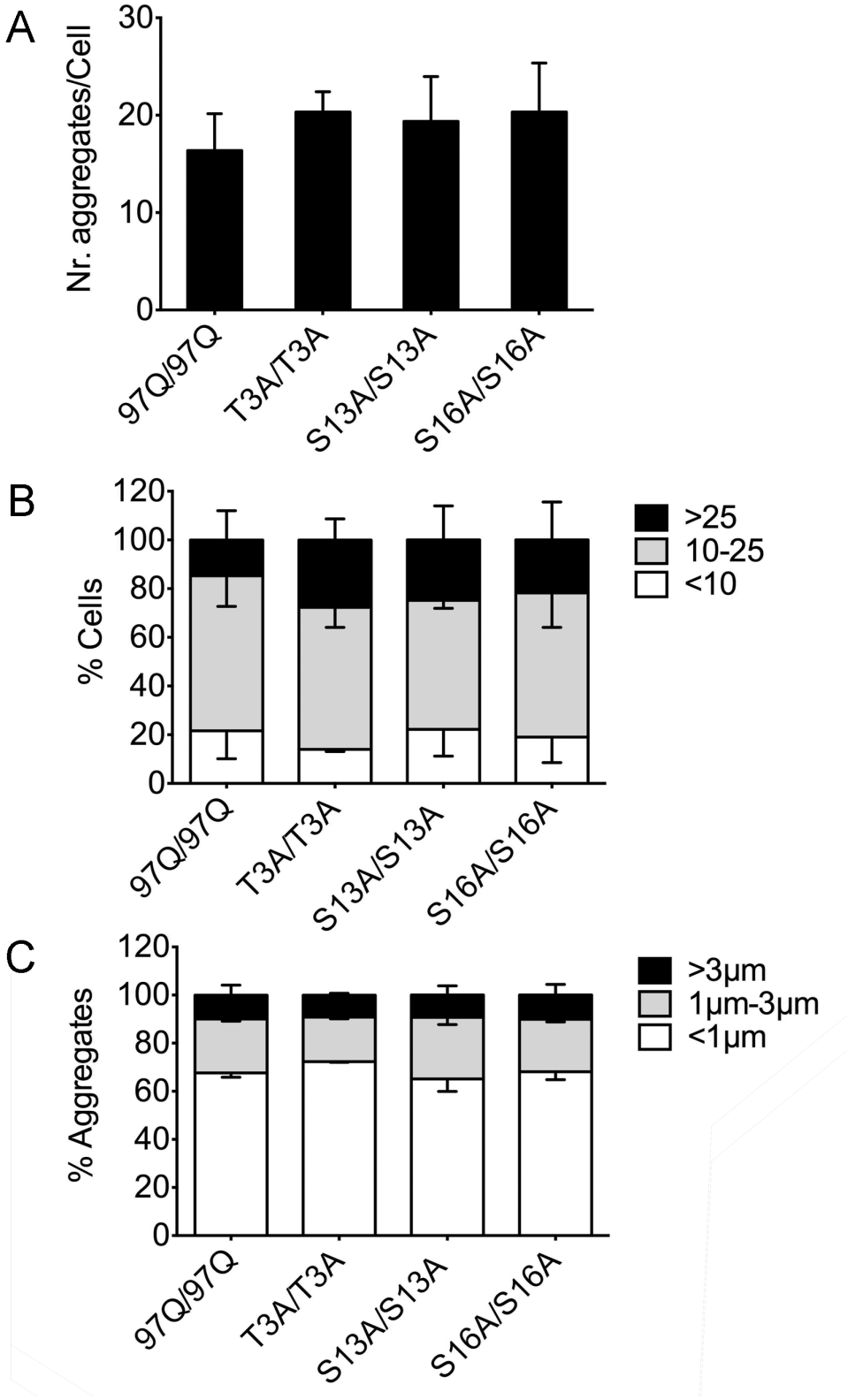

Figure S1. Single N17 phosphoresistant mutations do not alter HTTex1 aggregation pattern. Graphic representations from microscopy data of H4 cells transfected with the corresponding HTTex1-Venus BiFC pairs. Single phosphoresistant mutations did not change significantly the number of aggregates per cell (A), the distribution and number of aggregates per cell (B) or the size of aggregates (C).

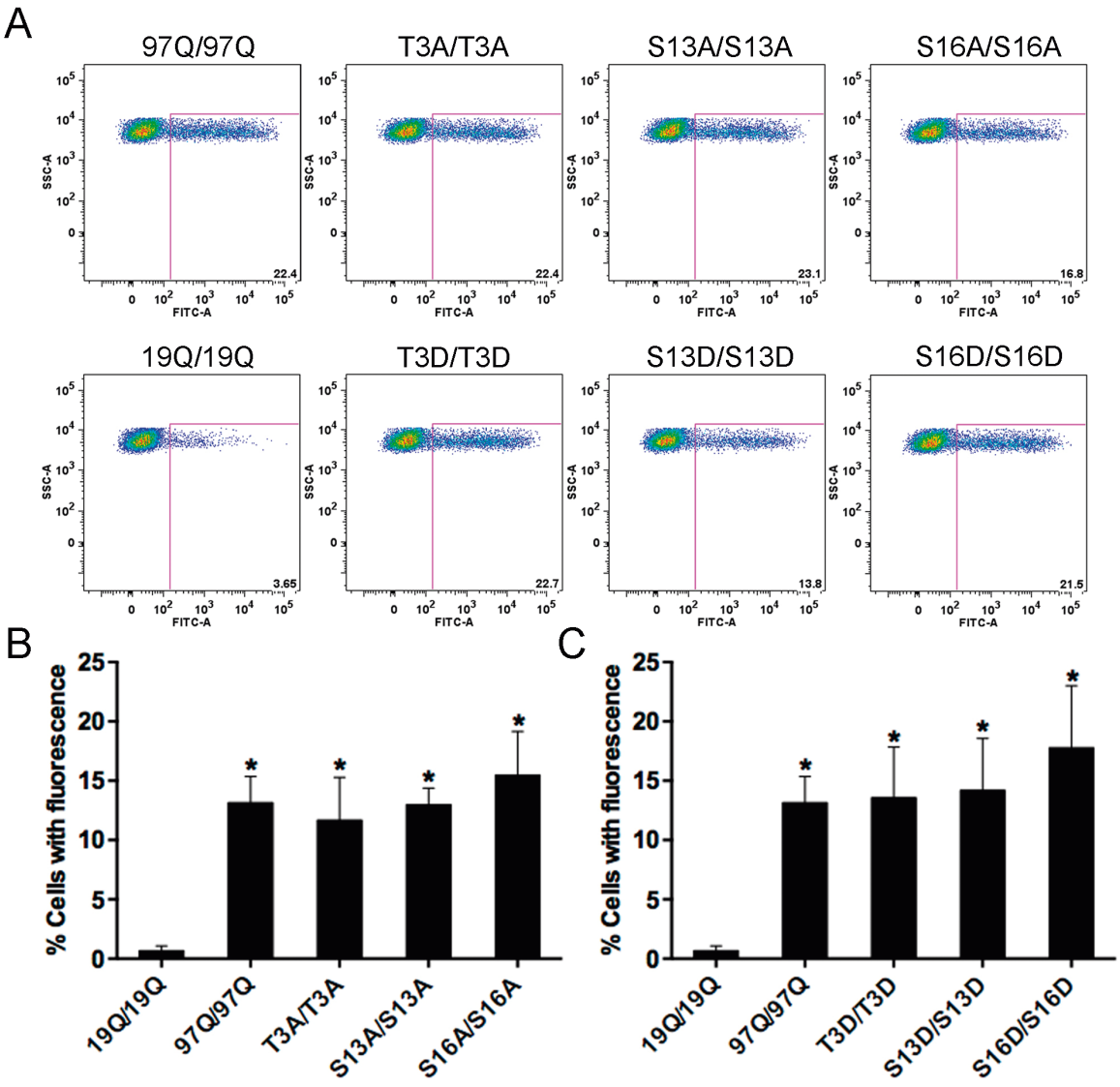

Figure S2. N17 phopho-mutations do not affect HTTex1 oligomerization. (A) Flow cytometry charts of H4 cells transfected with the indicated HTTex1-Venus BiFC pair. Y axis represents the side scatter (SSC) signal, and the X axis represents the signal in the FITC channel. Both scales are logarithmic. (B and C) Graphic representation of quantitative flow cytometry results. *significant versus 19QHTTex1 pair, $p<0.05$.

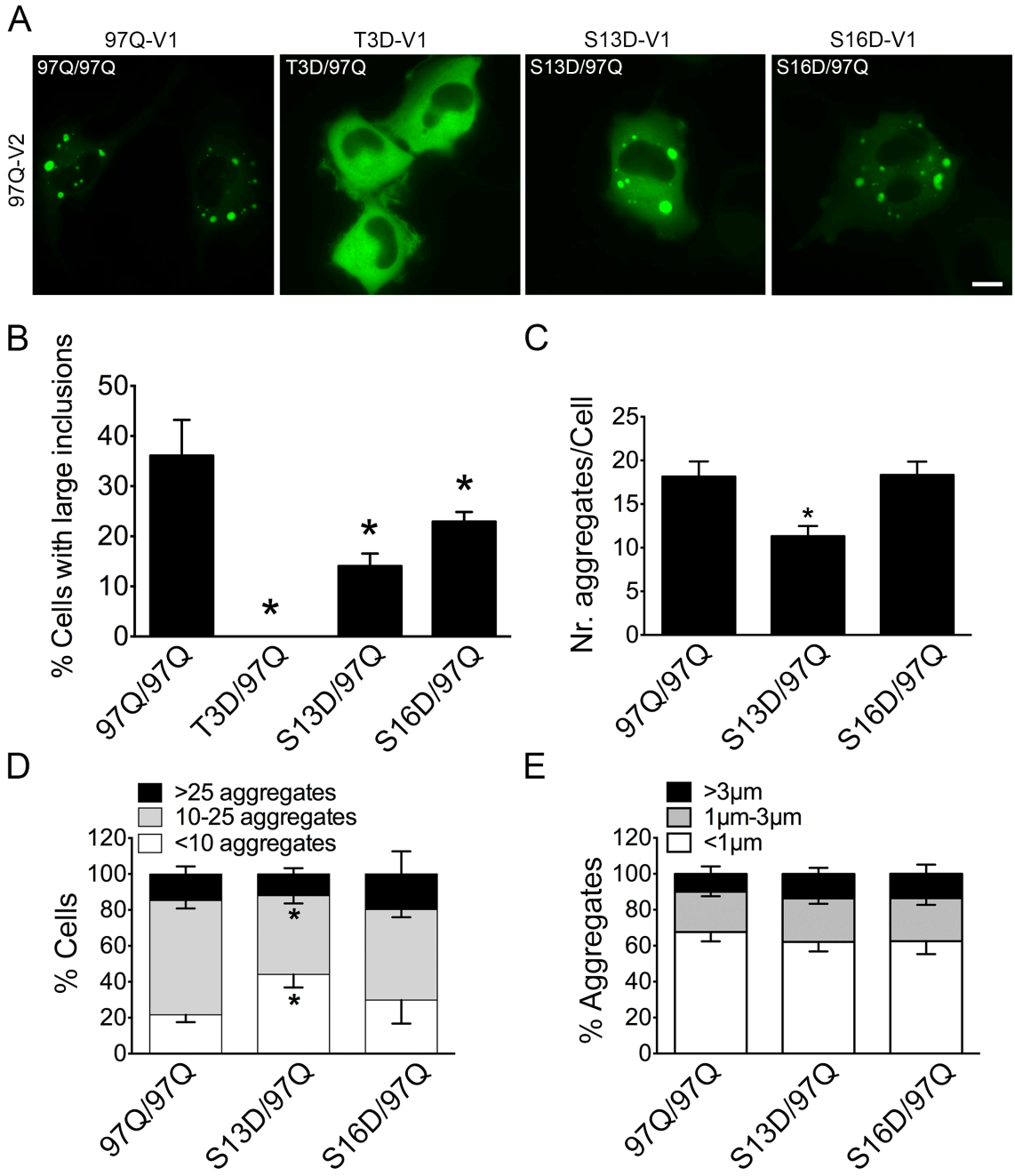

Figure S3. Relative contribution of N17 phosphorylatable residues towards HTTex1 aggregation. (A) Representative pictures of H4 cells transfected with different combinations of phosphomimics with non-mutated 97QHTTex1-Venus constructs. These combinations produced mixed phenotypes in terms of aggregation. Quantitative analyses of microscopy pictures confirmed that expression of T3D/97Q resulted in a total absence of cells with inclusions (B). (C) Average number of aggregates per cell. (D) Percentage of cells showing less than 10, between 10 and 25, and more than 25 aggregates. (E) Percentage of aggregates smaller than 1 μm, larger than 1 μm but smaller than 3 μm, and larger than 3 μm. *, significant versus 97Q/97Q, $p<0.05$. Scale bar, 20 μm.

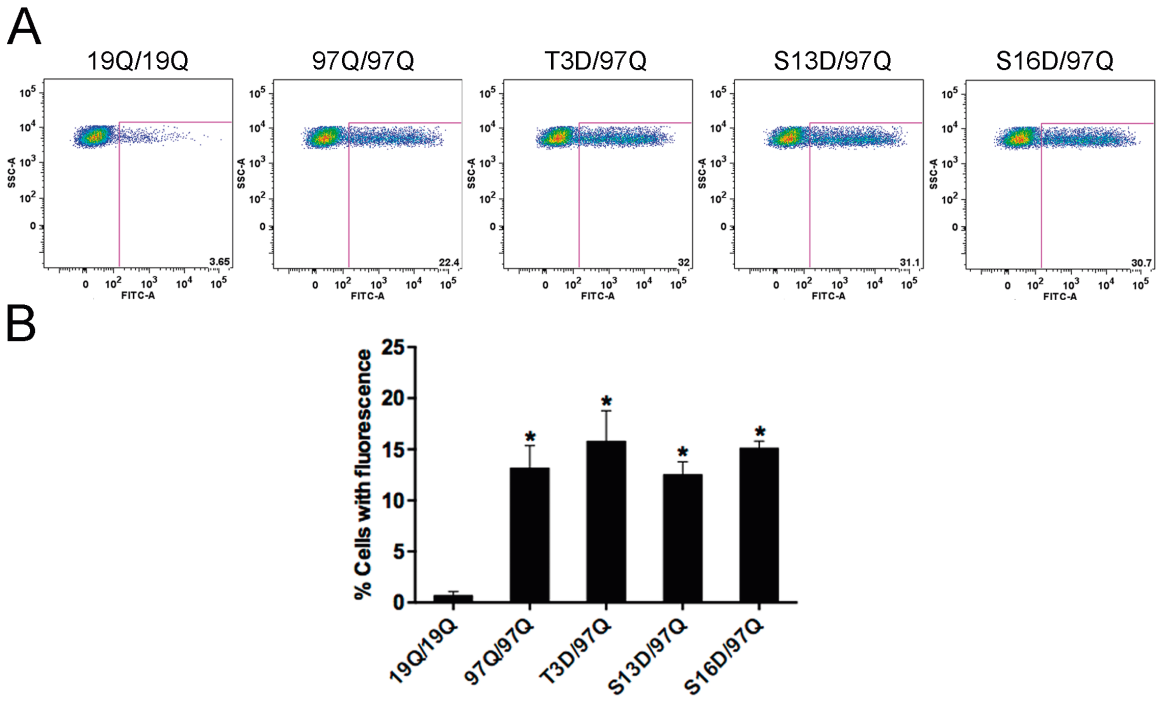

Figure S4. Combinations of phosphomimics and non-mutated 97QHTTex1 produce similar levels of fluorescence. (A) Representative flow cytometry profiles of cells co-transfected with different combinations of phosphomimic mutants and non-mutated 97QHTTex1 BiFC constructs. (B) Quantitative analysis of flow cytometry data. *significant versus 19QHTTex1 pair, $p<0.05$.

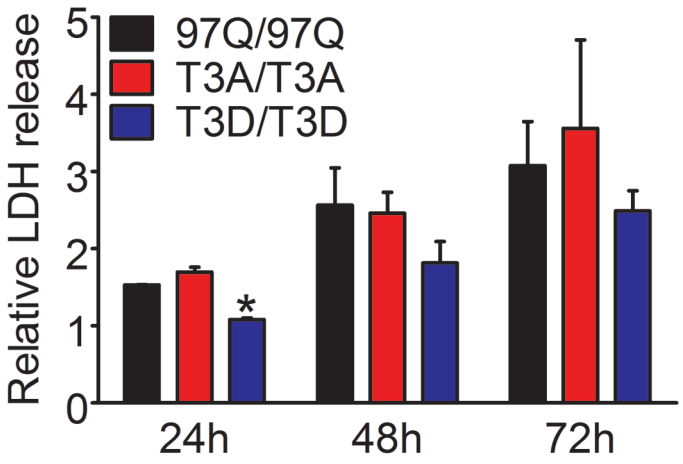

Figure S5. LDH activity of T3 phosphomutants measured over 24 h intervals. LDH release was measured in the supernatants of cells expressing non-mutated 97QHTTex1 (black bars), T3A (red bars) or T3D (blue bars) pairs, at different time points after transfection. Expression of T3D pair was protective at 24 h post-transfection, but no significant differences were observed at 48 h or 72 h comparing to the non-mutated 97QHTTex1. *significant versus 97Q/97Q, $p<0.05$.

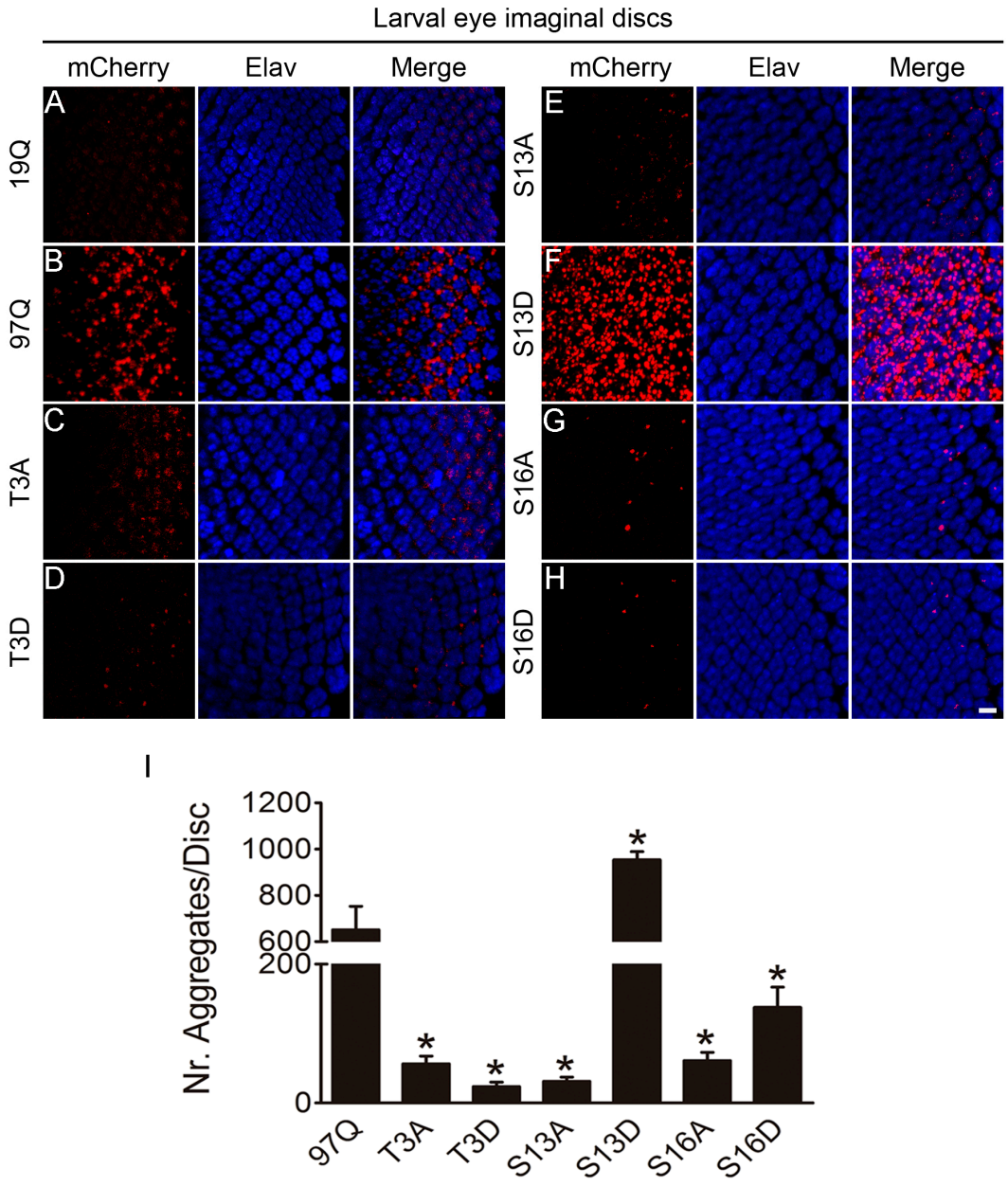

Figure S6. Aggregation patterns of HTTex1 phosphomutants in 3rd instar larval eye imaginal discs. Confocal microscopy images of eye imaginal discs in larvae expressing HTTex1-mCherry under the control of GMRGAL4. HTTex1-mCherry is shown in red, and photoreceptors (anti-Elav) are shown in blue. Wild-type 19QHTTex1 showed a diffuse pattern of expression (A), whereas non-mutated 97QHTTex1 produced high number of inclusions (B). Mutations in the N17 phosphorylatable residues reduced 97QHTTex1-mCherry aggregation in larvae (C-E and G-H), with the exception of S13D (F), which showed increased number of aggregates versus non-mutated 97QHTTex1 (B). (I) Quantitative analyses of confocal pictures. Average number of aggregates and standard deviations were calculated for at least 5 imaginal discs per genotype. *significant versus GMRGAL4>UAS-97QHTTex1-mCherry, $p<0.05$. Scale bar, 10 μm.

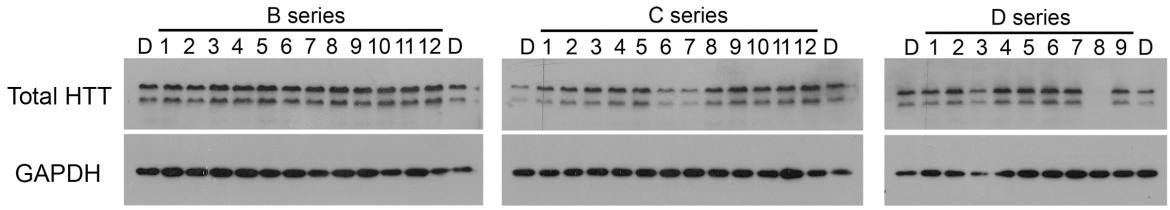

Figure S7. Effect of phosphatase inhibitors on HTTex1 expression. Representative blots of total protein extracts from H4 cells transfected with non-mutated 97QHTTex1-Venus BiFC constructs and incubated with the indicated phosphatase inhibitors for 24 h. Membranes were probed with anti-HTT and anti-GAPDH antibodies, as indicated. Corresponds to Table S1. D, DMSO.

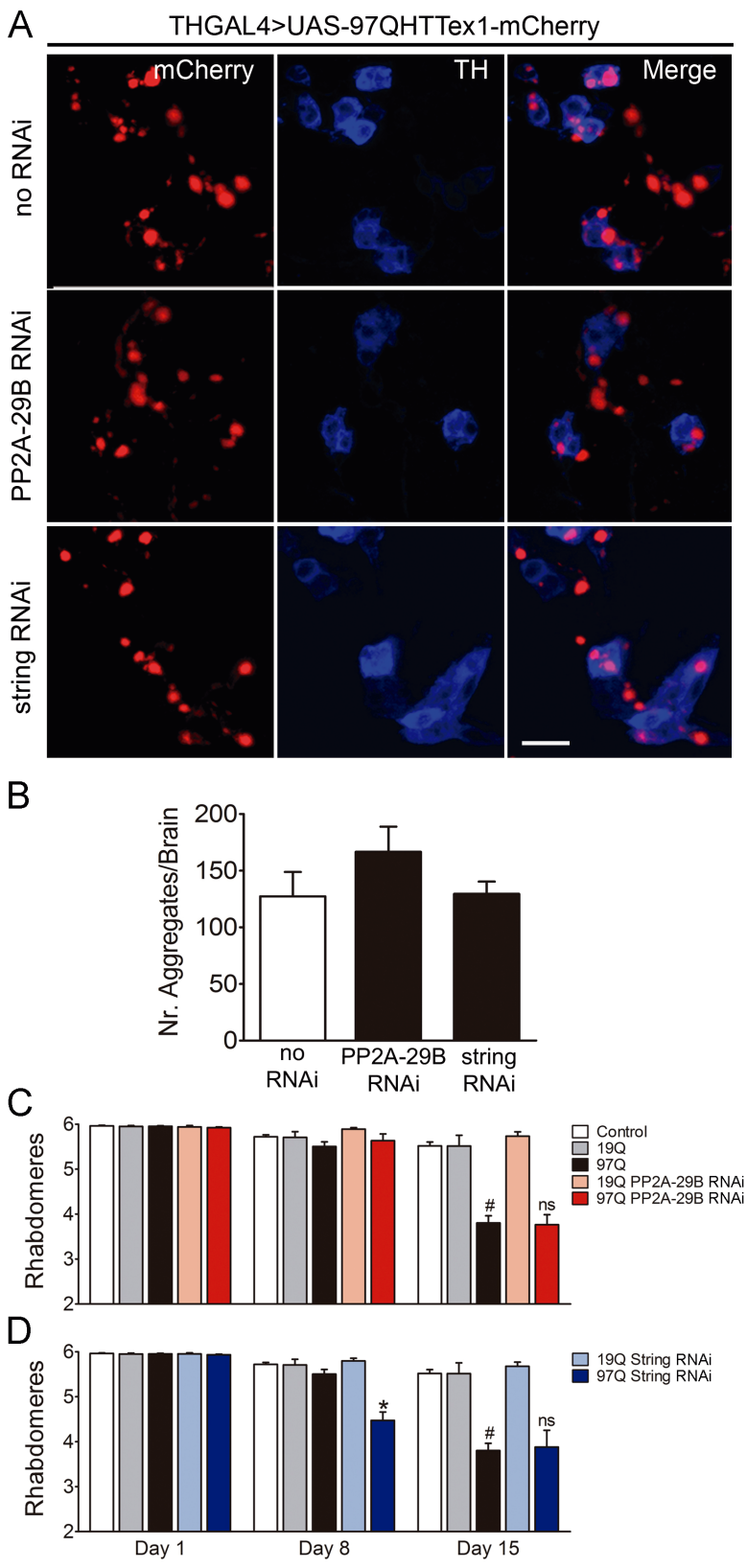

Figure S8. Knockdown of PP2A or *string* does not affect 97QHTTex1 aggregation or toxicity in *Drosophila*. (A) Imaging of adult dopaminergic neurons in RNAi transgenic flies expressing 97QHTTex1 under the control of THGAL4. *PP2A-29B* or *string* RNAi knockdown flies showed no overt phenotype in terms of aggregation when compared to 97QHTTex1 no RNAi control. (B) Quantitative analyses of confocal pictures. Data are average number of aggregates ± SEM. Scale bar, 10 µm. *PP2A-29B* (C) or *string* (D) downregulation did not affect progressive photoreceptor loss observed in 97QHTTex1 flies. *significant versus 97Q, #significant versus 97Q at day 1 and day 8, $p<0.05$. ns, no significant versus 97Q at day 15.

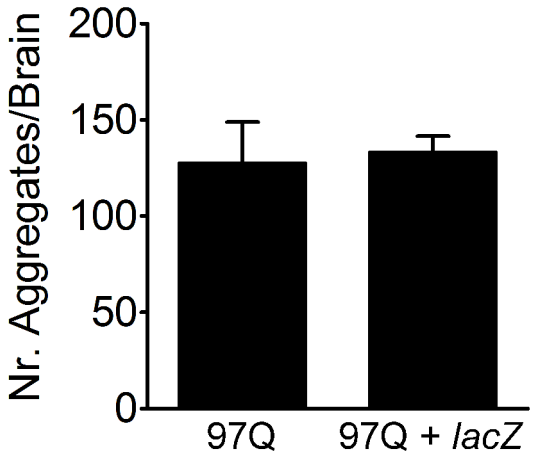

Figure S9. Double UAS control flies do not exhibit changes in aggregate phenotypic responses to THGAL4>UAS-97QHTTex1-mCherry expression. Quantification of average (±SEM) number of aggregates per brain in flies expressing both UAS-97QHTTex1-mCherry and UAS-*lacZ* constructs (97Q + *lacZ*), in comparison to single UAS-97QHTTex1-mCherry transgenic flies (97Q).

Supplemental information II

Inventory

Figure S10, related to Figure 20

Figure S11

Figure S12

Figure S13

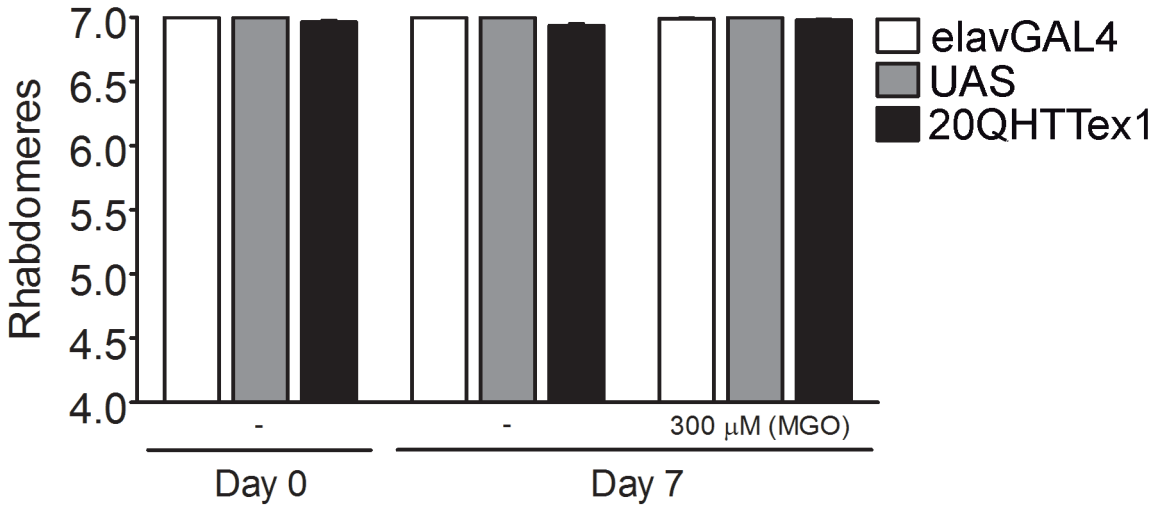

Figure S10. Control flies do not exhibit neuronal loss when treated with MGO. Quantification of mean rhabdomeres (± SEM) per ommatidium in driver and UAS control flies. Flies expressing a WT version of HTT (20QHTTex1) were also analyzed. The pseudopupil assay was performed in untreated flies (-) at the day of pupae hatching (day 0) and following 7 days (day 7). A group of at least 30 flies per genotype were separated upon eclosion and treated with the highest dose of MGO used in this study (300 μg). After 7 days of treatment, flies were handled for rhabdomere quantification.

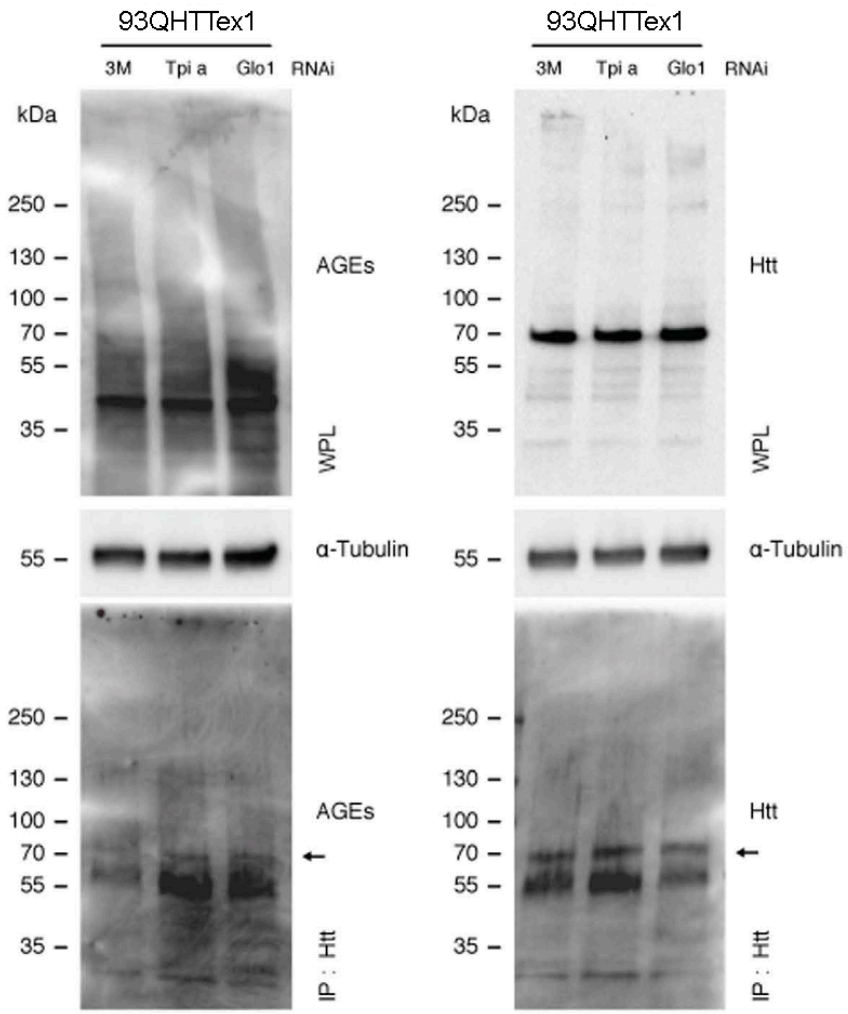

Figure S11. Knockdown of Glo1 or Tpi causes increased protein glycation and accumulation of AGEs in HD flies. One hundred heads from flies expressing 93QHTTex1 and knocked down for Tpi, Glo1 or 3M (as control) were lysed and immunoprecipitated (IP) with anti-HTT antibody (bottom panels). The whole protein lysates (WPL) (n = 3) and IP samples (n = 2) were probed for AGEs (left panels) or HTT (right panels). Arrow indicates 93QHTTex1 MW. Corresponding loading controls (α-tubulin) are shown.

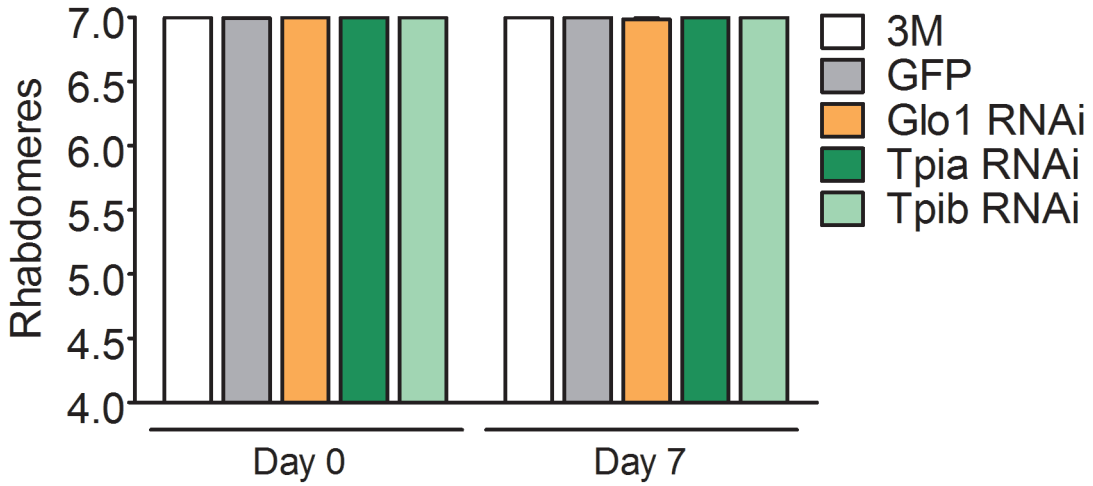

Figure S12. Knockdown of Glo1 or Tpi does not induce neurotoxicity in WT background flies. Number of rhabdomeres per ommatidium in WT flies with pan-neuronal knockdown of Glo1 or Tpi is presented at day 0 and 7 post-eclosion, with no neurodegeneration observed. Control flies expressing 3M or GFP also do not exhibit degeneration of rhabdomeres. Data is mean ± SEM.

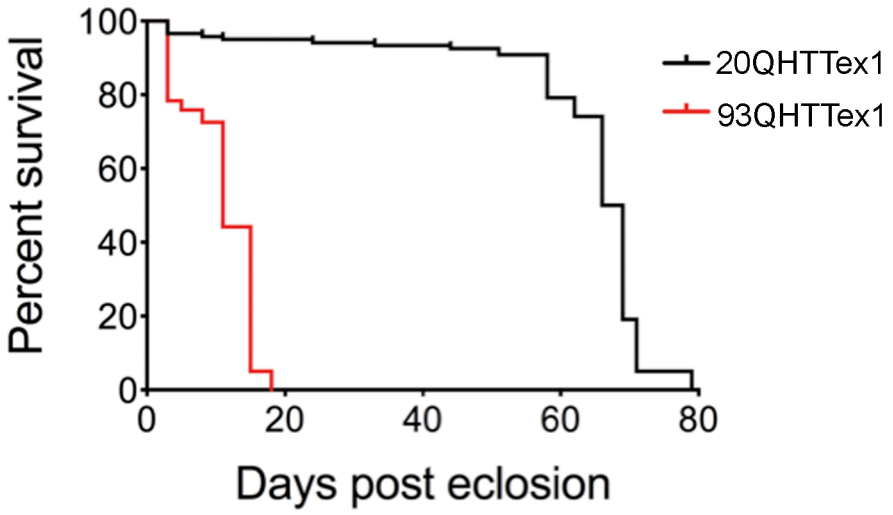

Figure S13. Pan-neuronal expression of 93QHTTex1 causes a dramatic decrease in lifespan. Survival curves of flies expressing 20QHTTex1 or 93QHTTex1 under the control of *elavGAL4*. Data is presented as mean ± SEM.

Supplemental information III

Inventory

Figure S14, related to Figure 22

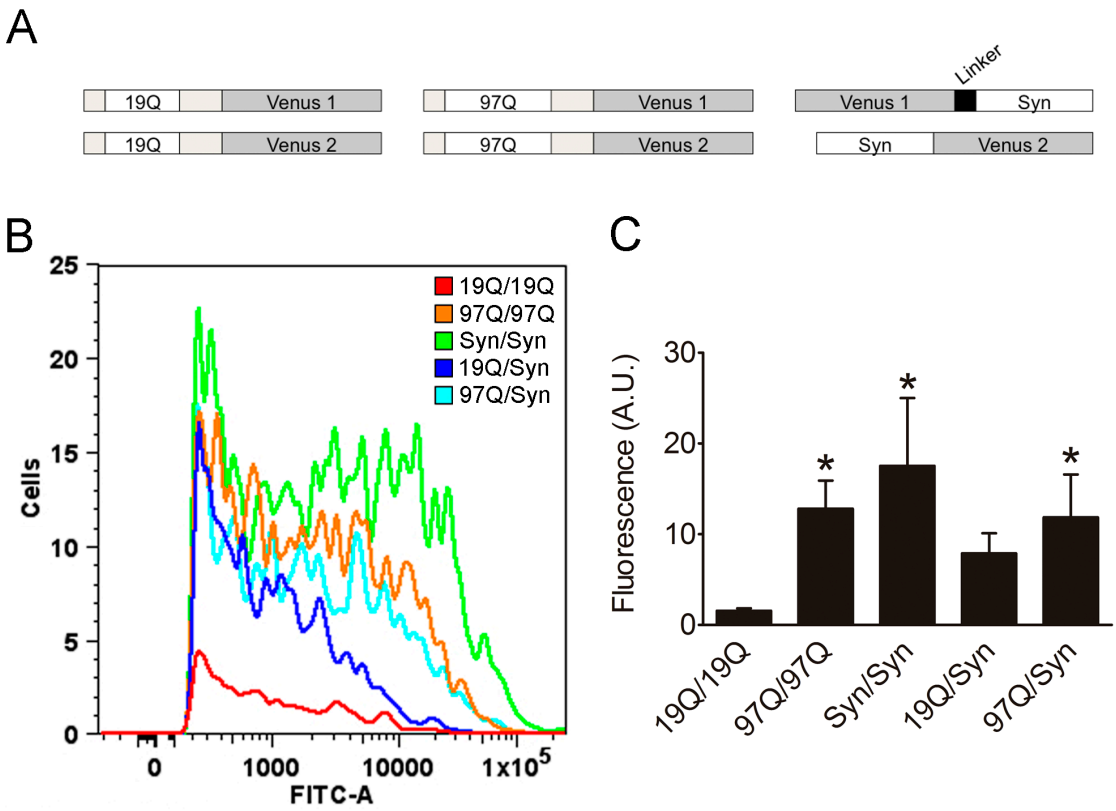

Figure S14. Alpha-synuclein interacts with HTT in living cells. H4 cells were transfected with different combinations of 19Q, 97Q and/or Syn-Venus BiFC plasmids (A). Twenty-four hours post-transfection, cells were analysed by means of flow cytometry (B and C). Co-expression of mutant HTT and α-syn produces similar levels of oligomerization in comparison to the 97Q/97Q control, as indicated by flow cytometry measurements of number of fluorescence cells (B) and total average fluorescence (C). Data is mean ± SD. *significant versus 19Q/19Q, $p<0.05$. AU, arbitrary units.

Supplemental information IV

Inventory

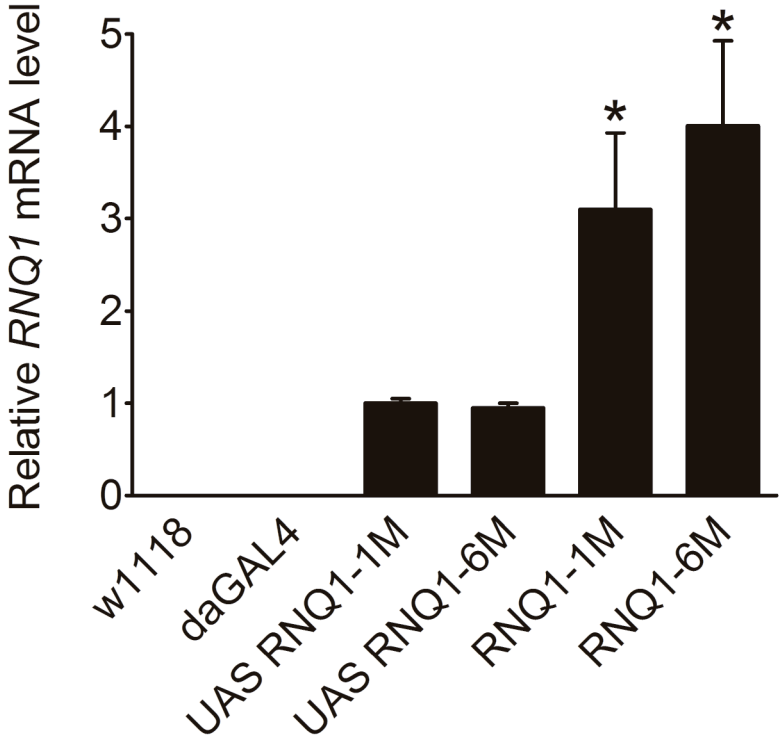

Figure S15. Quantification of *RNQ1* mRNA levels in *Drosophila* transgenic lines. Expression levels of *daGAL4*>UAS-RNQ1-1M and *daGAL4*>UAS-RNQ1-6M lines were compared to white background (w^{1118}), driver (*daGAL4*) and UAS controls, by means of QPCR. Levels of Rnq1 mRNA are increased ~3-4 fold in RNQ1-1M or RNQ1-6M expressing flies versus UAS controls. Data are represented as mean ± SEM of mRNA levels of *RNQ1* transgene relative to *rpl32* housekeeping gene. N = 30 flies per genotype. *significant versus respective UAS control, $p<0.05$.

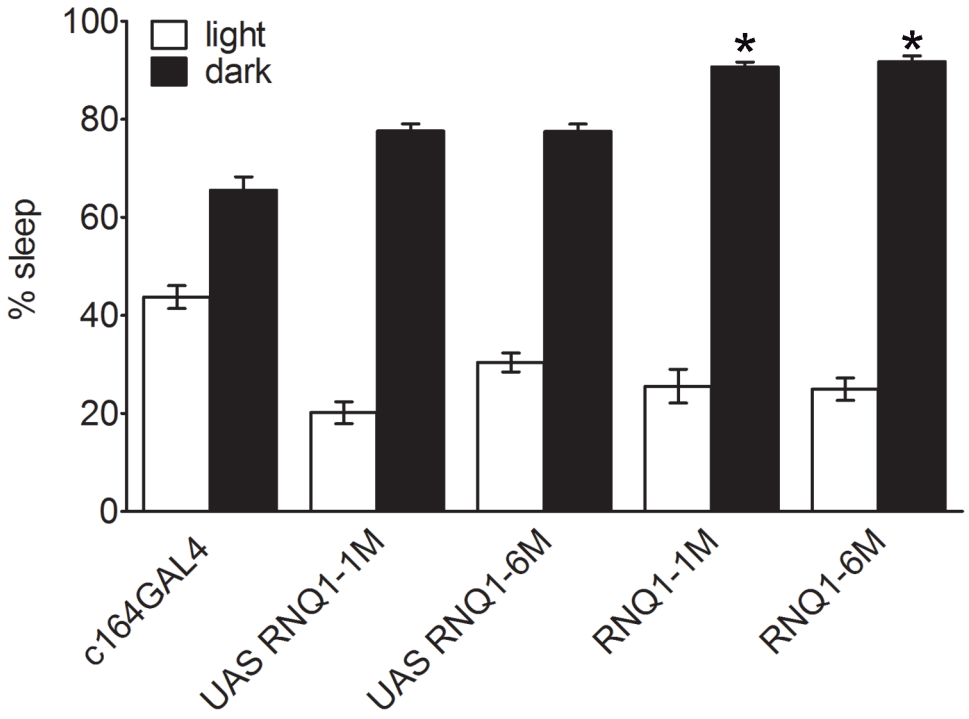

Figure S16. Rnq1 expressing flies exhibit increased sleep-like behavior during nighttime. Total rest was assayed in newly-emerged flies using Trikinetics *Drosophila* activity monitors. Activity data was recorded over 7 days in 12 h light/dark cycles and collected in 5 min time bins. Total sleep like-behavior is expressed as the average number of 5 min intervals with 0 activity counts. Flies expressing Rnq1 in the motor neurons show an increased number of rest periods throughout the night in comparison to controls. N = 26 - 32 flies per genotype. Data are mean ± SEM. *significant versus *c164GAL4* and UAS controls, $p<0.05$.

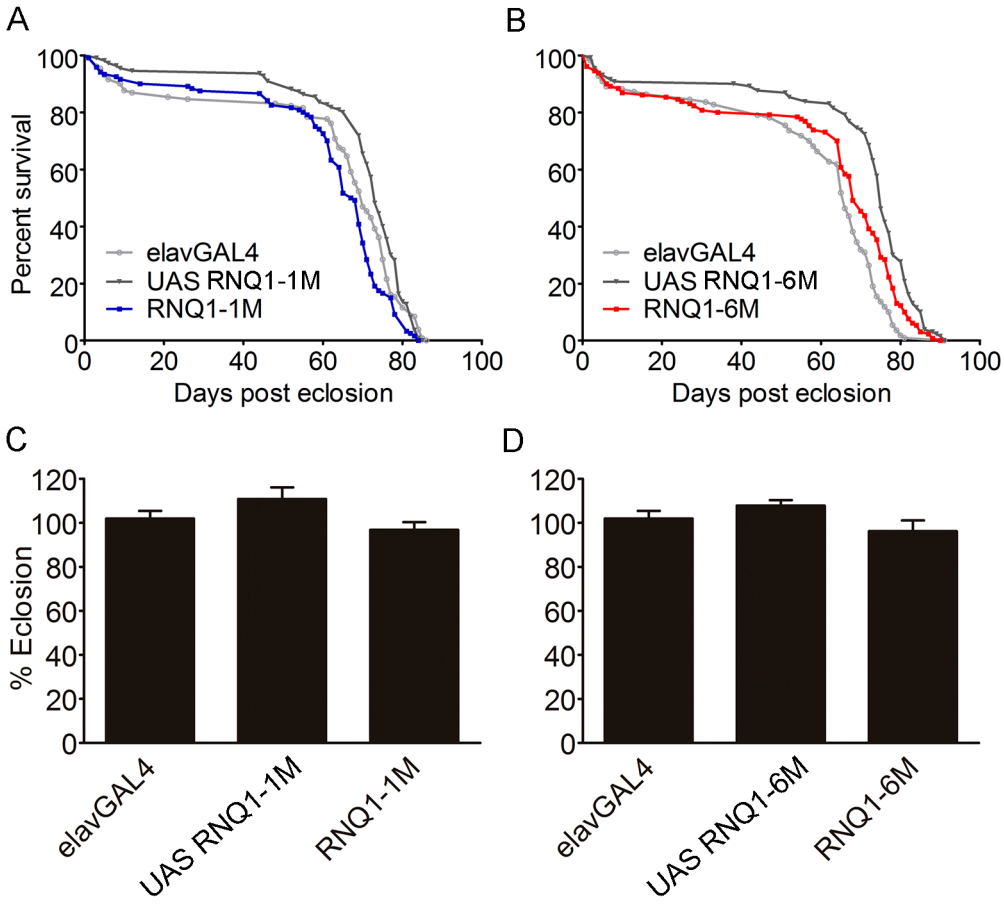

Figure S17. Rnq1 expression does not affect longevity or viability of WT background flies. Lifespan (A, B) and eclosion ratio (C, D) were evaluated in flies expressing RNQ1-1M or RNQ1-6M transgenes via the *elav* promotor. (A) *elavGAL4* (mean = 70 days), UAS RNQ1-1M (mean = 73 days), RNQ1-1M (mean = 67.5 days). (B) *elavGAL4* (mean = 66 days), UAS RNQ1-6M (mean = 75 days), RNQ1-1M (mean = 68 days). No differences were observed versus controls. Data are mean ± SEM.

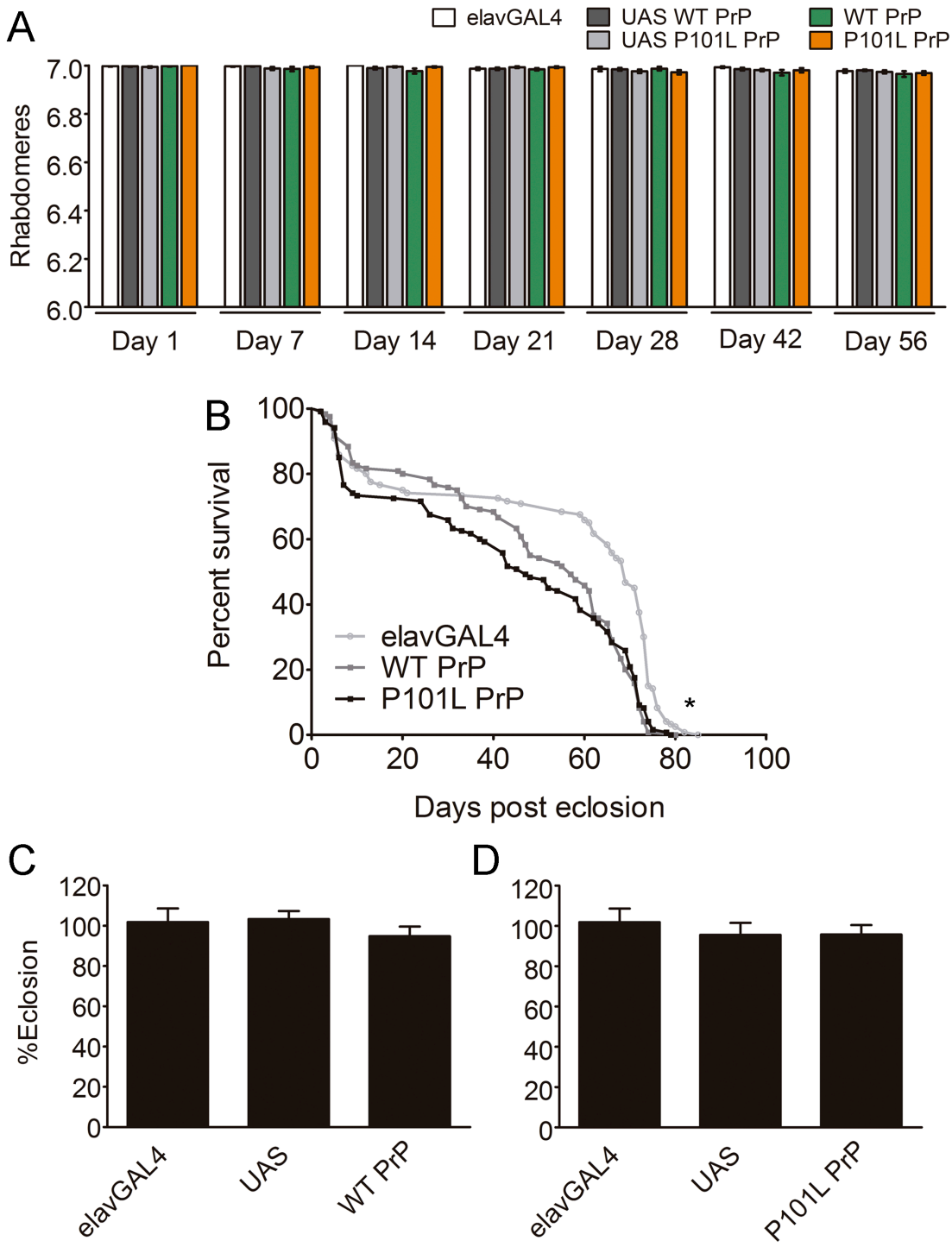

Figure S18. Expression of murine prion protein does not induce neurotoxicity in WT background flies. (A) Quantification of rhabdomeres per ommatidium in flies expressing wild-type (WT PrP) or a mutated version (P101L PrP) of the murine prion over 56 days post-eclosion. Pan-neuronal expression of PrP did not induce age-dependent neuronal loss (A) but decreased lifespan in WT background, as determined by percentage of surviving flies (B). Mean survival values are: elavGAL4 (mean=69 days), WT PrP (mean=57 days), P101L PrP (mean=47 days). (C and D) Percentage of eclosion was calculated by the mean ratio between emerging PrP expressing females versus control males hatching out of pupal case. Eclosion ratio was not affected in *elav*-driven PrP expressing flies. All data are mean ± SEM.

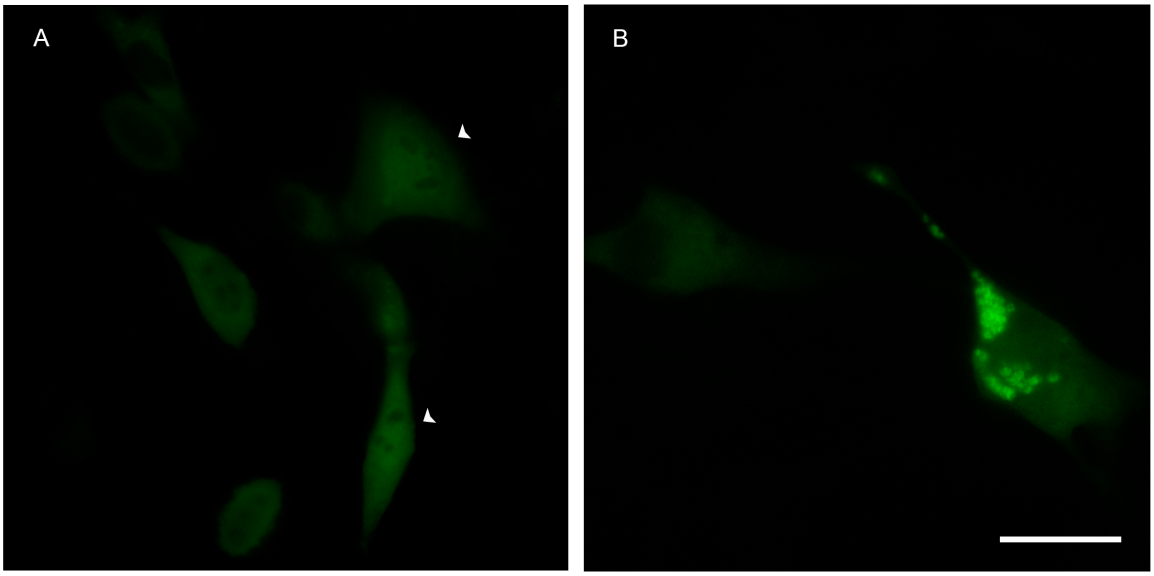

Figure S19. Rnq1 changes subcellular localization of mutant HTT and alters its aggregation in living cells. HT22 cells in (A) and (B) were co-transfected with RNQ1-Venus and 97QHTTex1-Venus plasmids. (A) 97QHTTex1 localizes to the nucleus in the presence of Rnq1. (B) Small cytosolic puncta formed upon interaction of Rnq1 with 97QHTTex1 are deposited together near the nucleus. Scale bar, 20 μm.

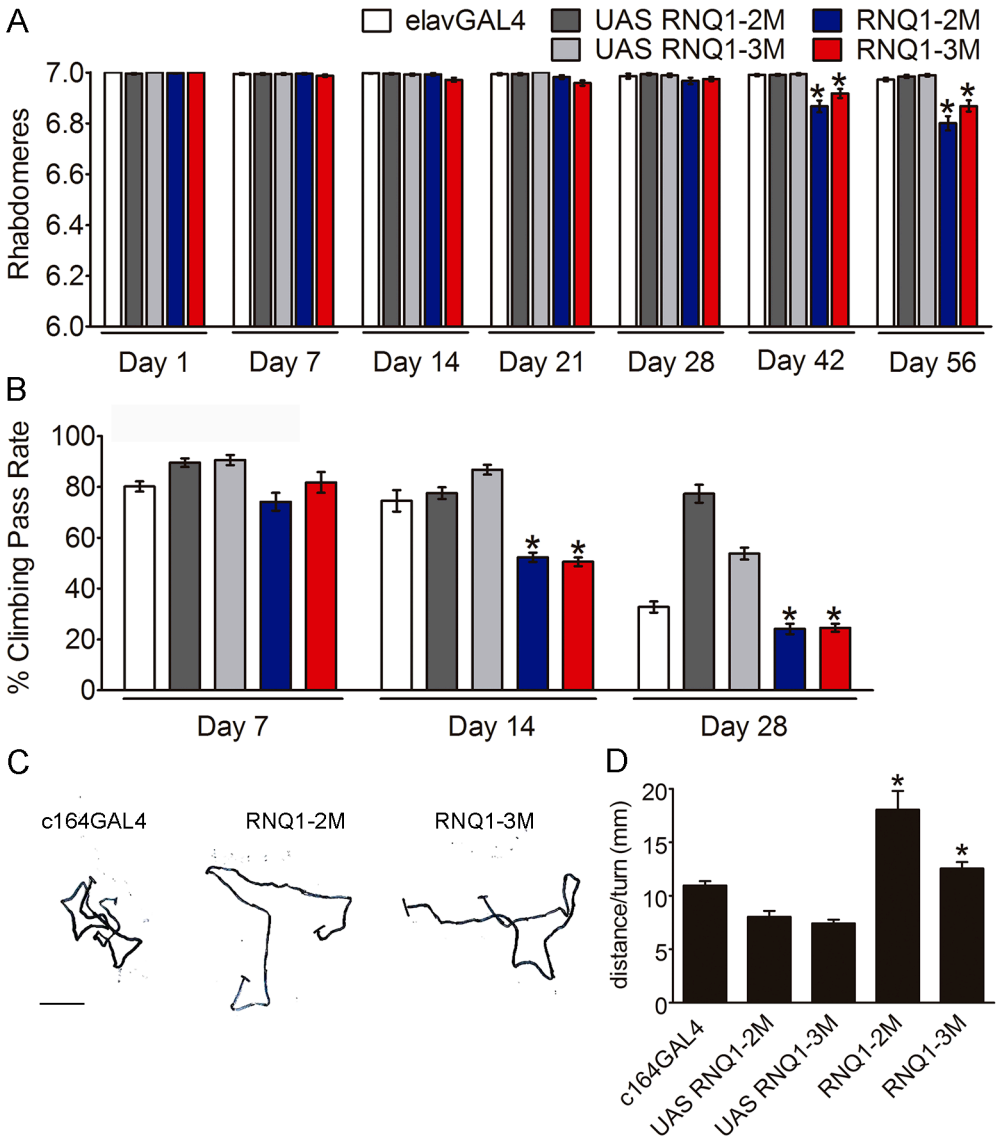

Figure S20. Phenotypic characterization of *Drosophila* lines carrying *RNQ1* transgene in the 3rd chromosome. Additional UAS-*RNQ1* transgenic lines (RNQ1-2M and RNQ1-3M) were analyzed for age-dependent neurodegeneration (A) and locomotor defects in both adults (B) and larvae (C, D). RNQ1-2M or RNQ1-3M expressing flies produced similar disease-relevant phenotypes exhibited by RNQ1-1M and RNQ1-6M lines. All data are mean ± SEM. *significant versus *elavGAL4* or *c164GAL4*, p <0.05. Scale bar, 10 mm.

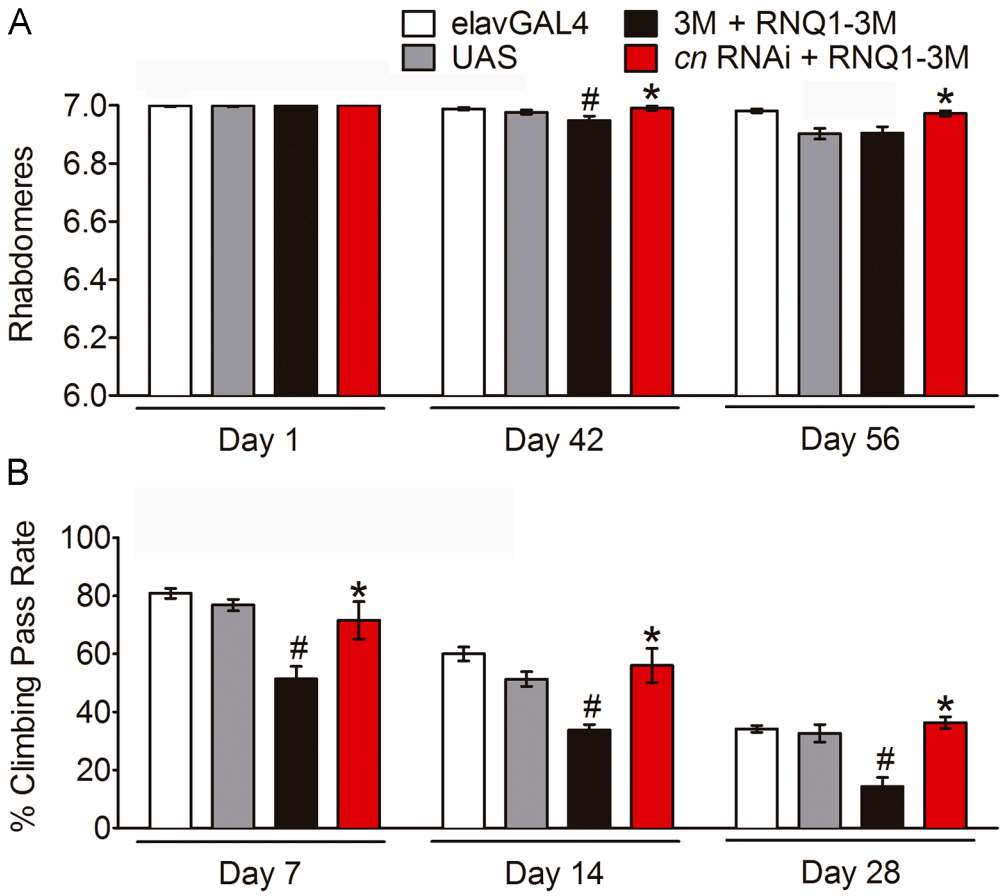

Figure S21. *cn* silencing improves disease-related phenotypes in the RNQ1-3M line. (A) Average number of rhabdomeres per ommatidium in aging flies. (B) Mean climbing pass rate at different post-eclosion ages. All data are mean ± SEM. *significant versus 3M + RNQ1-3M, #significant *elavGAL4* and UAS 3M + RNQ1-3M control, $p<0.05$.

VI.

References

Adjou, K. T., Allix, S., Ouidja, M. O., Backer, S., Couquet, C., Cornuejols, M. J., Deslys, J. P., Brugere, H., Brugere-Picoux, J., El-Hachimi, K. H. 2007. Alpha-synuclein accumulates in the brain of scrapie-affected sheep and goats. *J Comp Pathol,* 137**,** 78-81.

Agorogiannis, E. I., Agorogiannis, G. I., Papadimitriou, A., Hadjigeorgiou, G. M. 2004. Protein misfolding in neurodegenerative diseases. *Neuropathol Appl Neurobiol,* 30**,** 215-224.

Aguzzi, A., Rajendran, L. 2009. The transcellular spread of cytosolic amyloids, prions, and prionoids. *Neuron,* 64**,** 783-790.

Aharony, I., Ehrnhoefer, D. E., Shruster, A., Qiu, X., Franciosi, S., Hayden, M. R., Offen, D. 2015. A Huntingtin-based peptide inhibitor of caspase-6 provides protection from mutant Huntingtin-induced motor and behavioral deficits. *Hum Mol Genet,* 24**,** 2604-2614.

Ahmed, N., Battah, S., Karachalias, N., Babaei-Jadidi, R., Horanyi, M., Baroti, K., Hollan, S., Thornalley, P. J. 2003. Increased formation of methylglyoxal and protein glycation, oxidation and nitrosation in triosephosphate isomerase deficiency. *Biochim Biophys Acta,* 1639**,** 121-132.

Aiken, C. T., Steffan, J. S., Guerrero, C. M., Khashwji, H., Lukacsovich, T., Simmons, D., Purcell, J. M., Menhaji, K., Zhu, Y. Z., Green, K., Laferla, F., Huang, L., Thompson, L. M., Marsh, J. L. 2009. Phosphorylation of threonine 3: implications for Huntingtin aggregation and neurotoxicity. *J Biol Chem,* 284**,** 29427-29436.

Alberti, S., Halfmann, R., King, O., Kapila, A., Lindquist, S. 2009. A systematic survey identifies prions and illuminates sequence features of prionogenic proteins. *Cell,* 137**,** 146-158.

Amador, F. C., Henriques, A. G., da Cruz, E. S. O. A., da Cruz, E. S. E. F. 2004. Monitoring protein phosphatase 1 isoform levels as a marker for cellular stress. *Neurotoxicol Teratol,* 26**,** 387-395.

Amaral, J. D., Herrera, F., Rodrigues, P. M., Dionisio, P. A., Outeiro, T. F., Rodrigues, C. M. 2013. Live-cell imaging of p53 interactions using a novel Venus-based bimolecular fluorescence complementation system. *Biochem Pharmacol,* 85**,** 745-752.

Ambegaokar, S. S., Roy, B., Jackson, G. R. 2010. Neurodegenerative models in Drosophila: polyglutamine disorders, Parkinson disease, and amyotrophic lateral sclerosis. *Neurobiol Dis,* 40**,** 29-39.

Ambrose CM, D. M., Barnes G, Bates GP, Lin CS, Srinidhi J, Baxendale S,, Hummerich H, L. H., Altherr M, 1994. Structure and expression of the Huntington's disease gene: evidence against simple inactivation due to an expanded CAG repeat. *Somat Cell Mol Genet,* 20**,** 27-38.

Andre, E. A., Braatz, E. M., Liu, J. P., Zeitlin, S. O. 2017. Generation and Characterization of Knock-in Mouse Models Expressing Versions of Huntingtin with Either an N17 or a Combined PolyQ and Proline-Rich Region Deletion. *J Huntingtons Dis,* 6**,** 47-62.

Andreassen, O. A., Dedeoglu, A., Stanojevic, V., Hughes, D. B., Browne, S. E., Leech, C. A., Ferrante, R. J., Habener, J. F., Beal, M. F., Thomas, M. K. 2002. Huntington's disease of the endocrine pancreas: insulin deficiency and diabetes mellitus due to impaired insulin gene expression. *Neurobiol Dis,* 11**,** 410-424.

Anne, S. L., Saudou, F., Humbert, S. 2007. Phosphorylation of huntingtin by cyclin-dependent kinase 5 is induced by DNA damage and regulates wild-type and mutant huntingtin toxicity in neurons. *J Neurosci,* 27**,** 7318-7328.

Ansaloni, A., Wang, Z. M., Jeong, J. S., Ruggeri, F. S., Dietler, G., Lashuel, H. A. 2014. One-pot semisynthesis of exon 1 of the Huntingtin protein: new tools for elucidating the role of posttranslational modifications in the pathogenesis of Huntington's disease. *Angew Chem Int Ed Engl,* 53**,** 1928-1933.

Anzilotti, S., Giampa, C., Laurenti, D., Perrone, L., Bernardi, G., Melone, M. A., Fusco, F. R. 2012. Immunohistochemical localization of receptor for advanced glycation end (RAGE) products in the R6/2 mouse model of Huntington's disease. *Brain Res Bull,* 87**,** 350-358.

Arai, T., Hasegawa, M., Akiyama, H., Ikeda, K., Nonaka, T., Mori, H., Mann, D., Tsuchiya, K., Yoshida, M., Hashizume, Y., Oda, T. 2006. TDP-43 is a component of ubiquitin-positive tau-negative inclusions in frontotemporal lobar degeneration and amyotrophic lateral sclerosis. *Biochem Biophys Res Commun,* 351**,** 602-611.

Arango, M., Holbert, S., Zala, D., Brouillet, E., Pearson, J., Regulier, E., Thakur, A. K., Aebischer, P., Wetzel, R., Deglon, N., Neri, C. 2006. CA150 expression delays striatal cell death in overexpression and knock-in conditions for mutant huntingtin neurotoxicity. *J Neurosci,* 26**,** 4649-4659.

Arias, C., Montiel, T., Pena, F., Ferrera, P., Tapia, R. 2002. Okadaic acid induces epileptic seizures and hyperphosphorylation of the NR2B subunit of the NMDA receptor in rat hippocampus in vivo. *Exp Neurol,* 177**,** 284-291.

Arndt, J. R., Kondalaji, S. G., Maurer, M. M., Parker, A., Legleiter, J., Valentine, S. J. 2015. Huntingtin N-Terminal Monomeric and Multimeric Structures Destabilized by Covalent Modification of Heteroatomic Residues. *Biochemistry,* 54**,** 4285-4296.

Arrasate, M., Mitra, S., Schweitzer, E. S., Segal, M. R., Finkbeiner, S. 2004. Inclusion body formation reduces levels of mutant huntingtin and the risk of neuronal death. *Nature,* 431**,** 805-810.

Arslan, F., Hong, J. Y., Kanneganti, V., Park, S. K., Liebman, S. W. 2015. Heterologous aggregates promote de novo prion appearance via more than one mechanism. *PLoS Genet,* 11**,** e1004814.

Arzberger, T., Krampfl, K., Leimgruber, S., Weindl, A. 1997. Changes of NMDA receptor subunit (NR1, NR2B) and glutamate transporter (GLT1) mRNA expression in Huntington's disease--an in situ hybridization study. *J Neuropathol Exp Neurol,* 56**,** 440-454.

Askanas, V., Engel, W. K., Nogalska, A. 2012. Pathogenic considerations in sporadic inclusion-body myositis, a degenerative muscle disease associated with aging and abnormalities of myoproteostasis. *J Neuropathol Exp Neurol,* 71**,** 680-693.

Atwal, R. S., Desmond, C. R., Caron, N., Maiuri, T., Xia, J., Sipione, S., Truant, R. 2011. Kinase inhibitors modulate huntingtin cell localization and toxicity. *Nat Chem Biol,* 7**,** 453-460.

Atwal, R. S., Xia, J., Pinchev, D., Taylor, J., Epand, R. M., Truant, R. 2007. Huntingtin has a membrane association signal that can modulate huntingtin aggregation, nuclear entry and toxicity. *Hum Mol Genet,* 16**,** 2600-2615.

Auerbach, W., Hurlbert, M. S., Hilditch-Maguire, P., Wadghiri, Y. Z., Wheeler, V. C., Cohen, S. I., Joyner, A. L., MacDonald, M. E., Turnbull, D. H. 2001. The HD mutation causes progressive lethal neurological disease in mice expressing reduced levels of huntingtin. *Hum Mol Genet,* 10**,** 2515-2523.

Ayers, J. I., Fromholt, S. E., O'Neal, V. M., Diamond, J. H., Borchelt, D. R. 2016. Prion-like propagation of mutant SOD1 misfolding and motor neuron disease spread along neuroanatomical pathways. *Acta Neuropathol,* 131**,** 103-114.

Babcock, D. T., Ganetzky, B. 2015. Transcellular spreading of huntingtin aggregates in the Drosophila brain. *Proc Natl Acad Sci U S A,* 112**,** E5427-5433.

Badiola, N., de Oliveira, R. M., Herrera, F., Guardia-Laguarta, C., Goncalves, S. A., Pera, M., Suarez-Calvet, M., Clarimon, J., Outeiro, T. F., Lleo, A. 2011. Tau enhances alpha-synuclein aggregation and toxicity in cellular models of synucleinopathy. *PLoS One,* 6**,** e26609.

Bae, B. I., Xu, H., Igarashi, S., Fujimuro, M., Agrawal, N., Taya, Y., Hayward, S. D., Moran, T. H., Montell, C., Ross, C. A., Snyder, S. H., Sawa, A. 2005. p53 mediates cellular dysfunction and behavioral abnormalities in Huntington's disease. *Neuron,* 47**,** 29-41.

Bailey, C. D., Johnson, G. V. 2005. Tissue transglutaminase contributes to disease progression in the R6/2 Huntington's disease mouse model via aggregate-independent mechanisms. *J Neurochem,* 92**,** 83-92.

Baksi, S., Jana, N. R., Bhattacharyya, N. P., Mukhopadhyay, D. 2013. Grb2 is regulated by foxd3 and has roles in preventing accumulation and aggregation of mutant huntingtin. *PLoS One,* 8**,** e76792.

Balchin, D., Hayer-Hartl, M., Hartl, F. U. 2016. In vivo aspects of protein folding and quality control. *Science,* 353**,** aac4354.

Banerjee, M., Datta, M., Bhattacharyya, N. P. 2017. Modulation of mutant Huntingtin aggregates and toxicity by human myeloid leukemia factors. *Int J Biochem Cell Biol,* 82**,** 1-9.

Bao, J., Sharp, A. H., Wagster, M. V., Becher, M., Schilling, G., Ross, C. A., Dawson, V. L., Dawson, T. M. 1996. Expansion of polyglutamine repeat in huntingtin leads to abnormal protein interactions involving calmodulin. *Proc Natl Acad Sci U S A,* 93**,** 5037-5042.

Bartels, T., Choi, J. G., Selkoe, D. J. 2011. alpha-Synuclein occurs physiologically as a helically folded tetramer that resists aggregation. *Nature,* 477**,** 107-110.

Bates, G. P., Dorsey, R., Gusella, J. F., Hayden, M. R., Kay, C., Leavitt, B. R., Nance, M., Ross, C. A., Scahill, R. I., Wetzel, R., Wild, E. J., Tabrizi, S. J. 2015. Huntington disease. *Nat Rev Dis Primers,* 1**,** 15005.

Bates, G. P., Mangiarini, L., Davies, S. W. 1998. Transgenic mice in the study of polyglutamine repeat expansion diseases. *Brain Pathol,* 8**,** 699-714.

Behrens, P. F., Franz, P., Woodman, B., Lindenberg, K. S., Landwehrmeyer, G. B. 2002. Impaired glutamate transport and glutamate-glutamine cycling: downstream effects of the Huntington mutation. *Brain,* 125**,** 1908-1922.

Ben Haim, L., Carrillo-de Sauvage, M. A., Ceyzeriat, K., Escartin, C. 2015. Elusive roles for reactive astrocytes in neurodegenerative diseases. *Front Cell Neurosci,* 9**,** 278.

Ben-Gedalya, T., Lyakhovetsky, R., Yedidia, Y., Bejerano-Sagie, M., Kogan, N. M., Karpuj, M. V., Kaganovich, D., Cohen, E. 2011. Cyclosporin-A-induced prion protein aggresomes are dynamic quality-control cellular compartments. *J Cell Sci,* 124**,** 1891-1902.

Bennett, D., Lyulcheva, E., Alphey, L., Hawcroft, G. 2006. Towards a comprehensive analysis of the protein phosphatase 1 interactome in Drosophila. *J Mol Biol,* 364**,** 196-212.

Berger, C., Renner, S., Luer, K., Technau, G. M. 2007. The commonly used marker ELAV is transiently expressed in neuroblasts and glial cells in the Drosophila embryonic CNS. *Dev Dyn,* 236**,** 3562-3568.

Bhattacharyya, A., Thakur, A. K., Chellgren, V. M., Thiagarajan, G., Williams, A. D., Chellgren, B. W., Creamer, T. P., Wetzel, R. 2006. Oligoproline effects on polyglutamine conformation and aggregation. *J Mol Biol,* 355**,** 524-535.

Bjorkqvist, M., Fex, M., Renstrom, E., Wierup, N., Petersen, A., Gil, J., Bacos, K., Popovic, N., Li, J. Y., Sundler, F., Brundin, P., Mulder, H. 2005. The R6/2 transgenic mouse model of Huntington's disease develops diabetes due to deficient beta-cell mass and exocytosis. *Hum Mol Genet,* 14**,** 565-574.

Blum, D., Herrera, F., Francelle, L., Mendes, T., Basquin, M., Obriot, H., Demeyer, D., Sergeant, N., Gerhardt, E., Brouillet, E., Buee, L., Outeiro, T. F. 2015. Mutant huntingtin alters Tau phosphorylation and subcellular distribution. *Hum Mol Genet,* 24**,** 76-85.

Bodner, R. A., Outeiro, T. F., Altmann, S., Maxwell, M. M., Cho, S. H., Hyman, B. T., McLean, P. J., Young, A. B., Housman, D. E., Kazantsev, A. G. 2006. Pharmacological promotion of

inclusion formation: a therapeutic approach for Huntington's and Parkinson's diseases. *Proc Natl Acad Sci U S A,* 103**,** 4246-4251.

Bollen, M., Peti, W., Ragusa, M. J., Beullens, M. 2010. The extended PP1 toolkit: designed to create specificity. *Trends Biochem Sci,* 35**,** 450-458.

Bolte, S., Cordelieres, F. P. 2006. A guided tour into subcellular colocalization analysis in light microscopy. *J Microsc,* 224**,** 213-232.

Borrell-Pages, M., Zala, D., Humbert, S., Saudou, F. 2006. Huntington's disease: from huntingtin function and dysfunction to therapeutic strategies. *Cell Mol Life Sci,* 63**,** 2642-2660.

Boutell, J. M., Thomas, P., Neal, J. W., Weston, V. J., Duce, J., Harper, P. S., Jones, A. L. 1999. Aberrant interactions of transcriptional repressor proteins with the Huntington's disease gene product, huntingtin. *Hum Mol Genet,* 8**,** 1647-1655.

Boutell, J. M., Wood, J. D., Harper, P. S., Jones, A. L. 1998. Huntingtin interacts with cystathionine beta-synthase. *Hum Mol Genet,* 7**,** 371-378.

Bradford, J., Shin, J. Y., Roberts, M., Wang, C. E., Li, X. J., Li, S. 2009. Expression of mutant huntingtin in mouse brain astrocytes causes age-dependent neurological symptoms. *Proc Natl Acad Sci U S A,* 106**,** 22480-22485.

Bradford, J., Shin, J. Y., Roberts, M., Wang, C. E., Sheng, G., Li, S., Li, X. J. 2010. Mutant huntingtin in glial cells exacerbates neurological symptoms of Huntington disease mice. *J Biol Chem,* 285**,** 10653-10661.

Braithwaite, S. P., Stock, J. B., Lombroso, P. J., Nairn, A. C. 2012. Protein phosphatases and Alzheimer's disease. *Prog Mol Biol Transl Sci,* 106**,** 343-379.

Branco-Santos, J., Herrera, F., Pocas, G. M., Pires-Afonso, Y., Giorgini, F., Domingos, P. M., Outeiro, T. F. 2017. Protein phosphatase 1 regulates huntingtin exon 1 aggregation and toxicity. *Hum Mol Genet,* 26**,** 3763-3775.

Brand, A. H., Perrimon, N. 1993. Targeted gene expression as a means of altering cell fates and generating dominant phenotypes. *Development,* 118**,** 401-415.

Breda, C., Nugent, M. L., Estranero, J. G., Kyriacou, C. P., Outeiro, T. F., Steinert, J. R., Giorgini, F. 2015. Rab11 modulates alpha-synuclein-mediated defects in synaptic transmission and behaviour. *Hum Mol Genet,* 24**,** 1077-1091.

Breda, C., Sathyasaikumar, K. V., Sograte Idrissi, S., Notarangelo, F. M., Estranero, J. G., Moore, G. G., Green, E. W., Kyriacou, C. P., Schwarcz, R., Giorgini, F. 2016. Tryptophan-2,3-dioxygenase (TDO) inhibition ameliorates neurodegeneration by modulation of kynurenine pathway metabolites. *Proc Natl Acad Sci U S A,* 113**,** 5435-5440.

Brenner, M., Johnson, A. B., Boespflug-Tanguy, O., Rodriguez, D., Goldman, J. E., Messing, A. 2001. Mutations in GFAP, encoding glial fibrillary acidic protein, are associated with Alexander disease. *Nat Genet,* 27**,** 117-120.

Brettschneider, J., Del Tredici, K., Lee, V. M., Trojanowski, J. Q. 2015. Spreading of pathology in neurodegenerative diseases: a focus on human studies. *Nat Rev Neurosci,* 16**,** 109-120.

Bruce, K. L., Chernoff, Y. O. 2011. Sequence specificity and fidelity of prion transmission in yeast. *Semin Cell Dev Biol,* 22**,** 444-451.

Brundin, P., Melki, R., Kopito, R. 2010. Prion-like transmission of protein aggregates in neurodegenerative diseases. *Nat Rev Mol Cell Biol,* 11**,** 301-307.

Burke, K. A., Hensal, K. M., Umbaugh, C. S., Chaibva, M., Legleiter, J. 2013a. Huntingtin disrupts lipid bilayers in a polyQ-length dependent manner. *Biochim Biophys Acta,* 1828**,** 1953-1961.

Burke, K. A., Kauffman, K. J., Umbaugh, C. S., Frey, S. L., Legleiter, J. 2013b. The interaction of polyglutamine peptides with lipid membranes is regulated by flanking sequences associated with huntingtin. *J Biol Chem,* 288**,** 14993-15005.

Burnett, B. G., Andrews, J., Ranganathan, S., Fischbeck, K. H., Di Prospero, N. A. 2008. Expression of expanded polyglutamine targets profilin for degradation and alters actin dynamics. *Neurobiol Dis,* 30**,** 365-374.

Bustamante, M. B., Ansaloni, A., Pedersen, J. F., Azzollini, L., Cariulo, C., Wang, Z. M., Petricca, L., Verani, M., Puglisi, F., Park, H., Lashuel, H., Caricasole, A. 2015. Detection of huntingtin exon 1 phosphorylation by Phos-Tag SDS-PAGE: Predominant phosphorylation on threonine 3 and regulation by IKKbeta. *Biochem Biophys Res Commun,* 463**,** 1317-1322.

Campesan, S., Green, E. W., Breda, C., Sathyasaikumar, K. V., Muchowski, P. J., Schwarcz, R., Kyriacou, C. P., Giorgini, F. 2011. The kynurenine pathway modulates neurodegeneration in a Drosophila model of Huntington's disease. *Curr Biol,* 21**,** 961-966.

Caparros-Lefebvre, D., Kerdraon, O., Devos, D., Dhaenens, C. M., Blum, D., Maurage, C. A., Delacourte, A., Sablonniere, B. 2009. Association of corticobasal degeneration and Huntington's disease: can Tau aggregates protect Huntingtin toxicity? *Mov Disord,* 24**,** 1089-1090.

Cariulo, C., Azzollini, L., Verani, M., Martufi, P., Boggio, R., Chiki, A., Deguire, S. M., Cherubini, M., Gines, S., Marsh, J. L., Conforti, P., Cattaneo, E., Santimone, I., Squitieri, F., Lashuel, H. A., Petricca, L., Caricasole, A. 2017a. Phosphorylation of huntingtin at residue T3 is decreased in Huntington's disease and modulates mutant huntingtin protein conformation. *Proc Natl Acad Sci U S A*, in press.

Cariulo, C., Azzollini, L., Verani, M., Martufi, P., Boggio, R., Chiki, A., Deguire, S. M., Cherubini, M., Gines, S., Marsh, J. L., Conforti, P., Cattaneo, E., Santimone, I., Squitieri, F., Lashuel, H. A., Petricca, L., Caricasole, A. 2017b. Phosphorylation of huntingtin at residue T3 is decreased in Huntington's disease and modulates mutant huntingtin protein conformation. *Proc Natl Acad Sci U S A,* 114**,** E10809-E10818.

Caron, N. S., Desmond, C. R., Xia, J., Truant, R. 2013. Polyglutamine domain flexibility mediates the proximity between flanking sequences in huntingtin. *Proc Natl Acad Sci U S A,* 110**,** 14610-14615.

Caron, N. S., Hung, C. L., Atwal, R. S., Truant, R. 2014. Live cell imaging and biophotonic methods reveal two types of mutant huntingtin inclusions. *Hum Mol Genet,* 23**,** 2324-2338.

Carroll, J. B., Bates, G. P., Steffan, J., Saft, C., Tabrizi, S. J. 2015. Treating the whole body in Huntington's disease. *Lancet Neurol,* 14**,** 1135-1142.

Cataldo, A. M., Petanceska, S., Peterhoff, C. M., Terio, N. B., Epstein, C. J., Villar, A., Carlson, E. J., Staufenbiel, M., Nixon, R. A. 2003. App gene dosage modulates endosomal abnormalities of Alzheimer's disease in a segmental trisomy 16 mouse model of down syndrome. *J Neurosci,* 23**,** 6788-6792.

Cecchi, C., Stefani, M. 2013. The amyloid-cell membrane system. The interplay between the biophysical features of oligomers/fibrils and cell membrane defines amyloid toxicity. *Biophys Chem,* 182**,** 30-43.

Chan, H. Y., Warrick, J. M., Gray-Board, G. L., Paulson, H. L., Bonini, N. M. 2000. Mechanisms of chaperone suppression of polyglutamine disease: selectivity, synergy and modulation of protein solubility in Drosophila. *Hum Mol Genet,* 9**,** 2811-2820.

Charles, V., Mezey, E., Reddy, P. H., Dehejia, A., Young, T. A., Polymeropoulos, M. H., Brownstein, M. J., Tagle, D. A. 2000. Alpha-synuclein immunoreactivity of huntingtin polyglutamine aggregates in striatum and cortex of Huntington's disease patients and transgenic mouse models. *Neurosci Lett,* 289**,** 29-32.

Chartier-Harlin, M. C., Kachergus, J., Roumier, C., Mouroux, V., Douay, X., Lincoln, S., Levecque, C., Larvor, L., Andrieux, J., Hulihan, M., Waucquier, N., Defebvre, L.,

Amouyel, P., Farrer, M., Destee, A. 2004. Alpha-synuclein locus duplication as a cause of familial Parkinson's disease. *Lancet,* 364**,** 1167-1169.

Chatterjee, J., Beullens, M., Sukackaite, R., Qian, J., Lesage, B., Hart, D. J., Bollen, M., Köhn, M. 2012. Development of a Peptide that Selectively Activates Protein Phosphatase-1 in Living Cells. *Angewandte Chemie International Edition,* 51**,** 10054-10059.

Chatterjee, J., Kohn, M. 2013. Targeting the untargetable: recent advances in the selective chemical modulation of protein phosphatase-1 activity. *Curr Opin Chem Biol,* 17**,** 361-368.

Chen, C. D., Oh, S. Y., Hinman, J. D., Abraham, C. R. 2006a. Visualization of APP dimerization and APP-Notch2 heterodimerization in living cells using bimolecular fluorescence complementation. *J Neurochem,* 97**,** 30-43.

Chen, K., Maley, J., Yu, P. H. 2006b. Potential inplications of endogenous aldehydes in beta-amyloid misfolding, oligomerization and fibrillogenesis. *J Neurochem,* 99**,** 1413-1424.

Chen, M., Wolynes, P. G. 2017. Aggregation landscapes of Huntingtin exon 1 protein fragments and the critical repeat length for the onset of Huntington's disease. *Proc Natl Acad Sci U S A,* 114**,** 4406-4411.

Chen, X., Walker, D. G., Schmidt, A. M., Arancio, O., Lue, L. F., Yan, S. D. 2007. RAGE: a potential target for Abeta-mediated cellular perturbation in Alzheimer's disease. *Curr Mol Med,* 7**,** 735-742.

Chien, S., Reiter, L. T., Bier, E., Gribskov, M. 2002. Homophila: human disease gene cognates in Drosophila. *Nucleic Acids Res,* 30**,** 149-151.

Chiki, A., DeGuire, S. M., Ruggeri, F. S., Sanfelice, D., Ansaloni, A., Wang, Z. M., Cendrowska, U., Burai, R., Vieweg, S., Pastore, A., Dietler, G., Lashuel, H. A. 2017. Mutant Exon1 Huntingtin Aggregation is Regulated by T3 Phosphorylation-Induced Structural Changes and Crosstalk between T3 Phosphorylation and Acetylation at K6. *Angew Chem Int Ed Engl*, in press.

Chiti, F., Dobson, C. M. 2006. Protein misfolding, functional amyloid, and human disease. *Annu Rev Biochem,* 75**,** 333-366.

Cho, K., Cho, M. H., Seo, J. H., Peak, J., Kong, K. H., Yoon, S. Y., Kim, D. H. 2015. Calpain-mediated cleavage of DARPP-32 in Alzheimer's disease. *Aging Cell,* 14**,** 878-886.

Choi, J. K., Jeon, Y. C., Lee, D. W., Oh, J. M., Lee, H. P., Jeong, B. H., Carp, R. I., Koh, Y. H., Kim, Y. S. 2010. A Drosophila model of GSS syndrome suggests defects in active zones are responsible for pathogenesis of GSS syndrome. *Hum Mol Genet,* 19**,** 4474-4489.

Choi, Y. G., Kim, J. I., Jeon, Y. C., Park, S. J., Choi, E. K., Rubenstein, R., Kascsak, R. J., Carp, R. I., Kim, Y. S. 2004. Nonenzymatic glycation at the N terminus of pathogenic prion protein in transmissible spongiform encephalopathies. *J Biol Chem,* 279**,** 30402-30409.

Choudhury, K. R., Bhattacharyya, N. P. 2015. Chaperone protein HYPK interacts with the first 17 amino acid region of Huntingtin and modulates mutant HTT-mediated aggregation and cytotoxicity. *Biochem Biophys Res Commun,* 456**,** 66-73.

Chun, W., Lesort, M., Tucholski, J., Faber, P. W., MacDonald, M. E., Ross, C. A., Johnson, G. V. 2001a. Tissue transglutaminase selectively modifies proteins associated with truncated mutant huntingtin in intact cells. *Neurobiol Dis,* 8**,** 391-404.

Chun, W., Lesort, M., Tucholski, J., Ross, C. A., Johnson, G. V. 2001b. Tissue transglutaminase does not contribute to the formation of mutant huntingtin aggregates. *J Cell Biol,* 153**,** 25-34.

Chun, W., Waldo, G. S., Johnson, G. V. 2011. Split GFP complementation assay for quantitative measurement of tau aggregation in situ. *Methods Mol Biol,* 670**,** 109-123.

Cicchetti, F., Lacroix, S., Cisbani, G., Vallieres, N., Saint-Pierre, M., St-Amour, I., Tolouei, R., Skepper, J. N., Hauser, R. A., Mantovani, D., Barker, R. A., Freeman, T. B. 2014. Mutant

huntingtin is present in neuronal grafts in Huntington disease patients. *Ann Neurol,* 76**,** 31-42.

Cicchetti, F., Saporta, S., Hauser, R. A., Parent, M., Saint-Pierre, M., Sanberg, P. R., Li, X. J., Parker, J. R., Chu, Y., Mufson, E. J., Kordower, J. H., Freeman, T. B. 2009. Neural transplants in patients with Huntington's disease undergo disease-like neuronal degeneration. *Proc Natl Acad Sci U S A,* 106**,** 12483-12488.

Ciriacy, M., Breitenbach, I. 1979. Physiological effects of seven different blocks in glycolysis in Saccharomyces cerevisiae. *J Bacteriol,* 139**,** 152-160.

Clavaguera, F., Akatsu, H., Fraser, G., Crowther, R. A., Frank, S., Hench, J., Probst, A., Winkler, D. T., Reichwald, J., Staufenbiel, M., Ghetti, B., Goedert, M., Tolnay, M. 2013. Brain homogenates from human tauopathies induce tau inclusions in mouse brain. *Proc Natl Acad Sci U S A,* 110**,** 9535-9540.

Clavaguera, F., Bolmont, T., Crowther, R. A., Abramowski, D., Frank, S., Probst, A., Fraser, G., Stalder, A. K., Beibel, M., Staufenbiel, M., Jucker, M., Goedert, M., Tolnay, M. 2009. Transmission and spreading of tauopathy in transgenic mouse brain. *Nat Cell Biol,* 11**,** 909-913.

Clinton, L. K., Blurton-Jones, M., Myczek, K., Trojanowski, J. Q., LaFerla, F. M. 2010. Synergistic Interactions between Abeta, tau, and alpha-synuclein: acceleration of neuropathology and cognitive decline. *J Neurosci,* 30**,** 7281-7289.

Colby, D. W., Prusiner, S. B. 2011. Prions. *Cold Spring Harb Perspect Biol,* 3**,** a006833.

Colin, E., Zala, D., Liot, G., Rangone, H., Borrell-Pages, M., Li, X. J., Saudou, F., Humbert, S. 2008. Huntingtin phosphorylation acts as a molecular switch for anterograde/retrograde transport in neurons. *EMBO J,* 27**,** 2124-2134.

Collinge, J. 2001. Prion diseases of humans and animals: their causes and molecular basis. *Annu Rev Neurosci,* 24**,** 519-550.

Collinge, J., Clarke, A. R. 2007. A general model of prion strains and their pathogenicity. *Science,* 318**,** 930-936.

Colom-Cadena, M., Gelpi, E., Charif, S., Belbin, O., Blesa, R., Marti, M. J., Clarimon, J., Lleo, A. 2013. Confluence of alpha-synuclein, tau, and beta-amyloid pathologies in dementia with Lewy bodies. *J Neuropathol Exp Neurol,* 72**,** 1203-1212.

Cong, S. Y., Pepers, B. A., Evert, B. O., Rubinsztein, D. C., Roos, R. A., van Ommen, G. J., Dorsman, J. C. 2005. Mutant huntingtin represses CBP, but not p300, by binding and protein degradation. *Mol Cell Neurosci,* 30**,** 12-23.

Cong, X., Held, J. M., DeGiacomo, F., Bonner, A., Chen, J. M., Schilling, B., Czerwieniec, G. A., Gibson, B. W., Ellerby, L. M. 2011. Mass spectrometric identification of novel lysine acetylation sites in huntingtin. *Mol Cell Proteomics,* 10**,** M111 009829.

Conway, K. A., Harper, J. D., Lansbury, P. T. 1998. Accelerated in vitro fibril formation by a mutant alpha-synuclein linked to early-onset Parkinson disease. *Nat Med,* 4**,** 1318-1320.

Cornett, J., Cao, F., Wang, C. E., Ross, C. A., Bates, G. P., Li, S. H., Li, X. J. 2005. Polyglutamine expansion of huntingtin impairs its nuclear export. *Nat Genet,* 37**,** 198-204.

Corrochano, S., Renna, M., Carter, S., Chrobot, N., Kent, R., Stewart, M., Cooper, J., Brown, S. D., Rubinsztein, D. C., Acevedo-Arozena, A. 2012a. alpha-Synuclein levels modulate Huntington's disease in mice. *Hum Mol Genet,* 21**,** 485-494.

Corrochano, S., Renna, M., Tomas-Zapico, C., Brown, S. D., Lucas, J. J., Rubinsztein, D. C., Acevedo-Arozena, A. 2012b. alpha-Synuclein levels affect autophagosome numbers in vivo and modulate Huntington disease pathology. *Autophagy,* 8**,** 431-432.

Costanzo, M., Abounit, S., Marzo, L., Danckaert, A., Chamoun, Z., Roux, P., Zurzolo, C. 2013. Transfer of polyglutamine aggregates in neuronal cells occurs in tunneling nanotubes. *J Cell Sci,* 126**,** 3678-3685.

Costanzo, M., Zurzolo, C. 2013. The cell biology of prion-like spread of protein aggregates: mechanisms and implication in neurodegeneration. *Biochem J,* 452**,** 1-17.

Crick, S. L., Ruff, K. M., Garai, K., Frieden, C., Pappu, R. V. 2013. Unmasking the roles of N- and C-terminal flanking sequences from exon 1 of huntingtin as modulators of polyglutamine aggregation. *Proc Natl Acad Sci U S A,* 110**,** 20075-20080.

Crotti, A., Benner, C., Kerman, B. E., Gosselin, D., Lagier-Tourenne, C., Zuccato, C., Cattaneo, E., Gage, F. H., Cleveland, D. W., Glass, C. K. 2014. Mutant Huntingtin promotes autonomous microglia activation via myeloid lineage-determining factors. *Nat Neurosci,* 17**,** 513-521.

Crunkhorn, S. 2012. Neurodegenerative disease: Taming the RAGE of Alzheimer's disease. *Nat Rev Drug Discov,* 11**,** 351.

da Cruz e Silva, E. F., da Cruz e Silva, O. A., Zaia, C. T., Greengard, P. 1995a. Inhibition of protein phosphatase 1 stimulates secretion of Alzheimer amyloid precursor protein. *Mol Med,* 1**,** 535-541.

da Cruz e Silva, E. F., Fox, C. A., Ouimet, C. C., Gustafson, E., Watson, S. J., Greengard, P. 1995b. Differential expression of protein phosphatase 1 isoforms in mammalian brain. *J Neurosci,* 15**,** 3375-3389.

Darnell, G., Orgel, J. P., Pahl, R., Meredith, S. C. 2007. Flanking polyproline sequences inhibit beta-sheet structure in polyglutamine segments by inducing PPII-like helix structure. *J Mol Biol,* 374**,** 688-704.

Darrow, M. C., Sergeeva, O. A., Isas, J. M., Galaz-Montoya, J. G., King, J. A., Langen, R., Schmid, M. F., Chiu, W. 2015. Structural Mechanisms of Mutant Huntingtin Aggregation Suppression by the Synthetic Chaperonin-like CCT5 Complex Explained by Cryoelectron Tomography. *J Biol Chem,* 290**,** 17451-17461.

Das, I., Krzyzosiak, A., Schneider, K., Wrabetz, L., D'Antonio, M., Barry, N., Sigurdardottir, A., Bertolotti, A. 2015. Preventing proteostasis diseases by selective inhibition of a phosphatase regulatory subunit. *Science,* 348**,** 239-242.

Davis, J. K., Sindi, S. S. 2016. A mathematical model of the dynamics of prion aggregates with chaperone-mediated fragmentation. *J Math Biol,* 72**,** 1555-1578.

de Pril, R., Fischer, D. F., Roos, R. A., van Leeuwen, F. W. 2007. Ubiquitin-conjugating enzyme E2-25K increases aggregate formation and cell death in polyglutamine diseases. *Mol Cell Neurosci,* 34**,** 10-19.

De Strooper, B. 2007. Loss-of-function presenilin mutations in Alzheimer disease. Talking Point on the role of presenilin mutations in Alzheimer disease. *EMBO Rep,* 8**,** 141-146.

Dehay, B., Bertolotti, A. 2006. Critical role of the proline-rich region in Huntingtin for aggregation and cytotoxicity in yeast. *J Biol Chem,* 281**,** 35608-35615.

Deleault, N. R., Dolph, P. J., Feany, M. B., Cook, M. E., Nishina, K., Harris, D. A., Supattapone, S. 2003. Post-transcriptional suppression of pathogenic prion protein expression in Drosophila neurons. *J Neurochem,* 85**,** 1614-1623.

Derkatch, I. L., Bradley, M. E., Hong, J. Y., Liebman, S. W. 2001. Prions affect the appearance of other prions: the story of [PIN(+)]. *Cell,* 106**,** 171-182.

Derkatch, I. L., Bradley, M. E., Masse, S. V., Zadorsky, S. P., Polozkov, G. V., Inge-Vechtomov, S. G., Liebman, S. W. 2000. Dependence and independence of [PSI(+)] and [PIN(+)]: a two-prion system in yeast? *EMBO J,* 19**,** 1942-1952.

Derkatch, I. L., Bradley, M. E., Zhou, P., Chernoff, Y. O., Liebman, S. W. 1997. Genetic and environmental factors affecting the de novo appearance of the [PSI+] prion in Saccharomyces cerevisiae. *Genetics,* 147**,** 507-519.

Derkatch, I. L., Uptain, S. M., Outeiro, T. F., Krishnan, R., Lindquist, S. L., Liebman, S. W. 2004. Effects of Q/N-rich, polyQ, and non-polyQ amyloids on the de novo formation of the [PSI+] prion in yeast and aggregation of Sup35 in vitro. *Proc Natl Acad Sci U S A,* 101**,** 12934-12939.

Desplats, P., Lee, H. J., Bae, E. J., Patrick, C., Rockenstein, E., Crews, L., Spencer, B., Masliah, E., Lee, S. J. 2009. Inclusion formation and neuronal cell death through neuron-to-neuron transmission of alpha-synuclein. *Proc Natl Acad Sci U S A,* 106**,** 13010-13015.

Dettmer, U., Newman, A. J., Luth, E. S., Bartels, T., Selkoe, D. 2013. In vivo cross-linking reveals principally oligomeric forms of alpha-synuclein and beta-synuclein in neurons and non-neural cells. *J Biol Chem,* 288**,** 6371-6385.

Di Pardo, A., Maglione, V., Alpaugh, M., Horkey, M., Atwal, R. S., Sassone, J., Ciammola, A., Steffan, J. S., Fouad, K., Truant, R., Sipione, S. 2012. Ganglioside GM1 induces phosphorylation of mutant huntingtin and restores normal motor behavior in Huntington disease mice. *Proc Natl Acad Sci U S A,* 109**,** 3528-3533.

Dietz, K. N., Di Stefano, L., Maher, R. C., Zhu, H., Macdonald, M. E., Gusella, J. F., Walker, J. A. 2015. The Drosophila Huntington's disease gene ortholog dhtt influences chromatin regulation during development. *Hum Mol Genet,* 24**,** 330-345.

Dietzl, G., Chen, D., Schnorrer, F., Su, K. C., Barinova, Y., Fellner, M., Gasser, B., Kinsey, K., Oppel, S., Scheiblauer, S., Couto, A., Marra, V., Keleman, K., Dickson, B. J. 2007. A genome-wide transgenic RNAi library for conditional gene inactivation in Drosophila. *Nature,* 448**,** 151-156.

DiFiglia, M., Sapp, E., Chase, K. O., Davies, S. W., Bates, G. P., Vonsattel, J. P., Aronin, N. 1997. Aggregation of huntingtin in neuronal intranuclear inclusions and dystrophic neurites in brain. *Science,* 277**,** 1990-1993.

Doi, H., Koyano, S., Suzuki, Y., Nukina, N., Kuroiwa, Y. 2010. The RNA-binding protein FUS/TLS is a common aggregate-interacting protein in polyglutamine diseases. *Neurosci Res,* 66**,** 131-133.

Dombradi, V., Axton, J. M., Barker, H. M., Cohen, P. T. 1990. Protein phosphatase 1 activity in Drosophila mutants with abnormalities in mitosis and chromosome condensation. *FEBS Lett,* 275**,** 39-43.

Douglas, P. M., Summers, D. W., Ren, H. Y., Cyr, D. M. 2009. Reciprocal efficiency of RNQ1 and polyglutamine detoxification in the cytosol and nucleus. *Mol Biol Cell,* 20**,** 4162-4173.

Douglas, P. M., Treusch, S., Ren, H. Y., Halfmann, R., Duennwald, M. L., Lindquist, S., Cyr, D. M. 2008. Chaperone-dependent amyloid assembly protects cells from prion toxicity. *Proc Natl Acad Sci U S A,* 105**,** 7206-7211.

Duan, W., Guo, Z., Jiang, H., Ware, M., Li, X. J., Mattson, M. P. 2003. Dietary restriction normalizes glucose metabolism and BDNF levels, slows disease progression, and increases survival in huntingtin mutant mice. *Proc Natl Acad Sci U S A,* 100**,** 2911-2916.

Dudek, N. L., Dai, Y., Muma, N. A. 2008. Protective effects of interrupting the binding of calmodulin to mutant huntingtin. *J Neuropathol Exp Neurol,* 67**,** 355-365.

Duennwald, M. L., Jagadish, S., Giorgini, F., Muchowski, P. J., Lindquist, S. 2006a. A network of protein interactions determines polyglutamine toxicity. *Proc Natl Acad Sci U S A,* 103**,** 11051-11056.

Duennwald, M. L., Jagadish, S., Muchowski, P. J., Lindquist, S. 2006b. Flanking sequences profoundly alter polyglutamine toxicity in yeast. *Proc Natl Acad Sci U S A,* 103**,** 11045-11050.

Duffy, J. B. 2002. GAL4 system in Drosophila: a fly geneticist's Swiss army knife. *Genesis,* 34**,** 1-15.

Duim, W. C., Jiang, Y., Shen, K., Frydman, J., Moerner, W. E. 2014. Super-resolution fluorescence of huntingtin reveals growth of globular species into short fibers and coexistence of distinct aggregates. *ACS Chem Biol,* 9**,** 2767-2778.

Dunah, A. W., Jeong, H., Griffin, A., Kim, Y. M., Standaert, D. G., Hersch, S. M., Mouradian, M. M., Young, A. B., Tanese, N., Krainc, D. 2002. Sp1 and TAFII130 transcriptional activity disrupted in early Huntington's disease. *Science,* 296**,** 2238-2243.

Durham, H. D., Roy, J., Dong, L., Figlewicz, D. A. 1997. Aggregation of mutant Cu/Zn superoxide dismutase proteins in a culture model of ALS. *J Neuropathol Exp Neurol,* 56**,** 523-530.

Duyao, M. P., Auerbach, A. B., Ryan, A., Persichetti, F., Barnes, G. T., McNeil, S. M., Ge, P., Vonsattel, J. P., Gusella, J. F., Joyner, A. L., et al. 1995. Inactivation of the mouse Huntington's disease gene homolog Hdh. *Science,* 269**,** 407-410.

Eaglestone, S. S., Cox, B. S., Tuite, M. F. 1999. Translation termination efficiency can be regulated in Saccharomyces cerevisiae by environmental stress through a prion-mediated mechanism. *EMBO J,* 18**,** 1974-1981.

Ehrlich, M. E. 2012. Huntington's disease and the striatal medium spiny neuron: cell-autonomous and non-cell-autonomous mechanisms of disease. *Neurotherapeutics,* 9**,** 270-284.

Ehrnhoefer, D. E., Sutton, L., Hayden, M. R. 2011. Small changes, big impact: posttranslational modifications and function of huntingtin in Huntington disease. *Neuroscientist,* 17**,** 475-492.

Eisele, Y. S., Monteiro, C., Fearns, C., Encalada, S. E., Wiseman, R. L., Powers, E. T., Kelly, J. W. 2015. Targeting protein aggregation for the treatment of degenerative diseases. *Nat Rev Drug Discov,* 14**,** 759-780.

Elie, A., Prezel, E., Guerin, C., Denarier, E., Ramirez-Rios, S., Serre, L., Andrieux, A., Fourest-Lieuvin, A., Blanchoin, L., Arnal, I. 2015. Tau co-organizes dynamic microtubule and actin networks. *Sci Rep,* 5**,** 9964.

Elliott, D. A., Brand, A. H. 2008. The GAL4 system : a versatile system for the expression of genes. *Methods Mol Biol,* 420**,** 79-95.

Emmer, K. L., Waxman, E. A., Covy, J. P., Giasson, B. I. 2011. E46K human alpha-synuclein transgenic mice develop Lewy-like and tau pathology associated with age-dependent, detrimental motor impairment. *J Biol Chem,* 286**,** 35104-35118.

Ermak, G., Hench, K. J., Chang, K. T., Sachdev, S., Davies, K. J. 2009. Regulator of calcineurin (RCAN1-1L) is deficient in Huntington disease and protective against mutant huntingtin toxicity in vitro. *J Biol Chem,* 284**,** 11845-11853.

Esler, W. P., Wolfe, M. S. 2001. A portrait of Alzheimer secretases--new features and familiar faces. *Science,* 293**,** 1449-1454.

Faber, P. W., Barnes, G. T., Srinidhi, J., Chen, J., Gusella, J. F., MacDonald, M. E. 1998. Huntingtin interacts with a family of WW domain proteins. *Hum Mol Genet,* 7**,** 1463-1474.

Fan, H. C., Ho, L. I., Chi, C. S., Chen, S. J., Peng, G. S., Chan, T. M., Lin, S. Z., Harn, H. J. 2014. Polyglutamine (PolyQ) diseases: genetics to treatments. *Cell Transplant,* 23**,** 441-458.

Fan, J., Cowan, C. M., Zhang, L. Y., Hayden, M. R., Raymond, L. A. 2009. Interaction of postsynaptic density protein-95 with NMDA receptors influences excitotoxicity in the yeast artificial chromosome mouse model of Huntington's disease. *J Neurosci,* 29**,** 10928-10938.

Farrer, L. A. 1985. Diabetes mellitus in Huntington disease. *Clin Genet,* 27**,** 62-67.

Feany, M. B., Bender, W. W. 2000. A Drosophila model of Parkinson's disease. *Nature,* 404**,** 394-398.

Feng, Z., Jin, S., Zupnick, A., Hoh, J., de Stanchina, E., Lowe, S., Prives, C., Levine, A. J. 2006. p53 tumor suppressor protein regulates the levels of huntingtin gene expression. *Oncogene,* 25**,** 1-7.

Fernandez-Funez, P., Zhang, Y., Casas-Tinto, S., Xiao, X., Zou, W. Q., Rincon-Limas, D. E. 2010. Sequence-dependent prion protein misfolding and neurotoxicity. *J Biol Chem,* 285**,** 36897-36908.

Fernandez-Nogales, M., Cabrera, J. R., Santos-Galindo, M., Hoozemans, J. J., Ferrer, I., Rozemuller, A. J., Hernandez, F., Avila, J., Lucas, J. J. 2014. Huntington's disease is a four-repeat tauopathy with tau nuclear rods. *Nat Med,* 20**,** 881-885.

Ferreira, D. G., Temido-Ferreira, M., Miranda, H. V., Batalha, V. L., Coelho, J. E., Szego, E. M., Marques-Morgado, I., Vaz, S. H., Rhee, J. S., Schmitz, M., Zerr, I., Lopes, L. V., Outeiro, T. F. 2017. alpha-synuclein interacts with PrPC to induce cognitive impairment through mGluR5 and NMDAR2B. *Nat Neurosci*, in press.

Ferrer, I. 2004. Stress kinases involved in tau phosphorylation in Alzheimer's disease, tauopathies and APP transgenic mice. *Neurotox Res,* 6**,** 469-475.

Fiumara, F., Fioriti, L., Kandel, E. R., Hendrickson, W. A. 2010. Essential role of coiled coils for aggregation and activity of Q/N-rich prions and PolyQ proteins. *Cell,* 143**,** 1121-1135.

Fong, V. H., Vieira, A. 2013. Transthyretin aggregates induce production of reactive nitrogen species. *Neurodegener Dis,* 11**,** 42-48.

Forloni, G., Terreni, L., Bertani, I., Fogliarino, S., Invernizzi, R., Assini, A., Ribizzi, G., Negro, A., Calabrese, E., Volonte, M. A., Mariani, C., Franceschi, M., Tabaton, M., Bertoli, A. 2002. Protein misfolding in Alzheimer's and Parkinson's disease: genetics and molecular mechanisms. *Neurobiol Aging,* 23**,** 957-976.

Foroud, T., Gray, J., Ivashina, J., Conneally, P. M. 1999. Differences in duration of Huntington's disease based on age at onset. *J Neurol Neurosurg Psychiatry,* 66**,** 52-56.

Freese, A., Finklestein, S. P., DiFiglia, M. 1992. Basic fibroblast growth factor protects striatal neurons in vitro from NMDA-receptor mediated excitotoxicity. *Brain Res,* 575**,** 351-355.

Frim, D. M., Uhler, T. A., Short, M. P., Ezzedine, Z. D., Klagsbrun, M., Breakefield, X. O., Isacson, O. 1993. Effects of biologically delivered NGF, BDNF and bFGF on striatal excitotoxic lesions. *Neuroreport,* 4**,** 367-370.

Fuentealba, R. A., Udan, M., Bell, S., Wegorzewska, I., Shao, J., Diamond, M. I., Weihl, C. C., Baloh, R. H. 2010. Interaction with polyglutamine aggregates reveals a Q/N-rich domain in TDP-43. *J Biol Chem,* 285**,** 26304-26314.

Fung, J., Frost, D., Chakrabartty, A., McLaurin, J. 2004. Interaction of human and mouse Abeta peptides. *J Neurochem,* 91**,** 1398-1403.

Furlong, R. A., Narain, Y., Rankin, J., Wyttenbach, A., Rubinsztein, D. C. 2000. Alpha-synuclein overexpression promotes aggregation of mutant huntingtin. *Biochem J,* 346 Pt 3**,** 577-581.

Gajula Balija, M. B., Griesinger, C., Herzig, A., Zweckstetter, M., Jackle, H. 2011. Pre-fibrillar alpha-synuclein mutants cause Parkinson's disease-like non-motor symptoms in Drosophila. *PLoS One,* 6**,** e24701.

Galasko, D., Bell, J., Mancuso, J. Y., Kupiec, J. W., Sabbagh, M. N., van Dyck, C., Thomas, R. G., Aisen, P. S., Alzheimer's Disease Cooperative, S. 2014. Clinical trial of an inhibitor of RAGE-Abeta interactions in Alzheimer disease. *Neurology,* 82**,** 1536-1542.

Galpern, W. R., Lang, A. E. 2006. Interface between tauopathies and synucleinopathies: a tale of two proteins. *Ann Neurol,* 59**,** 449-458.

Gao, Y. G., Yang, H., Zhao, J., Jiang, Y. J., Hu, H. Y. 2014. Autoinhibitory structure of the WW domain of HYPB/SETD2 regulates its interaction with the proline-rich region of huntingtin. *Structure,* 22**,** 378-386.

Gauthier, L. R., Charrin, B. C., Borrell-Pages, M., Dompierre, J. P., Rangone, H., Cordelieres, F. P., De Mey, J., MacDonald, M. E., Lessmann, V., Humbert, S., Saudou, F. 2004. Huntingtin controls neurotrophic support and survival of neurons by enhancing BDNF vesicular transport along microtubules. *Cell,* 118**,** 127-138.

Gavin, B. A., Dolph, M. J., Deleault, N. R., Geoghegan, J. C., Khurana, V., Feany, M. B., Dolph, P. J., Supattapone, S. 2006. Accelerated accumulation of misfolded prion protein and spongiform degeneration in a Drosophila model of Gerstmann-Straussler-Scheinker syndrome. *J Neurosci,* 26**,** 12408-12414.

Gentleman, S. M. 2013. Review: microglia in protein aggregation disorders: friend or foe? *Neuropathol Appl Neurobiol,* 39**,** 45-50.

Gervais, F. G., Singaraja, R., Xanthoudakis, S., Gutekunst, C. A., Leavitt, B. R., Metzler, M., Hackam, A. S., Tam, J., Vaillancourt, J. P., Houtzager, V., Rasper, D. M., Roy, S., Hayden, M. R., Nicholson, D. W. 2002. Recruitment and activation of caspase-8 by the Huntingtin-interacting protein Hip-1 and a novel partner Hippi. *Nat Cell Biol,* 4**,** 95-105.

Ghosh, I., Hamilton, A. D., Lynne, R. 2000. Antiparallel Leucine Zipper-Directed Protein Reassembly: Application to the Green Fluorescent Protein. *J Am Chem Soc,* 122**,** 1.

Giasson, B. I., Forman, M. S., Higuchi, M., Golbe, L. I., Graves, C. L., Kotzbauer, P. T., Trojanowski, J. Q., Lee, V. M. 2003. Initiation and synergistic fibrillization of tau and alpha-synuclein. *Science,* 300**,** 636-640.

Gillis, J., Schipper-Krom, S., Juenemann, K., Gruber, A., Coolen, S., van den Nieuwendijk, R., van Veen, H., Overkleeft, H., Goedhart, J., Kampinga, H. H., Reits, E. A. 2013. The DNAJB6 and DNAJB8 protein chaperones prevent intracellular aggregation of polyglutamine peptides. *J Biol Chem,* 288**,** 17225-17237.

Giorgini, F., Guidetti, P., Nguyen, Q., Bennett, S. C., Muchowski, P. J. 2005. A genomic screen in yeast implicates kynurenine 3-monooxygenase as a therapeutic target for Huntington disease. *Nat Genet,* 37**,** 526-531.

Giorgini, F., Moller, T., Kwan, W., Zwilling, D., Wacker, J. L., Hong, S., Tsai, L. C., Cheah, C. S., Schwarcz, R., Guidetti, P., Muchowski, P. J. 2008. Histone deacetylase inhibition modulates kynurenine pathway activation in yeast, microglia, and mice expressing a mutant huntingtin fragment. *J Biol Chem,* 283**,** 7390-7400.

Giorgini, F., Muchowski, P. J. 2005. Connecting the dots in Huntington's disease with protein interaction networks. *Genome Biol,* 6**,** 210.

Gleixner, A. M., Pulugulla, S. H., Pant, D. B., Posimo, J. M., Crum, T. S., Leak, R. K. 2014. Impact of aging on heat shock protein expression in the substantia nigra and striatum of the female rat. *Cell Tissue Res,* 357**,** 43-54.

Glozak, M. A., Sengupta, N., Zhang, X., Seto, E. 2005. Acetylation and deacetylation of non-histone proteins. *Gene,* 363**,** 15-23.

Goehler, H., Lalowski, M., Stelzl, U., Waelter, S., Stroedicke, M., Worm, U., Droege, A., Lindenberg, K. S., Knoblich, M., Haenig, C., Herbst, M., Suopanki, J., Scherzinger, E., Abraham, C., Bauer, B., Hasenbank, R., Fritzsche, A., Ludewig, A. H., Bussow, K., Coleman, S. H., Gutekunst, C. A., Landwehrmeyer, B. G., Lehrach, H., Wanker, E. E. 2004. A protein interaction network links GIT1, an enhancer of huntingtin aggregation, to Huntington's disease. *Mol Cell,* 15**,** 853-865.

Goers, J., Manning-Bog, A. B., McCormack, A. L., Millett, I. S., Doniach, S., Di Monte, D. A., Uversky, V. N., Fink, A. L. 2003. Nuclear localization of alpha-synuclein and its interaction with histones. *Biochemistry,* 42**,** 8465-8471.

Goffredo, D., Rigamonti, D., Tartari, M., De Micheli, A., Verderio, C., Matteoli, M., Zuccato, C., Cattaneo, E. 2002. Calcium-dependent cleavage of endogenous wild-type huntingtin in primary cortical neurons. *J Biol Chem,* 277**,** 39594-39598.

Gomes, R. A., Sousa Silva, M., Vicente Miranda, H., Ferreira, A. E., Cordeiro, C. A., Freire, A. P. 2005. Protein glycation in Saccharomyces cerevisiae. Argpyrimidine formation and methylglyoxal catabolism. *FEBS J,* 272**,** 4521-4531.

Goncalves, S. A., Matos, J. E., Outeiro, T. F. 2010. Zooming into protein oligomerization in neurodegeneration using BiFC. *Trends Biochem Sci,* 35**,** 643-651.

Gong, C. X., Shaikh, S., Wang, J. Z., Zaidi, T., Grundke-Iqbal, I., Iqbal, K. 1995. Phosphatase activity toward abnormally phosphorylated tau: decrease in Alzheimer disease brain. *J Neurochem,* 65**,** 732-738.

Goodman, A. O., Barker, R. A. 2011. Body composition in premanifest Huntington's disease reveals lower bone density compared to controls. *PLoS Curr,* 3**,** RRN1214.

Gotz, J., Chen, F., van Dorpe, J., Nitsch, R. M. 2001. Formation of neurofibrillary tangles in P3011 tau transgenic mice induced by Abeta 42 fibrils. *Science,* 293**,** 1491-1495.

Gousset, K., Schiff, E., Langevin, C., Marijanovic, Z., Caputo, A., Browman, D. T., Chenouard, N., de Chaumont, F., Martino, A., Enninga, J., Olivo-Marin, J. C., Mannel, D., Zurzolo, C. 2009. Prions hijack tunnelling nanotubes for intercellular spread. *Nat Cell Biol,* 11**,** 328-336.

Graham, R. K., Deng, Y., Slow, E. J., Haigh, B., Bissada, N., Lu, G., Pearson, J., Shehadeh, J., Bertram, L., Murphy, Z., Warby, S. C., Doty, C. N., Roy, S., Wellington, C. L., Leavitt, B. R., Raymond, L. A., Nicholson, D. W., Hayden, M. R. 2006. Cleavage at the caspase-6 site is required for neuronal dysfunction and degeneration due to mutant huntingtin. *Cell,* 125**,** 1179-1191.

Gratuze, M., Cisbani, G., Cicchetti, F., Planel, E. 2016. Is Huntington's disease a tauopathy? *Brain,* 139**,** 1014-1025.

Gratuze, M., Noel, A., Julien, C., Cisbani, G., Milot-Rousseau, P., Morin, F., Dickler, M., Goupil, C., Bezeau, F., Poitras, I., Bissonnette, S., Whittington, R. A., Hebert, S. S., Cicchetti, F., Parker, J. A., Samadi, P., Planel, E. 2015. Tau hyperphosphorylation and deregulation of calcineurin in mouse models of Huntington's disease. *Hum Mol Genet,* 24**,** 86-99.

Green, E. W., Campesan, S., Breda, C., Sathyasaikumar, K. V., Muchowski, P. J., Schwarcz, R., Kyriacou, C. P., Giorgini, F. 2012. Drosophila eye color mutants as therapeutic tools for Huntington disease. *Fly (Austin),* 6**,** 117-120.

Green, E. W., Giorgini, F. 2012. Choosing and using Drosophila models to characterize modifiers of Huntington's disease. *Biochem Soc Trans,* 40**,** 739-745.

Greten-Harrison, B., Polydoro, M., Morimoto-Tomita, M., Diao, L., Williams, A. M., Nie, E. H., Makani, S., Tian, N., Castillo, P. E., Buchman, V. L., Chandra, S. S. 2010. alphabetagamma-Synuclein triple knockout mice reveal age-dependent neuronal dysfunction. *Proc Natl Acad Sci U S A,* 107**,** 19573-19578.

Groth, A. C., Fish, M., Nusse, R., Calos, M. P. 2004. Construction of transgenic Drosophila by using the site-specific integrase from phage phiC31. *Genetics,* 166**,** 1775-1782.

Gu, X., Cantle, J. P., Greiner, E. R., Lee, C. Y., Barth, A. M., Gao, F., Park, C. S., Zhang, Z., Sandoval-Miller, S., Zhang, R. L., Diamond, M., Mody, I., Coppola, G., Yang, X. W. 2015. N17 Modifies mutant Huntingtin nuclear pathogenesis and severity of disease in HD BAC transgenic mice. *Neuron,* 85**,** 726-741.

Gu, X., Greiner, E. R., Mishra, R., Kodali, R., Osmand, A., Finkbeiner, S., Steffan, J. S., Thompson, L. M., Wetzel, R., Yang, X. W. 2009. Serines 13 and 16 are critical determinants of full-length human mutant huntingtin induced disease pathogenesis in HD mice. *Neuron,* 64**,** 828-840.

Guerreiro, P. S., Huang, Y., Gysbers, A., Cheng, D., Gai, W. P., Outeiro, T. F., Halliday, G. M. 2013. LRRK2 interactions with alpha-synuclein in Parkinson's disease brains and in cell models. *J Mol Med (Berl),* 91**,** 513-522.

Guix, F. X., Ill-Raga, G., Bravo, R., Nakaya, T., de Fabritiis, G., Coma, M., Miscione, G. P., Villa-Freixa, J., Suzuki, T., Fernandez-Busquets, X., Valverde, M. A., de Strooper, B., Munoz, F. J. 2009. Amyloid-dependent triosephosphate isomerase nitrotyrosination induces glycation and tau fibrillation. *Brain,* 132**,** 1335-1345.

Gunawardena, S., Her, L. S., Brusch, R. G., Laymon, R. A., Niesman, I. R., Gordesky-Gold, B., Sintasath, L., Bonini, N. M., Goldstein, L. S. 2003. Disruption of axonal transport by loss of huntingtin or expression of pathogenic polyQ proteins in Drosophila. *Neuron,* 40**,** 25-40.

Guo, J. L., Covell, D. J., Daniels, J. P., Iba, M., Stieber, A., Zhang, B., Riddle, D. M., Kwong, L. K., Xu, Y., Trojanowski, J. Q., Lee, V. M. 2013. Distinct alpha-synuclein strains differentially promote tau inclusions in neurons. *Cell,* 154**,** 103-117.

Guo, J. P., Arai, T., Miklossy, J., McGeer, P. L. 2006. Abeta and tau form soluble complexes that may promote self aggregation of both into the insoluble forms observed in Alzheimer's disease. *Proc Natl Acad Sci U S A,* 103**,** 1953-1958.

Guo, Q., Bin, H., Cheng, J., Seefelder, M., Engler, T., Pfeifer, G., Oeckl, P., Otto, M., Moser, F., Maurer, M., Pautsch, A., Baumeister, W., Fernandez-Busnadiego, R., Kochanek, S. 2018. The cryo-electron microscopy structure of huntingtin. *Nature*, in press.

Guo, T., Noble, W., Hanger, D. P. 2017. Roles of tau protein in health and disease. *Acta Neuropathol,* 133**,** 665-704.

Gusella, J. F., MacDonald, M. E. 2009. Huntington's disease: the case for genetic modifiers. *Genome Med,* 1**,** 80.

Hackam, A. S., Yassa, A. S., Singaraja, R., Metzler, M., Gutekunst, C. A., Gan, L., Warby, S., Wellington, C. L., Vaillancourt, J., Chen, N., Gervais, F. G., Raymond, L., Nicholson, D. W., Hayden, M. R. 2000. Huntingtin interacting protein 1 induces apoptosis via a novel caspase-dependent death effector domain. *J Biol Chem,* 275**,** 41299-41308.

Hageman, J., Rujano, M. A., van Waarde, M. A., Kakkar, V., Dirks, R. P., Govorukhina, N., Oosterveld-Hut, H. M., Lubsen, N. H., Kampinga, H. H. 2010. A DNAJB chaperone subfamily with HDAC-dependent activities suppresses toxic protein aggregation. *Mol Cell,* 37**,** 355-369.

Haik, S., Privat, N., Adjou, K. T., Sazdovitch, V., Dormont, D., Duyckaerts, C., Hauw, J. J. 2002. Alpha-synuclein-immunoreactive deposits in human and animal prion diseases. *Acta Neuropathol,* 103**,** 516-520.

Haque, N. S., Isacson, O. 2000. Neurotrophic factors NGF and FGF-2 alter levels of huntingtin (IT15) in striatal neuronal cell cultures. *Cell Transplant,* 9**,** 623-627.

Harjes, P., Wanker, E. E. 2003. The hunt for huntingtin function: interaction partners tell many different stories. *Trends Biochem Sci,* 28**,** 425-433.

Hartl, F. U., Bracher, A., Hayer-Hartl, M. 2011. Molecular chaperones in protein folding and proteostasis. *Nature,* 475**,** 324-332.

Hassel, B., Tessler, S., Faull, R. L., Emson, P. C. 2008. Glutamate uptake is reduced in prefrontal cortex in Huntington's disease. *Neurochem Res,* 33**,** 232-237.

Hattori, N., Mizuno, Y. 2004. Pathogenetic mechanisms of parkin in Parkinson's disease. *Lancet,* 364**,** 722-724.

Hattula, K., Peranen, J. 2000. FIP-2, a coiled-coil protein, links Huntingtin to Rab8 and modulates cellular morphogenesis. *Curr Biol,* 10**,** 1603-1606.

Havel, L. S., Wang, C. E., Wade, B., Huang, B., Li, S., Li, X. J. 2011. Preferential accumulation of N-terminal mutant huntingtin in the nuclei of striatal neurons is regulated by phosphorylation. *Hum Mol Genet,* 20**,** 1424-1437.

Hayashi, M., Kobayashi, K., Furuta, H. 2003. Immunohistochemical study of neuronal intranuclear and cytoplasmic inclusions in Machado-Joseph disease. *Psychiatry Clin Neurosci,* 57**,** 205-213.

He, W. T., Xue, W., Gao, Y. G., Hong, J. Y., Yue, H. W., Jiang, L. L., Hu, H. Y. 2017. HSP90 recognizes the N-terminus of huntingtin involved in regulation of huntingtin aggregation by USP19. *Sci Rep,* 7**,** 14797.

Heegaard, N. H. 2009. beta(2)-microglobulin: from physiology to amyloidosis. *Amyloid,* 16**,** 151-173.

Heemskerk, A. W., Roos, R. A. 2012. Aspiration pneumonia and death in Huntington's disease. *PLoS Curr,* 4**,** RRN1293.

Helwig, M., Klinkenberg, M., Rusconi, R., Musgrove, R. E., Majbour, N. K., El-Agnaf, O. M., Ulusoy, A., Di Monte, D. A. 2016. Brain propagation of transduced alpha-synuclein involves non-fibrillar protein species and is enhanced in alpha-synuclein null mice. *Brain,* 139**,** 856-870.

Henshall, T. L., Tucker, B., Lumsden, A. L., Nornes, S., Lardelli, M. T., Richards, R. I. 2009. Selective neuronal requirement for huntingtin in the developing zebrafish. *Hum Mol Genet,* 18**,** 4830-4842.

Heppner, F. L., Ransohoff, R. M., Becher, B. 2015. Immune attack: the role of inflammation in Alzheimer disease. *Nat Rev Neurosci,* 16**,** 358-372.

Hermel, E., Gafni, J., Propp, S. S., Leavitt, B. R., Wellington, C. L., Young, J. E., Hackam, A. S., Logvinova, A. V., Peel, A. L., Chen, S. F., Hook, V., Singaraja, R., Krajewski, S., Goldsmith, P. C., Ellerby, H. M., Hayden, M. R., Bredesen, D. E., Ellerby, L. M. 2004. Specific caspase interactions and amplification are involved in selective neuronal vulnerability in Huntington's disease. *Cell Death Differ,* 11**,** 424-438.

Herrera, F., Gonçalves, S., Branco dos Santos, J., Fleming Outeiro, T. 2014. Studying the Molecular Determinants of Protein Oligomerization in Neurodegenerative Disorders by Bimolecular Fluorescence Complementation. in press.**,** 133-145.

Herrera, F., Outeiro, T. F. 2012. alpha-Synuclein modifies huntingtin aggregation in living cells. *FEBS Lett,* 586**,** 7-12.

Herrera, F., Tenreiro, S., Miller-Fleming, L., Outeiro, T. F. 2011. Visualization of cell-to-cell transmission of mutant huntingtin oligomers. *PLoS Curr,* 3**,** RRN1210.

Hinton, D. R., Polk, R. K., Linse, K. D., Weiss, M. H., Kovacs, K., Garner, J. A. 1997. Characterization of spherical amyloid protein from a prolactin-producing pituitary adenoma. *Acta Neuropathol,* 93**,** 43-49.

Hipp, M. S., Park, S. H., Hartl, F. U. 2014. Proteostasis impairment in protein-misfolding and -aggregation diseases. *Trends Cell Biol,* 24**,** 506-514.

Hipp, M. S., Patel, C. N., Bersuker, K., Riley, B. E., Kaiser, S. E., Shaler, T. A., Brandeis, M., Kopito, R. R. 2012. Indirect inhibition of 26S proteasome activity in a cellular model of Huntington's disease. *J Cell Biol,* 196**,** 573-587.

Hirth, F. 2010. Drosophila melanogaster in the study of human neurodegeneration. *CNS Neurol Disord Drug Targets,* 9**,** 504-523.

Hirth, F., Reichert, H. 1999. Conserved genetic programs in insect and mammalian brain development. *Bioessays,* 21**,** 677-684.

Ho, L. W., Brown, R., Maxwell, M., Wyttenbach, A., Rubinsztein, D. C. 2001. Wild type Huntingtin reduces the cellular toxicity of mutant Huntingtin in mammalian cell models of Huntington's disease. *J Med Genet,* 38**,** 450-452.

Holbert, S., Dedeoglu, A., Humbert, S., Saudou, F., Ferrante, R. J., Neri, C. 2003. Cdc42-interacting protein 4 binds to huntingtin: neuropathologic and biological evidence for a role in Huntington's disease. *Proc Natl Acad Sci U S A,* 100**,** 2712-2717.

Holbert, S., Denghien, I., Kiechle, T., Rosenblatt, A., Wellington, C., Hayden, M. R., Margolis, R. L., Ross, C. A., Dausset, J., Ferrante, R. J., Neri, C. 2001. The Gln-Ala repeat transcriptional activator CA150 interacts with huntingtin: neuropathologic and genetic evidence for a role in Huntington's disease pathogenesis. *Proc Natl Acad Sci U S A,* 98**,** 1811-1816.

Hollan, S., Fujii, H., Hirono, A., Hirono, K., Karro, H., Miwa, S., Harsanyi, V., Gyodi, E., Inselt-Kovacs, M. 1993. Hereditary triosephosphate isomerase (TPI) deficiency: two severely affected brothers one with and one without neurological symptoms. *Hum Genet,* 92**,** 486-490.

Hoop, C. L., Lin, H. K., Kar, K., Hou, Z., Poirier, M. A., Wetzel, R., van der Wel, P. C. 2014. Polyglutamine amyloid core boundaries and flanking domain dynamics in huntingtin fragment fibrils determined by solid-state nuclear magnetic resonance. *Biochemistry,* 53**,** 6653-6666.

Horvath, J., Burkhard, P. R., Herrmann, F. R., Bouras, C., Kovari, E. 2014. Neuropathology of parkinsonism in patients with pure Alzheimer's disease. *J Alzheimers Dis,* 39**,** 115-120.

Houlden, H., Johnson, J., Gardner-Thorpe, C., Lashley, T., Hernandez, D., Worth, P., Singleton, A. B., Hilton, D. A., Holton, J., Revesz, T., Davis, M. B., Giunti, P., Wood, N. W. 2007. Mutations in TTBK2, encoding a kinase implicated in tau phosphorylation, segregate with spinocerebellar ataxia type 11. *Nat Genet,* 39**,** 1434-1436.

Hu, C. D., Chinenov, Y., Kerppola, T. K. 2002. Visualization of interactions among bZIP and Rel family proteins in living cells using bimolecular fluorescence complementation. *Mol Cell,* 9**,** 789-798.

Hu, C. D., Kerppola, T. K. 2003. Simultaneous visualization of multiple protein interactions in living cells using multicolor fluorescence complementation analysis. *Nat Biotechnol,* 21**,** 539-545.

Huang, B., Lucas, T., Kueppers, C., Dong, X., Krause, M., Bepperling, A., Buchner, J., Voshol, H., Weiss, A., Gerrits, B., Kochanek, S. 2015. Scalable production in human cells and biochemical characterization of full-length normal and mutant huntingtin. *PLoS One,* 10**,** e0121055.

Huang, C. C., Faber, P. W., Persichetti, F., Mittal, V., Vonsattel, J. P., MacDonald, M. E., Gusella, J. F. 1998. Amyloid formation by mutant huntingtin: threshold, progressivity and recruitment of normal polyglutamine proteins. *Somat Cell Mol Genet,* 24**,** 217-233.

Huang, Z., Xu, Z., Wu, Y., Zhou, Y. 2011. Determining nuclear localization of alpha-synuclein in mouse brains. *Neuroscience,* 199**,** 318-332.

Huang, Z. N., Her, L. S. 2016. The Ubiquitin Receptor ADRM1 Modulates HAP40-Induced Proteasome Activity. *Mol Neurobiol*, in press.

Humbert, S., Bryson, E. A., Cordelieres, F. P., Connors, N. C., Datta, S. R., Finkbeiner, S., Greenberg, M. E., Saudou, F. 2002. The IGF-1/Akt pathway is neuroprotective in Huntington's disease and involves Huntingtin phosphorylation by Akt. *Dev Cell,* 2**,** 831-837.

Huntington, G. 1872. On Chorea. *Medical and Surgical Reporter*, 26, 320-321.

Hurlbert, M. S., Zhou, W., Wasmeier, C., Kaddis, F. G., Hutton, J. C., Freed, C. R. 1999. Mice transgenic for an expanded CAG repeat in the Huntington's disease gene develop diabetes. *Diabetes,* 48**,** 649-651.

Huynh, D. P., Del Bigio, M. R., Ho, D. H., Pulst, S. M. 1999. Expression of ataxin-2 in brains from normal individuals and patients with Alzheimer's disease and spinocerebellar ataxia 2. *Ann Neurol,* 45**,** 232-241.

Irwin, D. J., Abrams, J. Y., Schonberger, L. B., Leschek, E. W., Mills, J. L., Lee, V. M., Trojanowski, J. Q. 2013. Evaluation of potential infectivity of Alzheimer and Parkinson disease proteins in recipients of cadaver-derived human growth hormone. *JAMA Neurol,* 70**,** 462-468.

Ishizawa, T., Mattila, P., Davies, P., Wang, D., Dickson, D. W. 2003. Colocalization of tau and alpha-synuclein epitopes in Lewy bodies. *J Neuropathol Exp Neurol,* 62**,** 389-397.

Iwaki, T., Iwaki, A., Tateishi, J., Sakaki, Y., Goldman, J. E. 1993. Alpha B-crystallin and 27-kd heat shock protein are regulated by stress conditions in the central nervous system and accumulate in Rosenthal fibers. *Am J Pathol,* 143**,** 487-495.

Jackson, G. R., Salecker, I., Dong, X., Yao, X., Arnheim, N., Faber, P. W., MacDonald, M. E., Zipursky, S. L. 1998. Polyglutamine-expanded human huntingtin transgenes induce degeneration of Drosophila photoreceptor neurons. *Neuron,* 21**,** 633-642.

Jakubowski, B. R., Longoria, R. A., Shubeita, G. T. 2012. A high throughput and sensitive method correlates neuronal disorder genotypes to Drosophila larvae crawling phenotypes. *Fly (Austin),* 6**,** 303-308.

Jana, N. R., Dikshit, P., Goswami, A., Kotliarova, S., Murata, S., Tanaka, K., Nukina, N. 2005. Co-chaperone CHIP associates with expanded polyglutamine protein and promotes their degradation by proteasomes. *J Biol Chem,* 280**,** 11635-11640.

Jana, N. R., Tanaka, M., Wang, G., Nukina, N. 2000. Polyglutamine length-dependent interaction of Hsp40 and Hsp70 family chaperones with truncated N-terminal huntingtin: their role in suppression of aggregation and cellular toxicity. *Hum Mol Genet,* 9**,** 2009-2018.

Jayaraman, M., Kodali, R., Sahoo, B., Thakur, A. K., Mayasundari, A., Mishra, R., Peterson, C. B., Wetzel, R. 2012. Slow amyloid nucleation via alpha-helix-rich oligomeric intermediates in short polyglutamine-containing huntingtin fragments. *J Mol Biol,* 415**,** 881-899.

Jenkins, B. G., Klivenyi, P., Kustermann, E., Andreassen, O. A., Ferrante, R. J., Rosen, B. R., Beal, M. F. 2000. Nonlinear decrease over time in N-acetyl aspartate levels in the absence of neuronal loss and increases in glutamine and glucose in transgenic Huntington's disease mice. *J Neurochem,* 74**,** 2108-2119.

Jensen, P. H., Hager, H., Nielsen, M. S., Hojrup, P., Gliemann, J., Jakes, R. 1999. alpha-synuclein binds to Tau and stimulates the protein kinase A-catalyzed tau phosphorylation of serine residues 262 and 356. *J Biol Chem,* 274**,** 25481-25489.

Jeong, H., Then, F., Melia, T. J., Jr., Mazzulli, J. R., Cui, L., Savas, J. N., Voisine, C., Paganetti, P., Tanese, N., Hart, A. C., Yamamoto, A., Krainc, D. 2009. Acetylation targets mutant huntingtin to autophagosomes for degradation. *Cell,* 137**,** 60-72.

Johnston, J. A., Ward, C. L., Kopito, R. R. 1998. Aggresomes: a cellular response to misfolded proteins. *J Cell Biol,* 143**,** 1883-1898.

Joiner, W. J., Crocker, A., White, B. H., Sehgal, A. 2006. Sleep in Drosophila is regulated by adult mushroom bodies. *Nature,* 441**,** 757-760.

Kaganovich, D., Kopito, R., Frydman, J. 2008. Misfolded proteins partition between two distinct quality control compartments. *Nature,* 454**,** 1088-1095.

Kahlem, P., Green, H., Djian, P. 1998. Transglutaminase action imitates Huntington's disease: selective polymerization of Huntingtin containing expanded polyglutamine. *Mol Cell,* 1**,** 595-601.

Kalchman, M. A., Graham, R. K., Xia, G., Koide, H. B., Hodgson, J. G., Graham, K. C., Goldberg, Y. P., Gietz, R. D., Pickart, C. M., Hayden, M. R. 1996. Huntingtin is ubiquitinated and interacts with a specific ubiquitin-conjugating enzyme. *J Biol Chem,* 271**,** 19385-19394.

Kalchman, M. A., Koide, H. B., McCutcheon, K., Graham, R. K., Nichol, K., Nishiyama, K., Kazemi-Esfarjani, P., Lynn, F. C., Wellington, C., Metzler, M., Goldberg, Y. P., Kanazawa, I., Gietz, R. D., Hayden, M. R. 1997. HIP1, a human homologue of S. cerevisiae Sla2p, interacts with membrane-associated huntingtin in the brain. *Nat Genet,* 16**,** 44-53.

Kane, M. D., Lipinski, W. J., Callahan, M. J., Bian, F., Durham, R. A., Schwarz, R. D., Roher, A. E., Walker, L. C. 2000. Evidence for seeding of beta -amyloid by intracerebral infusion of Alzheimer brain extracts in beta -amyloid precursor protein-transgenic mice. *J Neurosci,* 20**,** 3606-3611.

Kantcheva, R. B., Mason, R., Giorgini, F. 2014. Aggregation-prone proteins modulate huntingtin inclusion body formation in yeast. *PLoS Curr,* 6.

Karpinar, D. P., Balija, M. B., Kugler, S., Opazo, F., Rezaei-Ghaleh, N., Wender, N., Kim, H. Y., Taschenberger, G., Falkenburger, B. H., Heise, H., Kumar, A., Riedel, D., Fichtner, L., Voigt, A., Braus, G. H., Giller, K., Becker, S., Herzig, A., Baldus, M., Jackle, H., Eimer, S., Schulz, J. B., Griesinger, C., Zweckstetter, M. 2009. Pre-fibrillar alpha-synuclein variants with impaired beta-structure increase neurotoxicity in Parkinson's disease models. *EMBO J,* 28**,** 3256-3268.

Katorcha, E., Makarava, N., Lee, Y. J., Lindberg, I., Monteiro, M. J., Kovacs, G. G., Baskakov, I. V. 2017. Cross-seeding of prions by aggregated alpha-synuclein leads to transmissible spongiform encephalopathy. *PLoS Pathog,* 13**,** e1006563.

Kayatekin, C., Matlack, K. E., Hesse, W. R., Guan, Y., Chakrabortee, S., Russ, J., Wanker, E. E., Shah, J. V., Lindquist, S. 2014. Prion-like proteins sequester and suppress the toxicity of huntingtin exon 1. *Proc Natl Acad Sci U S A,* 111**,** 12085-12090.

Kazemi-Esfarjani, P., Benzer, S. 2000. Genetic suppression of polyglutamine toxicity in Drosophila. *Science,* 287**,** 1837-1840.

Kegel, K. B., Meloni, A. R., Yi, Y., Kim, Y. J., Doyle, E., Cuiffo, B. G., Sapp, E., Wang, Y., Qin, Z. H., Chen, J. D., Nevins, J. R., Aronin, N., DiFiglia, M. 2002. Huntingtin is present in the nucleus, interacts with the transcriptional corepressor C-terminal binding protein, and represses transcription. *J Biol Chem,* 277**,** 7466-7476.

Kegel, K. B., Sapp, E., Yoder, J., Cuiffo, B., Sobin, L., Kim, Y. J., Qin, Z. H., Hayden, M. R., Aronin, N., Scott, D. L., Isenberg, G., Goldmann, W. H., DiFiglia, M. 2005. Huntingtin associates with acidic phospholipids at the plasma membrane. *J Biol Chem,* 280**,** 36464-36473.

Kelley, N. W., Huang, X., Tam, S., Spiess, C., Frydman, J., Pande, V. S. 2009. The predicted structure of the headpiece of the Huntingtin protein and its implications on Huntingtin aggregation. *J Mol Biol,* 388**,** 919-927.

Kerppola, T. K. 2008. Bimolecular fluorescence complementation (BiFC) analysis as a probe of protein interactions in living cells. *Annu Rev Biophys,* 37**,** 465-487.

Khoshnan, A., Ko, J., Watkin, E. E., Paige, L. A., Reinhart, P. H., Patterson, P. H. 2004. Activation of the IkappaB kinase complex and nuclear factor-kappaB contributes to mutant huntingtin neurotoxicity. *J Neurosci,* 24**,** 7999-8008.

Kierdorf, K., Erny, D., Goldmann, T., Sander, V., Schulz, C., Perdiguero, E. G., Wieghofer, P., Heinrich, A., Riemke, P., Holscher, C., Muller, D. N., Luckow, B., Brocker, T., Debowski, K., Fritz, G., Opdenakker, G., Diefenbach, A., Biber, K., Heikenwalder, M., Geissmann, F., Rosenbauer, F., Prinz, M. 2013. Microglia emerge from erythromyeloid precursors via Pu.1- and Irf8-dependent pathways. *Nat Neurosci,* 16**,** 273-280.

Kim, S., Kim, K. T. 2014. Therapeutic Approaches for Inhibition of Protein Aggregation in Huntington's Disease. *Exp Neurobiol,* 23**,** 36-44.

Kim, Y., Kim, C., Son, S. M., Song, H., Hong, H. S., Han, S. H., Mook-Jung, I. 2016. The novel RAGE interactor PRAK is associated with autophagy signaling in Alzheimer's disease pathogenesis. *Mol Neurodegener,* 11**,** 4.

Kim, Y. J., Yi, Y., Sapp, E., Wang, Y., Cuiffo, B., Kegel, K. B., Qin, Z. H., Aronin, N., DiFiglia, M. 2001. Caspase 3-cleaved N-terminal fragments of wild-type and mutant huntingtin are present in normal and Huntington's disease brains, associate with membranes, and undergo calpain-dependent proteolysis. *Proc Natl Acad Sci U S A,* 98**,** 12784-12789.

King, O. D., Gitler, A. D., Shorter, J. 2012. The tip of the iceberg: RNA-binding proteins with prion-like domains in neurodegenerative disease. *Brain Res,* 1462**,** 61-80.

Kino, Y., Washizu, C., Kurosawa, M., Yamada, M., Doi, H., Takumi, T., Adachi, H., Katsuno, M., Sobue, G., Hicks, G. G., Hattori, N., Shimogori, T., Nukina, N. 2016. FUS/TLS acts as an aggregation-dependent modifier of polyglutamine disease model mice. *Sci Rep,* 6**,** 35236.

Kirchner, J., Gross, S., Bennett, D., Alphey, L. 2007a. Essential, overlapping and redundant roles of the Drosophila protein phosphatase 1 alpha and 1 beta genes. *Genetics,* 176**,** 273-281.

Kirchner, J., Gross, S., Bennett, D., Alphey, L. 2007b. The nonmuscle myosin phosphatase PP1beta (flapwing) negatively regulates Jun N-terminal kinase in wing imaginal discs of Drosophila. *Genetics,* 175**,** 1741-1749.

Knowles, T. P., Vendruscolo, M., Dobson, C. M. 2014. The amyloid state and its association with protein misfolding diseases. *Nat Rev Mol Cell Biol,* 15**,** 384-396.

Koeppen, A. H. 2011. Friedreich's ataxia: pathology, pathogenesis, and molecular genetics. *J Neurol Sci,* 303**,** 1-12.

Kontopoulos, E., Parvin, J. D., Feany, M. B. 2006. Alpha-synuclein acts in the nucleus to inhibit histone acetylation and promote neurotoxicity. *Hum Mol Genet,* 15**,** 3012-3023.

Kostylev, M. A., Kaufman, A. C., Nygaard, H. B., Patel, P., Haas, L. T., Gunther, E. C., Vortmeyer, A., Strittmatter, S. M. 2015. Prion-Protein-interacting Amyloid-beta Oligomers of High Molecular Weight Are Tightly Correlated with Memory Impairment in Multiple Alzheimer Mouse Models. *J Biol Chem,* 290**,** 17415-17438.

Kotzbauer, P. T., Giasson, B. I., Kravitz, A. V., Golbe, L. I., Mark, M. H., Trojanowski, J. Q., Lee, V. M. 2004. Fibrillization of alpha-synuclein and tau in familial Parkinson's disease caused by the A53T alpha-synuclein mutation. *Exp Neurol,* 187**,** 279-288.

Koukoui, S. D., Chaudhuri, A. 2007. Neuroanatomical, molecular genetic, and behavioral correlates of fragile X syndrome. *Brain Res Rev,* 53**,** 27-38.

Kovacs, G. G., Rahimi, J., Strobel, T., Lutz, M. I., Regelsberger, G., Streichenberger, N., Perret-Liaudet, A., Hoftberger, R., Liberski, P. P., Budka, H., Sikorska, B. 2017. Tau pathology in Creutzfeldt-Jakob disease revisited. *Brain Pathol,* 27**,** 332-344.

Krainc, D. 2010. Huntington's disease: tagged for clearance. *Nat Med,* 16**,** 32-33.

Krench, M., Littleton, J. T. 2013. Modeling Huntington disease in Drosophila: Insights into axonal transport defects and modifiers of toxicity. *Fly (Austin),* 7**,** 229-236.

Krobitsch, S., Lindquist, S. 2000. Aggregation of huntingtin in yeast varies with the length of the polyglutamine expansion and the expression of chaperone proteins. *Proc Natl Acad Sci U S A,* 97**,** 1589-1594.

Kuehnen, P., Laubner, K., Raile, K., Schofl, C., Jakob, F., Pilz, I., Path, G., Seufert, J. 2011. Protein phosphatase 1 (PP-1)-dependent inhibition of insulin secretion by leptin in INS-1 pancreatic beta-cells and human pancreatic islets. *Endocrinology,* 152**,** 1800-1808.

Kuemmerle, S., Gutekunst, C. A., Klein, A. M., Li, X. J., Li, S. H., Beal, M. F., Hersch, S. M., Ferrante, R. J. 1999. Huntington aggregates may not predict neuronal death in Huntington's disease. *Ann Neurol,* 46**,** 842-849.

Kuiper, E. F. E., de Mattos, E. P., Jardim, L. B., Kampinga, H. H., Bergink, S. 2017. Chaperones in Polyglutamine Aggregation: Beyond the Q-Stretch. *Frontiers in Neuroscience,* 11.

Kulkarni, M. J., Korwar, A. M., Mary, S., Bhonsle, H. S., Giri, A. P. 2013. Glycated proteome: from reaction to intervention. *Proteomics Clin Appl,* 7**,** 155-170.

Kumar, A., Singh, P. K., Parihar, R., Dwivedi, V., Lakhotia, S. C., Ganesh, S. 2014. Decreased O-linked GlcNAcylation protects from cytotoxicity mediated by huntingtin exon1 protein fragment. *J Biol Chem,* 289**,** 13543-13553.

Kumar, V., Sami, N., Kashav, T., Islam, A., Ahmad, F., Hassan, M. I. 2016. Protein aggregation and neurodegenerative diseases: From theory to therapy. *Eur J Med Chem,* 124**,** 1105-1120.

Kuo, Y., Ren, S., Lao, U., Edgar, B. A., Wang, T. 2013. Suppression of polyglutamine protein toxicity by co-expression of a heat-shock protein 40 and a heat-shock protein 110. *Cell Death Dis,* 4**,** e833.

Kwiatkowski, T. J., Jr., Bosco, D. A., Leclerc, A. L., Tamrazian, E., Vanderburg, C. R., Russ, C., Davis, A., Gilchrist, J., Kasarskis, E. J., Munsat, T., Valdmanis, P., Rouleau, G. A., Hosler, B. A., Cortelli, P., de Jong, P. J., Yoshinaga, Y., Haines, J. L., Pericak-Vance, M. A., Yan, J., Ticozzi, N., Siddique, T., McKenna-Yasek, D., Sapp, P. C., Horvitz, H. R., Landers, J. E., Brown, R. H., Jr. 2009. Mutations in the FUS/TLS gene on chromosome 16 cause familial amyotrophic lateral sclerosis. *Science,* 323**,** 1205-1208.

Labbadia, J., Morimoto, R. I. 2013. Huntington's disease: underlying molecular mechanisms and emerging concepts. *Trends Biochem Sci,* 38**,** 378-385.

Lajoie, P., Snapp, E. L. 2010. Formation and toxicity of soluble polyglutamine oligomers in living cells. *PLoS One,* 5**,** e15245.

Landles, C., Sathasivam, K., Weiss, A., Woodman, B., Moffitt, H., Finkbeiner, S., Sun, B., Gafni, J., Ellerby, L. M., Trottier, Y., Richards, W. G., Osmand, A., Paganetti, P., Bates, G. P. 2010. Proteolysis of mutant huntingtin produces an exon 1 fragment that accumulates as an aggregated protein in neuronal nuclei in Huntington disease. *J Biol Chem,* 285**,** 8808-8823.

Lashuel, H. A., Hartley, D. M., Petre, B. M., Wall, J. S., Simon, M. N., Walz, T., Lansbury, P. T., Jr. 2003. Mixtures of wild-type and a pathogenic (E22G) form of Abeta40 in vitro accumulate protofibrils, including amyloid pores. *J Mol Biol,* 332**,** 795-808.

Leavitt, B. R., Guttman, J. A., Hodgson, J. G., Kimel, G. H., Singaraja, R., Vogl, A. W., Hayden, M. R. 2001. Wild-type huntingtin reduces the cellular toxicity of mutant huntingtin in vivo. *Am J Hum Genet,* 68**,** 313-324.

Leavitt, B. R., van Raamsdonk, J. M., Shehadeh, J., Fernandes, H., Murphy, Z., Graham, R. K., Wellington, C. L., Raymond, L. A., Hayden, M. R. 2006. Wild-type huntingtin protects neurons from excitotoxicity. *J Neurochem,* 96**,** 1121-1129.

Lee, H. J., Suk, J. E., Patrick, C., Bae, E. J., Cho, J. H., Rho, S., Hwang, D., Masliah, E., Lee, S. J. 2010. Direct transfer of alpha-synuclein from neuron to astroglia causes inflammatory responses in synucleinopathies. *J Biol Chem,* 285**,** 9262-9272.

Lee, J. Y., Song, J., Kwon, K., Jang, S., Kim, C., Baek, K., Kim, J., Park, C. 2012. Human DJ-1 and its homologs are novel glyoxalases. *Hum Mol Genet,* 21**,** 3215-3225.

Lee, K. J., Panzera, A., Rogawski, D., Greene, L. E., Eisenberg, E. 2007. Cellular prion protein (PrPC) protects neuronal cells from the effect of huntingtin aggregation. *J Cell Sci,* 120**,** 2663-2671.

Lee, W. C., Yoshihara, M., Littleton, J. T. 2004. Cytoplasmic aggregates trap polyglutamine-containing proteins and block axonal transport in a Drosophila model of Huntington's disease. *Proc Natl Acad Sci U S A,* 101**,** 3224-3229.

Lemere, C. A., Blusztajn, J. K., Yamaguchi, H., Wisniewski, T., Saido, T. C., Selkoe, D. J. 1996. Sequence of deposition of heterogeneous amyloid beta-peptides and APO E in Down syndrome: implications for initial events in amyloid plaque formation. *Neurobiol Dis,* 3**,** 16-32.

Lessing, D., Bonini, N. M. 2009. Maintaining the brain: insight into human neurodegeneration from Drosophila melanogaster mutants. *Nat Rev Genet,* 10**,** 359-370.

Leverenz, J. B., Quinn, J. F., Zabetian, C., Zhang, J., Montine, K. S., Montine, T. J. 2009. Cognitive impairment and dementia in patients with Parkinson disease. *Curr Top Med Chem,* 9**,** 903-912.

Lewis, J., Dickson, D. W., Lin, W. L., Chisholm, L., Corral, A., Jones, G., Yen, S. H., Sahara, N., Skipper, L., Yager, D., Eckman, C., Hardy, J., Hutton, M., McGowan, E. 2001. Enhanced neurofibrillary degeneration in transgenic mice expressing mutant tau and APP. *Science,* 293**,** 1487-1491.

Li, H., Li, S. H., Johnston, H., Shelbourne, P. F., Li, X. J. 2000. Amino-terminal fragments of mutant huntingtin show selective accumulation in striatal neurons and synaptic toxicity. *Nat Genet,* 25**,** 385-389.

Li, J., Henning Jensen, P., Dahlstrom, A. 2002a. Differential localization of alpha-, beta- and gamma-synucleins in the rat CNS. *Neuroscience,* 113**,** 463-478.

Li, L. B., Xu, K., Bonini, N. M. 2007. Suppression of polyglutamine toxicity by the yeast Sup35 prion domain in Drosophila. *J Biol Chem,* 282**,** 37694-37701.

Li, S. H., Cheng, A. L., Zhou, H., Lam, S., Rao, M., Li, H., Li, X. J. 2002b. Interaction of Huntington disease protein with transcriptional activator Sp1. *Mol Cell Biol,* 22**,** 1277-1287.

Li, S. H., Li, X. J. 1998. Aggregation of N-terminal huntingtin is dependent on the length of its glutamine repeats. *Hum Mol Genet,* 7**,** 777-782.

Li, W., West, N., Colla, E., Pletnikova, O., Troncoso, J. C., Marsh, L., Dawson, T. M., Jakala, P., Hartmann, T., Price, D. L., Lee, M. K. 2005. Aggregation promoting C-terminal truncation of alpha-synuclein is a normal cellular process and is enhanced by the familial Parkinson's disease-linked mutations. *Proc Natl Acad Sci U S A,* 102**,** 2162-2167.

Li, X. H., Du, L. L., Cheng, X. S., Jiang, X., Zhang, Y., Lv, B. L., Liu, R., Wang, J. Z., Zhou, X. W. 2013. Glycation exacerbates the neuronal toxicity of beta-amyloid. *Cell Death Dis,* 4**,** e673.

Li, X. J., Li, S. H., Sharp, A. H., Nucifora, F. C., Jr., Schilling, G., Lanahan, A., Worley, P., Snyder, S. H., Ross, C. A. 1995. A huntingtin-associated protein enriched in brain with implications for pathology. *Nature,* 378**,** 398-402.

Li, Z., Karlovich, C. A., Fish, M. P., Scott, M. P., Myers, R. M. 1999. A putative Drosophila homolog of the Huntington's disease gene. *Hum Mol Genet,* 8**,** 1807-1815.

Liao, H., Li, Y., Brautigan, D. L., Gundersen, G. G. 1998. Protein phosphatase 1 is targeted to microtubules by the microtubule-associated protein Tau. *J Biol Chem,* 273**,** 21901-21908.

Liao, L., Cheng, D., Wang, J., Duong, D. M., Losik, T. G., Gearing, M., Rees, H. D., Lah, J. J., Levey, A. I., Peng, J. 2004. Proteomic characterization of postmortem amyloid plaques isolated by laser capture microdissection. *J Biol Chem,* 279**,** 37061-37068.

Liebman, S. W., Meredith, S. C. 2010. Protein folding: sticky N17 speeds huntingtin pile-up. *Nat Chem Biol,* 6**,** 7-8.

Lievens, J. C., Woodman, B., Mahal, A., Spasic-Boscovic, O., Samuel, D., Kerkerian-Le Goff, L., Bates, G. P. 2001. Impaired glutamate uptake in the R6 Huntington's disease transgenic mice. *Neurobiol Dis,* 8**,** 807-821.

Lin, H. K., Boatz, J. C., Krabbendam, I. E., Kodali, R., Hou, Z., Wetzel, R., Dolga, A. M., Poirier, M. A., van der Wel, P. C. A. 2017. Fibril polymorphism affects immobilized non-amyloid flanking domains of huntingtin exon1 rather than its polyglutamine core. *Nat Commun,* 8**,** 15462.

Lippincott-Schwartz, J., Snapp, E., Kenworthy, A. 2001. Studying protein dynamics in living cells. *Nat Rev Mol Cell Biol,* 2**,** 444-456.

Liscic, R. M., Grinberg, L. T., Zidar, J., Gitcho, M. A., Cairns, N. J. 2008. ALS and FTLD: two faces of TDP-43 proteinopathy. *Eur J Neurol,* 15**,** 772-780.

Liu, Y. F., Deth, R. C., Devys, D. 1997. SH3 domain-dependent association of huntingtin with epidermal growth factor receptor signaling complexes. *J Biol Chem,* 272**,** 8121-8124.

Lobbestael, E., Zhao, J., Rudenko, I. N., Beylina, A., Gao, F., Wetter, J., Beullens, M., Bollen, M., Cookson, M. R., Baekelandt, V., Nichols, R. J., Taymans, J. M. 2013. Identification of protein phosphatase 1 as a regulator of the LRRK2 phosphorylation cycle. *Biochem J,* 456**,** 119-128.

Lodi, R., Schapira, A. H., Manners, D., Styles, P., Wood, N. W., Taylor, D. J., Warner, T. T. 2000. Abnormal in vivo skeletal muscle energy metabolism in Huntington's disease and dentatorubropallidoluysian atrophy. *Ann Neurol,* 48**,** 72-76.

Lopez, N., Aron, R., Craig, E. A. 2003. Specificity of class II Hsp40 Sis1 in maintenance of yeast prion [RNQ+]. *Mol Biol Cell,* 14**,** 1172-1181.

Luk, K. C., Kehm, V., Carroll, J., Zhang, B., O'Brien, P., Trojanowski, J. Q., Lee, V. M. 2012. Pathological alpha-synuclein transmission initiates Parkinson-like neurodegeneration in nontransgenic mice. *Science,* 338**,** 949-953.

Lundmark, K., Westermark, G. T., Olsen, A., Westermark, P. 2005. Protein fibrils in nature can enhance amyloid protein A amyloidosis in mice: Cross-seeding as a disease mechanism. *Proc Natl Acad Sci U S A,* 102**,** 6098-6102.

Lunkes, A., Lindenberg, K. S., Ben-Haiem, L., Weber, C., Devys, D., Landwehrmeyer, G. B., Mandel, J. L., Trottier, Y. 2002. Proteases acting on mutant huntingtin generate cleaved products that differentially build up cytoplasmic and nuclear inclusions. *Mol Cell,* 10**,** 259-269.

Luo, S., Mizuta, H., Rubinsztein, D. C. 2008. p21-activated kinase 1 promotes soluble mutant huntingtin self-interaction and enhances toxicity. *Hum Mol Genet,* 17**,** 895-905.

Luo, S., Rubinsztein, D. C. 2009. Huntingtin promotes cell survival by preventing Pak2 cleavage. *J Cell Sci,* 122**,** 875-885.

Luo, S., Vacher, C., Davies, J. E., Rubinsztein, D. C. 2005. Cdk5 phosphorylation of huntingtin reduces its cleavage by caspases: implications for mutant huntingtin toxicity. *J Cell Biol,* 169**,** 647-656.

Ma, L., Nicholson, L. F. 2004. Expression of the receptor for advanced glycation end products in Huntington's disease caudate nucleus. *Brain Res,* 1018**,** 10-17.

Ma, T. C., Buescher, J. L., Oatis, B., Funk, J. A., Nash, A. J., Carrier, R. L., Hoyt, K. R. 2007. Metformin therapy in a transgenic mouse model of Huntington's disease. *Neurosci Lett,* 411**,** 98-103.

Maddison, D. C., Giorgini, F. 2015. The kynurenine pathway and neurodegenerative disease. *Semin Cell Dev Biol,* 40**,** 134-141.

Madine, J., Middleton, D. A. 2010. Comparison of aggregation enhancement and inhibition as strategies for reducing the cytotoxicity of the aortic amyloid polypeptide medin. *Eur Biophys J,* 39**,** 1281-1288.

Maiuri, T., Woloshansky, T., Xia, J., Truant, R. 2013. The huntingtin N17 domain is a multifunctional CRM1 and Ran-dependent nuclear and cilial export signal. *Hum Mol Genet,* 22**,** 1383-1394.

Maksimovic, I. D., Jovanovic, M. D., Colic, M., Mihajlovic, R., Micic, D., Selakovic, V., Ninkovic, M., Malicevic, Z., Rusic-Stojiljkovic, M., Jovicic, A. 2001. Oxidative damage and metabolic dysfunction in experimental Huntington's disease: selective vulnerability of the striatum and hippocampus. *Vojnosanit Pregl,* 58**,** 237-242.

Maksimovic, I. D., Jovanovic, M. D., Malicevic, Z., Colic, M., Ninkovic, M. 2002. Effects of nerve and fibroblast growth factors on the production of nitric oxide in experimental model of Huntington's disease. *Vojnosanit Pregl,* 59**,** 119-123.

Mangiarini, L., Sathasivam, K., Seller, M., Cozens, B., Harper, A., Hetherington, C., Lawton, M., Trottier, Y., Lehrach, H., Davies, S. W., Bates, G. P. 1996. Exon 1 of the HD gene with an expanded CAG repeat is sufficient to cause a progressive neurological phenotype in transgenic mice. *Cell,* 87**,** 493-506.

Mannini, B., Cascella, R., Zampagni, M., van Waarde-Verhagen, M., Meehan, S., Roodveldt, C., Campioni, S., Boninsegna, M., Penco, A., Relini, A., Kampinga, H. H., Dobson, C. M., Wilson, M. R., Cecchi, C., Chiti, F. 2012. Molecular mechanisms used by chaperones to reduce the toxicity of aberrant protein oligomers. *Proc Natl Acad Sci U S A,* 109**,** 12479-12484.

Mansson, C., Kakkar, V., Monsellier, E., Sourigues, Y., Harmark, J., Kampinga, H. H., Melki, R., Emanuelsson, C. 2014. DNAJB6 is a peptide-binding chaperone which can suppress amyloid fibrillation of polyglutamine peptides at substoichiometric molar ratios. *Cell Stress Chaperones,* 19**,** 227-239.

Mansuy, I. M., Shenolikar, S. 2006. Protein serine/threonine phosphatases in neuronal plasticity and disorders of learning and memory. *Trends Neurosci,* 29**,** 679-686.

Marion, S., Urs, N. M., Peterson, S. M., Sotnikova, T. D., Beaulieu, J. M., Gainetdinov, R. R., Caron, M. G. 2014. Dopamine D2 receptor relies upon PPM/PP2C protein phosphatases to dephosphorylate huntingtin protein. *J Biol Chem,* 289**,** 11715-11724.

Maroni, G., Laurie-Ahlberg, C. C. 1983. Genetic control of Adh expression in Drosophila melanogaster. *Genetics,* 105**,** 921-933.

Marsh, J. L., Pallos, J., Thompson, L. M. 2003. Fly models of Huntington's disease. *Hum Mol Genet,* 12 Spec No 2**,** R187-193.

Martin, B., Golden, E., Carlson, O. D., Pistell, P., Zhou, J., Kim, W., Frank, B. P., Thomas, S., Chadwick, W. A., Greig, N. H., Bates, G. P., Sathasivam, K., Bernier, M., Maudsley, S., Mattson, M. P., Egan, J. M. 2009. Exendin-4 improves glycemic control, ameliorates brain and pancreatic pathologies, and extends survival in a mouse model of Huntington's disease. *Diabetes,* 58**,** 318-328.

Marui, W., Iseki, E., Ueda, K., Kosaka, K. 2000. Occurrence of human alpha-synuclein immunoreactive neurons with neurofibrillary tangle formation in the limbic areas of patients with Alzheimer's disease. *J Neurol Sci,* 174**,** 81-84.

Masliah, E., Rockenstein, E., Veinbergs, I., Sagara, Y., Mallory, M., Hashimoto, M., Mucke, L. 2001. beta-amyloid peptides enhance alpha-synuclein accumulation and neuronal deficits in a transgenic mouse model linking Alzheimer's disease and Parkinson's disease. *Proc Natl Acad Sci U S A,* 98**,** 12245-12250.

Mason, R. P., Casu, M., Butler, N., Breda, C., Campesan, S., Clapp, J., Green, E. W., Dhulkhed, D., Kyriacou, C. P., Giorgini, F. 2013. Glutathione peroxidase activity is neuroprotective in models of Huntington's disease. *Nat Genet,* 45**,** 1249-1254.

Mason, R. P., Giorgini, F. 2011. Modeling Huntington disease in yeast: perspectives and future directions. *Prion,* 5**,** 269-276.

Mead, S., Reilly, M. M. 2015. A new prion disease: relationship with central and peripheral amyloidoses. *Nat Rev Neurol,* 11**,** 90-97.

Meriin, A. B., Zhang, X., He, X., Newnam, G. P., Chernoff, Y. O., Sherman, M. Y. 2002. Huntington toxicity in yeast model depends on polyglutamine aggregation mediated by a prion-like protein Rnq1. *J Cell Biol,* 157**,** 997-1004.

Merlini, G., Seldin, D. C., Gertz, M. A. 2011. Amyloidosis: pathogenesis and new therapeutic options. *J Clin Oncol,* 29**,** 1924-1933.

Metzler, M., Gan, L., Mazarei, G., Graham, R. K., Liu, L., Bissada, N., Lu, G., Leavitt, B. R., Hayden, M. R. 2010. Phosphorylation of huntingtin at Ser421 in YAC128 neurons is associated with protection of YAC128 neurons from NMDA-mediated excitotoxicity and is modulated by PP1 and PP2A. *J Neurosci,* 30**,** 14318-14329.

Meunier, C., Merienne, N., Jolle, C., Deglon, N., Pellerin, L. 2016. Astrocytes are key but indirect contributors to the development of the symptomatology and pathophysiology of Huntington's disease. *Glia,* 64**,** 1841-1856.

Michalek, M., Salnikov, E. S., Werten, S., Bechinger, B. 2013. Membrane interactions of the amphipathic amino terminus of huntingtin. *Biochemistry,* 52**,** 847-858.

Miller, B. R., Dorner, J. L., Shou, M., Sari, Y., Barton, S. J., Sengelaub, D. R., Kennedy, R. T., Rebec, G. V. 2008. Up-regulation of GLT1 expression increases glutamate uptake and attenuates the Huntington's disease phenotype in the R6/2 mouse. *Neuroscience,* 153**,** 329-337.

Mishra, R., Hoop, C. L., Kodali, R., Sahoo, B., van der Wel, P. C., Wetzel, R. 2012. Serine phosphorylation suppresses huntingtin amyloid accumulation by altering protein aggregation properties. *J Mol Biol,* 424**,** 1-14.

Miyazono, M., Kitamoto, T., Iwaki, T., Tateishi, J. 1992. Colocalization of prion protein and beta protein in the same amyloid plaques in patients with Gerstmann-Straussler syndrome. *Acta Neuropathol,* 83**,** 333-339.

Modregger, J., DiProspero, N. A., Charles, V., Tagle, D. A., Plomann, M. 2002. PACSIN 1 interacts with huntingtin and is absent from synaptic varicosities in presymptomatic Huntington's disease brains. *Hum Mol Genet,* 11**,** 2547-2558.

Monsellier, E., Redeker, V., Ruiz-Arlandis, G., Bousset, L., Melki, R. 2015. Molecular interaction between the chaperone Hsc70 and the N-terminal flank of huntingtin exon 1 modulates aggregation. *J Biol Chem,* 290**,** 2560-2576.

Morales, R., Moreno-Gonzalez, I., Soto, C. 2013. Cross-seeding of misfolded proteins: implications for etiology and pathogenesis of protein misfolding diseases. *PLoS Pathog,* 9**,** e1003537.

Muchowski, P. J., Schaffar, G., Sittler, A., Wanker, E. E., Hayer-Hartl, M. K., Hartl, F. U. 2000. Hsp70 and hsp40 chaperones can inhibit self-assembly of polyglutamine proteins into amyloid-like fibrils. *Proc Natl Acad Sci U S A,* 97**,** 7841-7846.

Mummery-Widmer, J. L., Yamazaki, M., Stoeger, T., Novatchkova, M., Bhalerao, S., Chen, D., Dietzl, G., Dickson, B. J., Knoblich, J. A. 2009. Genome-wide analysis of Notch signalling in Drosophila by transgenic RNAi. *Nature,* 458**,** 987-992.

Murali, A., Maue, R. A., Dolph, P. J. 2014. Reversible symptoms and clearance of mutant prion protein in an inducible model of a genetic prion disease in Drosophila melanogaster. *Neurobiol Dis,* 67**,** 71-78.

Myeku, N., Clelland, C. L., Emrani, S., Kukushkin, N. V., Yu, W. H., Goldberg, A. L., Duff, K. E. 2016. Tau-driven 26S proteasome impairment and cognitive dysfunction can be prevented early in disease by activating cAMP-PKA signaling. *Nat Med,* 22**,** 46-53.

Nagai, T., Ibata, K., Park, E. S., Kubota, M., Mikoshiba, K., Miyawaki, A. 2002. A variant of yellow fluorescent protein with fast and efficient maturation for cell-biological applications. *Nat Biotechnol,* 20**,** 87-90.

Nagaraj, R. H., Oya-Ito, T., Padayatti, P. S., Kumar, R., Mehta, S., West, K., Levison, B., Sun, J., Crabb, J. W., Padival, A. K. 2003. Enhancement of chaperone function of alpha-crystallin by methylglyoxal modification. *Biochemistry,* 42**,** 10746-10755.

Nakao, N., Odin, P., Lindvall, O., Brundin, P. 1996. Differential trophic effects of basic fibroblast growth factor, insulin-like growth factor-1, and neurotrophin-3 on striatal neurons in culture. *Exp Neurol,* 138**,** 144-157.

Narayan, P., Ehsani, S., Lindquist, S. 2014. Combating neurodegenerative disease with chemical probes and model systems. *Nat Chem Biol,* 10**,** 911-920.

Nasir, J., Floresco, S. B., O'Kusky, J. R., Diewert, V. M., Richman, J. M., Zeisler, J., Borowski, A., Marth, J. D., Phillips, A. G., Hayden, M. R. 1995. Targeted disruption of the Huntington's disease gene results in embryonic lethality and behavioral and morphological changes in heterozygotes. *Cell,* 81**,** 811-823.

Neveklovska, M., Clabough, E. B., Steffan, J. S., Zeitlin, S. O. 2012. Deletion of the huntingtin proline-rich region does not significantly affect normal huntingtin function in mice. *J Huntingtons Dis,* 1**,** 71-87.

New, L., Jiang, Y., Zhao, M., Liu, K., Zhu, W., Flood, L. J., Kato, Y., Parry, G. C., Han, J. 1998. PRAK, a novel protein kinase regulated by the p38 MAP kinase. *EMBO J,* 17**,** 3372-3384.

Ni, J. Q., Zhou, R., Czech, B., Liu, L. P., Holderbaum, L., Yang-Zhou, D., Shim, H. S., Tao, R., Handler, D., Karpowicz, P., Binari, R., Booker, M., Brennecke, J., Perkins, L. A., Hannon, G. J., Perrimon, N. 2011. A genome-scale shRNA resource for transgenic RNAi in Drosophila. *Nat Methods,* 8**,** 405-407.

Niwa, J., Ishigaki, S., Hishikawa, N., Yamamoto, M., Doyu, M., Murata, S., Tanaka, K., Taniguchi, N., Sobue, G. 2002. Dorfin ubiquitylates mutant SOD1 and prevents mutant SOD1-mediated neurotoxicity. *J Biol Chem,* 277**,** 36793-36798.

Nixon, R. A. 2013. The role of autophagy in neurodegenerative disease. *Nat Med,* 19**,** 983-997.

Nubling, G., Bader, B., Levin, J., Hildebrandt, J., Kretzschmar, H., Giese, A. 2012. Synergistic influence of phosphorylation and metal ions on tau oligomer formation and coaggregation with alpha-synuclein at the single molecule level. *Mol Neurodegener,* 7**,** 35.

Nussbaum, R. L., Polymeropoulos, M. H. 1997. Genetics of Parkinson's disease. *Hum Mol Genet,* 6**,** 1687-1691.

Oddo, S., Billings, L., Kesslak, J. P., Cribbs, D. H., LaFerla, F. M. 2004. Abeta immunotherapy leads to clearance of early, but not late, hyperphosphorylated tau aggregates via the proteasome. *Neuron,* 43**,** 321-332.

Okamoto, S., Pouladi, M. A., Talantova, M., Yao, D., Xia, P., Ehrnhoefer, D. E., Zaidi, R., Clemente, A., Kaul, M., Graham, R. K., Zhang, D., Vincent Chen, H. S., Tong, G., Hayden, M. R., Lipton, S. A. 2009. Balance between synaptic versus extrasynaptic NMDA receptor activity influences inclusions and neurotoxicity of mutant huntingtin. *Nat Med,* 15**,** 1407-1413.

Orosz, F., Olah, J., Ovadi, J. 2009. Triosephosphate isomerase deficiency: new insights into an enigmatic disease. *Biochim Biophys Acta,* 1792**,** 1168-1174.

Osherovich, L. Z., Weissman, J. S. 2001. Multiple Gln/Asn-rich prion domains confer susceptibility to induction of the yeast [PSI(+)] prion. *Cell,* 106**,** 183-194.

Outeiro, T. F., Putcha, P., Tetzlaff, J. E., Spoelgen, R., Koker, M., Carvalho, F., Hyman, B. T., McLean, P. J. 2008. Formation of toxic oligomeric alpha-synuclein species in living cells. *PLoS One,* 3**,** e1867.

Oya-Ito, T., Liu, B. F., Nagaraj, R. H. 2006. Effect of methylglyoxal modification and phosphorylation on the chaperone and anti-apoptotic properties of heat shock protein 27. *J Cell Biochem,* 99**,** 279-291.

Ozawa, D., Kaji, Y., Yagi, H., Sakurai, K., Kawakami, T., Naiki, H., Goto, Y. 2011. Destruction of amyloid fibrils of keratoepithelin peptides by laser irradiation coupled with amyloid-specific thioflavin T. *J Biol Chem,* 286**,** 10856-10863.

Pal, A., Severin, F., Lommer, B., Shevchenko, A., Zerial, M. 2006. Huntingtin-HAP40 complex is a novel Rab5 effector that regulates early endosome motility and is up-regulated in Huntington's disease. *J Cell Biol,* 172**,** 605-618.

Pang, T. Y., Stam, N. C., Nithianantharajah, J., Howard, M. L., Hannan, A. J. 2006. Differential effects of voluntary physical exercise on behavioral and brain-derived neurotrophic factor expression deficits in Huntington's disease transgenic mice. *Neuroscience,* 141**,** 569-584.

Pardo, R., Colin, E., Regulier, E., Aebischer, P., Deglon, N., Humbert, S., Saudou, F. 2006. Inhibition of calcineurin by FK506 protects against polyglutamine-huntingtin toxicity through an increase of huntingtin phosphorylation at S421. *J Neurosci,* 26**,** 1635-1645.

Park, S. H., Kukushkin, Y., Gupta, R., Chen, T., Konagai, A., Hipp, M. S., Hayer-Hartl, M., Hartl, F. U. 2013. PolyQ proteins interfere with nuclear degradation of cytosolic proteins by sequestering the Sis1p chaperone. *Cell,* 154**,** 134-145.

Park, Y., Kim, W., Kim, A. Y., Choi, H. J., Choi, J. K., Park, N., Koh, E. K., Seo, J., Koh, Y. H. 2011. Normal prion protein in Drosophila enhances the toxicity of pathogenic polyglutamine proteins and alters susceptibility to oxidative and autophagy signaling modulators. *Biochem Biophys Res Commun,* 404**,** 638-645.

Patel, B. K., Liebman, S. W. 2007. "Prion-proof" for [PIN+]: infection with in vitro-made amyloid aggregates of Rnq1p-(132-405) induces [PIN+]. *J Mol Biol,* 365**,** 773-782.

Pearce, M. M. 2017. Prion-like transmission of pathogenic protein aggregates in genetic models of neurodegenerative disease. *Curr Opin Genet Dev,* 44**,** 149-155.

Pearce, M. M., Spartz, E. J., Hong, W., Luo, L., Kopito, R. R. 2015. Prion-like transmission of neuronal huntingtin aggregates to phagocytic glia in the Drosophila brain. *Nat Commun,* 6**,** 6768.

Pecho-Vrieseling, E., Rieker, C., Fuchs, S., Bleckmann, D., Esposito, M. S., Botta, P., Goldstein, C., Bernhard, M., Galimberti, I., Muller, M., Luthi, A., Arber, S., Bouwmeester, T., van der Putten, H., Di Giorgio, F. P. 2014. Transneuronal propagation of mutant huntingtin contributes to non-cell autonomous pathology in neurons. *Nat Neurosci,* 17**,** 1064-1072.

Pepys, M. B., Hawkins, P. N., Booth, D. R., Vigushin, D. M., Tennent, G. A., Soutar, A. K., Totty, N., Nguyen, O., Blake, C. C., Terry, C. J., et al. 1993. Human lysozyme gene mutations cause hereditary systemic amyloidosis. *Nature,* 362**,** 553-557.

Perkins, L. A., Holderbaum, L., Tao, R., Hu, Y., Sopko, R., McCall, K., Yang-Zhou, D., Flockhart, I., Binari, R., Shim, H. S., Miller, A., Housden, A., Foos, M., Randkelv, S., Kelley, C., Namgyal, P., Villalta, C., Liu, L. P., Jiang, X., Huan-Huan, Q., Wang, X., Fujiyama, A., Toyoda, A., Ayers, K., Blum, A., Czech, B., Neumuller, R., Yan, D., Cavallaro, A., Hibbard, K., Hall, D., Cooley, L., Hannon, G. J., Lehmann, R., Parks, A., Mohr, S. E.,

Ueda, R., Kondo, S., Ni, J. Q., Perrimon, N. 2015. The Transgenic RNAi Project at Harvard Medical School: Resources and Validation. *Genetics,* 201**,** 843-852.

Perrett, S., Jones, G. W. 2008. Insights into the mechanism of prion propagation. *Curr Opin Struct Biol,* 18**,** 52-59.

Peters, P. J., Ning, K., Palacios, F., Boshans, R. L., Kazantsev, A., Thompson, L. M., Woodman, B., Bates, G. P., D'Souza-Schorey, C. 2002. Arfaptin 2 regulates the aggregation of mutant huntingtin protein. *Nat Cell Biol,* 4**,** 240-245.

Pfaff, D. H., Fleming, T., Nawroth, P., Teleman, A. A. 2017. Evidence Against a Role for the Parkinsonism-associated Protein DJ-1 in Methylglyoxal Detoxification. *J Biol Chem,* 292**,** 685-690.

Pfaffl, M. W., Horgan, G. W., Dempfle, L. 2002. Relative expression software tool (REST) for group-wise comparison and statistical analysis of relative expression results in real-time PCR. *Nucleic Acids Res,* 30**,** e36.

Phillips, S. A., Thornalley, P. J. 1993. The formation of methylglyoxal from triose phosphates. Investigation using a specific assay for methylglyoxal. *Eur J Biochem,* 212**,** 101-105.

Pichaud, F., Desplan, C. 2001. A new visualization approach for identifying mutations that affect differentiation and organization of the Drosophila ommatidia. *Development,* 128**,** 815-826.

Pineda, J. R., Pardo, R., Zala, D., Yu, H., Humbert, S., Saudou, F. 2009. Genetic and pharmacological inhibition of calcineurin corrects the BDNF transport defect in Huntington's disease. *Mol Brain,* 2**,** 33.

Pinsonneault, R. L., Mayer, N., Mayer, F., Tegegn, N., Bainton, R. J. 2011. Novel models for studying the blood-brain and blood-eye barriers in Drosophila. *Methods Mol Biol,* 686**,** 357-369.

Pires, R. H., Karsai, A., Saraiva, M. J., Damas, A. M., Kellermayer, M. S. 2012. Distinct annular oligomers captured along the assembly and disassembly pathways of transthyretin amyloid protofibrils. *PLoS One,* 7**,** e44992.

Plomann, M., Lange, R., Vopper, G., Cremer, H., Heinlein, U. A., Scheff, S., Baldwin, S. A., Leitges, M., Cramer, M., Paulsson, M., Barthels, D. 1998. PACSIN, a brain protein that is upregulated upon differentiation into neuronal cells. *Eur J Biochem,* 256**,** 201-211.

Pocas, G. M., Branco-Santos, J., Herrera, F., Outeiro, T. F., Domingos, P. M. 2015. alpha-Synuclein modifies mutant huntingtin aggregation and neurotoxicity in Drosophila. *Hum Mol Genet,* 24**,** 1898-1907.

Podolsky, S., Leopold, N. A., Sax, D. S. 1972. Increased frequency of diabetes mellitus in patients with Huntington's chorea. *Lancet,* 1**,** 1356-1358.

Posey, A. E., Ruff, K. M., Harmon, T. S., Crick, S. L., Li, A., Diamond, M. I., Pappu, R. V. 2018. Profilin reduces aggregation and phase separation of huntingtin N-terminal fragments by preferentially binding to soluble monomers and oligomers. *J Biol Chem*, in press.

Preisinger, E., Jordan, B. M., Kazantsev, A., Housman, D. 1999. Evidence for a recruitment and sequestration mechanism in Huntington's disease. *Philos Trans R Soc Lond B Biol Sci,* 354**,** 1029-1034.

Purves, D. C., Brachmann, C. 2007. Dissection of imaginal discs from 3rd instar Drosophila larvae. *J Vis Exp*, in press.**,** 140.

Puyal, J., Ginet, V., Grishchuk, Y., Truttmann, A. C., Clarke, P. G. 2012. Neuronal autophagy as a mediator of life and death: contrasting roles in chronic neurodegenerative and acute neural disorders. *Neuroscientist,* 18**,** 224-236.

Qin, Z. H., Wang, Y., Sapp, E., Cuiffo, B., Wanker, E., Hayden, M. R., Kegel, K. B., Aronin, N., DiFiglia, M. 2004. Huntingtin bodies sequester vesicle-associated proteins by a polyproline-dependent interaction. *J Neurosci,* 24**,** 269-281.

Raha-Chowdhury, R., Andrews, S. R., Gruen, J. R. 2005. CAT 53: a protein phosphatase 1 nuclear targeting subunit encoded in the MHC Class I region strongly expressed in regions of the brain involved in memory, learning, and Alzheimer's disease. *Brain Res Mol Brain Res,* 138**,** 70-83.

Rahimi, J., Kovacs, G. G. 2014. Prevalence of mixed pathologies in the aging brain. *Alzheimers Res Ther,* 6**,** 82.

Rajan, R. S., Illing, M. E., Bence, N. F., Kopito, R. R. 2001. Specificity in intracellular protein aggregation and inclusion body formation. *Proc Natl Acad Sci U S A,* 98**,** 13060-13065.

Rangone, H., Pardo, R., Colin, E., Girault, J. A., Saudou, F., Humbert, S. 2005. Phosphorylation of arfaptin 2 at Ser260 by Akt Inhibits PolyQ-huntingtin-induced toxicity by rescuing proteasome impairment. *J Biol Chem,* 280**,** 22021-22028.

Rangone, H., Poizat, G., Troncoso, J., Ross, C. A., MacDonald, M. E., Saudou, F., Humbert, S. 2004. The serum- and glucocorticoid-induced kinase SGK inhibits mutant huntingtin-induced toxicity by phosphorylating serine 421 of huntingtin. *Eur J Neurosci,* 19**,** 273-279.

Ratovitski, T., Chighladze, E., Arbez, N., Boronina, T., Herbrich, S., Cole, R. N., Ross, C. A. 2012. Huntingtin protein interactions altered by polyglutamine expansion as determined by quantitative proteomic analysis. *Cell Cycle,* 11**,** 2006-2021.

Ravikumar, B., Imarisio, S., Sarkar, S., O'Kane, C. J., Rubinsztein, D. C. 2008. Rab5 modulates aggregation and toxicity of mutant huntingtin through macroautophagy in cell and fly models of Huntington disease. *J Cell Sci,* 121**,** 1649-1660.

Ravikumar, B., Vacher, C., Berger, Z., Davies, J. E., Luo, S., Oroz, L. G., Scaravilli, F., Easton, D. F., Duden, R., O'Kane, C. J., Rubinsztein, D. C. 2004. Inhibition of mTOR induces autophagy and reduces toxicity of polyglutamine expansions in fly and mouse models of Huntington disease. *Nat Genet,* 36**,** 585-595.

Raychaudhuri, S., Sinha, M., Mukhopadhyay, D., Bhattacharyya, N. P. 2008. HYPK, a Huntingtin interacting protein, reduces aggregates and apoptosis induced by N-terminal Huntingtin with 40 glutamines in Neuro2a cells and exhibits chaperone-like activity. *Hum Mol Genet,* 17**,** 240-255.

Raymond, L. A., Andre, V. M., Cepeda, C., Gladding, C. M., Milnerwood, A. J., Levine, M. S. 2011. Pathophysiology of Huntington's disease: time-dependent alterations in synaptic and receptor function. *Neuroscience,* 198**,** 252-273.

Reaume, A. G., Elliott, J. L., Hoffman, E. K., Kowall, N. W., Ferrante, R. J., Siwek, D. F., Wilcox, H. M., Flood, D. G., Beal, M. F., Brown, R. H., Jr., Scott, R. W., Snider, W. D. 1996. Motor neurons in Cu/Zn superoxide dismutase-deficient mice develop normally but exhibit enhanced cell death after axonal injury. *Nat Genet,* 13**,** 43-47.

Reither, G., Chatterjee, J., Beullens, M., Bollen, M., Schultz, C., Kohn, M. 2013. Chemical activators of protein phosphatase-1 induce calcium release inside intact cells. *Chem Biol,* 20**,** 1179-1186.

Ren, P. H., Lauckner, J. E., Kachirskaia, I., Heuser, J. E., Melki, R., Kopito, R. R. 2009. Cytoplasmic penetration and persistent infection of mammalian cells by polyglutamine aggregates. *Nat Cell Biol,* 11**,** 219-225.

Resenberger, U. K., Harmeier, A., Woerner, A. C., Goodman, J. L., Muller, V., Krishnan, R., Vabulas, R. M., Kretzschmar, H. A., Lindquist, S., Hartl, F. U., Multhaup, G., Winklhofer, K. F., Tatzelt, J. 2011. The cellular prion protein mediates neurotoxic signalling of beta-sheet-rich conformers independent of prion replication. *EMBO J,* 30**,** 2057-2070.

Resende, C. G., Outeiro, T. F., Sands, L., Lindquist, S., Tuite, M. F. 2003. Prion protein gene polymorphisms in Saccharomyces cerevisiae. *Mol Microbiol,* 49**,** 1005-1017.

Revesz, T., Holton, J. L., Lashley, T., Plant, G., Frangione, B., Rostagno, A., Ghiso, J. 2009. Genetics and molecular pathogenesis of sporadic and hereditary cerebral amyloid angiopathies. *Acta Neuropathol,* 118**,** 115-130.

Rey, N. L., Steiner, J. A., Maroof, N., Luk, K. C., Madaj, Z., Trojanowski, J. Q., Lee, V. M., Brundin, P. 2016. Widespread transneuronal propagation of alpha-synucleinopathy triggered in olfactory bulb mimics prodromal Parkinson's disease. *J Exp Med,* 213**,** 1759-1778.

Ribchester, R. R., Thomson, D., Wood, N. I., Hinks, T., Gillingwater, T. H., Wishart, T. M., Court, F. A., Morton, A. J. 2004. Progressive abnormalities in skeletal muscle and neuromuscular junctions of transgenic mice expressing the Huntington's disease mutation. *Eur J Neurosci,* 20**,** 3092-3114.

Richard, J. P. 1991. Kinetic parameters for the elimination reaction catalyzed by triosephosphate isomerase and an estimation of the reaction's physiological significance. *Biochemistry,* 30**,** 4581-4585.

Richards, F. M. 1958. On the Enzymic Activity of Subtilisin-Modified Ribonuclease. *Proc Natl Acad Sci U S A,* 44**,** 162-166.

Richarme, G., Mihoub, M., Dairou, J., Bui, L. C., Leger, T., Lamouri, A. 2015. Parkinsonism-associated protein DJ-1/Park7 is a major protein deglycase that repairs methylglyoxal- and glyoxal-glycated cysteine, arginine, and lysine residues. *J Biol Chem,* 290**,** 1885-1897.

Ripaud, L., Chumakova, V., Antonin, M., Hastie, A. R., Pinkert, S., Korner, R., Ruff, K. M., Pappu, R. V., Hornburg, D., Mann, M., Hartl, F. U., Hipp, M. S. 2014. Overexpression of Q-rich prion-like proteins suppresses polyQ cytotoxicity and alters the polyQ interactome. *Proc Natl Acad Sci U S A,* 111**,** 18219-18224.

Ritz, C., Spiess, A. N. 2008. qpcR: an R package for sigmoidal model selection in quantitative real-time polymerase chain reaction analysis. *Bioinformatics,* 24**,** 1549-1551.

Robinson, S. W., Nugent, M. L., Dinsdale, D., Steinert, J. R. 2014. Prion protein facilitates synaptic vesicle release by enhancing release probability. *Hum Mol Genet,* 23**,** 4581-4596.

Rochet, J. C. 2007. Novel therapeutic strategies for the treatment of protein-misfolding diseases. *Expert Rev Mol Med,* 9**,** 1-34.

Rockabrand, E., Slepko, N., Pantalone, A., Nukala, V. N., Kazantsev, A., Marsh, J. L., Sullivan, P. G., Steffan, J. S., Sensi, S. L., Thompson, L. M. 2007. The first 17 amino acids of Huntingtin modulate its sub-cellular localization, aggregation and effects on calcium homeostasis. *Hum Mol Genet,* 16**,** 61-77.

Rosenblatt, A., Kumar, B. V., Mo, A., Welsh, C. S., Margolis, R. L., Ross, C. A. 2012. Age, CAG repeat length, and clinical progression in Huntington's disease. *Mov Disord,* 27**,** 272-276.

Rosenstock, T. R., de Brito, O. M., Lombardi, V., Louros, S., Ribeiro, M., Almeida, S., Ferreira, I. L., Oliveira, C. R., Rego, A. C. 2011. FK506 ameliorates cell death features in Huntington's disease striatal cell models. *Neurochem Int,* 59**,** 600-609.

Ross, C. A., Aylward, E. H., Wild, E. J., Langbehn, D. R., Long, J. D., Warner, J. H., Scahill, R. I., Leavitt, B. R., Stout, J. C., Paulsen, J. S., Reilmann, R., Unschuld, P. G., Wexler, A., Margolis, R. L., Tabrizi, S. J. 2014. Huntington disease: natural history, biomarkers and prospects for therapeutics. *Nat Rev Neurol,* 10**,** 204-216.

Ross, C. A., Poirier, M. A. 2004. Protein aggregation and neurodegenerative disease. *Nat Med,* 10 Suppl**,** S10-17.

Ross, C. A., Poirier, M. A. 2005. Opinion: What is the role of protein aggregation in neurodegeneration? *Nat Rev Mol Cell Biol,* 6**,** 891-898.

Ross, C. A., Tabrizi, S. J. 2011. Huntington's disease: from molecular pathogenesis to clinical treatment. *Lancet Neurol,* 10**,** 83-98.

Rossetti, G., Cossio, P., Laio, A., Carloni, P. 2011. Conformations of the Huntingtin N-term in aqueous solution from atomistic simulations. *FEBS Lett,* 585**,** 3086-3089.

Roy, B., Jackson, G. R. 2014. Interactions between Tau and alpha-synuclein augment neurotoxicity in a Drosophila model of Parkinson's disease. *Hum Mol Genet,* 23**,** 3008-3023.

Roze, E., Cahill, E., Martin, E., Bonnet, C., Vanhoutte, P., Betuing, S., Caboche, J. 2011. Huntington's Disease and Striatal Signaling. *Front Neuroanat,* 5**,** 55.

Rubinsztein, D. C. 2002. Lessons from animal models of Huntington's disease. *Trends Genet,* 18**,** 202-209.

Rubinsztein, D. C., Codogno, P., Levine, B. 2012. Autophagy modulation as a potential therapeutic target for diverse diseases. *Nat Rev Drug Discov,* 11**,** 709-730.

Rui, Y. N., Xu, Z., Patel, B., Chen, Z., Chen, D., Tito, A., David, G., Sun, Y., Stimming, E. F., Bellen, H. J., Cuervo, A. M., Zhang, S. 2015. Huntingtin functions as a scaffold for selective macroautophagy. *Nat Cell Biol,* 17**,** 262-275.

Sabate, R., Rousseau, F., Schymkowitz, J., Ventura, S. 2015. What makes a protein sequence a prion? *PLoS Comput Biol,* 11**,** e1004013.

Sahoo, B., Arduini, I., Drombosky, K. W., Kodali, R., Sanders, L. H., Greenamyre, J. T., Wetzel, R. 2016. Folding Landscape of Mutant Huntingtin Exon1: Diffusible Multimers, Oligomers and Fibrils, and No Detectable Monomer. *PLoS One,* 11**,** e0155747.

Sajjad, M. U., Green, E. W., Miller-Fleming, L., Hands, S., Herrera, F., Campesan, S., Khoshnan, A., Outeiro, T. F., Giorgini, F., Wyttenbach, A. 2014. DJ-1 modulates aggregation and pathogenesis in models of Huntington's disease. *Hum Mol Genet,* 23**,** 755-766.

Sakahira, H., Breuer, P., Hayer-Hartl, M. K., Hartl, F. U. 2002. Molecular chaperones as modulators of polyglutamine protein aggregation and toxicity. *Proc Natl Acad Sci U S A,* 99 Suppl 4**,** 16412-16418.

Sakudo, A., Onodera, T. 2014. Prion protein (PrP) gene-knockout cell lines: insight into functions of the PrP. *Front Cell Dev Biol,* 2**,** 75.

Salazar, S. V., Strittmatter, S. M. 2017. Cellular prion protein as a receptor for amyloid-beta oligomers in Alzheimer's disease. *Biochem Biophys Res Commun,* 483**,** 1143-1147.

Sarell, C. J., Stockley, P. G., Radford, S. E. 2013. Assessing the causes and consequences of co-polymerization in amyloid formation. *Prion,* 7**,** 359-368.

Sathasivam, K., Neueder, A., Gipson, T. A., Landles, C., Benjamin, A. C., Bondulich, M. K., Smith, D. L., Faull, R. L., Roos, R. A., Howland, D., Detloff, P. J., Housman, D. E., Bates, G. P. 2013. Aberrant splicing of HTT generates the pathogenic exon 1 protein in Huntington disease. *Proc Natl Acad Sci U S A,* 110**,** 2366-2370.

Sato, Y., Mariot, P., Detimary, P., Gilon, P., Henquin, J. C. 1998. Okadaic acid-induced decrease in the magnitude and efficacy of the Ca2+ signal in pancreatic beta cells and inhibition of insulin secretion. *Br J Pharmacol,* 123**,** 97-105.

Satyal, S. H., Schmidt, E., Kitagawa, K., Sondheimer, N., Lindquist, S., Kramer, J. M., Morimoto, R. I. 2000. Polyglutamine aggregates alter protein folding homeostasis in Caenorhabditis elegans. *Proc Natl Acad Sci U S A,* 97**,** 5750-5755.

Saudou, F., Finkbeiner, S., Devys, D., Greenberg, M. E. 1998. Huntingtin acts in the nucleus to induce apoptosis but death does not correlate with the formation of intranuclear inclusions. *Cell,* 95**,** 55-66.

Saudou, F., Humbert, S. 2016. The Biology of Huntingtin. *Neuron,* 89**,** 910-926.

Scappini, E., Koh, T. W., Martin, N. P., O'Bryan, J. P. 2007. Intersectin enhances huntingtin aggregation and neurodegeneration through activation of c-Jun-NH2-terminal kinase. *Hum Mol Genet,* 16**,** 1862-1871.

Scherzinger, E., Sittler, A., Schweiger, K., Heiser, V., Lurz, R., Hasenbank, R., Bates, G. P., Lehrach, H., Wanker, E. E. 1999. Self-assembly of polyglutamine-containing huntingtin fragments into amyloid-like fibrils: implications for Huntington's disease pathology. *Proc Natl Acad Sci U S A,* 96**,** 4604-4609.

Schilling, B., Gafni, J., Torcassi, C., Cong, X., Row, R. H., LaFevre-Bernt, M. A., Cusack, M. P., Ratovitski, T., Hirschhorn, R., Ross, C. A., Gibson, B. W., Ellerby, L. M. 2006. Huntingtin phosphorylation sites mapped by mass spectrometry. Modulation of cleavage and toxicity. *J Biol Chem,* 281**,** 23686-23697.

Schindelin, J., Arganda-Carreras, I., Frise, E., Kaynig, V., Longair, M., Pietzsch, T., Preibisch, S., Rueden, C., Saalfeld, S., Schmid, B., Tinevez, J. Y., White, D. J., Hartenstein, V., Eliceiri, K., Tomancak, P., Cardona, A. 2012. Fiji: an open-source platform for biological-image analysis. *Nat Methods,* 9**,** 676-682.

Schonberger, S. J., Jezdic, D., Faull, R. L., Cooper, G. J. 2013. Proteomic analysis of the human brain in Huntington's Disease indicates pathogenesis by molecular processes linked to other neurodegenerative diseases and to type-2 diabetes. *J Huntingtons Dis,* 2**,** 89-99.

Schumacher, J. M., Short, M. P., Hyman, B. T., Breakefield, X. O., Isacson, O. 1991. Intracerebral implantation of nerve growth factor-producing fibroblasts protects striatum against neurotoxic levels of excitatory amino acids. *Neuroscience,* 45**,** 561-570.

Schwab, C., Arai, T., Hasegawa, M., Yu, S., McGeer, P. L. 2008. Colocalization of transactivation-responsive DNA-binding protein 43 and huntingtin in inclusions of Huntington disease. *J Neuropathol Exp Neurol,* 67**,** 1159-1165.

Senechal, Y., Kelly, P. H., Dev, K. K. 2008. Amyloid precursor protein knockout mice show age-dependent deficits in passive avoidance learning. *Behav Brain Res,* 186**,** 126-132.

Shahmoradian, S. H., Galaz-Montoya, J. G., Schmid, M. F., Cong, Y., Ma, B., Spiess, C., Frydman, J., Ludtke, S. J., Chiu, W. 2013. TRiC's tricks inhibit huntingtin aggregation. *Elife,* 2**,** e00710.

Shattuck, J. E., Waechter, A. C., Ross, E. D. 2017. The effects of glutamine/asparagine content on aggregation and heterologous prion induction by yeast prion-like domains. *Prion,* 11**,** 249-264.

Shekhawat, S. S., Ghosh, I. 2011. Split-protein systems: beyond binary protein-protein interactions. *Curr Opin Chem Biol,* 15**,** 789-797.

Sherizen, D., Jang, J. K., Bhagat, R., Kato, N., McKim, K. S. 2005. Meiotic recombination in Drosophila females depends on chromosome continuity between genetically defined boundaries. *Genetics,* 169**,** 767-781.

Shin, J. Y., Fang, Z. H., Yu, Z. X., Wang, C. E., Li, S. H., Li, X. J. 2005. Expression of mutant huntingtin in glial cells contributes to neuronal excitotoxicity. *J Cell Biol,* 171**,** 1001-1012.

Shyu, Y. J., Suarez, C. D., Hu, C. D. 2008. Visualization of AP-1 NF-kappaB ternary complexes in living cells by using a BiFC-based FRET. *Proc Natl Acad Sci U S A,* 105**,** 151-156.

Si, X., Pu, J., Zhang, B. 2017. Structure, Distribution, and Genetic Profile of alpha-Synuclein and Their Potential Clinical Application in Parkinson's Disease. *J Mov Disord,* 10**,** 69-79.

Sideri, T. C., Koloteva-Levine, N., Tuite, M. F., Grant, C. M. 2011. Methionine oxidation of Sup35 protein induces formation of the [PSI+] prion in a yeast peroxiredoxin mutant. *J Biol Chem,* 286**,** 38924-38931.

Sikora, J., Towpik, J., Graczyk, D., Kistowski, M., Rubel, T., Poznanski, J., Langridge, J., Hughes, C., Dadlez, M., Boguta, M. 2009. Yeast prion [PSI+] lowers the levels of mitochondrial prohibitins. *Biochim Biophys Acta,* 1793**,** 1703-1709.

Singaraja, R. R., Hadano, S., Metzler, M., Givan, S., Wellington, C. L., Warby, S., Yanai, A., Gutekunst, C. A., Leavitt, B. R., Yi, H., Fichter, K., Gan, L., McCutcheon, K., Chopra, V.,

Michel, J., Hersch, S. M., Ikeda, J. E., Hayden, M. R. 2002. HIP14, a novel ankyrin domain-containing protein, links huntingtin to intracellular trafficking and endocytosis. *Hum Mol Genet,* 11**,** 2815-2828.

Siskova, Z., Mahad, D. J., Pudney, C., Campbell, G., Cadogan, M., Asuni, A., O'Connor, V., Perry, V. H. 2010. Morphological and functional abnormalities in mitochondria associated with synaptic degeneration in prion disease. *Am J Pathol,* 177**,** 1411-1421.

Sittler, A., Walter, S., Wedemeyer, N., Hasenbank, R., Scherzinger, E., Eickhoff, H., Bates, G. P., Lehrach, H., Wanker, E. E. 1998. SH3GL3 associates with the Huntingtin exon 1 protein and promotes the formation of polygln-containing protein aggregates. *Mol Cell,* 2**,** 427-436.

Sivanandam, V. N., Jayaraman, M., Hoop, C. L., Kodali, R., Wetzel, R., van der Wel, P. C. 2011. The aggregation-enhancing huntingtin N-terminus is helical in amyloid fibrils. *J Am Chem Soc,* 133**,** 4558-4566.

Slow, E. J., Graham, R. K., Osmand, A. P., Devon, R. S., Lu, G., Deng, Y., Pearson, J., Vaid, K., Bissada, N., Wetzel, R., Leavitt, B. R., Hayden, M. R. 2005. Absence of behavioral abnormalities and neurodegeneration in vivo despite widespread neuronal huntingtin inclusions. *Proc Natl Acad Sci U S A,* 102**,** 11402-11407.

Solomon, J. P., Page, L. J., Balch, W. E., Kelly, J. W. 2012. Gelsolin amyloidosis: genetics, biochemistry, pathology and possible strategies for therapeutic intervention. *Crit Rev Biochem Mol Biol,* 47**,** 282-296.

Sondheimer, N., Lindquist, S. 2000. Rnq1: an epigenetic modifier of protein function in yeast. *Mol Cell,* 5**,** 163-172.

Sorensen, S. A., Fenger, K. 1992. Causes of death in patients with Huntington's disease and in unaffected first degree relatives. *J Med Genet,* 29**,** 911-914.

Sousa Silva, M., Gomes, R. A., Ferreira, A. E., Ponces Freire, A., Cordeiro, C. 2013. The glyoxalase pathway: the first hundred years... and beyond. *Biochem J,* 453**,** 1-15.

Southwell, A. L., Khoshnan, A., Dunn, D. E., Bugg, C. W., Lo, D. C., Patterson, P. H. 2008. Intrabodies binding the proline-rich domains of mutant huntingtin increase its turnover and reduce neurotoxicity. *J Neurosci,* 28**,** 9013-9020.

Stamatakos, M., Paraskeva, P., Stefanaki, C., Katsaronis, P., Lazaris, A., Safioleas, K., Kontzoglou, K. 2011. Medullary thyroid carcinoma: The third most common thyroid cancer reviewed. *Oncol Lett,* 2**,** 49-53.

Steffan, J. S., Agrawal, N., Pallos, J., Rockabrand, E., Trotman, L. C., Slepko, N., Illes, K., Lukacsovich, T., Zhu, Y. Z., Cattaneo, E., Pandolfi, P. P., Thompson, L. M., Marsh, J. L. 2004. SUMO modification of Huntingtin and Huntington's disease pathology. *Science,* 304**,** 100-104.

Steffan, J. S., Bodai, L., Pallos, J., Poelman, M., McCampbell, A., Apostol, B. L., Kazantsev, A., Schmidt, E., Zhu, Y. Z., Greenwald, M., Kurokawa, R., Housman, D. E., Jackson, G. R., Marsh, J. L., Thompson, L. M. 2001. Histone deacetylase inhibitors arrest polyglutamine-dependent neurodegeneration in Drosophila. *Nature,* 413**,** 739-743.

Steffan, J. S., Kazantsev, A., Spasic-Boskovic, O., Greenwald, M., Zhu, Y. Z., Gohler, H., Wanker, E. E., Bates, G. P., Housman, D. E., Thompson, L. M. 2000. The Huntington's disease protein interacts with p53 and CREB-binding protein and represses transcription. *Proc Natl Acad Sci U S A,* 97**,** 6763-6768.

Stein, K. C., True, H. L. 2011. The [RNQ+] prion: a model of both functional and pathological amyloid. *Prion,* 5**,** 291-298.

Steiner, I., Hajkova, P. 2006. Patterns of isolated atrial amyloid: a study of 100 hearts on autopsy. *Cardiovasc Pathol,* 15**,** 287-290.

Steinert, J. R., Campesan, S., Richards, P., Kyriacou, C. P., Forsythe, I. D., Giorgini, F. 2012. Rab11 rescues synaptic dysfunction and behavioural deficits in a Drosophila model of Huntington's disease. *Hum Mol Genet,* 21**,** 2912-2922.

Stewart, K. L., Radford, S. E. 2017. Amyloid plaques beyond Abeta: a survey of the diverse modulators of amyloid aggregation. *Biophys Rev,* 9**,** 405-419.

Stopschinski, B. E., Diamond, M. I. 2017. The prion model for progression and diversity of neurodegenerative diseases. *Lancet Neurol,* 16**,** 323-332.

Stout, J. C., Paulsen, J. S., Queller, S., Solomon, A. C., Whitlock, K. B., Campbell, J. C., Carlozzi, N., Duff, K., Beglinger, L. J., Langbehn, D. R., Johnson, S. A., Biglan, K. M., Aylward, E. H. 2011. Neurocognitive signs in prodromal Huntington disease. *Neuropsychology,* 25**,** 1-14.

Strehlow, A. N., Li, J. Z., Myers, R. M. 2007. Wild-type huntingtin participates in protein trafficking between the Golgi and the extracellular space. *Hum Mol Genet,* 16**,** 391-409.

Subramaniam, S., Sixt, K. M., Barrow, R., Snyder, S. H. 2009. Rhes, a striatal specific protein, mediates mutant-huntingtin cytotoxicity. *Science,* 324**,** 1327-1330.

Sun, L., Liu, S. Y., Zhou, X. W., Wang, X. C., Liu, R., Wang, Q., Wang, J. Z. 2003. Inhibition of protein phosphatase 2A- and protein phosphatase 1-induced tau hyperphosphorylation and impairment of spatial memory retention in rats. *Neuroscience,* 118**,** 1175-1182.

Sun, Y., Savanenin, A., Reddy, P. H., Liu, Y. F. 2001. Polyglutamine-expanded huntingtin promotes sensitization of N-methyl-D-aspartate receptors via post-synaptic density 95. *J Biol Chem,* 276**,** 24713-24718.

Svenningsson, P., Nishi, A., Fisone, G., Girault, J. A., Nairn, A. C., Greengard, P. 2004. DARPP-32: an integrator of neurotransmission. *Annu Rev Pharmacol Toxicol,* 44**,** 269-296.

Sweeney, P., Park, H., Baumann, M., Dunlop, J., Frydman, J., Kopito, R., McCampbell, A., Leblanc, G., Venkateswaran, A., Nurmi, A., Hodgson, R. 2017. Protein misfolding in neurodegenerative diseases: implications and strategies. *Transl Neurodegener,* 6**,** 6.

Szatmari, E., Habas, A., Yang, P., Zheng, J. J., Hagg, T., Hetman, M. 2005. A positive feedback loop between glycogen synthase kinase 3beta and protein phosphatase 1 after stimulation of NR2B NMDA receptors in forebrain neurons. *J Biol Chem,* 280**,** 37526-37535.

Tagawa, K., Marubuchi, S., Qi, M. L., Enokido, Y., Tamura, T., Inagaki, R., Murata, M., Kanazawa, I., Wanker, E. E., Okazawa, H. 2007. The induction levels of heat shock protein 70 differentiate the vulnerabilities to mutant huntingtin among neuronal subtypes. *J Neurosci,* 27**,** 868-880.

Takano, H., Gusella, J. F. 2002. The predominantly HEAT-like motif structure of huntingtin and its association and coincident nuclear entry with dorsal, an NF-kB/Rel/dorsal family transcription factor. *BMC Neurosci,* 3**,** 15.

Takeda, A., Hashimoto, M., Mallory, M., Sundsumo, M., Hansen, L., Masliah, E. 2000. C-terminal alpha-synuclein immunoreactivity in structures other than Lewy bodies in neurodegenerative disorders. *Acta Neuropathol,* 99**,** 296-304.

Tam, S., Geller, R., Spiess, C., Frydman, J. 2006. The chaperonin TRiC controls polyglutamine aggregation and toxicity through subunit-specific interactions. *Nat Cell Biol,* 8**,** 1155-1162.

Tam, S., Spiess, C., Auyeung, W., Joachimiak, L., Chen, B., Poirier, M. A., Frydman, J. 2009. The chaperonin TRiC blocks a huntingtin sequence element that promotes the conformational switch to aggregation. *Nat Struct Mol Biol,* 16**,** 1279-1285.

Tan, J. M., Wong, E. S., Lim, K. L. 2009. Protein misfolding and aggregation in Parkinson's disease. *Antioxid Redox Signal,* 11**,** 2119-2134.

Tanaka, M., Chien, P., Naber, N., Cooke, R., Weissman, J. S. 2004a. Conformational variations in an infectious protein determine prion strain differences. *Nature,* 428**,** 323-328.

Tanaka, M., Kim, Y. M., Lee, G., Junn, E., Iwatsubo, T., Mouradian, M. M. 2004b. Aggresomes formed by alpha-synuclein and synphilin-1 are cytoprotective. *J Biol Chem,* 279**,** 4625-4631.

Tang, T. S., Tu, H., Chan, E. Y., Maximov, A., Wang, Z., Wellington, C. L., Hayden, M. R., Bezprozvanny, I. 2003. Huntingtin and huntingtin-associated protein 1 influence neuronal calcium signaling mediated by inositol-(1,4,5) triphosphate receptor type 1. *Neuron,* 39**,** 227-239.

Tappan, E., Chamberlin, A. R. 2008. Activation of protein phosphatase 1 by a small molecule designed to bind to the enzyme's regulatory site. *Chem Biol,* 15**,** 167-174.

Tauffenberger, A., Chitramuthu, B. P., Bateman, A., Bennett, H. P., Parker, J. A. 2013. Reduction of polyglutamine toxicity by TDP-43, FUS and progranulin in Huntington's disease models. *Hum Mol Genet,* 22**,** 782-794.

Taylor, C. T., Furuta, G. T., Synnestvedt, K., Colgan, S. P. 2000. Phosphorylation-dependent targeting of cAMP response element binding protein to the ubiquitin/proteasome pathway in hypoxia. *Proc Natl Acad Sci U S A,* 97**,** 12091-12096.

Taylor, J. P., Hardy, J., Fischbeck, K. H. 2002. Toxic proteins in neurodegenerative disease. *Science,* 296**,** 1991-1995.

Taylor, J. P., Tanaka, F., Robitschek, J., Sandoval, C. M., Taye, A., Markovic-Plese, S., Fischbeck, K. H. 2003. Aggresomes protect cells by enhancing the degradation of toxic polyglutamine-containing protein. *Hum Mol Genet,* 12**,** 749-757.

Telling, G. C., Scott, M., Mastrianni, J., Gabizon, R., Torchia, M., Cohen, F. E., DeArmond, S. J., Prusiner, S. B. 1995. Prion propagation in mice expressing human and chimeric PrP transgenes implicates the interaction of cellular PrP with another protein. *Cell,* 83**,** 79-90.

Tenreiro, S., Eckermann, K., Outeiro, T. F. 2014. Protein phosphorylation in neurodegeneration: friend or foe? *Front Mol Neurosci,* 7**,** 42.

Teoh, C. L., Griffin, M. D., Howlett, G. J. 2011. Apolipoproteins and amyloid fibril formation in atherosclerosis. *Protein Cell,* 2**,** 116-127.

Thakur, A. K., Jayaraman, M., Mishra, R., Thakur, M., Chellgren, V. M., Byeon, I. J., Anjum, D. H., Kodali, R., Creamer, T. P., Conway, J. F., Gronenborn, A. M., Wetzel, R. 2009. Polyglutamine disruption of the huntingtin exon 1 N terminus triggers a complex aggregation mechanism. *Nat Struct Mol Biol,* 16**,** 380-389.

The Huntington's Disease Collaborative Research Group 1993. A novel gene containing a trinucleotide repeat that is expanded and unstable on Huntington's disease chromosomes. *Cell,* 72**,** 971-983.

Thompson, L. M., Aiken, C. T., Kaltenbach, L. S., Agrawal, N., Illes, K., Khoshnan, A., Martinez-Vincente, M., Arrasate, M., O'Rourke, J. G., Khashwji, H., Lukacsovich, T., Zhu, Y. Z., Lau, A. L., Massey, A., Hayden, M. R., Zeitlin, S. O., Finkbeiner, S., Green, K. N., LaFerla, F. M., Bates, G., Huang, L., Patterson, P. H., Lo, D. C., Cuervo, A. M., Marsh, J. L., Steffan, J. S. 2009. IKK phosphorylates Huntingtin and targets it for degradation by the proteasome and lysosome. *J Cell Biol,* 187**,** 1083-1099.

Tian, R., Gregor, M., Wiche, G., Goldman, J. E. 2006. Plectin regulates the organization of glial fibrillary acidic protein in Alexander disease. *Am J Pathol,* 168**,** 888-897.

Tomas-Zapico, C., Diez-Zaera, M., Ferrer, I., Gomez-Ramos, P., Moran, M. A., Miras-Portugal, M. T., Diaz-Hernandez, M., Lucas, J. J. 2012. alpha-Synuclein accumulates in huntingtin inclusions but forms independent filaments and its deficiency attenuates early phenotype in a mouse model of Huntington's disease. *Hum Mol Genet,* 21**,** 495-510.

Tomita, T. 2012. Islet amyloid polypeptide in pancreatic islets from type 2 diabetic subjects. *Islets,* 4**,** 223-232.

Tonoki, A., Kuranaga, E., Ito, N., Nekooki-Machida, Y., Tanaka, M., Miura, M. 2011. Aging causes distinct characteristics of polyglutamine amyloids in vivo. *Genes Cells,* 16**,** 557-564.

Toombs, J. A., McCarty, B. R., Ross, E. D. 2010. Compositional determinants of prion formation in yeast. *Mol Cell Biol,* 30**,** 319-332.

Torroja, L., Packard, M., Gorczyca, M., White, K., Budnik, V. 1999. The Drosophila beta-amyloid precursor protein homolog promotes synapse differentiation at the neuromuscular junction. *J Neurosci,* 19**,** 7793-7803.

Trevino, R. S., Lauckner, J. E., Sourigues, Y., Pearce, M. M., Bousset, L., Melki, R., Kopito, R. R. 2012. Fibrillar structure and charge determine the interaction of polyglutamine protein aggregates with the cell surface. *J Biol Chem,* 287**,** 29722-29728.

True, H. L., Berlin, I., Lindquist, S. L. 2004. Epigenetic regulation of translation reveals hidden genetic variation to produce complex traits. *Nature,* 431**,** 184-187.

True, H. L., Lindquist, S. L. 2000. A yeast prion provides a mechanism for genetic variation and phenotypic diversity. *Nature,* 407**,** 477-483.

Tsigelny, I. F., Crews, L., Desplats, P., Shaked, G. M., Sharikov, Y., Mizuno, H., Spencer, B., Rockenstein, E., Trejo, M., Platoshyn, O., Yuan, J. X., Masliah, E. 2008. Mechanisms of hybrid oligomer formation in the pathogenesis of combined Alzheimer's and Parkinson's diseases. *PLoS One,* 3**,** e3135.

Tsvetkov, A. S., Arrasate, M., Barmada, S., Ando, D. M., Sharma, P., Shaby, B. A., Finkbeiner, S. 2013. Proteostasis of polyglutamine varies among neurons and predicts neurodegeneration. *Nat Chem Biol,* 9**,** 586-592.

Tuite, M. F., Mundy, C. R., Cox, B. S. 1981. Agents that cause a high frequency of genetic change from [psi+] to [psi-] in Saccharomyces cerevisiae. *Genetics,* 98**,** 691-711.

Tyebji, S., Hannan, A. J. 2017. Synaptopathic mechanisms of neurodegeneration and dementia: Insights from Huntington's disease. *Prog Neurobiol,* 153**,** 18-45.

Tyedmers, J., Mogk, A., Bukau, B. 2010a. Cellular strategies for controlling protein aggregation. *Nat Rev Mol Cell Biol,* 11**,** 777-788.

Tyedmers, J., Treusch, S., Dong, J., McCaffery, J. M., Bevis, B., Lindquist, S. 2010b. Prion induction involves an ancient system for the sequestration of aggregated proteins and heritable changes in prion fragmentation. *Proc Natl Acad Sci U S A,* 107**,** 8633-8638.

Urrea, L., Segura-Feliu, M., Masuda-Suzukake, M., Hervera, A., Pedraz, L., Garcia Aznar, J. M., Vila, M., Samitier, J., Torrents, E., Ferrer, I., Gavin, R., Hagesawa, M., Del Rio, J. A. 2017. Involvement of Cellular Prion Protein in alpha-Synuclein Transport in Neurons. *Mol Neurobiol*, in press.

van der Burg, J. M., Bjorkqvist, M., Brundin, P. 2009. Beyond the brain: widespread pathology in Huntington's disease. *Lancet Neurol,* 8**,** 765-774.

van der Burg, J. M., Winqvist, A., Aziz, N. A., Maat-Schieman, M. L., Roos, R. A., Bates, G. P., Brundin, P., Bjorkqvist, M., Wierup, N. 2011. Gastrointestinal dysfunction contributes to weight loss in Huntington's disease mice. *Neurobiol Dis,* 44**,** 1-8.

van Rooijen, B. D., Claessens, M. M., Subramaniam, V. 2009. Lipid bilayer disruption by oligomeric alpha-synuclein depends on bilayer charge and accessibility of the hydrophobic core. *Biochim Biophys Acta,* 1788**,** 1271-1278.

van Roon-Mom, W. M., Reid, S. J., Jones, A. L., MacDonald, M. E., Faull, R. L., Snell, R. G. 2002. Insoluble TATA-binding protein accumulation in Huntington's disease cortex. *Brain Res Mol Brain Res,* 109**,** 1-10.

Vasconcelos, B., Stancu, I. C., Buist, A., Bird, M., Wang, P., Vanoosthuyse, A., Van Kolen, K., Verheyen, A., Kienlen-Campard, P., Octave, J. N., Baatsen, P., Moechars, D., Dewachter,

I. 2016. Heterotypic seeding of Tau fibrillization by pre-aggregated Abeta provides potent seeds for prion-like seeding and propagation of Tau-pathology in vivo. *Acta Neuropathol,* 131**,** 549-569.

Veldman, M. B., Rios-Galdamez, Y., Lu, X. H., Gu, X., Qin, W., Li, S., Yang, X. W., Lin, S. 2015. The N17 domain mitigates nuclear toxicity in a novel zebrafish Huntington's disease model. *Mol Neurodegener,* 10**,** 67.

Venken, K. J., Simpson, J. H., Bellen, H. J. 2011. Genetic manipulation of genes and cells in the nervous system of the fruit fly. *Neuron,* 72**,** 202-230.

Verma, U. N., Yamamoto, Y., Prajapati, S., Gaynor, R. B. 2004. Nuclear role of I kappa B Kinase-gamma/NF-kappa B essential modulator (IKK gamma/NEMO) in NF-kappa B-dependent gene expression. *J Biol Chem,* 279**,** 3509-3515.

Vicente Miranda, H., El-Agnaf, O. M., Outeiro, T. F. 2016a. Glycation in Parkinson's disease and Alzheimer's disease. *Mov Disord,* 31**,** 782-790.

Vicente Miranda, H., Gomes, M. A., Branco-Santos, J., Breda, C., Lazaro, D. F., Lopes, L. V., Herrera, F., Giorgini, F., Outeiro, T. F. 2016b. Glycation potentiates neurodegeneration in models of Huntington's disease. *Sci Rep,* 6**,** 36798.

Vicente Miranda, H., Outeiro, T. F. 2010. The sour side of neurodegenerative disorders: the effects of protein glycation. *J Pathol,* 221**,** 13-25.

Vicente Miranda, H., Szego, E. M., Oliveira, L. M. A., Breda, C., Darendelioglu, E., de Oliveira, R. M., Ferreira, D. G., Gomes, M. A., Rott, R., Oliveira, M., Munari, F., Enguita, F. J., Simoes, T., Rodrigues, E. F., Heinrich, M., Martins, I. C., Zamolo, I., Riess, O., Cordeiro, C., Ponces-Freire, A., Lashuel, H. A., Santos, N. C., Lopes, L. V., Xiang, W., Jovin, T. M., Penque, D., Engelender, S., Zweckstetter, M., Klucken, J., Giorgini, F., Quintas, A., Outeiro, T. F. 2017. Glycation potentiates alpha-synuclein-associated neurodegeneration in synucleinopathies. *Brain,* 140**,** 1399-1419.

Vicente Miranda, H., Xiang, W., de Oliveira, R. M., Simoes, T., Pimentel, J., Klucken, J., Penque, D., Outeiro, T. F. 2013. Heat-mediated enrichment of alpha-synuclein from cells and tissue for assessing post-translational modifications. *J Neurochem,* 126**,** 673-684.

Victoria, G. S., Zurzolo, C. 2017. The spread of prion-like proteins by lysosomes and tunneling nanotubes: Implications for neurodegenerative diseases. *J Cell Biol,* 216**,** 2633-2644.

Virshup, D. M., Shenolikar, S. 2009. From promiscuity to precision: protein phosphatases get a makeover. *Mol Cell,* 33**,** 537-545.

Vital, A., Canron, M. H., Gil, R., Hauw, J. J., Vital, C. 2007. A sporadic case of Creutzfeldt-Jakob disease with beta-amyloid deposits and alpha-synuclein inclusions. *Neuropathology,* 27**,** 273-277.

Vuono, R., Winder-Rhodes, S., de Silva, R., Cisbani, G., Drouin-Ouellet, J., Network, R. I. o. t. E. H. s. D., Spillantini, M. G., Cicchetti, F., Barker, R. A. 2015. The role of tau in the pathological process and clinical expression of Huntington's disease. *Brain,* 138**,** 1907-1918.

Wacker, J. L., Zareie, M. H., Fong, H., Sarikaya, M., Muchowski, P. J. 2004. Hsp70 and Hsp40 attenuate formation of spherical and annular polyglutamine oligomers by partitioning monomer. *Nat Struct Mol Biol,* 11**,** 1215-1222.

Wang, J. W., Sylwester, A. W., Reed, D., Wu, D. A., Soll, D. R., Wu, C. F. 1997. Morphometric description of the wandering behavior in Drosophila larvae: aberrant locomotion in Na+ and K+ channel mutants revealed by computer-assisted motion analysis. *J Neurogenet,* 11**,** 231-254.

Wang, Y., Cui, J., Sun, X., Zhang, Y. 2011. Tunneling-nanotube development in astrocytes depends on p53 activation. *Cell Death Differ,* 18**,** 732-742.

Wanker, E. E., Rovira, C., Scherzinger, E., Hasenbank, R., Walter, S., Tait, D., Colicelli, J., Lehrach, H. 1997. HIP-I: a huntingtin interacting protein isolated by the yeast two-hybrid system. *Hum Mol Genet,* 6**,** 487-495.

Warby, S. C., Chan, E. Y., Metzler, M., Gan, L., Singaraja, R. R., Crocker, S. F., Robertson, H. A., Hayden, M. R. 2005. Huntingtin phosphorylation on serine 421 is significantly reduced in the striatum and by polyglutamine expansion in vivo. *Hum Mol Genet,* 14**,** 1569-1577.

Waxman, E. A., Giasson, B. I. 2011. Induction of intracellular tau aggregation is promoted by alpha-synuclein seeds and provides novel insights into the hyperphosphorylation of tau. *J Neurosci,* 31**,** 7604-7618.

Wellington, C. L., Ellerby, L. M., Gutekunst, C. A., Rogers, D., Warby, S., Graham, R. K., Loubser, O., van Raamsdonk, J., Singaraja, R., Yang, Y. Z., Gafni, J., Bredesen, D., Hersch, S. M., Leavitt, B. R., Roy, S., Nicholson, D. W., Hayden, M. R. 2002. Caspase cleavage of mutant huntingtin precedes neurodegeneration in Huntington's disease. *J Neurosci,* 22**,** 7862-7872.

Wetzel, R. 2006. Nucleation of huntingtin aggregation in cells. *Nat Chem Biol,* 2**,** 297-298.

Weyand, C. M. 2007. Immunopathologic aspects of rheumatoid arthritis: who is the conductor and who plays the immunologic instrument? *J Rheumatol Suppl,* 79**,** 9-14.

White, J. K., Auerbach, W., Duyao, M. P., Vonsattel, J. P., Gusella, J. F., Joyner, A. L., MacDonald, M. E. 1997. Huntingtin is required for neurogenesis and is not impaired by the Huntington's disease CAG expansion. *Nat Genet,* 17**,** 404-410.

Wickner, R. B., Dyda, F., Tycko, R. 2008. Amyloid of Rnq1p, the basis of the [PIN+] prion, has a parallel in-register beta-sheet structure. *Proc Natl Acad Sci U S A,* 105**,** 2403-2408.

Wild, E. J., Boggio, R., Langbehn, D., Robertson, N., Haider, S., Miller, J. R., Zetterberg, H., Leavitt, B. R., Kuhn, R., Tabrizi, S. J., Macdonald, D., Weiss, A. 2015. Quantification of mutant huntingtin protein in cerebrospinal fluid from Huntington's disease patients. *J Clin Invest,* 125**,** 1979-1986.

Wild, E. J., Tabrizi, S. J. 2014. Targets for future clinical trials in Huntington's disease: what's in the pipeline? *Mov Disord,* 29**,** 1434-1445.

Williamson, T. E., Vitalis, A., Crick, S. L., Pappu, R. V. 2010. Modulation of polyglutamine conformations and dimer formation by the N-terminus of huntingtin. *J Mol Biol,* 396**,** 1295-1309.

Winner, B., Jappelli, R., Maji, S. K., Desplats, P. A., Boyer, L., Aigner, S., Hetzer, C., Loher, T., Vilar, M., Campioni, S., Tzitzilonis, C., Soragni, A., Jessberger, S., Mira, H., Consiglio, A., Pham, E., Masliah, E., Gage, F. H., Riek, R. 2011. In vivo demonstration that alpha-synuclein oligomers are toxic. *Proc Natl Acad Sci U S A,* 108**,** 4194-4199.

Wiseman, F. K., Al-Janabi, T., Hardy, J., Karmiloff-Smith, A., Nizetic, D., Tybulewicz, V. L., Fisher, E. M., Strydom, A. 2015. A genetic cause of Alzheimer disease: mechanistic insights from Down syndrome. *Nat Rev Neurosci,* 16**,** 564-574.

Wong, B. K., Ehrnhoefer, D. E., Graham, R. K., Martin, D. D., Ladha, S., Uribe, V., Stanek, L. M., Franciosi, S., Qiu, X., Deng, Y., Kovalik, V., Zhang, W., Pouladi, M. A., Shihabuddin, L. S., Hayden, M. R. 2015a. Partial rescue of some features of Huntington Disease in the genetic absence of caspase-6 in YAC128 mice. *Neurobiol Dis,* 76**,** 24-36.

Wong, P. M., Feng, Y., Wang, J., Shi, R., Jiang, X. 2015b. Regulation of autophagy by coordinated action of mTORC1 and protein phosphatase 2A. *Nat Commun,* 6**,** 8048.

Wong, Y. C., Holzbaur, E. L. 2014. The regulation of autophagosome dynamics by huntingtin and HAP1 is disrupted by expression of mutant huntingtin, leading to defective cargo degradation. *J Neurosci,* 34**,** 1293-1305.

Wu, J. S., Luo, L. 2006. A protocol for dissecting Drosophila melanogaster brains for live imaging or immunostaining. *Nat Protoc,* 1**,** 2110-2115.

Xia, J., Lee, D. H., Taylor, J., Vandelft, M., Truant, R. 2003. Huntingtin contains a highly conserved nuclear export signal. *Hum Mol Genet,* 12**,** 1393-1403.

Yamamoto, A., Cremona, M. L., Rothman, J. E. 2006. Autophagy-mediated clearance of huntingtin aggregates triggered by the insulin-signaling pathway. *J Cell Biol,* 172**,** 719-731.

Yamanaka, T., Miyazaki, H., Oyama, F., Kurosawa, M., Washizu, C., Doi, H., Nukina, N. 2008. Mutant Huntingtin reduces HSP70 expression through the sequestration of NF-Y transcription factor. *EMBO J,* 27**,** 827-839.

Yan, Y., Peng, D., Tian, J., Chi, J., Tan, J., Yin, X., Pu, J., Xia, K., Zhang, B. 2011. Essential sequence of the N-terminal cytoplasmic localization-related domain of huntingtin and its effect on huntingtin aggregates. *Sci China Life Sci,* 54**,** 342-350.

Yanai, A., Huang, K., Kang, R., Singaraja, R. R., Arstikaitis, P., Gan, L., Orban, P. C., Mullard, A., Cowan, C. M., Raymond, L. A., Drisdel, R. C., Green, W. N., Ravikumar, B., Rubinsztein, D. C., El-Husseini, A., Hayden, M. R. 2006. Palmitoylation of huntingtin by HIP14 is essential for its trafficking and function. *Nat Neurosci,* 9**,** 824-831.

Yang, H., Hu, H. Y. 2016. Sequestration of cellular interacting partners by protein aggregates: implication in a loss-of-function pathology. *FEBS J,* 283**,** 3705-3717.

Yin, H., Kuret, J. 2006. C-terminal truncation modulates both nucleation and extension phases of tau fibrillization. *FEBS Lett,* 580**,** 211-215.

Yu, A., Shibata, Y., Shah, B., Calamini, B., Lo, D. C., Morimoto, R. I. 2014. Protein aggregation can inhibit clathrin-mediated endocytosis by chaperone competition. *Proc Natl Acad Sci U S A,* 111**,** E1481-1490.

Zainelli, G. M., Ross, C. A., Troncoso, J. C., Fitzgerald, J. K., Muma, N. A. 2004. Calmodulin regulates transglutaminase 2 cross-linking of huntingtin. *J Neurosci,* 24**,** 1954-1961.

Zeitlin, S., Liu, J. P., Chapman, D. L., Papaioannou, V. E., Efstratiadis, A. 1995. Increased apoptosis and early embryonic lethality in mice nullizygous for the Huntington's disease gene homologue. *Nat Genet,* 11**,** 155-163.

Zhang, J., Dong, X. P. 2012. Dysfunction of microtubule-associated proteins of MAP2/tau family in Prion disease. *Prion,* 6**,** 334-338.

Zhang, S., Feany, M. B., Saraswati, S., Littleton, J. T., Perrimon, N. 2009. Inactivation of Drosophila Huntingtin affects long-term adult functioning and the pathogenesis of a Huntington's disease model. *Dis Model Mech,* 2**,** 247-266.

Zhang, Y., Leavitt, B. R., van Raamsdonk, J. M., Dragatsis, I., Goldowitz, D., MacDonald, M. E., Hayden, M. R., Friedlander, R. M. 2006. Huntingtin inhibits caspase-3 activation. *EMBO J,* 25**,** 5896-5906.

Zheng, Z., Li, A., Holmes, B. B., Marasa, J. C., Diamond, M. I. 2013. An N-terminal nuclear export signal regulates trafficking and aggregation of Huntingtin (Htt) protein exon 1. *J Biol Chem,* 288**,** 6063-6071.

Zhong, S. C., Luo, X., Chen, X. S., Cai, Q. Y., Liu, J., Chen, X. H., Yao, Z. X. 2010. Expression and subcellular location of alpha-synuclein during mouse-embryonic development. *Cell Mol Neurobiol,* 30**,** 469-482.

Zhou, H., Li, S. H., Li, X. J. 2001. Chaperone suppression of cellular toxicity of huntingtin is independent of polyglutamine aggregation. *J Biol Chem,* 276**,** 48417-48424.

Zhu, X., Siedlak, S. L., Smith, M. A., Perry, G., Chen, S. G. 2006. LRRK2 protein is a component of Lewy bodies. *Ann Neurol,* 60**,** 617-618; author reply 618-619.

Zhuchenko, O., Bailey, J., Bonnen, P., Ashizawa, T., Stockton, D. W., Amos, C., Dobyns, W. B., Subramony, S. H., Zoghbi, H. Y., Lee, C. C. 1997. Autosomal dominant cerebellar ataxia

(SCA6) associated with small polyglutamine expansions in the alpha 1A-voltage-dependent calcium channel. *Nat Genet,* 15**,** 62-69.

Zondler, L., Miller-Fleming, L., Repici, M., Goncalves, S., Tenreiro, S., Rosado-Ramos, R., Betzer, C., Straatman, K. R., Jensen, P. H., Giorgini, F., Outeiro, T. F. 2014. DJ-1 interactions with alpha-synuclein attenuate aggregation and cellular toxicity in models of Parkinson's disease. *Cell Death Dis,* 5**,** e1350.

Zuccato, C., Ciammola, A., Rigamonti, D., Leavitt, B. R., Goffredo, D., Conti, L., MacDonald, M. E., Friedlander, R. M., Silani, V., Hayden, M. R., Timmusk, T., Sipione, S., Cattaneo, E. 2001. Loss of huntingtin-mediated BDNF gene transcription in Huntington's disease. *Science,* 293**,** 493-498.

Zuccato, C., Tartari, M., Crotti, A., Goffredo, D., Valenza, M., Conti, L., Cataudella, T., Leavitt, B. R., Hayden, M. R., Timmusk, T., Rigamonti, D., Cattaneo, E. 2003. Huntingtin interacts with REST/NRSF to modulate the transcription of NRSE-controlled neuronal genes. *Nat Genet,* 35**,** 76-83.

Zuccato, C., Valenza, M., Cattaneo, E. 2010. Molecular mechanisms and potential therapeutical targets in Huntington's disease. *Physiol Rev,* 90**,** 905-981.

Zucchelli, S., Marcuzzi, F., Codrich, M., Agostoni, E., Vilotti, S., Biagioli, M., Pinto, M., Carnemolla, A., Santoro, C., Gustincich, S., Persichetti, F. 2011. Tumor necrosis factor receptor-associated factor 6 (TRAF6) associates with huntingtin protein and promotes its atypical ubiquitination to enhance aggregate formation. *J Biol Chem,* 286**,** 25108-25117.

Zuchner, T., Brundin, P. 2008. Mutant huntingtin can paradoxically protect neurons from death. *Cell Death Differ,* 15**,** 435-442.

Zwilling, D., Huang, S. Y., Sathyasaikumar, K. V., Notarangelo, F. M., Guidetti, P., Wu, H. Q., Lee, J., Truong, J., Andrews-Zwilling, Y., Hsieh, E. W., Louie, J. Y., Wu, T., Scearce-Levie, K., Patrick, C., Adame, A., Giorgini, F., Moussaoui, S., Laue, G., Rassoulpour, A., Flik, G., Huang, Y., Muchowski, J. M., Masliah, E., Schwarcz, R., Muchowski, P. J. 2011. Kynurenine 3-monooxygenase inhibition in blood ameliorates neurodegeneration. *Cell,* 145**,** 863-874.

VII.

Facsimile of Published Articles

OXFORD

Human Molecular Genetics, 2017, Vol. 26, No. 19 3763–3775

doi: 10.1093/hmg/ddx260
Advance Access Publication Date: 7 July 2017
Original Article

ORIGINAL ARTICLE

Protein phosphatase 1 regulates huntingtin exon 1 aggregation and toxicity

Joana Branco-Santos[1,2,3,§], Federico Herrera[1,*,§], Gonçalo M. Poças[2,†], Yolanda Pires-Afonso[2,‡], Flaviano Giorgini[3], Pedro M. Domingos[2,*] and Tiago F. Outeiro[4,5,*]

[1]Laboratory of Cell Structure and Dynamics, Instituto de Tecnologia Química e Biológica, Oeiras, Portugal, [2]Laboratory of Cell Signaling in Drosophila, Instituto de Tecnologia Química e Biológica, Oeiras, Portugal, [3]Department of Genetics & Genome Biology, University of Leicester, Leicester, UK, [4]Department of Experimental Neurodegeneration, Center for Nanoscale Microscopy and Molecular Physiology of the Brain, Center for Biostructural Imaging of Neurodegeneration, University Medical Center Gottingen, Göttingen, Germany and [5]Max Planck Institute for Experimental Medicine, Göttingen, Germany

* To whom correspondence should be addressed at: Laboratory of Cell Structure and Dynamics, ITQB-NOVA, Av. Da República, Estação Agronómica Nacional, 2780-157 Oeiras, Portugal. Tel: +351 214469300; Email: fherrera@itqb.unl.pt (F.H.); Laboratory of Cell Signalling in *Drosophila*, ITQB-NOVA, Av. Da República, Estação Agronómica Nacional, 2780-157 Oeiras, Portugal. Tel: +351 211157781; Fax: +351 214411277; Email: domingp@itqb.unl.pt (P.M.D.); Department Experimental Neurodegeneration, Waldweg 33, 37073 Göttingen, Germany. Tel: +49 5513913545; Fax: +49 5513922693; Email: touteir@gwdg.de (T.F.O.)

Abstract

Huntington's disease is neurodegenerative disorder caused by a polyglutamine expansion in the N-terminal region of the huntingtin protein (N17). Here, we analysed the relative contribution of each phosphorylatable residue in the N17 region (T3, S13 and S16) towards huntingtin exon 1 (HTTex1) oligomerization, aggregation and toxicity in human cells and *Drosophila* neurons. We used bimolecular fluorescence complementation to show that expression of single phosphomimic mutations completely abolished HTTex1 aggregation in human cells. In *Drosophila*, mimicking phosphorylation at T3 decreased HTTex1 aggregation both in larvae and adult flies. Interestingly, pharmacological or genetic inhibition of protein phosphatase 1 (PP1) prevented HTTex1 aggregation in both human cells and *Drosophila* while increasing neurotoxicity in flies. Our findings suggest that PP1 modulates HTTex1 aggregation by regulating phosphorylation on T3. In summary, our study suggests that modulation of HTTex1 single phosphorylation events by PP1 could constitute an efficient and direct molecular target for therapeutic interventions in Huntington's disease.

Introduction

Huntington's disease (HD) is characterized by the loss of medium spiny neurons in the striatum. The main histopathological hallmark of HD is the misfolding and subsequent intracellular aggregation of a mutant form of huntingtin (HTT) (1). HTT is a very large protein (~350 kDa), but expression of exon 1 is sufficient to produce HD-like features in various cellular and animal models (2–4). HTT exon 1 (HTTex1) contains a polyglutamine (polyQ) tract that, in normal conditions, is constituted by 6–35 glutamine residues. An expansion of the polyQ tract beyond 35 glutamines induces the misfolding and

[†]Present address: School of Biological Sciences, Monash University, Clayton, Victoria, Australia.
[‡]Present address: Department of Oncology, Luxembourg Institute of Health, University of Luxembourg, Esch-Belval, Luxembourg.
[§]These authors contributed equally to this work.

Received: May 18, 2017. **Revised:** June 28, 2017. **Accepted:** June 30, 2017

aggregation of mutant HTT and causes HD (5,6). Mutant HTT with longer polyQ expansions is more prone to aggregate, and leads to earlier onset of the disease (2,7,8).

The polyQ tract is preceded by an N-terminal sequence of 17 amino acids (N17 domain) that is highly conserved, suggesting that this domain plays an important role in the function of HTT (9–15). The N17 domain plays a key role in the aggregation pathway of HTT, where the protein associates first into alpha-helical oligomers and acts as a seed to concentrate and facilitate the formation of larger aggregates and fibrils (16–20). Deletion or posttranslational modifications such as phosphorylation, ubiquitination and SUMOylation in the N17 produce striking effects in the stability and aggregation of HTT, as well as in cell viability (21–34). The N17 domain has three phosphorylatable amino acid residues—threonine at position 3 (T3), and serine residues at positions 13 and 16 (S13 and S16). Constitutive phosphorylation of T3 enhances mutant HTT aggregation, but its role in HTT toxicity remains unclear (29). Previous studies have focused on double S13/S16 phosphorylation (30,31,35–38), despite the fact that double S13/S16 phosphorylation is less frequent than single T3 or S13 phosphorylation (39,40), and that overexpression of particular kinases is required in order to achieve double S13/S16 phosphorylation (30).

Single phosphorylation and phosphomimetic modifications in S13 or S16 modulates the formation of HTT fibrils and reduces the oligomerization rate in cell-free systems, just as the double S13/S16 phosphorylation does, both *in vitro* and *in vivo* (26,28,30,31). Casein kinase 2 (CK2) inhibitors reduce S13/S16 phosphorylation and enhance toxicity (37), while GM1 ganglioside induces S13/S16 phosphorylation and restores motor and molecular deficits in HD mice (36). IKK, a kinase involved in inflammatory responses, also regulates T3 and S13/S16 phosphorylation and modulates HTT aggregation (30,37,39,41). While several protein phosphatases control HTT dephosphorylation beyond exon 1 and modulate its toxicity (42–46), it is not known which protein phosphatases, if any, regulate phosphorylation of the N17 domain.

Here, we elucidate the contribution of single N17 phosphorylation events towards HTTex1 oligomerization, aggregation and toxicity. We screened a collection of protein phosphatase chemical inhibitors to identify modulators of HTTex1 oligomerization and aggregation in human cells. Inhibition of PP1 prevents HTTex1 aggregation but not oligomerization in human cells. In addition, downregulation of PP1 in *Drosophila* neurons reduces HTTex1 aggregation and increases its toxicity. In total, our findings point to a critical role of T3 phosphorylation in HTTex1 aggregation and support the targeting of PP1 for therapeutic interventions in HD.

Results

Single N17 phosphomutants modulate HTTex1 aggregation in human cells

In order to investigate the contribution of each phosphorylatable residue within the N17 region (T3, S13 and S16) towards HTTex1 aggregation, we used the bimolecular complementation assay (BiFC) system for the visualization of both oligomeric species and inclusion bodies of HTTex1 in living cells, which we have previously described (47–49). In this system, wild-type (19Q) or disease-causing (97Q) HTTex1 are fused to non-fluorescent halves of the Venus fluorescent protein (Fig. 1A). Thus, upon dimerization of HTTex1 fragments, the Venus halves are brought together and reconstitute the functional fluorophore. Therefore, fluorescence is proportional to the extent of HTTex1 dimerization/oligomerization. We introduced point mutations in each of the phosphorylatable residues within the N17, changing these amino acids to either alanine (A mutants, which cannot be phosphorylated—phosphoresistant) or to aspartic acid (D mutants, which mimic the phosphorylated state—phosphomimic). Importantly, these phosphomutants behave like phosphorylated peptides in terms of their aggregation in cell-free systems and primary neuronal cultures (26,28).

We had previously shown that 97QHTTex1-Venus BiFC pairs oligomerize and aggregate more readily than wild-type 19QHTTex1-Venus BiFC pairs (49). Strikingly, all single phosphomimic mutations of 97QHTTex1-Venus BiFC constructs (T3D, S13D, S16D) completely abolished the formation of inclusion bodies in human cells (Fig. 1B and C) while the phosphoresistant mutants (T3A, S13A, S16A) behaved similarly to non-mutated 97QHTTex1-Venus BiFC pairs (Fig. 1B and C and Supplementary Material, Fig. S1). These phenotypes were further confirmed by filter trap assays, where non-mutated 97QHTTex1 and phosphoresistant pairs appear as large SDS-insoluble aggregates, as opposed to wild-type 19QHTTex1 and phosphomimic pairs [Fig. 1D, filter trap (FT)]. No differences in oligomerization/fluorescence levels were observed between the phosphomutants, and non-mutated 97QHTTex1, as determined by flow cytometry (Supplementary Material, Fig. S2). Native-PAGE analyses confirmed that all phosphomutants formed oligomeric species (Fig. 1D). These results are consistent with a recent report where expanded HTTex1 was shown to exist as tetramers but not monomers (50).

Owing to its dynamic nature, phosphorylation usually affects only a fraction of the total pool of any given protein. Thus, we hypothesized that subpopulations or pools of 97QHTTex1 with different extents of phosphorylation may co-exist in cells. In order to determine whether 97QHTTex1 fragments with different phosphorylation status interacted in living cells, we took advantage of the unique features of our BiFC system to screen all possible pairwise combinations of phosphomutants and non-mutated 97QHTTex1 control (Table 1). Combinations of phosphomimic with non-mutated 97QHTTex1 oligomerized to the same extent as the non-mutated 97QHTTex1 pair, as determined by flow cytometry (Supplementary Material, Fig. S3). However, phosphomimic pairs did not form inclusions, independently of the mutated residue (Table 1). Combinations of phosphomimics with non-mutated 97QHTTex1 (Table 1 and Fig. 2A and B) or phosphoresistant mutants (Table 1) resulted in intermediate aggregation phenotypes, depending on which residue was mutated. Combinations including T3D, S13D or S16D resulted in 0%, 14.1–22.0% or 19.8–29.1% of cells with inclusions, respectively (Table 1), which is significantly less than the percentage of cells with inclusions observed with the non-mutated 97QHTTex1 pair (36.1%). In contrast, phosphoresistant pairs generally resulted in an increased percentage of cells displaying inclusions (43.5–48.5% cells with inclusions), with the exception of the S13A/S16A combination (35.3%) (Table 1).

Importantly, the effect of phosphomimic mutants on 97QHTTex1 aggregation appears to be protein-specific (Fig. 2). We and others have recently shown that HTTex1 co-aggregates with alpha-synuclein (α-syn) and Tau, and that these interactions change the aggregation profile of HTTex1 (47,48,51,52). Combinations of phosphomimic 97QHTTex1 with α-syn BiFC constructs resulted in a residue-dependent reduction in the percentage of cells with inclusions, with the T3D/Syn showing no inclusions (Fig. 2A and C). On the other hand, combinations of Tau-Venus plasmids showed the same aggregation pattern independently of the mutated residue (Fig. 2A and D). These

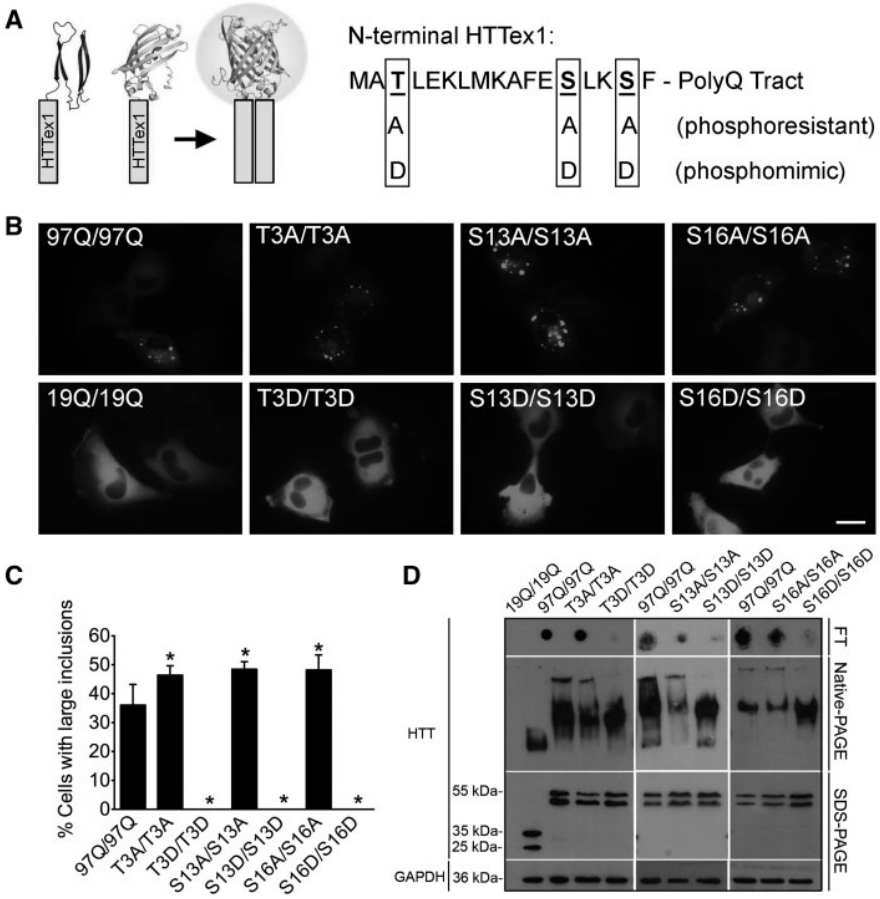

Figure 1. Single N17 phosphomimic mutations modulate 97QHTTex1 aggregation but not oligomerization in human H4 glioma cells. (**A**) HTTex1 (grey bars) was fused to two non-fluorescent halves of the Venus protein. When HTTex1 dimerizes, Venus recovers fluorescence. The three N17 phosphorylatable residues were mutated to mimic phosphorylation or dephosphorylation. (**B**) Cells transfected with phosphoresistant BiFC pairs resemble the non-mutated 97QHTTex1 phenotype in terms of aggregation, while phosphomimic pairs showed a total absence of aggregates. (**C**) Quantitative analyses of microscopy pictures. *Significant versus 97Q/97Q, $P < 0.05$. (**D**) Filter trap assays (FT) were consistent with microscopy results. Phosphomimic pairs did not produce insoluble aggregates (FT), but showed similar levels of oligomeric species (Native-PAGE) comparing to non-mutated 97QHTTex1. Expression levels of each pair were evaluated by SDS-PAGE. Scale bar, 20 μm.

observations further support that single N17 phosphomutants modulate HTTex1 aggregation, and that the T3D is the most restrictive modification in preventing HTTex1 aggregation.

Increased dynamics of 97QHTTex1 inclusions containing S13 or S16 phosphomimic mutants

We next analysed the dynamics of 97QHTTex1 inclusions using fluorescence recovery after photobleaching (FRAP). We observed a faster fluorescence recovery in inclusions formed by pairs containing phosphomimic mutants (S13D or S16D) and non-mutated 97QHTTex1 in comparison to inclusions formed exclusively by non-mutated 97QHTTex1 (Fig. 3A and B; Supplementary Material, Videos S1–S3). The phosphoresistant (T3A or S13A)/97QHTTex1 pairs, but not the S16A/97QHTTex1, presented slower fluorescence recovery in inclusions (Fig. 3C). Phosphomimic-containing inclusions often had less defined boundaries, appearing rather continuous with the cytosolic fluorescence, consistent with areas of more dynamic exchange of HTT protein. Inclusions formed by the S13D/97QHTTex1 combination (Fig. 3D and Supplementary Material, Video S4) showed a fluid-like behaviour as opposed to the more rigid behaviour of the inclusions formed by combinations containing phosphoresistant mutants (Supplementary Material, Video S5) or non-mutated 97QHTTex1 BiFC pairs (Supplementary Material, Video S6).

Overall, the results suggest that single phosphorylation events within N17 domain prevent HTTex1 aggregation but not its oligomerization, and that phosphorylation at the T3 residue might play a critical role in modulating HTTex1 aggregation. In addition, our observations support the idea that inclusions might be composed of non-phosphorylated HTT or mixtures of non-phosphorylated and phosphorylated pools of molecules, consistent with data indicating that disease-causing HTT is hypophosphorylated in the N17 region (29,37).

Protein phosphatases regulate HTTex1 aggregation in human cells

The results above indicate that single N17 phosphorylation can modulate HTTex1 aggregation, which is consistent with the idea that N17 phosphorylation might be enhanced by the activation of kinases (30,37,39) or, alternatively, by the inhibition of phosphatases. In order to identify protein phosphatases that might mediate HTTex1 dephosphorylation, we screened a library of 33 phosphatase chemical inhibitors for their effect on HTTex1 aggregation and oligomerization, using our 97QHTTex1-Venus BiFC

Table 1. Percentage of cells containing HTT inclusions (average ± SEM) when co-transfected with different combinations of HTTex1-, α-syn- or Tau-Venus BiFC plasmids

		Venus 2								
		T3D	S13D	S16D	T3A	S13A	S16A	97Q	α-syn	Tau
Venus 1	T3D	0	0	0	0	0	0	0	0	15.5±2.2
	S13D		0	0	22.0±3.4	17.1±2.3	14.5±1.2	14.1±1.3	5.6±1.7	15.7±2.2
	S16D			0	27.5±1.5	29.1±3.6	19.8±3.0	22.9±1.0	10.0±4.8	16.5±1.7
	T3A				46.4±1.3	43.5±3.6	45.9±2.5	34.5±2.2	N/D	N/D
	S13A					48.5±1.3	35.3±2.4	37.8±1.9	N/D	N/D
	S16A						48.2±2.6	36.6±6.1	N/D	N/D
	97Q							36.1±2.2	39.3±3.9	16.2±1.3

N/D, not determined.

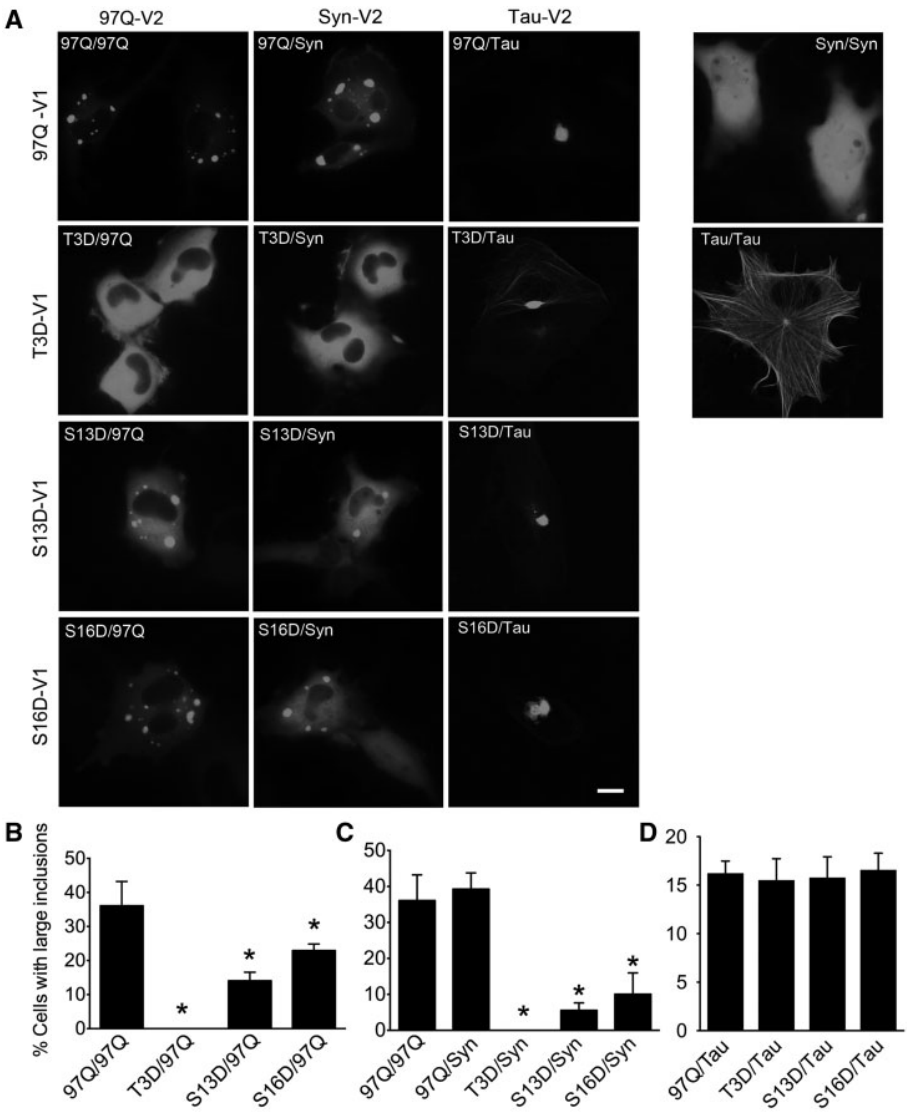

Figure 2. Effect of phosphomimic mutants on 97QHTTex1 aggregation is protein-specific. (**A**) Combinations of 97QHTTex1-Venus 1 BiFC constructs with synuclein- or tau-Venus 2 BiFC constructs revealed different co-aggregation responses to phosphomimic constructs. 97QHTTex1 (**B**) and synuclein (**C**) showed similar patterns of aggregation in the presence of single phosphomimic mutations, with T3D being the most restrictive for decreasing aggregation. (**D**) Tau co-aggregated with 97QHTTex1 regardless of the N17 mutation. *Significant versus 97Q/97Q (B) or 97Q/Syn (C), $P < 0.05$. Scale bar, 20 μm.

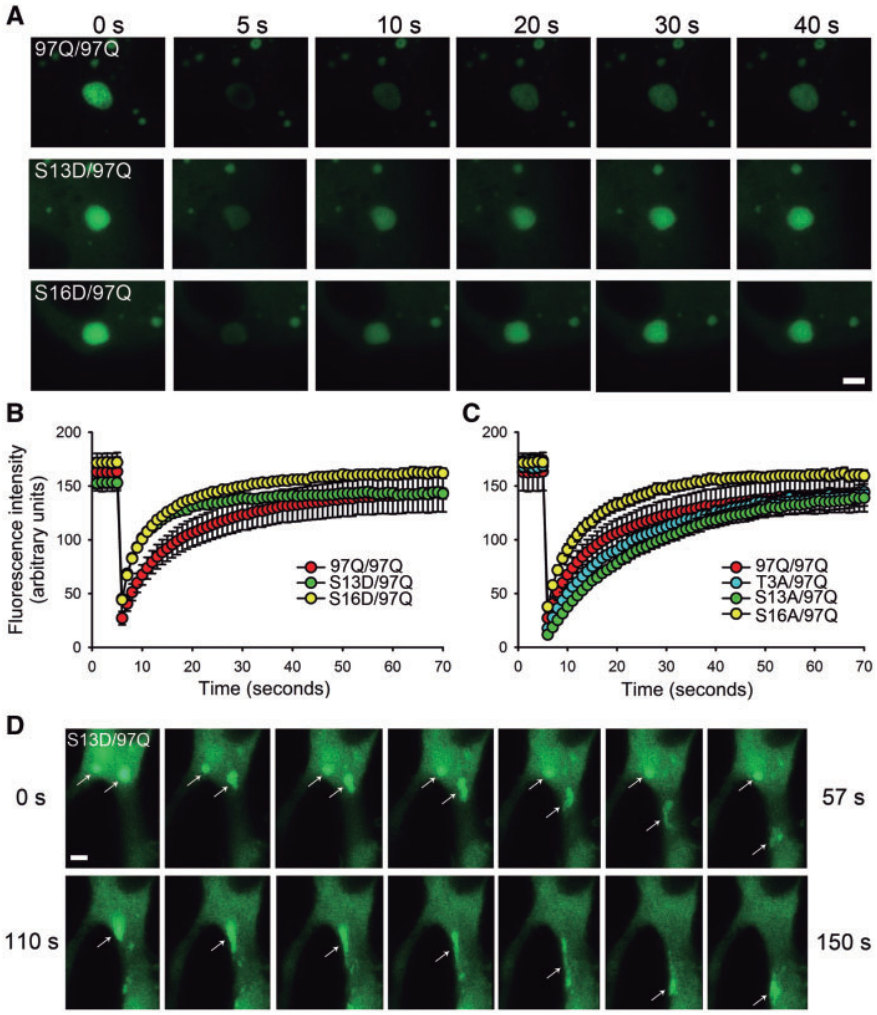

Figure 3. Phosphomimic-containing inclusions of 97QHTTex1 are more dynamic. (**A**) Time lapse of FRAP experiments on aggregates containing non-mutated 97QHTTex1 alone or in combination with phosphomimic mutant in H4 glioma cells. T3D mutants produced no aggregates under any circumstance. (**B**) Aggregates containing S13D or S16D mutants recovered significantly faster than the non-mutated 97QHTTex1. (**C**) Aggregates combining non-mutated 97QHTTex1 with T3A or S13A recovered more slowly than aggregates made only of non-mutated 97QHTTex1, with the exception of the S16A/97Q combination. (**D**) Time lapse of aggregates formed by non-mutated 97QHTTex1 and S13D (Supplementary Material, Video S4). Aggregates containing phosphomimic versions are highly dynamic and flexible, and move (arrow indicates moving aggregate in each frame) through the cell with more freedom than non-mutated 97QHTTex1 aggregates (Supplementary Material, Video S1). Scale bars, 20 μm.

system (Fig. 4 and Supplementary Material, Table S1). We found that inhibitors of PP1/PP2A, CD45, and Cdc25 prevented 97QHTTex1 aggregation as determined by filter trap assay (Fig. 4A). These results were confirmed by fluorescence microscopy, where we observed that inhibitors for those phosphatases significantly decreased the percentage of cells with inclusions (Fig. 4B). Interestingly, the decrease in oligomerization upon treatment with these phosphatase inhibitors was much less dramatic than the reduction observed in aggregation levels (B01, B02, B07, B08 and C04). Although a slight reduction in fluorescence/oligomerization was observed for 28 out of the 33 inhibitors assayed, the few exceptions where a striking decrease was observed (C06, D01 and D03) were owing to cytotoxicity (Supplementary Material, Table S1). Importantly, cells treated with CD45 inhibitors showed reduced levels of HTTex1 expression and increased toxicity (Supplementary Material, Table S1), and were therefore excluded from the study.

Single N17 phosphomutants modulate HTTex1 aggregation in *Drosophila*

To further investigate the role of N17 phosphorylation on HTTex1 aggregation, we expressed single phosphoresistant or phosphomimic versions of 97QHTTex1 in *Drosophila* and assessed for the formation of inclusions. We generated flies expressing different phosphomutant versions of 97QHTTex1 fused to mCherry in adult dopaminergic neurons, under the control of tyrosine hydroxylase (TH)-GAL4 (Fig. 5, columns 1–3), or in larval imaginal discs using the eye-specific glass multiple reporter (GMR)-GAL4 driver (Supplementary Material, Fig. S4). Both T3A (Fig. 5B) and T3D (Fig. 5E) mutants formed fewer inclusions than non-mutated 97QHTTex1 (Fig. 5A), while S13D (Fig. 5F) and S16D (Fig. 5G) mutants showed a significantly larger number of aggregates (quantification in Fig. 5O). S13A (Fig. 5C) and S16A (Fig. 5D) showed no difference in the number of

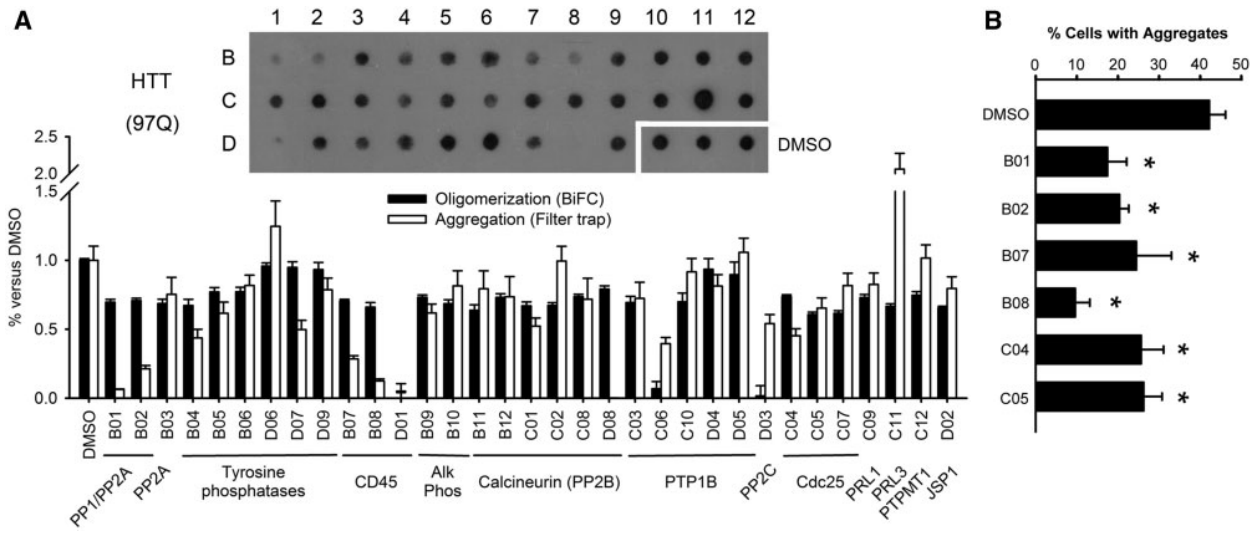

Figure 4. Protein phosphatases regulate HTTex1 aggregation in mammalian cells. **(A)** Representative filter trap of protein extracts from cells transfected with non-mutated 97QHTTex1 BiFC constructs and treated with chemical inhibitors of protein phosphatases. The graph shows oligomerization levels as determined by flow cytometry (black bars) and aggregation levels as determined by optic density of filter trap dots (white bars). The names of phosphatase inhibitors (Enzo Life Sciences) and the concentrations used are described in Supplementary Material, Table S1. **(B)** Selected inhibitors PP1/PP2A (B01 and B02) and Cdc25 (C04 and C05) also reduced the percentage of H4 cells with large HTTex1 inclusions as determined by quantitative analyses of microscopy pictures. *Significant versus DMSO, $P < 0.05$.

inclusions in comparison with non-mutated 97QHTTex1 (Fig. 5O). In the larval eye imaginal discs, all phosphomutants showed decreased aggregation, with the exception of the S13D mutant that formed more inclusions than the non-mutated 97QHTTex1 (Supplementary Material, Fig. S4).

These findings indicate that expression of N17 phosphomutants can modulate 97QHTTex1 aggregation in *Drosophila*, depending on the developmental stage and cellular context.

PP1 regulates HTTex1 aggregation and neurotoxicity in *Drosophila*

In order to test if protein phosphatases also regulate HTTex1 aggregation in *Drosophila*, we performed RNAi knockdown experiments for the homologues of PP1, PP2A and Cdc25 in flies expressing 97QHTTex1 in dopaminergic neurons (Fig. 5, columns 4–6, and Supplementary Material, Fig. S5). These three phosphatases caused the stronger decrease in HTTex1 aggregation in mammalian cells, upon chemical inhibition. PP1 knockdown flies showed a significant decrease in 97QHTTex1 aggregation (Fig. 5H), while PP2A or string (Cdc25 homologue) downregulation had no effect on 97QHTTex1 aggregation (Supplementary Material, Fig. S5A and B). PP1 downregulation prevented 97QHTTex1 aggregation in the presence of serine-phosphoresistant mutants (S13A or S16A) (Fig. 5J and K), but not T3A, where we did not observe any statistically significant change in the number of aggregates when compared with T3A in the absence of PP1 RNAi (Fig. 5O). These results indicate that the effect of PP1 RNAi on 97QHTTex1 aggregation might be mostly mediated by T3 phosphorylation. On the other hand, PP1 knockdown caused an increased number of aggregates in T3D background, and a reduction in the number of aggregates in S13D and S16D backgrounds (Fig. 5O). Since HTTex1 does not contain any phosphorylatable residue beyond N17 domain, the increased aggregation observed in the T3D background upon PP1 inhibition suggests that S13 and/or S16 might also be target for phosphorylation to modulate 97QHTTex1 aggregation, in our *Drosophila* model.

We next analysed the effect of PP1, PP2A or string RNAi knockdown on HTTex1 toxicity in the *Drosophila* eye photoreceptor neurons (Fig. 6 and Supplementary Material, Fig. S5). Importantly, genetic inhibition of PP1 did not compromise rhabdomere viability in flies expressing wild-type (19Q) HTTex1 under the control of rhodopsin 1 (Rh1)-GAL4 [Fig. 6A (column 4) and D]. However, PP1 knockdown significantly enhanced 97QHTTex1 toxicity, further reducing the number of rhabdomeres in an age dependent manner [Fig. 6A–C (column 5) and C]. PP2A or string RNAi had no effect in the number of rhabdomeres upon co-expression with 19QHTTex1 or 97QHTTex1 (Supplementary Material, Fig. S5C and D).

Discussion

Protein misfolding and aggregation are intimately involved in the pathogenesis of HD and other neurodegenerative disorders. Despite extensive research in the field, the precise molecular mechanisms by which misfolded proteins aggregate and form toxic species remain elusive. Increasing evidence suggests that targeting phosphorylation events in the N17 domain of mutant HTT can influence the pathological function of the protein (28,30,36–38). However, the significance of single N17 phosphorylation events in HTT oligomerization, aggregation and toxicity is still poorly understood.

Here, we report that single N17 phosphorylation can prevent HTTex1 aggregation, but not oligomerization. We propose that each residue has a different ‘strength’ in modulating HTTex1 aggregation. Importantly, we found that protein phosphatase 1 can control HTTex1 aggregation and toxicity, suggesting that N17 phosphorylation might be mediated by this protein phosphatase. The fact that single N17 phosphorylation events are sufficient to abolish HTTex1 aggregation could be very important from an HD therapeutic perspective, since a single N17

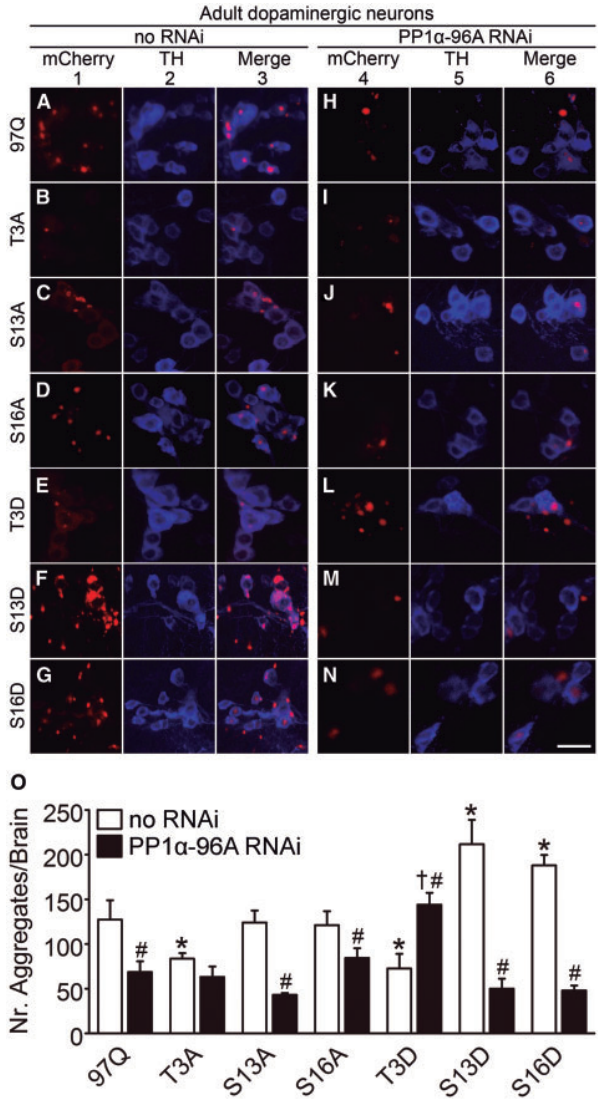

Figure 5. PP1 knockdown prevents 97QHTTex1 aggregation in *Drosophila*. Confocal microscopy images of dopaminergic neurons in adult *Drosophila* brains expressing non-mutated 97QHTTex1-mCherry or the different phosphomutants (**A–G**) under the control of TH-GAL4. (**H–N**) Co-expression of *PP1α-96A* RNAi together with 97QHTTex1-mCherry or phosphomutants. 97HTTex1-mCherry is shown in red (columns 1 and 4), and dopaminergic cells (columns 2 and 5, anti-TH) are shown in blue. T3A (B) and T3D (E) prevented 97HTTex1-mCherry aggregation, while phosphomimic mutations at S13 or S16 produced a significant increase of 97HTTex1-mCherry inclusion bodies (F and G). *PP1α-96A* RNAi decreased the number of 97HTTex1-mCherry inclusions, with the exception of T3A (I), where no change was observed, and T3D (L) expressing flies, which showed a significant increase in 97HTTex1-mCherry aggregation, all in comparison to the respective no RNAi expressing genotype. (O) Quantification of average number of aggregates (±SEM) in each brain. *Significant versus TH-GAL4>97QHTTex1, #Significant versus their 'no RNAi' transgenic control (white bars), †significant versus TH-GAL4>97QHTT/*PP1α-96A* RNAi, $P < 0.05$. Scale bar, 10 μm.

phosphorylation could provide a simpler molecular target than double phosphorylation.

We show that single phosphomimic mutation in T3, S13 or S16 allow 97QHTTex1 to oligomerize but not to form large inclusions in human cells (Fig. 1 and Supplementary Material, Fig. S2). Double S13/S16 phosphorylation prevents aggregation both *in vitro* and *in vivo*, and toxicity *in vivo* (22,26). However, double S13/S16 phosphorylation is less abundant than single phosphorylation events (39), and may require the overexpression of specific kinases (30), which may confound therapeutic efforts based on this approach. Although some studies reported on the effect of single S13 or S16 phosphorylation events on HTTex1 intracellular localization, they did not focus on HTTex1 oligomerization, aggregation or toxicity (28,37). Results from cell-free systems indicate that single S13- or S16-phosphorylated HTTex1 behave similarly to double S13/S16-phosphorylated HTTex1 in terms of aggregation, being unable to form mature fibrils (26). Our findings in living human cells provide additional biological support for those *in vitro* studies.

The unique properties of our BiFC cellular model allowed us to analyse the relative contribution of each phosphorylatable residue towards HTTex1 oligomerization and aggregation. We found that T3D completely abolished 97QHTTex1 aggregation in the presence of any other phosphomutant or non-mutated 97QHTTex1 molecules, while S13D or S16D only had a partial reduction effect (Fig. 2 and Table 1). These results, together with the higher abundance of T3-phosphorylated pools (39,40), highlight the relevance of this residue in modulating the aggregation of HTTex1, and strongly support T3 as a promising target for HD intervention (29). Our results also suggest that, HTTex1 might be predominantly unphosphorylated under pathological conditions (29,37), as phosphoresistant combinations behave more similarly to the non-mutated 97QHTTex1 pair than to the phosphomimics, regarding their aggregation pattern (Fig. 1 and Table 1).

Previous *in vitro* studies demonstrate that N17 phosphorylation inhibits β-sheet conformation of mutant HTTex1 and suppresses its fibrillization, stabilizing the α-helical structure of the N17 domain which could led to altered aggregation dynamics (41,53). In FRAP experiments, we show that combinations of phosphomimic and non-mutated 97QHTTex1 induced the formation of inclusions that were more dynamic, diffuse and fluid than regular 97QHTTex1 aggregates, resembling an intermediate stage between oligomers and mature inclusions (Fig. 3, Supplementary Material, Videos S1–S4 and S6). Additionally, non-mutated 97QHTTex1 pairs did not aggregate to the same extent as the phosphoresistant combinations (Fig. 1C and Table 1). Thus, we propose a model where unphosphorylated HTTex1 fragments oligomerize and form inclusions that grow into mature fibrils until enough phosphorylated HTTex1 molecules are intercalated in the structure to interfere with the process, acting as a 'brake'. This could explain the existence of aggregates of various sizes and morphologies.

Genetic and pharmacological inhibition of PP1 resulted in lower 97QHTTex1 aggregation and increased toxicity (Figs 4–6). Protein phosphatases PP2B/3 (Calcineurin), PP2C and PP1/PP2A have been also shown to regulate HTT phosphorylation at several residues beyond exon 1, as well as HTT toxicity (42–46). It is important to note that HTTex1 does not contain any phosphorylatable residue beyond the N17 domain and, therefore, any direct effect of protein phosphatases should happen on T3, S13 or S16. Our results indicate that PP1 affects 97QHTTex1 aggregation by regulating T3 phosphorylation. In *Drosophila* dopaminergic neurons, PP1 knockdown in serine-phosphomutant backgrounds leads to a decrease in 97QHTTex1 aggregation, regardless the phosphorylation-like state of these residues (Fig. 5O). Moreover, PP1 RNAi does not cause any further reduction of 97QHTTex1 aggregation when co-expressed with T3A mutant. Together, these data suggest that the effect of PP1 inhibition on HTTex1 aggregation is primarily mediated by T3 phosphorylation. However, an

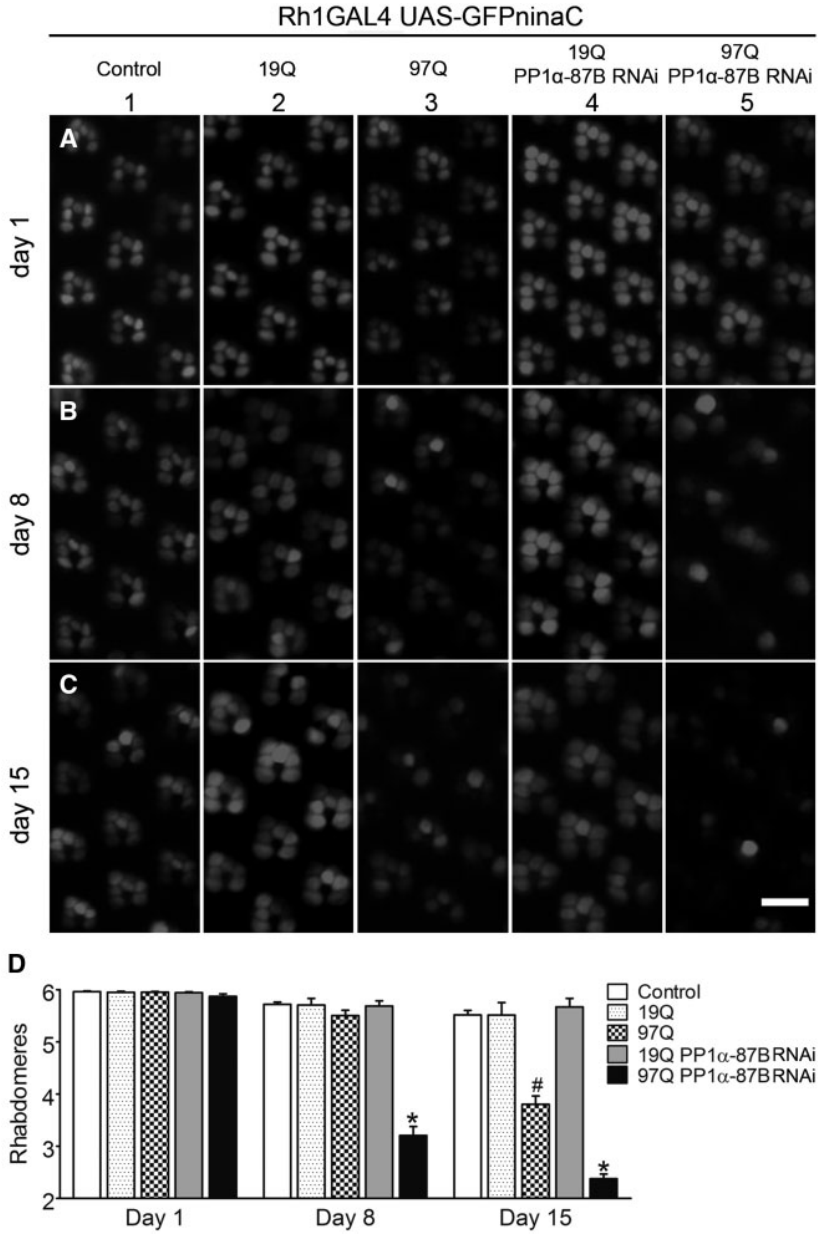

Figure 6. Downregulation of PP1 potentiates HTTex1 neurotoxicity in adult fly photoreceptor neurons. (**A–C**) Representative pictures of photoreceptors observed by water immersion live imaging of the retinas. Wild-type flies, HD flies and flies expressing *PP1α-87B* RNAi together with 19QHTTex1 or 97QHTTex1 were analysed at Day 1, 8 and 15 post-eclosion. Wild-type and 19QHTTex1 expressing flies showed normal retinal morphology as the six outer photoreceptors were visible per ommatidium (columns 1 and 2). Flies expressing 97QHTTex1 exhibited age-dependent neurodegeneration with progressive loss of rhabdomeres from 8 to 15 days after eclosion (B and C, column 3). *PP1α-87B* downregulation caused an increase of neurotoxicity in flies expressing 97QHTTex1 (B and C, column 5) and did not affect photoreceptor integrity of 19QHTTex1 flies (column 4). Visualization of the rhabdomeres was done using Rh1-Gal4>UAS-GFP^{ninaC}, as described in Materials and Methods. (**D**) Quantification of mean rhabdomeres (±SEM) per ommatidium. *Significant versus 97Q, #Significant versus 97Q at days 1 and 8, $P < 0.05$. Scale bar, 10 μm.

increase in 97QHTTex1 aggregation is observed when PP1 RNAi is co-expressed with T3D mutant (Fig. 5L and O), indicating that S13 and S16 might also be target for PP1 regulation. Since S13D or S16D increase 97QHTTex1 aggregation (Fig. 5F, G and O), we hypothesize that PP1 modulates S13 or S16 phosphorylation upon T3 phosphorylation. In fact, it is likely that different N17 mutations may contribute to subsequent phosphorylation events in other residues. For example, IKK-mediated S16 phosphorylation is facilitated by previous phosphorylation of S13 (30).

Interestingly, the striking decrease in 97QHTTex1 aggregation observed when PP1 RNAi was co-expressed with S13D or S16D mutants versus S13D or S16D alone (no RNAi) (Fig. 5O), suggests that T3 phosphorylation is dominant over S13 or S16 phosphorylation. Our human cell data also supports this hypothesis, since S13D or S16D BiFC combinations with non-mutated 97QHTTex1 still shows aggregates, while T3D BiFC combinations with any other mutant completely abolishes aggregation (Fig. 2 and Table 1).

HTT N17 phosphorylation modulates neurotoxicity in several HD models by preventing HTT aggregation (31). However, this finding remains controversial (29,30,37). Currently, there is still debate on whether large, insoluble aggregates are the cause of neuropathology or a byproduct of accumulated misfolded HTT. Though these aggregates were originally thought to be neurotoxic, accumulating evidence suggests that the formation of large aggregates might be part of a protective cellular mechanism to sequester soluble toxic species (54–57). Our data here suggest that N17 phosphorylation modulation of HTTex1 neurotoxicity and the appearance of large aggregates are not necessarily related. Interestingly, polyQ-dependent toxicity varies widely depending on the cellular environment and cell-type specificity, indicating that additional factors may contribute to HTTex1 toxicity (58). Moreover, studies on other post-translational modifications in the N17 region reveal a complex cross-talk among these different modifications in modulating aggregation, and suggest that neurotoxicity may be owing to different mechanisms dependent upon the modifier site (30,33).

Altered PP1 activity has been linked to a variety of diseases, including several neurodegenerative disorders, such as Parkinson's and Alzheimer's diseases (59–61). In fact, PP1 is normally highly expressed in the brain, and is particularly abundant in medium spiny neurons, known to be significantly affected in HD (62). Based on these findings, it is possible that PP1 malfunction increases the susceptibility of certain types of neurons to mutant HTTex1-induced degeneration. Not surprisingly, inhibition of PP1 resulted in increased age-dependent neuronal loss in our *Drosophila* HD model, suggesting that PP1 activity imbalance might precede HTTex1 neurotoxicity. Despite considerable efforts to develop specific chemical activators of PP1 (63,64), further investigations will be necessary to clarify the relationship between PP1 activity impairment, aggregation and neurotoxicity in the context of HD and other polyQ misfolding disorders.

In summary, our results support a strong role for single N17 phosphorylation events on HTTex1 aggregation, dynamics and toxicity, and uncover the regulatory role of PP1 in these events. Ultimately, our study opens novel avenues for the therapeutic targeting of PP1 and N17 phosphorylation in HD.

Materials and Methods

Cell culture, plasmids and treatments

Human H4 glioma cells (ATCC HTB-148, LGC Standards, Barcelona, Spain) were maintained in OPTI-MEM I culture medium (Gibco, Invitrogen, Barcelona, Spain) supplemented with 10% (v/v) fetal bovine serum and 1% (w/v) of a penicillin/streptomycin commercial antibiotic mixture (Gibco), under controlled conditions of temperature and humidity (37 °C, 5% CO_2). Different types of cell culture dishes were used for cell seeding depending on the application. For flow cytometry and toxicity assays, cells were grown on 6-well plates (35 mm diameter, Techno Plastic Cultures AG, Switzerland). For microscopy, cells were seeded on glass-bottom 35 mm dishes (10 mm glass surface diameter, MatTek Corporation, Ashland, MA, USA). And, for protein extraction (PAGE and filter trap assays), cells were seeded on 100 mm dishes (Techno Plastic Cultures AG, Switzerland). For all experiments, cells were counted and seeded at a density of 10 000 cells/cm^2 regardless dish size. Generation of HTTex1- and tau-Venus BiFC constructs was described in detail elsewhere (47,49). Alpha-synuclein-Venus BiFC plasmids were a kind gift from Pamela J. McLean (Department of Neurology, Alzheimer's Disease Research Unit, Massachusetts General Hospital, MA, USA). Phosphomimic (T3, S13 or S16 mutated to aspartic acid) and phosphoresistant (T3, S13 or S16 mutated to alanine) constructs were produced by PCR-based site-directed mutagenesis using 97QHTTex1-Venus plasmids as templates. Plasmid transfection was performed by means of the X-tremeGene 9 reagent (Roche diagnostics, Mannheim, Germany), following manufacturer's instructions. Twenty-four hours after transfection, cells were collected and analysed for oligomerization, aggregation and toxicity as described below. Pharmacological inhibition of protein phosphatases was performed using a phosphatase inhibitor library (Enzo Life Sciences, Lausen, Switzerland). Briefly, cells were treated with 33 different phosphatase inhibitors upon transfection of 97QHTTex1 BiFC constructs. Phosphatase inhibitors were dissolved in DMSO and added to culture medium at variable concentrations, according to the IC50 described in manufacturer's instructions (Supplementary Material, Table S1).

Flow cytometry

Cells were washed with Ca^{2+} and Mg^{2+} free phosphate buffer saline (PBS) (Gibco) and collected by trypsinization (0.05% w/v trypsin, 5 min, 37 °C) into BD Falcon Round-Bottom tubes (BD Biosciences, San Jose, CA, USA). Cell pellet was resuspended in PBS and analysed by means of a LSR Fortessa flow cytometer (Beckton Dickinson, Franklin Lakes, NJ, USA). Ten thousand cells were examined per experimental group. The FlowJo software (Tree Star, Inc., Ashland, OR, USA) was used for data analyses and representation.

Fluorescence microscopy and FRAP experiments

Images of living H4 cells were acquired using an Axiovert 200M widefield fluorescence microscope equipped with a CCD camera (Carl Zeiss MicroImaging GmbH, Germany). Pictures of a total of 100–150 cells per sample were scored for aggregate quantification using the ImageJ free software (http://rsbweb.nih.gov/ij/). FRAP experiments were performed using a META LSM 510 confocal microscope. Briefly, protein aggregates were focused at the central focal plane and adjusted to avoid pixel saturation. Experiments lasted for 70–150 s, taking one picture every second. After establishing the basal signal, aggregates were bleached using the 488 nm laser line at 100% laser transmission on a circular region of interest with a diameter of 30 pixels (1.31 μm radius) for 5 s (10 iterations). Fluorescence recovery was then monitored for 60–140 s with LSM software. Images were analysed and prepared for publication by means of the ImageJ free software.

Immunoblotting

Proteins were extracted in native or denaturing conditions according to the requirements of each technique. Briefly, cells were washed with PBS 1× and collected by scraping. Cells were incubated with lysis buffer and sonicated for 10 s at 5 mA using a Soniprep 150 sonicator (Albra, Milano, Italy). For denaturalizing conditions, the lysis buffer was 1% Triton X-100, 150 mM NaCl, 50 mM Tris pH 7.4, supplemented with a protease inhibitor cocktail (Roche diagnostics). For native conditions, the lysis buffer was 173 mM NaCl, 50 mM Tris pH 7.4, 5 mM EDTA, also supplemented with protease inhibitor cocktail. Proteins were collected after cell lysate centrifugation at 10 000 *g* for 10 min at 4 °C and quantified by means of the BCA Protein Assay Reagent Kit (Thermo Fisher

Scientific, Inc., Rockford, IL, USA), following manufacturer's instructions. For SDS- or Native-PAGE immunoblotting, 15 μg of total protein extracts were prepared and separated by electrophoresis using a 12% SDS-polyacrylamide gel or a 5% SDS-free-polyacrylamide gel, respectively. For denaturing conditions, samples were boiled in standard loading buffer (200 mM Tris–HCl pH 6.8, 8% SDS, 40% glycerol, 6.3% β-mercaptoethanol, 0.4% bromophenol blue) for 5 min at 95 °C. For native conditions, extracts were mixed with SDS- and mercaptoethanol free loading buffer (200 mM Tris–HCl pH 6.8; 40% glycerol; 0.4% bromophenol blue) and the boiling step was omitted. Proteins were transferred onto PVDF membranes and blocked with 5% (w/v) non-fat dry milk in Tris–HCl buffer saline-Tween solution (TBS-T) (150 mM NaCl, 50 mM Tris pH 7.4, 0.5% Tween-20) for 1 h at room temperature. Membranes were incubated with primary antibodies against HTT (1:500, Millipore, Billerica, MA, USA) and GAPDH (1:30 000, Ambion, Austin, TX, USA) as specified. A secondary mouse IgG Horseradish Peroxidase-linked antibody (1:10 000, GE Healthcare Life Sciences, Uppsala, Sweden) was used for 1 h incubation at room temperature. Immunoblots were developed with enhanced chemiluminescence reagents (Millipore) and exposed to X-ray films.

Filter trap assays

Cells were pelleted by centrifugation at 700 g for 10 min and cell lysates collected in native conditions as described above. One hundred micrograms of native protein extracts were mixed with SDS to a final concentration of 0.4% (w/v). Samples were loaded on a dot-blotting device and filtered by vacuum through cellulose acetate membranes (0.22 μm pore; GE Water & Process Technologies, Fairfield, CT, USA), previously incubated with 1% (w/v) SDS solution in PBS. After filtration, membranes were washed two times and processed for immublotting detection of HTT, as described above. In these conditions, only large SDS-insoluble aggregates are retained in the filter and therefore HTT signal is proportional to the presence of large insoluble species. Analyses and quantification of blots signal were performed using ImageJ software. HTTex1 aggregation levels (Fig. 4) were calculated by densitometry analyses and normalized to total HTT expression levels and GAPDH loading control.

Drosophila stocks, genetics and crosses

Flies were maintained at 25 °C and raised on standard cornmeal medium in a light/dark cycle of 12 h. We generated eight constructs encoding for different versions of HTTex1 fused to mCherry: a wild-type version with a polyQ tail containing 19 glutamines, a mutant version with 97 glutamines, and 6 constructs encoding phosphomutant versions (T3A/D, S13A/D and S16A/D) with 97 glutamines. To establish transgenic UAS-HTTex1-mCherry lines, our constructs were cloned into pWalium10-roe by the Gateway cloning technology (Thermo Fisher Scientific), and then injected into y^1w^{1118} embryos using phiC31 integrase-mediated DNA recombination (BestGene strain #9723, attP landing site at 2L-28E7). For genetic knockdown experiments in *Drosophila*, we employed UAS-RNAi-targeted lines of four phosphatases: *string* (homolog of cdc25 phosphatase, BL34831, HMS00146), *PP1α-96A* (alpha-1 isoform of PP1 catalytic subunit, BL42641, HMS02477), *PP1α-87B* (alpha-2 isoform of PP1 catalytic subunit, BL32414, HMS00409), and *PP2A-29B* (PP2A regulatory subunit, BL43283, HMS01921). RNAi stocks were obtained from the TRiP (Transgenic RNAi Project) library (65,66), courtesy of the Bloomington Drosophila Stock Center (Indiana University, Bloomington, IN, USA). Three different driver lines were used: TH-GAL4 (active in dopaminergic neurons, under the control of the TH promotor), GMR-GAL4 (active in the eye) and Rh1-GAL4 (active in the photoreceptors R1-R6, under the control of Rh1 promotor). To analyse the effect of RNAi downregulation of specific phosphatases upon HTTex1 aggregation and toxicity, UAS-97QHTTmCherry/CyO;THGAL4/TM6B was crossed with UAS-RNAi-targeted lines. Adult flies carrying UAS-97QHTTmCherry/+;TH-GAL4/UAS-*string*RNAi, UAS-97QHTTmCherry/+;TH-GAL4/UAS-*PP1α-87B*RNAi, UAS-97QHTTmCherry/UAS-*PP1α-96A*;TH-GAL4/+ and UAS-97QHTTmCherry/+;TH-GAL4/UAS-*PP2A-29B*RNAi were selected and analysed. Unless specified otherwise, flies carrying UAS-lacZ targeted to the same location were used as controls. For deep pseudopupil (DPP) analysis, Rh1-GAL4;UAS-green fluorescent protein^{ninaC} (GFP^{ninaC})/UAS-19QHTTmCherry;UAS-*PP1-87B*RNAi/+ and Rh1-GAL4;UAS-GFP^{ninaC}/UAS-97QHTTmCherry;UAS-*PP1-87B*RNAi/+ adult flies were selected and analysed. Rh1-GAL4;UAS-GFP^{ninaC}, Rh1-GAL4;UAS-GFP^{ninaC}/UAS-19QHTTmCherry;UAS-GFP and Rh1-GAL4;UAS-GFP^{ninaC}/UAS-97QHTTmCherry;UAS-GFP were used as controls.

Immunohistochemistry and confocal microscopy

For confocal imaging of adult brains, 10-day-old flies were dissected and brains prepared as previously described (51). Briefly, adult flies were anesthetized with CO_2 and brains isolated in PBS 1× from the head cuticles before being fixed in 4% paraformaldehyde-containing PBS. Dopaminergic neurons were stained by incubation for 48 h at 4 °C with mouse anti-TH antibody (1:100, Immunostar, Hudson, WI, USA) in PBST (1× PBS, 0.3% Triton X-100) containing 5% (v/v) normal goat serum. Samples were washed three times for 15 min in PBST. Mouse anti-Cy5 (1:200, Jackson ImmunoResearch, West Grove, PA, USA) was diluted in PBST-containing 5% (v/v) normal goat serum and used as secondary antibody by incubation for 24 h at 4 °C. For larva immunohistochemistry, eye imaginal discs of third instar larvae were dissected in PBS 1× and fixed for 1 h in 4% paraformaldehyde as described (67). Samples were then washed three times for 15 min in PBST and incubated overnight at 4 °C with rat anti-Elav antibody (1:100, Developmental Studies Hybridoma Bank, University of Iowa, USA). Imaginal discs were washed three times for 15 min in PBST and incubated for 2 h with rat anti-Cy5 secondary antibody (1:200, Jackson ImmunoResearch). Finally, all samples were submitted to a last step of washing and mounted in 80% glycerol PBS solution, followed by confocal microscopy analyses. Z-stack images were acquired using a LSM 710 Meta Zeiss confocal microscope (resolution of 1024 × 1024, slice thickness of 1 μm, frame average of 2). Z-projections were generated and merged using ImageJ free software and images were prepared on Adobe Photoshop CS6 (Adobe Systems Incorporated, San Jose, CA, USA). For quantification of aggregates, mCherry Z-stack images were analysed by means of the Fiji software (68) and aggregation was measured using 3D Objects Counter plugin (69). The minimum threshold value was defined as 0.144 μm^3 to exclude signal from soluble HTT in the count. Volume (μm^3) occupied per each aggregate, average number of aggregates and standard error were calculated for at least five imaginal discs or adult brains per genotype.

Live imaging of adult *Drosophila* eye

DPP analysis was performed in living animals as previously described (51,70). Briefly, flies at age of 1, 8 or 15 days were

anaesthetized with CO_2 and then placed on a 50-mm petri dish, previously poured with 2% (w/v) agarose at 40 °C. Once the agarose was solidified, the anesthetized flies were covered with cool water to keep anaesthetic conditions. Adult compound eye integrity of at least five flies per genotype was examined by fluorescence microscopy with a water immersion objective (HC APO L40X/0.80W U-V-I, Leica Microsystems, Wetzlar, Germany). Images were obtained using a Leica DM5500 B microscope (Leica Microsystems) and an Andor Luca R DL-604M camera (Andor Technology Ltd., Belfast, UK). Images were analysed using Image J free software and number of fluorescing rhabdomeres was scored for >15 ommatidia per fly.

Statistical analyses

GraphPad Prism 5 (GraphPad Software, Inc., La Jolla, CA, USA) or Sigmaplot software (Systat Software, Inc., San Jose, CA, USA) were used to perform the statistical analysis and graphical representation of data. *In vitro* results are shown as the average ± standard deviation (SD) of at least three independent experiments and *Drosophila* results as the average ± standard error (SEM), unless specified otherwise. Cell culture data were analysed by means of a one-way ANOVA followed by a post hoc Tukey test for average comparison. Aggregates quantification in *Drosophila* was analysed by means of a one-way ANOVA with Newman–Keuls post hoc test. DPP assays were analysed by means of a two-way ANOVA followed by a Bonferroni post hoc test. Results were in all cases considered significant only when $P < 0.05$.

Authors' Contributions

J.B.S. and F.H. carried out the experiments in mammalian cells. J.B.S., G.M.P. and Y.P.A. performed the *Drosophila* experiments, under supervision of P.M.D. and F.G. F.H., J.B.S., P.M.D. and T.F.O. wrote the manuscript, which was edited by all authors. J.B.S. and F.H. prepared the figures. F.H. and T.F.O. had the original idea, supervised the work in mammalian cells and coordinated the different teams.

Supplementary Material

Supplementary Material is available at *HMG* online.

Acknowledgements

The authors thank the Bloomington Drosophila Stock Center and the Developmental Studies Hybridoma Bank for fly stocks and antibodies, respectively. The authors also thank Bioimaging Unit from Instituto de Medicina Molecular and Advance Imaging Unit from Instituto Gulbenkian de Ciência for support with imaging.

Conflict of Interest statement. None declared.

Funding

T.F.O. and F.H. were supported by a seed grant from the European Huntington Disease Network (EHDN). T.F.O. is currently supported by the DFG Center for Nanoscale Microscopy and Molecular Physiology of the Brain. P.M.D. was supported by grants FCT-ANR/NEU-NMC/0006/2013, PTDC/NEU-NMC/2459/2014 and IF/00697/2014. F.H. and P.M.D. were also supported by Project LISBOA-01-0145-FEDER-007660 (Cellular Structural and Molecular Microbiology) funded by FEDER funds through COMPETE2020 - Programa Operacional Competitividade e Internacionalização (POCI) and by national funds through Fundação para a Ciência e Tecnologia (Refs SFRH/BPD/63530/2009, IF/00094/2013/CP1173/CT0005 and UID/CBQ/04612/2013). J.B.S. was supported by Fundação para a Ciência e a Tecnologia (Ref SFRH/BD/85275/2012) and FCT/MCTES (Ref CBQ/04612/ICL3535, to F.H. and P.M.D.). F.G. thanks the Medical Research Council (MRC) for funding that provided valuable infrastructure supporting this work.

References

1. Rochet, J.C. (2007) Novel therapeutic strategies for the treatment of protein-misfolding diseases. *Expert Rev. Mol. Med*, **9**, 1–34.
2. Bates, G.P., Dorsey, R., Gusella, J.F., Hayden, M.R., Kay, C., Leavitt, B.R., Nance, M., Ross, C.A., Scahill, R.I., Wetzel, R. *et al.* (2015) Huntington disease. *Nat. Rev. Dis. Primers*, **1**, 15005.
3. Bates, G.P., Mangiarini, L. and Davies, S.W. (1998) Transgenic mice in the study of polyglutamine repeat expansion diseases. *Brain. Pathol.*, **8**, 699–714.
4. Mangiarini, L., Sathasivam, K., Seller, M., Cozens, B., Harper, A., Hetherington, C., Lawton, M., Trottier, Y., Lehrach, H., Davies, S.W. *et al.* (1996) Exon 1 of the HD gene with an expanded CAG repeat is sufficient to cause a progressive neurological phenotype in transgenic mice. *Cell*, **87**, 493–506.
5. The Huntington's Disease Collaborative Research Group. (1993) A novel gene containing a trinucleotide repeat that is expanded and unstable on Huntington's disease chromosomes. *Cell*, **72**, 971–983.
6. Ambrose, C.M., D.M., Barnes, G., Bates, G.P., Lin, C.S., Srinidhi, J., Baxendale, S., Hummerich, H., L.H. and Altherr, M. (1994) Structure and expression of the Huntington's disease gene: evidence against simple inactivation due to an expanded CAG repeat. *Somat. Cell Mol. Genet.*, **20**, 27–38.
7. Krobitsch, S. and Lindquist, S. (2000) Aggregation of huntingtin in yeast varies with the length of the polyglutamine expansion and the expression of chaperone proteins. *Proc. Natl. Acad. Sci. U.S.A.*, **97**, 1589–1594.
8. DiFiglia, M., Sapp, E., Chase, K.O., Davies, S.W., Bates, G.P., Vonsattel, J.P. and Aronin, N. (1997) Aggregation of huntingtin in neuronal intranuclear inclusions and dystrophic neurites in brain. *Science*, **277**, 1990–1993.
9. Kuiper, E.F.E., de Mattos, E.P., Jardim, L.B., Kampinga, H.H. and Bergink, S. (2017) Chaperones in polyglutamine aggregation: beyond the Q-stretch. *Front. Neurosci.*, **11**.
10. Burke, K.A., Kauffman, K.J., Umbaugh, C.S., Frey, S.L. and Legleiter, J. (2013) The interaction of polyglutamine peptides with lipid membranes is regulated by flanking sequences associated with huntingtin. *J. Biol. Chem.*, **288**, 14993–15005.
11. Michalek, M., Salnikov, E.S., Werten, S. and Bechinger, B. (2013) Membrane interactions of the amphipathic amino terminus of huntingtin. *Biochemistry*, **52**, 847–858.
12. Atwal, R.S., Xia, J., Pinchev, D., Taylor, J., Epand, R.M. and Truant, R. (2007) Huntingtin has a membrane association signal that can modulate huntingtin aggregation, nuclear entry and toxicity. *Hum. Mol. Genet.*, **16**, 2600–2615.
13. Rockabrand, E., Slepko, N., Pantalone, A., Nukala, V.N., Kazantsev, A., Marsh, J.L., Sullivan, P.G., Steffan, J.S., Sensi, S.L. and Thompson, L.M. (2007) The first 17 amino acids of Huntingtin modulate its sub-cellular localization,

aggregation and effects on calcium homeostasis. *Hum. Mol. Genet.*, **16**, 61–77.
14. Cornett, J., Cao, F., Wang, C.E., Ross, C.A., Bates, G.P., Li, S.H. and Li, X.J. (2005) Polyglutamine expansion of huntingtin impairs its nuclear export. *Nat. Genet.*, **37**, 198–204.
15. Xia, J., Lee, D.H., Taylor, J., Vandelft, M. and Truant, R. (2003) Huntingtin contains a highly conserved nuclear export signal. *Hum. Mol. Genet.*, **12**, 1393–1403.
16. Crick, S.L., Ruff, K.M., Garai, K., Frieden, C. and Pappu, R.V. (2013) Unmasking the roles of N- and C-terminal flanking sequences from exon 1 of huntingtin as modulators of polyglutamine aggregation. *Proc. Natl. Acad. Sci. U.S.A.*, **110**, 20075–20080.
17. Jayaraman, M., Kodali, R., Sahoo, B., Thakur, A.K., Mayasundari, A., Mishra, R., Peterson, C.B. and Wetzel, R. (2012) Slow amyloid nucleation via alpha-helix-rich oligomeric intermediates in short polyglutamine-containing huntingtin fragments. *J. Mol. Biol.*, **415**, 881–899.
18. Williamson, T.E., Vitalis, A., Crick, S.L. and Pappu, R.V. (2010) Modulation of polyglutamine conformations and dimer formation by the N-terminus of huntingtin. *J. Mol. Biol.*, **396**, 1295–1309.
19. Thakur, A.K., Jayaraman, M., Mishra, R., Thakur, M., Chellgren, V.M., Byeon, I.J., Anjum, D.H., Kodali, R., Creamer, T.P., Conway, J.F. *et al.* (2009) Polyglutamine disruption of the huntingtin exon 1 N terminus triggers a complex aggregation mechanism. *Nat. Struct. Mol. Biol.*, **16**, 380–389.
20. Wetzel, R. (2006) Nucleation of huntingtin aggregation in cells. *Nat. Chem. Biol.*, **2**, 297–298.
21. Veldman, M.B., Rios-Galdamez, Y., Lu, X.H., Gu, X., Qin, W., Li, S., Yang, X.W. and Lin, S. (2015) The N17 domain mitigates nuclear toxicity in a novel zebrafish Huntington's disease model. *Mol. Neurodegener.*, **10**, 67.
22. Gu, X., Cantle, J.P., Greiner, E.R., Lee, C.Y., Barth, A.M., Gao, F., Park, C.S., Zhang, Z., Sandoval-Miller, S., Zhang, R.L. *et al.* (2015) N17 Modifies mutant Huntingtin nuclear pathogenesis and severity of disease in HD BAC transgenic mice. *Neuron*, **85**, 726–741.
23. Choudhury, K.R. and Bhattacharyya, N.P. (2015) Chaperone protein HYPK interacts with the first 17 amino acid region of Huntingtin and modulates mutant HTT-mediated aggregation and cytotoxicity. *Biochem. Biophys. Res. Commun.*, **456**, 66–73.
24. Maiuri, T., Woloshansky, T., Xia, J. and Truant, R. (2013) The huntingtin N17 domain is a multifunctional CRM1 and Ran-dependent nuclear and cilial export signal. *Hum. Mol. Genet.*, **22**, 1383–1394.
25. Zheng, Z., Li, A., Holmes, B.B., Marasa, J.C. and Diamond, M.I. (2013) An N-terminal nuclear export signal regulates trafficking and aggregation of Huntingtin (Htt) protein exon 1. *J. Biol. Chem.*, **288**, 6063–6071.
26. Mishra, R., Hoop, C.L., Kodali, R., Sahoo, B., van der Wel, P.C. and Wetzel, R. (2012) Serine phosphorylation suppresses huntingtin amyloid accumulation by altering protein aggregation properties. *J. Mol. Biol.*, **424**, 1–14.
27. Zucchelli, S., Marcuzzi, F., Codrich, M., Agostoni, E., Vilotti, S., Biagioli, M., Pinto, M., Carnemolla, A., Santoro, C., Gustincich, S. *et al.* (2011) Tumor necrosis factor receptor-associated factor 6 (TRAF6) associates with huntingtin protein and promotes its atypical ubiquitination to enhance aggregate formation. *J. Biol. Chem.*, **286**, 25108–25117.
28. Havel, L.S., Wang, C.E., Wade, B., Huang, B., Li, S. and Li, X.J. (2011) Preferential accumulation of N-terminal mutant huntingtin in the nuclei of striatal neurons is regulated by phosphorylation. *Hum. Mol. Genet.*, **20**, 1424–1437.
29. Aiken, C.T., Steffan, J.S., Guerrero, C.M., Khashwji, H., Lukacsovich, T., Simmons, D., Purcell, J.M., Menhaji, K., Zhu, Y.Z., Green, K. *et al.* (2009) Phosphorylation of threonine 3: implications for Huntingtin aggregation and neurotoxicity. *J. Biol. Chem.*, **284**, 29427–29436.
30. Thompson, L.M., Aiken, C.T., Kaltenbach, L.S., Agrawal, N., Illes, K., Khoshnan, A., Martinez-Vincente, M., Arrasate, M., O'Rourke, J.G., Khashwji, H. *et al.* (2009) IKK phosphorylates Huntingtin and targets it for degradation by the proteasome and lysosome. *J. Cell Biol.*, **187**, 1083–1099.
31. Gu, X., Greiner, E.R., Mishra, R., Kodali, R., Osmand, A., Finkbeiner, S., Steffan, J.S., Thompson, L.M., Wetzel, R. and Yang, X.W. (2009) Serines 13 and 16 are critical determinants of full-length human mutant huntingtin induced disease pathogenesis in HD mice. *Neuron*, **64**, 828–840.
32. Jana, N.R., Dikshit, P., Goswami, A., Kotliarova, S., Murata, S., Tanaka, K. and Nukina, N. (2005) Co-chaperone CHIP associates with expanded polyglutamine protein and promotes their degradation by proteasomes. *J. Biol. Chem.*, **280**, 11635–11640.
33. Steffan, J.S., Agrawal, N., Pallos, J., Rockabrand, E., Trotman, L.C., Slepko, N., Illes, K., Lukacsovich, T., Zhu, Y.Z., Cattaneo, E. *et al.* (2004) SUMO modification of Huntingtin and Huntington's disease pathology. *Science*, **304**, 100–104.
34. Steffan, J.S., Bodai, L., Pallos, J., Poelman, M., McCampbell, A., Apostol, B.L., Kazantsev, A., Schmidt, E., Zhu, Y.Z., Greenwald, M. *et al.* (2001) Histone deacetylase inhibitors arrest polyglutamine-dependent neurodegeneration in Drosophila. *Nature*, **413**, 739–743.
35. Caron, N.S., Hung, C.L., Atwal, R.S. and Truant, R. (2014) Live cell imaging and biophotonic methods reveal two types of mutant huntingtin inclusions. *Hum. Mol. Genet.*, **23**, 2324–2338.
36. Di Pardo, A., Maglione, V., Alpaugh, M., Horkey, M., Atwal, R.S., Sassone, J., Ciammola, A., Steffan, J.S., Fouad, K., Truant, R. *et al.* (2012) Ganglioside GM1 induces phosphorylation of mutant huntingtin and restores normal motor behavior in Huntington disease mice. *Proc. Natl. Acad. Sci. U.S.A.*, **109**, 3528–3533.
37. Atwal, R.S., Desmond, C.R., Caron, N., Maiuri, T., Xia, J., Sipione, S. and Truant, R. (2011) Kinase inhibitors modulate huntingtin cell localization and toxicity. *Nat. Chem. Biol.*, **7**, 453–460.
38. Khoshnan, A., Ko, J., Watkin, E.E., Paige, L.A., Reinhart, P.H. and Patterson, P.H. (2004) Activation of the IkappaB kinase complex and nuclear factor-kappaB contributes to mutant huntingtin neurotoxicity. *J. Neurosci.*, **24**, 7999–8008.
39. Bustamante, M.B., Ansaloni, A., Pedersen, J.F., Azzollini, L., Cariulo, C., Wang, Z.M., Petricca, L., Verani, M., Puglisi, F., Park, H. *et al.* (2015) Detection of huntingtin exon 1 phosphorylation by Phos-Tag SDS-PAGE: Predominant phosphorylation on threonine 3 and regulation by IKKbeta. *Biochem. Biophys. Res. Commun.*, **463**, 1317–1322.
40. Huang, B., Lucas, T., Kueppers, C., Dong, X., Krause, M., Bepperling, A., Buchner, J., Voshol, H., Weiss, A., Gerrits, B. *et al.* (2015) Scalable production in human cells and biochemical characterization of full-length normal and mutant huntingtin. *PLoS One*, **10**, e0121055.
41. Caron, N.S., Desmond, C.R., Xia, J. and Truant, R. (2013) Polyglutamine domain flexibility mediates the proximity between flanking sequences in huntingtin. *Proc. Natl. Acad. Sci. U.S.A.*, **110**, 14610–14615.

42. Marion, S., Urs, N.M., Peterson, S.M., Sotnikova, T.D., Beaulieu, J.M., Gainetdinov, R.R. and Caron, M.G. (2014) Dopamine D2 receptor relies upon PPM/PP2C protein phosphatases to dephosphorylate huntingtin protein. *J. Biol. Chem.*, **289**, 11715–11724.
43. Rosenstock, T.R., de Brito, O.M., Lombardi, V., Louros, S., Ribeiro, M., Almeida, S., Ferreira, I.L., Oliveira, C.R. and Rego, A.C. (2011) FK506 ameliorates cell death features in Huntington's disease striatal cell models. *Neurochem. Int.*, **59**, 600–609.
44. Pineda, J.R., Pardo, R., Zala, D., Yu, H., Humbert, S. and Saudou, F. (2009) Genetic and pharmacological inhibition of calcineurin corrects the BDNF transport defect in Huntington's disease. *Mol. Brain*, **2**, 33.
45. Ermak, G., Hench, K.J., Chang, K.T., Sachdev, S. and Davies, K.J. (2009) Regulator of calcineurin (RCAN1-1L) is deficient in Huntington disease and protective against mutant huntingtin toxicity in vitro. *J. Biol. Chem.*, **284**, 11845–11853.
46. Pardo, R., Colin, E., Regulier, E., Aebischer, P., Deglon, N., Humbert, S. and Saudou, F. (2006) Inhibition of calcineurin by FK506 protects against polyglutamine-huntingtin toxicity through an increase of huntingtin phosphorylation at S421. *J. Neurosci.*, **26**, 1635–1645.
47. Blum, D., Herrera, F., Francelle, L., Mendes, T., Basquin, M., Obriot, H., Demeyer, D., Sergeant, N., Gerhardt, E., Brouillet, E. *et al.* (2015) Mutant huntingtin alters Tau phosphorylation and subcellular distribution. *Hum. Mol. Genet.*, **24**, 76–85.
48. Herrera, F. and Outeiro, T.F. (2012) alpha-Synuclein modifies huntingtin aggregation in living cells. *FEBS Lett.*, **586**, 7–12.
49. Herrera, F., Tenreiro, S., Miller-Fleming, L. and Outeiro, T.F. (2011) Visualization of cell-to-cell transmission of mutant huntingtin oligomers. *PLoS Curr.*, **3**, RRN1210.
50. Sahoo, B., Arduini, I., Drombosky, K.W., Kodali, R., Sanders, L.H., Greenamyre, J.T. and Wetzel, R. (2016) Folding landscape of mutant huntingtin exon1: diffusible multimers, oligomers and fibrils, and no detectable monomer. *PLoS One*, **11**, e0155747.
51. Pocas, G.M., Branco-Santos, J., Herrera, F., Outeiro, T.F. and Domingos, P.M. (2015) alpha-Synuclein modifies mutant huntingtin aggregation and neurotoxicity in Drosophila. *Hum. Mol. Genet.*, **24**, 1898–1907.
52. Furlong, R.A., Narain, Y., Rankin, J., Wyttenbach, A. and Rubinsztein, D.C. (2000) Alpha-synuclein overexpression promotes aggregation of mutant huntingtin. *Biochem. J.*, **346(Pt 3)**, 577–581.
53. Chiki, A., DeGuire, S.M., Ruggeri, F.S., Sanfelice, D., Ansaloni, A., Wang, Z.M., Cendrowska, U., Burai, R., Vieweg, S., Pastore, A. *et al.* (2017) Mutant exon 1 Huntingtin aggregation is regulated by T3 phosphorylation-induced structural changes and crosstalk between T3 phosphorylation and acetylation at K6. *Angew. Chem. Int. Ed.*, **56**, 1–6.
54. Kuemmerle, S., Gutekunst, C.A., Klein, A.M., Li, X.J., Li, S.H., Beal, M.F., Hersch, S.M. and Ferrante, R.J. (1999) Huntington aggregates may not predict neuronal death in Huntington's disease. *Ann. Neurol.*, **46**, 842–849.
55. Arrasate, M., Mitra, S., Schweitzer, E.S., Segal, M.R. and Finkbeiner, S. (2004) Inclusion body formation reduces levels of mutant huntingtin and the risk of neuronal death. *Nature*, **431**, 805–810.
56. Slow, E.J., Graham, R.K., Osmand, A.P., Devon, R.S., Lu, G., Deng, Y., Pearson, J., Vaid, K., Bissada, N., Wetzel, R. *et al.* (2005) Absence of behavioral abnormalities and neurodegeneration in vivo despite widespread neuronal huntingtin inclusions. *Proc. Natl. Acad. Sci. U.S.A.*, **102**, 11402–11407.
57. Bodner, R.A., Outeiro, T.F., Altmann, S., Maxwell, M.M., Cho, S.H., Hyman, B.T., McLean, P.J., Young, A.B., Housman, D.E. and Kazantsev, A.G. (2006) Pharmacological promotion of inclusion formation: a therapeutic approach for Huntington's and Parkinson's diseases. *Proc. Natl. Acad. Sci. U.S.A.*, **103**, 4246–4251.
58. Tsvetkov, A.S., Arrasate, M., Barmada, S., Ando, D.M., Sharma, P., Shaby, B.A. and Finkbeiner, S. (2013) Proteostasis of polyglutamine varies among neurons and predicts neurodegeneration. *Nat. Chem. Biol.*, **9**, 586–592.
59. Lobbestael, E., Zhao, J., Rudenko, I.N., Beylina, A., Gao, F., Wetter, J., Beullens, M., Bollen, M., Cookson, M.R., Baekelandt, V. *et al.* (2013) Identification of protein phosphatase 1 as a regulator of the LRRK2 phosphorylation cycle. *Biochem. J.*, **456**, 119–128.
60. Braithwaite, S.P., Stock, J.B., Lombroso, P.J. and Nairn, A.C. (2012) Protein phosphatases and Alzheimer's disease. *Prog. Mol. Biol. Transl. Sci.*, **106**, 343–379.
61. Gong, C.X., Shaikh, S., Wang, J.Z., Zaidi, T., Grundke-Iqbal, I. and Iqbal, K. (1995) Phosphatase activity toward abnormally phosphorylated tau: decrease in Alzheimer disease brain. *J. Neurochem.*, **65**, 732–738.
62. da Cruz e Silva, E.F., Fox, C.A., Ouimet, C.C., Gustafson, E., Watson, S.J. and Greengard, P. (1995) Differential expression of protein phosphatase 1 isoforms in mammalian brain. *J. Neurosci.*, **15**, 3375–3389.
63. Tappan, E. and Chamberlin, A.R. (2008) Activation of protein phosphatase 1 by a small molecule designed to bind to the enzyme's regulatory site. *Chem. Biol.*, **15**, 167–174.
64. Chatterjee, J., Beullens, M., Sukackaite, R., Qian, J., Lesage, B., Hart, D.J., Bollen, M. and Köhn, M. (2012) Development of a peptide that selectively activates protein phosphatase-1 in living cells. *Angew. Chem. Int. Ed.*, **51**, 10054–10059.
65. Perkins, L.A., Holderbaum, L., Tao, R., Hu, Y., Sopko, R., McCall, K., Yang-Zhou, D., Flockhart, I., Binari, R., Shim, H.S. *et al.* (2015) The Transgenic RNAi Project at Harvard Medical School: resources and validation. *Genetics*, **201**, 843–852.
66. Ni, J.Q., Zhou, R., Czech, B., Liu, L.P., Holderbaum, L., Yang-Zhou, D., Shim, H.S., Tao, R., Handler, D., Karpowicz, P. *et al.* (2011) A genome-scale shRNA resource for transgenic RNAi in Drosophila. *Nat. Methods*, **8**, 405–407.
67. Purves, D.C. and Brachmann, C. (2007) Dissection of imaginal discs from 3rd instar Drosophila larvae. *J. Vis. Exp.*, **2**, 140.
68. Schindelin, J., Arganda-Carreras, I., Frise, E., Kaynig, V., Longair, M., Pietzsch, T., Preibisch, S., Rueden, C., Saalfeld, S., Schmid, B. *et al.* (2012) Fiji: an open-source platform for biological-image analysis. *Nat. Methods*, **9**, 676–682.
69. Bolte, S. and Cordelieres, F.P. (2006) A guided tour into subcellular colocalization analysis in light microscopy. *J. Microsc.*, **224**, 213–232.
70. Pichaud, F. and Desplan, C. (2001) A new visualization approach for identifying mutations that affect differentiation and organization of the Drosophila ommatidia. *Development*, **128**, 815–826.

SCIENTIFIC REPORTS

OPEN

Glycation potentiates neurodegeneration in models of Huntington's disease

Received: 25 May 2016
Accepted: 21 October 2016
Published: 18 November 2016

Hugo Vicente Miranda[1,2], Marcos António Gomes[2], Joana Branco-Santos[3,4], Carlo Breda[3], Diana F. Lázaro[5], Luísa Vaqueiro Lopes[2], Federico Herrera[4], Flaviano Giorgini[3] & Tiago Fleming Outeiro[1,5,6]

Protein glycation is an age-dependent posttranslational modification associated with several neurodegenerative disorders, including Alzheimer's and Parkinson's diseases. By modifying amino-groups, glycation interferes with folding of proteins, increasing their aggregation potential. Here, we studied the effect of pharmacological and genetic manipulation of glycation on huntingtin (HTT), the causative protein in Huntington's disease (HD). We observed that glycation increased the aggregation of mutant HTT exon 1 fragments associated with HD (HTT72Q and HTT103Q) in yeast and mammalian cell models. We found that glycation impairs HTT clearance thereby promoting its intracellular accumulation and aggregation. Interestingly, under these conditions autophagy increased and the levels of mutant HTT released to the culture medium decreased. Furthermore, increased glycation enhanced HTT toxicity in human cells and neurodegeneration in fruit flies, impairing eclosion and decreasing life span. Overall, our study provides evidence that glycation modulates HTT exon-1 aggregation and toxicity, and suggests it may constitute a novel target for therapeutic intervention in HD.

Huntington's disease (HD) is an autosomal-dominant neurodegenerative disorder affecting 5–10 per 100 000 individuals[1–3]. Its clinical features include progressive motor dysfunction, cognitive impairment, and psychiatric disturbance and dementia[4]. HD is caused by a CAG triplet repeat expansion in exon 1 of the *HTT* gene, which encodes a polyglutamine (polyQ) stretch in huntingtin (HTT) protein. The number of CAG repeats varies from 16 to 35 in healthy individuals, while expansions of >35 CAG repeats are found in HD patients[1]. The length of the polyQ tract in the protein modulates HTT aggregation, thereby causing cytotoxicity by mechanisms that are still not fully understood, with medium spiny neurons in the striatum particularly affected[5].

Glucose is the major energy supply of neurons and is essential for their survival. However, impaired glucose metabolism can also damage neurons and lead to neurodegeneration. For example, diabetic patients who neglect their circulating glucose levels frequently develop severe neuropathy that results in the amputation of limbs[6,7]. Glucose metabolism drives the formation of by-products that are highly reactive with free amino-groups of proteins. This non-enzymatic reaction, named glycation, induces the formation of advanced glycation end-products (AGEs) that frequently have deleterious effects on proteins[8,9]. For example, glycation has been reported in several neurodegenerative disorders such as Alzheimer's and Parkinson's diseases, where it potentiates the aggregation and toxicity of proteins such as amyloid-β (Aβ) and α-synuclein, respectively[8,9].

Methylglyoxal (MGO) is an unavoidable by-product of glycolysis and the most reactive glycation agent. It is mainly produced by the non-enzymatic decomposition of the phosphate group of the triose phosphates (glyceraldeyde 3-phosphate and dihydroxyacetone phosphate)[8]. MGO can also arise from the interconversion between

[1]CEDOC, Chronic Diseases Research Centre, NOVA Medical School | Faculdade de Ciências Médicas, Universidade NOVA de Lisboa, Campo dos Mártires da Pátria, 130, 1169-056, Lisboa, Portugal. [2]Instituto de Medicina Molecular, Faculdade de Medicina, Universidade de Lisboa, Lisboa, Portugal. [3]Department of Genetics, University of Leicester, Leicester LE1 7RH, United Kingdom. [4]Instituto de Tecnologia Química e Biológica, Universidade Nova de Lisboa, Estação Agronomica Nacional, Av. da República, Oeiras 2780-157, Portugal. [5]Department of Neurodegeneration and Restorative Research, Center for Nanoscale Microscopy and Molecular Physiology of the Brain (CNMPB), University Medical Center Göttingen, Waldweg 33, 37073 Göttingen, Germany. [6]Max Planck Institute for Experimental Medicine, Göttingen, Germany. Correspondence and requests for materials should be addressed to T.F.O. (email: touteir@gwdg.de)

glyceraldeyde 3-phosphate and dihydroxyacetone phosphate by the triose phosphate isomerase (Tpi), where the enediolate intermediate may leak from the active site of Tpi in a paracatalytical reaction[10]. Moreover, decreased Tpi activity results in an accumulation of dihydroxyacetone phosphate and MGO[11,12]. MGO is detoxified by the glyoxalase system [glyoxalases I (Glo1) and II (Glo2)] and by aldose reductases[13]. In particular, we previously showed that Glo1 inactivation induces a strong increase in MGO levels in yeast[14]. TPI1 deficiency increases the levels of DHAP[15] and, consequently, increases the levels of MGO[16,17]. Notably, TPI deficiency in humans results in increased levels of MGO[18]. We recently demonstrated that glycation of α-synuclein - a central player in Parkinson's disease - potentiates its aggregation and toxicity (submitted manuscript). Thus, we hypothesized that glycation might act as a common cellular mechanism modulating pathogenesis in several neurodegenerative diseases. Although HD is a genetic disorder, both genetic and environmental factors have been found to modulate the age of disease onset and severity of HD[19–22]. Although no direct correlation between glycation and the pathogenesis of HD has been established thus far, the levels of the receptors for AGEs (RAGE) are increased in HD brains[23] and in mouse models[24]. In addition, we also found that DJ-1 - an enzyme with glyoxalase and deglycase activity - modulates HTT toxicity[25]. Here, we show that glycation potentiates HTT aggregation, impairs protein clearance and increases neuronal loss in various established models of HD.

Results

Glycation induces HTT aggregation in yeast cells. We started by investigating the effects of MGO in a highly tractable yeast model of HD based on the expression of GFP-tagged HTT exon 1 fragments[26] with normal (HTT25Q) or expanded (HTT72Q and HTT103Q) polyQ stretches, which lead to HTT aggregation and toxicity[27,28]. Interestingly, we observed that glycating conditions (using MGO as the glycating agent) potentiated the formation of HTT72Q and HTT103Q inclusions in a dose-dependent manner, an effect that was potentiated by genetic deletion of Tpi (Fig. 1a,b).

We also modulated MGO levels genetically using *Glo1* (Δ*glo1*) or *Tpi* (Δ*tpi*) knockout strains. Deletion of these genes increases the intracellular levels of MGO and promotes the accumulation of AGEs[14,16,17]. Remarkably, in protein extracts from Δ*glo1* and Δ*tpi* strains, HTT was retained in the wells of SDS-PAGE gels (Fig. 1c), further demonstrating that glycation promotes aggregation of mutant HTT. HTT aggregation is also a function of HTT intracellular concentration, as overexpression of normal 25QHTT can also lead to aggregation[29]. Consistently, MGO also increased the intracellular HTT levels in a dose-dependent manner (Fig. 1c,d).

MGO increases HTT levels, aggregation, and toxicity in human cells. To further investigate the effects of glycation on HTT, we used transfected human H4 cells with variants of GFP-tagged HTT exon 1 fragments encoding for 25 (HTT25Q) or 104 (HTT104Q) glutamines. To increase protein glycation, cells were treated with 0.5 mM of MGO, a working concentration widely used in various studies[30–32]. We found that this treatment increased protein glycation without increasing overall cytotoxicity (submitted manuscript). We confirmed that MGO treatment increased overall glycation levels of cells expressing either HTT25Q or HTT104Q (Fig. 2a). Moreover, using immunoprecipitation, we detected a consistent increase in the levels of AGEs in both HTT25Q and HTT104Q (Fig. 2a). Treatment with MGO induced a significant increase in the percentage of cells displaying HTT inclusions (1.33 fold) (Fig. 2b,c) and SDS-insoluble aggregates (1.5 fold), as assessed by filter trap assays (Fig. 2d,e). The levels of both HTT25Q and HTT104Q increased significantly under glycating conditions (1.33 and 1.95 fold, respectively) (Fig. 2f,g). Notably, treatment of cells with MGO also specifically increased HTT104Q toxicity (1.5 fold) (Fig. 2h) and decreased cell viability of both HTT25Q and HTT104Q expressing cells (Fig. S1).

MGO impairs HTT clearance. Since MGO increased the intracellular levels of HTT, we next investigated the possible involvement of protein clearance pathways. First, we monitored the rate of clearance of the different HTT variants upon blocking *de novo* protein synthesis using cycloheximide (CHX). Interestingly, clearance of both HTT25Q (Fig. 3a,b) and HTT104Q (Fig. 3c,d) was impaired under MGO-induced glycating conditions.

Second, we assessed the effect of MGO in the autophagy lysosome pathway (ALP). For this, we blocked the ALP system with ammonium chloride (NH_4Cl) in vehicle or MGO-treated cells, and evaluated the activation of ALP by measuring the accumulation of LC3-II levels[33]. Treatment of cells expressing HTT25Q with MGO reduced the activation of ALP (0.4 fold) (Fig. 3e,f). In contrast, in cells expressing HTT104Q we observed increased activation of ALP (6.6 fold) in response to MGO (Fig. 3g,h).

Third, we evaluated the effects of MGO on the UPS system using an unstable version of GFP (GFPu) that indicates the overall activity of the UPS[34]. Briefly, when the UPS is functioning properly, low levels of GFPu accumulation are expected. As a positive control, we blocked the proteasome function with MG132 and observed a dose-dependent increase in the fluorescence levels, indicating proteasome inhibition (Fig. S2). The levels of GFPu were not altered in cells expressing either HTT25Q or HTT104Q upon MGO treatment (Fig. 3i,j).

Finally, we asked whether glycating conditions affected the cellular release of different HTT exon 1 variants. Conditioned media from HTT104Q-expressing cells treated with MGO showed a significant reduction in the total amount of HTT (less than 0.5 fold), but no changes were observed in the conditioned media from HTT25Q-expressing cells (Fig. 3k,l).

These results suggest that glycation impairs HTT clearance, causing it to accumulate and aggregate within cells.

Glycation enhances toxicity in *Drosophila* models of HD. Given that MGO increased HTT aggregation and toxicity in cell models, we next investigated whether glycation also affected neuronal loss *in vivo*, employing a *Drosophila* model of HD based upon the pan-neuronal expression of a HTT exon 1 fragment with 93 or 20 glutamines (HTT93Q or HTT20Q) via the GAL4/UAS system[35]. HTT93Q flies exhibit a variety of HD-relevant phenotypes, including decreased lifespan, locomotor defects, degeneration of photoreceptor

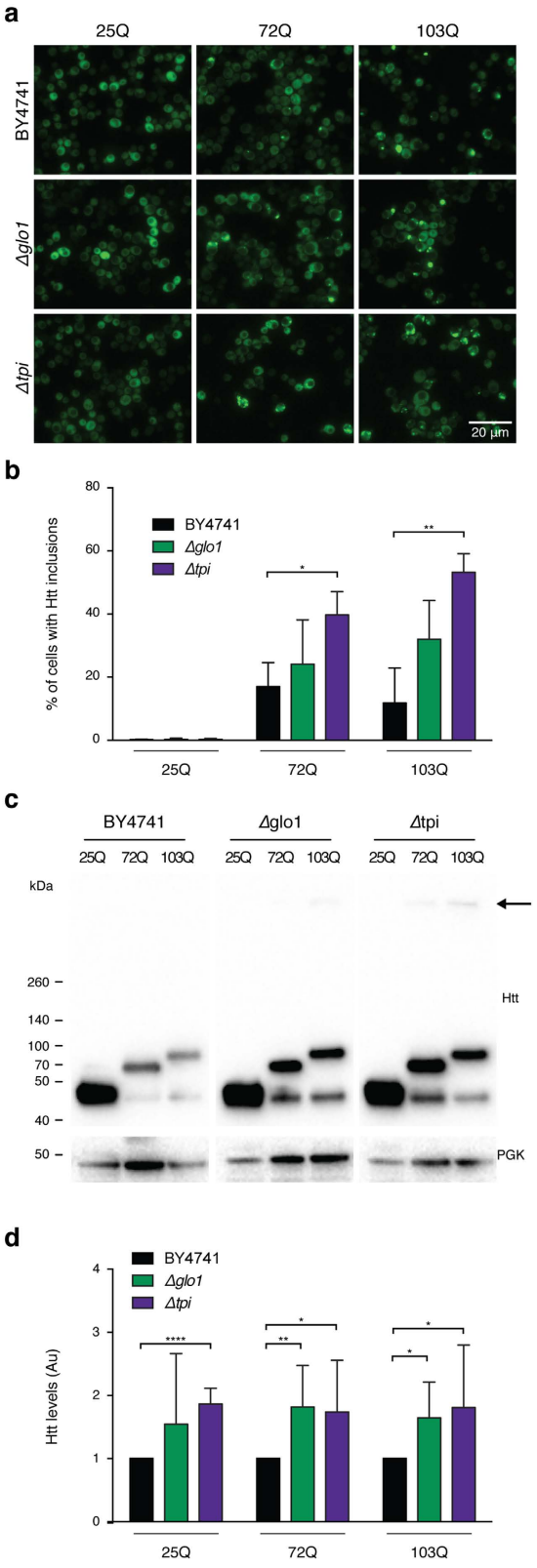

Figure 1. Glycation increases HTT levels and inclusion formation in yeast. (a) Fluorescence micrographs of BY4741 (Ctrl), *glo1*Δ and *tpi*Δ yeast strains transformed with HTT 25Q, 72Q or 103Q variants fused to GFP (scale bar 20µm). **(b)** % of yeast cells displaying HTT inclusions (at least n = 3 per condition). **(c)** Yeast protein extracts were immunoblotted with an anti-GFP antibody. Arrow indicates HTT aggregates. **(d)** Corresponding HTT levels are presented in arbitrary units (at least n = 3 per condition). Data in all panels are average ± SD, $^{*}p < 0.05$, $^{**}p < 0.01$, $^{***}p < 0.001$, $^{****}p < 0.0001$. For (*D*), unpaired two-tailed t-test with equal SD.

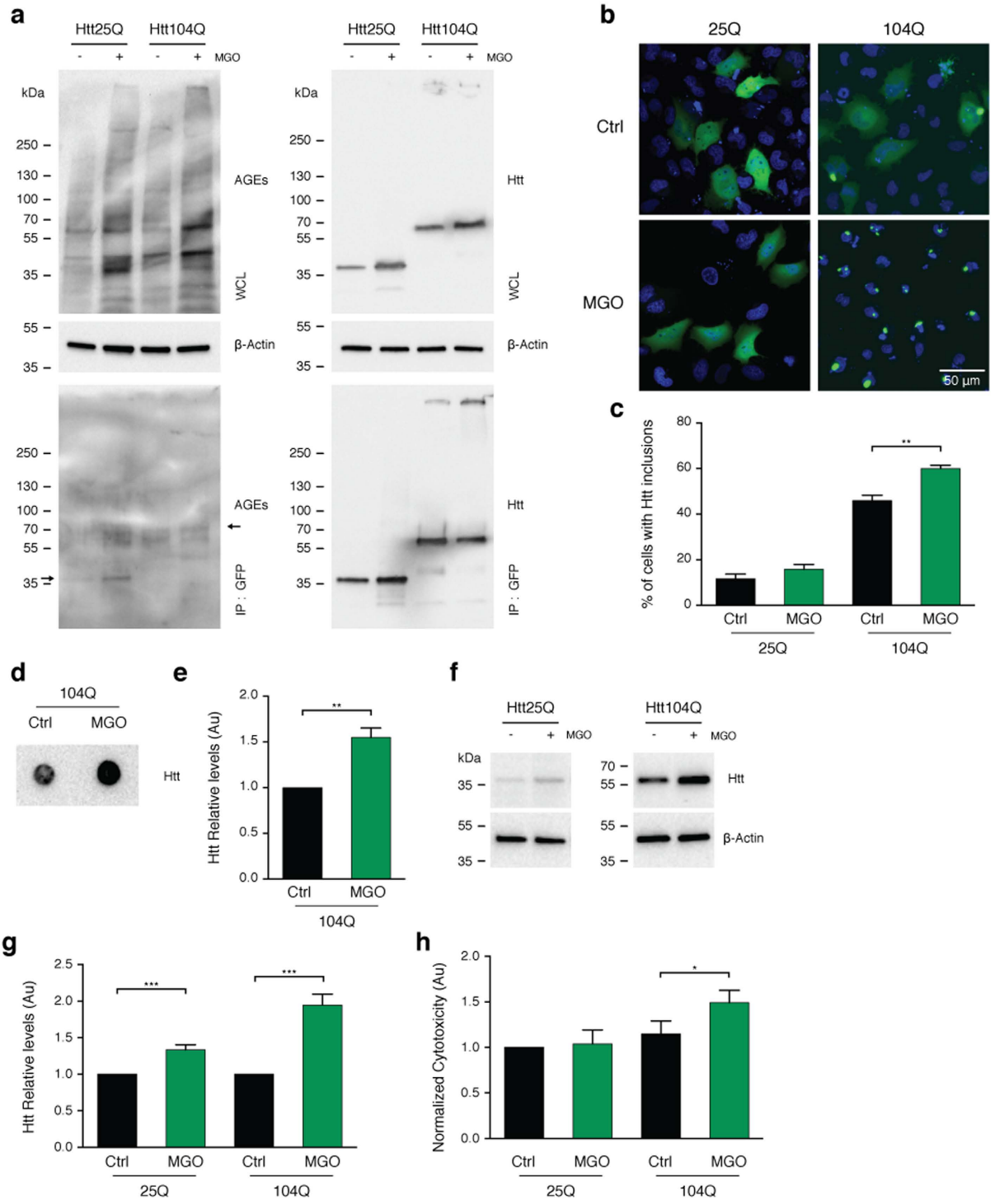

Figure 2. MGO induces HTT aggregation and toxicity in H4 cells. (a) Human H4 cells expressing HTT 25Q or 104Q were treated with vehicle (Ctrl) or MGO (0.5 mM) for 16 h. Cells were lysed and immunoprecipitated (IP) with GFP-trap (bottom panels). The whole cell lysates (WCL) and IP samples were probed for AGEs (left panels) or GFP (right panels). Arrow indicates HTT 25Q and HTT 104Q MW. Corresponding loading controls (β-actin) are presented (n = 3). **(b)** H4 cells expressing HTT 25Q or 104Q fused with GFP were treated with vehicle (Ctrl) or MGO (0.5 mM) for 16 h. After treatment, cells were probed with Hoechst and imaged *in vivo*. Fluorescence micrographs and **(c)** corresponding % of cells with HTT inclusions are presented. Scale barm 50 μm. **(d)** Representative filter trap assay and **(e)** corresponding HTT levels of cells expressing HTT 104Q treated with vehicle or MGO for 16 h and immunoblotted with an anti-GFP antibody. **(f)** Protein extracts were immunoblotted with an anti-GFP antibody. **(g)** The corresponding HTT levels are presented (at least n = 3 per condition). **(h)** Toxicity of vehicle (Ctrl) or MGO measured by LDH release (n = 3) and normalized to 25Q. Data in all panels are average ± SD, *$p < 0.05$, **$p < 0.01$, ***$p < 0.001$, ****$p < 0.0001$. For (**c,e,g,h**), unpaired two-tailed t-test with equal SD.

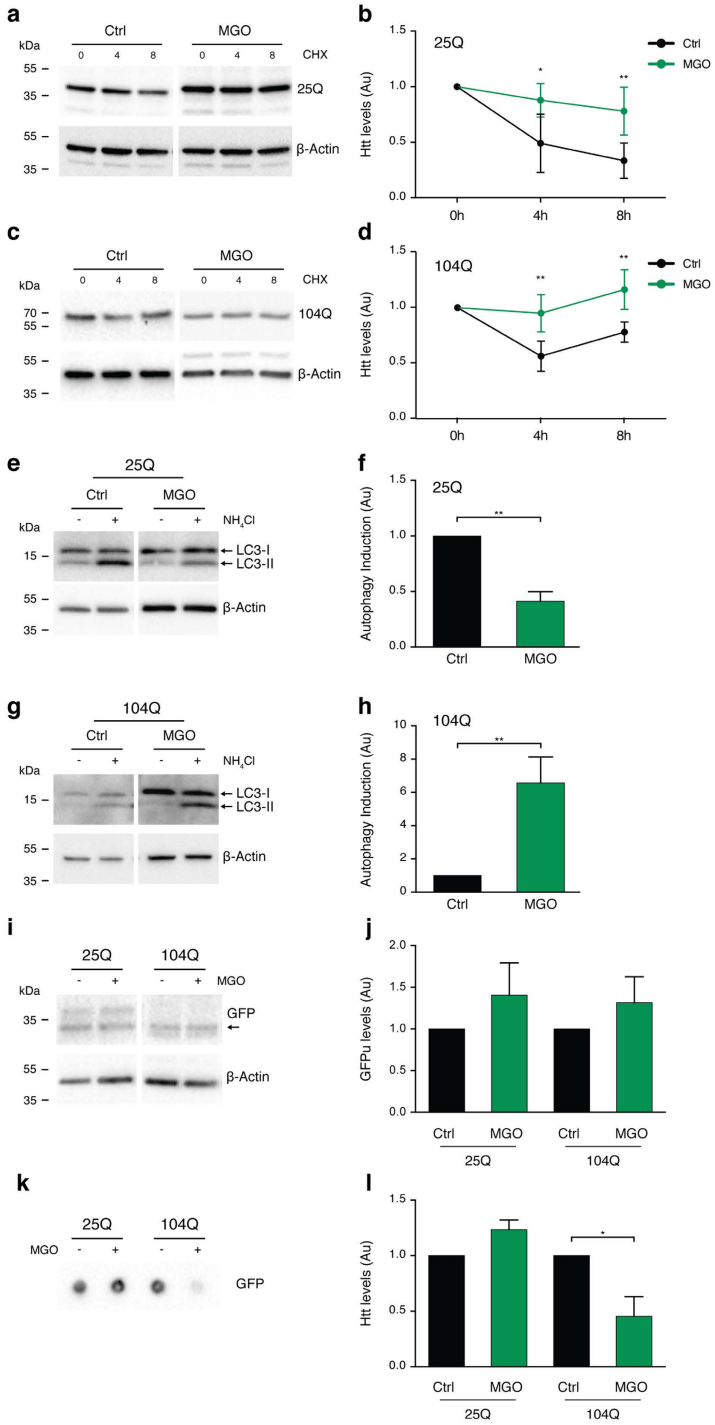

Figure 3. Glycation impairs HTT clearance. H4 cells expressing HTT 25Q (**a,b**) or 104Q **(c,d)** for 24 h were pre-treated with vehicle (Ctrl) or MGO (0.5 mM) for 16 h. Cells were treated with vehicle or MGO for 24 h together with CHX. Protein extracts were probed for GFP and β-actin, for normalization, and protein levels are presented (at least n = 3). HTT 25Q **(e,f)** and 104Q **(g,h)** expressing cells were pre-treated with vehicle (Ctrl) or MGO (0.5 mM) for 16 h. Cells were treated with vehicle or MGO for 2 h together with vehicle (−) or NH_4Cl (+). Protein extracts were probed for LC3 (I and II) and β-actin. LC3-II levels (lower band) were normalized to β-actin and as a metric for autophagy induction, the difference between NH_4Cl and vehicle treatments was calculated. The ratio between MGO and Ctrl is presented as autophagy induction ratio (at least n = 3). **(i)** HTT 25Q and GFPu 104Q and GFPu cells were treated with vehicle (−) or MGO (0.5 mM) (+) for 16 h. Protein extracts were probed for GFP and β-actin (at least n = 3). Arrow indicates GFPu. **(j)** Normalized GFPu levels are presented. **(k)** HTT 25Q or 104Q were treated with vehicle (−) or MGO (0.5 mM) (+) for 16h. Fresh media was conditioned for 6 h in the same cells (−) or (+) and probed in a dotblot system for GFP (n = 3). **(l)** Normalized Htt released levels are presented. Data in all panels are average ± SD, *p < 0.05, **p < 0.01. For (**b,d,f,h,j**), unpaired two-tailed t-test with equal SD.

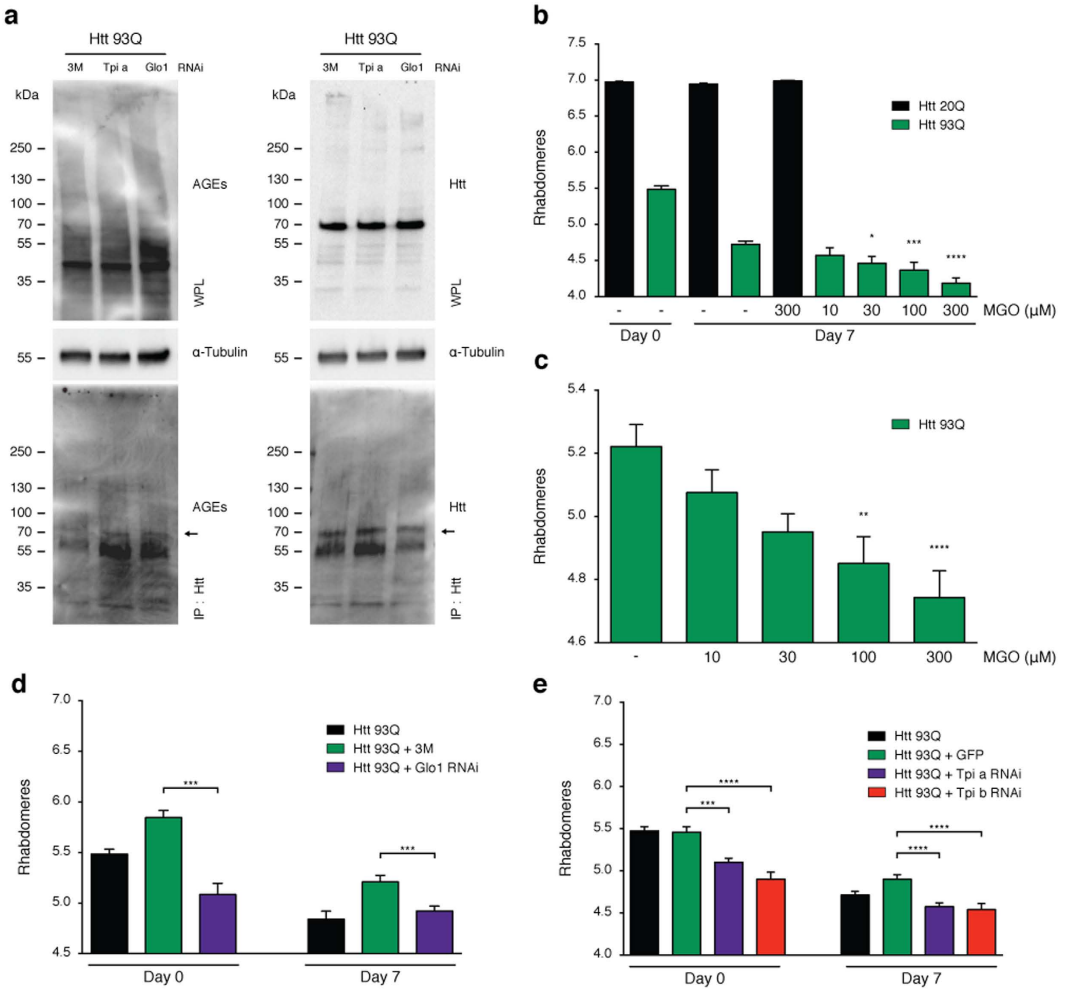

Figure 4. Knockdown of *Glo1* or *Tpi* induces neurotoxicity and decreases lifespan and survival in HTT93Q expressing flies. (a) 100 heads of flies expressing Htt93Q and knocked down for *Tpi*, *Glo1* or 3 M (as control) were lysed and immunoprecipitated with anti-HTT antibody (bottom panels). The whole protein lysates (WPL) (n = 3) and IP samples (n = 2) were probed for AGEs (left panels) or HTT (right panels). Arrow indicates HTT93Q MW. Corresponding loading controls (α-tubulin) are shown. **(b)** Adult flies expressing HTT93Q were treated with different concentrations of MGO. Quantification of mean rhabdomeres per ommatidium is presented. **(c)** Flies were treated during development with MGO. Quantification of rhabdomeres per ommatidium upon eclosion is presented. Number of rhabdomeres per ommatidium in HTT expressing flies with pan-neuronal knockdown of *Glo1* **(d)** or *Tpi* **(e)** is presented at day 0 or 7 post-eclosion. *3M + Htt93Q* and *GFP + Htt93Q* were used as titration controls for *Glo1* and *Tpi* silencing lines, respectively. Data in all panels are mean ± SEM, *$p < 0.05$, **$p < 0.01$, ***$p < 0.001$, ****$p < 0.0001$; one-way ANOVA with Newman-Keuls post-hoc test.

neurons (rhabdomeres), and impaired emergence of the adult fly from the pupal case (eclosion)[36,37]. We manipulated glycation in fruit flies either via MGO administration or genetic knockdown of either *Glo1* or *Tpi*. Importantly, silencing of *Tpi* or *Glo1* in flies expressing HTT93Q displayed an overall increase in glycation and an increase in the levels of AGEs (Fig. 4a). Adult HTT93Q-expressing flies displayed a dose-dependent reduction in the number of rhabdomeres per ommatidium when treated with MGO for 7 days (Fig. 4b). Moreover, we found that treatment of HTT93Q larvae during development with MGO resulted in a significant reduction in the number of rhabdomeres upon eclosion (Fig. 4c). RNAi knockdown of either *Glo1* or *Tpi* in WT flies did not modulate neurodegeneration (Fig. S3). However, in HTT93Q expressing flies, knockdown of either *Glo1* or *Tpi* caused a significant increase in neurodegeneration of rhabdomeres at both 0 and 7 days after eclosion (Fig. 4d,e) when compared to their relative titration controls. Remarkably, we observed a significant reduction in the percentage of eclosion in both *Glo1* and *Tpi* knockdown lines (Fig. 5a,b) and a 6-day reduction in the lifespan in the *Glo1* knockdown line (Fig. 5c,d). These results strongly suggest that glycation can act as an important environmental modifier of HTT toxicity and HD.

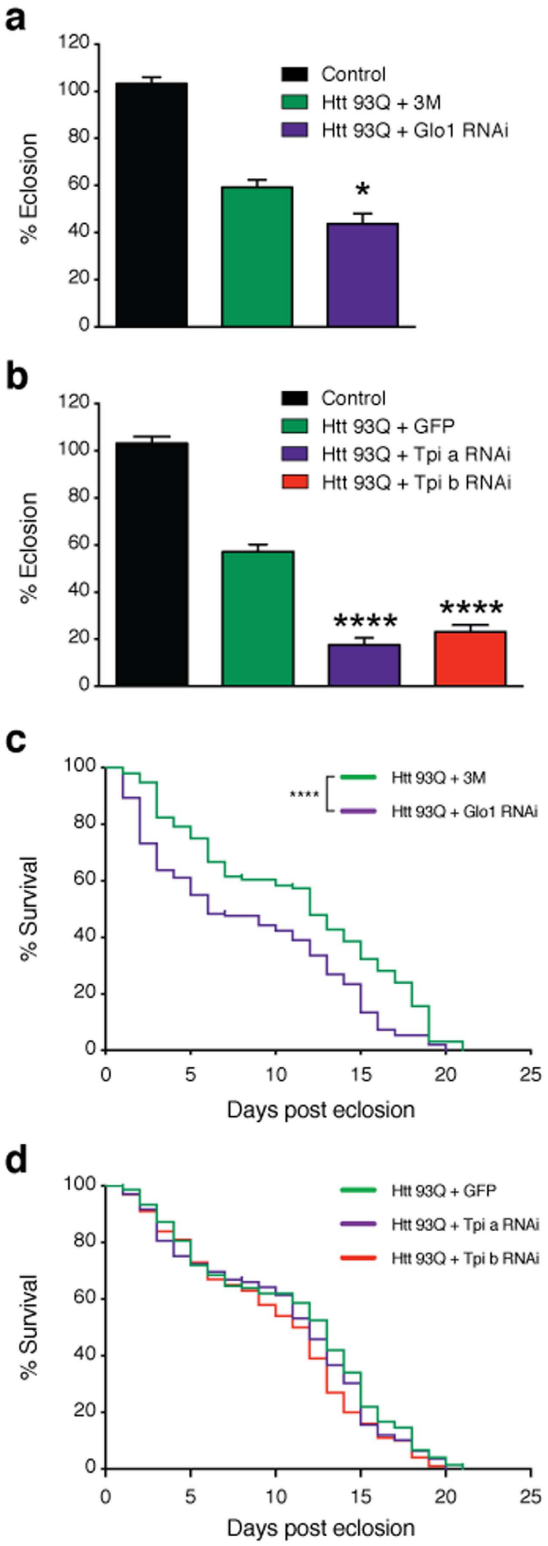

Figure 5. Knockdown of *Glo1* or *Tpi* impairs development and reduces lifespan in flies. RNAi silencing of *Glo1* **(a)** or *Tpi* **(b)** caused a reduction in the percentage of flies emerging from the pupal case. Flies carrying a single copy of the driver (*elavGAL4*) are shown as a control. Data in panels (**a,b**) are mean ± SEM. Survival rate was evaluated in flies with pan-neuronal knockdown of *Glo1* **(c)** or *Tpi* **(d)** in mutant HTT backgrounds (n = 100–150 flies per genotype). *3M* + *Htt93Q* and *GFP* + *Htt93Q* were used in experiments as titration controls for *GloI* and *Tpi* silencing lines, respectively. *Htt93Q* + *Glo1* RNAi (mean = 6); *Htt93Q* + *3M* (mean = 12); *Htt93Q* + *Tpi* a RNAi (mean = 12); *Htt93Q* + *Tpi* b RNAi (mean = 11.5); *Htt93Q* + GFP (mean = 13). *$p < 0.05$, **$p < 0.01$, ****$p < 0.0001$; for (**a,b**) Ordinary one-way ANOVA with Newman-Keuls multiple comparisons test; for (**c,d**) Log-rank (Mantel-Cox) test.

Discussion

The precise mechanisms through which HTT mutations cause HD are still unknown. However, accumulation of HTT plays an important role in the disease and strategies aimed at reducing its levels constitute attractive strategies for therapeutic intervention and are currently being explored in ongoing clinical trials[38].

Different posttranslational modifications (PTMs) are known to modulate the levels, aggregation propensity and clearance of HTT, and could play a role in the development of HD[39–41]. For example, phosphorylation of HTT on Ser13 and Ser16 is protective in mouse models of HD[42] enhancing the clearance of HTT via the proteasome and chaperone-mediated autophagy[43]. Acetylation of Lys9 and Lys444 promotes HTT clearance via the autophagy lysosome pathway (ALP)[44]. On the other hand, SUMOylation leads to HTT accumulation and translocation into the nucleus[45].

Using established yeast, mammalian cell and fly models of HD, we found that both pharmacological and genetic induction of glycation plays a deleterious role in HD models by decreasing HTT clearance, increasing the intracellular levels of HTT and enhancing its aggregation and toxicity, either directly or indirectly (through the increase in the levels of HTT). Impaired clearance of HTT via the proteasome was previously associated with HD[2]. Strikingly, we observed different effects of glycation on normal (25Q) vs. mutant (104Q) HTT variants. While glycation impaired the activation of the ALP system in cells expressing HTT25Q, we observed increased activation of the ALP system in cells expressing HTT104Q. Although we cannot completely exclude an indirect effect of general protein glycation, we clearly observed distinct phenotypes between 25Q and 104Q HTT. The increased ALP activation suggests a compensatory mechanism for the cell to cope with aggregated HTT that is normally cleared via the ALP system[46,47].

Diabetes is a risk factor for neurodegenerative diseases such as Alzheimer's and Parkinson's[8,9]. A major consequence of diabetes is glucose metabolism imbalance and consequent hyperglycemia. Glucose and its byproducts have the ability to react with amino groups, forming AGEs that can impact the function of target proteins. Glycation exacerbates the accumulation, aggregation and toxicity of Aβ and α-synuclein[8,48]. Therefore, it is reasonable to hypothesize that glycation might constitute a common mechanism contributing to the development of neurodegenerative diseases by acting as a "second hit" that tips the proteostasis balance of cells, causing dysfunction of multiple essential cellular pathways, and leading to premature death. Interestingly, and in agreement with our hypothesis, drugs used for the treatment of diabetes were already shown to be protective in HD. For example, metformin was shown to prolong the survival of HD male mice[49]. In addition, exendin-4 decreased HTT aggregation, suppressed cellular pathology in both brain and pancreas, improved motor function, and extended survival in a mouse model of HD[50]. In fact, the prevalence of diabetes is higher in HD patients[51,52]. Mouse models of HD develop hyperglycemia[53,54], possibly due to the accumulation of intranuclear HTT inclusions in pancreatic β cells that produce insulin[55,56]. Consistently, HD brains differentially express several proteins linked to type-2 diabetes[57]. However, whether diabetes is a contributing factor to pathogenesis or a consequence of HD is still unclear, as is the role of HTT glycation.

Although activation of autophagy could clear aggregated proteins and is considered an important therapeutic approach for several neurodegenerative disorders[58], autophagy could also lead to neuronal death. Overactivation of ALP can lead to apoptosis or autophagic cell death[59]. Therefore, promoting glycation in HTT104Q expressing cells might account for the observed increase in HTT cytotoxicity by overactivating the ALP.

We did not observe alterations in the UPS, suggesting that, under the conditions tested, glycation does not affect HTT clearance by the proteasome. Interestingly, we observed that glycation reduces the release of HTT104Q, which may account for the observed intracellular accumulation of HTT104Q, increased aggregation and toxicity.

In vivo, feeding of mutant HTT exon-1-expressing flies with MGO, reduced the number of rhabdomeres per omatidium, demonstrating a dose-dependent and selective effect. The deleterious effect of MGO was also observed in a reduction of eclosion, suggesting that glycation exacerbates HTT-toxicity during development. Importantly, genetic manipulation of pathways controlling MGO levels, through *Glo1* or *Tpi1* knockdown, also resulted in increased neurotoxicity of mutant HTT93Q, and reduced survival. In *Tpi* RNAi flies, we observed a significant reduction in eclosion, and in *Glo1* RNAi flies we observed a significant reduction in eclosion and survival rate. Altogether, our data clearly suggest that increased glycation exacerbates the toxicity of mutant HTT, and that this can occur already during developmental stages.

In this study we demonstrate for the first time that glycation plays an important role in HTT homeostasis, contributing to its neurotoxicity, accumulation and aggregation, as well as potentiating several disease-relevant phenotypes in a *Drosophila* model of HD (Fig. 6). Therefore, we hypothesize that hyperglycemia, and the unavoidable glycation of proteins including HTT, may not only be a consequence but also a contributing factor in HD pathogenesis.

Interestingly, we recently showed that DJ-1 overexpression protects against HTT toxicity in yeast and fruit flies[25]. Although mutations in the DJ-1 gene are associated with recessive forms of Parkinson's disease, DJ-1 was recently described as an anti-MGO enzyme with glyoxalase activity[60]. Moreover, DJ-1 was also suggested to act as a protein deglycase that repairs MGO-glycated proteins[61]. These findings are consistent with our study, further supporting a connection between protein glycation and HD. Altogether, our study suggests that glycation might contribute to HTT dysfunction and that modulation of glycation may constitute a novel target for therapeutic intervention in HD.

Materials and Methods

HTT protein levels and aggregation in yeast. The parental *Saccharomyces cerevisiae* strain BY4741 (*MAT a*, *his3*Δ, *leu2*Δ, *met15*Δ, *ura3*Δ), and deletion mutants *glo1*Δ and *tpi*Δ strains were used (Euroscarf collection). Cells were grown and transformed as in ref. 13 using GFP fusion constructs with a mutant HTT fragment with an expanded polyQ stretch of either 25, 72 or 103 in p416 vector under the regulation of the GPD

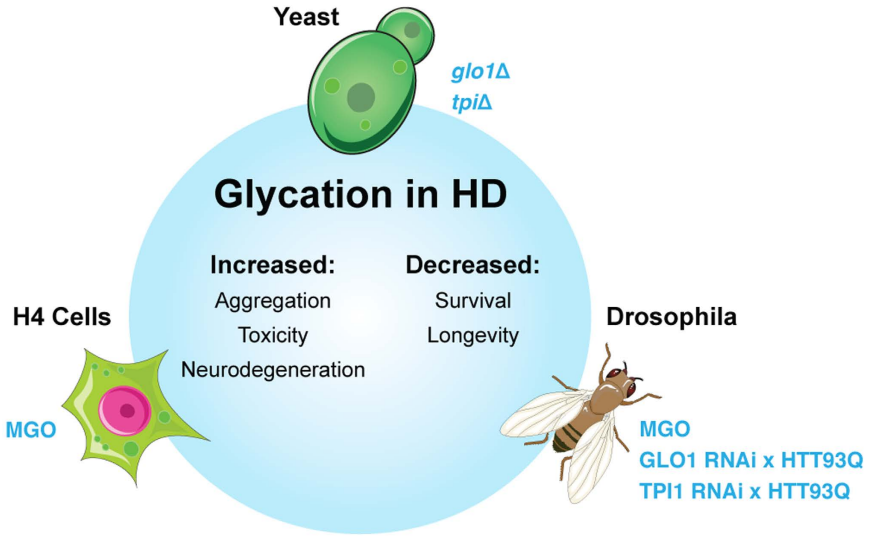

Figure 6. Schematic representation of the effects of MGO glycation in models of HD. Glycation increases HTT intracellular levels and inclusion formation in yeast and H4. Ultimately, it increases HTT-dependent toxicity, leading to neurodegeneration and reduced viability and lifespan in flies.

promoter as in ref. 26. Protein extraction was performed as in ref. 13. Fluorescence microscopy was performed using a Zeiss Axiovert 200 M.

MGO purification. MGO was produced as described in ref. 14.

Immunoprecipitation, microscopy, immunoblotting, toxicity, viability and aggregation assays. H4 neuroglioma cells were maintained, grown and transfected with HTT exon-1 fragments with a polyQ expansions of either 25 or 104 fused to GFP as in ref. 26. Twenty-four hours after HTT25Q or HTT104Q transfection, cells in 35 mm imaging dishes (Ibidi), 60 mm or 100 mm dishes (Corning) were treated with vehicle (PBS) or MGO (0.5 mM) for 16 h. Total protein lysates were obtained as in ref. 13. Htt was immunoprecipitated using GFP-trap (Chromotek) according to the manufacturer instructions. Widefield fluorescent microscope Zeiss Axiovert 200 M (Carl Zeiss MicroImaging) or point scanning confocal microscope Zeiss LSM 710 (Carl Zeiss MicroImaging) were used to visualize HTT inclusions. Immunobloting was performed according to standard procedures as in ref. 13 using the following antibodies: anti GFP (NeuroMab, P42212, 1:3000); anti AGEs (Cosmobio, KAL-KH-001, 1:500); anti LC3 (Nano Tools, 0260-100/LC3-2G6, 1:2000) and anti β-actin (Ambion, AM4302, 1:5000). Cytotoxicity was measured by means of the LDH kit (Clontech), following manufacturer´s instructions. Cell viability was determined using the MTT assay according to standard procedures. Evaluation of HTT aggregation profiles by filter retardation assay was performed as in ref. 62. Briefly, cellulose acetate membranes retain aggregates that are not soluble in SDS (1%) and that are larger than 0.22 μm.

HTT clearance assay. For CHX chase experiments, H4 cells were transfected as previously[13] with either HTT25Q or HTT104Q. After 24 h, cells were treated with vehicle (PBS) or MGO (0.5 mM) for 16 h. Media was renewed and cells re-challenged with vehicle or MGO for 24 h in the presence of CHX (100 μM, added at given time points). Protein extracts were immunobloted. Proteasome impairment was assessed as the amount of GFPu accumulation. H4 cells were cotransfected with E.V. with GFPu; HTT25Q with GFPu or HTT104Q with GFPu. 24 h post transfection, media was renewed and cells treated with vehicle (PBS) or MGO (0.5 mM) for 16 h and processed for immunobloting with anti-GFP antibody (NeuroMab, P42212). As positive control, H4 cells were transfected with GFPu and treated with increasing concentrations of MG132 for 24 hours. GFPu average fluorescence level was analyzed by epifluorescence microscopy. For autophagy impairment studies, H4 cells were transfected with HTT25Q or HTT104Q. 24 h post transfection, media was renewed and cells treated for 16 h with vehicle (PBS) or MGO (0.5 mM). Media was again renewed and cells were re-challenged with vehicle or MGO during autophagy blockage with ammonium chloride (20 mM) for 2 h. Autophagy activity was measured as the amount of accumulated LC3-II after treatment with autophagy blockers[33]. For HTT release studies, H4 cells, transfected with HTT25Q or HTT104Q for 24 h were treated with MGO (0.5 mM) for 16 h. Media was renewed, and cells were again treated with MGO (0.5 mM) for 6 h, media collected, applied onto nitrocellulose membranes (0.22 μm, Millipore) using a dot blot apparatus, and immunobloted with anti-GFP by standard procedures.

Drosophila lines. Flies were raised at 25 °C in LD12:12 on standard maize food. The *elav-GAL4* (c155) and *w; UASeGFP*; + (5431) lines were obtained from the Bloomington Stock Center (Bloomington, Indiana). The *w; +; UASHTT93Q* and *w; +; UASHTT20Q* transgenic line was kindly provided by J. Lawrence Marsh and Leslie Thompson (University of California, Irvine)[35]. RNAi transgenic lines were obtained from the Vienna *Drosophila* RNAi Center (VDRC). For *Glo1* knockdown, the 101560 line from the KK Library (phiC31-based transgenes at

a single, defined site) was used. For *Tpi* knockdown, two lines were employed from the GD Library (P-element based, random insertion sites): 25643 and 25644. The *UASeGFP* and *w; 3M; +* (carrying an empty vector located in the KK site) lines were used in the experiment as titration controls.

Immunoprecipitation of HTT expressed in flies. Flies were processed for IP 7 days post-eclosion. Briefly, heads were separated using standard procedures, and protein extracts prepared by vigorous homogenization with a tissue grinder followed by liquid nitrogen freeze and thaw cycles. 750 μg of protein were used for IP, as we previously described[63]. 10 μl per IP of anti Htt antibody was used (Millipore, MAB5374). IP and whole protein lysate (WPL) were probed using anti AGEs (Cosmobio, KAL-KH-001, 1:500); anti-Htt (Millipore, MAB5374, 1:1000) and anti α-tubulin (Sigma, T5168, 1:15000).

Drosophila eclosion and longevity assays. Eclosion of fly lines was assessed as previously described in ref. 64. Male flies carrying the *elavGAL4* driver were crossed to virgin females carrying the UASHTT93Q transgene in order to generate females expressing HTT93Q and control males in the F1 generation. 10–35 crosses were set up in separate vials for each condition and parental flies were removed 5 days after mating. The number of female or male progeny emerging was scored over 10 days post-eclosion and the percentage of eclosion per vial was calculated using the following ratio: (number of female/number of male flies) × 100. For longevity assays, newly emerged female flies of the desired genotype were collected and kept in groups of 10 in separate vials. Flies were moved to fresh food every 2–3 days and the number of dead individuals scored daily.

Treatment of Drosophila with MGO. MGO was dissolved in H_2O and added to standard maize media at the required doses (10, 30, 100 or 300 μM). For treatment during development, crosses were set up and flies were grown on standard maize media previously supplemented with MGO. Flies expressing the desired genotype were collected upon eclosion and analyzed for both eclosion percentage and rhabdomere number. For adult feeding experiments, newly emerged flies were transferred to MGO-supplemented food and moved daily to fresh vials with appropriate MGO treatment concentration. Rhabdomeres were scored in flies fed with different concentrations of MGO during 7 days, newly emerged untreated flies and 7 days-old untreated flies.

Pseudopupil analysis. The number of visible rhabdomeres per ommatidium was measured as described in ref. 37. Briefly, the number of rhabdomeres was scored for a minimum of 50 ommatidia per fly, in at least 12 flies per condition at day 0 or 7 post-eclosion. Heads from adult flies were removed and fixed to glass slides using clear fingernail polish and rhabdomeres were examined at 500X magnification using an Olympus BH2 light microscope.

References

1. MacDonald, M. E. *et al.* A novel gene containing a trinucleotide repeat that is expanded and unstable on Huntington's disease chromosomes. *Cell* **72,** 971–983, doi: http://dx.doi.org/10.1016/0092-8674(93)90585-E (1993).
2. Labbadia, J. & Morimoto, R. I. Huntington's disease: underlying molecular mechanisms and emerging concepts. *Trends in biochemical sciences* **38,** 378–385, doi: 10.1016/j.tibs.2013.05.003 (2013).
3. Munoz-Sanjuan, I. & Bates, G. P. The importance of integrating basic and clinical research toward the development of new therapies for Huntington disease. *The Journal of clinical investigation* **121,** 476–483, doi: 10.1172/JCI45364 (2011).
4. Walker, F. O. Huntington's disease. *Lancet* **369,** 218–228, doi: 10.1016/S0140-6736(07)60111-1 (2007).
5. Li, S. H. & Li, X. J. Aggregation of N-terminal huntingtin is dependent on the length of its glutamine repeats. *Human molecular genetics* **7,** 777–782 (1998).
6. Javed, S., Petropoulos, I. N., Alam, U. & Malik, R. A. Treatment of painful diabetic neuropathy. *Ther Adv Chronic Dis* **6,** 15–28, doi: 10.1177/2040622314552071 (2015).
7. Schreiber, A. K., Nones, C. F., Reis, R. C., Chichorro, J. G. & Cunha, J. M. Diabetic neuropathic pain: Physiopathology and treatment. *World J Diabetes* **6,** 432–444, doi: 10.4239/wjd.v6.i3.432 (2015).
8. Vicente Miranda, H., El-Agnaf, O. M. & Outeiro, T. F. Glycation in Parkinson's disease and Alzheimer's disease. *Mov Disord*, doi: 10.1002/mds.26566 (2016).
9. Vicente Miranda, H. & Outeiro, T. F. The sour side of neurodegenerative disorders: the effects of protein glycation. *The Journal of pathology* **221,** 13–25, doi: 10.1002/path.2682 (2010).
10. Richard, J. P. Kinetic parameters for the elimination reaction catalyzed by triosephosphate isomerase and an estimation of the reaction's physiological significance. *Biochemistry* **30,** 4581–4585 (1991).
11. Guix, F. X. *et al.* Amyloid-dependent triosephosphate isomerase nitrotyrosination induces glycation and tau fibrillation. *Brain* **132,** 1335–1345, doi: 10.1093/brain/awp023 (2009).
12. Orosz, F., Olah, J. & Ovadi, J. Triosephosphate isomerase deficiency: new insights into an enigmatic disease. *Biochim Biophys Acta* **1792,** 1168–1174, doi: 10.1016/j.bbadis.2009.09.012 (2009).
13. Vicente Miranda, H. *et al.* Heat-mediated enrichment of alpha-synuclein from cells and tissue for assessing post-translational modifications. *Journal of neurochemistry* **126,** 673–684, doi: 10.1111/jnc.12251 (2013).
14. Gomes, R. A. *et al.* Protein glycation in Saccharomyces cerevisiae. Argpyrimidine formation and methylglyoxal catabolism. *FEBS J* **272,** 4521–4531, doi: 10.1111/j.1742-4658.2005.04872.x (2005).
15. Ciriacy, M. & Breitenbach, I. Physiological effects of seven different blocks in glycolysis in Saccharomyces cerevisiae. *J Bacteriol* **139,** 152–160 (1979).
16. Hollan, S. *et al.* Hereditary triosephosphate isomerase (TPI) deficiency: two severely affected brothers one with and one without neurological symptoms. *Hum Genet* **92,** 486–490 (1993).
17. Phillips, S. A. & Thornalley, P. J. The formation of methylglyoxal from triose phosphates. Investigation using a specific assay for methylglyoxal. *Eur J Biochem* **212,** 101–105 (1993).
18. Ahmed, N. *et al.* Increased formation of methylglyoxal and protein glycation, oxidation and nitrosation in triosephosphate isomerase deficiency. *Biochim Biophys Acta* **1639,** 121–132 (2003).
19. Correia, K. *et al.* The Genetic Modifiers of Motor OnsetAge (GeM MOA) Website: Genome-wide Association Analysis for Genetic Modifiers of Huntington's Disease. *Journal of Huntington's disease* **4,** 279–284, doi: 10.3233/JHD-150169 (2015).
20. Lee, J.-M. *et al.* Identification of Genetic Factors that Modify Clinical Onset of Huntington's Disease. *Cell* **162,** 516–526, doi: http://dx.doi.org/10.1016/j.cell.2015.07.003 (2015).

21. Mo, C., Hannan, A. J. & Renoir, T. Environmental factors as modulators of neurodegeneration: insights from gene-environment interactions in Huntington's disease. *Neuroscience and biobehavioral reviews* **52,** 178–192, doi: 10.1016/j.neubiorev.2015.03.003 (2015).
22. van Dellen, A. & Hannan, A. J. Genetic and environmental factors in the pathogenesis of Huntington's disease. *Neurogenetics* **5,** 9–17, doi: 10.1007/s10048-003-0169-5 (2004).
23. Ma, L. & Nicholson, L. F. Expression of the receptor for advanced glycation end products in Huntington's disease caudate nucleus. *Brain research* **1018,** 10–17, doi: 10.1016/j.brainres.2004.05.052 (2004).
24. Anzilotti, S. *et al.* Immunohistochemical localization of receptor for advanced glycation end (RAGE) products in the R6/2 mouse model of Huntington's disease. *Brain Res Bull* **87,** 350–358, doi: 10.1016/j.brainresbull.2011.01.009 (2012).
25. Sajjad, M. U. *et al.* DJ-1 modulates aggregation and pathogenesis in models of Huntington's disease. *Human molecular genetics* **23,** 755–766, doi: 10.1093/hmg/ddt466 (2014).
26. Krobitsch, S. & Lindquist, S. Aggregation of huntingtin in yeast varies with the length of the polyglutamine expansion and the expression of chaperone proteins. *Proceedings of the National Academy of Sciences of the United States of America* **97,** 1589–1594 (2000).
27. Duennwald, M. L., Jagadish, S., Muchowski, P. J. & Lindquist, S. Flanking sequences profoundly alter polyglutamine toxicity in yeast. *Proceedings of the National Academy of Sciences of the United States of America* **103,** 11045–11050, doi: 10.1073/pnas.0604547103 (2006).
28. Meriin, A. B. *et al.* Aggregation of expanded polyglutamine domain in yeast leads to defects in endocytosis. *Molecular and cellular biology* **23,** 7554–7565 (2003).
29. Herrera, F., Tenreiro, S., Miller-Fleming, L. & Outeiro, T. F. Visualization of cell-to-cell transmission of mutant huntingtin oligomers. *PLoS Curr* **3,** RRN1210, doi: 10.1371/currents.RRN1210 (2011).
30. Chang, T. J. *et al.* Glucagon-like peptide-1 prevents methylglyoxal-induced apoptosis of beta cells through improving mitochondrial function and suppressing prolonged AMPK activation. *Sci Rep* **6,** 23403, doi: 10.1038/srep23403 (2016).
31. Hansen, F. *et al.* Methylglyoxal and carboxyethyllysine reduce glutamate uptake and S100B secretion in the hippocampus independently of RAGE activation. *Amino Acids* **48,** 375–385, doi: 10.1007/s00726-015-2091-1 (2016).
32. Nass, N. *et al.* Differential response to alpha-oxoaldehydes in tamoxifen resistant MCF-7 breast cancer cells. *PLoS One* **9,** e101473, doi: 10.1371/journal.pone.0101473 (2014).
33. Klionsky, D. J. *et al.* Guidelines for the use and interpretation of assays for monitoring autophagy (3rd edition). *Autophagy* **12,** 1–222, doi: 10.1080/15548627.2015.1100356 (2016).
34. Bence, N. F., Sampat, R. M. & Kopito, R. R. Impairment of the ubiquitin-proteasome system by protein aggregation. *Science* **292,** 1552–1555, doi: 10.1126/science.292.5521.1552 (2001).
35. Steffan, J. S. *et al.* Histone deacetylase inhibitors arrest polyglutamine-dependent neurodegeneration in Drosophila. *Nature* **413,** 739–743, doi: 10.1038/35099568 (2001).
36. Green, E. W. & Giorgini, F. Choosing and using Drosophila models to characterize modifiers of Huntington's disease. *Biochem Soc Trans* **40,** 739–745, doi: 10.1042/BST20120072 (2012).
37. Mason, R. P. *et al.* Glutathione peroxidase activity is neuroprotective in models of Huntington's disease. *Nature genetics* **45,** 1249–1254, doi: 10.1038/ng.2732 (2013).
38. Wild, E. J. & Tabrizi, S. J. Targets for future clinical trials in Huntington's disease: what's in the pipeline? *Mov Disord* **29,** 1434–1445, doi: 10.1002/mds.26007 (2014).
39. Ehrnhoefer, D. E., Sutton, L. & Hayden, M. R. Small changes, big impact: posttranslational modifications and function of huntingtin in Huntington disease. *The Neuroscientist: a review journal bringing neurobiology, neurology and psychiatry* **17,** 475–492, doi: 10.1177/1073858410390378 (2011).
40. Krainc, D. Huntington's disease: tagged for clearance. *Nature medicine* **16,** 32–33, doi: 10.1038/nm0110-32 (2010).
41. Saudou, F. & Humbert, S. The Biology of Huntingtin. *Neuron* **89,** 910–926, doi: 10.1016/j.neuron.2016.02.003 (2016).
42. Gu, X. *et al.* Serines 13 and 16 are critical determinants of full-length human mutant huntingtin induced disease pathogenesis in HD mice. *Neuron* **64,** 828–840, doi: 10.1016/j.neuron.2009.11.020 (2009).
43. Thompson, L. M. *et al.* IKK phosphorylates Huntingtin and targets it for degradation by the proteasome and lysosome. *The Journal of cell biology* **187,** 1083–1099, doi: 10.1083/jcb.200909067 (2009).
44. Jeong, H. *et al.* Acetylation targets mutant huntingtin to autophagosomes for degradation. *Cell* **137,** 60–72, doi: 10.1016/j.cell.2009.03.018 (2009).
45. Wang, Y., Lin, F. & Qin, Z. H. The role of post-translational modifications of huntingtin in the pathogenesis of Huntington's disease. *Neuroscience bulletin* **26,** 153–162, doi: 10.1007/s12264-010-1118-6 (2010).
46. Nixon, R. A. The role of autophagy in neurodegenerative disease. *Nature medicine* **19,** 983–997, doi: 10.1038/nm.3232 (2013).
47. Yamamoto, A., Cremona, M. L. & Rothman, J. E. Autophagy-mediated clearance of huntingtin aggregates triggered by the insulin-signaling pathway. *The Journal of cell biology* **172,** 719–731, doi: 10.1083/jcb.200510065 (2006).
48. Li, X. H. *et al.* Glycation exacerbates the neuronal toxicity of beta-amyloid. *Cell death & disease* **4,** e673, doi: 10.1038/cddis.2013.180 (2013).
49. Ma, T. C. *et al.* Metformin therapy in a transgenic mouse model of Huntington's disease. *Neuroscience letters* **411,** 98–103, doi: 10.1016/j.neulet.2006.10.039 (2007).
50. Martin, B. *et al.* Exendin-4 improves glycemic control, ameliorates brain and pancreatic pathologies, and extends survival in a mouse model of Huntington's disease. *Diabetes* **58,** 318–328, doi: 10.2337/db08-0799 (2009).
51. Farrer, L. A. Diabetes mellitus in Huntington disease. *Clinical genetics* **27,** 62–67 (1985).
52. Podolsky, S., Leopold, N. A. & Sax, D. S. Increased frequency of diabetes mellitus in patients with Huntington's chorea. *Lancet* **1,** 1356–1358 (1972).
53. Hurlbert, M. S. *et al.* Mice transgenic for an expanded CAG repeat in the Huntington's disease gene develop diabetes. *Diabetes* **48,** 649–651 (1999).
54. Jenkins, B. G. *et al.* Nonlinear decrease over time in N-acetyl aspartate levels in the absence of neuronal loss and increases in glutamine and glucose in transgenic Huntington's disease mice. *Journal of neurochemistry* **74,** 2108–2119 (2000).
55. Andreassen, O. A. *et al.* Huntington's disease of the endocrine pancreas: insulin deficiency and diabetes mellitus due to impaired insulin gene expression. *Neurobiology of disease* **11,** 410–424 (2002).
56. Bjorkqvist, M. *et al.* The R6/2 transgenic mouse model of Huntington's disease develops diabetes due to deficient beta-cell mass and exocytosis. *Human molecular genetics* **14,** 565–574, doi: 10.1093/hmg/ddi053 (2005).
57. Schonberger, S. J., Jezdic, D., Faull, R. L. & Cooper, G. J. Proteomic analysis of the human brain in Huntington's Disease indicates pathogenesis by molecular processes linked to other neurodegenerative diseases and to type-2 diabetes. *Journal of Huntington's disease* **2,** 89–99, doi: 10.3233/JHD-120044 (2013).
58. Harris, H. & Rubinsztein, D. C. Control of autophagy as a therapy for neurodegenerative disease. *Nature reviews. Neurology* **8,** 108–117, doi: 10.1038/nrneurol.2011.200 (2012).
59. Puyal, J., Ginet, V., Grishchuk, Y., Truttmann, A. C. & Clarke, P. G. Neuronal autophagy as a mediator of life and death: contrasting roles in chronic neurodegenerative and acute neural disorders. *The Neuroscientist: a review journal bringing neurobiology, neurology and psychiatry* **18,** 224–236, doi: 10.1177/1073858411404948 (2012).

60. Lee, J. Y. *et al.* Human DJ-1 and its homologs are novel glyoxalases. *Human molecular genetics* **21,** 3215–3225, doi: 10.1093/hmg/dds155 (2012).
61. Richarme, G. *et al.* Parkinsonism-associated protein DJ-1/Park7 is a major protein deglycase that repairs methylglyoxal- and glyoxal-glycated cysteine, arginine, and lysine residues. *The Journal of biological chemistry* **290,** 1885–1897, doi: 10.1074/jbc.M114.597815 (2015).
62. Herrera, F. & Outeiro, T. F. Alpha-Synuclein modifies huntingtin aggregation in living cells. *FEBS letters* **586,** 7–12, doi: 10.1016/j.febslet.2011.11.019 (2012).
63. Guerreiro, P. S. *et al.* LRRK2 interactions with alpha-synuclein in Parkinson's disease brains and in cell models. *J Mol Med* (*Berl*) **91,** 513–522, doi: 10.1007/s00109-012-0984-y (2013).
64. Breda, C. *et al.* Tryptophan-2,3-dioxygenase (TDO) inhibition ameliorates neurodegeneration by modulation of kynurenine pathway metabolites. *Proceedings of the National Academy of Sciences of the United States of America* **113,** 5435–5440, doi: 10.1073/pnas.1604453113 (2016).

Acknowledgements

We thank Professor Rui Moreira and Dr. Susana Lucas for MGO purification. Authors were supported by: HVM (Fundação para a Ciência e Tecnologia (FCT), Portugal SFRH/BPD/64702/2009 and SFRH/BPD/109347/2015); JBS (SFRH/BD/85275/2012); FH (SFRH/BPD/63530/2009 and IF/00094/2013); TFO (EMBO Installation Grant; Marie Curie IRG, Neurofold). TFO is supported by the DFG Center for Nanoscale Microscopy and Molecular Physiology of the Brain (CNMPB). FG is supported by grants from the Medical Research Council (MRC) and the CHDI Foundation, Inc.

Author Contributions

Yeast experiments were designed by H.V.M. and T.F.O., performed by H.V.M. and M.A.G. and analyzed by H.V.M., M.A.G. and T.F.O. H4 experiments were designed by H.V.M. and T.F.O., performed by H.V.M., M.A.G. and D.F.L. and analyzed by H.V.M., M.A.G., L.V.L. and T.F.O. *Drosophila* experiments were designed by H.V.M., F.G. and T.F.O., performed by J.B.S., C.B. and H.V.M. and analyzed by H.V.M., J.B.S., C.B., F.H., F.G. and T.F.O. H.V.M. and T.F.O. wrote the manuscript. All authors proofread the manuscript.

Additional Information

Supplementary information accompanies this paper at http://www.nature.com/srep

Competing financial interests: The authors declare no competing financial interests.

How to cite this article: Vicente Miranda, H. *et al.* Glycation potentiates neurodegeneration in models of Huntington's disease. *Sci. Rep.* **6**, 36798; doi: 10.1038/srep36798 (2016).

Publisher's note: Springer Nature remains neutral with regard to jurisdictional claims in published maps and institutional affiliations.

Human Molecular Genetics, 2015, Vol. 24, No. 7 1898–1907

doi: 10.1093/hmg/ddu606
Advance Access Publication Date: 1 December 2014
Original Article

ORIGINAL ARTICLE

α-Synuclein modifies mutant huntingtin aggregation and neurotoxicity in *Drosophila*

Gonçalo M. Poças[1], Joana Branco-Santos[1,2], Federico Herrera[1,2], Tiago Fleming Outeiro[2,3], and Pedro M. Domingos[1,*]

[1]Instituto de Tecnologia Química e Biológica, Universidade Nova de Lisboa, Av. da República, Oeiras 2780-157, Portugal, [2]Cell and Molecular Neuroscience Unit, Instituto de Medicina Molecular, Faculdade de Medicina da Universidade de Lisboa, Av. Prof. Egas Moniz, Lisboa 1649-029, Portugal, and [3]Department of Neurodegeneration and Restorative Research, Center for Nanoscale Microscopy and Molecular Physiology of the Brain, University Medical Center Goettingen, Waldweg 33, Goettingen 37073, Germany

*To whom correspondence should be addressed at: Pedro Domingos, Laboratory Cell Signalling in Drosophila, ITQB, LAO Building, Rua da Quinta Grande 6, Oeiras 2780-156, Portugal. Tel: +351 211157781; Email: domingp@itqb.unl.pt

Abstract

Protein misfolding and aggregation is a major hallmark of neurodegenerative disorders such as Alzheimer's disease (AD), Parkinson's disease (PD) and Huntington's disease (HD). Until recently, the consensus was that each aggregation-prone protein was characteristic of each disorder [α-synuclein (α-syn)/PD, mutant huntingtin (Htt)/HD, Tau and amyloid beta peptide/AD]. However, growing evidence indicates that aggregation-prone proteins can actually co-aggregate and modify each other's behavior and toxicity, suggesting that this process may also contribute to the overlap in clinical symptoms across different diseases. Here, we show that α-syn and mutant Htt co-aggregate *in vivo* when co-expressed in *Drosophila* and produce a synergistic age-dependent increase in neurotoxicity associated to a decline in motor function and life span. Altogether, our results suggest that the co-existence of α-syn and Htt in the same neuronal cells worsens aggregation-related neuropathologies and accelerates disease progression.

Introduction

The presence of protein aggregates in the brain is a common hallmark for several neurodegenerative diseases, such as Alzheimer's disease (AD), Parkinson's disease (PD) and Huntington's disease (HD). The specific subcellular location and composition of protein aggregates are characteristics for each disorder. PD hallmarks are the formation of Lewy bodies, intracytoplasmic inclusions of misfolded proteins containing mainly α-synuclein (α-syn) and the demise of dopaminergic neurons in the substantia nigra. In AD, deposits of amyloid-beta and tau proteins in the brain lead to hippocampal degeneration, cognitive impairment and dementia. In HD, mutant huntingtin (Htt) with polyglutamine (polyQ) repeat expansion accumulates in cytoplasmic and intranuclear aggregates leading to neurodegeneration in the striatum (1).

Although each neurodegenerative disorder has its characteristic pathophysiology, current evidence indicates that there is also significant overlap between apparently different disorders. For example, α-syn is the protein that characteristically aggregates in PD, but it was originally discovered as a constituent of amyloid plaques in AD (2) and, later on, was found in protein aggregates in diverse pathologies of the central nervous system, such as HD, trisomy of chromosome 21, progressive supranuclear palsy and frontotemporal dementia (3–7). Tau, an AD-associated protein, was detected in protein aggregates in patients with PD, sporadic dementia with Lewy bodies and multiple system atrophy, as well as in some animal models for synucleinopathies (8–14).

Received: September 23, 2014. **Revised and Accepted:** November 27, 2014

This apparent convergence of the molecular and cellular phenomena is accompanied by an overlap in the symptoms. For instance, patients suffering from diseases that affect movement control and coordination, as is the case of PD and HD, may also exhibit dementia in more advanced stages of disease (15). Conversely, patients afflicted by dementia can also show PD- or HD-like motor symptoms (16).

There is growing evidence that co-occurrence of aggregate-prone proteins may decisively influence the pathophysiology and severity of neural disorders. Tau and α-syn interact and co-aggregate, and this is associated with an increase in neurotoxicity in cellular and *Drosophila* models (17,18). Htt has been recently shown to co-aggregate with proteins associated with synucleinopathies and tauopathies (19–22). Mutant Htt induces Tau hyperphosphorylation and aggregation, preventing its association to the microtubular network and producing large ring-like aggregates close to the microtubular network (19,20). DJ-1, which is associated with familial PD, interacts and co-aggregates with α-syn and Htt, modulating their toxicity in models of PD and HD (20,22).

We have previously shown that α-syn modifies the dynamics and aggregation pattern of mutant Htt in cells in culture (23). Here, we expand those studies and report that co-existence of α-syn and mutant Htt *in vivo* strongly enhances PD- and HD-related neuropathology in *Drosophila melanogaster*, suggesting that the interplay between the two proteins deserves further investigation in the context of HD and PD.

Results

Co-expression of mutant Htt and α-syn alters Htt aggregation pattern

Expression of normal (25Q) Htt or α-syn bimolecular fluorescence complementation (BiFC) pairs in human (H4) cells produced mostly homogeneous fluorescence, Htt being more often restricted to the cytosol and α-syn spreading both through nucleus and cytosol (Fig. 1A). On the other hand, mutant (103Q) Htt BiFC pairs produced protein aggregates. The combination of mutant Htt/α-syn also produced aggregates, but they seemed fewer and larger than pure 103Q aggregates. This was confirmed quantitatively (Fig. 1B–D), as the number of aggregates per cell was reduced 2-fold in mutant Htt/α-syn combinations (Fig. 1B), and the number of cells with <10 aggregates grew at the expense of cells with >25 aggregates (Fig. 1C). Finally, the percentage of aggregates larger than 3 µm increased in mutant Htt/α-syn combinations at the expense of aggregates smaller than 1 µm (Fig. 1D). The proportion of cells with 10–25 aggregates and of aggregates between 1 and 3 µm remained unchanged.

Both mutant Htt and α-syn increased cell death 24 h after transfection of H4 cells with the corresponding combinations of BiFC constructs (Fig. 1E). However, and in spite of the clear changes induced by α-syn on mutant Htt aggregation pattern, we did not observe changes at the viability level, even 72 h after transfection (data not shown). Longer experiments are extremely difficult to carry out in this experimental setup.

Htt103Q-mCherry and α-syn-EGFP co-localize and co-aggregate in dopaminergic neurons and in photoreceptors

In order to confirm our results with human cells in culture and to be able to measure neurotoxic effects of Htt/α-syn combinations during longer periods of time, we performed assays using transgenic overexpression in *Drosophila*. Co-expression of a mutant version of Htt containing 103 glutamines (Htt103Q-mCherry) and wild-type α-syn-EGFP in dopaminergic neurons (TH-GAL4) showed co-localization and co-aggregation of these two proteins (Fig. 2), confirming our results in cultured human cells. In terms of subcellular location, we found that these α-syn-EGFP/Htt103Q-mCherry aggregates accumulate both in cell bodies (Fig. 2A) and neurites (Fig. 2B) of dopaminergic neurons. In contrast, flies co-expressing α-syn-EGFP with a wild-type version of Htt (Htt25Q-mCherry) do not show aggregates (Fig. 2C), suggesting that only mutant Htt stimulates the deposition of α-syn in these aggregates. Flies expressing α-syn-EGFP or wild-type Htt25Q-mCherry alone did not show aggregates (Fig. 2D and E).

Using sGMR-GAL4 we induced the co-expression of Htt103Q-mCherry and α-syn-EGFP in eye imaginal discs of third instar larvae (Fig. 3). We observed co-localization and co-aggregation of α-syn and mutant Htt in the cytoplasm of the photoreceptors (Fig. 3A and A′), and also in the axonal projections of the photoreceptors in the larval brain (Fig. 3B).

Htt103Q-mCherry and α-syn-EGFP are physically interacting

Mutant Htt103Q-mCherry was co-immunoprecipitated with α-syn-EGFP, using an antibody against the green fluorescent protein (GFP) tag, further demonstrating that mutant Htt103Q-mCherry and α-syn-EGFP interact and co-aggregate in *Drosophila* cells (Fig. 4A). In order to analyze the solubility status of these proteins when they are co-expressed, we performed a Triton-X solubility experiment using protein extracts from 8 days old adult heads. We found that the levels of α-syn-EGFP and Htt103Q-mCherry in the Triton insoluble fraction increased when these proteins are co-expressed, in comparison when they are expressed alone (Fig. 4B). This result indicates that co-expression of α-syn-EGFP and Htt103Q-mCherry causes an increase in the formation of insoluble aggregates containing these two proteins.

Co-expression of Htt103Q-mCherry and α-syn-EGFP produces premature and severe degeneration in the photoreceptors

Next, we expressed Htt103Q-mCherry and α-syn-EGFP in the eye using sGMR-GAL4 and analyzed the external morphology of the adult eye in 8 days old flies (Fig. 5A–D). Expression of the GFP tag alone had no effect on eye development or viability as the eyes looked normal (Fig. 5A). Flies expressing α-syn-EGFP alone also developed a normal eye, identical to control flies (Fig. 5B). On the other hand, flies expressing mutant Htt103Q-mCherry, alone or in combination with α-syn-EGFP, showed striking retinal degeneration, producing a strong rough eye phenotype (Fig. 5C and D). Co-expression of mutant Htt103Q-mCherry and α-syn-EGFP did not worsen the rough eye phenotype in comparison with Htt103Q-mCherry alone. However, co-expression of Htt103Q-mCherry and α-syn-EGFP specifically in the photoreceptors R1–R6, using Rh1-GAL4, showed a stronger and premature degeneration phenotype (Fig. 5G) in comparison with Htt103Q-mCherry alone (Fig. 5H). In this case, control GFP or α-syn-EGFP alone did not show any degeneration phenotype (Fig. 5E and F). These results indicate that co-expression of α-syn-EGFP and mutant Htt103Q-mCherry enhances neurodegeneration of the *Drosophila* photoreceptors *in vivo*.

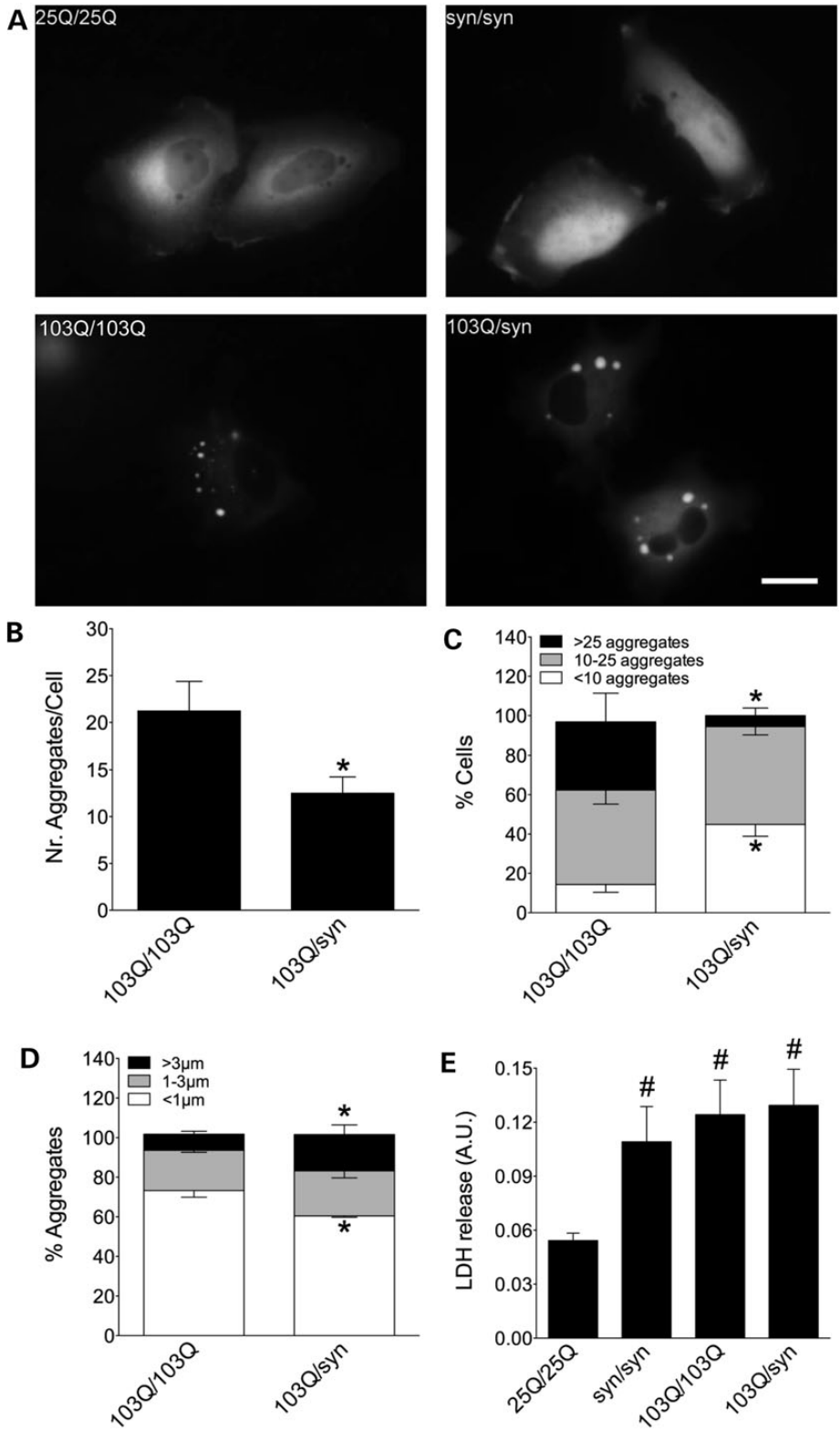

Figure 1. Co-expression of mutant Htt and α-syn alters Htt aggregation pattern. (**A**) H4 cells transfected with different combinations of α-syn- and Htt-Venus BiFC constructs. Cells transfected with a Htt25Q-Venus BiFC pair of plasmids show homogeneous fluorescence indicative of oligomeric species, while a Htt103Q-Venus BiFC pair produces both oligomeric species and large intracellular fluorescent aggregates with variable size and morphology. Htt location is primarily cytosolic. α-Syn-Venus BiFC pair produces homogeneous fluorescence distributed throughout all cellular compartments, including the nucleus. When α-syn and Htt103Q BiFC constructs were combined, there is a change in the aggregation pattern of both proteins, quantified in **B**–**D**. Co-transfection of Htt103Q with α-syn BiFC constructs decreases the average number of aggregates per cell (B and C) and increases the average size of aggregates (D). (**E**) The α-syn pair or the Htt103Q pair are more toxic than the wild-type Htt pair and combining α-syn with Htt103Q does not enhance toxicity in this model. *Significant versus 103Q/103Q, $P < 0.01$; #Significant versus 25Q/25Q, $P < 0.001$. Scale bar, 20 µm. AU, arbitrary units.

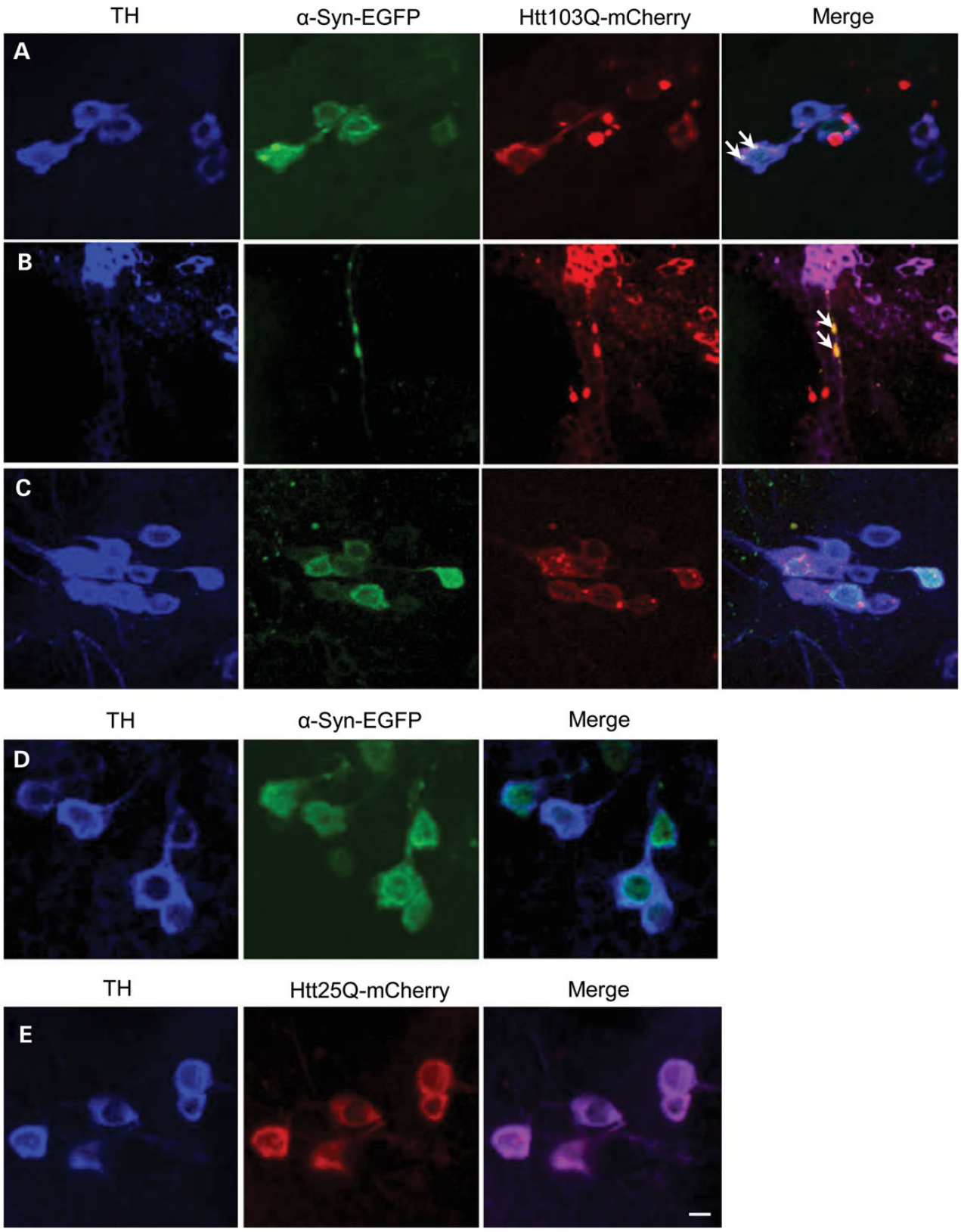

Figure 2. Htt103Q-mCherry and α-syn-EGFP co-localize and co-aggregate when expressed in dopaminergic neurons. (**A**) Co-localization of Htt103Q-mCherry and α-syn-EGFP aggregates in cell bodies of dopaminergic neurons (arrows). (**B**) Co-localization of Htt103Q-mCherry and α-syn-EGFP aggregates in neurites of dopaminergic neurons (arrows). (**C**) Wild-type Htt (Htt25Q-mCherry) does not form aggregates with α-syn-EGFP. (**D** and **E**) The expression of α-syn-EGFP alone or Htt25Q-mCherry does not induce the formation of aggregates. The images in A–E show dopaminergic neurons in the paired posterior lateral 1 (PPL1) cluster marked by an anti-TH antibody (against tyrosine hydroxylase). Genotypes: (A, B) TH-GAL4, UAS-α-syn-EGFP/ UAS-Htt103Q-mCherry, (C) TH-GAL4, UAS-α-syn-EGFP/UAS-Htt25Q-mCherry, (D) TH-GAL4, UAS-α-syn-EGFP and (E) TH-GAL4, UAS-Htt25Q-mCherry. Scale bars represent 10 μm.

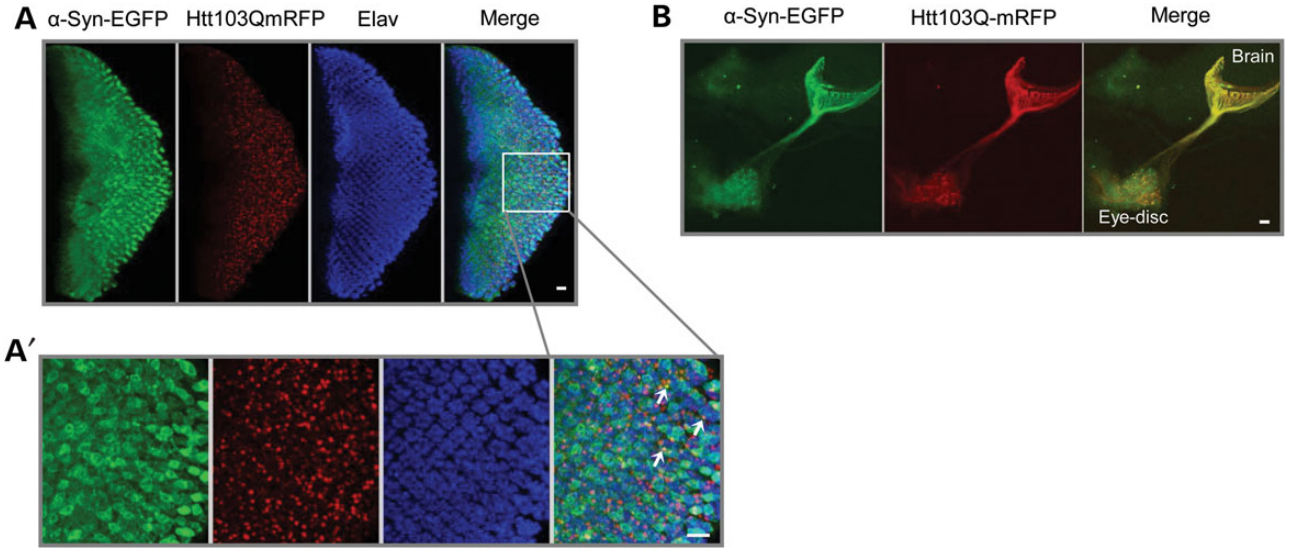

Figure 3. Htt103Q-mCherry and α-syn-EGFP co-localize and co-aggregate in the eye discs of third instar larvae. (**A**) Third instar larval eye disc from double transgenics stained with the pan-neuronal marker anti-elav. α-Syn-EGFP co-localized and co-aggregated with Htt103Q-mCherry aggregates in the cytoplasm of larval photoreceptors. (**A′**) Magnified area delimited by the box in (A). Arrows indicate foci of co-aggregated proteins. (**B**) Htt103Q-mCherry and α-syn-EGFP co-localized in the photoreceptors' axonal projections in the larval brain. Genotype: sGMR-GAL4, UAS-α-syn-EGFP/UAS-Htt103Q-mCherry. Scale bars represent 10 μm.

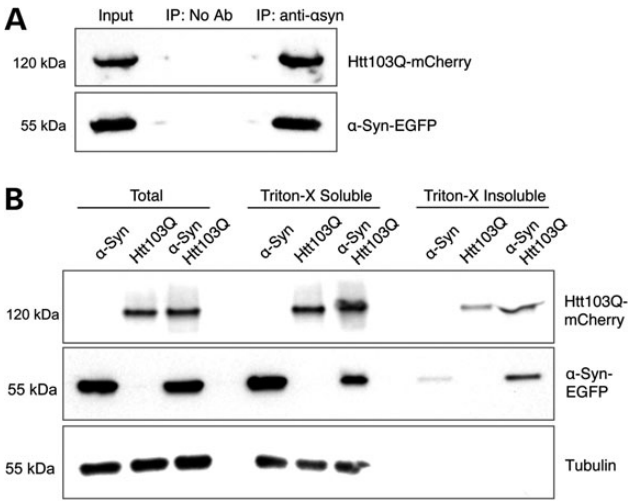

Figure 4. Htt103Q-mCherry and α-syn-EGFP are physically interacting. (**A**) Immunoprecipitation of α-syn-EGFP with an antibody against the EGFP tag pulled down Htt103Q-mCherry from dopaminergic neurons, showed by immunoblotting analysis. (**B**) Immunoblotting of Total, Triton-X soluble and Triton-X insoluble fractions of α-syn-EGFP and Htt103Q-mCherry from adult heads of flies co-expressing these two proteins. The levels of α-syn-EGFP and Htt103Q-mCherry in the insoluble fraction are higher when these proteins are co-expressed. Genotypes: (A) TH-GAL4, UAS-α-syn-EGFP/UAS-Htt103Q-mCherry. (B) α-Syn: sGMR-GAL4, UAS-α-syn-EGFP. Htt103Q: sGMR-GAL4, UAS-Htt103Q-mCherry. α-Syn/Htt103Q-mCherry: sGMR-GAL4, UAS-α-syn-EGFP/UAS-Htt103Q-mCherry.

Co-expression of Htt103Q-mCherry and α-syn-EGFP in the nervous system causes severe motor dysfunction and a decrease in life span

We evaluated the motor function and life span of flies co-expressing mutant Htt103Q-mCherry and α-syn-EGFP in the central nervous system, using nSyb-GAL4 (Fig. 6). To test motor function we used 'climbing assays', where flies of different genotypes were tapped to the bottom of the vial and allowed to climb up the walls (Fig. 6A). We recorded the climbing time when five flies crossed a 15-cm finish line. Eight days old flies co-expressing Htt103Q-mCherry and α-syn-EGFP took, on average, four more seconds to reach the finish line than the other genotypes tested. The motor ability of flies co-expressing Htt103Q-mCherry/α-syn-EGFP deteriorated more and faster than the other genotypes, with the difference in climbing times reaching 32 s by day 30.

Flies co-expressing Htt103Q-mCherry and α-syn-EGFP also showed a dramatic decrease in life span, with 44 days of maximum survival (Fig. 6B). Flies co-expressing Htt25Q-mCherry and α-syn-EGFP had a maximum survival of 71 days. Maximum survival of flies expressing GFP, α-syn-EGFP, Htt25Q-mCherry or Htt103Q-mCherry alone ranged from 59 to 83 days. Interestingly, neurotoxicity, motor dysfunction and fly death started around days 8–15 and their increase occurred in parallel, indicating an association between these events. These results suggest that co-expression of α-syn and mutant Htt synergistically enhances each other's toxicity, eventually accelerating the progression of the disorder.

Discussion

Here, we show that α-syn and mutant Htt, two proteins associated with PD and HD, respectively, can interact and co-aggregate *in vivo*. Furthermore, their co-expression produced a synergistic deterioration of neural tissue, motor function and life span in *Drosophila*. The effects of α-syn/Htt co-expression under the different promoters are summarized in Table 1. While co-expression of other proteins associated with human neurodegenerative diseases has also shown deleterious effects in different models (17,18,23,24), this is the first demonstration that co-expression of α-syn and mutant Htt can enhance neurodegeneration in *Drosophila*.

Our results support the idea that the co-occurrence of these two different aggregation-prone proteins in neural cells can produce striking changes in the pathology, symptoms and disease progression. Moreover, our study may give some clues why some patients suffering with a specific neuropathology may

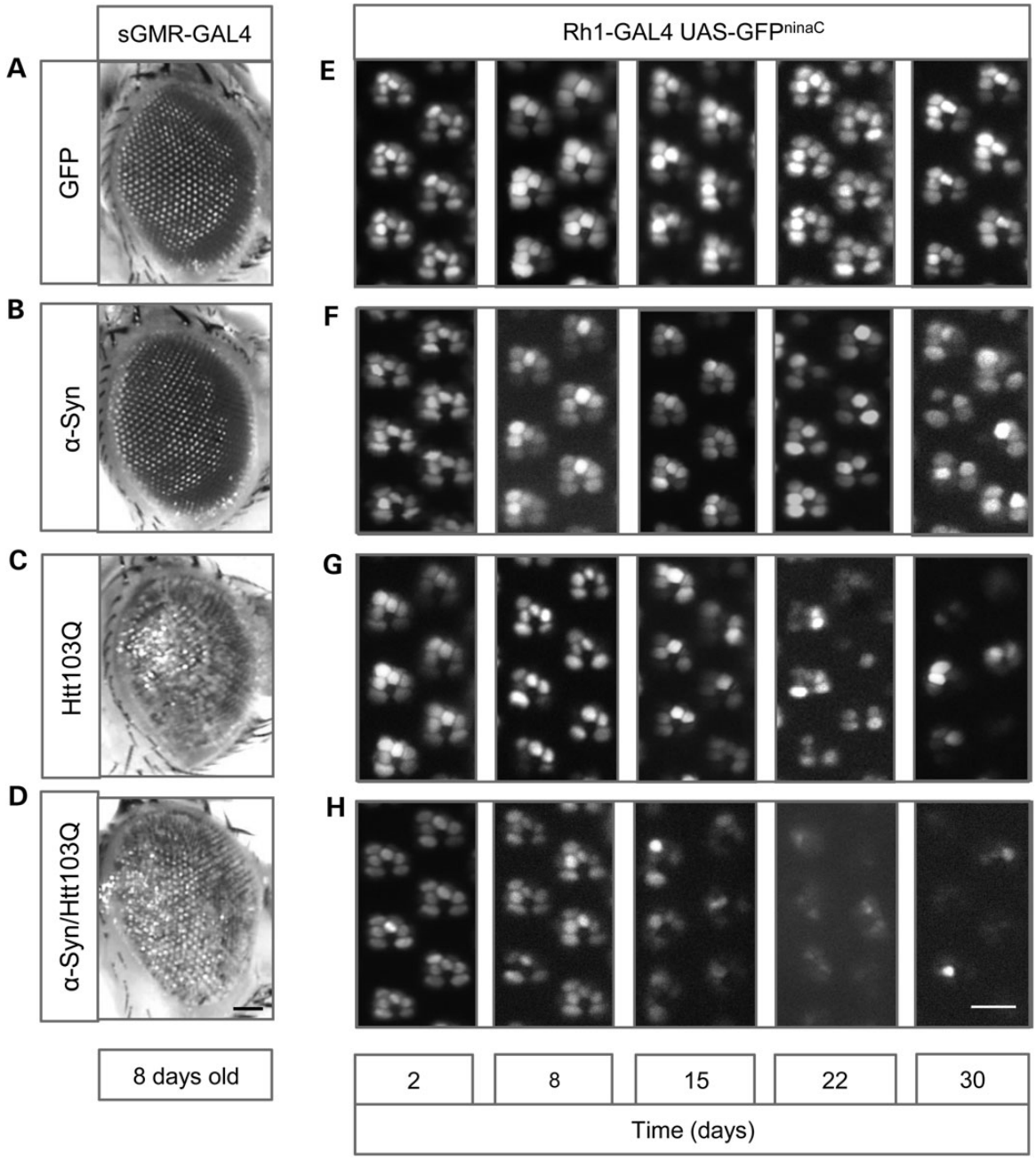

Figure 5. Co-expression of Htt103Q-mCherry and α-syn-EGFP produces premature and severe degeneration in the photoreceptors. (**A–D**) External morphology of the adult eye. (A and B) Expression of GFP or α-syn-EGFP does not affect external eye morphology. (C and D) Co-expression of Htt103Q-mCherry and α-syn-EGFP produces a rough eye phenotype identical to the one induced by the single expression of Htt103Q-mCherry. (**E–H**) Photoreceptors neurodegeneration in the adult eye, analyzed by water immersion microscopy assay of the retinas. (E) Expression of GFP did not induce degeneration of the photoreceptors, with the six photoreceptors being present in the ommatidial clusters; (F, G) flies expressing α-syn-EGFP or Htt103Q-mCherry showed progressive degeneration of the photoreceptors. (H) Co-expression of Htt103Q-mCherry and α-syn-EGFP induced severe and early degeneration of the photoreceptors. Genotypes are indicated in the boxes on top and lateral of the figures: (A) sGMR-GAL4, UAS-GFP, (B) sGMR-GAL4, UAS-α-syn-EGFP, (C) sGMR-GAL4, UAS-Htt103Q-mCherry, (D) sGMR-GAL4, UAS-α-syn-EGFP/UAS-Htt103Q-mCherry, (E) Rh1-GAL4, UAS-GFP, (F) Rh1-GAL4, UAS-α-syn-EGFP, (G) Rh1-GAL4, UAS-Htt103Q-mCherry and (H) Rh1-GAL4, UAS-α-syn-EGFP/UAS-Htt103Q-mCherry. Scale bars represent 50 μm (A–D) and 10 μm (E–H).

show, at the symptomatic level, a significant overlap between different human neurodegenerative diseases. It is possible that a HD patient containing a mutant version of the Htt gene (expansion of the trinucleotide CAG) and thereby suffering from the consequences of mutant Htt aggregation and toxicity may be also in risk of developing aggregation of α-syn and therefore being affected by some of the symptoms associated with PD. This could occur as a consequence of the propensity of mutant Htt and α-syn to interact, co-aggregate and interfere with their normal biological roles in cells. In addition, the two most affected brain regions in patients with PD and HD, the substantia nigra and striatum, respectively, are anatomically and functionally interconnected, reinforcing the interest of studying the crosstalk between these two neuropathologies. Finally, the models established in this work may constitute useful tools to screen and discover new candidate drugs against PD and HD.

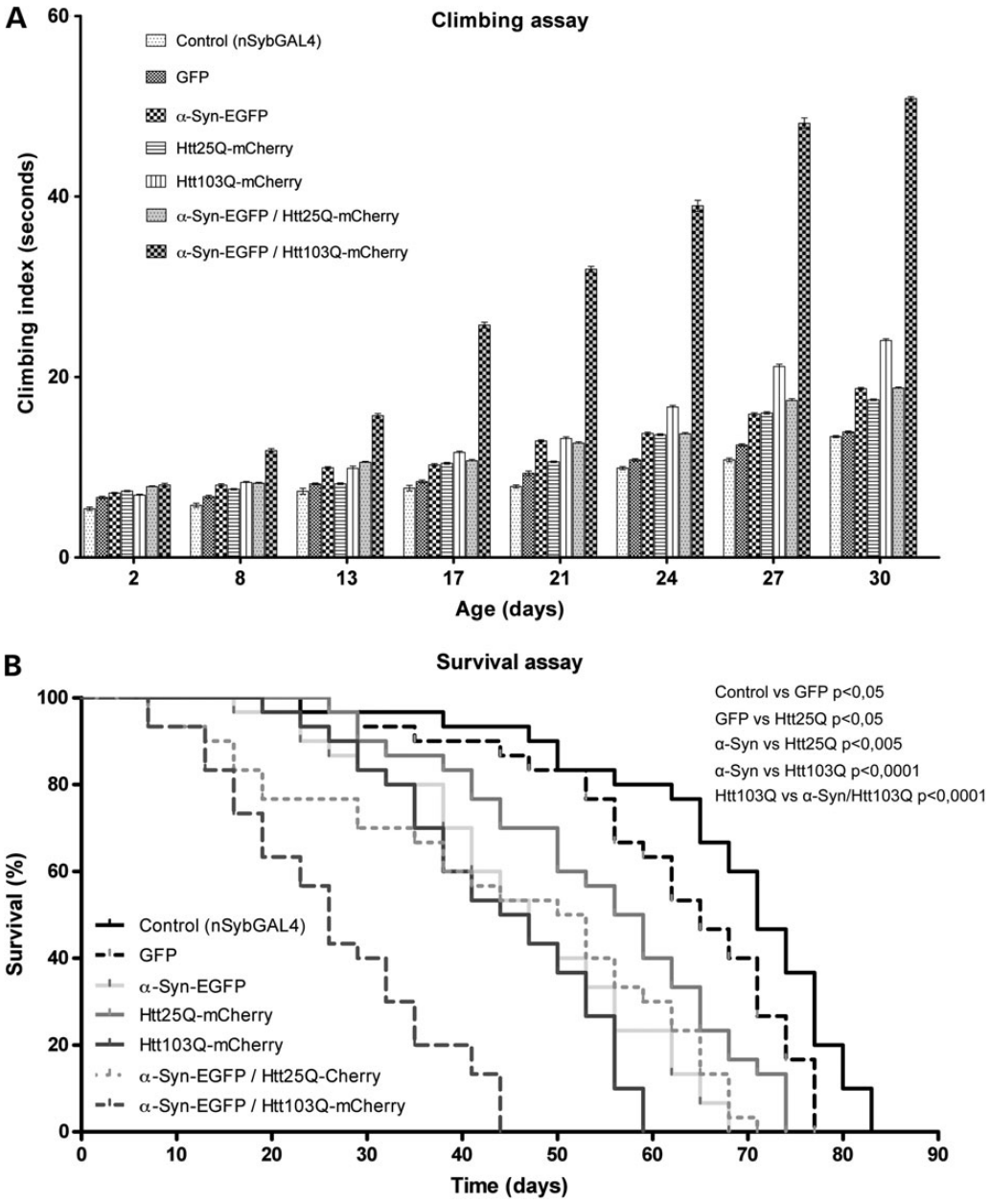

Figure 6. Co-expression of Htt103Q-mCherry and α-syn-EGFP in the nervous system causes severe motor dysfunction and a decrease in life span. (**A**) Flies co-expressing Htt103Q-mCherry and α-syn-EGFP under the control of nSyb-GAL4 show a strong impairment of the motor abilities compared with the rest of the genotypes tested. The Y-axis represents the time (in seconds), it took for five males to climb 15 cm (mean ± SEM). Statistically significant values, comparing each of genotypes, were calculated by doing two-way ANOVA with Bonferroni post-test. With very few exceptions, all the differences detected between the genotypes tested in this assay were statistically significant with a $P < 0.001$ (except the difference between the genotypes Htt25Q-mCherry and α-Syn-EGFP/Htt25Q-mCherry which is significant for a $P < 0.01$). The differences not statistically significant ($P > 0.05$) were GFP versus Htt25Q-mCherry at day 13; α-Syn-EGFP versus Htt103Q-mCherry at day 13; α-Syn-EGFP versus α-Syn-EGFP/Htt25Q-mCherry at days 24 and 30; Htt103Q-mCherry versus α-Syn-EGFP/Htt25Q-mCherry at day 8. (**B**) Flies co-expressing Htt103Q-mCherry and α-syn-EGFP under the control of nSyb-GAL4 have a life span significantly shorter in comparison with the rest of the genotypes tested. Values on the Y-axis represent the percentage of flies alive at each time point analyzed. The maximum survival (in days) is indicated for each genotype (the mean values indicate the number of days it took for half of the flies to die): control (nSyb-GAL4) 83 (mean = 70), GFP (nSyb-GAL4, UAS-GFP) 77 (mean = 64), α-syn-EGFP (nSyb-GAL4, UAS-α-syn-EGFP) 68 (mean = 45), Htt25Q-mCherry (nSyb-GAL4, UAS- Htt25Q-mCherry) 74 (mean = 56), Htt103Q-mCherry (nSyb-GAL4, UAS-Htt103Q-mCherry) 59 (mean = 44), α-syn-EGFP/Htt25Q-mCherry (nSyb-GAL4, UAS-α-syn-EGFP/UAS-Htt25Q-mCherry) 71 (mean = 50) and α-syn-EGFP/Htt103Q-mCherry (nSyb-GAL4, UAS-α-syn-EGFP/UAS-Htt103Q-mCherry) 44 (mean = 25). Statistical significance is indicated in the graph (log-rank, Mantel–Cox test).

Material and Methods

Cell culture and BiFC plasmids

Maintenance of H4 human glioma cells and Htt and α-syn BiFC constructs were previously described in detail (23,25). Briefly, in our BiFC systems, Htt and α-syn were fused to two non-fluorescent halves of the Venus protein (Venus 1, amino acids 1–157; and Venus 2, amino acids 158–239). When the Htt and α-syn dimerize, the Venus halves get together and reconstitute a functional fluorophore. Fluorescence is therefore proportional to the

Table 1. GAL4 lines used in this study and respective phenotypes

GAL4 line	Tissue	Phenotype (co-expression of α-syn and mutant Htt)
TH-GAL4	Dopaminergic neurons	Co-localization, interaction and co-aggregation of α-syn and Htt
nSyb-GAL4	Nervous system	Impairment of motor abilities and reduced life span
sGMR-GAL4	Eye	Co-localization, co-aggregation and retinal degeneration
Rh1-GAL4	Photoreceptors R1-R6	Premature degeneration of the photoreceptors

amount of Htt/α-syn dimers and oligomers. H4 cells were transfected with the corresponding BiFC pairs and 24 h later pictures were taken on a Zeiss Axiovert 200M. A total of 150 cells from three independent experiments were analyzed. Graphs of Figure 1 show mean ± SD of three independent experiments.

Drosophila stocks

To generate UAS-α-Syn-EGFP, we fused α-syn with EGFP and cloned into pUAST using the *Bgl*II and *Acc*65I restriction sites. The transgenic flies were generated by BestGene, USA. We generated two different UAS-Htt-mCherry lines, one encoding a wild-type version of Htt (exon 1) with a 25 polyQ tail and the other encoding a mutant version of Htt with a 103 polyQ tail. These two constructs were cloned into pWalium10-roe and transgenic lines were generated using phiC31 integrase-mediated DNA integration (BestGene Strain #9723, attP acceptor site in 28E7).

Four different drivers were obtained from the Bloomington Stock Center (Indiana University, Bloomington, IN, USA): nSyb-GAL4 (active in the entire nervous system, under the control of the Synaptobrevin promoter), TH-GAL4 (active in dopaminergic neurons, under the control of the tyrosine hydroxylase promoter), GMR-GAL4 (active in the eye, under the control of the glass multiple reporter) and Rh1-GAL4 (active in the photoreceptors R1–R6, under the control of the rhodopsin1 promoter). *Drosophila* stocks were maintained at 25°C on standard cornmeal media in an incubator with a 12 h light/dark cycle.

Immunohistochemistry and microscopy

Brain preparations for confocal microscopy imaging were done as previously described (26). Briefly, adult flies were anesthetized with CO_2 and the brains were isolated from the head cuticles and fixed in phosphate buffered saline (PBS) containing 4% paraformaldehyde.

Dopaminergic neurons were stained by incubation for 48 h at 4°C with mouse anti-TH antibody (Immunostar, Hudson, WI, USA) diluted 1:50 in PBST (1× PBS + 0.3% Triton X-100) containing 5% (v/v) normal goat serum. Three 10-min washes with PBST were done before incubation with a secondary anti-mouse Cy5 (Jackson ImmunoResearch), also diluted in PBST-containing 5% (v/v) normal goat serum.

Brain samples were analyzed and images were collected using a LSM 710 Meta Zeiss confocal microscope. Images were acquired with a resolution of 1024 × 1024, with a slice thickness of 1 µm and a line-average of 4. Z-projections were generated using ImageJ and the images were processed using Adobe Photoshop.

The degenerative effects caused by co-expression of α-syn and mutant Htt were assessed in the photoreceptors of adult eyes. To analyze external eye morphology, we used a Leica Z16 APO macroscope and a Leica DFC 420C camera. To analyze photoreceptor degeneration, we performed water immersion microscopy as previously described (27). Images were obtained using a Leica DM5500 B microscope and an Andor LucaR camera.

Immunoprecipitation, Triton-X solubility and immunoblotting analysis

Flies were transferred to 50-ml tubes, frozen in liquid nitrogen and immediately decapitated by vigorous vortexing. Isolated heads were collected to 1.5-ml tubes and maintained in dry ice. Proteins were extracted in lysis buffer supplemented with Complete Protease Inhibitor Cocktail tablets from Roche (Basel, Switzerland). Total protein was quantified using the DC Protein Assay, from Bio-Rad (CA, USA). In the immunoprecipitation experiments, α-syn-EGFP was pulled down from 1 mg of total protein extract, using GFP-Trap_A beads or blocked agarose beads (No Ab, no antibody negative control), following manufacturer's instructions (Chromotek, Munich, Germany). α-syn-EGFP pull-down and Htt103Q-mCherry co-immunoprecipitation were analyzed by immunoblotting using anti-GFP (3H9) and anti-RFP (5F8) antibodies from Chromotek, both diluted 1:1000 in PBS. Input lane corresponds to 30 µg of total protein extract and co-IP lane corresponds to one-fifth of the immunoprecipitated material.

The Triton-X solubility experiment was performed as previously described (28). Briefly, 200 µg of total protein extract was incubated with 1% Triton X-100 on ice during 30 min. Triton soluble and insoluble proteins fractions were separated by a 60-min centrifugation step at 15 000*g* at 4°C. The supernatant, containing the soluble proteins fraction (Triton-X soluble), was carefully collected and the pellet, containing the insoluble proteins fraction (Triton-X insoluble), was resuspended in 40 µl of 2% sodium dodecyl sulfate Tris–HCl buffer pH 7.4 by pipetting and sonication for 10 s. For the immunoblotting analysis, equal volumes of each fraction were loaded and the presence of α-syn-EGFP and Htt103Q-mCherry in the total, soluble and insoluble fractions was detected using anti-GFP (3H9) and anti-RFP (5F8). Additionally, anti-α-tubulin (AA4.3) from Developmental Studies Hybridoma Bank (IA, USA), diluted 1:500 in PBS, was used as loading control.

Climbing assays and survival assays

Motor function was analyzed by startle-induced locomotion and negative geotaxis response assays, commonly called climbing assays, as previously described (29). Briefly, groups of 10 males of the same age of each genotype of interest were placed into 18-cm-long vials, at room temperature for environmental acclimatization, and 30 min later they were gently tapped to the bottom of the vial (a minimum number of 30 males per genotype was tested). We recorded the climbing time when five flies crossed the 15-cm finish line. For each genotype we tested three independent groups of males and performed five trials for each time point. Results are the average climbing time ± SEM of these independent experiments.

For survival assays, flies were maintained in a humid incubator at 25°C under a 12 h light/dark cycle. Thirty adult females of the same age were placed in three vials (10 flies per vial) containing fresh food. Each 3 days the flies were transferred into vials with fresh food and the number of living flies was registered.

Statistical analysis

Statistical analyses were done using GraphPad Prism software version 5 (San Diego, CA, USA). For BiFC we performed a one-way ANOVA followed by a post-hoc Tukey test for average comparison. For climbing assays, we performed a two-way ANOVA followed by a Bonferroni post-test. For the survival assays, we performed a Log-rank (Mantel–Cox) test.

Acknowledgements

We thank Maria Luísa Vasconcelos, Rui Martinho and the Bloomington Stock Centre for *Drosophila* stocks. We thank the TRiP at Harvard Medical School (NIH/NIGMS R01-GM084947) for providing plasmid vectors used in this study. We thank Developmental Studies Hybridoma Bank for antibodies.

Conflict of Interest statement. None declared.

Funding

This work was supported by grant FCT-ANR/NEU-NMC/0006/2013 from Fundação para a Ciência e a Tecnologia, Portugal. G.M.P. was supported by a doctoral fellowship from the Fundação para a Ciência e a Tecnologia (SFRH/BD/61477/2009). J.B.S. and F.H. were supported by fellowships from the Fundação para a Ciência e a Tecnologia (SFRH/BD/85275/2012 and SFRH/BPD/63530/2009, respectively). F.H. and T.F.O. were also supported by seed funds from the European Huntington's Disease Network (EHDN). T.F.O. is supported by the DFG Center for Nanoscale Microscopy and Molecular Physiology of the Brain.

References

1. Soto, C. and Estrada, L.D. (2008) Protein misfolding and neurodegeneration. *Arch. Neurol.*, **65**, 184–189.
2. Yoshimoto, M., Iwai, A., Kang, D., Otero, D.A., Xia, Y. and Saitoh, T. (1995) NACP, the precursor protein of the non-amyloid beta/A4 protein (A beta) component of Alzheimer disease amyloid, binds A beta and stimulates A beta aggregation. *Proc. Natl. Acad. Sci. USA*, **92**, 9141–9145.
3. Wilhelmsen, K.C., Forman, M.S., Rosen, H.J., Alving, L.I., Goldman, J., Feiger, J., Lee, J.V., Segall, S.K., Kramer, J.H., Lomen-Hoerth, C. *et al.* (2004) 17q-linked frontotemporal dementia-amyotrophic lateral sclerosis without tau mutations with tau and alpha-synuclein inclusions. *Arch. Neurol.*, **61**, 398–406.
4. Hamilton, R.L. (2000) Lewy bodies in Alzheimer's disease: a neuropathological review of 145 cases using alpha-synuclein immunohistochemistry. *Brain Pathol.*, **10**, 378–384.
5. Raghavan, R., Khin-Nu, C., Brown, A., Irving, D., Ince, P.G., Day, K., Tyrer, S.P. and Perry, R.H. (1993) Detection of Lewy bodies in Trisomy 21 (Down's syndrome). *Can. J. Neurol. Sci.*, **20**, 48–51.
6. Judkins, A.R., Forman, M.S., Uryu, K., Hinkle, D.A., Asbury, A. K., Lee, V.M. and Trojanowski, J.Q. (2002) Co-occurrence of Parkinson's disease with progressive supranuclear palsy. *Acta Neuropathol.*, **103**, 526–530.
7. Charles, V., Mezey, E., Reddy, P.H., Dehejia, A., Young, T.A., Polymeropoulos, M.H., Brownstein, M.J. and Tagle, D.A. (2000) Alpha-synuclein immunoreactivity of huntingtin polyglutamine aggregates in striatum and cortex of Huntington's disease patients and transgenic mouse models. *Neurosci. Lett.*, **289**, 29–32.
8. Galpern, W.R. and Lang, A.E. (2006) Interface between tauopathies and synucleinopathies: a tale of two proteins. *Ann. Neurol.*, **59**, 449–458.
9. Clarimon, J., Molina-Porcel, L., Gomez-Isla, T., Blesa, R., Guardia-Laguarta, C., Gonzalez-Neira, A., Estorch, M., Ma Grau, J., Barraquer, L., Roig, C. *et al.* (2009) Early-onset familial lewy body dementia with extensive tauopathy: a clinical, genetic, and neuropathological study. *J Neuropathol. Exp. Neurol.*, **68**, 73–82.
10. Galloway, P.G., Grundke-Iqbal, I., Iqbal, K. and Perry, G. (1988) Lewy bodies contain epitopes both shared and distinct from Alzheimer neurofibrillary tangles. *J. Neuropathol. Exp. Neurol.*, **47**, 654–663.
11. Giasson, B.I., Forman, M.S., Higuchi, M., Golbe, L.I., Graves, C. L., Kotzbauer, P.T., Trojanowski, J.Q. and Lee, V.M. (2003) Initiation and synergistic fibrillization of tau and alpha-synuclein. *Science*, **300**, 636–640.
12. Ishizawa, T., Mattila, P., Davies, P., Wang, D. and Dickson, D. W. (2003) Colocalization of tau and alpha-synuclein epitopes in Lewy bodies. *J. Neuropathol. Exp. Neurol.*, **62**, 389–397.
13. Wills, J., Jones, J., Haggerty, T., Duka, V., Joyce, J.N. and Sidhu, A. (2010) Elevated tauopathy and alpha-synuclein pathology in postmortem Parkinson's disease brains with and without dementia. *Exp. Neurol.*, **225**, 210–218.
14. Haggerty, T., Credle, J., Rodriguez, O., Wills, J., Oaks, A.W., Masliah, E. and Sidhu, A. (2011) Hyperphosphorylated Tau in an alpha-synuclein-overexpressing transgenic model of Parkinson's disease. *Eur. J. Neurosci.*, **33**, 1598–1610.
15. Perry, R.J. and Hodges, J.R. (1996) Spectrum of memory dysfunction in degenerative disease. *Curr. Opin. Neurol.*, **9**, 281–285.
16. Tsolaki, M., Kokarida, K., Iakovidou, V., Stilopoulos, E., Meimaris, J. and Kazis, A. (2001) Extrapyramidal symptoms and signs in Alzheimer's disease: prevalence and correlation with the first symptom. *Am. J. Alzheimers* Dis. Other Demen., **16**, 268–278.
17. Roy, B. and Jackson, G.R. (2014) Interactions between Tau and alpha-synuclein augment neurotoxicity in a Drosophila model of Parkinson's disease. *Hum. Mol. Genet.*, **23**, 3008–3023.
18. Badiola, N., de Oliveira, R.M., Herrera, F., Guardia-Laguarta, C., Goncalves, S.A., Pera, M., Suarez-Calvet, M., Clarimon, J., Outeiro, T.F. and Lleo, A. (2011) Tau enhances alpha-synuclein aggregation and toxicity in cellular models of synucleinopathy. *PLoS One*, **6**, e26609.
19. Blum, D., Herrera, F., Francelle, L., Mendes, T., Basquin, M., Obriot, H., Demeyer, D., Sergeant, N., Gerhardt, E., Brouillet, E. *et al.* (2015) Mutant huntingtin alters Tau phosphorylation and subcellular distribution. *Hum. Mol. Genet.*, **24**, 76–85.
20. Sajjad, M.U., Green, E.W., Miller-Fleming, L., Hands, S., Herrera, F., Campesan, S., Khoshnan, A., Outeiro, T.F., Giorgini, F. and Wyttenbach, A. (2014) DJ-1 modulates aggregation and pathogenesis in models of Huntington's disease. *Hum. Mol. Genet.*, **23**, 755–766.
21. Gratuze, M., Noel, A., Julien, C., Cisbani, G., Milot-Rousseau, P., Morin, F., Dickler, M., Goupil, C., Bezeau, F., Poitras, I. *et al.* (2015) Tau hyperphosphorylation and deregulation of calcineurin in mouse models of Huntington's disease. *Hum. Mol. Genet.*, **24**, 86–89.
22. Zondler, L., Miller-Fleming, L., Repici, M., Goncalves, S., Tenreiro, S., Rosado-Ramos, R., Betzer, C., Straatman, K.R., Jensen, P.H., Giorgini, F. *et al.* (2014) DJ-1 interactions with alpha-synuclein attenuate aggregation and cellular toxicity in models of Parkinson's disease. *Cell Death Dis.*, **5**, e1350.

23. Herrera, F. and Outeiro, T.F. (2012) Alpha-synuclein modifies huntingtin aggregation in living cells. *FEBS Lett.*, **586**, 7–12.
24. Corrochano, S., Renna, M., Carter, S., Chrobot, N., Kent, R., Stewart, M., Cooper, J., Brown, S.D., Rubinsztein, D.C. and Acevedo-Arozena, A. (2012) Alpha-synuclein levels modulate Huntington's disease in mice. *Hum. Mol. Genet.*, **21**, 485–494.
25. Herrera, F., Tenreiro, S., Miller-Fleming, L. and Outeiro, T.F. (2011) Visualization of cell-to-cell transmission of mutant huntingtin oligomers. *PLoS Curr.*, **3**, RRN1210.
26. Wu, J.S. and Luo, L. (2006) A protocol for dissecting *Drosophila melanogaster* brains for live imaging or immunostaining. *Nat. Protoc.*, **1**, 2110–2115.
27. Pichaud, F. and Desplan, C. (2001) A new visualization approach for identifying mutations that affect differentiation and organization of the *Drosophila ommatidia*. *Development*, **128**, 815–826.
28. Tenreiro, S., Reimao-Pinto, M.M., Antas, P., Rino, J., Wawrzycka, D., Macedo, D., Rosado-Ramos, R., Amen, T., Waiss, M., Magalhaes, F. *et al.* (2014) Phosphorylation modulates clearance of alpha-synuclein inclusions in a yeast model of Parkinson's disease. *PLoS Genet*, **10**, e1004302.
29. Park, J., Lee, S.B., Lee, S., Kim, Y., Song, S., Kim, S., Bae, E., Kim, J., Shong, M., Kim, J.M. *et al.* (2006) Mitochondrial dysfunction in Drosophila PINK1 mutants is complemented by parkin. *Nature*, **441**, 1157–1161.

Chapter 12

Studying the Molecular Determinants of Protein Oligomerization in Neurodegenerative Disorders by Bimolecular Fluorescence Complementation

Federico Herrera, Susana Gonçalves and Joana Branco dos Santos
Cell and Molecular Neuroscience Unit, Instituto de Medicina Molecular, Lisboa, Portugal

Tiago Fleming Outeiro
Cell and Molecular Neuroscience Unit, Instituto de Medicina Molecular, Lisboa, Portugal; Instituto de Fisiologia, Faculdade de Medicina da Universidade de Lisboa, Lisboa, Portugal; Department of Neurodegeneration and Restorative Research, Center for Molecular Physiology of the Brain, University of Göttingen, Göttingen, Germany

Chapter Outline

INTRODUCTION

Protein–protein interactions are at the root of all biologic processes in both physiologic and pathologic conditions. Our ability to study such interactions relied for a long time on biochemical assays such as immunoprecipitation or immunocytochemistry, performed on cell or tissue lysates or fixed cells or tissue. While these assays are extremely informative, accurate and widely used, they do not enable the study of the dynamics of protein–protein interactions in living cells and organisms. Additionally, they are not well suited for high-throughput screens because they are usually rather laborious and time consuming. Advances in the last two decades have made it possible to characterize the full interactome of a single protein, visualize multiple protein–protein interactions in living organisms, or carry out high-throughput genetic and pharmacologic screens for the identification of modifiers of protein interactions [1–4]. Such technologies include fluorescence, bioluminescence and protein complementation assays, and hold the promise for a more complete understanding of normal and aberrant protein–protein interactions in health and disease.

In this chapter, we focus on the bimolecular fluorescence complementation assay and its application to the study of aberrant protein oligomerization in neurodegenerative

Bio-nanoimaging. http://dx.doi.org/10.1016/B978-0-12-394431-3.00012-2

disorders such as Alzheimer's disease, Parkinson's disease and Huntington's disease.

An online video is linked to this chapter (see Online video 1).

NEURODEGENERATIVE DISORDERS AND PROTEIN MISFOLDING

Neurodegenerative disorders are a family of age-related pathologies caused by a progressive loss of neurons in specific areas of the nervous system. Therefore, clinical symptoms are characteristic of each disorder (Table 12.1). However, they share several molecular, cellular and histopathologic features such as inflammation, oxidative stress, mitochondrial dysfunction and the accumulation of β-sheet-rich proteinaceous inclusions [5]. These events are closely interrelated, but the initial trigger of neurodegenerative disorders remains unclear in most cases.

A great deal of evidence supports the idea that protein misfolding is the initial trigger of neurodegenerative disorders [6–8]. Single-gene mutations have been identified as the primary cause of some neurodegenerative disorders, such as familial Parkinson's disease (PD), familial Alzheimer's disease (AD), familial amyotrophic lateral sclerosis (ALS) or Huntington's disease (HD) [8–15]. These mutations lead invariably to protein misfolding, aggregation and neurotoxicity in cell and animal models. Point mutations in α-synuclein, parkin, and LRRK2, among a few other genes, cause PD [8,10–12]. α-Synuclein is the main component of the Lewy bodies, proteinaceous inclusions characteristic of the disorder. Presenilin mutations cause the accumulation of β-amyloid peptide in AD [8]. Mutations in superoxide dismutase, TDP-43 or FUS induce the aggregation and toxicity of these proteins in familial ALS [13–15]. Elongation of the polyglutamine tract of the huntingtin protein beyond 35 glutamines is the cause of HD, where huntingtin inclusions are also present [9,16]. Protein aggregation and toxicity is also dependent on protein concentration because duplications and triplications of the genes encoding α-synuclein or amyloid precursor protein (APP) cause PD and AD, respectively [17–19].

PROTEIN OLIGOMERIZATION, AGGREGATION AND TOXICITY

The large proteinaceous deposits found in cells and tissues were originally thought to be the toxic forms. However, the formation of large amyloid structures has also been hypothesized as a natural mechanism for storing peptidic hormones and factors to be released to the medium [20] or for scavenging dysfunctional proteins before they are degraded by the ubiquitin–proteasome and lysosome–autophagy systems [21,22]. Current evidence strongly indicates that large amyloid deposits constitute an attempt by cells to neutralize the toxicity of smaller, more soluble aggregated species known as dimers and oligomers [16,23,24]. (For the sake of simplicity, we will refer to both species as oligomers or oligomeric species throughout the text.) While large aggregates occupy specific cellular sites and do not move substantially, oligomeric species are able to move more freely within cells and across membranes. Their solubility and dynamic properties should, in theory, allow them to interfere with biologic processes more effectively than larger, more static, protein inclusions. Soluble oligomeric species could even spread throughout tissues and act as seeds for the generation of protein aggregates and toxicity in different areas of the brain, as happens in prion disorders [25–27].

Large protein inclusions are easily observed by classic microscopy and protein labeling procedures. However, the dynamics and behavior of oligomeric species remain poorly understood due, at least in part, to the lack of suitable experimental models for the study of oligomeric species in living cells. We and others have recently used protein complementation approaches for the visualization of oligomers in living cells [27–32].

PROTEIN COMPLEMENTATION ASSAYS: HISTORY AND LATEST DEVELOPMENTS

Protein complementation was discovered by Frederic M Richards as early as 1958 [33]. He realized that a ribonuclease digested with subtilisin produced two fragments without activity when they were isolated, but recovered activity when they were mixed together. In the mid 1960s, Agnes Ullmann and Nobel Prize winners François Jacob and Jacques Monod used this principle to produce β-galactosidase fragments which would complement in bacteria [34]. Many proteins have since been shown to display this property and have been used with different purposes (Table 12.2). Johnsson and Varshavsky pioneered the yeast two-hybrid system based on split-ubiquitin for the detection of protein–protein interactions between both soluble and membrane-bound proteins [35]. In 2000, Ghosh et al described for the first time a complementation assay with a fluorescent protein, the green fluorescent protein (GFP) (Fig. 12.1A), when they studied the interaction of artificial peptides in bacteria [36]. Nagai et al used the complementation properties of the green and yellow fluorescent proteins to develop genetically-encoded calcium sensors [37–39]. Kerppola and colleagues then used fluorescence complementation for the analysis of protein–protein interaction in mammalian cells and named the method bimolecular fluorescence complementation (BiFC) assay (Fig. 12.1) [40].

In the following decade, BiFC systems evolved considerably. There are currently BiFC systems with virtually every fluorescent protein in the spectrum (Table 12.2), and their advantages and disadvantages have been extensively analyzed. Probably the greatest advantage of BiFC assays

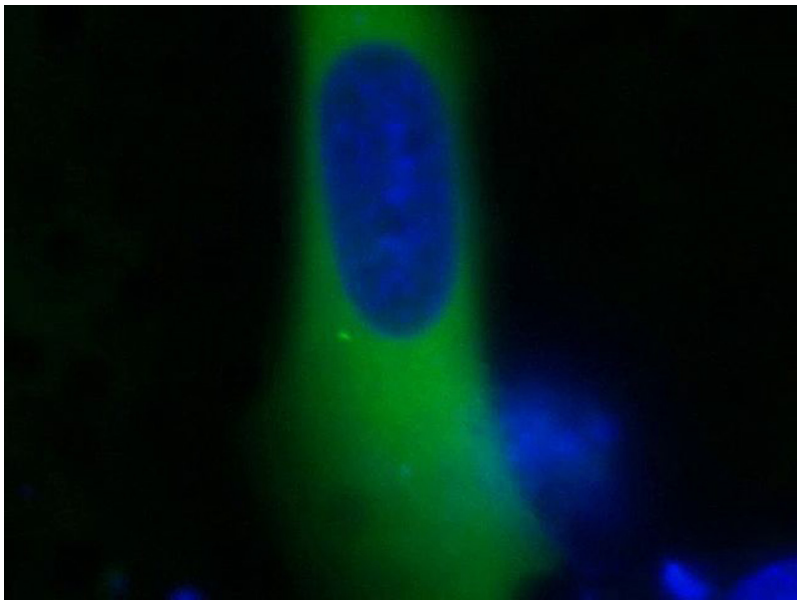

ONLINE VIDEO 1

TABLE 12.1 Selected Protein Misfolding Disorders

Neurologic disorders				
Disease	**Location**	**Aggregate Types**	**Major protein components**	**References**
Parkinson's disease	Substantia nigra; Cerebral cortex	Cytoplasmic Lewy bodies	α-synuclein Ubiquitin LRRK2	6, 8, 11, 12, 56
Alzheimer's disease	Neocortex Limbic region	Extracellular amyloid plaques and intracellular Tau tangles	β-amyloid HSP90 tau protein Ubiquitin	7, 8, 18, 57
Huntington's disease	Striatal and cortical areas	Nuclear and cytoplasmic aggregates	Huntingtin Ubiquitin	7, 9, 16
Spinocerebellar ataxias	Cerebellum, spinal cord and brainstem	Cytoplasmic or intranuclear inclusions	Ataxins CACNA1A tau protein TBP ATN1	58–61
Friedreich ataxia	Dentate nucleus, dorsal root ganglia	Cytoplasmatic inclusions in neurons	Frataxin	62
ALS	Motor neurons	Cytoplasmatic aggregates in neurons and astrocytes	SOD I TDP-43 FUS/TLS Ubiquitin	13, 63, 64
Alexander's disease	Astrocytes	Rosenthal fibers	GFAP CRYAB HSP27 Plectin	65–67
Fragile X syndrome	Neocortex Hippocampus	Intranuclear inclusions	FMRP Ubiquitin	68
Transmissible spongiform encephalopathy (TSEs)	Cerebral cortex	Fibrillar amyloid deposits	Prion protein (PrP) MAP2 Tau protein	22, 69
Familial amyloid polyneuropathy	Sensory and motor nerve fibers Autonomic ganglions	Amyloid deposits	Transthyretin	70
Prolactinomas	Pituitary gland	Amyloid deposits	Prolactin	71
Non-neurologic disorders				
Disease	**Location**	**Aggregate types**	**Composition**	**References**
Aortic medial amyloid	Circulatory system	Amyloid deposits	Medin	72
Atherosclerosis	Circulatory system	Amyloid deposits	Apolipoprotein AI	73
Cardiac arrhythmias, isolated atrial amyloidosis	Circulatory system	Atrial amyloid deposits	Atrial natriuretic factor	74
Cerebral amyloid angiopathy	Circulatory system	Amyloid deposits	Beta amyloid, Cystatin	75

Continued

TABLE 12.1 Selected Protein Misfolding Disorders—cont'd

Non-neurologic disorders				
Disease	**Location**	**Aggregate types**	**Composition**	**References**
Diabetes mellitus type 2	Pancreas	Amyloid deposits	Amylin	76
Dialysis related amyloidosis	Systemic	Amyloid deposits in osteoarticular structures	Beta 2 microglobulin	77
Finnish amyloidosis	Systemic	Amyloid deposits	Gelsolin	78
Hereditary non-neuropathic systemic amyloidosis	Systemic	Amyloid deposits	Lysozyme	79
Lattice corneal dystrophy	Eye	Amyloid deposits	Keratoepithelin	80
Medullary carcinoma of the thyroid	Thyroid gland	Nuclear, cytoplasmic and extracellular amyloid deposits	Calcitonin	81
Rheumatoid arthritis	Bones and joints	B and T cell aggregates	Serum amyloid A	82
Sporadic inclusion body myositis	Muscle	Multiprotein aggregates: Aβ42, Tau, α-synuclein	S-IBM	83
Systemic AL amyloidosis	Systemic	Amyloid deposits	Immunoglobulin light chain AL	84

over other complementation assays is the fact that the signal is produced and visualized simply by the reconstitution of the fluorescent protein, without adding any substrate. First- and second-generation fluorescent proteins reconstitute the fluorophore much more efficiently at temperatures below 30°C, and were therefore suitable for studies in plants, worms, *Xenopus* and *in vitro* assays with purified proteins [3,41,42]. However, mammalian cells do not respond well to temperatures below 37°C. This limitation was overcome by the development of third-generation fluorescent proteins, such as Venus and Cerulean, which are brighter and able to efficiently reconstitute the fluorophore at 37°C (Fig. 12.1B). On the other hand, third-generation fluorophores often show lower signal-to-noise ratios because they have higher levels of spontaneous binding of the split proteins, i.e. binding not mediated by the interaction of the proteins of interest [42–44]. Point mutations in these proteins, or different partitions of the fluorophore, are able to improve signal-to-noise ratios by decreasing spontaneous binding and background signal, but there is still room for further improvement [42,43,45,46]. Another major limitation of some BiFC systems is that they are fundamentally irreversible once the functional fluorophore is formed, unlike complementation systems based on luciferase, β-lactamase or DHFR [36]. This feature complicates the visualization of reversible interactions, but it can be useful for trapping and visualization of rare complexes, or to test the effect of the accumulation of oligomers in living cells and organisms. There is a delay between the actual interaction between the proteins of interest and the reconstitution of the fluorophore, probably in the range of minutes. This makes it difficult to monitor phenomena that occur in the range of miliseconds or seconds in real time. Finally, original BiFC systems were limited to the study of the interaction between two proteins simultaneously, but current multicolor BiFC systems allow the analysis of multiple alternative protein–protein interactions simultaneously (Fig. 12.1C) [3,4]. Multicolor BiFC is based on the fact that different N-terminal fragments from different GFP-derived proteins have different excitation/emission spectra when combined with the same C-terminal fragment (Fig. 12.1C). For instance, N-terminal fragments of mLumin, Cerulean, or Venus can be used to identify three protein–protein interactions simultaneously in the same cell, using them in combination with the C-terminal fragment from ECFP. BiFC systems can be also combined with FRET/FLIM platforms to analyze the interaction between more than two proteins simultaneously [47].

ADVANTAGES OF BiFC SYSTEMS FOR STUDYING PROTEIN INTERACTIONS

BiFC systems have many advantages over other methods for the visualization of protein–protein interactions. First, they enable the visualization of actual protein–protein

TABLE 12.2 Proteins Used for Complementation Studies and Their Applications. We have Focused Mostly on Those Reports of Protein Complementation Systems Aimed at Studying Protein–Protein Interactions. For an Extensive Review of the Current Uses and Future Potential of Protein Complementation Assays, Please See Shekhawat and Ghosh (2011) [36]

Protein		Partitions	Aim	Reference
Ribonuclease A		20/21	First description of protein complementation	33
Beta-galactosidase		147/148	Protein–protein interaction	34, 85
Ubiquitin		35/36	Protein–protein interaction	35
Dihydrofolate reductase (DHFR)		107/108	Protein–protein interaction	86
Tobacco etch virus (TEV)-protease		118/119	Protein–protein interaction	87
Beta-lactamase		196/197	Protein–protein interaction DNA methylation	88, 89
Chorismate mutase		21/22	Protein–protein interaction	90
DnaE (intein)		123/124	Protein–protein interaction	91
Herpes Simplex Virus 1 (HSV1)-Thymidine kinase		265/266	Protein–protein interaction *in vivo* (combined with PET)	92
			Kills cells in the presence of ganciclovir	93
Luciferases	Firefly	437/438	Protein–protein interaction	94
	Gaussia	105/106	Protein–protein interaction	95
	Renilla	229/230	Protein–protein interaction	96
Fluorescent proteins	GFP	155/156 213/214	Protein–protein interaction	3, 51
	EGFP	157/158	Protein–protein interaction	97
	BFP	172/173	Protein–protein interaction	3
	ECFP	154/155, 172/173	Protein–protein interaction Production of genetically encoded calcium sensors	4, 38
	Cerulean	154/155, 172/173	Protein–protein interaction	53
	EYFP	154/155, 172/173	Protein–protein interaction	4
	Venus	144/145, 154/155, 158/159, 172/173, 210/211	Protein–protein interaction Production of genetically encoded calcium sensors	37–39, 42, 43, 45, 46, 53
	mCitrine	154/155, 172/173	Protein–protein interaction	53
	Kusabira Orange	–	Protein–protein interaction	Su et al 2006, oral communication[a]
	mRFP1	154/155, 168/169	Protein–protein interaction	3, 98
	mCherry	159/160	Protein–protein interaction	99
	mKate	151/152, 165/166	Protein–protein interaction	100
	mLumin	151/152, 165/167	Protein–protein interaction	100

[a] *http://www.dmphotonics.com/PW2011/PW2011BiFC.htm*

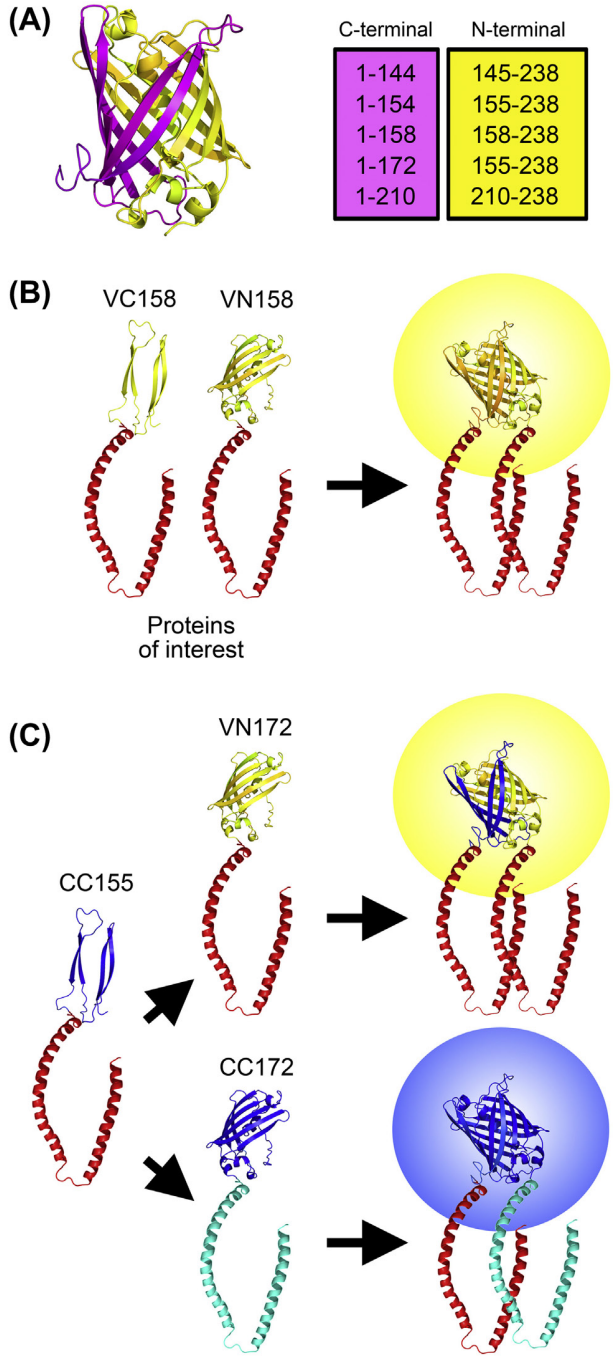

FIGURE 12.1 The principle of bimolecular fluorescence complementation (BiFC) assays. (A) Proteins from the family of the green fluorescent protein can be split in two non-fluorescent fragments. In the appropiate conditions, these fragments can physically interact and reconstitute the functional fluorophore. The fragments are not necessarily sequential. For example, the N-terminal fragment comprising amino acids 1–172 can be combined successfully with a C-terminal fragment comprising amino acids 155–238. (B) In single-color BiFC assays, the non-fluorescent fragments are fused to two proteins of interest. If the proteins dimerize, the non-fluorescent fragments are close enough to each other to reconstitute the fluorophore and emit fluorescence. (C) Interactions between more than two proteins can be studied by multicolor BiFC. In multicolor BiFC, the proteins of interest are fused to the N-terminal fragments of fluorophores with compatible excitation/emission spectra or to the C-terminal fragment of one of the fluorophores. Because the excitation/emission spectrum is determined by the largest fragment (N-terminal), each protein interaction will produce a different type of fluorescence.

interactions in the cell. This is an advantage over microscopy techniques that use co-localization of signals as an indication of protein–protein interaction. Microscopic co-localization does not necessarily mean that there is an interaction between the proteins of interest, as most light microscopy techniques do not afford enough resolution. Co-localization has a spatial resolution above 250 nm, and therefore proteins can co-localize and actually be very far from each other or in different planes. FRET-FLIM techniques enable the determination of whether two proteins actually interact, because the transfer of energy can occur only if the distance between the proteins is less than 10 nm. However, the distance between the two interactors is calculated based on the difference between the life-time of the two fluorophores and, therefore, the identification of the interaction between the proteins of interest is not as direct as in BiFC assays. Second, BiFC systems allow studies in living cells. Immunoprecipitation and immunoblotting techniques are excellent as biochemical proofs of interaction and/or oligomerization, but they cannot be used on living cells. The same happens with immunocytochemistry when samples are fixed and exposed to antibodies, procedures that introduce several additional artifacts and sources of bias in the experimental design. FRET-FLIM is also possible for studies in living cells. Finally, BiFC systems are much more suitable for high-throughput analyses than are immunoprecipitation, immunocytochemistry or FRET-FLIM methods. There are a few examples of FRET-based high-throughput screening of compounds that modify the interaction between two proteins, but their setup is far more complex, expensive and time-consuming than BiFC models [48,49]. Although the design and development of BiFC systems may be time-consuming, once it is established it can greatly save time and resources in large-scale analyses. Most of the time required would correspond to the cloning for the generation of the system (1–3 months), although there are now new tools available that could make this task easier, such as the Gateway BiFC vectors [50]. Preparation of samples for flow cytometry and their analysis can take as little as 2 hours (30–50 samples at a good cell concentration), and are also amenable to automation. If the analyzer is a fluorescence microscope, samples may not need any further handling (living cells) or just fixation (dead cells), but data acquisition, analysis and interpretation is not as straightforward as it is in flow cytometry analyses. This is also the main advantage of BiFC over FRET/FLIM assays. The same screening by immunoprecipitation or immunocytochemistry would greatly increase the costs due to the requirement of antibodies, and would require much more time for the processing of samples. Thus, the larger the study, the more cost-effective becomes a BiFC system.

Further toxicity and biochemical assays should complement results of the initial BiFC screening in order to characterize both the nature and toxicity of oligomeric species and the levels of expression of the constructs. If insoluble

aggregates are formed, Triton-X-soluble and -insoluble fractions, sucrose gradients or filter trap assays can be used to more accurately characterize larger inclusions [27,28].

PROTEIN COMPLEMENTATION ASSAYS FOR THE STUDY OF NEURODEGENERATIVE DISORDERS

We have recently developed BiFC models for the visualization of α-synuclein and huntingtin oligomerization in living cells [27–29]. Other groups developed similar models for the study of the oligomerization of APP, tau protein and huntingtin [30–32]. The principle of the success of these systems is the simplicity of the technique and the fact that we know *a priori* that the proteins of interest oligomerize and, therefore, finding the optimal combination of BiFC constructs is just a matter of time.

In BiFC models, monomers are not fluorescent, and only dimers, oligomers and larger inclusions – if they are formed – produce fluorescence (Fig. 12.2). This 'all or nothing' difference makes it possible to monitor closely the first steps of aggregation, i.e. oligomerization, because cells pass from a non-fluorescent to a fluorescent state progressively over time. Additionally, oligomers and large inclusions can be observed on a microscope as relatively different entities. Fluorescence from oligomers is homogeneously distributed, while large inclusions are foci of concentrated, intense fluorescence (Fig. 12.2). This allows the determination of the number, size and subcellular location of large inclusions [28] and the assessment of the dynamics of oligomeric species and inclusions of different sizes over time, for example. We have also used successfully our huntingtin BiFC system to show cell-to-cell transmission of huntingtin in living cells by flow cytometry [27]. In that study, two independent populations of cells were transfected with each of the BiFC constructs. When these cell populations were isolated, they did not display fluorescence, as determined by flow cytometry. However, when cell populations were mixed, some fluorescent cells appeared, demonstrating the traffic of mutant huntingtin between cells. Another possible, but yet unexplored use for these systems would be to include a localization signal in one of the BiFC constructs, such as a nuclear import signal or a mitochondrial localization signal, and study the dynamics of proteins between organelles and cytoplasm.

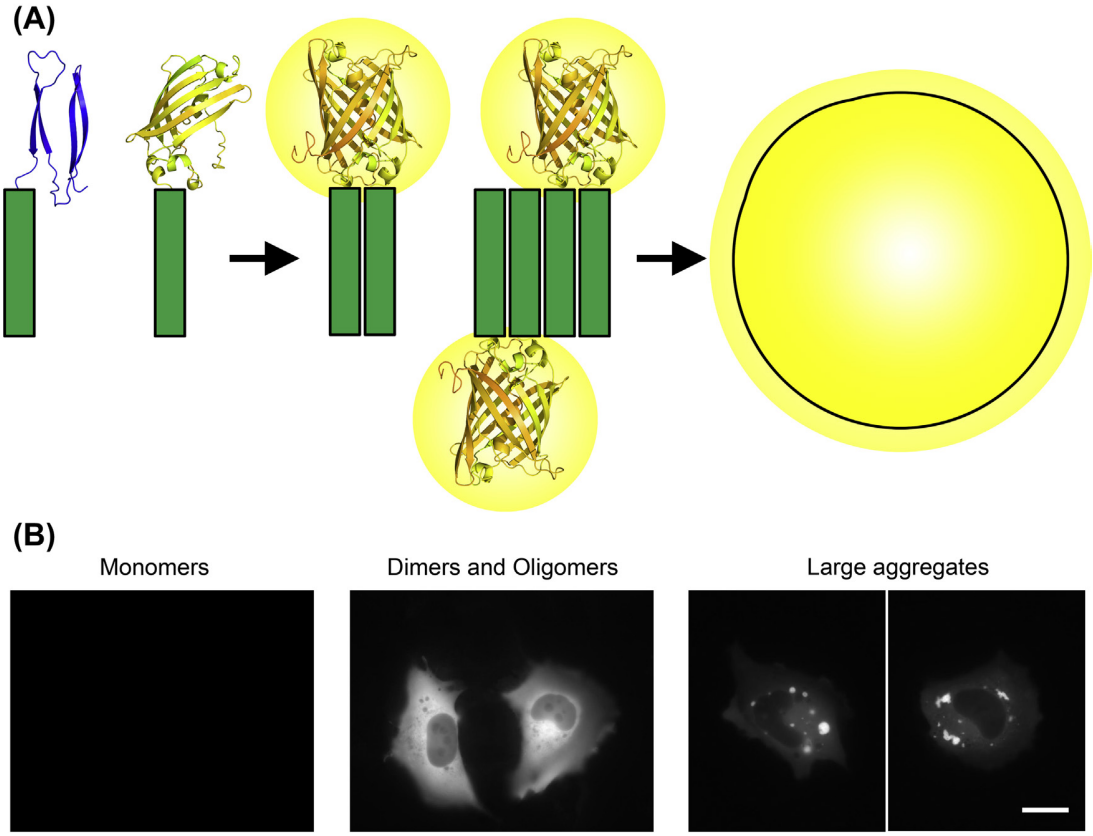

FIGURE 12.2 BiFC models of neurodegenerative disorders. (A) In these models, monomers do not show fluorescence. Dimers and oligomers show a homogeneously distributed fluorescence in the subcellular compartment where they are formed; larger inclusions are observed as brighter regions with different morphologies that 'scavenge' fluorescence from the rest of the cell. The localization of the oligomers and aggregates depends on the protein of interest and the particular experimental conditions. (B) In the huntingtin BiFC model, fluorescence is mostly restricted to the cytoplasm and aggregates are very frequent. Scale bar: 20 μm.

METHODS

Design

The first step for the design of a BiFC system is to choose the reporter protein. As mentioned before, basically every fluorescent protein can be split and used for BiFC (Table 12.2). However, they behave differently in many aspects that could be relevant to each particular experimental paradigm. First- and second-generation fluorophores, such as GFP, YFP, EGFP and EYFP, are less bright and fold with decreased efficiency at temperatures over 30°C. Although there is a BiFC system with a superfolder version of GFP, it is not clear whether this version is able to reconstitute the fluorophore at 30°C [51]. Third-generation fluorophores overcome the temperature issue but they produce more nonspecific background. Some point mutations in Venus, such as V150A or I152L, can improve signal-to-noise ratios of third-generation fluorophores in different experimental paradigms [42,46](Table 12,2). A recent report described a new partition of Venus (Aa 1–210 and Aa 210–238) that shows lower levels of spontaneous binding and higher signal-to-noise ratios [43]. Interestingly, the superfolder GFP BiFC also uses a partition in this interval (Aa 1–213 and Aa 214–238) [51].

While the lower brightness of first- and second-generation fluorophores is a disadvantage if the interaction is very weak, the higher brightness of third-generation fluorophores can also be a problem if interactions are strong. The former may produce a signal which is too low, masking the effect of conditions that inhibit oligomerization; the latter may produce saturating signals close to the upper limit of detection of the analyzers, thus masking conditions that enhance oligomerization. In theory, this could be compensated for by the use of stronger or weaker promoters or by transfecting cells with higher or lower numbers of plasmids.

There are additional particular properties specific for each fluorophore that could be of interest – or a disadvantage – for our BiFC system. For example, mCherry is more resistant to low pH than are the green proteins, a property that has been used to develop reporter systems in lysosomal and autophagy-related proteins [52]. On the other hand, mCherry and other fluorescent proteins have a strong tendency to aggregate themselves into tetramers, which is not desirable when analyzing protein–protein interactions.

The excitation and emission wavelengths of the fluorescent proteins can also pose limitations, especially when the BiFC system is to be used in combination with other fluorochromes or in multicolor BiFC. The C-terminal fragment is shorter and extremely similar among the different fluorescent proteins, while the N-terminal region is responsible for the excitation and emission properties of the final fluorophore. Multicolor BiFC takes advantage of this feature. In multicolor BiFC, one protein of interest is fused to a C-terminal fragment, and the other two (or more, in theory) are fused to two N-terminal fragments from different fluorescent proteins (Fig. 12.2B). The most popular combination for multicolor BiFC is Cerulean and Venus (amino acids 1–172, N-terminal) with the C-terminal region of ECFP (amino acids 155–238). While the combination of Cerulean with ECFP emits in the blue spectrum (max. ex. 439 nm; max. em. 479 nm), Venus with ECFP displays yellow/green fluorescence (max.ex. 504 nm; max. em. 513 nm) [4,53].

The optimal relative orientation of the protein of interest and the reporter protein cannot be currently predicted from their amino acid sequence or tertiary structure. Therefore, it has to be determined empirically by testing all possible combinations (Fig. 12.3). Producing and testing the different combinations of constructs is time-consuming and adds to the costs involved. However, testing can be very often restricted to two or three combinations on the basis of the properties of the protein of interest. This is illustrated by the following two examples. Proteins such as caspases, or the amyloid precursor protein, suffer post-translational cleavage. If the goal is to study the interaction of one of the cleavage fragments, then it is important to make sure that the reporter protein remains fused to the fragment of interest after cleavage. Other proteins are not functional when tags are located in their terminal regions. For example, some intermediate filaments, such as desmin or GFAP, may form aberrant aggregates or lose their ability to generate functional oligomers when tags are fused to their C-terminal side [54,55]. If the objective is to produce a BiFC system with intermediate filaments, the combinations should be therefore restricted to N-terminal fusions.

A series of controls should be included in the cloning plan and experimental design, especially to have an estimate of binding specificity and background (noise) signal caused by spontaneous binding of the halves of the reporter protein. Ideal controls would be fusion proteins that are unable to interact, such as versions of the proteins of interest which lack the interacting region or have a substitution in it. According to the original developers of BiFC and to our own experience, the non-fluorescent fragments of any fluorescent protein cannot be used as negative controls without being fused to a protein as they might produce higher background due to non-specific assembly (http://people.pharmacy.purdue.edu/~hu1/). In spite of these measures, researchers should expect some degree of noise, even with the least bright fluorescent proteins. This is especially enhanced when fusion proteins are overexpressed, because their higher intracellular concentration will increase the chance that the two non-fluorescent halves will meet and bind spontaneously. It is expected that physiologic promoters or less potent promoters would give lower background signals. Nevertheless, the very potent cytomegalovirus (CMV) promoter is still the most common promoter used in mammalian BiFC systems.

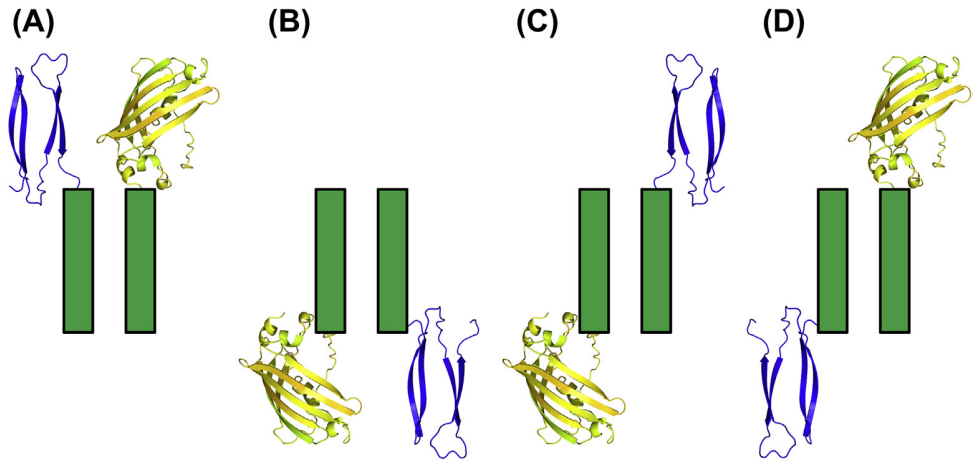

FIGURE 12.3 Basic constructs for the development of a BiFC system. They are represented from the N-terminal end (top) to the C-terminal end (bottom). The protein of interest is represented by the green rectangles, and the fluorophore fragments are represented by three-dimensional protein structures (blue, C-terminal fragment; yellow, N-terminal fragment). (A) Both fluorophore fragments fused to the C-terminal region of the proteins of interest. (B) Both fluorophore fragments fused to the N-terminal region of the proteins of interest. (C) The N-terminal fragment of the fluorophore fused to the C-terminal end of the proteins of interest, and the C-terminal fragment fused to the N-terminal end of the proteins of interest. (D) The reverse of option C.

In the case of BiFC models of neurodegenerative disorders, it can be relevant to compare wild type versus mutant, disease-related proteins. For example, in the case of our huntingtin BiFC model, we and others compare the oligomerization of HD-related mutant huntingtin (with a 103Q glutamine tract) versus the oligomerization of a wild type form of the protein (with a 25Q glutamine tract) [27,30].

In summary, the design of a BiFC system is not trivial and should be considered thoroughly before starting the production of constructs. Spending some time elaborating the best strategy for our experimental paradigm can prove advantageous in the development of the BiFC system.

Development

One of the most appealing features of BiFC systems is that they can be developed and optimized with reagents and equipment found in virtually every laboratory suited to cell and molecular biology, or in the core facilities of most institutions. This is further facilitated by the fact that research laboratories and some plasmid repositories have made available to the scientific community a few BiFC constructs where any protein of interest can be cloned (http://people.pharmacy.purdue.edu/~hu1/; http://www.addgene.org). Additionally, there are Gateway BiFC vectors available that can accelerate the cloning [50].

If the available constructs are not suitable for the particular experimental conditions, it is relatively easy to make home-made BiFC systems. The sequences of the protein of interest and the reporter protein, a vector, and cloning reagents and equipment are enough to produce the constructs. In order to test and optimize the BiFC system, needs are reduced to common cell culture materials and equipment such as simple flow cytometry analyzers and/or a wide-field/confocal fluorescence microscope that can be currently found in most laboratories. Detailed protocols of these sets of techniques are common knowledge and their explanation is beyond the scope of this chapter.

Troubleshooting

No Signal

A biologic cause for this is highly unlikely because (a) the protein of interest is known to interact with itself to form oligomers (in the case of protein misfolding disorders), and (b) there is always some background derived from the spontaneous binding of the halves of the reporter protein. Therefore, the cause of this problem should be of a technical nature. One could:

1. Check the DNA sequence of your constructs for possible frameshift mutations. Frameshift mutations, due to errors during cloning, will convert part of the reporter protein into a totally different protein unable to reconstitute a functional fluorophore.
2. Confirm that both BiFC constructs are efficiently transfected. Some cells are reluctant to be efficiently transfected with more than one plasmid, e.g. primary neurons or astrocytes. Cells transfected with only one BiFC construct will not give any signal.
3. Test other possible combinations of constructs, including molecular linkers of different size between the protein of interest and the reporter protein. The molecular linkers will increase the flexibility of the protein and improve the chances that the non-fluorescent halves will reconstitute the fluorophore.

Low Signal

The fluorescence of the BiFC system is, in theory, proportional to the oligomerization of the protein. However, there are many factors that could affect the amount of signal. In this case, one should:

1. Check transfection efficiency.
2. Verify the effect of temperature. Although it is not the optimal temperature for mammalian cells, reconstitution of the fluorophore is more efficient at lower temperatures.
3. Confirm that cultures are reasonably viable. If the protein of interest is very toxic it can kill those cells that express it and therefore give a lower signal. The situation could be improved by transfecting lower amounts of BiFC constructs or putting the fusion proteins under a less potent promoter. It could also be avoided by using cells more resistant to the toxicity of the protein.
4. Verify the time-frame for flurophore maturation. We detect fluorescent cells as soon as 4–6 hours after transfection by flow cytometry, but we need at least 8 hours to see a few fluorescent cells by microscopy.
5. Test combinations of constructs, including molecular linkers, in order to improve the chances that the fluorophore will be reconstituted.

If none of these measures improve the signal, the protein of interest may be interfering with the reconstitution of the fluorophore. This must be determined empirically, and may have no easy solution.

Low Signal-to-Noise Ratio (High Background)

In order to have an estimate of the spontaneous reconstitution of the BiFC fragments, a series of controls should be included in the experimental design.

1. Ideally, constructs containing a mutant protein of interest that is deficient for interaction should be used to establish the background line.
2. If available, inhibitors or activators of the interaction could be helpful to establish the specificity of the interaction as well as the upper and lower limits of signal.
3. If the background is still very high, one may need to change the fluorophore, modify the partition of the fluorophore, or look for point mutants that reduce its spontaneous reconstitution and thus improve the signal-to-noise ratio. Such partitions and mutations have been described for several fluorophores, Venus being probably the most studied in this sense.

NOTE: BiFC halves of the fluorophore should not be used without being fused to a protein of interest as background controls. They frequently show higher levels of fluorescence than when they are fused to proteins. The use of constructs containing third proteins, known to interact or not interact with the proteins of interest as a reference or basal line, is possible but not recommended. Each protein–protein interaction has a particular fluorescence pattern that can be altered by many factors, such as intracellular localization.

ACKNOWLEDGMENTS

SG is supported by a PhD Fellowship from AXA Research Fund, France, and by Fundação para a Ciência e Tecnologia (SFRH/BD/79337/2011). FH is supported by Fundação para a Ciência e Tecnologia (SFRH/BPD/63530/2009). TFO was supported by a Marie Curie International Reintegration Grant (Neurofold), an EMBO Installation Grant, and Fundação para a Ciência e Tecnologia.

REFERENCES

[1] Wang LJ, Hsu CW, Chen CC, Liang Y, Chen LC, Ojcius DM, et al. Interactome-wide analysis identifies end-binding protein 1 as a crucial component for the speck-like particle formation of activated AIM2 inflammasomes. Mol Cell Proteom 2012;11:1230–44.
[2] Kristensen AR, Gsponer J, Foster LJ. A high-throughput approach for measuring temporal changes in the interactome. Nat Methods 2012 Sep;9(9):907–9.
[3] Kodama Y, Wada M. Simultaneous visualization of two protein complexes in a single plant cell using multicolor fluorescence complementation analysis. Plant Mol Biol 2009;70(1–2):211–7.
[4] Hu CD, Kerppola TK. Simultaneous visualization of multiple protein interactions in living cells using multicolor fluorescence complementation analysis. Nat Biotechnol 2003;21(5):539–45.
[5] Jellinger KA. General aspects of neurodegeneration. J Neural Transm Suppl 2003;65:101–44.
[6] Tan JM, Wong ES, Lim KL. Protein misfolding and aggregation in Parkinson's disease. Antioxid Redox Signal 2009;11(9):2119–34.
[7] Agorogiannis EI, Agorogiannis GI, Papadimitriou A, Hadjigeorgiou GM. Protein misfolding in neurodegenerative diseases. Neuropathol Appl Neurobiol 2004;30(3):215–24.
[8] Forloni G, Terreni L, Bertani I, Fogliarino S, Invernizzi R, Assini A, et al. Protein misfolding in Alzheimer's and Parkinson's disease: genetics and molecular mechanisms. Neurobiol Aging 2002;23(5):957–76.
[9] The Huntington's Disease Collaborative Research Group. A novel gene containing a trinucleotide repeat that is expanded and unstable on Huntington's disease chromosomes. Cell 1993;72(6):971–83.
[10] Hattori N, Mizuno Y. Pathogenetic mechanisms of parkin in Parkinson's disease. Lancet 2004;364(9435):722–4.
[11] Conway KA, Harper JD, Lansbury PT. Accelerated in vitro fibril formation by a mutant alpha-synuclein linked to early-onset Parkinson disease. Nat Med 1998;4(11):1318–20.
[12] Nussbaum RL, Polymeropoulos MH. Genetics of Parkinson's disease. Hum Mol Genet 1997;6(10):1687–91.
[13] Kwiatkowski Jr TJ, Bosco DA, Leclerc AL, Tamrazian E, Vanderburg CR, Russ C, et al. Mutations in the FUS/TLS gene on chromosome 16 cause familial amyotrophic lateral sclerosis. Science 2009;323(5918):1205–8.
[14] Liscic RM, Grinberg LT, Zidar J, Gitcho MA, Cairns NJ. ALS and FTLD: two faces of TDP-43 proteinopathy. Eur J Neurol 2008;15(8):772–80.
[15] Durham HD, Roy J, Dong L, Figlewicz DA. Aggregation of mutant Cu/Zn superoxide dismutase proteins in a culture model of ALS. J Neuropathol Exp Neurol 1997;56(5):523–30.

[16] Arrasate M, Mitra S, Schweitzer ES, Segal MR, Finkbeiner S. Inclusion body formation reduces levels of mutant huntingtin and the risk of neuronal death. Nature 2004;431(7010):805–10.
[17] Chartier-Harlin MC, Kachergus J, Roumier C, Mouroux V, Douay X, Lincoln S, et al. Alpha-synuclein locus duplication as a cause of familial Parkinson's disease. Lancet 2004;364(9440):1167–9.
[18] Cataldo AM, Petanceska S, Peterhoff CM, Terio NB, Epstein CJ, Villar A, et al. App gene dosage modulates endosomal abnormalities of Alzheimer's disease in a segmental trisomy 16 mouse model of down syndrome. J Neurosci 2003;23(17):6788–92.
[19] Lemere CA, Blusztajn JK, Yamaguchi H, Wisniewski T, Saido TC, Selkoe DJ. Sequence of deposition of heterogeneous amyloid beta-peptides and APO E in Down syndrome: implications for initial events in amyloid plaque formation. Neurobiol Dis 1996;3(1):16–32.
[20] Maji SK, Perrin MH, Sawaya MR, Jessberger S, Vadodaria K, Rissman RA, et al. Functional amyloids as natural storage of peptide hormones in pituitary secretory granules. Science 2009;325(5938):328–32.
[21] Gamerdinger M, Kaya AM, Wolfrum U, Clement AM, Behl C. BAG3 mediates chaperone-based aggresome-targeting and selective autophagy of misfolded proteins. EMBO Rep 2011;12(2):149–56.
[22] Ben-Gedalya T, Lyakhovetsky R, Yedidia Y, Bejerano-Sagie M, Kogan NM, Karpuj MV, et al. Cyclosporin-A-induced prion protein aggresomes are dynamic quality-control cellular compartments. J Cell Sci 2011;124(Pt 11):1891–902.
[23] Bodner RA, Outeiro TF, Altmann S, Maxwell MM, Cho SH, Hyman BT, et al. Pharmacological promotion of inclusion formation: a therapeutic approach for Huntington's and Parkinson's diseases. Proc Natl Acad Sci USA 2006;103(11):4246–51.
[24] Winner B, Jappelli R, Maji SK, Desplats PA, Boyer L, Aigner S, et al. In vivo demonstration that alpha-synuclein oligomers are toxic. Proc Natl Acad Sci USA 2011;108(10):4194–9.
[25] Hansen C, Angot E, Bergström AL, Steiner JA, Pieri L, Paul G, et al. alpha-Synuclein propagates from mouse brain to grafted dopaminergic neurons and seeds aggregation in cultured human cells. J Clin Invest 2011;121(2):715–25.
[26] Lee SJ, Desplats P, Sigurdson C, Tsigelny I, Masliah E. Cell-to-cell transmission of non-prion protein aggregates. Nat Rev Neurol 2010;6(12):702–6.
[27] Herrera F, Tenreiro S, Miller-Fleming L, Outeiro TF. Visualization of cell-to-cell transmission of mutant huntingtin oligomers. PLoS Curr 2011;3:RRN1210.
[28] Herrera F, Outeiro TF. alpha-Synuclein modifies huntingtin aggregation in living cells. FEBS Lett 2012;586(1):7–12.
[29] Outeiro TF, Putcha P, Tetzlaff JE, Spoelgen R, Koker M, Carvalho F, et al. Formation of toxic oligomeric alpha-synuclein species in living cells. PLoS One 2008;3(4):e1867.
[30] Lajoie P, Snapp EL. Formation and toxicity of soluble polyglutamine oligomers in living cells. PLoS One 2010;5(12):e15245.
[31] Chen CD, Oh SY, Hinman JD, Abraham CR. Visualization of APP dimerization and APP-Notch2 heterodimerization in living cells using bimolecular fluorescence complementation. J Neurochem 2006;97(1):30–43.
[32] Chun W, Waldo GS, Johnson GV. Split GFP complementation assay for quantitative measurement of tau aggregation in situ. Methods Mol Biol 2011;670:109–23.
[33] Richards FM. On the enzymic activity of subtilisin-modified ribonuclease. Proc Natl Acad Sci USA 1958;44(2):162–6.
[34] Ullmann A, Jacob F, Monod J. Characterization by in vitro complementation of a peptide corresponding to an operator-proximal segment of the beta-galactosidase structural gene of Escherichia coli. J Mol Biol 1967;24(2):339–43.
[35] Johnsson N, Varshavsky A. Split ubiquitin as a sensor of protein interactions in vivo. Proc Natl Acad Sci USA 1994;91(22):10340–4.
[36] Shekhawat SS, Ghosh I. Split-protein systems: beyond binary protein–protein interactions. Curr Opin Chem Biol 2011;15(6):789–97.
[37] Nagai T, Sawano A, Park ES, Miyawaki A. Circularly permuted green fluorescent proteins engineered to sense Ca^{2+}. Proc Natl Acad Sci USA 2001;98(6):3197–202.
[38] Nagai T, Yamada S, Tominaga T, Ichikawa M, Miyawaki A. Expanded dynamic range of fluorescent indicators for Ca(2+) by circularly permuted yellow fluorescent proteins. Proc Natl Acad Sci USA 2004;101(29):10554–9.
[39] Nagai T, Ibata K, Park ES, Kubota M, Mikoshiba K, Miyawaki A. A variant of yellow fluorescent protein with fast and efficient maturation for cell-biological applications. Nat Biotechnol 2002;20(1):87–90.
[40] Hu CD, Chinenov Y, Kerppola TK. Visualization of interactions among bZIP and Rel family proteins in living cells using bimolecular fluorescence complementation. Mol Cell 2002;9(4):789–98.
[41] Shyu YJ, Hiatt SM, Duren HM, Ellis RE, Kerppola TK, Hu CD. Visualization of protein interactions in living *Caenorhabditis elegans* using bimolecular fluorescence complementation analysis. Nat Protoc 2008;3(4):588–96.
[42] Saka Y, Hagemann AI, Smith JC. Visualizing protein interactions by bimolecular fluorescence complementation in *Xenopus*. Methods 2008;45(3):192–5.
[43] Ohashi K, Kiuchi T, Shoji K, Sampei K, Mizuno K. Visualization of cofilin-actin and Ras-Raf interactions by bimolecular fluorescence complementation assays using a new pair of split Venus fragments. Biotechniques 2012;52(1):45–50.
[44] Robida AM, Kerppola TK. Bimolecular fluorescence complementation analysis of inducible protein interactions: effects of factors affecting protein folding on fluorescent protein fragment association. J Mol Biol 2009;394(3):391–409.
[45] Kodama Y, Hu CD. An improved bimolecular fluorescence complementation assay with a high signal-to-noise ratio. Biotechniques 2010;49(5):793–805.
[46] Nakagawa C, Inahata K, Nishimura S, Sugimoto K. Improvement of a Venus-based bimolecular fluorescence complementation assay to visualize bFos-bJun interaction in living cells. Biosci Biotechnol Biochem 2011;75(7):1399–401.
[47] Shyu YJ, Suarez CD, Hu CD. Visualization of AP-1 NF-kappaB ternary complexes in living cells by using a BiFC-based FRET. Proc Natl Acad Sci USA 2008;105(1):151–6.
[48] Song Y, Madahar V, Liao J. Development of FRET assay into quantitative and high-throughput screening technology platforms for protein-protein interactions. Ann Biomed Eng 2011;39(4):1224–34.
[49] Rogers MS, Cryan LM, Habeshian KA, Bazinet L, Caldwell TP, Ackroyd PC, et al. A FRET-based high-throughput screening assay to identify inhibitors of anthrax protective antigen binding to capillary morphogenesis gene 2 protein. PLoS One 2012;7(6):e39911.
[50] Gehl C, Waadt R, Kudla J, Mendel RR, Hansch R. New GATEWAY vectors for high throughput analyses of protein–protein interactions by bimolecular fluorescence complementation. Mol Plant 2009;2(5):1051–8.

[51] Zhou J, Lin J, Zhou C, Deng X, Xia B. An improved bimolecular fluorescence complementation tool based on superfolder green fluorescent protein. Acta Biochim Biophys Sin (Shanghai) 2011;43(3):239–44.
[52] Tresse E, Salomons FA, Vesa J, Bott LC, Kimonis V, Yao TP, et al. VCP/p97 is essential for maturation of ubiquitin-containing autophagosomes and this function is impaired by mutations that cause IBMPFD. Autophagy 2010;6(2):217–27.
[53] Shyu YJ, Liu H, Deng X, Hu CD. Identification of new fluorescent protein fragments for bimolecular fluorescence complementation analysis under physiological conditions. Biotechniques 2006;40(1):61–6.
[54] Flint D, Li R, Webster LS, Naidu S, Kolodny E, Percy A, et al. Splice site, frameshift, and chimeric GFAP mutations in Alexander disease. Hum Mutat 2012;33(7):1141–8.
[55] Haubold K, Herrmann H, Langer SJ, Evans RM, Leinwand LA, Klymkowsky MW. Acute effects of desmin mutations on cytoskeletal and cellular integrity in cardiac myocytes. Cell Motil Cytoskeleton 2003;54(2):105–21.
[56] Zhu X, Siedlak SL, Smith MA, Perry G, Chen SG. LRRK2 protein is a component of Lewy bodies. Ann Neurol 2006;60(5):617–8.
[57] Liao L, Cheng D, Wang J, Duong DM, Losik TG, Gearing M, et al. Proteomic characterization of postmortem amyloid plaques isolated by laser capture microdissection. J Biol Chem 2004 Aug 27;279(35):37061–8.
[58] Huynh DP, Del Bigio MR, Ho DH, Pulst SM. Expression of ataxin-2 in brains from normal individuals and patients with Alzheimer's disease and spinocerebellar ataxia 2. Ann Neurol 1999 Feb;45(2):232–41.
[59] Hayashi M, Kobayashi K, Furuta H. Immunohistochemical study of neuronal intranuclear and cytoplasmic inclusions in Machado-Joseph disease. Psychiatry Clin Neurosci 2003 Apr;57(2):205–13.
[60] Zhuchenko O, Bailey J, Bonnen P, Ashizawa T, Stockton DW, Amos C, et al. Autosomal dominant cerebellar ataxia (SCA6) associated with small polyglutamine expansions in the alpha 1A-voltage-dependent calcium channel. Nat Genet. 1997 Jan;15(1):62–9.
[61] Houlden H, Johnson J, Gardner-Thorpe C, Lashley T, Hernandez D, Worth P, et al. Mutations in TTBK2, encoding a kinase implicated in tau phosphorylation, segregate with spinocerebellar ataxia type 11. Nat Genet. 2007 Dec;39(12):1434–6.
[62] Koeppen AH. Friedreich's ataxia: pathology, pathogenesis, and molecular genetics. J Neurol Sci 2011 Apr 15;303(1–2):1–2.
[63] Arai T, Hasegawa M, Akiyama H, Ikeda K, Nonaka T, Mori H, et al. TDP-43 is a component of ubiquitin-positive tau-negative inclusions in frontotemporal lobar degeneration and amyotrophic lateral sclerosis. Biochem Biophys Res Commun 2006;351(3):602–11.
[64] Niwa J, Ishigaki S, Hishikawa N, Yamamoto M, Doyu M, Murata S, et al. Dorfin ubiquitylates mutant SOD1 and prevents mutant SOD1-mediated neurotoxicity. J Biol Chem. 2002 Sep 27;277(39):36793–8.
[65] Brenner M, Johnson AB, Boespflug-Tanguy O, Rodriguez D, Goldman JE, Messing A. Mutations in GFAP, encoding glial fibrillary acidic protein, are associated with Alexander disease. Nat Genet 2001 Jan;27(1):117–20.
[66] Iwaki T, Iwaki A, Tateishi J, Sakaki Y, Goldman JE. Alpha B-crystallin and 27-kd heat shock protein are regulated by stress conditions in the central nervous system and accumulate in Rosenthal fibers. Am J Pathol 1993 Aug;143(2):487–95.
[67] Tian R, Gregor M, Wiche G, Goldman JE. Plectin regulates the organization of glial fibrillary acidic protein in Alexander disease. Am J Pathol 2006 Mar;168(3):888–97.
[68] Koukoui SD, Chaudhuri A. Neuroanatomical, molecular genetic, and behavioral correlates of fragile X syndrome. Brain Res Rev. 2007 Jan;53(1):27–38.
[69] Zhang J, Dong XP. Dysfunction of microtubule-associated proteins of MAP2/tau family in Prion disease. Prion 2012 Sep-Oct;6(4):334–8.
[70] Fong VH, Vieira A. Transthyretin aggregates induce production of reactive nitrogen species. Neurodegener Dis 2013;11(1):42–8.
[71] Hinton DR, Polk RK, Linse KD, Weiss MH, Kovacs K, Garner JA. Characterization of spherical amyloid protein from a prolactin-producing pituitary adenoma. Acta Neuropathol 1997 Jan;93(1):43–9.
[72] Madine J, Middleton DA. Comparison of aggregation enhancement and inhibition as strategies for reducing the cytotoxicity of the aortic amyloid polypeptide medin. Eur Biophys J 2010 Aug;39(9):1281–8.
[73] Teoh CL, Griffin MD, Howlett GJ. Apolipoproteins and amyloid fibril formation in atherosclerosis. Protein Cell 2011 Feb;2(2):116–27.
[74] Steiner I, Hajkova P. Patterns of isolated atrial amyloid: a study of 100 hearts on autopsy. Cardiovasc Pathol 2006 Sep-Oct;15(5):287–90.
[75] Revesz T, Holton JL, Lashley T, Plant G, Frangione B, Rostagno A, et al. Genetics and molecular pathogenesis of sporadic and hereditary cerebral amyloid angiopathies. Acta Neuropathol 2009 Jul;118(1):115–30.
[76] Tomita T. Islet amyloid polypeptide in pancreatic islets from type 2 diabetic subjects. Islets 2012 May-Jun;4(3):223–32.
[77] Heegaard NH. beta(2)-microglobulin: from physiology to amyloidosis. Amyloid 2009;16(3):151–73.
[78] Solomon JP, Page LJ, Balch WE, Kelly JW. Gelsolin amyloidosis: genetics, biochemistry, pathology and possible strategies for therapeutic intervention. Crit Rev Biochem Mol Biol 2012 May-Jun;47(3):282–96.
[79] Pepys MB, Hawkins PN, Booth DR, Vigushin DM, Tennent GA, Soutar AK, et al. Human lysozyme gene mutations cause hereditary systemic amyloidosis. Nature 1993 Apr 8;362(6420):553–7.
[80] Ozawa D, Kaji Y, Yagi H, Sakurai K, Kawakami T, Naiki H, et al. Destruction of amyloid fibrils of keratoepithelin peptides by laser irradiation coupled with amyloid-specific thioflavin T. J Biol Chem. 2011 Mar 25;286(12):10856–63.
[81] Stamatakos M, Paraskeva P, Stefanaki C, Katsaronis P, Lazaris A, Safioleas K, et al. Medullary thyroid carcinoma: The third most common thyroid cancer reviewed. Oncol Lett. 2011 Jan;2(1):49–53; Epub 2010 Nov 23.
[82] Weyand CM. Immunopathologic aspects of rheumatoid arthritis: who is the conductor and who plays the immunologic instrument? J Rheumatol Suppl 2007 Jul;79:9–14.
[83] Askanas V, Engel WK, Nogalska A. Pathogenic considerations in sporadic inclusion-body myositis, a degenerative muscle disease associated with aging and abnormalities of myoproteostasis. J Neuropathol Exp Neurol 2012 Aug;71(8):680–93.
[84] Merlini G, Seldin DC, Gertz MA. Amyloidosis: pathogenesis and new therapeutic options. J Clin Oncol 2011 May 10;29(14):1924–33.
[85] Rossi F, Charlton CA, Blau HM. Monitoring protein-protein interactions in intact eukaryotic cells by beta-galactosidase complementation. Proc Natl Acad Sci USA 1997 Aug 5;94(16):8405–10.
[86] Pelletier JN, Campbell-Valois FX, Michnick SW. Oligomerization domain-directed reassembly of active dihydrofolate reductase from rationally designed fragments. Proc Natl Acad Sci USA 1998;95(21):12141–6.

[87] Wehr MC, Laage R, Bolz U, Fischer TM, Grünewald S, Scheek S, et al. Monitoring regulated protein-protein interactions using split TEV. Nat Methods 2006 Dec;3(12):985–93.
[88] Porter JR, Stains CI, Segal DJ, Ghosh I. Split beta-lactamase sensor for the sequence-specific detection of DNA methylation. Anal Chem 2007;79(17):6702–8.
[89] Spotts JM, Dolmetsch RE, Greenberg ME. Time-lapse imaging of a dynamic phosphorylation-dependent protein-protein interaction in mammalian cells. Proc Natl Acad Sci USA 2002;99(23):15142–7.
[90] Muller MM, Kries H, Csuhai E, Kast P, Hilvert D. Design, selection, and characterization of a split chorismate mutase. Protein Sci 2010 May;19(5):1000–10.
[91] Kanno A, Ozawa T, Umezawa Y. Intein-mediated reporter gene assay for detecting protein-protein interactions in living mammalian cells. Anal Chem 2006;78(2):556–60.
[92] Massoud TF, Paulmurugan R, Gambhir SS. A molecularly engineered split reporter for imaging protein-protein interactions with positron emission tomography. Nat Med 2010;16(8):921–6.
[93] Okada T, Caplen NJ, Ramsey WJ, Onodera M, Shimazaki K, Nomoto T, et al. In situ generation of pseudotyped retroviral progeny by adenovirus-mediated transduction of tumor cells enhances the killing effect of HSV-tk suicide gene therapy in vitro and in vivo. J Gene Med 2004;6(3):288–99.
[94] Paulmurugan R, Umezawa Y, Gambhir SS. Noninvasive imaging of protein–protein interactions in living subjects by using reporter protein complementation and reconstitution strategies. Proc Natl Acad Sci USA 2002 Nov 26;99(24):15608–13.
[95] Kim SB, Sato M, Tao H. Split Gaussia luciferase-based bioluminescence template for tracing protein dynamics in living cells. Anal Chem 2009;81(1):67–74.
[96] Paulmurugan R, Gambhir SS. Monitoring protein–protein interactions using split synthetic renilla luciferase protein-fragment-assisted complementation. Anal Chem 2003;75(7):1584–9.
[97] Barnard E, McFerran NV, Trudgett A, Nelson J, Timson DJ. Development and implementation of split-GFP-based bimolecular fluorescence complementation (BiFC) assays in yeast. Biochem Soc Trans 2008;36(Pt 3):479–82.
[98] Jach G, Pesch M, Richter K, Frings S, Uhrig JF. An improved mRFP1 adds red to bimolecular fluorescence complementation. Nat Methods 2006;3(8):597–600.
[99] Fan JY, Cui ZQ, Wei HP, Zhang ZP, Zhou YF, Wang YP, et al. Split mCherry as a new red bimolecular fluorescence complementation system for visualizing protein–protein interactions in living cells. Biochem Biophys Res Commun 2008;367(1):47–53.
[100] Chu J, Zhang Z, Zheng Y, Yang J, Qin L, Lu J, et al. A novel far-red bimolecular fluorescence complementation system that allows for efficient visualization of protein interactions under physiological conditions. Biosens Bioelectron 2009;25(1):234–9.